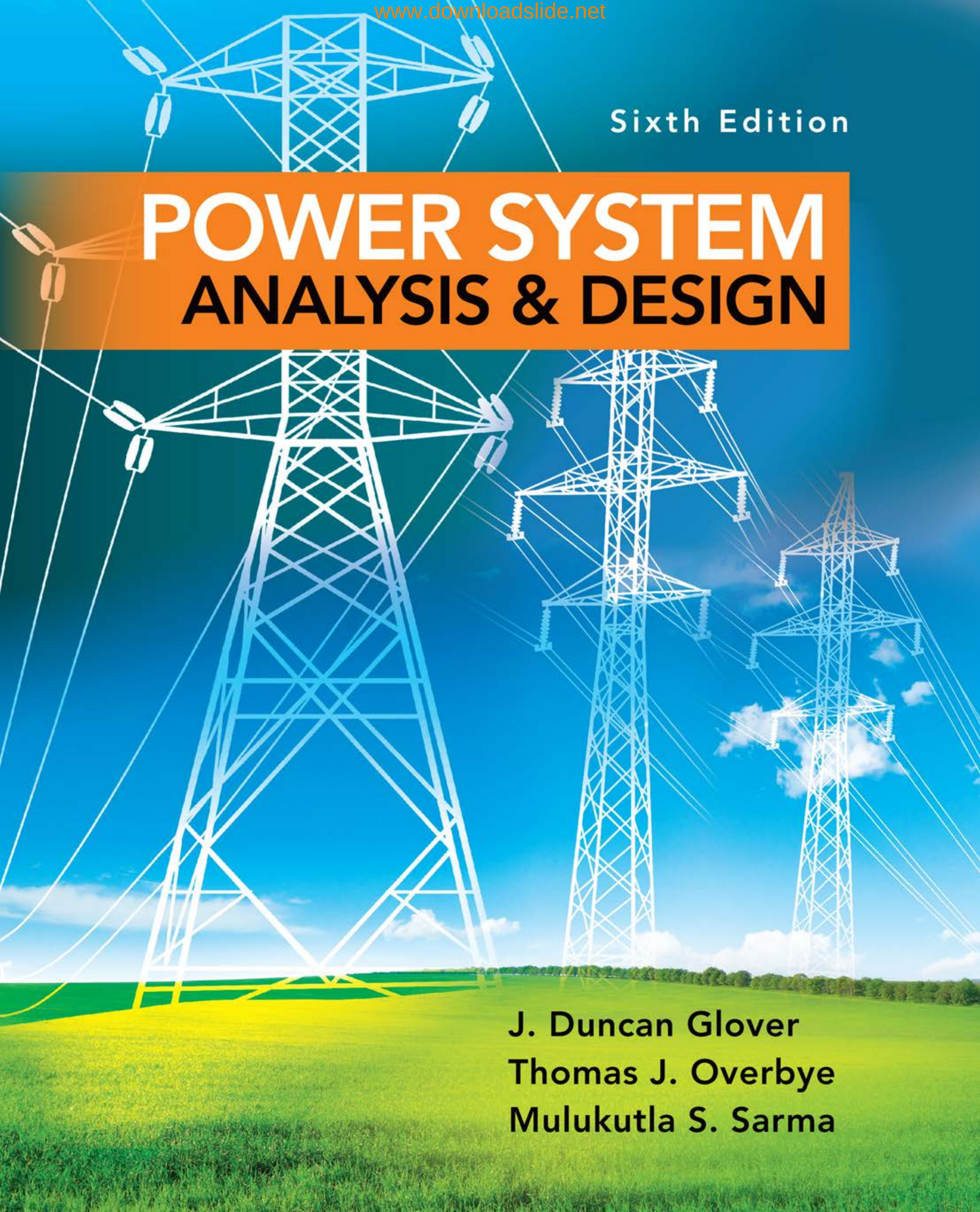

Sixth Edition

POWER SYSTEM
ANALYSIS & DESIGN

J. Duncan Glover
Thomas J. Overbye
Mulukutla S. Sarma

POWER SYSTEM ANALYSIS & DESIGN

SIXTH EDITION

J. DUNCAN GLOVER
Failure Electrical, LLC

THOMAS J. OVERBYE
University of Illinois

MULUKUTLA S. SARMA
Northeastern University

CENGAGE
Learning®

Australia • Brazil • Japan • Korea • Mexico • Singapore • Spain • United Kingdom • United States

Copyright 2017 Cengage Learning. All Rights Reserved. May not be copied, scanned, or duplicated, in whole or in part. Due to electronic rights, some third party content may be suppressed from the eBook and/or eChapter(s). Editorial review has deemed that any suppressed content does not materially affect the overall learning experience. Cengage Learning reserves the right to remove additional content at any time if subsequent rights restrictions require it.

This is an electronic version of the print textbook. Due to electronic rights restrictions, some third party content may be suppressed. Editorial review has deemed that any suppressed content does not materially affect the overall learning experience. The publisher reserves the right to remove content from this title at any time if subsequent rights restrictions require it. For valuable information on pricing, previous editions, changes to current editions, and alternate formats, please visit www.cengage.com/highered to search by ISBN#, author, title, or keyword for materials in your areas of interest.

Important Notice: Media content referenced within the product description or the product text may not be available in the eBook version.

Copyright 2017 Cengage Learning. All Rights Reserved. May not be copied, scanned, or duplicated, in whole or in part. Due to electronic rights, some third party content may be suppressed from the eBook and/or eChapter(s). Editorial review has deemed that any suppressed content does not materially affect the overall learning experience. Cengage Learning reserves the right to remove additional content at any time if subsequent rights restrictions require it.

CENGAGE
Learning®

***Power System Analysis & Design*, Sixth Edition**

J. Duncan Glover, Thomas J. Overbye, and Mulukutla S. Sarma

Product Director, Global Engineering: Timothy L. Anderson

Senior Content Developer: Mona Zeftel

Associate Media Content Developer: Ashley Kaupert

Product Assistant: Alexander Sham

Marketing Manager: Kristin Stine

Director, Content and Media Production: Sharon L. Smith

Content Project Manager: D. Jean Buttrom

Production Service: RPK Editorial Services, Inc.

Copyeditor: Warren Hapke

Proofreaders: Martha McMaster and Shelly Gerger-Knechtl

Indexer: RPK Editorial Services

Compositor: MPS Limited

Senior Art Director: Michelle Kunkler

Internal Designer: Carmela Pereira

Cover Designer: Itzhack Shelomi

Cover Image: High voltage power lines and pylon, kstudija/ShutterStock.com; Picturesque Green Field and Blue Sky, AlinaMD/ShutterStock.com; Power high voltage tower, kstudija /ShutterStock.com

Intellectual Property
  Analyst: Christine Myaskovsky
  Project Manager: Sarah Shainwald

Text and Image Permissions Researcher: Kristiina Paul

Senior Manufacturing Planner: Doug Wilke

WCN: 02-200-203

ALL RIGHTS RESERVED. No part of this work covered by the copyright herein may be reproduced or distributed in any form or by any means, except as permitted by U.S. copyright law, without the prior written permission of the copyright owner.

For product information and technology assistance, contact us at **Cengage Learning Customer & Sales Support, 1-800-354-9706**.

For permission to use material from this text or product, submit all requests online at **www.cengage.com/permissions**. Further permissions questions can be emailed to **permissionrequest@cengage.com**.

Library of Congress Control Number: 2015956452

ISBN: 978-1-305-63213-4

Cengage Learning
20 Channel Center Street
Boston, MA 02210
USA

Cengage Learning is a leading provider of customized learning solutions with employees residing in nearly 40 different countries and sales in more than 125 countries around the world. Find your local representative at **www.cengage.com.**

Cengage Learning products are represented in Canada by Nelson Education Ltd.

To learn more about Cengage Learning Solutions, visit **www.cengage.com/engineering**.

Purchase any of our products at your local college store or at our preferred online store **www.cengagebrain.com**.

Unless otherwise noted, all items © Cengage Learning.

Printed in the United States of America
Print Number: 01 Print Year: 2015

Copyright 2017 Cengage Learning. All Rights Reserved. May not be copied, scanned, or duplicated, in whole or in part. Due to electronic rights, some third party content may be suppressed from the eBook and/or eChapter(s). Editorial review has deemed that any suppressed content does not materially affect the overall learning experience. Cengage Learning reserves the right to remove additional content at any time if subsequent rights restrictions require it.

In loving memory of my mentors Professor Fred C. Schweppe [1933–1988] and Dr. Alexander Kusko [1921–2013]. You taught me, you guided me, you set the bar for which I continue to strive. You shall not be forgotten.

My Guardian Poet[s]

A guardian poet you have been to me
Much like an angel, there protecting me
When I was silent, lost in dark of night
You read my words and brought me back to light

You told me that my words were ever true
That in my writes were thoughts profound and new
You would not let me simply drift away
A word of hope you'd send to greet each day

Your name is there below each thing I write
To tear dimmed eyes you brought a vision bright
"The Queen of Passion," how I love the name
You gave to me and life is not the same

To you, my Guardian Poet, thanks I bring
You fool me not; I see your angel wing

Eileen Manassian Ghali

To Jo, Tim, Hannah, and Amanda

Copyright 2017 Cengage Learning. All Rights Reserved. May not be copied, scanned, or duplicated, in whole or in part. Due to electronic rights, some third party content may be suppressed from the eBook and/or eChapter(s). Editorial review has deemed that any suppressed content does not materially affect the overall learning experience. Cengage Learning reserves the right to remove additional content at any time if subsequent rights restrictions require it.

Copyright 2017 Cengage Learning. All Rights Reserved. May not be copied, scanned, or duplicated, in whole or in part. Due to electronic rights, some third party content may be suppressed from the eBook and/or eChapter(s). Editorial review has deemed that any suppressed content does not materially affect the overall learning experience. Cengage Learning reserves the right to remove additional content at any time if subsequent rights restrictions require it.

Contents

Preface xi

List of Symbols, Units, and Notation xvii

CHAPTER 1 Introduction 1

Case Study: How the Free Market Rocked the Grid 2

1.1 History of Electric Power Systems 10

1.2 Present and Future Trends 17

1.3 Electric Utility Industry Structure 20

1.4 Computers in Power System Engineering 21

1.5 PowerWorld Simulator 22

CHAPTER 2 Fundamentals 31

Case Study: Key Connections 32

2.1 Phasors 40

2.2 Instantaneous Power in Single-Phase AC Circuits 42

2.3 Complex Power 47

2.4 Network Equations 52

2.5 Balanced Three-Phase Circuits 55

2.6 Power in Balanced Three-Phase Circuits 63

2.7 Advantages of Balanced Three-Phase versus Single-Phase Systems 68

CHAPTER 3 Power Transformers 87

Case Study: Power Transformers—Life Management and Extension 88

3.1 The Ideal Transformer 95

3.2 Equivalent Circuits for Practical Transformers 101

Copyright 2017 Cengage Learning. All Rights Reserved. May not be copied, scanned, or duplicated, in whole or in part. Due to electronic rights, some third party content may be suppressed from the eBook and/or eChapter(s). Editorial review has deemed that any suppressed content does not materially affect the overall learning experience. Cengage Learning reserves the right to remove additional content at any time if subsequent rights restrictions require it.

3.3 The Per-Unit System 107
3.4 Three-Phase Transformer Connections and Phase Shift 115
3.5 Per-Unit Equivalent Circuits of Balanced Three-Phase Two-Winding Transformers 120
3.6 Three-Winding Transformers 125
3.7 Autotransformers 129
3.8 Transformers with Off-Nominal Turns Ratios 131

CHAPTER 4 Transmission Line Parameters 161

Case Study: Integrating North America's Power Grid 162
Case Study: Grid Congestion - Unclogging the Arteries of North America's Power Grid 167
4.1 Transmission Line Design Considerations 173
4.2 Resistance 178
4.3 Conductance 181
4.4 Inductance: Solid Cylindrical Conductor 181
4.5 Inductance: Single-Phase Two-Wire Line and Three-Phase Three-Wire Line with Equal Phase Spacing 186
4.6 Inductance: Composite Conductors, Unequal Phase Spacing, Bundled Conductors 188
4.7 Series Impedances: Three-Phase Line with Neutral Conductors and Earth Return 196
4.8 Electric Field and Voltage: Solid Cylindrical Conductor 201
4.9 Capacitance: Single-Phase Two-Wire Line and Three-Phase Three-Wire Line with Equal Phase Spacing 204
4.10 Capacitance: Stranded Conductors, Unequal Phase Spacing, Bundled Conductors 206
4.11 Shunt Admittances: Lines with Neutral Conductors and Earth Return 210
4.12 Electric Field Strength at Conductor Surfaces and at Ground Level 215
4.13 Parallel Circuit Three-Phase Lines 218

Copyright 2017 Cengage Learning. All Rights Reserved. May not be copied, scanned, or duplicated, in whole or in part. Due to electronic rights, some third party content may be suppressed from the eBook and/or eChapter(s). Editorial review has deemed that any suppressed content does not materially affect the overall learning experience. Cengage Learning reserves the right to remove additional content at any time if subsequent rights restrictions require it.

CHAPTER 5 **Transmission Lines: Steady-State Operation 237**

Case Study: The ABCs of HVDC Transmission Technologies: An Overview of High Voltage Direct Current Systems and Applications 238
5.1 Medium and Short Line Approximations 258
5.2 Transmission-Line Differential Equations 265
5.3 Equivalent π Circuit 271
5.4 Lossless Lines 274
5.5 Maximum Power Flow 282
5.6 Line Loadability 284
5.7 Reactive Compensation Techniques 289

CHAPTER 6 **Power Flows 309**

Case Study: Finding Flexibility—Cycling the Conventional Fleet 310
6.1 Direct Solutions to Linear Algebraic Equations: Gauss Elimination 330
6.2 Iterative Solutions to Linear Algebraic Equations: Jacobi and Gauss-Seidel 334
6.3 Iterative Solutions to Nonlinear Algebraic Equations: Newton-Raphson 340
6.4 The Power Flow Problem 345
6.5 Power Flow Solution by Gauss-Seidel 351
6.6 Power Flow Solution by Newton-Raphson 353
6.7 Control of Power Flow 363
6.8 Sparsity Techniques 369
6.9 Fast Decoupled Power Flow 372
6.10 The “DC” Power Flow 372
6.11 Power Flow Modeling of Wind Generation 374
6.12 Economic Dispatch 376
6.13 Optimal Power Flow 389
Design Projects 1–3 404–412

CHAPTER 7 **Symmetrical Faults 415**

Case Study: Short-Circuit Modeling of a Wind Power Plant 416
7.1 Series R–L Circuit Transients 435

Copyright 2017 Cengage Learning. All Rights Reserved. May not be copied, scanned, or duplicated, in whole or in part. Due to electronic rights, some third party content may be suppressed from the eBook and/or eChapter(s). Editorial review has deemed that any suppressed content does not materially affect the overall learning experience. Cengage Learning reserves the right to remove additional content at any time if subsequent rights restrictions require it.

7.2 Three-Phase Short Circuit—Unloaded Synchronous Machine 438
7.3 Power System Three-Phase Short Circuits 442
7.4 Bus Impedance Matrix 445
7.5 Circuit Breaker and Fuse Selection 455
Design Project 3 (*continued*) 472

CHAPTER 8 **Symmetrical Components 475**

Case Study: Technological Progress in High-Voltage Gas-Insulated Substations 476
8.1 Definition of Symmetrical Components 493
8.2 Sequence Networks of Impedance Loads 499
8.3 Sequence Networks of Series Impedances 506
8.4 Sequence Networks of Three-Phase Lines 508
8.5 Sequence Networks of Rotating Machines 510
8.6 Per-Unit Sequence Models of Three-Phase Two-Winding Transformers 516
8.7 Per-Unit Sequence Models of Three-Phase Three-Winding Transformers 522
8.8 Power in Sequence Networks 524

CHAPTER 9 **Unsymmetrical Faults 539**

Case Study: Innovative Medium Voltage Switchgear for Today's Applications 540
9.1 System Representation 547
9.2 Single Line-to-Ground Fault 553
9.3 Line-to-Line Fault 557
9.4 Double Line-to-Ground Fault 560
9.5 Sequence Bus Impedance Matrices 567
Design Project 3 (*continued*) 588
Design Project 4 589

CHAPTER 10 **System Protection 593**

Case Study: Upgrading Relay Protection Be Prepared for the Next Replacement or Upgrade Project 594
10.1 System Protection Components 612

Copyright 2017 Cengage Learning. All Rights Reserved. May not be copied, scanned, or duplicated, in whole or in part. Due to electronic rights, some third party content may be suppressed from the eBook and/or eChapter(s). Editorial review has deemed that any suppressed content does not materially affect the overall learning experience. Cengage Learning reserves the right to remove additional content at any time if subsequent rights restrictions require it.

10.2 Instrument Transformers 614
10.3 Overcurrent Relays 620
10.4 Radial System Protection 625
10.5 Reclosers and Fuses 629
10.6 Directional Relays 633
10.7 Protection of a Two-Source System with Directional Relays 634
10.8 Zones of Protection 635
10.9 Line Protection with Impedance (Distance) Relays 639
10.10 Differential Relays 645
10.11 Bus Protection with Differential Relays 647
10.12 Transformer Protection with Differential Relays 648
10.13 Pilot Relaying 653
10.14 Numeric Relaying 654

CHAPTER 11 **Transient Stability 669**

Case Study: Down, but Not Out 671
11.1 The Swing Equation 689
11.2 Simplified Synchronous Machine Model and System Equivalents 695
11.3 The Equal-Area Criterion 697
11.4 Numerical Integration of the Swing Equation 707
11.5 Multimachine Stability 711
11.6 A Two-Axis Synchronous Machine Model 719
11.7 Wind Turbine Machine Models 724
11.8 Design Methods for Improving Transient Stability 730

CHAPTER 12 **Power System Controls 739**

Case Study: No Light in August: Power System Restoration Following the 2003 North American Blackout 742
12.1 Generator-Voltage Control 757
12.2 Turbine-Governor Control 761
12.3 Load-Frequency Control 767

Copyright 2017 Cengage Learning. All Rights Reserved. May not be copied, scanned, or duplicated, in whole or in part. Due to electronic rights, some third party content may be suppressed from the eBook and/or eChapter(s). Editorial review has deemed that any suppressed content does not materially affect the overall learning experience. Cengage Learning reserves the right to remove additional content at any time if subsequent rights restrictions require it.

CHAPTER 13 **Transmission Lines: Transient Operation 779**

Case Study: Surge Arresters 780
Case Study: Emergency Response 794
13.1 Traveling Waves on Single-Phase Lossless Lines 809
13.2 Boundary Conditions for Single-Phase Lossless Lines 813
13.3 Bewley Lattice Diagram 822
13.4 Discrete-Time Models of Single-Phase Lossless Lines and Lumped RLC Elements 828
13.5 Lossy Lines 834
13.6 Multiconductor Lines 838
13.7 Power System Overvoltages 841
13.8 Insulation Coordination 847

CHAPTER 14 **Power Distribution 859**

Case Study: It's All in the Plans 860
14.1 Introduction to Distribution 875
14.2 Primary Distribution 878
14.3 Secondary Distribution 885
14.4 Transformers in Distribution Systems 890
14.5 Shunt Capacitors in Distribution Systems 900
14.6 Distribution Software 905
14.7 Distribution Reliability 906
14.8 Distribution Automation 910
14.9 Smart Grids 913

Appendix 921
Index 925

Copyright 2017 Cengage Learning. All Rights Reserved. May not be copied, scanned, or duplicated, in whole or in part. Due to electronic rights, some third party content may be suppressed from the eBook and/or eChapter(s). Editorial review has deemed that any suppressed content does not materially affect the overall learning experience. Cengage Learning reserves the right to remove additional content at any time if subsequent rights restrictions require it.

Preface

The objective of this book is to present methods of power system analysis and design, particularly with the aid of a personal computer, in sufficient depth to give the student the basic theory at the undergraduate level. The approach is designed to develop students' thinking processes, enabling them to reach a sound understanding of a broad range of topics related to power system engineering, while motivating their interest in the electrical power industry. Because we believe that fundamental physical concepts underlie creative engineering and form the most valuable and permanent part of an engineering education, we highlight physical concepts while giving due attention to mathematical techniques. Both theory and modeling are developed from simple beginnings so that they can be readily extended to new and complex situations.

NEW TO THIS EDITION

New chapter-opening case studies bring principles to life for students by providing practical, real-world engineering applications for the material discussed in each chapter.

Comprehensively revised problem sets ensure students have the practice they need to master critical skills.

Updated Instructor Resources

These resources include

- Instructor's Solutions Manual with solutions to all problems
- Comprehensive Test Bank offering additional problems
- Annotated Lecture Note PowerPoint Slides
- Lesson Plans that detail how to most effectively use this edition
- Updated PowerWorld Simulator Software
- Student PowerPoint Notes

New design projects in this edition meet Accreditation Board for Engineering and Technology (ABET) requirements to provide valuable hands-on experience and to help ensure students are receiving an education that meets globally recognized accreditation standards.

The latest version of the valuable PowerWorld Simulator (version 19) is included and integrated throughout the text.

Copyright 2017 Cengage Learning. All Rights Reserved. May not be copied, scanned, or duplicated, in whole or in part. Due to electronic rights, some third party content may be suppressed from the eBook and/or eChapter(s). Editorial review has deemed that any suppressed content does not materially affect the overall learning experience. Cengage Learning reserves the right to remove additional content at any time if subsequent rights restrictions require it.

KEY FEATURES

The text presents present-day, practical applications and new technologies along with ample coverage of the ongoing restructuring of the electric utility industry. It is supported by an ample number of worked examples, including illustrations, covering most of the theoretical points raised. It also includes PowerWorld Simulator version 19 to extend fully worked examples into computer implementations of the solutions. Version 19 includes power flow, optimal power flow, contingency analysis, short circuit, and transient stability.

The text includes a chapter on Power Distribution with content on Smart Grids.

It also includes discussions on modeling of wind turbines in power flow and transient stability.

Four design projects are included, all of which meet ABET requirements.

POWERWORLD SIMULATOR

One of the most challenging aspects of engineering education is giving students an intuitive feel for the systems they are studying. Engineering systems are, for the most part, complex. While paper-and-pencil exercises can be quite useful for highlighting the fundamentals, they often fall short in imparting the desired intuitive insight. To help provide this insight, the book uses PowerWorld Simulator version 19 to integrate computer-based examples, problems, and design projects throughout the text.

PowerWorld Simulator was originally developed at the University of Illinois at Urbana-Champaign to teach the basics of power systems to nontechnical people involved in the electricity industry, with version 1.0 introduced in June 1994. The program's interactive and graphical design made it an immediate hit as an educational tool, but a funny thing happened—its interactive and graphical design also appealed to engineers doing analysis of real power systems. To meet the needs of a growing group of users, PowerWorld Simulator was commercialized in 1996 by the formation of PowerWorld Corporation. Thus while retaining its appeal for education, over the years PowerWorld Simulator has evolved into a top-notch analysis package, able to handle power systems of any size. PowerWorld Simulator is now used throughout the power industry, with a range of users encompassing universities, utilities of all sizes, government regulators, power marketers, and consulting firms.

In integrating PowerWorld Simulator with the text, our design philosophy has been to use the software to extend, rather than replace, the fully worked examples provided in previous editions. Therefore, except when the problem size makes it impractical, each PowerWorld Simulator example includes a fully worked hand solution of the problem along with a PowerWorld Simulator case. This format allows students to simultaneously see the details of how a problem is solved and a computer implementation of the solution. The added benefit from PowerWorld Simulator is its ability to easily extend the example. Through its interactive design, students can quickly vary example parameters and immediately see the impact such changes have on the solution. By reworking the examples with the new parameters, students get immediate feedback on whether they understand the solution process.

Copyright 2017 Cengage Learning. All Rights Reserved. May not be copied, scanned, or duplicated, in whole or in part. Due to electronic rights, some third party content may be suppressed from the eBook and/or eChapter(s). Editorial review has deemed that any suppressed content does not materially affect the overall learning experience. Cengage Learning reserves the right to remove additional content at any time if subsequent rights restrictions require it.

The interactive and visual design of PowerWorld Simulator also makes it an excellent tool for instructors to use for in-class demonstrations. With numerous examples utilizing PowerWorld Simulator instructors can easily demonstrate many of the text topics. Additional PowerWorld Simulator functionality is introduced in the text problems and design projects.

PREREQUISITES

As background for this course, it is assumed that students have had courses in electric network theory (including transient analysis) and ordinary differential equations and have been exposed to linear systems, matrix algebra, and computer programming. In addition, it would be helpful, but not necessary, to have had an electric machines course.

ORGANIZATION

The text is intended to be fully covered in a two-semester or three-quarter course offered to seniors and first-year graduate students. The organization of chapters and individual sections is flexible enough to give the instructor sufficient latitude in choosing topics to cover, especially in a one-semester course. The text is supported by an ample number of worked examples covering most of the theoretical points raised. The many problems to be worked with a calculator as well as problems to be worked using a personal computer have been revised in this edition.

After an introduction to the history of electric power systems along with present and future trends, *Chapter 2* orients the students to the terminology and serves as a brief review of fundamentals. The chapter reviews phasor concepts, power, and single-phase as well as three-phase circuits.

Chapters 3 through 5 examine power transformers including the per-unit system, transmission-line parameters, and steady-state operation of transmission lines. *Chapter 6* examines power flows including the Newton-Raphson method, power-flow modeling of wind generation, economic dispatch, and optimal power flow. These chapters provide a basic understanding of power systems under balanced three-phase, steady-state, normal operating conditions.

Chapters 7 through 10, which cover symmetrical faults, symmetrical components, unsymmetrical faults, and system protection, come under the general heading of power system short-circuit protection. *Chapter 11* examines transient stability, which includes the swing equation, the equal-area criterion, and multi-machine stability with modeling of wind-energy systems. *Chapter 12* covers power system controls, including generator-voltage control, turbine-governor control, and load-frequency control. *Chapter 13* examines transient operation of transmission lines including power system overvoltages and surge protection.

Chapter 14 introduces the basic features of primary and secondary distribution systems as well as basic distribution components including distribution substation transformers, distribution transformers, and shunt capacitors. We list some of the major distribution software vendors followed by an introduction to distribution reliability, distribution automation, and smart grids.

Copyright 2017 Cengage Learning. All Rights Reserved. May not be copied, scanned, or duplicated, in whole or in part. Due to electronic rights, some third party content may be suppressed from the eBook and/or eChapter(s). Editorial review has deemed that any suppressed content does not materially affect the overall learning experience. Cengage Learning reserves the right to remove additional content at any time if subsequent rights restrictions require it.

ADDITIONAL RESOURCES

Companion websites for this book are available for both students and instructors. These websites provide useful links and other support material.

Student Website

The **Student Companion Site** includes a link to download the free student version of PowerWorld and Student PowerPoint Notes.

Instructor Resource Center

The **Instructor Companion Site** includes

- Instructor's Solutions Manual
- Annotated PowerPoint Slides
- Lecture Notes
- Test Banks

To access the support material described here along with all additional course materials, please visit https://sso.cengage.com.

MINDTAP ONLINE COURSE AND READER

This textbook is also available online through Cengage Learning's MindTap, a personalized learning program. Students who purchase the MindTap have access to the book's multimedia-rich electronic Reader and are able to complete homework and assessment material online, on their desktops, laptops, or iPads. Instructors who use a Learning Management System (such as Blackboard, Canvas, or Moodle) for tracking course content, assignments, and grading, can seamlessly access the MindTap suite of content and assessments for this course.

With MindTap, instructors can

- Personalize the Learning Path to match the course syllabus by rearranging content or appending original material to the online content
- Connect a Learning Management System portal to the online course and Reader
- Customize online assessments and assignments
- Track student engagement, progress and comprehension
- Promote student success through interactivity, multimedia, and exercises

Additionally, students can listen to the text through ReadSpeaker, take notes in the digital Reader, study from and create their own Flashcards, highlight content for easy reference, and check their understanding of the material through practice quizzes and automatically-graded homework.

ACKNOWLEDGMENTS

The material in this text was gradually developed to meet the needs of classes taught at universities in the United States and abroad over the past 35 years. The original 13 chapters were written by the first author, J. Duncan Glover, *Failure Electrical LLC*,

Copyright 2017 Cengage Learning. All Rights Reserved. May not be copied, scanned, or duplicated, in whole or in part. Due to electronic rights, some third party content may be suppressed from the eBook and/or eChapter(s). Editorial review has deemed that any suppressed content does not materially affect the overall learning experience. Cengage Learning reserves the right to remove additional content at any time if subsequent rights restrictions require it.

who is indebted to many people who helped during the planning and writing of this book. The profound influence of earlier texts written on power systems, particularly by W. D. Stevenson, Jr., and the developments made by various outstanding engineers are gratefully acknowledged. Details of sources can only be made through references at the end of each chapter, as they are otherwise too numerous to mention.

Chapter 14 *(Power Distribution)* was a collaborative effort between Dr. Glover (Sections 14.1-14.7) and Co-author Thomas J. Overbye (Sections 14.8 & 14.9). Professor Overbye, *University of Illinois at Urbana-Champaign* updated Chapter 6 *(Power Flows) and* Chapter 11 *(Transient Stability)*. He also provided the examples and problems using PowerWorld Simulator as well as three design projects. Co-author Mulukutla Sarma, *Northeastern University,* contributed to end-of-chapter multiple-choice questions and problems.

We commend the following Global Engineering team members at Cengage Learning: Timothy Anderson, Product Director; Mona Zeftel, Senior Content Developer; and Kristiina Paul, Freelance Permissions Researcher; as well as Rose Kernan of RPK Editorial Services, Inc. for their broad knowledge, skills, and ingenuity in publishing this edition. We also thank Jean Buttrom, Content Project Manager; Kristin Stine, Marketing Manager; Elizabeth Murphy, Engagement Specialist; Ashley Kaupert, Associate Media Content Developer; Teresa Versaggi and Alexander Sham, Product Assistants.

The reviewers for the sixth edition are as follows: Ross Baldick, *University of Texas at Austin*; François Bouffard, *McGill University*; Venkata Dinavahi, *University of Alberta*; Seyed Pouyan Jazayeri, *University of Calgary*; Bruno Osorno, *California State University at Northridge*, Zeb Tate, *University of Toronto*; and Mahyar Zarghami, *California State University at Sacramento.*

Substantial contributions to prior editions of this text were made by a number of invaluable reviewers, as follows:

Fifth Edition: Thomas L. Baldwin, *Florida State University;* Ali Emadi, *Illinois Institute of Technology;* Reza Iravani, *University of Toronto;* Surya Santoso, *University of Texas at Austin;* Ali Shaban, *California Polytechnic State University, San Luis Obispo;* and Dennis O. Wiitanen, *Michigan Technological University,* and Hamid Jaffari, *Danvers Electric.*

Fourth Edition: Robert C. Degeneff, *Rensselaer Polytechnic Institute;* Venkata Dina-vahi, *University of Alberta;* Richard G. Farmer, *Arizona State University;* Steven M. Hietpas, *South Dakota State University;* M. Hashem Nehrir, *Montana State University;* Anil Pahwa, *Kansas State University;* and Ghadir Radman, *Tennessee Technical University.*

Third Edition: Sohrab Asgarpoor, *University of Nebraska-Lincoln;* Mariesa L. Crow, *University of Missouri-Rolla;* Ilya Y. Grinberg, *State University of New York, College at Buffalo;* Iqbal Husain, *The University of Akron;* W. H. Kersting, *New Mexico State University;* John A. Palmer, *Colorado School of Mines;* Satish J. Ranada, *New Mexico State University;* and Shyama C. Tandon, *California Polytechnic State University.*

Second Edition: Max D. Anderson, *University of Missouri-Rolla;* Sohrab Asgarpoor, *University of Nebraska-Lincoln;* Kaveh Ashenayi, *University of Tulsa;* Richard D. Christie, Jr., *University of Washington;* Mariesa L. Crow, *University of Missouri-Rolla;* Richard G. Farmer, *Arizona State University;* Saul Goldberg, *California Polytechnic*

Copyright 2017 Cengage Learning. All Rights Reserved. May not be copied, scanned, or duplicated, in whole or in part. Due to electronic rights, some third party content may be suppressed from the eBook and/or eChapter(s). Editorial review has deemed that any suppressed content does not materially affect the overall learning experience. Cengage Learning reserves the right to remove additional content at any time if subsequent rights restrictions require it.

University; Clifford H. Grigg, *Rose-Hulman Institute of Technology;* Howard B. Hamilton, *University of Pittsburgh;* Leo Holzenthal, Jr., *University of New Orleans;* Walid Hubbi, *New Jersey Institute of Technology;* Charles W. Isherwood, *University of Massachusetts-Dartmouth;* W. H. Kersting, *New Mexico State University;* Wayne E. Knabach, *South Dakota State University;* Pierre-Jean Lagace, *IREQ Institut de Reserche a"Hydro-Quebec;* James T. Lancaster, *Alfred University;* Kwang Y. Lee, *Pennsylvania State University;* Mohsen Lotfalian, *University of Evansville;* Rene B. Marxheimer, *San Francisco State University,* Lamine Mili, *Virginia Polytechnic Institute and State University;* Osama A. Mohammed, *Florida International University;* Clifford C. Mosher, *Washington State University,* Anil Pahwa, *Kansas State University;* M. A. Pai, *University of Illinois at Urbana-Champaign;* R. Ramakumar, *Oklahoma State University;* Teodoro C. Robles, *Milwaukee School of Engineering,* Ronald G. Schultz, *Cleveland State University;* Stephen A. Sebo, *Ohio State University;* Raymond Shoults, *University of Texas at Arlington,* Richard D. Shultz, *University of Wisconsin at Platteville;* Charles Slivinsky, *University of Missouri-Columbia;* John P. Stahl, *Ohio Northern University;* E. K. Stanek, *University of Missouri-Rolla;* Robert D. Strattan, *University of Tulsa;* Tian-Shen Tang, *Texas A&M University-Kingsville;* S. S. Venkata, *University of Washington;* Francis M. Wells, *Vanderbilt University;* Bill Wieserman, *University of Pennsylvania-Johnstown;* Stephen Williams, *U.S. Naval Postgraduate School;* and Salah M. Yousif, *California State University-Sacramento.*

First Edition: Frederick C. Brockhurst, *Rose-Hulman Institute of Technology;* Bell A. Cogbill. *Northeastern University;* Saul Goldberg, *California Polytechnic State University;* Mack Grady, *University of Texas at Austin;* Leonard F. Grigsby, *Auburn University;* Howard Hamilton, *University of Pittsburgh;* William F. Horton, *California Polytechnic State University;* W. H. Kersting, *New Mexico State University;* John Pavlat, *Iowa State University;* R. Ramakumar, *Oklahoma State University;* B. Don Russell, *Texas A&M;* Sheppard Salon, *Rensselaer Polytechnic Institute;* Stephen A. Sebo, *Ohio State University;* and Dennis O. Wiitanen, *Michigan Technological University.*

In conclusion, the objective in writing this text and the accompanying software package will have been fulfilled if the book is considered to be student-oriented, comprehensive, and up to date, with consistent notation and necessary detailed explanation at the level for which it is intended.

J. Duncan Glover

Thomas J. Overbye

Mulukutla S. Sarma

Copyright 2017 Cengage Learning. All Rights Reserved. May not be copied, scanned, or duplicated, in whole or in part. Due to electronic rights, some third party content may be suppressed from the eBook and/or eChapter(s). Editorial review has deemed that any suppressed content does not materially affect the overall learning experience. Cengage Learning reserves the right to remove additional content at any time if subsequent rights restrictions require it.

List of Symbols, Units, and Notation

Symbol	Description	Symbol	Description
a	operator 1/120°	P	real power
a_t	transformer turns ratio	q	Charge
A	area	Q	reactive power
A	transmission line parameter	r	radius
$\boldsymbol{A}$	symmetrical components	R	resistance
	transformation matrix	R	turbine-governor regulation
B	loss coefficient		constant
B	frequency bias constant	$\mathbf{R}$	resistance matrix
B	phasor magnetic flux density	s	Laplace operator
B	transmission line parameter	S	apparent power
C	capacitance	S	complex power
C	transmission line parameter	t	time
D	damping	T	period
D	distance	T	temperature
D	transmission line parameter	T	torque
E	phasor source voltage	$v(t)$	instantaneous voltage
E	phasor electric field strength	V	voltage magnitude (rms unless
$\boldsymbol{f}$	frequency		otherwise indicated)
G	conductance	V	phasor voltage
$\mathbf{G}$	conductance matrix	$\boldsymbol{V}$	vector of phasor voltages
H	normalized inertia constant	X	reactance
H	phasor magnetic field intensity	$\mathbf{X}$	reactance matrix
$i(t)$	instantaneous current	Y	phasor admittance
I	current magnitude (rms unless	$\boldsymbol{Y}$	admittance matrix
	otherwise indicated)	Z	phasor impedance
I	phasor current	$\boldsymbol{Z}$	impedance matrix
$\boldsymbol{I}$	vector of phasor currents	α	angular acceleration
j	operator 1/90°	α	transformer phase
J	moment of inertia		shift angle
l	length	β	current angle

Copyright 2017 Cengage Learning. All Rights Reserved. May not be copied, scanned, or duplicated, in whole or in part. Due to electronic rights, some third party content may be suppressed from the eBook and/or eChapter(s). Editorial review has deemed that any suppressed content does not materially affect the overall learning experience. Cengage Learning reserves the right to remove additional content at any time if subsequent rights restrictions require it.

Symbol	Description	Symbol	Description
l	length	β	area frequency response characteristic
L	inductance		
L	inductance matrix	δ	voltage angle
N	number (of buses, lines, turns, etc.)	δ	torque angle
p.f.	power factor	ε	permittivity
$p(t)$	instantaneous power	Γ	reflection or refraction coefficient
λ	magnetic flux linkage		
λ	Penalty factor	θ	impedance angle
Φ	magnetic flux	θ	angular position
ρ	resistivity	μ	permeability
τ	time in cycles	υ	velocity of propagation
τ	transmission line transit time	ω	radian frequency

SI Units

A	ampere
C	coulomb
F	farad
H	henry
Hz	hertz
J	joule
kg	kilogram
m	meter
N	newton
rad	radian
s	second
S	siemen
VA	voltampere
var	voltampere reactive
W	watt
Wb	weber
Ω	ohm

English Units

BTU	British thermal unit
Cmil	circular mil
ft	foot
hp	horsepower
in	inch
mi	mile

Notation

Lowercase letters such as v(t) and i(t) indicate instantaneous values.
Uppercase letters such as V and I indicate rms values.
Uppercase letters in italic such as *V* and *I* indicate rms phasors.
Matrices and vectors with real components such as **R** and **I** are indicated by boldface type.
Matrices and vectors with complex components such as ***Z*** and ***I*** are indicated by boldface italic type.
Superscript T denotes vector or matrix transpose.
Asterisk (*) denotes complex conjugate.
PW highlights problems that utilize PowerWorld Simulator.

Copyright 2017 Cengage Learning. All Rights Reserved. May not be copied, scanned, or duplicated, in whole or in part. Due to electronic rights, some third party content may be suppressed from the eBook and/or eChapter(s). Editorial review has deemed that any suppressed content does not materially affect the overall learning experience. Cengage Learning reserves the right to remove additional content at any time if subsequent rights restrictions require it.

1 Introduction

Blundell geothermal power plant near Milford, UT, USA. This 38-MW plant consists of two generating units powered by geothermal steam. Steam is created from water heated by magma at depths up to 6100 meters below Earth's surface. (Courtesy of PacifiCorp.)

Electrical engineers are concerned with every step in the process of generation, transmission, distribution, and utilization of electrical energy. The electric utility industry is probably the largest and most complex industry in the world. The electrical engineer who works in that industry encounters challenging problems in designing future power systems to deliver increasing amounts of electrical energy in a safe, clean, and economical manner.

The objectives of this chapter are to review briefly the history of the electric utility industry, to discuss present and future trends in electric power systems, to describe

Copyright 2017 Cengage Learning. All Rights Reserved. May not be copied, scanned, or duplicated, in whole or in part. Due to electronic rights, some third party content may be suppressed from the eBook and/or eChapter(s). Editorial review has deemed that any suppressed content does not materially affect the overall learning experience. Cengage Learning reserves the right to remove additional content at any time if subsequent rights restrictions require it.

the restructuring of the electric utility industry, and to introduce PowerWorld Simulator—a power system analysis and simulation software package.

CASE STUDY

The following article describes the deregulation of the electric utility industry that has been taking place in the United States, including the benefits and problems that have been encountered with deregulation. During the last two decades, deregulation has had both good and bad effects. It has changed the mix of fuels in the U.S. generation fleet, shifting it away from coal and nuclear power toward natural gas and has opened the door to greener forms of electricity generation. It has also made many companies that provide electricity more efficient by increasing the reliability of power plants and reducing labor costs. However, wholesale prices of electricity have increased dramatically in some areas of the United States, market-based investments in transmission have been problematic, and rolling blackouts have been encountered [8].

How the Free Market Rocked the Grid*

Seth Blumsack Pennsylvania State University

It led to higher rates and rolling blackouts, but it also opened the door to greener forms of electricity generation.

Most of us take for granted that the lights will work when we flip them on, without worrying too much about the staggeringly complex things needed to make that happen. Thank the engineers who designed and built the power grids for that—but don't thank them too much. Their main goal was reliability; keeping the cost of electricity down was less of a concern. That's in part why so many people in the United States complain about high electricity prices. Some armchair economists (and a quite a few real ones) have long argued that the solution is deregulation. After all, many other U.S. industries have been deregulated—take, for instance, oil, natural gas, or trucking—and greater competition in those sectors swiftly brought prices down. Why not electricity?

Such arguments were compelling enough to convince two dozen or so U.S. states to deregulate their electric industries. Most began in the mid-1990s, and problems emerged soon after, most famously in the rolling blackouts that Californians suffered through in the summer of 2000 and the months that followed. At the root of these troubles is the fact that free markets can be messy and volatile, something few took into account when deregulation began. But the consequences have since proved so

© 2010 IEEE. Reprinted, with permission, from Seth Blumsack, "How the Free Market Rocked the Grid," IEEE Spectrum, December 2010, pp. 44–59.

---

*How the Free Market Rocked the Grid by Seth Blumsack, © 2010 IEEE. Reprinted, with permission, from *IEEE Spectrum* (December 2010), pg. 44–48, 57–59.

Copyright 2017 Cengage Learning. All Rights Reserved. May not be copied, scanned, or duplicated, in whole or in part. Due to electronic rights, some third party content may be suppressed from the eBook and/or eChapter(s). Editorial review has deemed that any suppressed content does not materially affect the overall learning experience. Cengage Learning reserves the right to remove additional content at any time if subsequent rights restrictions require it.

chaotic that a quarter of these states have now suspended plans to revamp the way they manage their electric utilities, and few (if any) additional states are rushing to jump on the deregulation bandwagon.

The United States is far from being the only nation that has struggled with electricity deregulation. But the U.S. experience is worth exploring because it highlights many of the challenges that can arise when complex industries such as electric power generation and distribution are subject to competition.

Unlike many other nations grappling with electricity deregulation, the United States has never had one governmentowned electric utility running the whole country. Instead, a patchwork of for-profit utilities, publicly owned municipal utilities, and electric cooperatives keeps the nation's lights on. The story of how that mixture has evolved over the last 128 years helps to explain why deregulation hasn't made electric power as cheap and plentiful as many had hoped.

The 1882 opening of Thomas Edison's Pearl Street generation station in New York City marks the birth of the American electric utility industry. That station produced low-voltage direct current, which had to be consumed close to the point of production, because sending it farther would have squandered most of the power as heat in the connecting wires.

Edison's approach prevailed for a while, with different companies scrambling to build neighborhood power stations. They were regulated only to the extent that their owners had to obtain licenses from local officials. Municipalities handed these licenses out freely, showing the prevailing laissez-faire attitude toward competition. Also, politicians wanted to see the cost of electricity drop. (A kilowatt-hour in the late 1800s cost about U.S. $5.00 in today's dollars; now it averages just 12 cents.)

It didn't take long, though, before Samuel Insull, a former Edison employee who became a utility entrepreneur in the Midwest, realized that the technology George Westinghouse was advocating—large steam or hydroelectric turbines linked to long-distance ac transmission lines—could provide electricity at lower cost. Using such equipment, his company soon drove its competitors out of business. Other big utilities followed Insull's lead and came to monopolize the electricity markets in New York, New Jersey, and the Southeast. But the rise of these companies was ultimately a bane to consumers, who had to pay exorbitant prices after the competition had been quashed.

Angered by the steep rates, consumers formed electricity cooperatives and municipal utilities. That in turn led Insull and his counterparts to plead with state officials for protection from this "ruinous" competition. Politicians complied, passing laws that granted the large electric power companies exclusive franchises in their areas in exchange for regulation of their prices and profits. The municipal utilities and electricity cooperatives continued to operate but in most cases never grew as large as the regulated for-profit (investor-owned) utilities.

This basic structure remained in place until the oil shocks of the 1970s. Real electricity prices rose by almost 50 percent during that

Copyright 2017 Cengage Learning. All Rights Reserved. May not be copied, scanned, or duplicated, in whole or in part. Due to electronic rights, some third party content may be suppressed from the eBook and/or eChapter(s). Editorial review has deemed that any suppressed content does not materially affect the overall learning experience. Cengage Learning reserves the right to remove additional content at any time if subsequent rights restrictions require it.

troubled decade, despite having fallen virtually every year since the opening of Edison's Pearl Street station. One culprit was the widespread use of imported oil. The United States then generated almost 20 percent of its electricity using fuel oil; today that figure is less than 1 percent. And many utilities had made some poor investments—primarily in nuclear power—which their customers had to pay for.

The 1970s also exposed problems in how the electric power industry was regulated. Power grids were growing in complexity as different utilities began interconnecting, and many regulators—particularly those whose appointments were political favors—didn't understand the technical implications of their decisions. The combination of rising prices and obvious mismanagement led many large industrial consumers of electricity to push for deregulation.

The Public Utility Regulatory Policies Act of 1978 was the first shot fired in the ensuing battle. The new federal law allowed nonutility companies to generate electricity from "alternative" fuel sources (mostly natural gas), and it required utilities to sign long-term supply contracts with these new generating companies. The Energy Policy Act of 1992 expanded the pool of players in the wholesale electricity market by allowing financial institutions—Morgan Stanley being the first—to buy and sell bulk electric power. Yet neither act was effective in curbing electricity prices.

Two states, California and Pennsylvania, then decided to take more drastic measures. They established centralized spot markets for electricity and allowed individual customers to choose their electricity suppliers. While Pennsylvania's experiment has largely run smoothly, California's experience was quite different. After two years of reasonably stable operation, wholesale prices exploded in 2000, from a few cents per kilowatt-hour to more than a dollar per kilowatt-hour. One reason for those astronomical prices was that power-trading companies like Enron Corp. had figured out how to game the system. With retail prices capped by law at 6.7 cents per kilowatt-hour, two of the state's three investor-owned utilities, Pacific Gas & Electric and Southern California Edison, ran out of money to pay for electricity. That triggered a second power crisis the following year, which forced the state to buy electricity from producers. The long-term contracts signed during that period of panic buying saddled California taxpayers with a debt of some $40 billion.

■ ■ ■ ■

For Californians, at least, deregulation had lost its gloss. This turned out to be temporary: The state recently reintroduced centralized wholesale markets modeled after Pennsylvania's. But has deregulation on the whole made things better or worse? Dozens of studies have attempted to answer that question. But you can't simply compare states that have aggressively deregulated with ones that haven't. That would ignore the fact that some states have built-in advantages that keep prices low: proximity to natural resources,

Copyright 2017 Cengage Learning. All Rights Reserved. May not be copied, scanned, or duplicated, in whole or in part. Due to electronic rights, some third party content may be suppressed from the eBook and/or eChapter(s). Editorial review has deemed that any suppressed content does not materially affect the overall learning experience. Cengage Learning reserves the right to remove additional content at any time if subsequent rights restrictions require it.

a large base of generation capacity, and so forth. It also ignores what utilities and regulators would have done if deregulation had never happened.

To answer the question properly, you'd need to figure out what things would have been like in the absence of deregulation. And that's well-nigh impossible. Of the various studies that have attempted to assess the impacts of deregulation, most have come from groups with a stake in the outcome of the regulatory reform process. So they tend to be either strongly for deregulation or strongly against it. In reality, deregulation has had both good and bad effects.

Consider a simple variable like the price of electricity. That competition will lead to lower prices is about as close to a universal truth as economics gets. But electricity seems to be an exception.

Here's why: Under regulation, each generating plant is paid for its electricity based on its average cost plus some prescribed rate of return. In a competitive market, supply and demand set the price. That means that the last plant coming online to handle the load determines the wholesale price of electricity. All generators in the system are then paid that same amount for each kilowatt-hour they inject into the grid.

That might seem only fair, but you have to remember that not all electricity generators are created equal. In most places, coal and nuclear plants, which can't be ramped up and down easily, produce the roughly constant baseload power feeding the grid. If more is needed, natural gas turbines then kick in. So in deregulated markets, the price of gas, which has historically been higher than that of coal or nuclear fuel, ends up controlling the wholesale price of electricity—allowing the owners of nuclear plants and efficient coal plants to earn much higher profits than they did under regulation. That's why electricity prices in many places rose so sharply when natural gas prices skyrocketed at the turn of the millennium.

Other strange dynamics also come into play. For example, state political leaders realize that escalating or erratic electricity prices are bad for economic development (and their own chances of reelection). So they've fought hard to keep them low and stable by imposing rate caps and freezes. But many of these same states also compelled their electric utilities to divest themselves of generating capacity in an attempt to spur competition. And when electricity demand is high and the utilities don't have enough of their own generating capacity, they're forced to buy more on the spot market, where prices are volatile. The results have not been pretty. In 2000, one of California's two largest utilities went bankrupt, and the other nearly did. And when regulators in Maryland finally allowed retail electricity rates in Baltimore to float with wholesale electricity prices, the local utility immediately announced a rate increase of 72 percent, leading to consumer outrage and eventually to the summary firing of the entire public utility commission.

Copyright 2017 Cengage Learning. All Rights Reserved. May not be copied, scanned, or duplicated, in whole or in part. Due to electronic rights, some third party content may be suppressed from the eBook and/or eChapter(s). Editorial review has deemed that any suppressed content does not materially affect the overall learning experience. Cengage Learning reserves the right to remove additional content at any time if subsequent rights restrictions require it.

UNITED KINGDOM
GERMANY
FRANCE
AUSTRALIA
ARGENTINA

DEREGULATION IS ALL OVER THE MAP
Countries have deregulated their electric power industries to different degrees, as these five examples show.

Argentina

Privatization of electricity generation in Argentina began in 1992, followed the next year by privatization of that nation's six transmission companies. Argentine law did not allow any of the resultant for-profit power companies to control more than 10 percent of the country's generation capacity, ensuring considerable competition among them.

United Kingdom

Electricity restructuring in the UK began under Margaret Thatcher, with the Electricity Act of 1983, which gave independent power producers access to the national grid. Government-owned generators were then fully privatized in the 1990s.

France

France began a very modest program of reform in 2001, but for the most part electricity supply remains completely dominated by the state electricity company, Électricité de France.

Germany

In response to a 1996 European directive, Germany abolished its law exempting electricity from competition in 1998. But most of that country's electricity still comes from just a few vertically integrated power companies, with comparatively little electricity trading on open exchanges.

Australia

The Australian state of Victoria privatized its electricity sector in 1994. Some other Australian states soon followed suit. And Australia established a national wholesale electricity market in December 1998.

Copyright 2017 Cengage Learning. All Rights Reserved. May not be copied, scanned, or duplicated, in whole or in part. Due to electronic rights, some third party content may be suppressed from the eBook and/or eChapter(s). Editorial review has deemed that any suppressed content does not materially affect the overall learning experience. Cengage Learning reserves the right to remove additional content at any time if subsequent rights restrictions require it.

Clearly, deregulation hasn't been at all successful in bringing prices down. But has it made the companies that provide electricity more efficient? Very probably. Their labor costs have fallen, mostly through reductions in staff, while the reliability of their power plants has improved. The champions in this regard are the nuclear power stations, whose uptimes have risen from around 65 percent in the 1980s to over 90 percent today. This shouldn't be a surprise. Because the construction costs of most of these plants have been paid off and because nuclear generators have very low operating expenses, the plants have become extraordinarily profitable. So their owners strive to have them online as much as possible, investing as needed to keep them well maintained.

Maintaining some other parts of the grid infrastructure has, however, proved to be more of a struggle. In the old days, investments in transmission lines and generating stations were determined by consensus between each utility and its regulator. Deregulation's architects envisioned a different scenario—that entrepreneurial firms would automatically make the needed investments in hopes of profiting from them. That didn't exactly happen. One thing deregulation definitely did do, though, was to change the mix of fuels in the U.S. generation fleet, shifting it away from coal and nuclear power toward natural gas. That's because gas units are quick to build, and many are flexible enough to operate only when prices are high enough to warrant throwing their switches on. It helps, too, that natural gas is a cleaner fuel than coal and less controversial than nuclear power, which helps with public approval. Also, because companies generating electricity in a free market need to demonstrate a return on investment within 5 to 10 years, building big nuclear and coal plants, which usually take over a decade to complete, just isn't an option. So more and more of the grid's power comes from gas turbines, despite the high fuel costs.

The changing investment environment has also inflated the cost of building new infrastructure. The reason is obvious once you think about it. Regulated utilities can spread the burden of investment among all their customers, and the government guarantees that these companies can charge enough to recover their initial outlay and make a decent profit on it. So there's little financial risk in building a new plant or transmission line, allowing the companies to attract low-priced capital. Not so with unregulated utilities, whose fortunes depend on an uncertain market. The greater risk they face means they must offer higher returns to attract investors, and these increased financing costs make capital projects more expensive.

Depending on market-based investment in transmission lines has proved especially problematic. Deregulation's proponents believed that for-profit companies would recover the money they invested in transmission lines through "congestion

Copyright 2017 Cengage Learning. All Rights Reserved. May not be copied, scanned, or duplicated, in whole or in part. Due to electronic rights, some third party content may be suppressed from the eBook and/or eChapter(s). Editorial review has deemed that any suppressed content does not materially affect the overall learning experience. Cengage Learning reserves the right to remove additional content at any time if subsequent rights restrictions require it.

pricing"—charging more when demand for these lines is high. Instead, lucrative congestion revenues have only given the owners of existing transmission lines an incentive *not* to build more capacity. And the general aversion people have to high-tension cables nearby—the "not in my backyard" effect—has made it almost impossible to construct new lines.

No great wonder, then, that investment in transmission lines and equipment has mostly been falling since the 1970s. Many people paid little notice to that fact, but the Northeast blackout of 2003 was a wake-up call. It began on a hot August afternoon with several seemingly trivial outages of transmission lines in Ohio, but by nighttime a series of cascading failures grew to plunge more than 50 million people in the Midwest, the Northeast, and Ontario into darkness. This episode convinced even skeptics that investment in the nation's electricity grid was lagging.

■ ■ ■ ■

Given deregulation's checkered record, you have to wonder how well competitive electricity markets will handle upcoming challenges. In particular, how will they reconcile the need for reliable, low-cost power with the environmental costs of producing it?

One much-discussed way to use markets to benefit the environment is to put a price on emissions of carbon dioxide and other greenhouse gases. Many countries have already done this. But unless the price is set a lot higher than in Europe, U.S. utilities and generating companies aren't going to be abandoning their carbon-spewing coal plants anytime soon—they're just too profitable. Putting a dollar value on greenhouse gases might encourage some generators to invest in less carbon-intensive power sources where they can, but only if proper laws and regulations are in place to lower the risk. And that won't happen overnight.

In the meantime, 32 of the 50 U.S. states are trying to boost the use of renewables by mandating "renewable portfolio standards." These standards force utilities to buy considerable quantities of wind and solar power but also give them the freedom to shop for the least expensive sources. Also, the U.S. Department of Energy wants 20 percent of the nation's electricity to come from wind power by 2030. Government bodies are taking these actions because consumer demand alone hasn't sparked much renewable generation. That's not surprising. The wind and sun are notoriously fickle, which forces system operators to maintain plants that can fill in when necessary. Those backup generators are expensive, as are the transmission lines needed to link most renewable resources, which are located in sparsely populated areas, to the people using electricity. So the cost of generating "green" electricity is generally higher than the price it can command.

Renewable portfolio standards create a not-so-free market (but a market nevertheless) for wind and solar power while also pressuring these producers to keep their prices down.

Copyright 2017 Cengage Learning. All Rights Reserved. May not be copied, scanned, or duplicated, in whole or in part. Due to electronic rights, some third party content may be suppressed from the eBook and/or eChapter(s). Editorial review has deemed that any suppressed content does not materially affect the overall learning experience. Cengage Learning reserves the right to remove additional content at any time if subsequent rights restrictions require it.

Policymakers in both regulated and deregulated states are also hoping to harness other market-based approaches to reducing electricity consumption. Using less electricity not only helps the environment, it can be just as effective as increasing supply in maintaining the reliability of the grid. And it's less expensive to boot.

The most straightforward way to discourage electricity use is, of course, to charge a lot for it. But U.S. consumers, and the lawmakers who represent them, are never too keen on that. Another strategy now being explored—one that's less of a political hot potato—is to have utility operators offer their customers compensation for reducing their demand for electricity during times of peak use. A reduction in demand allows utilities to avoid having to buy so much electricity when wholesale costs are at their highest. This approach provides an enticement to consumers to react to market signals, even if they are not yet ready to face them squarely in the form of higher prices.

Another advance that probably wouldn't have come about without deregulation is the emergence of small-scale, distributed generation, particularly from renewable sources such as rooftop solar panels. What's happening in many places is that customers are producing some electricity on their own while still attached to the grid. So they can offset some of the electricity they would otherwise consume, perhaps even spinning their meters backward at times. Although this practice competes with the electricity that the utility sells, more and more utilities are nevertheless allowing it to a greater or lesser degree.

■ ■ ■ ■

In hindsight, the electricity crisis in California and the myriad problems with deregulation in other parts of the country could have been anticipated. Given the complex market rules, concentrated supply, and largely inelastic demand, it's really no wonder that Enron, other energy-trading companies, and the electricity suppliers themselves found clever ways to manipulate markets.

Would U.S. consumers have been better off if the industry had remained strictly regulated? It all depends. If your goal is low electricity rates, maybe the answer is yes—but don't forget that bad regulatory decisions helped drive up electricity prices in the first place. If, however, you want the ability to feed power from your rooftop solar panels into the grid, the answer is probably no.

The real question facing the United States now is whether it can maintain reliable electricity grids without building lots of new transmission lines and big power plants. The only realistic alternative to such massive construction projects is for the generation of electricity to become more widely distributed, coupled with substantial efforts in energy efficiency. Electricity markets will surely have to become more expansive and open to accommodate that inevitable evolution. And they will also require new technical standards and, yes, some new forms of regulation. ■

Copyright 2017 Cengage Learning. All Rights Reserved. May not be copied, scanned, or duplicated, in whole or in part. Due to electronic rights, some third party content may be suppressed from the eBook and/or eChapter(s). Editorial review has deemed that any suppressed content does not materially affect the overall learning experience. Cengage Learning reserves the right to remove additional content at any time if subsequent rights restrictions require it.

1.1 HISTORY OF ELECTRIC POWER SYSTEMS

In 1878, Thomas A. Edison began work on the electric light and formulated the concept of a centrally located power station with distributed lighting serving a surrounding area. He perfected his light by October 1879, and the opening of his historic Pearl Street Station in New York City on September 4, 1882, marked the beginning of the electric utility industry (see Figure 1.1). At Pearl Street, dc generators, then called dynamos, were driven by steam engines to supply an initial load of 30 kW for 110-V incandescent lighting to 59 customers in a one-square-mile area. From this beginning in 1882 through 1972, the electric utility industry grew at a remarkable pace—a growth based on continuous reductions in the price of electricity due primarily to technological accomplishment and creative engineering.

The introduction of the practical dc motor by Sprague Electric, as well as the growth of incandescent lighting, promoted the expansion of Edison's dc systems. The development of three-wire, 220-V dc systems allowed load to increase somewhat, but as transmission distances and loads continued to increase, voltage problems were

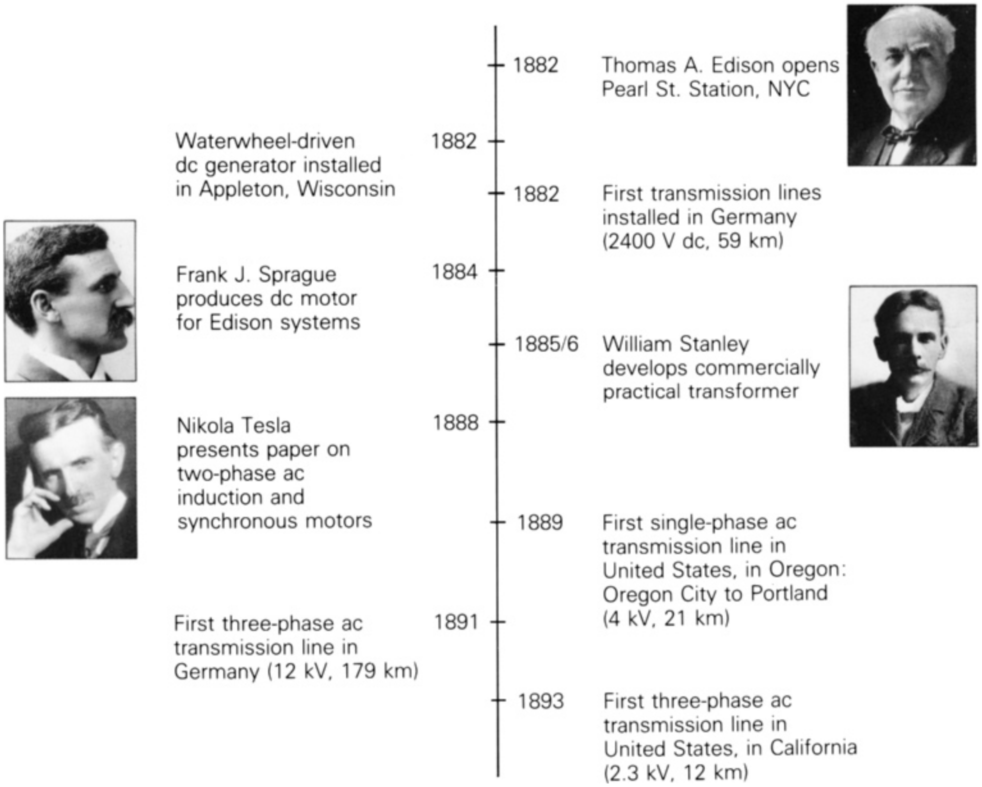
1882 Thomas A. Edison opens Pearl St. Station, NYC
Waterwheel-driven dc generator installed in Appleton, Wisconsin 1882
1882 First transmission lines installed in Germany (2400 V dc, 59 km)
Frank J. Sprague produces dc motor for Edison systems 1884
1885/6 William Stanley develops commercially practical transformer
Nikola Tesla presents paper on two-phase ac induction and synchronous motors 1888
1889 First single-phase ac transmission line in United States, in Oregon: Oregon City to Portland (4 kV, 21 km)
First three-phase ac transmission line in Germany (12 kV, 179 km) 1891
1893 First three-phase ac transmission line in United States, in California (2.3 kV, 12 km)

FIGURE 1.1

Milestones of the early electric utility industry [1]. (H.M. Rustebakke et al., *Electric Utility Systems Practice*, 4th Ed. (New York: Wiley, 1983). Reprinted with permission of John Wiley & Sons, Inc. Photos courtesy of Westinghouse Historical Collection.) (Photos courtesy of Westinghouse Historical Collection.) (Based on H.M. Rustebakke et al., Electric Utility Systems Practice, 4th. Ed. (New York: Wiley, 1983).)

Copyright 2017 Cengage Learning. All Rights Reserved. May not be copied, scanned, or duplicated, in whole or in part. Due to electronic rights, some third party content may be suppressed from the eBook and/or eChapter(s). Editorial review has deemed that any suppressed content does not materially affect the overall learning experience. Cengage Learning reserves the right to remove additional content at any time if subsequent rights restrictions require it.

encountered. These limitations of maximum distance and load were overcome in 1885 by William Stanley's development of a commercially practical transformer. Stanley installed an ac distribution system in Great Barrington, Massachusetts, to supply 150 lamps. With the transformer, the ability to transmit power at high voltage with corresponding lower current and lower line-voltage drops made ac more attractive than dc. The first single-phase ac line in the United States operated in 1889 in Oregon, between Oregon City and Portland—21 km at 4 kV.

The growth of ac systems, further encouraged in 1888 when Nikola Tesla presented a paper at a meeting of the American Institute of Electrical Engineers describing two-phase induction and synchronous motors, made evident the advantages of polyphase versus single-phase systems. The first three-phase line in Germany became operational in 1891, transmitting power 179 km at 12 kV. The first three-phase line in the United States (in California) became operational in 1893, transmitting power 12 km at 2.3 kV. The three-phase induction motor conceived by Tesla went on to become the workhorse of the industry.

In the same year that Edison's steam-driven generators were inaugurated, a waterwheel-driven generator was installed in Appleton, Wisconsin. Since then, most electric energy has been generated in steam-powered and in water-powered (called hydro) turbine plants. Today, steam turbines account for more than 85% of U.S. electric energy generation, whereas hydro turbines account for about 7%. Gas turbines are used in some cases to meet peak loads. Also, the addition of wind turbines and solar cells into the bulk power system is expected to grow considerably in the near future.

Steam plants are fueled primarily by coal, gas, oil, and uranium. Of these, coal is the most widely used fuel in the United States due to its abundance in the country. Although many of these coal-fueled power plants were converted to oil during the early 1970s, that trend reversed back to coal after the 1973–74 oil embargo, which caused an oil shortage and created a national desire to reduce dependency on foreign oil. More recently, electric companies have been retiring older, coal-fueled power plants. In 2012, approximately 37% of electricity in the United States was generated from coal [2].

In 1957, nuclear units with 90-MW steam-turbine capacity, fueled by uranium, were installed, and today nuclear units with 1312-MW steam-turbine capacity are in service. In 2012, approximately 19% of electricity in the United States was generated from uranium from 104 nuclear power plants. However, the growth of nuclear capacity in the United States has been halted by rising construction costs, licensing delays, and public opinion. Although there are no emissions associated with nuclear power generation, there are safety issues and environmental issues, such as the disposal of used nuclear fuel and the impact of heated cooling-tower water on aquatic habitats. Future technologies for nuclear power are concentrated on safety and environmental issues [2, 3, 7].

Starting in the 1990s, the choice of fuel for new power plants in the United States has been natural gas due to its availability and low cost as well as the higher efficiency, lower emissions, shorter construction-lead times, safety, and lack of controversy associated with power plants that use natural gas. Natural gas is used to generate electricity by the following processes:

1. Gas combustion turbines use natural gas directly to fire the turbine.
2. Steam turbines burn natural gas to create steam in a boiler, which is then run through the steam turbine.

Copyright 2017 Cengage Learning. All Rights Reserved. May not be copied, scanned, or duplicated, in whole or in part. Due to electronic rights, some third party content may be suppressed from the eBook and/or eChapter(s). Editorial review has deemed that any suppressed content does not materially affect the overall learning experience. Cengage Learning reserves the right to remove additional content at any time if subsequent rights restrictions require it.

3. Combined cycle units use a gas combustion turbine by burning natural gas, and the hot exhaust gases from the combustion turbine are used to boil water that operates a steam turbine.
4. Fuel cells powered by natural gas generate electricity using electrochemical reactions by passing streams of natural gas and oxidants over electrodes that are separated by an electrolyte. In 2012, approximately 30% of electricity in the United States was generated from natural gas [2, 3, 7].

Renewable energy sources have the advantage of providing a more sustainable use of finite energy sources with little or no contribution to polluting emissions. Renewable sources include conventional hydroelectric (water power), geothermal, wood, wood waste, all municipal waste, landfill gas, other biomass, solar, and wind power. In 2012, in the United States, approximately 12% of electricity was generated by renewable sources [2, 3]. Germany, which has an official governmental goal to generate 100% of electricity from renewable sources by 2050, achieved 31% in 2014 [14].

Substantial research efforts have shown nuclear fusion energy to be a promising technology for producing safe, pollution-free, and economical electric energy later in the 21st century and beyond. The fuel consumed in a nuclear fusion reaction is deuterium, of which a virtually inexhaustible supply is present in seawater.

The early ac systems operated at various frequencies including 25, 50, 60, and 133 Hz. In 1891, it was proposed that 60 Hz be the standard frequency in the United States. In 1893, 25-Hz systems were introduced with the synchronous converter. However, these systems were used primarily for railroad electrification (and many are now retired) because they had the disadvantage of causing incandescent lights to flicker. In California, the Los Angeles Department of Power and Water operated at 50 Hz but converted to 60 Hz when power from the Hoover Dam became operational in 1937. In 1949, Southern California Edison also converted from 50 to 60 Hz. Today, the two standard frequencies for generation, transmission, and distribution of electric power in the world are 60 Hz (in the United States, Canada, Mexico, and Brazil) and 50 Hz (in Europe, the former Soviet republics, China, South America, except Brazil, and India). In Japan, the western part of the country, including Kyoto, uses 60 Hz, while the eastern part, including Tokyo, uses 50 Hz. The advantage of 60-Hz systems is that generators, motors, and transformers in these systems are generally smaller than 50-Hz equipment with the same ratings. The advantage of 50-Hz systems is that transmission lines and transformers have smaller reactances at 50 Hz than at 60 Hz.

As shown in Figure 1.2, the rate of growth of electric energy in the United States was approximately 7% per year from 1902 to 1972. This corresponds to a doubling of electric energy consumption every 10 years over the 70-year period. In other words, every 10 years, the industry installed a new electric system equal in energy-producing capacity to the total of what it had built since the industry began. The annual growth rate slowed after the oil embargo of 1973 to 1974. Kilowatt-hour consumption in the United States increased by 3.4% per year from 1972 to 1980, and by only 0.7% per year from 2000 to 2011. In 2012, total U.S. electricity generation was 4.05×10^{12} kilowatt-hours (kWh), a 1.3% decrease from 2011.

Along with increases in load growth, there have been continuing increases in the size of generating units (Table 1.1). The principal incentive to build larger units has been economy of scale—that is, a reduction in installed cost per kilowatt

Copyright 2017 Cengage Learning. All Rights Reserved. May not be copied, scanned, or duplicated, in whole or in part. Due to electronic rights, some third party content may be suppressed from the eBook and/or eChapter(s). Editorial review has deemed that any suppressed content does not materially affect the overall learning experience. Cengage Learning reserves the right to remove additional content at any time if subsequent rights restrictions require it.

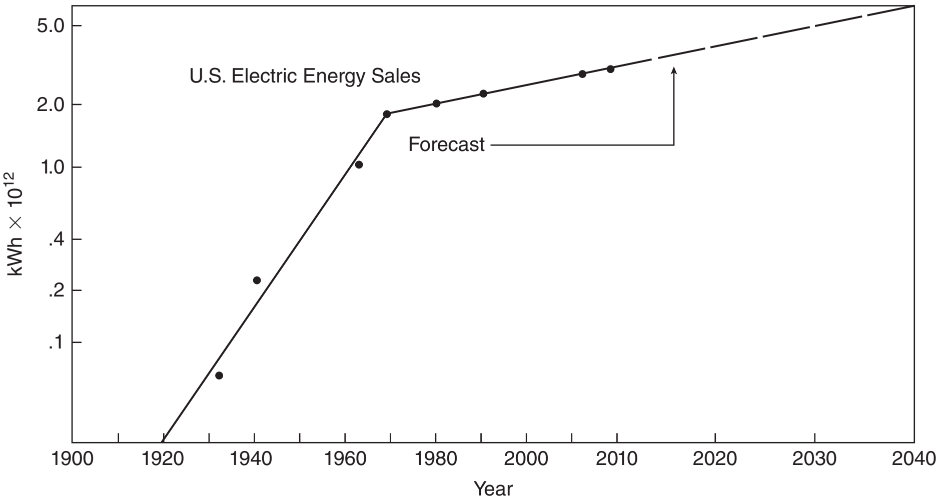

FIGURE 1.2

Growth of U.S. electric energy consumption [3]. (www.eia.gov, U.S. Energy Information Administration, Annual Energy Outlook 2010 Early Release Overview, M. P. Barhman and B.K. Johnson, "The ABC's of HVDC Transmission Technologies" IEEE Power & Energy Magazine, 5, 2, (March/April 2007) pp. 33–44.)

of capacity for larger units. However, there have also been steady improvements in generation efficiency. For example, in 1934 the average heat rate for steam generation in the U.S. electric industry was 17,950 BTU/kWh, which corresponds to 19% efficiency. By 1991, the average heat rate was 10,367 BTU/kWh, which corresponds to 33% efficiency. These improvements in thermal efficiency due to increases in unit size and in steam temperature and pressure, as well as to the use of steam reheat, have resulted in savings in fuel costs and overall operating costs.

There have been continuing increases, too, in transmission voltages (Table 1.2). From Edison's 220-V three-wire dc grid to 4-kV single-phase and 2.3-kV three-phase transmission, ac transmission voltages in the United States have risen progressively to 150, 230, 345, 500, and now 765 kV. And in 2009 in China, the first 1000 kV ultra-high voltage (UHV) ac transmission line, a 650-km line from Shaanxi Province

Hydroelectric Generators		Generators Driven by Single-Shaft, 3600 r/min Fossil-Fueled Steam Turbines	
Size (MVA)	Year of Installation	Size (MVA)	Year of Installation
4	1895	5	1914
108	1941	50	1937
158	1966	216	1953
232	1973	506	1963
615	1975	907	1969
718	1978	1120	1974

TABLE 1.1

Growth of generator sizes in the United States [1].

(*Source:* Based on H.M. Rustebakke et al., Electric Utility Systems Practice, 4th. Ed. (New York: Wiley, 1983).

Copyright 2017 Cengage Learning. All Rights Reserved. May not be copied, scanned, or duplicated, in whole or in part. Due to electronic rights, some third party content may be suppressed from the eBook and/or eChapter(s). Editorial review has deemed that any suppressed content does not materially affect the overall learning experience. Cengage Learning reserves the right to remove additional content at any time if subsequent rights restrictions require it.

to Hubei Province, began commercial operation [15]. The incentives for increasing transmission voltages have been: (1) increases in transmission distance and transmission capacity; (2) smaller line-voltage drops; (3) reduced line losses; (4) reduced right-of-way requirements per MW transfer; and (5) lower capital and operating costs of transmission. Today, one 765-kV three-phase line can transmit thousands of megawatts over hundreds of kilometers.

Voltage (kV)	Year of Installation
2.3	1893
44	1897
150	1913
165	1922
230	1923
287	1935
345	1953
500	1965
765	1969

TABLE 1.2

History of increases in three-phase transmission voltages in the United States [1].

(*Source:* Based on H.M. Rustebakke et al., Electric Utility Systems Practice, 4th. Ed. (New York: Wiley, 1983).

The technological developments that have occurred in conjunction with ac transmission, including developments in insulation, protection, and control, are in themselves important. The following examples are noteworthy:

1. The suspension insulator;
2. The high-speed relay system, currently capable of detecting short-circuit currents within one cycle (0.017 s);
3. High-speed, extra-high-voltage (EHV) circuit breakers, capable of interrupting up to 63-kA three-phase, short-circuit currents within two cycles (0.033 s);
4. High-speed reclosure of EHV lines, which enables automatic return to service within a fraction of a second after a fault has been cleared;
5. The EHV surge arrester, which provides protection against transient overvoltages due to lightning strikes and line-switching operations;
6. Power-line carrier, microwave, and fiber optics as communication mechanisms for protecting, controlling, and metering transmission lines;
7. The principle of insulation coordination applied to the design of an entire transmission system;
8. Energy control centers with supervisory control and data acquisition (SCADA) and with automatic generation control (AGC) for centralized computer monitoring and control of generation, transmission, and distribution;
9. Automated distribution features, including advanced metering infrastructure (AMI), reclosers, and remotely controlled sectionalizing switches with fault-indicating capability, along with automated mapping/facilities management (AM/FM) and geographic information systems (GIS) for quick isolation and identification of outages and for rapid restoration of customer services; and
10. Digital relays capable of circuit breaker control, data logging, fault locating, self-checking, fault analysis, remote query, and relay event monitoring/recording.

In 1954, the first modern high-voltage dc (HVDC) transmission line was put into commercial operation in Sweden between Vastervik and the island of Gotland in the Baltic Sea; it operated at 100 kV for a distance of 100 km. The first HVDC line in the United States was the ±400-kV (now ±500 kV), 1360-km Pacific Intertie line, installed between Oregon and California in 1970. As of 2014, seven other HVDC lines up to ±500 kV and 13 back-to-back ac-dc links had been installed in the

Copyright 2017 Cengage Learning. All Rights Reserved. May not be copied, scanned, or duplicated, in whole or in part. Due to electronic rights, some third party content may be suppressed from the eBook and/or eChapter(s). Editorial review has deemed that any suppressed content does not materially affect the overall learning experience. Cengage Learning reserves the right to remove additional content at any time if subsequent rights restrictions require it.

United States, and a total of 111 HVDC lines up to ±800 kV had been installed worldwide [4]. And in 2015 in China, the first ±1000 kV UHVDC transmission line, a 2600-km line from Xingjiang Province to Sichuan Province, is planned for commercial operation [16].

For an HVDC line embedded in an ac system, solid-state converters at both ends of the dc line operate as rectifiers and inverters. Since the cost of an HVDC transmission line is less than that of an ac line with the same capacity, the additional cost of converters for dc transmission is offset when the line is long enough. Studies have shown that overhead HVDC transmission is economical in the United States for transmission distances longer than about 600 km. However, HVDC also has the advantage that it may be the only feasible method to:

1. interconnect two asynchronous networks;
2. utilize long underground or underwater cable circuits;
3. bypass network congestion;
4. reduce fault currents;
5. share utility rights-of-way without degrading reliability; and mitigate environmental concerns [5].

In the United States, electric utilities grew first as isolated systems, with new ones continuously starting up throughout the country. Gradually, however, neighboring electric utilities began to interconnect, to operate in parallel. This improved both reliability and economy. Figure 1.3 shows major 115-kV and higher-voltage, interconnected transmission in the United States. An interconnected system has many advantages. An interconnected utility can draw upon another's rotating generator reserves during a time of need (such as a sudden generator outage or load increase), thereby maintaining continuity of service, increasing reliability, and reducing the total number of generators that need to be kept running under no-load conditions. Also, interconnected utilities can schedule power transfers during normal periods to take advantage of energy-cost differences in respective areas, load diversity, time zone differences, and seasonal conditions. For example, utilities whose generation is primarily hydro can supply low-cost power during high-water periods in spring/summer and can receive power from the interconnection during low-water periods in fall/winter. Interconnections also allow shared ownership of larger, more efficient generating units.

While sharing the benefits of interconnected operation, each utility is obligated to help neighbors who are in trouble, to maintain scheduled intertie transfers during normal periods, and to participate in system frequency regulation.

In addition to the benefits and obligations of interconnected operation, there are disadvantages. Interconnections, for example, have increased fault currents that occur during short circuits, thus requiring the use of circuit breakers with higher interrupting capability. Furthermore, although overall system reliability and economy have improved dramatically through interconnection, there is a remote possibility that an initial disturbance may lead to a regional blackout, such as the one that occurred in August 2003 in the northeastern United States and Canada.

Copyright 2017 Cengage Learning. All Rights Reserved. May not be copied, scanned, or duplicated, in whole or in part. Due to electronic rights, some third party content may be suppressed from the eBook and/or eChapter(s). Editorial review has deemed that any suppressed content does not materially affect the overall learning experience. Cengage Learning reserves the right to remove additional content at any time if subsequent rights restrictions require it.

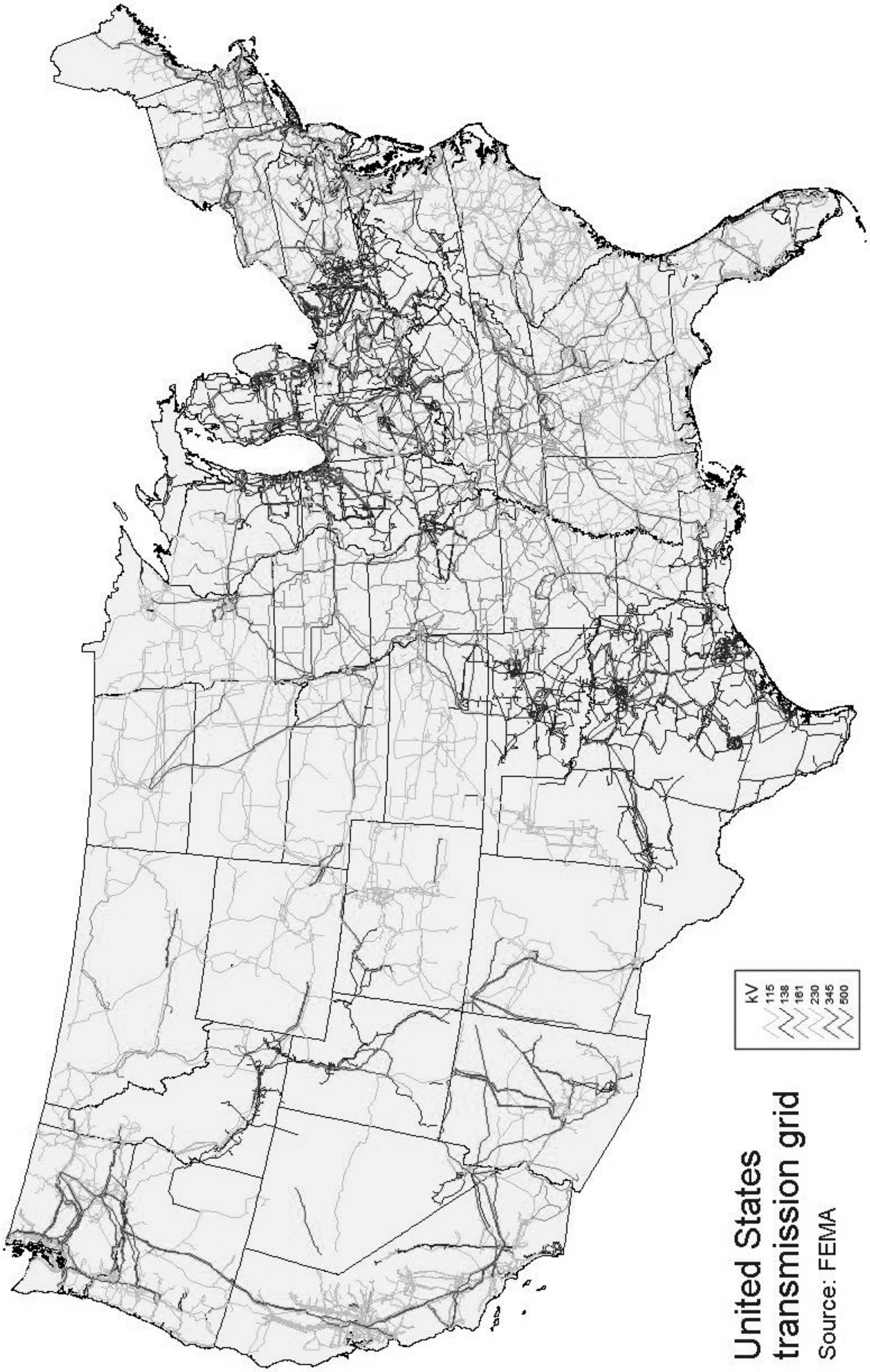

United States transmission grid

Source: FEMA

FIGURE 1.3

Major transmission in the United States (FEMA).

Copyright 2017 Cengage Learning. All Rights Reserved. May not be copied, scanned, or duplicated, in whole or in part. Due to electronic rights, some third party content may be suppressed from the eBook and/or eChapter(s). Editorial review has deemed that any suppressed content does not materially affect the overall learning experience. Cengage Learning reserves the right to remove additional content at any time if subsequent rights restrictions require it.

1.2 PRESENT AND FUTURE TRENDS

Present trends indicate that the United States is becoming more electrified as it shifts away from a dependence on the direct use of fossil fuels. The electric power industry advances economic growth, promotes business development and expansion, provides solid employment opportunities, enhances the quality of life for its users, and powers the world. Increasing electrification in the United States is evidenced in part by the ongoing digital revolution. Today the United States electric power industry is a robust, $840-billion-plus industry that employs nearly 500,000 workers. In the United States economy, the industry represents approximately 3% of real gross domestic product (GDP) [6].

As shown in Figure 1.2, the growth rate in the use of electricity in the United States is projected to increase by about 1% per year from 2012 to 2025 [2]. Although electricity forecasts for the next thirteen years are based on economic and social factors that are subject to change, 1% annual growth rate is considered necessary to generate the GDP anticipated over that period. Variations in longer-term forecasts of 0.7 to 1.3% annual growth from 2012 to 2040 are based on low-to-high ranges in economic growth. Average end-use price of electricity is projected to increase from 9.8 cents to 11.1 cents per kilowatt-hour from 2012 to 2040 [2, 3].

Figure 1.4 shows the percentages of various fuels used to meet U.S. electric energy requirements for 2012 and those projected for 2025 and 2040. Several trends are apparent in the chart. One is the continuing use of coal. This trend is due primarily to the large amount of U.S. coal reserves, which, according to some estimates, is

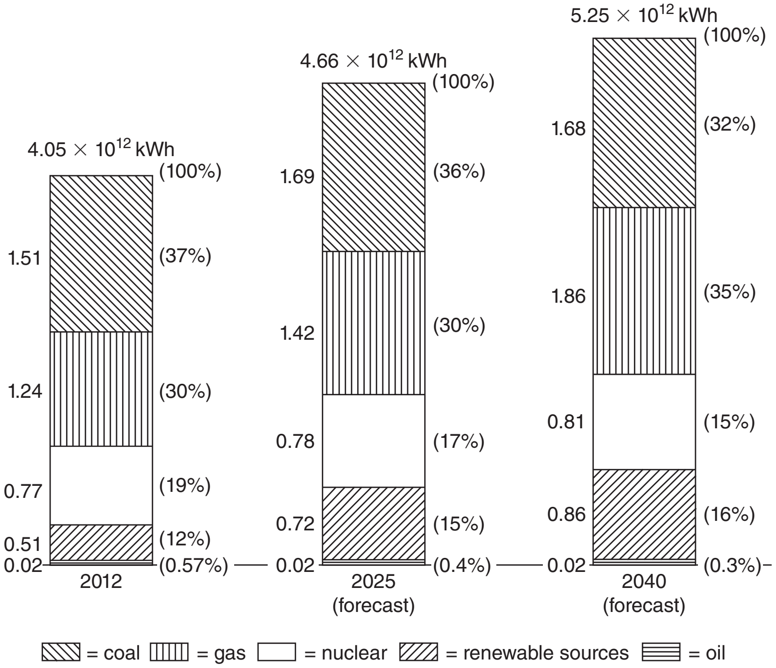

FIGURE 1.4

Electric energy generation in the United States, by principal fuel types [2, 3]. Renewable sources include conventional hydroelectric, geothermal, wood, wood waste, all municipal waste, landfill gas, other biomass, solar, and wind power. (U.S. Energy Information Administration, Electric power annual 2012, Dec 2013, U.S. Energy Information Administration, Annual Energy Outlook 2014, www.eia.gov.)

Copyright 2017 Cengage Learning. All Rights Reserved. May not be copied, scanned, or duplicated, in whole or in part. Due to electronic rights, some third party content may be suppressed from the eBook and/or eChapter(s). Editorial review has deemed that any suppressed content does not materially affect the overall learning experience. Cengage Learning reserves the right to remove additional content at any time if subsequent rights restrictions require it.

sufficient to meet U.S. energy needs for the next 500 years. Implementation of public policies that have been proposed to reduce carbon dioxide emissions and air pollution could reverse this trend. Another trend is the continuing consumption of natural gas in the long term with gas-fired turbines that are safe, clean, and more efficient than competing technologies. Regulatory policies to lower greenhouse gas emissions could accelerate a switchover from coal to gas, but that would require an increasing supply of deliverable natural gas. A slight percentage decrease in nuclear fuel consumption is also evident. No new nuclear plant has been ordered in the United States for more than 30 years. The projected growth from 0.77×10^{12} kWh in 2012 to 0.86×10^{12} kWh in 2040 in nuclear generation is based on uprates at existing plants and some new nuclear capacity that offsets early retirements. Safety concerns require passive or inherently safe reactor designs with standardized, modular construction of nuclear units. Also shown in Figure 1.4 is an accelerating increase in electricity generation from renewable resources in response to a variety of federal and state policies [2, 3].

Figure 1.5 shows the 2012 and projected 2025 U.S. generating capability by principal fuel type. As shown, total U.S. generating capacity is projected to reach 1110 GW (1 GW = 1000 MW) by the year 2025, which represents a 0.3% annual projected growth in generating capacity from 2013 to 2025. The projection assumes 131 GW of new capacity additions and 87 GW of cumulative capacity retirements from 2013 to 2025 [2, 3, 7].

As of 2012, there were 476,247 circuit miles of existing transmission (above 200 kV) in North America, which includes the continental United States, Canada,

FIGURE 1.5

Installed generating capability in the United States by principal fuel types [2, 3]. Net summer capacities of renewable sources include conventional and pumped storage hydroelectric, geothermal, wood, wood waste, all municipal waste, landfill gas, other biomass, solar, and wind power. (U.S. Energy Information Administration, electric power annual 2012, Dec 2013, U.S. Energy Information Administration, Annual Energy Outlook 2014, www.eia.gov.)

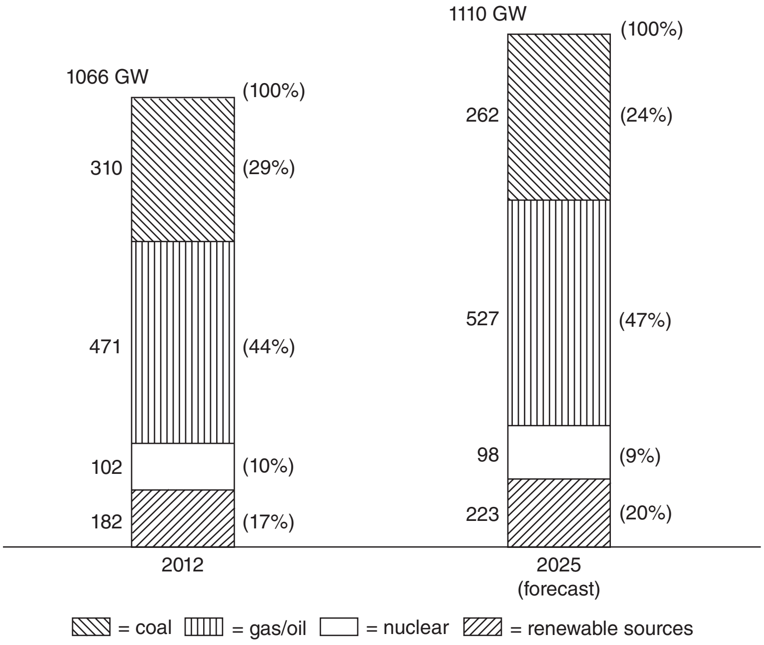

Copyright 2017 Cengage Learning. All Rights Reserved. May not be copied, scanned, or duplicated, in whole or in part. Due to electronic rights, some third party content may be suppressed from the eBook and/or eChapter(s). Editorial review has deemed that any suppressed content does not materially affect the overall learning experience. Cengage Learning reserves the right to remove additional content at any time if subsequent rights restrictions require it.

and the northern portion of Baja California, Mexico. Currently, 5100 circuit-miles are under construction and expected to be in service before 2015, and an additional 21,800 circuit-miles are planned with in-service dates before 2023. According to the North American Electric Reliability Corporation (NERC), new transmission projects are being driven primarily to enhance reliability. Other reasons include congestion alleviation and integration of renewable energy sources [7].

According to NERC, building new transmission is an ongoing challenge for the electricity industry. Transmission right-of-way issues required in the siting of new transmission lines that span multiple states and provinces are highly visible and require increased coordination among multiple regulating agencies and authorities. A lack of coordination regarding cost allocation, coupled with public opposition due to land use and property valuation concerns, has often resulted in extended delays in transmission construction. Further, ongoing state and provincial policies require continued integration of renewable resources, including wind and solar. These variable resources are most commonly built in remote areas where wind power densities and solar development are favorable. In many cases, the existing transmission network needs to be expanded to integrate these renewable resources and meet other state-wide goals [7].

Growth in distribution construction roughly correlates with growth in electric energy consumption. During the last three decades, many U.S. utilities converted older 2.4-, 4.1-, and 5-kV primary distribution systems to 12 or 15 kV. The 15-kV voltage class is widely preferred by U.S. utilities for new installations; higher primary distribution voltages including 25 kV and 34.5 kV are also utilized. Secondary distribution reduces the voltage for utilization by commercial and residential customers. Common secondary distribution voltages in the United States are 240/120 V, single-phase, three-wire; 208 Y/120 V, three-phase, four-wire; and 480 Y/277 V, three-phase, four-wire.

Transmission and distribution grids in the United States as well as other industrialized countries are aging and being stressed by operational uncertainties and challenges never envisioned when they were developed many decades ago. There is a growing consensus in the power industry and among many governments that smart grid technology is the answer to the uncertainties and challenges. A smart grid is characterized by the following attributes:

1. Self-healing from power system disturbances;
2. Enables active participation by consumers in demand response;
3. Operates resiliency against both physical and cyber attacks;
4. Provides quality power that meets 21st century needs;
5. Accommodates all generation and energy storage technologies;
6. Enables new products, services, and markets; and
7. Optimizes asset utilization and operating efficiency.

The objective of a smart grid is to provide reliable, high-quality electric power to digital societies in an environmentally friendly and sustainable manner [11].

According to recent studies, almost 62% of electric utility employees in the United States have the potential to retire or leave over the ten-year period from 2014 to 2024.

Copyright 2017 Cengage Learning. All Rights Reserved. May not be copied, scanned, or duplicated, in whole or in part. Due to electronic rights, some third party content may be suppressed from the eBook and/or eChapter(s). Editorial review has deemed that any suppressed content does not materially affect the overall learning experience. Cengage Learning reserves the right to remove additional content at any time if subsequent rights restrictions require it.

According to the Power Engineering Society (PES) of the Institute of Electrical Engineers (IEEE), of the 170 engineering faculty working full time in power engineering education and research in the United States, some 50 senior faculty members have retired during the 2009 to 2014 time frame. The continuing availability of qualified power system engineers is a critical resource to ensure that transmission and distribution systems are maintained and operated efficiently and reliably [9,10].

1.3 ELECTRIC UTILITY INDUSTRY STRUCTURE

The case study at the beginning of this chapter describes the restructuring of the electric utility industry that has been ongoing in the United States. The previous structure of large, vertically integrated monopolies that existed until the last decade of the twentieth century is being replaced by a horizontal structure with generating companies, transmission companies, and distribution companies as separate business facilities.

In 1992, the United States Congress passed the Energy Policy Act, which has shifted and continues to further shift regulatory power from the state level to the federal level. The 1992 Energy Policy Act mandates the Federal Energy Regulatory Commission (FERC) to ensure that adequate transmission and distribution access is available to exempt wholesale generators (EWGs) and nonutility generation (NUG). In 1996, FERC issued the "MegaRule," which regulates Transmission Open Access (TOA).

TOA was mandated in order to facilitate competition in wholesale generation. As a result, a broad range of independent power producers (IPPs) and cogenerators now submit bids and compete in energy markets to match electric energy supply and demand. Currently, the retail structure of power distribution is becoming similar to the existing structure of the telephone industry; that is, consumers choose which electric energy supplier to buy power from. Also, with demand-side metering, consumers know the retail price of electric energy at any given time and may choose when to purchase it.

Overall system reliability has become a major concern as the electric utility industry adapts to the new horizontal structure. The North American Electric Reliability Corporation (NERC) was created after the 1965 Northeast blackout and is responsible for maintaining system standards and reliability. NERC coordinates its efforts with FERC and governmental organizations in Canada [12].

As shown in Figure 1.3, the transmission system in North America is interconnected in a large power grid known as the North American Power Systems Interconnection. NERC divides this grid into eight regional entities including NPCC—the Northeast Power Coordinating Council, MRO—the Midwest Reliability Organization, and SPP—the Southwest Power Pool. Members of the regional entities come from all segments of the electric industry: investor-owned utilities; federal power agencies; rural electric cooperatives; state, municipal, and provincial utilities; independent power producers; power marketers; and end-use customers. These members jointly perform regional planning studies and operate jointly to schedule generation.

The basic premise of TOA is that transmission owners treat all transmission users on a nondiscriminatory and comparable basis. In December 1999, FERC issued

Copyright 2017 Cengage Learning. All Rights Reserved. May not be copied, scanned, or duplicated, in whole or in part. Due to electronic rights, some third party content may be suppressed from the eBook and/or eChapter(s). Editorial review has deemed that any suppressed content does not materially affect the overall learning experience. Cengage Learning reserves the right to remove additional content at any time if subsequent rights restrictions require it.

Order 2000, which calls for companies owning transmission systems to put transmission systems under the control of Regional Transmission Organizations (RTOs). Several of the NERC regions have either established independent system operators (ISOs) or planned for ISOs to operate the transmission system and facilitate transmission services. Maintenance of the transmission system remains the responsibility of the transmission owners.

At the time of the August 14, 2003, blackout in the northeastern United States and Canada, NERC reliability standards were voluntary. In August 2005, the U.S. Federal government passed the Energy Policy Act of 2005, which authorizes the creation of an electric reliability organization (ERO) with the statutory authority to enforce compliance with reliability standards among all market participants. As of June 18, 2007, FERC granted NERC the legal authority to enforce reliability standards with all users, owners, and operators of the bulk power system in the United States, and made compliance with those standards mandatory and enforceable. Currently, the legislative framework to make standards enforceable exists through action of the regulatory authority in the Canadian provinces of Alberta, British Columbia, Nova Scotia, and Quebec. In addition, standards become enforceable upon NERC board action in the Canadian provinces of Manitoba (Manitoba Hydro only), New Brunswick, Ontario, and Saskatchewan [12].

The objectives of electric utility restructuring are to increase competition, decrease regulation, and in the long run lower consumer prices. There is a concern that the benefits from breaking up the old, vertically integrated utilities are unrealized if the new unbundled generation and transmission companies are able to exert market power. Market power refers to the ability of one seller or group of sellers to maintain prices above competitive levels for a significant period of time, which could be done via collusion or by taking advantage of operational anomalies that create and exploit transmission congestion. Market power can be eliminated by independent supervision of generation and transmission companies, by ensuring that there are an ample number of generation companies, by eliminating transmission congestion, and by creating a truly competitive market, where the spot price at each node (bus) in the transmission system equals the marginal cost of providing energy at that node, where the energy provider is any generator bidding into the system [12].

1.4 COMPUTERS IN POWER SYSTEM ENGINEERING

As electric utilities have grown in size and the number of interconnections has increased, planning for future expansion has become increasingly complex. The increasing cost of additions and modifications has made it imperative that utilities consider a range of design options and perform detailed studies of the effects on the system of each option, based on a number of assumptions: normal and abnormal operating conditions, peak and off-peak loadings, and present and future years of operation. A large volume of network data must also be collected and accurately handled. To assist the engineer in this power system planning, digital computers and highly developed computer programs are used. Such programs include power-flow, stability, short-circuit, and transients programs.

Copyright 2017 Cengage Learning. All Rights Reserved. May not be copied, scanned, or duplicated, in whole or in part. Due to electronic rights, some third party content may be suppressed from the eBook and/or eChapter(s). Editorial review has deemed that any suppressed content does not materially affect the overall learning experience. Cengage Learning reserves the right to remove additional content at any time if subsequent rights restrictions require it.

Power-flow programs compute the voltage magnitudes, phase angles, and transmission-line power flows for a network under steady-state operating conditions. Other results, including transformer tap settings and generator reactive power outputs, are also computed. Today's computers have sufficient storage and speed to efficiently compute power-flow solutions for networks with 100,000 buses and 150,000 transmission lines. Results are usually viewed interactively on computer screens in the form of either tabular displays or single-line diagrams; the engineer uses these to modify the network with a mouse or from a keyboard and can readily visualize the results. The computer's large storage and high-speed capabilities allow the engineer to run the many different cases necessary to analyze and design transmission and generation-expansion options.

Stability programs are used to study power systems under disturbance conditions to determine whether synchronous generators and motors remain in synchronization. System disturbances can be caused by the sudden loss of a generator or transmission line, by sudden load increases or decreases, and by short circuits and switching operations. The stability program combines power-flow equations and machine-dynamic equations to compute the angular swings of machines during disturbances. The program also computes critical clearing times for network faults, and allows the engineer to investigate the effects of various machine parameters, network modifications, disturbance types, and control schemes.

Short-circuit programs are used to compute three-phase and line-to-ground faults in power system networks in order to select circuit breakers for fault interruption, select relays that detect faults and control circuit breakers, and determine relay settings. Short-circuit currents are computed for each relay and circuit-breaker location and for various system-operating conditions such as lines or generating units out of service in order to determine minimum and maximum fault currents.

Transients programs compute the magnitudes and shapes of transient overvoltages and currents that result from lightning strikes and line-switching operations. The planning engineer uses the results of a transients program to determine insulation requirements for lines, transformers, and other equipment, and to select surge arresters that protect equipment against transient overvoltages.

Other computer programs for power system planning include relay-coordination programs and distribution-circuits programs. Computer programs for generation-expansion planning include reliability analysis and loss-of-load probability (LOLP) programs, production cost programs, and investment cost programs.

1.5 POWERWORLD SIMULATOR

PowerWorld Simulator (PowerWorld) version 19 is a commercial-grade power system analysis and simulation package that accompanies this text. The purposes of integrating PowerWorld with the text are to provide computer solutions to examples in the text, to extend the examples, to demonstrate topics covered in the text, to provide a software tool for more realistic design projects, and to provide the readers with experience using a commercial grade power system analysis package. To use this software package, you must first install PowerWorld, along with all of the necessary

Copyright 2017 Cengage Learning. All Rights Reserved. May not be copied, scanned, or duplicated, in whole or in part. Due to electronic rights, some third party content may be suppressed from the eBook and/or eChapter(s). Editorial review has deemed that any suppressed content does not materially affect the overall learning experience. Cengage Learning reserves the right to remove additional content at any time if subsequent rights restrictions require it.

case files onto your computer. The PowerWorld software and case files can be downloaded by going to the www.powerworld.com/gloversarmaoverbye Web page, and clicking on the **DownLoad PowerWorld Software and Cases for the 6th Edition** button. The remainder of this section provides the necessary details to get up and running with PowerWorld.

EXAMPLE 1.1

Introduction to PowerWorld Simulator

After installing PowerWorld, double-click on the PW icon to start the program. Power system analysis requires, of course, that the user provide the program with a model of the power system. With PowerWorld, you can either build a new case (model) from scratch or start from an existing case. Most of the examples in the book, as in this case, initially start from an existing case. PowerWorld uses the common ribbon user interface in which common commands, such as opening or saving a case, are available by clicking on the items on the top of the screen. So to open a case click **File** and then select **Open Case**. This displays the Open Dialog. Select the Example 1_1 case in the Chapter 1 directory, and then click Open. The display should look similar to Figure 1.6.

FIGURE 1.6

Example power system

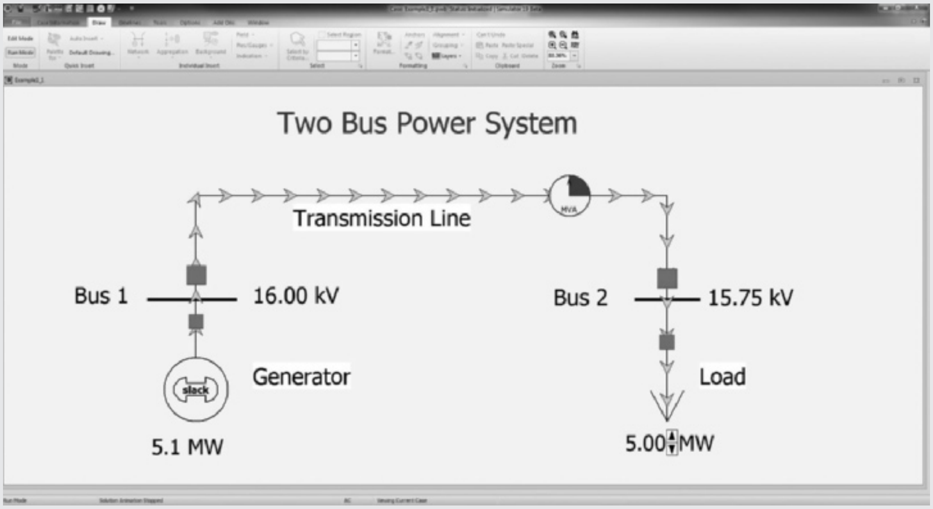

For users familiar with electric circuit schematics, it is readily apparent that Figure 1.6 does *not* look like a traditional schematic. This is because the system is drawn in what is called a oneline diagram form. A brief explanation is in order. Electric power systems range in size from small dc systems with peak power demands of perhaps a few milliwatts (mW) to large continent-spanning

(*Continued*)

Copyright 2017 Cengage Learning. All Rights Reserved. May not be copied, scanned, or duplicated, in whole or in part. Due to electronic rights, some third party content may be suppressed from the eBook and/or eChapter(s). Editorial review has deemed that any suppressed content does not materially affect the overall learning experience. Cengage Learning reserves the right to remove additional content at any time if subsequent rights restrictions require it.

interconnected ac systems with peak demands of hundreds of Giga-watts (GW) of demand (1 GW = 1 × 10^9 Watt). The subject of this book and also PowerWorld are the high-voltage, high-power, interconnected ac systems. Almost without exception these systems operate using three-phase ac power at either 50 or 60 Hz. As discussed in Chapter 2, a full analysis of an arbitrary three-phase system requires consideration of each of the three phases. Drawing such systems in full schematic form quickly gets excessively complicated. Thankfully, during normal operation, three-phase systems are usually balanced. This permits the system to be accurately modeled as an equivalent single-phase system (the details are discussed in Chapter 8, "Symmetrical Components"), Most power system analysis packages, including PowerWorld, use this approach. Then connections between devices are drawn with a single line joining the system devices, hence the term *oneline diagram*. However, do keep in mind that the actual systems are three-phase.

Figure 1.6 illustrates how the major power system components are represented in PowerWorld. Generators are shown as a circle with a "dog-bone" rotor, large arrows represent loads, and transmission lines are simply drawn as lines. In power system terminology, the nodes at which two or more devices join are called *buses*. In PowerWorld, thicker lines usually represent buses; the bus voltages are shown in kilovolts (kV) in the fields immediately to the right of the buses. In addition to voltages, power engineers are also concerned with how power flows through the system (the solution of the power flow problem is covered in Chapter 6, "Power Flows"). In PowerWorld, power flows can be visualized with arrows superimposed on the generators, loads, and transmission lines. The size and speed of the arrows indicate the direction of flow. One of the unique aspects of PowerWorld is its ability to animate power systems. To start the animation, select the **Tools** tab on the ribbon and then click on the green and black arrow button above **Solve** (i.e., the "Play" button). The oneline should come to life! While the oneline is being animated, you can interact with the system. Figure 1.6 represents a simple power system in which a generator is supplying power to a load through a 16-kV distribution system feeder. The solid red blocks on the line and load represent circuit breakers. To open a circuit breaker, simply click on it. Since the load is series-connected to the generator, clicking on any of the circuit breakers isolates the load from the generator resulting in a blackout. To restore the system, click again on the circuit breaker to close it and then again select the **Solve** button on the **Tools** ribbon. To vary the load, click on the up or down arrows between the load value and its "MW" field. Note that because of the impedance of the line, the load's voltage drops as its value is increased.

You can view additional information about most of the elements on the oneline by right-clicking on them. For example right-clicking on the generator symbol brings up a local menu of additional information about the generator, while right-clicking on the transmission line brings up local menu of information about the line. The meaning of many of these fields become clearer as you progress through the book. To modify the display itself, simply right-click on a blank area of the

Copyright 2017 Cengage Learning. All Rights Reserved. May not be copied, scanned, or duplicated, in whole or in part. Due to electronic rights, some third party content may be suppressed from the eBook and/or eChapter(s). Editorial review has deemed that any suppressed content does not materially affect the overall learning experience. Cengage Learning reserves the right to remove additional content at any time if subsequent rights restrictions require it.

oneline. This displays the Onelines local menu. Select **Oneline Display Options** to display the Oneline Display Options dialog. From this dialog you can customize many of the display features. For example, to change the animated flow arrow color, select Animated Flows from the options shown on the left side of the dialog. Then click on the green colored box next to the Actual MW field (towards the bottom of the dialog) to change its color.

There are several techniques for panning and/or zooming on the oneline. One method to pan is to first click in an empty portion of the display and then press the keyboard arrow keys in the direction you would like to move. To zoom, just hold down the Ctrl key while pressing the up arrow to zoom in or the down arrow to zoom out. Alternatively you can drag the oneline by clicking and holding the left mouse button down and then moving the mouse—the oneline should follow. To go to a favorite view from the Onelines local menu, select the **Go To View** to view a list of saved views.

If you would like to retain your changes after you exit PowerWorld, you need to save the results. To do this, select **File** in the upper-left portion of the ribbon and then **Save Case As;** enter a different file name so as to not overwrite the initial case. One important note: PowerWorld actually saves the information associated with the power system model itself in a different file from the information associated with the oneline. The power system model is stored in *.pwb files (PowerWorld Binary file) while the Oneline Display information is stored in *.pwd files (PowerWorld Display file). For all the cases discussed in this book, the names of both files should be the same (except the different extensions). The reason for the dual file system is to provide flexibility. With large system models, it is quite common for a system to be displayed using multiple oneline diagrams. Furthermore, a single oneline diagram might be used at different times to display information about different cases.

EXAMPLE 1.2

PowerWorld Simulator—Edit Mode

PowerWorld has two major modes of operations. The Run Mode, which was just introduced, is used for running simulations and performing analysis. The Edit Mode, which is used for modifying existing cases and building new cases, is introduced in this example. To switch to the Edit Mode, click on the **Edit Mode** button, which is located in the upper-left portion of the display immediately below the PowerWorld icon. Use the Edit Mode to add an additional bus and load, as well as two new lines, to the Example 1_1 system.

When switching to the Edit Mode notice that the ribbon changes slightly, with several of the existing buttons and icons disabled and others enabled. Also, the

(*Continued*)

Copyright 2017 Cengage Learning. All Rights Reserved. May not be copied, scanned, or duplicated, in whole or in part. Due to electronic rights, some third party content may be suppressed from the eBook and/or eChapter(s). Editorial review has deemed that any suppressed content does not materially affect the overall learning experience. Cengage Learning reserves the right to remove additional content at any time if subsequent rights restrictions require it.

oneline now has a superimposed grid to help with alignment (the grid can be customized using the Grid/Highlight Unlinked options category on the Oneline Display Options dialog). In the Edit Mode, first add a new bus to the system. This can be done graphically by first selecting the **Draw** tab, then clicking on the **Network** button and selecting **Bus**. Once this is done, move the mouse to the desired oneline location and click (note the **Draw** tab is only available in the Edit Mode). The Bus Options dialog then appears. This dialog is used to set the bus parameters. For now leave all the bus fields at their default values, except set Bus Name to "bus 3" and set the nominal voltage to 16.0; note that the number for this new bus was automatically set to the one greater than the highest bus number in the case. The oneline should look similar to Figure 1.7. You may wish to save your case now to avoid losing your changes.

FIGURE 1.7

Example 1.2—Edit Mode view with new bus

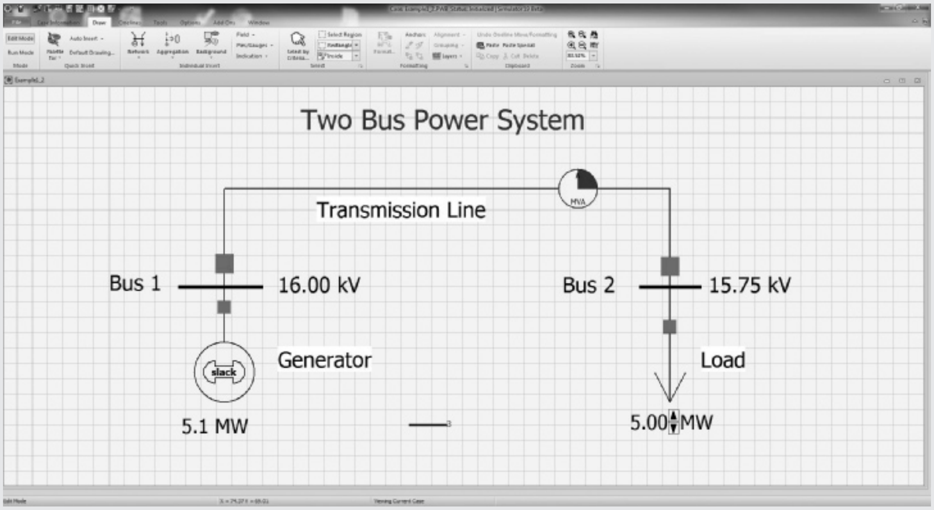

By default, when a new bus is inserted, a bus field is also inserted. *Bus fields* are used to show information about buses on the onelines. In this case the new field shows the bus name, although initially in rather small fonts. To change the field's font size, click on the field to select it, and then select the **Format** button (on the Draw ribbon) to display the Format dialog. Click on the **Font** tab and change the font's size to a larger value to make it easier to see. You can also change the size of the bus itself using the Format dialog, Display/Size tab. To see the bus voltage magnitude, add an additional bus field. On the Draw ribbon select **Field, Bus Field**, and then click near bus 3. This displays the Bus Field Options dialog. Make sure the bus number is set to 3, and that the "Type of Field" is Bus Voltage. Again, resize with the **Format, Font** dialog.

Next, insert some load at bus 3. This can be done graphically by selecting **Network, Load** and then clicking on bus 3. The Load Options dialog appears,

Copyright 2017 Cengage Learning. All Rights Reserved. May not be copied, scanned, or duplicated, in whole or in part. Due to electronic rights, some third party content may be suppressed from the eBook and/or eChapter(s). Editorial review has deemed that any suppressed content does not materially affect the overall learning experience. Cengage Learning reserves the right to remove additional content at any time if subsequent rights restrictions require it.

allowing you to set the load parameters. Note that the load was automatically assigned to bus 3. Leave all the fields at their default values, except set the orientation to "Down," and enter 10.0 in the Constant Power column MW Value field. As the name implies, a constant power load treats the load power as being independent of bus voltage; constant power load models are commonly used in power system analysis. By default, PowerWorld "anchors" each load symbol to its bus. This is a handy feature when changing a drawing, since when you drag the bus, the load and all associated fields move as well. Note that two fields showing the load's real (MW) and reactive (Mvar) power were also auto-inserted with the load. Select the reactive field right now, and then choose one. **Delete** (located towards the right side of the **Draw** ribbon) to remove it. You should also resize the MW field using the **Format, Font** command.

Now join the bus 3 load to the rest of the system. Do this by adding a line from bus 2 to bus 3. Select **Network, Transmission Line** and then click on bus 2. This begins the line drawing. During line drawing, PowerWorld adds a new line segment for each mouse click. After adding several segments place the cursor on bus 3 and double-click. The Transmission Line/Transformer Options dialog appears, allowing you to set the line's parameters. Note that PowerWorld should have automatically set the "from" and "to" bus numbers based upon the starting and ending buses (buses 2 and 3). If these values have not been set automatically, then you probably did not click exactly on bus 2 or bus 3; manually enter the values. Next, set the line's Series Resistance (R) field to 0.3, the Series Reactance (X) field to 0.6, and the MVA Limits Limit (A) field to 20 (the details of transformer and transmission line modeling is covered in Chapters 3 through 5). Select OK to close the dialog. Note that PowerWorld also auto-inserted two circuit breakers and a round "pie chart" symbol. The pie charts are used to show the percentage loading of the line. You can change the display size for these objects by right-clicking on them to display their option dialogs.

EXAMPLE 1.3

PowerWorld Simulator—Run Mode

Next, switch back to Run Mode to solve and animate the new system developed in Example 1.2. Click on the **Run Mode** button (immediately below the **Edit Mode** button), select the **Tools** on the ribbon, and then click the green-and-black button above **Solve** to start the simulation. You should see the arrows flow from bus 1 to bus 2 to bus 3. Note that the total generation is now about 15.4 MW, with 15 MW flowing to the two loads and 0.4 MW lost to the wire resistance. To add the load variation arrows to the bus 3 load, right click on the Load MW field (not the load

(Continued)

Copyright 2017 Cengage Learning. All Rights Reserved. May not be copied, scanned, or duplicated, in whole or in part. Due to electronic rights, some third party content may be suppressed from the eBook and/or eChapter(s). Editorial review has deemed that any suppressed content does not materially affect the overall learning experience. Cengage Learning reserves the right to remove additional content at any time if subsequent rights restrictions require it.

arrow itself) to display the field's local menu. Select **Load Field Information Dialog** to view the Load Field Options dialog. Set the Delta per Mouse Click field to 1.0, which changes the load by one MW per click on the up/down arrows. You may also like to set the Digits to Right of Decimal to 2 to see more digits in the load field. Be sure to save your case. The new system now has one generator and two loads. The system is still radial, meaning that a break anywhere on the wire joining bus 1 to bus 2 would result in a blackout of all the loads. Radial power systems are quite common in the lower voltage distribution systems. At higher voltage levels, networked systems are typically used. In a networked system, each load has at least two possible sources of power. Convert the system to a networked system simply by adding a new line from bus 1 to bus 3. To do this, switch back to Edit Mode, and then repeat the previous line insertion process except you should start at bus 1 and end at bus 3; use the same line parameters as for the bus 2 to 3 line. Also before returning to Run Mode, right click on the blue Two Bus Power System title and change it to Three Bus Power System. Return to Run Mode and again solve. Your final system should look similar to the system shown in Figure 1.8. Note that now you can open any single line and still supply both loads—a nice increase in reliability!

FIGURE 1.8

Example 1.3—New three-bus system

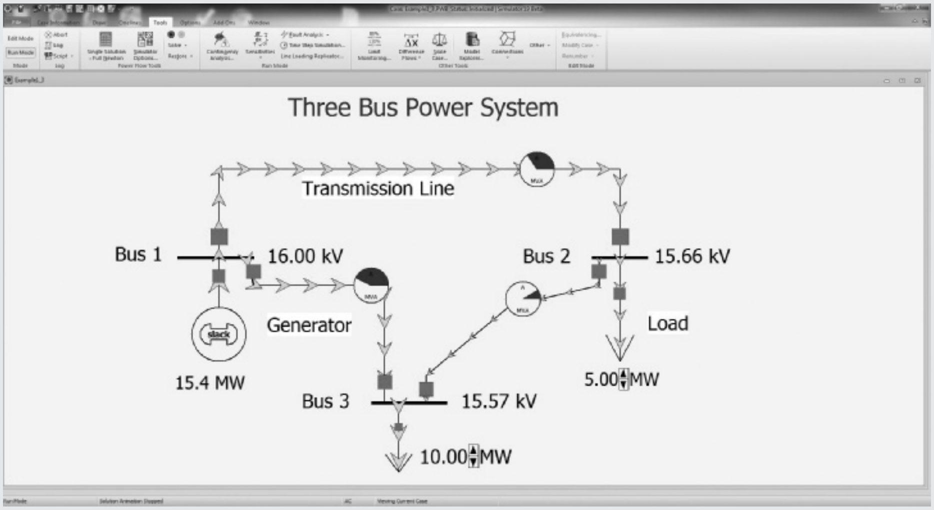

With this introduction, you now have the skills necessary to begin using PowerWorld to interactively learn about power systems. If you'd like to take a look at some of the larger systems you'll be studying, in the Chapter 6 directory open PowerWorld case Example 6_13. This case models a power system with 37 buses. Notice that when you open any line in the system, the flow of power immediately redistributes to continue to meet the total load demand. While the education version of PowerWorld is limited to 42 buses, the commercial version can handle cases with the tens of thousands of buses common in utility studies.

Copyright 2017 Cengage Learning. All Rights Reserved. May not be copied, scanned, or duplicated, in whole or in part. Due to electronic rights, some third party content may be suppressed from the eBook and/or eChapter(s). Editorial review has deemed that any suppressed content does not materially affect the overall learning experience. Cengage Learning reserves the right to remove additional content at any time if subsequent rights restrictions require it.

REFERENCES

1. H. M. Rustebakke et al., *Electric Utility Systems Practice,* 4th ed. (New York: Wiley. 1983). Photos courtesy of Westinghouse Historical Collection.
2. U.S. Energy Information Administration, *Electric Power Annual 2012—December 2013,* www.eia.gov.
3. U.S. Energy Information Administration, *Annual Energy Outlook 2014, April 2014,* www.eia.gov.
4. Wikipedia Encyclopedia, *List of HVDC Projects,* en.wikipedia.org.
5. M. P. Bahrman and B. K. Johnson, “The ABCs of HVDC Transmission Technologies,” *IEEE Power & Energy Magazine,* 5,2 (March/April 2007), pp. 33–44.
6. Edison Electric Institute, *Key Facts about the Electric Power Industry,* May 2013, www.eei.org.
7. North American Electric Reliability Corporation (NERC), *2013 Long-Term Reliability Assessment* (Atlanta, GA: www.nerc.com, December 2013).
8. Seth Blumsack, “How the Free Market Rocked the Grid,” *IEEE Spectrum,* 47, 12 (December, 2010), pp. 44–48, 57–59.
9. Utility Analytics Institute, *Aging Utility Workforce: Business Impacts and Strategies,* November 27, 2013, www.inin.com
10. IEEE Power & Energy Society, *Preparing the Foundation for Future Electric Energy Systems: A Strong Power and Energy Engineering Workforce,* U.S. Power & Energy Engineering Workforce Collaborative, April 2009, www.ieee-pes.org
11. E. Santacana, G. Rackliffe, L. Tang, and X. Feng, “Getting Smart,” *IEEE Power & Energy Magazine,* 8,2 (March/April 2010), pp. 41–48.
12. North American Electric Reliability Corporation (NERC), *About NERC* (Princeton, NJ: www.nerc.com).
13. T.J. Overbye and J. Weber, “Visualizing the Electric Grid,” *IEEE Spectrum,* 38,2 (February 2001), pp. 52–58.
14. *Solar Power in Germany,* en.wikipedia.com
15. “Focus on UHV AC: China shows the way by energising 1,000 kV line,” *Global Transmission Report,* www.globaltransmission.info, March 2, 2009.
16. J. Cao and J.Y. Cai, “HVDC in China,” *EPRI 2013 HVDC & Facts Conference,* Palo Alto, CA, www.cepri.com, August 28, and 29, 2013.

Copyright 2017 Cengage Learning. All Rights Reserved. May not be copied, scanned, or duplicated, in whole or in part. Due to electronic rights, some third party content may be suppressed from the eBook and/or eChapter(s). Editorial review has deemed that any suppressed content does not materially affect the overall learning experience. Cengage Learning reserves the right to remove additional content at any time if subsequent rights restrictions require it.

Copyright 2017 Cengage Learning. All Rights Reserved. May not be copied, scanned, or duplicated, in whole or in part. Due to electronic rights, some third party content may be suppressed from the eBook and/or eChapter(s). Editorial review has deemed that any suppressed content does not materially affect the overall learning experience. Cengage Learning reserves the right to remove additional content at any time if subsequent rights restrictions require it.

2 Fundamentals

Operations Center at PJM. PJM is a regional transmission organization (RTO) that coordinates the movement of wholesale electricity and ensures the reliability of the high-voltage electric power system serving 61 million people in all or parts of Delaware, Illinois, Indiana, Kentucky, Maryland, Michigan, New Jersey, North Carolina, Ohio, Pennsylvania, Tennessee, Virginia, West Virginia and the District of Columbia, USA (Courtesy of PJM Interconnection, LLC.)

The objective of this chapter is to review basic concepts and establish terminology and notation. In particular, we review phasors, instantaneous power, complex power, network equations, and elementary aspects of balanced three-phase circuits. Students who have already had courses in electric network theory and basic electric machines should find this chapter to be primarily refresher material.

Copyright 2017 Cengage Learning. All Rights Reserved. May not be copied, scanned, or duplicated, in whole or in part. Due to electronic rights, some third party content may be suppressed from the eBook and/or eChapter(s). Editorial review has deemed that any suppressed content does not materially affect the overall learning experience. Cengage Learning reserves the right to remove additional content at any time if subsequent rights restrictions require it.

CASE STUDY

Throughout most of the 20th century, electric utility companies built increasingly larger generation plants, primarily hydro or thermal (using coal, gas, oil, or nuclear fuel). At the end of the 20th century, following the ongoing deregulation of the electric utility industry with increased competition in the United States and in other countries, smaller generation sources that connect directly to distribution systems have emerged. Distributed energy resources are sources of energy including generation and storage devices that are located near local loads. Distributed generation sources include renewable technologies (including geothermal, ocean tides, solar, and wind) and nonrenewable technologies (including internal combustion engines, combustion turbines, combined cycle, microturbines, and fuel cells). Microgrids are systems that have distributed energy resources and associated loads that can form intentional islands in distribution systems. The following article provides an overview of ongoing microgrid activities undertaken by the Office of Electricity Delivery and Energy Reliability of the U.S. Department of Energy [5].

KEY CONNECTIONS

By Merrill Smith and Dan Ton

U.S. Department of Energy

Microgrids have been identified as key components of the smart grid for improving power reliability and quality, increasing system energy efficiency, and providing the possibility of grid independence to individual end-user sites. The Microgrid Exchange Group, an ad hoc group of experts and implementers of microgrid technology, has defined a microgrid as “a group of interconnected loads and distributed energy resources within clearly defined electrical boundaries that acts as a single controllable entity with respect to the grid. A microgrid can connect and disconnect from the grid to enable it to operate in both grid-connected or island mode.”

Microgrids have been described by other organizations using similar definitions, including the key concepts of a system made up of multiple loads along with generation and the ability to island from the grid. Microgrids provide multiple benefits that include:

- Enabling grid modernization and the integration of multiple smart grid technologies;

(Merrill Smith and Dan Ton, “Key Connections,” U.S. Deptartment of Energy, Washington DC, USA)

Copyright 2017 Cengage Learning. All Rights Reserved. May not be copied, scanned, or duplicated, in whole or in part. Due to electronic rights, some third party content may be suppressed from the eBook and/or eChapter(s). Editorial review has deemed that any suppressed content does not materially affect the overall learning experience. Cengage Learning reserves the right to remove additional content at any time if subsequent rights restrictions require it.

- Enhancing and easing the integration of distributed and renewable energy sources that help reduce peak load and also reduce losses by locating generation near demand;
- Meeting end-user needs by ensuring energy supply for critical loads, controlling power quality and reliability at the local level, and promoting customer participation through demand-side management and community involvement in electricity supply; and
- Supporting the macrogrid by handling sensitive loads and the variability of renewables locally and supplying ancillary services to the bulk power system.

Within the Office of Electricity Delivery and Energy Reliability (OE) of the U.S. Department of Energy (DOE), the Smart Grid R&D Program was established to accelerate the deployment and integration of the advanced communication, control, and information technologies needed to modernize the nation's electric delivery network. This modernization includes preparing the U.S. electric infrastructure to meet the challenges of the 21st-century economy. The Smart Grid R&D Program has two goals: to dynamically optimize grid operations and resources for a robust, flexible, and secure electric grid; and to fully integrate demand response and consumer participation into grid resource planning and operations. The program's microgrid activities support the achievement of both of these goals.

According to the DOE's September 2011 update of the *Smart Grid Research and Development Multi-Year Program Plan: 2010–2014* (available at http://events.energetics.com/SmartGridPeerReview2012/pdfs/SG_MYPP_2011.pdf), the microgrid initiative has established the following 2020 performance targets for costs, reliability, system energy efficiencies, and emissions to advance these grid modernization goals: "to develop commercial-scale microgrid systems (capacity <10 MW) capable of reducing [the] outage time of required loads by >98% at a cost comparable to nonintegrated baseline solutions (uninterrupted power supply…plus diesel genset) while reducing emissions by >20% and improving system energy efficiencies by >20%."

This article provides an overview of ongoing microgrid activities being undertaken by OE and its Smart Grid R&D Program. In addition, it discusses the process OE has undertaken to engage microgrid stakeholders to jointly identify the remaining areas in which there are R&D gaps and develop a plan to address those gaps.

Ongoing Microgrid Activities

The bulk of the DOE's microgrid R&D efforts to date have focused on demonstration activities to meet niche application needs, such as those for meeting peak load reduction, renewable energy mandates and directives, and energy surety and reliability at certain critical facilities,

Copyright 2017 Cengage Learning. All Rights Reserved. May not be copied, scanned, or duplicated, in whole or in part. Due to electronic rights, some third party content may be suppressed from the eBook and/or eChapter(s). Editorial review has deemed that any suppressed content does not materially affect the overall learning experience. Cengage Learning reserves the right to remove additional content at any time if subsequent rights restrictions require it.

including military installations. These ongoing microgrid demonstration projects consist of lab- and field-scale R&D test beds, renewable and distributed systems integration (RDSI) projects for peak load reduction, select Smart Grid Demonstration Program (SGDP) projects funded under the American Recovery and Reinvestment Act of 2009 (ARRA) as part of OE's implementation of grid modernization, and assessment and demonstration projects jointly supported by the U.S. Department of Defense (DOD) and the DOE.

OE is currently supporting nine RDSI projects with a total value exceeding U.S.$100 million (with approximately U.S.$55 million coming from the DOE). The two primary goals of these projects are to demonstrate at least 15% peak demand reduction at the distribution feeder or substation level through integrating distributed energy resources (DERs) and to demonstrate microgrids that can operate in both grid-parallel and islanded modes. These projects are proving out systems that can defer transmission and distribution investments and upgrades by utilizing local assets (generation and load reduction) in an integrated fashion. They are also increasing the reliability of the local distribution system by adding elements that make it more stable and reconfigurable. Other benefits being realized from these projects include addressing vulnerabilities in critical infrastructure, managing peak loads, lowering emissions, using fuel resources more efficiently, and helping customers manage energy costs. These RDSI projects are progressing toward achieving the goals of at least 15% in peak demand reductions and the ability to island. Some, such as the Illinois Institute of Technology, Chevron/Santa Rita Jail, and Ft. Collins FortZED projects, have already realized or exceeded the 15% reduction goal.

Under ARRA, SGDP has funded 16 smart grid regional demonstration projects to demonstrate emerging smart grid technologies and alternative architectures to validate business models and address regulatory and scalability issues. Among them, several projects are conducting demonstrations involving combinations of the following elements: renewable energy resources, distributed generation, energy storage, demand-side management, and charging schemes for plug-in electric vehicles. These projects include (but are not limited to) the Pacific Northwest Smart Grid Demonstration by Battelle Memorial Institute, which includes Portland General Electric's High Reliability Zone (a microgrid); the Energy Internet Demonstration by Pecan Street Project Inc. in Texas; and the Irvine Smart Grid Demonstration by Southern California Edison. Further information on the SGDP projects is available at http://www.smartgrid.gov/recovery_act/project_information?keys=&project%5B%5D=2.

There has also been a significant effort by national laboratories to produce microgrid designs, analyses, and demonstrations at test facilities and military bases. Lawrence Berkeley

Copyright 2017 Cengage Learning. All Rights Reserved. May not be copied, scanned, or duplicated, in whole or in part. Due to electronic rights, some third party content may be suppressed from the eBook and/or eChapter(s). Editorial review has deemed that any suppressed content does not materially affect the overall learning experience. Cengage Learning reserves the right to remove additional content at any time if subsequent rights restrictions require it.

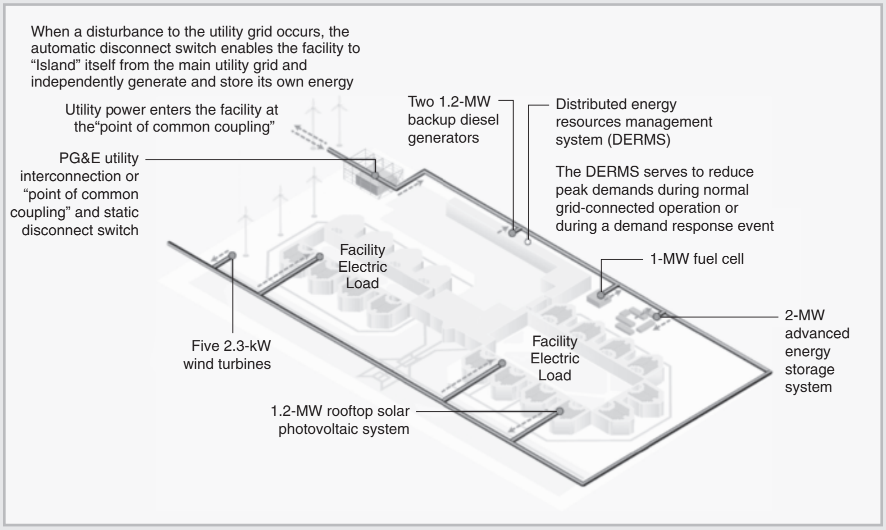
When a disturbance to the utility grid occurs, the automatic disconnect switch enables the facility to "Island" itself from the main utility grid and independently generate and store its own energy
Utility power enters the facility at the"point of common coupling"
PG&E utility interconnection or "point of common coupling" and static disconnect switch
Two 1.2-MW backup diesel generators
Distributed energy resources management system (DERMS)
The DERMS serves to reduce peak demands during normal grid-connected operation or during a demand response event
1-MW fuel cell
Facility Electric Load
Facility Electric Load
2-MW advanced energy storage system
Five 2.3-kW wind turbines
1.2-MW rooftop solar photovoltaic system

Figure 1 *Chevron Energy Solutions' project at the Santa Rita Jail in Dublin, California, to demonstrate commercial application of a CERTS microgrid (used with permission)* (Based on Chevron Energy Solutions.)

National Laboratory (LBNL) is teaming with American Electric Power (AEP), the University of Wisconsin, and Sandia National Laboratories (SNL) to apply Consortium for Electric Reliability Technology Solutions (CERTS) microgrid concepts in AEP's Dolan Technology Center at the Walnut Station Test Facility in Groveport, Ohio. The Sacramento Municipal Utility District, the Chevron Energy Solutions RDSI project (shown in Figure 1), and the DOD at Fort Sill and Maxwell Air Force Bases are also applying CERTS microgrid concepts in field demonstrations. LBNL has developed the distributed energy resources customer adoption model (DER-CAM), an economic model for predicting and optimizing the capacity and minimizing the cost of operating distributed generation in microgrids.

SNL has developed its energy surety microgrid (ESM) methodology, which uses cost and performance data from military bases to develop approaches for implementing high-reliability microgrids and to assist in planning for and analysis of the potential risks in future military and commercial projects. To date, 14 military bases have received assessments and/or conceptual microgrid designs using SNL's ESM methodology. From this work, SNL has developed a set of valuable lessons learned that, combined with its design methodology, provide a blueprint for future ESM microgrid implementation.

The ESM design work was the springboard for a larger joint microgrid deployment effort on the part of the DOE, the DOD, and the U.S. Department of Homeland Security (DHS). This joint effort,

Copyright 2017 Cengage Learning. All Rights Reserved. May not be copied, scanned, or duplicated, in whole or in part. Due to electronic rights, some third party content may be suppressed from the eBook and/or eChapter(s). Editorial review has deemed that any suppressed content does not materially affect the overall learning experience. Cengage Learning reserves the right to remove additional content at any time if subsequent rights restrictions require it.

known as a joint capabilities technology demonstration (JCTD), is the first of its kind for the DOE and will ultimately deploy three smart power infrastructure demonstration for energy reliability and security (SPIDERS) microgrids. Five national laboratories—Idaho, National Renewable Energy Laboratory, Oak Ridge National Laboratory (ORNL), Pacific Northwest National Laboratory (PNNL), and SNL—supported by the DOE are playing a pivotal role in the SPIDERS deployment through their work on the microgrid designs, the cyber designs, and the development of a transition plan that can be used to design and deploy microgrids at additional military facilities and in the private sector. The three SPIDERS microgrids will be deployed in phases at Joint Base Pearl Harbor-Hickam (Hawaii), Fort Carson (Colorado), and Camp Smith (Hawaii), respectively. The first phase, at Pearl Harbor-Hickam, has completed successful technical and operational demonstrations. A key element of SPIDERS is standardization of the design approach, contracting, installation, security, and operation of these microgrids to support future applications.

Other work at the national laboratories is also supporting the microgrid effort. ORNL's Distributed Energy Communications & Controls laboratory is developing controls for inverter-based DERs to provide local voltage, power, and power quality support for the ORNL campus distribution system. On the simulation side, PNNL has been developing GridLAB-D as a distribution system simulation tool that integrates grid operations at several levels, including microgrids.

As OE moves forward with microgrid R&D, it is coordinating the national laboratories' efforts on microgrids so they will be more cohesive and unified. The labs will be working on three major tasks. The focus will be on:

- Developing use cases (based on existing microgrids) to define the performance requirements and technology specifications of microgrids;
- Performing cost and benefit analysis to identify high-impact R&D for additional investments; and
- Creating integrated tool sets for developing conceptual and preliminary designs and controls and operations architectures.

In addition to meeting individual niche applications, the various DOE demonstrations also field-prove capabilities of current technologies and unveil lessons learned, challenges, and needed but unmet capabilities. Current technologies will clearly not be enough to meet the 2020 performance targets established by the DOE for microgrids. As part of its continuing effort to engage stakeholders in joint planning and implementation of R&D activities, the Smart Grid R&D Program convened two microgrid workshops, in 2011 and 2012, to seek stakeholder input on key areas for R&D and performance

Copyright 2017 Cengage Learning. All Rights Reserved. May not be copied, scanned, or duplicated, in whole or in part. Due to electronic rights, some third party content may be suppressed from the eBook and/or eChapter(s). Editorial review has deemed that any suppressed content does not materially affect the overall learning experience. Cengage Learning reserves the right to remove additional content at any time if subsequent rights restrictions require it.

Workshops to Engage Stakeholders for R&D Planning	• 2011 workshop affirmed DOE 2020 targets and defined R&D areas for component and system integration technologies • 2012 workshop integrated R&D areas (from 2011) into planning/design and operations/control and prioritized R&D topics in each
Rescoping Lab AOPs to Address Workshop Priority R&D Topics	• Use case development to define performance requirements and technology specifications • Cost and benefit analysis to ID high-impact R&D for investments • Integrated tool sets for conceptual/ preliminary designs • Integrated tool sets for controls and operations architecture
FY14 Microgrid R&D FOA	• In synergy with Lab AOPs to achieve cost parity for the identified microgrid use case

Figure 2 R&D pathway toward the DOE's 2020 microgrid performance targets

baselines, targets, and actionable plans. This input was incorporated into the DOE's 2012 *Smart Grid Research and Development Multi-Year Program Plan* to guide current and future DOE R&D efforts in microgrids (see Figure 2).

Microgrid Workshops

The DOE held its first microgrid workshop on August 30–31, 2011 in San Diego, California; a follow-up workshop was held on July 30–31, 2012 in Chicago. The purpose of the first workshop was to convene experts and practitioners to assist the DOE in identifying and prioritizing R&D areas in the field of microgrids. The second workshop was held in response to path-forward discussions that called for sharing lessons learned and best practices for system integration from existing projects in the United States

Copyright 2017 Cengage Learning. All Rights Reserved. May not be copied, scanned, or duplicated, in whole or in part. Due to electronic rights, some third party content may be suppressed from the eBook and/or eChapter(s). Editorial review has deemed that any suppressed content does not materially affect the overall learning experience. Cengage Learning reserves the right to remove additional content at any time if subsequent rights restrictions require it.

(including military microgrids) and elsewhere. In addition, the purpose of the second workshop was to delve more deeply into R&D topics gathered from the first workshop and subsequently determine system integration gap areas and functional requirements.

The 2011 Workshop

Two tracks were organized to address the potential cost reduction of major microgrid components and subcomponents. One track focused on microgrid components, with separate sessions on switch technologies, control and protection technologies, and inverters and converters. The second track focused on microgrid systems, with separate sessions on standards and protocols, system design and economic analysis tools, and system integration.

The 2012 Workshop

A working list of system integration issues, categorized in the two areas of planning and design and operations and control, was presented for input from the attendees, based on their experience. This brainstorming session resulted in 12 R&D topics for discussion. For each topic, participants discussed four aspects: the current status of the technology, needs and challenges, the scope of the needed R&D, and R&D metrics.

Conclusions from the breakout session discussions and the report-out presentations from the 2011 workshop were documented in the *DOE Microgrid Workshop Report*, available at http://energy.gov/sites/prod/files/Microgrid%20Workshop%20Report%20August%202011.pdf. The 2012 workshop program agenda with embedded presentation links is available at http://e2rg.com/events/agenda/. Table 1 lists the key R&D areas identified from the two workshops.

Conclusions and the Path Forward

The DOE's Smart Grid R&D Program considers microgrids to be key building blocks for smart grids and has established microgrid R&D as a key area of focus. A significant number of R&D needs and challenges have been identified for microgrids during the two workshops described above, with input from more than 170 experts and practitioners, representing a broad group of stakeholders in the United States, Canada, Europe, Japan, and Korea. At the two workshops, the scope of the R&D necessary to address the identified needs and challenges was outlined. The technical, economical, social, and environmental benefits that can result from successful development and deployment of microgrids became evident in the course of the workshop discussions and presentations.

Engaging stakeholders and knowledgeable practitioners to obtain input on R&D needs is a key part of the R&D topic development process. With the input collected, the Smart Grid R&D Program will further refine R&D requirements so as to plan and develop a competitive funding opportunity announcement, subject to available DOE funds. The DOE's

Copyright 2017 Cengage Learning. All Rights Reserved. May not be copied, scanned, or duplicated, in whole or in part. Due to electronic rights, some third party content may be suppressed from the eBook and/or eChapter(s). Editorial review has deemed that any suppressed content does not materially affect the overall learning experience. Cengage Learning reserves the right to remove additional content at any time if subsequent rights restrictions require it.

2011 Workshop		2012 Workshop	
R&D Areas			
Components	Systems	Planning and Design	Operations and Controls
Switch Technologies	**Standards and Protocols**	**System Architecture Development**	**Steady-State Control and Coordination**
Legacy grid-connection technologies to enable connection and disconnection from the grid	Universal microgrid communications and control standards	Definition of microgrid applications, interfaces, and services	Internal services within the microgrid
Requirements based on customer and utility needs	Microgrid protection, coordination, and safety	Open architectures that promote flexibility, scalability, and security	Interaction of the microgrid with utilities or other microgrids
Control and Protection Technologies	**System Design and Economic Analysis Tools**	**Modeling and Analysis**	**Transient State Control and Protection**
Best practices and specifications for protection and controls; information models	Microgrid multiobjective optimization framework	Performance optimization methods and uncertainty in the modeling and design process	Transient state control and protection
Reliable, low-cost protection	Designing an operations optimization methodology that takes uncertainty into account		
Switches to handle full fault current			
Inverters/Converters	**System Integration**	**Power System Design**	**Operational Optimization**
Topologies and control algorithms so that multiple inverters can operate in a microgrid	A common integration framework	DC power	Operational optimization of a single microgrid
Advanced power electronics technologies		Microgrid integration	Operational optimization of multiple microgrids

Table 1

Key R&D Areas Identified from the DOE's 2011 and 2012 Microgrid Workshops

Copyright 2017 Cengage Learning. All Rights Reserved. May not be copied, scanned, or duplicated, in whole or in part. Due to electronic rights, some third party content may be suppressed from the eBook and/or eChapter(s). Editorial review has deemed that any suppressed content does not materially affect the overall learning experience. Cengage Learning reserves the right to remove additional content at any time if subsequent rights restrictions require it.

microgrid R&D initiative hopes to advance microgrids, in partnership with industry and research experts, from conception through R&D execution.

For Further Reading

U.S. Department of Energy. Information/fact sheets on the smart grid projects (including the smart grid demonstration projects) funded through the American Recovery and Reinvestment Act of 2009. [Online]. Available: http://www.smartgrid.gov/recovery_act/project_information

U.S. Department of Energy. (2012, May 10). Smart grid R&D Program peer review June 7–8, 2012. [Online]. Available: http://energy.gov/oe/articles/smart-grid-rd-program-peer-review-june-7-8-2012

U.S. Department of Energy. Smart grid research & development multi-year program plan: 2010–2014. [Online]. Available: http://energy.gov/sites/prod/files/SG_MYPP_2012%20Update.pdf

U.S. Department of Energy. (2011). Microgrid workshop report. [Online]. Available: http://energy.gov/sites/prod/files/Microgrid%20Workshop%20Report%20August%202011.pdf

U.S. Department of Energy. (2012). Microgrid workshop agenda and presentations. [Online]. Available: http://e2rg.com/microgrid-2012/Workshop_Agenda-08092012.pdf

Sandia National Laboratories. SPIDERS: The smart power infrastructure demonstration for energy reliability and security. [Online]. Available: http://energy.sandia.gov/wp/wp-content/gallery/uploads/SPIDERS_Fact_Sheet_2012-1431P.pdf

Biographies

Merrill Smith is with the U.S. Department of Energy, Washington, D.C.

Dan Ton is with the U.S. Department of Energy, Washington, D.C. ■

2.1 PHASORS

A sinusoidal voltage or current at constant frequency is characterized by two parameters: a maximum value and a phase angle. A voltage

$$v(t) = \mathrm{V}_{\max}\cos(\omega t + \delta) \tag{2.1.1}$$

has a maximum value $\mathrm{V}_{\max}$ and a phase angle δ when referenced to $\cos(\omega t)$. The root-mean-square (rms) value, also called *effective value*, of the sinusoidal voltage is

$$\mathrm{V} = \frac{\mathrm{V}_{\max}}{\sqrt{2}} \tag{2.1.2}$$

Euler's identity, $e^{j\phi} = \cos\phi + j\sin\phi$, can be used to express a sinusoid in terms of a phasor. For the above voltage,

Copyright 2017 Cengage Learning. All Rights Reserved. May not be copied, scanned, or duplicated, in whole or in part. Due to electronic rights, some third party content may be suppressed from the eBook and/or eChapter(s). Editorial review has deemed that any suppressed content does not materially affect the overall learning experience. Cengage Learning reserves the right to remove additional content at any time if subsequent rights restrictions require it.

$$v(t) = \mathrm{Re}\left[\mathrm{V}_{\max} e^{j(\omega t+\delta)}\right]$$
$$= \mathrm{Re}\left[\sqrt{2}(\mathrm{V}e^{j\delta})e^{j\omega t}\right] \tag{2.1.3}$$

where $j = \sqrt{-1}$ and Re denotes "real part of." The rms phasor representation of the voltage is given in three forms—exponential, polar, and rectangular:

$$V = \underbrace{\mathrm{V}e^{j\delta}}_{\text{exponential}} = \underbrace{\mathrm{V}\underline{/\delta}}_{\text{polar}} = \underbrace{\mathrm{V}\cos\delta + j\mathrm{V}\sin\delta}_{\text{rectangular}} \tag{2.1.4}$$

A phasor can be easily converted from one form to another. Conversion from polar to rectangular is shown in the phasor diagram of Figure 2.1. Euler's identity can be used to convert from exponential to rectangular form. As an example, the voltage

$$v(t) = 169.7\cos(\omega t + 60°) \text{ volts} \tag{2.1.5}$$

has a maximum value $\mathrm{V}_{\max} = 169.7$ volts, a phase angle $\delta = 60°$ when referenced to $\cos(\omega t)$, and an rms phasor representation in polar form of

$$V = 120\underline{/60°} \quad \text{volts} \tag{2.1.6}$$

Also, the current

$$i(t) = 100\cos(\omega t + 45°) \text{ A} \tag{2.1.7}$$

has a maximum value $\mathrm{I}_{\max} = 100$ A, an rms value $\mathrm{I} = 100/\sqrt{2} = 70.7$ A, a phase angle of 45°, and a phasor representation

$$I = 70.7\underline{/45°} = 70.7e^{j45} = 50 + j50 \quad \text{A} \tag{2.1.8}$$

The relationships between the voltage and current phasors for the three passive elements—resistor, inductor, and capacitor—are summarized in Figure 2.2, where sinusoidal-steady-state excitation and constant values of R, L, and C are assumed.

When voltages and currents are discussed in this text, lowercase letters such as $v(t)$ and $i(t)$ indicate instantaneous values, uppercase letters such as V and I indicate rms values, and uppercase letters in italics such as V and I indicate rms phasors. When voltage or current values are specified, they shall be rms values unless otherwise indicated.

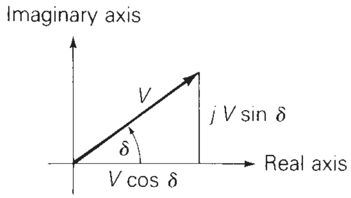

FIGURE 2.1

Phasor diagram for converting from polar to rectangular form

Copyright 2017 Cengage Learning. All Rights Reserved. May not be copied, scanned, or duplicated, in whole or in part. Due to electronic rights, some third party content may be suppressed from the eBook and/or eChapter(s). Editorial review has deemed that any suppressed content does not materially affect the overall learning experience. Cengage Learning reserves the right to remove additional content at any time if subsequent rights restrictions require it.

FIGURE 2.2

Summary of relationships between phasors *V* and *I* for constant R, L, and C elements with sinusoidal-steady-state excitation

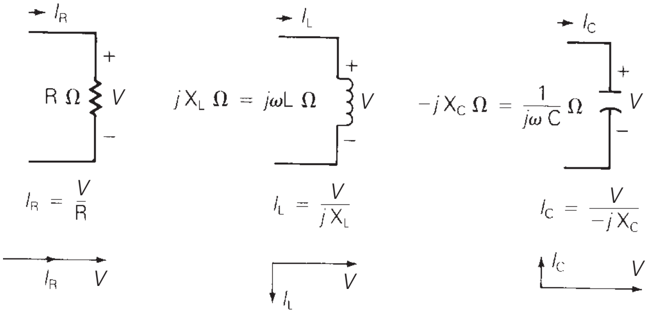

2.2 INSTANTANEOUS POWER IN SINGLE-PHASE AC CIRCUITS

Power is the rate of change of energy with respect to time. The unit of power is a watt, which is a joule per second. Instead of saying that a load absorbs energy at a rate given by the power, it is common practice to say that a load absorbs power. The instantaneous power in watts absorbed by an electrical load is the product of the instantaneous voltage across the load in volts and the instantaneous current into the load in amperes. Assume that the load voltage is

$$v(t) = V_{max}\cos(\omega t + \delta) \text{ volts} \tag{2.2.1}$$

We now investigate the instantaneous power absorbed by purely resistive, purely inductive, purely capacitive, and general RLC loads. We also introduce the concepts of real power, power factor, and reactive power. The physical significance of real and reactive power is also discussed.

PURELY RESISTIVE LOAD

For a purely resistive load, the current into the load is in phase with the load voltage, $I = V/R$, and the current into the resistive load is

$$i_R(t) = I_{Rmax}\cos(\omega t + \delta) \quad \text{A} \tag{2.2.2}$$

where $I_{Rmax} = V_{max}/R$. The instantaneous power absorbed by the resistor is

$$\begin{aligned} p_R(t) &= v(t)i_R(t) = V_{max}I_{Rmax}\cos^2(\omega t + \delta) \\ &= \tfrac{1}{2}V_{max}I_{Rmax}\{1 + \cos[2(\omega t + \delta)]\} \\ &= VI_R\{1 + \cos[2(\omega t + \delta)]\} \quad \text{W} \end{aligned} \tag{2.2.3}$$

As indicated by (2.2.3), the instantaneous power absorbed by the resistor has an average value

Copyright 2017 Cengage Learning. All Rights Reserved. May not be copied, scanned, or duplicated, in whole or in part. Due to electronic rights, some third party content may be suppressed from the eBook and/or eChapter(s). Editorial review has deemed that any suppressed content does not materially affect the overall learning experience. Cengage Learning reserves the right to remove additional content at any time if subsequent rights restrictions require it.

$$P_R = VI_R = \frac{V^2}{R} = I_R^2 R \quad \text{W} \tag{2.2.4}$$

plus a double-frequency term $VI_R \cos[2(\omega t + \delta)]$.

PURELY INDUCTIVE LOAD

For a purely inductive load, the current lags the voltage by 90°, $I_L = V/(jX_L)$, and

$$i_L(t) = I_{L\max} \cos(\omega t + \delta - 90°) \quad \text{A} \tag{2.2.5}$$

where $I_{L\max} = V_{\max}/X_L$, and $X_L = \omega L$ is the inductive reactance. The instantaneous power absorbed by the inductor is*

$$\begin{aligned} p_L(t) &= v(t) i_L(t) = V_{\max} I_{L\max} \cos(\omega t + \delta) \cos(\omega t + \delta - 90°) \\ &= \tfrac{1}{2} V_{\max} I_{L\max} \cos[2(\omega t + \delta) - 90°] \\ &= VI_L \sin[2(\omega t + \delta)] \quad \text{W} \end{aligned} \tag{2.2.6}$$

As indicated by (2.2.6), the instantaneous power absorbed by the inductor is a double-frequency sinusoid with *zero* average value.

PURELY CAPACITIVE LOAD

For a purely capacitive load, the current leads the voltage by 90°, $I_c = V/(-jX_C)$, and

$$i_C(t) = I_{C\max} \cos(\omega t + \delta + 90°) \quad \text{A} \tag{2.2.7}$$

where $I_{C\max} = V_{\max}/X_C$, and $X_C = 1/(\omega C)$ is the capacitive reactance. The instantaneous power absorbed by the capacitor is

$$\begin{aligned} p_C(t) &= v(t) i_C(t) = V_{\max} I_{C\max} \cos(\omega t + \delta) \cos(\omega t + \delta + 90°) \\ &= \tfrac{1}{2} V_{\max} I_{C\max} \cos[2(\omega t + \delta) + 90°)] \\ &= -VI_C \sin[2(\omega t + \delta)] \quad \text{W} \end{aligned} \tag{2.2.8}$$

The instantaneous power absorbed by a capacitor is also a double-frequency sinusoid with *zero* average value.

GENERAL RLC LOAD

For a general load composed of RLC elements under sinusoidal-steady-state excitation, the load current is of the form

$$i(t) = I_{\max} \cos(\omega t + \beta) \quad \text{A} \tag{2.2.9}$$

Copyright 2017 Cengage Learning. All Rights Reserved. May not be copied, scanned, or duplicated, in whole or in part. Due to electronic rights, some third party content may be suppressed from the eBook and/or eChapter(s). Editorial review has deemed that any suppressed content does not materially affect the overall learning experience. Cengage Learning reserves the right to remove additional content at any time if subsequent rights restrictions require it.

The instantaneous power absorbed by the load is then*

$$\begin{aligned} p(t) &= v(t)i(t) = \mathrm{V}_{\max}\mathrm{I}_{\max}\cos(\omega t+\delta)\cos(\omega t+\beta) \\ &= \tfrac{1}{2}\mathrm{V}_{\max}\mathrm{I}_{\max}\{\cos(\delta-\beta)+\cos[2(\omega t+\delta)-(\delta-\beta)]\} \\ &= \mathrm{VI}\cos(\delta-\beta)+\mathrm{VI}\cos(\delta-\beta)\cos[2(\omega t+\delta)] \\ &\quad + \mathrm{VI}\sin(\delta-\beta)\sin[2(\omega t-\delta)] \\ p(t) &= \mathrm{VI}\cos(\delta-\beta)\{1+\cos[2(\omega t+\delta)]\}+\mathrm{VI}\sin(\delta-\beta) \end{aligned}$$

Letting $\mathrm{I}\cos(\delta-\beta)=\mathrm{I_R}$ and $\mathrm{I}\sin(\delta-\beta)=\mathrm{I_X}$ gives

$$p(t) = \underbrace{\mathrm{VI_R}\{1+\cos[2(\omega t+\delta)]\}}_{p_\mathrm{R}(t)} + \underbrace{\mathrm{VI_X}\sin[2(\omega t+\delta)]}_{p_\mathrm{X}(t)} \tag{2.2.10}$$

As indicated by (2.2.10), the instantaneous power absorbed by the load has two components: One can be associated with the power $p_\mathrm{R}(t)$ absorbed by the resistive component of the load, and the other can be associated with the power $p_\mathrm{X}(t)$ absorbed by the reactive (inductive or capacitive) component of the load. The first component $p_\mathrm{R}(t)$ in (2.2.10) is identical to (2.2.3), where $\mathrm{I_R}=\mathrm{I}\cos(\delta-\beta)$ is the component of the load current in phase with the load voltage. The phase angle $(\delta-\beta)$ represents the angle between the voltage and current. The second component $p_\mathrm{X}(t)$ in (2.2.10) is identical to (2.2.6) or (2.2.8), where $\mathrm{I_x}=\mathrm{I}\sin(\delta-\beta)$ is the component of load current 90° out of phase with the voltage.

REAL POWER

Equation (2.2.10) shows that the instantaneous power $p_\mathrm{R}(t)$ absorbed by the resistive component of the load is a double-frequency sinusoid with average value P given by

$$\mathrm{P}=\mathrm{VI_R}=\mathrm{VI}\cos(\delta-\beta)\ \mathrm{W} \tag{2.2.11}$$

The *average power* P is also called *real power* or *active power.* All three terms indicate the same quantity P given by (2.2.11).

POWER FACTOR

The term $\cos(\delta-\beta)$ in (2.2.11) is called the *power factor.* The phase angle $(\delta-\beta)$, which is the angle between the voltage and current, is called the *power factor angle.* For dc circuits, the power absorbed by a load is the product of the dc load voltage and the dc load current; for ac circuits, the average power absorbed by a load is the product of the rms load voltage V, rms load current I, and the power factor $\cos(\delta-\beta)$, as shown by (2.2.11). For inductive loads, the current lags the voltage, which means β is less than δ, and the power factor is said to be *lagging.* For capacitive loads, the current leads the voltage, which means β is greater than δ, and the power factor is said to be *leading.* By convention, the power factor $\cos(\delta-\beta)$ is positive. If $|\delta-\beta|$

---

*Use the identity: $\cos\mathrm{A}\cos\mathrm{B}=\frac{1}{2}[\cos(\mathrm{A}-\mathrm{B})+\cos(\mathrm{A}+\mathrm{B})]$.

Copyright 2017 Cengage Learning. All Rights Reserved. May not be copied, scanned, or duplicated, in whole or in part. Due to electronic rights, some third party content may be suppressed from the eBook and/or eChapter(s). Editorial review has deemed that any suppressed content does not materially affect the overall learning experience. Cengage Learning reserves the right to remove additional content at any time if subsequent rights restrictions require it.

is greater than 90°, then the reference direction for current may be reversed, resulting in a positive value of $\cos(\delta - \beta)$.

REACTIVE POWER

The instantaneous power absorbed by the reactive part of the load, given by the component $p_X(t)$ in (2.2.10), is a double-frequency sinusoid with zero average value and with amplitude Q given by

$$Q = VI_X = VI\sin(\delta - \beta) \text{ var} \tag{2.2.12}$$

The term Q is given the name *reactive power.* Although it has the same units as real power, the usual practice is to define units of reactive power as volt-amperes reactive, or var.

EXAMPLE 2.1

Instantaneous, real, and reactive power and the power factor

The voltage $v(t) = 141.4\cos(\omega t)$ is applied to a load consisting of a 10-Ω resistor in parallel with an inductive reactance $X_L = \omega L = 3.77\ \Omega$. Calculate the instantaneous power absorbed by the resistor and by the inductor. Also calculate the real and reactive power absorbed by the load, and the power factor.

SOLUTION

The circuit and phasor diagram are shown in Figure 2.3(a). The load voltage is

$$V = \frac{141.4}{\sqrt{2}}\underline{/0^\circ} = 100\ \underline{/0^\circ} \text{ volts}$$

The resistor current is

$$I_R = \frac{V}{R} = \frac{100}{10}\underline{/0^\circ} = 10\underline{/0^\circ}\ \text{A}$$

The inductor current is

$$I_L = \frac{V}{jX_L} = \frac{100}{(j3.77)}\underline{/0^\circ} = 26.53\underline{/-90^\circ}\ \text{A}$$

The total load current is

$$I = I_R + I_L = 10 - j26.53 = 28.35\underline{/-69.34^\circ}\ \text{A}$$

The instantaneous power absorbed by the resistor is, from (2.2.3),

$$\begin{aligned} p_R(t) &= (100)\,(10)[1 + \cos(2\omega t)] \\ &= 1000\,[1 + \cos(2\omega t)] \quad \text{W} \end{aligned}$$

(Continued)

Copyright 2017 Cengage Learning. All Rights Reserved. May not be copied, scanned, or duplicated, in whole or in part. Due to electronic rights, some third party content may be suppressed from the eBook and/or eChapter(s). Editorial review has deemed that any suppressed content does not materially affect the overall learning experience. Cengage Learning reserves the right to remove additional content at any time if subsequent rights restrictions require it.

FIGURE 2.3

Circuit and phasor diagram for Example 2.1

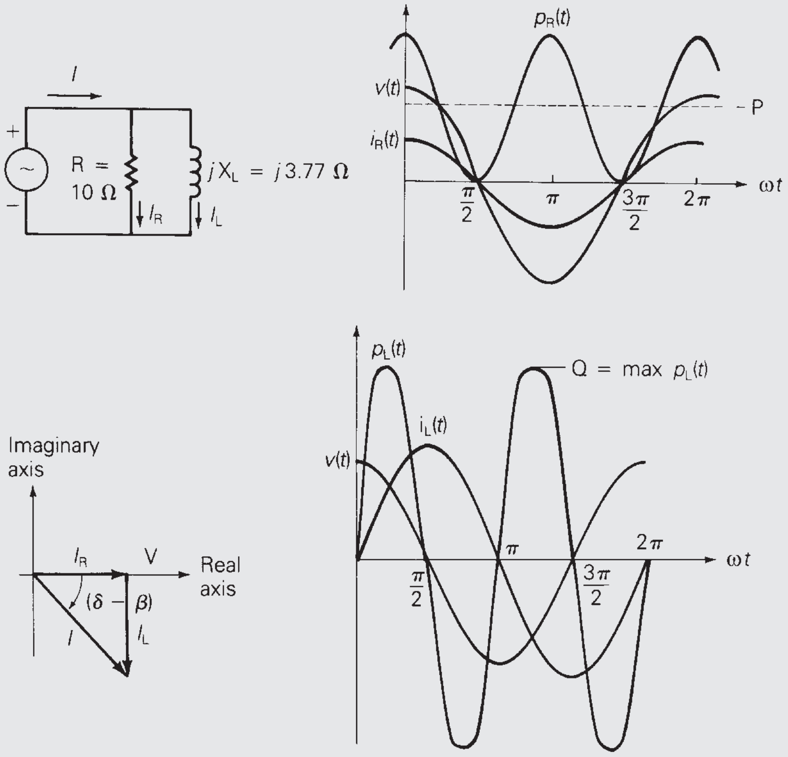
I
+
−
~
R =
10 Ω
I_R
$jX_L = j3.77\ \Omega$
I_L
Imaginary axis
I_R
V
Real axis
$(\delta - \beta)$
I
I_L
$p_R(t)$
v(t)
$i_R(t)$
P
ωt
$\frac{\pi}{2}$
π
$\frac{3\pi}{2}$
2π
$p_L(t)$
Q = max $p_L(t)$
$i_L(t)$
v(t)
π
2π
ωt
$\frac{\pi}{2}$
$\frac{3\pi}{2}$

(a) Circuit and phasor diagram

(b) Waveforms

The instantaneous power absorbed by the inductor is, from (2.2.6),

$$
\begin{aligned}
p_L(t) &= (100)(26.53)\sin(2\omega t) \\
&= 2653\sin(\omega t) \quad \text{W}
\end{aligned}
$$

The real power absorbed by the load is, from (2.2.11),

$$
\begin{aligned}
\text{P} &= \text{VI}\cos(\delta - \beta) = (100)(28.53)\cos(0° + 69.34°) \\
&= 1000 \text{ W}
\end{aligned}
$$

(*Note*: P is also equal to $\text{VI}_R = \text{V}^2/\text{R}$.)
The reactive power absorbed by the load is, from (2.2.12),

$$
\begin{aligned}
\text{Q} &= \text{VI}\sin(\delta - \beta) = (100)(28.53)\sin(0° + 69.34°) \\
&= 2653 \text{ var}
\end{aligned}
$$

(*Note*: Q is also equal to $\text{VI}_L = \text{V}^2/\text{X}_L$.)

Copyright 2017 Cengage Learning. All Rights Reserved. May not be copied, scanned, or duplicated, in whole or in part. Due to electronic rights, some third party content may be suppressed from the eBook and/or eChapter(s). Editorial review has deemed that any suppressed content does not materially affect the overall learning experience. Cengage Learning reserves the right to remove additional content at any time if subsequent rights restrictions require it.

The power factor is

$$\text{p.f.} = \cos(\delta - \beta) = \cos(69.34°) = 0.3528 \text{ lagging}$$

Voltage, current, and power waveforms are shown in Figure 2.3(b).

As shown for this parallel RL load, the resistor absorbs real power (1000 W) and the inductor absorbs reactive power (2653 vars). The resistor current $i_R(t)$ is in phase with the load voltage, and the inductor current $i_L(t)$ lags the load voltage by 90°. The power factor is lagging for an RL load.

Note $p_R(t)$ and $p_x(t)$, given by (2.2.10), are strictly valid only for a parallel R-X load. For a general RLC load, the voltages across the resistive and reactive components may not be in phase with the source voltage $v(t)$, resulting in additional phase shifts in $p_R(t)$ and $p_x(t)$ (see Problem 2.13). However, (2.2.11) and (2.2.12) for P and Q are valid for a general RLC load.

PHYSICAL SIGNIFICANCE OF REAL AND REACTIVE POWER

The physical significance of real power P is easily understood. The total energy absorbed by a load during a time interval T, consisting of one cycle of the sinusoidal voltage, is PT watt-seconds (Ws). During a time interval of n cycles, the energy absorbed is P(nT) watt-seconds, all of which is absorbed by the resistive component of the load. A kilowatt-hour meter is designed to measure the energy absorbed by a load during a time interval $(t_2 - t_1)$, consisting of an integral number of cycles, by integrating the real power P over the time interval $(t_2 - t_1)$.

The physical significance of reactive power Q is not as easily understood. Q refers to the maximum value of the instantaneous power absorbed by the reactive component of the load. The instantaneous reactive power, given by the second *term* $p_x(t)$ in (2.2.10), is alternately positive and negative, and it expresses the reversible flow of energy to and from the reactive component of the load. Q may be positive or negative, depending on the sign of $(\delta - \beta)$ in (2.2.12). Reactive power Q is a useful quantity when describing the operation of power systems (this will become evident in later chapters). As one example, shunt capacitors can be used in transmission systems to deliver reactive power and thereby increase voltage magnitudes during heavy load periods (see Chapter 5).

2.3 COMPLEX POWER

For circuits operating in sinusoidal-steady-state, real and reactive power are conveniently calculated from complex power, defined below. Let the voltage across a circuit element be $V = \text{V}\underline{/\delta}$, and the current into the element be $I = \text{I}\underline{/\beta}$. Then the complex power S is the product of the voltage and the conjugate of the current:

$$\begin{aligned} S &= VI^* = [\text{V}\underline{/\delta}]\,[\text{I}\underline{/\beta}]^* = \text{VI}\underline{/\delta - \beta} \\ &= \text{VI}\cos(\delta - \beta) + j\text{VI}\sin(\delta - \beta) \end{aligned} \qquad (2.3.1)$$

Copyright 2017 Cengage Learning. All Rights Reserved. May not be copied, scanned, or duplicated, in whole or in part. Due to electronic rights, some third party content may be suppressed from the eBook and/or eChapter(s). Editorial review has deemed that any suppressed content does not materially affect the overall learning experience. Cengage Learning reserves the right to remove additional content at any time if subsequent rights restrictions require it.

where $(\delta - \beta)$ is the angle between the voltage and current. Comparing (2.3.1) with (2.2.11) and (2.2.12), S is recognized as

$$S = P + jQ \tag{2.3.2}$$

The magnitude S = VI of the complex power S is called the *apparent power*. Although it has the same units as P and Q, it is common practice to define the units of apparent power S as volt-amperes or VA. The real power P is obtained by multiplying the apparent power S = VI by the power factor p.f. $= \cos(\delta - \beta)$.

The procedure for determining whether a circuit element absorbs or delivers power is summarized in Figure 2.4. Figure 2.4(a) shows the *load convention*, where the current *enters* the positive terminal of the circuit element, and the complex power *absorbed* by the circuit element is calculated from (2.3.1). This equation shows that, depending on the value of $(\delta - \beta)$, P may have either a positive or negative value. If P is positive, then the circuit element absorbs positive real power.

However, if P is negative, the circuit element absorbs negative real power, or alternatively, it delivers positive real power. Similarly, if Q is positive, the circuit element in Figure 2.4(a) absorbs positive reactive power. However, if Q is negative, the circuit element absorbs negative reactive power, or it delivers positive reactive power.

Figure 2.4(b) shows the *generator convention*, where the current *leaves* the positive terminal of the circuit element, and the complex power *delivered* is calculated from (2.3.1). When P is positive (negative) the circuit element *delivers* positive (negative) real power. Similarly, when Q is positive (negative), the circuit element *delivers* positive (negative) reactive power.

FIGURE 2.4

Load and generator conventions

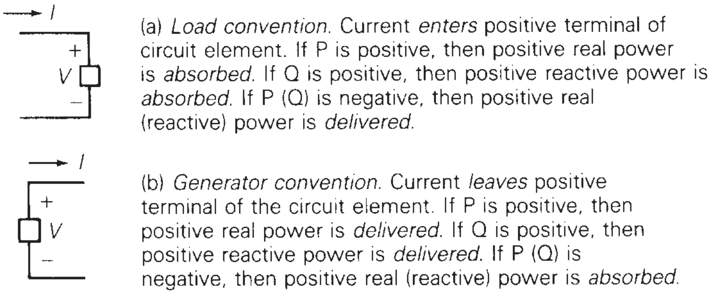

(a) *Load convention*. Current *enters* positive terminal of circuit element. If P is positive, then positive real power is *absorbed*. If Q is positive, then positive reactive power is *absorbed*. If P (Q) is negative, then positive real (reactive) power is *delivered*.

(b) *Generator convention*. Current *leaves* positive terminal of the circuit element. If P is positive, then positive real power is *delivered*. If Q is positive, then positive reactive power is *delivered*. If P (Q) is negative, then positive real (reactive) power is *absorbed*.

EXAMPLE 2.2

Real and reactive power, delivered or absorbed

A single-phase voltage source with $V = 100\underline{/130^\circ}$ volts delivers a current $I = 10\underline{/10^\circ}$ A, which leaves the positive terminal of the source. Calculate the source real and reactive power, and state whether the source delivers or absorbs each of these.

Copyright 2017 Cengage Learning. All Rights Reserved. May not be copied, scanned, or duplicated, in whole or in part. Due to electronic rights, some third party content may be suppressed from the eBook and/or eChapter(s). Editorial review has deemed that any suppressed content does not materially affect the overall learning experience. Cengage Learning reserves the right to remove additional content at any time if subsequent rights restrictions require it.

SOLUTION

Since I leaves the positive terminal of the source, the generator convention is assumed, and the complex power delivered is, from (2.3.1),

$$S = VI^* = [100\angle 130°]\,[10\angle 10°]^*$$

$$S = 1000\angle 120° = -500 + j866$$

$$\text{P} = \text{Re}[S] = -500 \quad \text{W}$$

$$\text{Q} = \text{Im}[S] = +866 \ \text{var}$$

where Im denotes "imaginary part of." The source absorbs 500 W and delivers 866 var. Readers familiar with electric machines will recognize that one example of this source is a synchronous motor. When a synchronous motor operates at a leading power factor, it absorbs real power and delivers reactive power.

The *load convention* is used for the RLC elements shown in Figure 2.2. Therefore, the complex power *absorbed* by any of these three elements can be calculated as follows. Assume a load voltage $V = V\angle\delta$. Then, from (2.3.1),

$$\text{resistor:} \quad S_{\text{R}} = VI_{\text{R}}^* = [\text{V}\angle\delta]\left[\frac{\text{V}}{\text{R}}\angle{-\delta}\right] = \frac{\text{V}^2}{\text{R}} \tag{2.3.3}$$

$$\text{indicator:} \quad S_{\text{L}} = VI_{\text{L}}^* = [\text{V}\angle\delta]\left[\frac{\text{V}}{-j\text{X}_{\text{L}}}\angle{-\delta}\right] = +j\frac{\text{V}^2}{\text{X}_{\text{L}}} \tag{2.3.4}$$

$$\text{capacitor:} \quad S_{\text{C}} = VI_{\text{C}}^* = [\text{V}\angle\delta]\left[\frac{\text{V}}{-j\text{X}_{\text{C}}}\angle{-\delta}\right] = -j\frac{\text{V}^2}{\text{X}_{\text{C}}} \tag{2.3.5}$$

From these complex power expressions, the following can be stated:

A (positive-valued) resistor absorbs (positive) real power, $\text{P}_{\text{R}} = \text{V}^2/\text{R}$ W, and zero reactive power, $\text{Q}_{\text{R}} = 0$ var.

An inductor absorbs zero real power, $\text{P}_{\text{L}} = 0$ W, and positive reactive power, $\text{Q}_{\text{L}} = \text{V}^2/\text{X}_{\text{L}}$ var.

A capacitor absorbs zero real power, $\text{P}_{\text{C}} = 0$ W, and *negative* reactive power, $\text{Q}_{\text{C}} = -\text{V}^2/\text{X}_{\text{C}}$ var. Alternatively, a capacitor *delivers positive* reactive power, $+\ \text{V}^2/\text{X}_{\text{C}}$.

For a general load composed of RLC elements, complex power S is also calculated from (2.3.1). The real power $\text{P} = \text{Re}(S)$ absorbed by a passive load is always positive. The reactive power $\text{Q} = \text{Im}(S)$ absorbed by a load may be either positive or negative. When the load is inductive, the current lags the voltage, which means β is less than δ in (2.3.1), and the reactive power absorbed is positive. When the load is

Copyright 2017 Cengage Learning. All Rights Reserved. May not be copied, scanned, or duplicated, in whole or in part. Due to electronic rights, some third party content may be suppressed from the eBook and/or eChapter(s). Editorial review has deemed that any suppressed content does not materially affect the overall learning experience. Cengage Learning reserves the right to remove additional content at any time if subsequent rights restrictions require it.

FIGURE 2.5

Power triangle

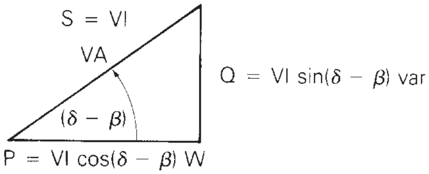

capacitive, the current leads the voltage, which means β is greater than δ, and the reactive power absorbed is negative; or, alternatively, the capacitive load delivers positive reactive power.

Complex power can be summarized graphically by use of the power triangle shown in Figure 2.5. As shown, the apparent power S, real power P, and reactive power Q form the three sides of the power triangle. The power factor angle $(\delta - \beta)$ is also shown, and the following expressions can be obtained:

$$S = \sqrt{P^2 + Q^2} \tag{2.3.6}$$

$$(\delta - \beta) = \tan^{-1}(Q/P) \tag{2.3.7}$$

$$Q = P\tan(\delta - \beta) \tag{2.3.8}$$

$$\text{p.f.} = \cos(\delta - \beta) = \frac{P}{S} = \frac{P}{\sqrt{P^2 + Q^2}} \tag{2.3.9}$$

EXAMPLE 2.3

Power triangle and power factor correction

A single-phase source delivers 100 kW to a load operating at a power factor of 0.8 lagging. Calculate the reactive power to be delivered by a capacitor connected in parallel with the load in order to raise the source power factor to 0.95 lagging. Also draw the power triangle for the source and load. Assume that the source voltage is constant, and neglect the line impedance between the source and load.

SOLUTION

The circuit and power triangle are shown in Figure 2.6. The real power $P = P_S = P_R$ delivered by the source and absorbed by the load is not changed when the capacitor is connected in parallel with the load, since the capacitor delivers only reactive power Q_C. For the load, the power factor angle, reactive power absorbed, and apparent power are

$$\theta_L = (\delta - \beta_L) = \cos^{-1}(0.8) = 36.87°$$

$$Q_L = P\tan\theta_L = 100\tan(36.87°) = 75 \quad \text{kvar}$$

$$S_L = \frac{P}{\cos\theta_L} = 125 \quad \text{kVA}$$

Copyright 2017 Cengage Learning. All Rights Reserved. May not be copied, scanned, or duplicated, in whole or in part. Due to electronic rights, some third party content may be suppressed from the eBook and/or eChapter(s). Editorial review has deemed that any suppressed content does not materially affect the overall learning experience. Cengage Learning reserves the right to remove additional content at any time if subsequent rights restrictions require it.

FIGURE 2.6

Circuit and power triangle for Example 2.3

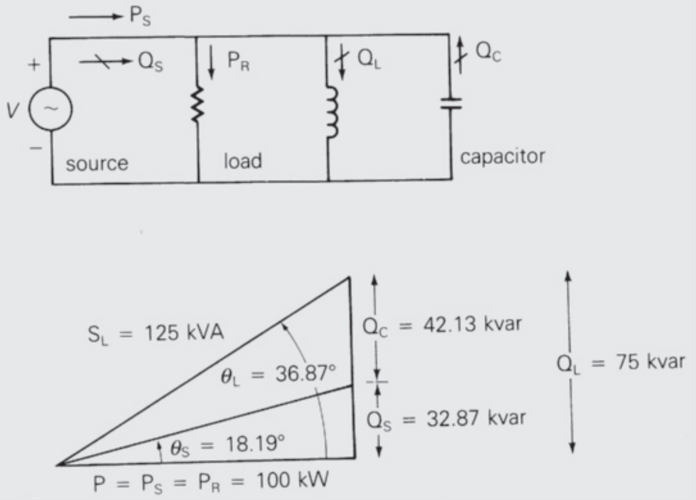

After the capacitor is connected, the power factor angle, reactive power delivered, and apparent power of the source are

$$\theta_S = (\delta - \beta_S) = \cos^{-1}(0.95) = 18.19°$$

$$Q_S = P \tan \theta_S = 100 \tan(18.19°) = 32.87 \quad \text{kvar}$$

$$S_S = \frac{P}{\cos \theta_S} = \frac{100}{0.95} = 105.6 \quad \text{kVA}$$

The capacitor delivers

$$Q_C = Q_L - Q_S = 75 - 32.87 = 42.13 \text{ kVA}$$

The method of connecting a capacitor in parallel with an inductive load is known as *power factor correction.* The effect of the capacitor is to increase the power factor of the source that delivers power to the load. Also, the source apparent power S_S decreases. As shown in Figure 2.6, the source apparent power for this example decreases from 125 kVA without the capacitor to 105.3 kVA with the capacitor. The source current $I_S = S_S/V$ also decreases. When line impedance between the source and load is included, the decrease in source current results in lower line losses and lower line-voltage drops. The end result of power factor correction is improved efficiency and improved voltage regulation.

To see an animated view of this example, open PowerWorld Simulator case Example 2_3 (see Figure 2.7). From the ribbon select the green-and-black Play button to begin the simulation. The speed and size of the green arrows are

(*Continued*)

Copyright 2017 Cengage Learning. All Rights Reserved. May not be copied, scanned, or duplicated, in whole or in part. Due to electronic rights, some third party content may be suppressed from the eBook and/or eChapter(s). Editorial review has deemed that any suppressed content does not materially affect the overall learning experience. Cengage Learning reserves the right to remove additional content at any time if subsequent rights restrictions require it.

FIGURE 2.7

Screen for Example 2.3

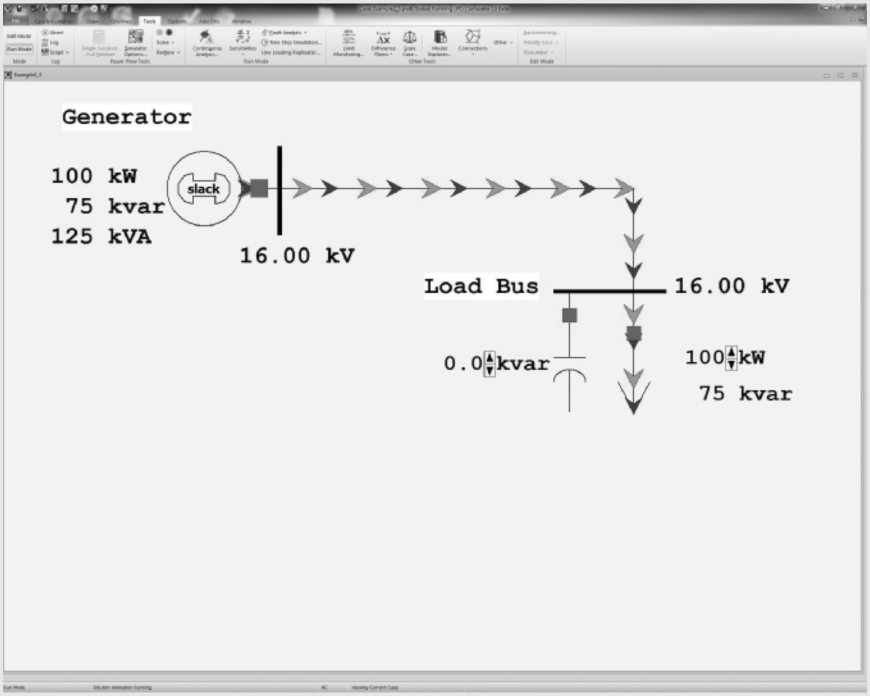

proportional to the real power supplied to the load bus, and the blue arrows are proportional to the reactive power. Here, reactive compensation can be supplied in discrete 20-kvar steps by clicking on the arrows in the capacitor's kvar field, and the load can be varied by clicking on the arrows in the load field. Notice that increasing the reactive compensation decreases both the reactive power flow on the supply line and the kVA power supplied by the generator; the real power flow is unchanged.

2.4 NETWORK EQUATIONS

For circuits operating in sinusoidal-steady-state, Kirchhoff's current law (KCL) and voltage law (KVL) apply to phasor currents and voltages. Thus the sum of all phasor currents entering any node is zero and the sum of the phasor voltage drops around any closed path is zero. Network analysis techniques based on Kirchhoff's laws, including nodal analysis, mesh or loop analysis, superposition, source transformations, and Thevenin's theorem or Norton's theorem, are useful for analyzing such circuits.

Copyright 2017 Cengage Learning. All Rights Reserved. May not be copied, scanned, or duplicated, in whole or in part. Due to electronic rights, some third party content may be suppressed from the eBook and/or eChapter(s). Editorial review has deemed that any suppressed content does not materially affect the overall learning experience. Cengage Learning reserves the right to remove additional content at any time if subsequent rights restrictions require it.

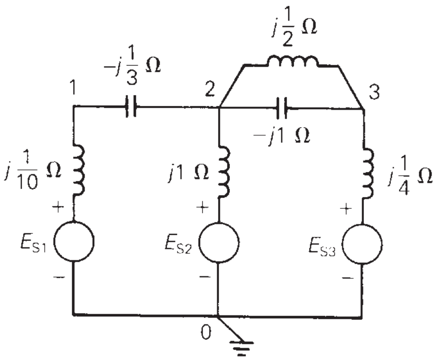

FIGURE 2.8 Circuit diagram for reviewing nodal analysis

Various computer solutions of power system problems are formulated from nodal equations, which can be systematically applied to circuits. The circuit shown in Figure 2.8, which is used here to review nodal analysis, is assumed to be operating in sinusoidal-steady-state; source voltages are represented by phasors E_{S1}, E_{S2}, and E_{S3}; circuit impedances are specified in ohms. Nodal equations are written in the following three steps:

STEP 1 For a circuit with $(N + 1)$ nodes (also called buses), select one bus as the reference bus and define the voltages at the remaining buses with respect to the reference bus.

The circuit in Figure 2.8 has four buses—that is, $N + 1 = 4$ or $N = 3$. Bus 0 is selected as the reference bus, and bus voltages V_{10}, V_{20}, and V_{30} are then defined with respect to bus 0.

STEP 2 Transform each voltage source in series with an impedance to an equivalent current source in parallel with that impedance. Also, show admittance values instead of impedance values on the circuit diagram. Each current source is equal to the voltage source divided by the source impedance.

In Figure 2.9, equivalent current sources I_1, I_2, and I_3 are shown, and all impedances are converted to corresponding admittances.

STEP 3 Write nodal equations in matrix format as follows:

$$\begin{bmatrix} Y_{11} & Y_{12} & Y_{13} & \cdots & Y_{1N} \\ Y_{21} & Y_{22} & Y_{23} & \cdots & Y_{2N} \\ Y_{31} & Y_{32} & Y_{33} & \cdots & Y_{3N} \\ \vdots & \vdots & \vdots & & \vdots \\ Y_{N1} & Y_{N2} & Y_{N3} & \cdots & Y_{NN} \end{bmatrix} \begin{bmatrix} V_{10} \\ V_{20} \\ V_{30} \\ \vdots \\ V_{N0} \end{bmatrix} = \begin{bmatrix} I_1 \\ I_2 \\ I_3 \\ \vdots \\ I_N \end{bmatrix} \tag{2.4.1}$$

Copyright 2017 Cengage Learning. All Rights Reserved. May not be copied, scanned, or duplicated, in whole or in part. Due to electronic rights, some third party content may be suppressed from the eBook and/or eChapter(s). Editorial review has deemed that any suppressed content does not materially affect the overall learning experience. Cengage Learning reserves the right to remove additional content at any time if subsequent rights restrictions require it.

FIGURE 2.9

Circuit of Figure 2.8 with equivalent current sources replacing voltage sources. Admittance values are also shown.

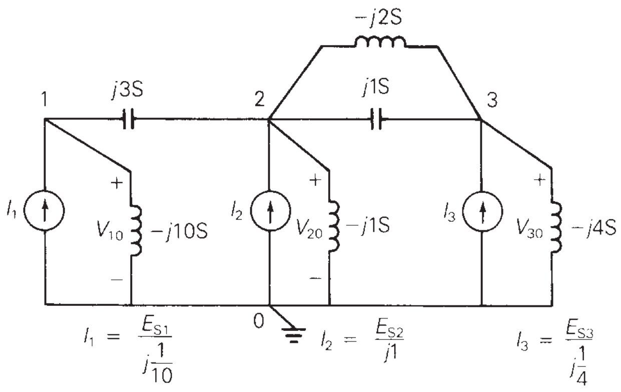
$-j2S$
1
$j3S$
2
$j1S$
3
I_1
$+$
V_{10}
$-j10S$
$-$
I_2
$+$
V_{20}
$-j1S$
$-$
I_3
$+$
V_{30}
$-j4S$
0
$I_1 = \frac{E_{S1}}{j\frac{1}{10}}$
$I_2 = \frac{E_{S2}}{j1}$
$I_3 = \frac{E_{S3}}{j\frac{1}{4}}$

Using matrix notation, (2.4.1) becomes

$$\boldsymbol{YV} = \boldsymbol{I} \tag{2.4.2}$$

where $\boldsymbol{Y}$ is the $N \times N$ bus admittance matrix, $\boldsymbol{V}$ is the column vector of N bus voltages, and $\boldsymbol{I}$ is the column vector of N current sources. The elements Y_{kn}, of the bus admittance matrix $\boldsymbol{Y}$ are formed as follows:

diagonal elements: Y_{kk} = sum of admittances connected to bus k $(k = 1, 2, \ldots, N)$ (2.4.3)

off-diagonal elements: $Y_{kn} = -$(sum of admittances connected between buses k and n) $(k \neq n)$ (2.4.4)

The diagonal element Y_{kk} is called the *self-admittance* or the *driving-point admittance* of bus k, and the off-diagonal element Y_{kn} for $k \neq n$ is called the *mutual admittance* or the *transfer admittance* between buses k and n. Since $Y_{kn} = Y_{kn}$, the matrix $\boldsymbol{Y}$ is symmetric.

For the circuit of Figure 2.9, (2.4.1) becomes

$$\left[\begin{array}{c|c|c} (j3-j10) & -(j3) & 0 \\ \hline -(j3) & (j3-j1+j1-j2) & -(j1-j2) \\ \hline 0 & -(j1-j2) & (j1-j2-j4) \end{array}\right] \begin{bmatrix} V_{10} \\ V_{20} \\ V_{30} \end{bmatrix} = \begin{bmatrix} I_1 \\ I_2 \\ I_3 \end{bmatrix}$$

$$j \begin{bmatrix} -7 & -3 & 0 \\ -3 & 1 & 1 \\ 0 & 1 & -5 \end{bmatrix} \begin{bmatrix} V_{10} \\ V_{20} \\ V_{30} \end{bmatrix} = \begin{bmatrix} I_1 \\ I_2 \\ I_3 \end{bmatrix} \tag{2.4.5}$$

Copyright 2017 Cengage Learning. All Rights Reserved. May not be copied, scanned, or duplicated, in whole or in part. Due to electronic rights, some third party content may be suppressed from the eBook and/or eChapter(s). Editorial review has deemed that any suppressed content does not materially affect the overall learning experience. Cengage Learning reserves the right to remove additional content at any time if subsequent rights restrictions require it.

The advantage of this method of writing nodal equations is that a digital computer can be used both to generate the admittance matrix $\boldsymbol{Y}$ and to solve (2.4.2) for the unknown bus voltage vector $\boldsymbol{V}$. Once a circuit is specified with the reference bus and other buses identified, the circuit admittances and their bus connections become computer input data for calculating the elements Y_{kn} via (2.4.3) and (2.4.4). After $\boldsymbol{Y}$ is calculated and the current source vector $\boldsymbol{I}$ is given as input, standard computer programs for solving simultaneous linear equations can then be used to determine the bus voltage vector $\boldsymbol{V}$.

When double subscripts are used to denote a voltage in this text, the voltage shall be that at the node identified by the first subscript with respect to the node identified by the second subscript. For example, the voltage V_{10} in Figure 2.9 is the voltage at node 1 with respect to node 0. Also, a current I_{ab} shall indicate the current from node a to node b. Voltage polarity marks (+/−) and current reference arrows (→) are not required when double subscript notation is employed. The polarity marks in Figure 2.9 for V_{10}, V_{20}, and V_{30}, although not required, are shown for clarity. The reference arrows for sources I_1, I_2, and I_3 in Figure 2.9 are required, however, since single subscripts are used for these currents. Matrices and vectors shall be indicated in this text by boldface type (for example, $\boldsymbol{Y}$ or $\boldsymbol{V}$).

2.5 BALANCED THREE-PHASE CIRCUITS

In this section, we introduce the following topics for balanced three-phase circuits: Y connections, line-to-neutral voltages, line-to-line voltages, line currents, Δ loads, Δ−Y conversions, and equivalent line-to-neutral diagrams.

BALANCED Y CONNECTIONS

Figure 2.10 shows a three-phase, Y-connected (or "wye-connected") voltage source feeding a balanced-Y-connected load. For a Y connection, the neutrals of each phase are connected. In Figure 2.10 the source neutral connection is labeled bus n and the load neutral connection is labeled bus N. The three-phase source is assumed to be ideal since source impedances are neglected. Also neglected are the

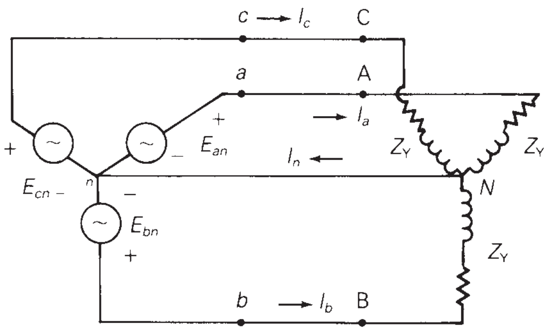

FIGURE 2.10

Circuit diagram of a three-phase Y-connected source feeding a balanced-Y load

Copyright 2017 Cengage Learning. All Rights Reserved. May not be copied, scanned, or duplicated, in whole or in part. Due to electronic rights, some third party content may be suppressed from the eBook and/or eChapter(s). Editorial review has deemed that any suppressed content does not materially affect the overall learning experience. Cengage Learning reserves the right to remove additional content at any time if subsequent rights restrictions require it.

line impedances between the source and load terminals, and the neutral impedance between buses n and N. The three-phase load is *balanced*, which means the load impedances in all three phases are identical.

BALANCED LINE-TO-NEUTRAL VOLTAGES

In Figure 2.10, the terminal buses of the three-phase source are labeled a, b, and c, and the source line-to-neutral voltages are labeled E_{an}, E_{bn}, and E_{cn}. The source is *balanced* when these voltages have equal magnitudes and an equal 120°-phase difference between any two phases. An example of balanced three-phase line-to-neutral voltages is

$$\begin{aligned} E_{an} &= 10\underline{/0^\circ} \\ E_{bn} &= 10\underline{/-120^\circ} = 10\underline{/+240^\circ} \\ E_{cn} &= 10\underline{/+120^\circ} = 10\underline{/-240^\circ} \text{ volts} \end{aligned} \tag{2.5.1}$$

where the line-to-neutral voltage magnitude is 10 volts and E_{an} is the reference phasor. The phase sequence is called *positive sequence* or *abc* sequence when E_{an} leads E_{bn} by 120° and E_{bn} leads E_{cn} by 120°. The phase sequence is called *negative sequence* or *acb* sequence when E_{an} leads E_{cn} by 120° and E_{cn} leads E_{bn} by 120°. The voltages in (2.5.1) are positive-sequence voltages, since E_{an} leads E_{bn} by 120°. The corresponding phasor diagram is shown in Figure 2.11.

BALANCED LINE-TO-LINE VOLTAGES

The voltages E_{ab}, E_{bc}, and E_{ca} between phases are called line-to-line voltages. Writing a KVL equation for a closed path around buses a, b, and n in Figure 2.10.

$$E_{ab} = E_{an} - E_{bn} \tag{2.5.2}$$

For the line-to-neutral voltages of (2.5.1),

$$\begin{aligned} E_{ab} &= 10\underline{/0^\circ} - 10\underline{/-120^\circ} = 10 - 10\left[\frac{-1 - j\sqrt{3}}{2}\right] \\ E_{ab} &= \sqrt{3}(10)\left(\frac{\sqrt{3} + j1}{2}\right) = \sqrt{3}(10\underline{/30^\circ}) \quad \text{volts} \end{aligned} \tag{2.5.3}$$

FIGURE 2.11

Phasor diagram of balanced positive-sequence line-to-neutral voltages with E_{an} as the reference

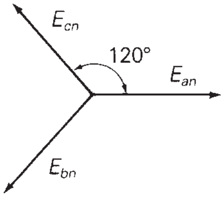

Similarly, the line-to-line voltages E_{bc} and E_{ca} are

$$\begin{aligned} E_{bc} &= E_{bn} - E_{cn} = 10\underline{/-120^\circ} - 10\underline{/+120^\circ} \\ &= \sqrt{3}(10\underline{/-90^\circ}) \quad \text{volts} \end{aligned} \tag{2.5.4}$$

$$\begin{aligned} E_{ca} &= E_{cn} - E_{an} = 10\underline{/+120^\circ} - 10\underline{/0^\circ} \\ &= \sqrt{3}(10\underline{/150^\circ}) \text{ volts} \end{aligned} \tag{2.5.5}$$

The line-to-line voltages of (2.5.3) through (2.5.5) are also balanced, since they have equal magnitudes of $\sqrt{3}$ (10) volts and 120° displacement between any two

Copyright 2017 Cengage Learning. All Rights Reserved. May not be copied, scanned, or duplicated, in whole or in part. Due to electronic rights, some third party content may be suppressed from the eBook and/or eChapter(s). Editorial review has deemed that any suppressed content does not materially affect the overall learning experience. Cengage Learning reserves the right to remove additional content at any time if subsequent rights restrictions require it.

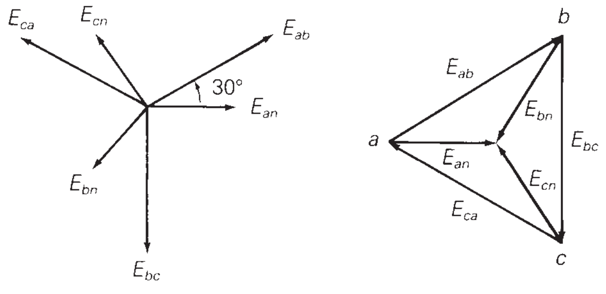

(a) Phasor diagram (b) Voltage triangle

FIGURE 2.12

Positive-sequence line-to-neutral and line-to-line voltages in a balanced three-phase, Y-connected system

phases. Comparison of these line-to-line voltages with the line-to-neutral voltages of (2.5.1) leads to the following conclusion:

> In a balanced three-phase Y-connected system with positive-sequence sources, the line-to-line voltages are $\sqrt{3}$ times the line-to-neutral voltages and lead by 30°. That is,

$$\begin{aligned} E_{ab} &= \sqrt{3}E_{an}\underline{/+30^\circ} \\ E_{bc} &= \sqrt{3}E_{bn}\underline{/+30^\circ} \\ E_{ca} &= \sqrt{3}E_{cn}\underline{/+30^\circ} \end{aligned} \tag{2.5.6}$$

This very important result is summarized in Figure 2.12. In Figure 2.12(a) each phasor begins at the origin of the phasor diagram. In Figure 2.12(b) the line-to-line voltages form an equilateral triangle with vertices labeled *a*, *b*, *c* corresponding to buses *a*, *b*, and *c* of the system; the line-to-neutral voltages begin at the vertices and end at the center of the triangle, which is labeled *n* for neutral bus *n*. Also, the clockwise sequence of the vertices *abc* in Figure 2.12(b) indicates positive-sequence voltages. In both diagrams, E_{an} is the reference. However, the diagrams could be rotated to align with any other reference.

Since the balanced line-to-line voltages form a closed triangle in Figure 2.12, their sum is zero. In fact, the sum of line-to-line voltages $(E_{ab} + E_{bc} + E_{ca})$ is *always* zero, even if the system is unbalanced, since these voltages form a closed path around buses *a*, *b*, and *c*. Also, in a balanced system, the sum of the line-to-neutral voltages $(E_{an} + E_{bn} + E_{cn})$ equals zero.

BALANCED LINE CURRENTS

Since the impedance between the source and load neutrals in Figure 2.10 is neglected, buses *n* and *N* are at the same potential, $E_{nN} = 0$. Accordingly, a separate KVL equation can be written for each phase, and the line currents can be written by inspection:

$$\begin{aligned} I_a &= E_{an}/Z_Y \\ I_b &= E_{bn}/Z_Y \\ I_c &= E_{cn}/Z_Y \end{aligned} \tag{2.5.7}$$

Copyright 2017 Cengage Learning. All Rights Reserved. May not be copied, scanned, or duplicated, in whole or in part. Due to electronic rights, some third party content may be suppressed from the eBook and/or eChapter(s). Editorial review has deemed that any suppressed content does not materially affect the overall learning experience. Cengage Learning reserves the right to remove additional content at any time if subsequent rights restrictions require it.

For example, if each phase of the Y-connected load has an impedance $Z_Y = 2\underline{/30^\circ}\ \Omega$, then

$$\begin{aligned} I_a &= \frac{10\underline{/0^\circ}}{2\underline{/30^\circ}} = 5\underline{/-30^\circ}\ \text{A} \\ I_b &= \frac{10\underline{/-120^\circ}}{2\underline{/30^\circ}} = 5\underline{/-150^\circ}\ \text{A} \\ I_c &= \frac{10\underline{/+120^\circ}}{2\underline{/30^\circ}} = 5\underline{/90^\circ}\ \text{A} \end{aligned} \tag{2.5.8}$$

FIGURE 2.13

Phasor diagram of line currents in a balanced three-phase system

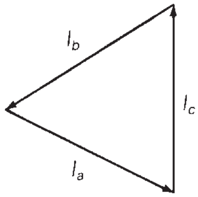

The line currents are also balanced, since they have equal magnitudes of 5 A and 120° displacement between any two phases. The neutral current I_n is determined by writing a KCL equation at bus N in Figure 2.10.

$$I_n = I_a + I_b + I_c \tag{2.5.9}$$

Using the line currents of (2.5.8),

$$\begin{aligned} I_n &= 5\underline{/-30^\circ} + 5\underline{/-150^\circ} + 5\underline{/90^\circ} \\ I_n &= 5\left(\frac{\sqrt{3} - j1}{2}\right) + 5\left(\frac{-\sqrt{3} - j1}{2}\right) + j5 = 0 \end{aligned} \tag{2.5.10}$$

The phasor diagram of the line currents is shown in Figure 2.13. Since these line currents form a closed triangle, their sum, which is the neutral current I_n, is zero. In general, the sum of any balanced three-phase set of phasors is zero, since balanced phasors form a closed triangle. Thus, although the impedance between neutrals n and N in Figure 2.10 is assumed to be zero, the neutral current will be zero for *any* neutral impedance ranging from short circuit (0 Ω) to open circuit (∞ Ω), as long as the system is balanced. If the system is not balanced—which could occur if the source voltages, load impedances, or line impedances were unbalanced—then the line currents will not be balanced, and a neutral current I_n may flow between buses n and N.

BALANCED-Δ LOADS

Figure 2.14 shows a three-phase Y-connected source feeding a balanced-Δ-connected (or "delta-connected") load. For a balanced-Δ connection, equal load impedances Z_Δ are connected in a triangle whose vertices form the buses, labeled A, B, and C in Figure 2.14. The Δ connection does not have a neutral bus.

Since the line impedances are neglected in Figure 2.14, the source line-to-line voltages are equal to the load line-to-line voltages, and the Δ-load currents I_{AB}, I_{BC} and I_{CA} are

$$\begin{aligned} I_{AB} &= E_{ab}/Z_\Delta \\ I_{BC} &= E_{bc}/Z_\Delta \\ I_{CA} &= E_{ca}/Z_\Delta \end{aligned} \tag{2.5.11}$$

Copyright 2017 Cengage Learning. All Rights Reserved. May not be copied, scanned, or duplicated, in whole or in part. Due to electronic rights, some third party content may be suppressed from the eBook and/or eChapter(s). Editorial review has deemed that any suppressed content does not materially affect the overall learning experience. Cengage Learning reserves the right to remove additional content at any time if subsequent rights restrictions require it.

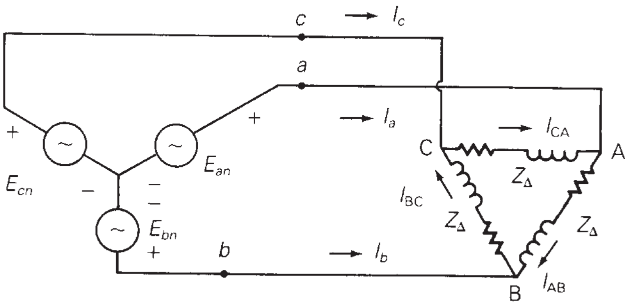

FIGURE 2.14

Circuit diagram of a Y-connected source feeding a balanced-Δ load

For example, if the line-to-line voltages are given by (2.5.3) through (2.5.5) and if $Z_\Delta = 5\angle 30^\circ\ \Omega$, then the Δ-load currents are

$$\begin{aligned} I_{AB} &= \sqrt{3}\left(\frac{10\angle -30^\circ}{5\angle 30^\circ}\right) = 3.464\angle 0^\circ \ \text{A} \\ I_{BC} &= \sqrt{3}\left(\frac{10\angle -90^\circ}{5\angle 30^\circ}\right) = 3.464\angle -120^\circ \ \text{A} \\ I_{CA} &= \sqrt{3}\left(\frac{10\angle 150^\circ}{5\angle 30^\circ}\right) = 3.464\angle +120^\circ \ \text{A} \end{aligned} \tag{2.5.12}$$

Also, the line currents can be determined by writing a KCL equation at each bus of the Δ load, as follows:

$$\begin{aligned} I_a &= I_{AB} - I_{CA} = 3.464\angle 0^\circ - 3.464\angle 120^\circ = \sqrt{3}(3.464\angle -30^\circ) \\ I_b &= I_{BC} - I_{AB} = 3.464\angle -120^\circ - 3.464\angle 0^\circ = \sqrt{3}(3.464\angle -150^\circ) \\ I_c &= I_{CA} - I_{BC} = 3.464\angle 120^\circ - 3.464\angle -120^\circ = \sqrt{3}(3.464\angle +90^\circ) \end{aligned} \tag{2.5.13}$$

Both the Δ-load currents given by (2.5.12) and the line currents given by (2.5.13) are balanced. Thus the sum of balanced Δ-load currents ($I_{AB} + I_{BC} + I_{CA}$) equals zero. The sum of line currents ($I_a + I_b + I_c$) is always zero for a Δ-connected load, even if the system is unbalanced, since there is no neutral wire. Comparison of (2.5.12) and (2.5.13) leads to the following conclusion:

For a balanced-Δ load supplied by a balanced positive-sequence source, the line currents into the load are $\sqrt{3}$ times the Δ-load currents and lag by 30°. That is,

$$\begin{aligned} I_a &= \sqrt{3} I_{AB}\angle -30^\circ \\ I_b &= \sqrt{3} I_{BC}\angle -30^\circ \\ I_c &= \sqrt{3} I_{CA}\angle -30^\circ \end{aligned} \tag{2.5.14}$$

This result is summarized in Figure 2.15.

Copyright 2017 Cengage Learning. All Rights Reserved. May not be copied, scanned, or duplicated, in whole or in part. Due to electronic rights, some third party content may be suppressed from the eBook and/or eChapter(s). Editorial review has deemed that any suppressed content does not materially affect the overall learning experience. Cengage Learning reserves the right to remove additional content at any time if subsequent rights restrictions require it.

FIGURE 2.15

Phasor diagram of line currents and load currents for a balanced-Δ load

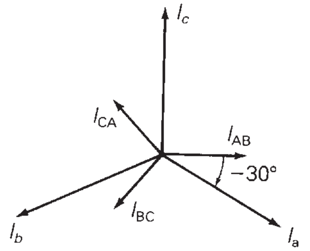

Δ–Y CONVERSION FOR BALANCED LOADS

Figure 2.16 shows the conversion of a balanced-Δ load to a balanced-Y load. If balanced voltages are applied, then these loads will be equivalent as viewed from their terminal buses A, B, and C when the line currents into the Δ load are the same as the line currents into the Y load. For the Δ load,

$$I_A = \sqrt{3}I_{AB}\underline{/-30°} = \frac{\sqrt{3}E_{AB}\underline{/-30°}}{Z_\Delta} \tag{2.5.15}$$

and for the Y load,

$$I_A = \frac{E_{AN}}{Z_Y} = \frac{E_{AB}\underline{/-30°}}{\sqrt{3}Z_Y} \tag{2.5.16}$$

Comparison of (2.5.15) and (2.5.16) indicates that I_A will be the same for both the Δ and Y loads when

$$Z_Y = \frac{Z_\Delta}{3} \tag{2.5.17}$$

Also, the other line currents I_B and I_C into the Y load will equal those into the Δ load when $Z_Y = Z_\Delta/3$, since these loads are balanced. Thus a balanced-Δ load can

FIGURE 2.16

Δ-Y conversion for balanced loads

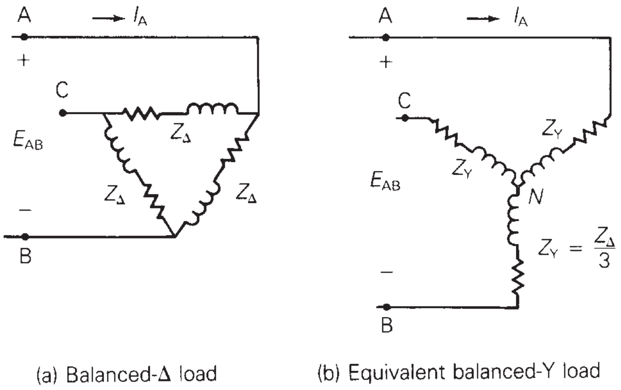

(a) Balanced-Δ load (b) Equivalent balanced-Y load

Copyright 2017 Cengage Learning. All Rights Reserved. May not be copied, scanned, or duplicated, in whole or in part. Due to electronic rights, some third party content may be suppressed from the eBook and/or eChapter(s). Editorial review has deemed that any suppressed content does not materially affect the overall learning experience. Cengage Learning reserves the right to remove additional content at any time if subsequent rights restrictions require it.

be converted to an equivalent balanced-Y load by dividing the Δ-load impedance by 3. The angles of these Δ- and equivalent Y-load impedances are the same. Similarly, a balanced-Y load can be converted to an equivalent balanced-Δ load using $Z_\Delta = 3Z_Y$.

EXAMPLE 2.4

Balanced-Δ and-Y loads

A balanced, positive-sequence, Y-connected voltage source with $E_{ab} = 480\angle 0^\circ$ volts is applied to a balanced-Δ load with $Z_\Delta = 30\angle 40^\circ\ \Omega$. The line impedance between the source and load is $Z_L = 1\angle 85^\circ\ \Omega$ for each phase. Calculate the line currents, the Δ-load currents, and the voltages at the load terminals.

SOLUTION

The solution is most easily obtained as follows. First, convert the Δ load to an equivalent Y. Then connect the source and Y-load neutrals with a zero-ohm neutral wire. The connection of the neutral wire has no effect on the circuit, since the neutral current $I_n = 0$ in a balanced system. The resulting circuit is shown in Figure 2.17. The line currents are

$$\begin{aligned}
I_A &= \frac{E_{an}}{Z_L + Z_Y} = \frac{\frac{480}{\sqrt{3}}\angle -30^\circ}{1\angle 85^\circ + \frac{30}{3}\angle 40^\circ} \\
&= \frac{277.1\angle -30^\circ}{(0.0872 + j0.9962) + (7.660 + j6.428)} \\
&= \frac{277.1\angle -30^\circ}{(7.748 + j7.424)} = \frac{277.1\angle -30^\circ}{10.73\angle 43.78^\circ} = 25.83\angle -73.78^\circ \text{ A} \\
I_B &= 25.83\angle 166.22^\circ \text{ A} \\
I_C &= 25.83\angle 46.22^\circ \text{ A}
\end{aligned} \tag{2.5.18}$$

The Δ-load currents are, from (2.5.14),

$$\begin{aligned}
I_{AB} &= \frac{I_a}{\sqrt{3}}\angle +30^\circ = \frac{25.83}{\sqrt{3}}\angle -73.78^\circ + 30^\circ = 14.91\angle -43.78^\circ \text{ A} \\
I_{BC} &= 14.91\angle -163.78^\circ \text{ A} \\
I_{CA} &= 14.91\angle +76.22^\circ \text{ A}
\end{aligned} \tag{2.5.19}$$

Copyright 2017 Cengage Learning. All Rights Reserved. May not be copied, scanned, or duplicated, in whole or in part. Due to electronic rights, some third party content may be suppressed from the eBook and/or eChapter(s). Editorial review has deemed that any suppressed content does not materially affect the overall learning experience. Cengage Learning reserves the right to remove additional content at any time if subsequent rights restrictions require it.

FIGURE 2.17

Circuit diagram for Example 2.4

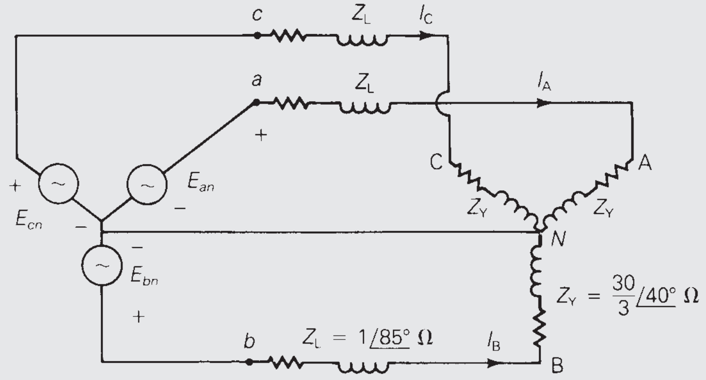
c
Z_L
I_C
a
Z_L
I_A
+
C
A
E_{an}
−
+
E_{cn}
−
Z_Y
Z_Y
N
−
E_{bn}
$Z_Y = \frac{30}{3}\underline{/40^\circ}\ \Omega$
+
b
$Z_L = 1\underline{/85^\circ}\ \Omega$
I_B
B

The voltages at the load terminals are

$$
\begin{aligned}
E_{AB} &= Z_\Delta I_{AB} = (30\underline{/40^\circ})(14.91\underline{/-43.78^\circ}) = 447.3\underline{/-3.78^\circ} \\
E_{BC} &= 447.3\underline{/-123.78^\circ} \qquad (2.5.20) \\
E_{CA} &= 447.3\underline{/116.22^\circ} \quad \text{volts}
\end{aligned}
$$

EQUIVALENT LINE-TO-NEUTRAL DIAGRAMS

When working with balanced three-phase circuits, only one phase need be analyzed. Δ loads can be converted to Y loads, and all source and load neutrals can be connected with a zero-ohm neutral wire without changing the solution. Then one phase of the circuit can be solved. The voltages and currents in the other two phases are equal in magnitude to and ±120° out of phase with those of the solved phase. Figure 2.18 shows an equivalent line-to-neutral diagram for one phase of the circuit in Example 2.4.

When discussing three-phase systems in this text, voltages shall be rms line-to-line voltages unless otherwise indicated. This is standard industry practice.

FIGURE 2.18

Equivalent line-to-neutral diagram for the circuit of Example 2.4

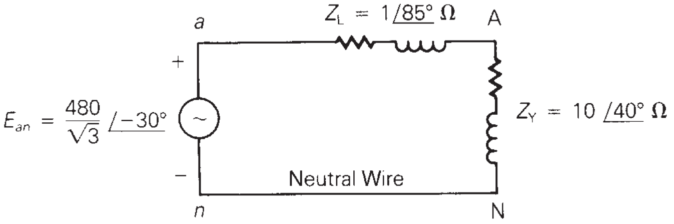
a
$Z_L = 1\underline{/85^\circ}\ \Omega$
A
+
$E_{an} = \frac{480}{\sqrt{3}}\underline{/-30^\circ}$
$Z_Y = 10\ \underline{/40^\circ}\ \Omega$
−
Neutral Wire
n
N

Copyright 2017 Cengage Learning. All Rights Reserved. May not be copied, scanned, or duplicated, in whole or in part. Due to electronic rights, some third party content may be suppressed from the eBook and/or eChapter(s). Editorial review has deemed that any suppressed content does not materially affect the overall learning experience. Cengage Learning reserves the right to remove additional content at any time if subsequent rights restrictions require it.

2.6 POWER IN BALANCED THREE-PHASE CIRCUITS

In this section, we discuss instantaneous power and complex power for balanced three-phase generators and motors and for balanced-Y and Δ-impedance loads.

INSTANTANEOUS POWER: BALANCED THREE-PHASE GENERATORS

Figure 2.19 shows a Y-connected generator represented by three voltage sources with their neutrals connected at bus n and by three identical generator impedances Z_g. Assume that the generator is operating under balanced steady-state conditions with the instantaneous generator terminal voltage given by

$$v_{an}(t) = \sqrt{2}\mathrm{V}_{\mathrm{LN}}\cos(\omega t + \delta) \quad \text{volts} \tag{2.6.1}$$

and with the instantaneous current leaving the positive terminal of phase a given by

$$i_a(t) = \sqrt{2}\mathrm{I}_{\mathrm{L}}\cos(\omega t + \beta) \ \ \mathrm{A} \tag{2.6.2}$$

where V_{LN} is the rms line-to-neutral voltage and I_{L} is the rms line current. The instantaneous power $p_a(t)$ delivered by phase a of the generator is

$$\begin{aligned} p_a(t) &= v_{an}(t)i_a(t) \\ &= 2\mathrm{V}_{\mathrm{LN}}\mathrm{I}_{\mathrm{L}}\cos(\omega t + \delta)\cos(\omega t + \beta) \\ &= \mathrm{V}_{\mathrm{LN}}\mathrm{I}_{\mathrm{L}}\cos(\delta - \beta) + \mathrm{V}_{\mathrm{LN}}\mathrm{I}_{\mathrm{L}}\cos(2\omega t + \delta + \beta) \quad \mathrm{W} \end{aligned} \tag{2.6.3}$$

Assuming balanced operating conditions, the voltages and currents of phases b and c have the same magnitudes as those of phase a and are $+120°$ out of phase with phase a. Therefore the instantaneous power delivered by phase b is

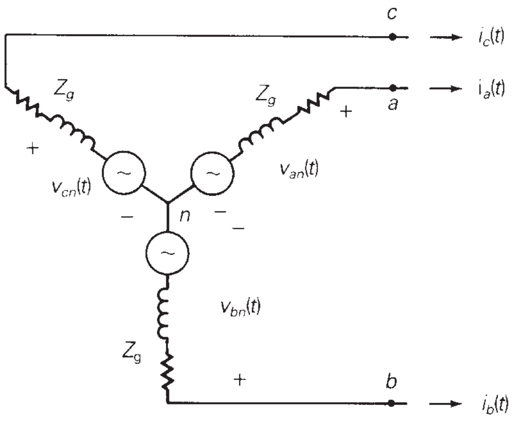

FIGURE 2.19

Y-connected generator

Copyright 2017 Cengage Learning. All Rights Reserved. May not be copied, scanned, or duplicated, in whole or in part. Due to electronic rights, some third party content may be suppressed from the eBook and/or eChapter(s). Editorial review has deemed that any suppressed content does not materially affect the overall learning experience. Cengage Learning reserves the right to remove additional content at any time if subsequent rights restrictions require it.

$$\begin{aligned} p_b(t) &= 2\mathrm{V_{LN}I_L}\cos(\omega t + \delta - 120°)\cos(\omega t + \beta - 120°) \\ &= \mathrm{V_{LN}I_L}\cos(\delta - \beta) + \mathrm{V_{LN}I_L}\cos(2\omega t + \delta + \beta - 240°) \quad \mathrm{W} \end{aligned} \tag{2.6.4}$$

and by phase c,

$$\begin{aligned} p_c(t) &= 2\mathrm{V_{LN}I_L}\cos(\omega t + \delta + 120°)\cos(\omega t + \beta + 120°) \\ &= \mathrm{V_{LN}I_L}\cos(\delta - \beta) + \mathrm{V_{LN}I_L}\cos(2\omega t + \delta + \beta + 240°) \quad \mathrm{W} \end{aligned} \tag{2.6.5}$$

The total instantaneous power $p_{3\phi}(t)$ delivered by the three-phase generator is the sum of the instantaneous powers delivered by each phase. Using (2.6.3) through (2.6.5):

$$\begin{aligned} p_{3\phi}(t) &= p_a(t) + p_b(t) + p_c(t) \\ &= 3\mathrm{V_{LN}I_L}\cos(\delta - \beta) + \mathrm{V_{LN}I_L}[\cos(2\omega t + \delta + \beta) \\ &\quad + \cos(2\omega t + \delta + \beta - 240°) \\ &\quad + \cos(2\omega t + \delta + \beta + 240°)] \;\; \mathrm{W} \end{aligned} \tag{2.6.6}$$

The three cosine terms within the brackets of (2.6.6) can be represented by a *balanced* set of three phasors. Therefore, the sum of these three terms is zero for any value of δ, for any value of β, and for all values of t. Equation (2.6.6) then reduces to

$$p_{3\phi}(t) = \mathrm{P}_{3\phi} = 3\mathrm{V_{LN}I_L}\cos(\delta - \beta) \quad \mathrm{W} \tag{2.6.7}$$

Equation (2.6.7) can be written in terms of the line-to-line voltage $\mathrm{V_{LL}}$ instead of the line-to-neutral voltage $\mathrm{V_{LN}}$. Under balanced operating conditions.

$$\mathrm{V_{LN}} = \mathrm{V_{LL}}/\sqrt{3} \quad \text{and} \quad \mathrm{P}_{3\phi} = \sqrt{3}\mathrm{V_{LL}I_L}\cos(\delta - \beta) \quad \mathrm{W} \tag{2.6.8}$$

Inspection of (2.6.8) leads to the following conclusion:

> The total instantaneous power delivered by a three-phase generator under balanced operating conditions is not a function of time, but a *constant*, $p_{3\phi}(t) = \mathrm{P}_{3\phi}$.

INSTANTANEOUS POWER: BALANCED THREE-PHASE MOTORS AND IMPEDANCE LOADS

The total instantaneous power absorbed by a three-phase motor under balanced steady-state conditions is also a constant. Figure 2.19 can be used to represent a three-phase motor by reversing the line currents to enter rather than leave the positive terminals. Then (2.6.1) through (2.6.8), valid for power *delivered* by a generator, are also valid for power *absorbed* by a motor. These equations are also valid for the instantaneous power absorbed by a balanced three-phase impedance load.

COMPLEX POWER: BALANCED THREE-PHASE GENERATORS

The phasor representations of the voltage and current in (2.6.1) and (2.6.2) are

$$V_{an} = \mathrm{V_{LN}}\underline{/\delta} \quad \text{volts} \tag{2.6.9}$$

$$I_a = \mathrm{I_L}\underline{/\beta} \quad \mathrm{A} \tag{2.6.10}$$

Copyright 2017 Cengage Learning. All Rights Reserved. May not be copied, scanned, or duplicated, in whole or in part. Due to electronic rights, some third party content may be suppressed from the eBook and/or eChapter(s). Editorial review has deemed that any suppressed content does not materially affect the overall learning experience. Cengage Learning reserves the right to remove additional content at any time if subsequent rights restrictions require it.

where I_a leaves positive terminal "a" of the generator. The complex power S_a delivered by phase a of the generator is

$$\begin{aligned} S_a &= V_{an}I_a^* = \mathrm{V_{LN}I_L}\underline{/(\delta - \beta)} \\ &= \mathrm{V_{LN}I_L}\cos(\delta - \beta) + j\mathrm{V_{LN}I_L}\sin(\delta - \beta) \end{aligned} \tag{2.6.11}$$

Under balanced operating conditions, the complex powers delivered by phases b and c are identical to S_a, and the total complex power $S_{3\phi}$ delivered by the generator is

$$\begin{aligned} S_{3\phi} &= S_a + S_b + S_c = 3S_a \\ &= 3\mathrm{V_{LN}I_L}\underline{/(\delta - \beta)} \\ &= 3\mathrm{V_{LN}I_L}\cos(\delta - \beta) + j3\mathrm{V_{LN}I_L}\sin(\delta - \beta) \end{aligned} \tag{2.6.12}$$

In terms of the total real and reactive powers,

$$S_{3\phi} = \mathrm{P}_{3\phi} + j\mathrm{Q}_{3\phi} \tag{2.6.13}$$

where

$$\begin{aligned} \mathrm{P}_{3\phi} &= \mathrm{Re}(S_{3\phi}) = 3\mathrm{V_{LN}I_L}\cos(\delta - \beta) \\ &= \sqrt{3}\mathrm{V_{LL}I_L}\cos(\delta - \beta) \quad \mathrm{W} \end{aligned} \tag{2.6.14}$$

and

$$\begin{aligned} \mathrm{Q}_{3\phi} &= \mathrm{Im}(S_{3\phi}) = 3\mathrm{V_{LN}I_L}\sin(\delta - \beta) \\ &= \sqrt{3}\mathrm{V_{LL}I_L}\sin(\delta - \beta) \quad \mathrm{var} \end{aligned} \tag{2.6.15}$$

Also, the total apparent power is

$$\mathrm{S}_{3\phi} = |S_{3\phi}| = 3\mathrm{V_{LN}I_L} = \sqrt{3}\mathrm{V_{LL}I_L} \quad \mathrm{VA} \tag{2.6.16}$$

COMPLEX POWER: BALANCED THREE-PHASE MOTORS

The preceding expressions for complex, real, reactive, and apparent power *delivered* by a three-phase generator are also valid for the complex, real, reactive, and apparent power *absorbed* by a three-phase motor.

COMPLEX POWER: BALANCED-Y AND BALANCED-Δ IMPEDANCE LOADS

Equations (2.6.13) through (2.6.16) are also valid for balanced-Y and -Δ impedance loads. For a balanced-Y load, the line-to-neutral voltage across the phase a load impedance and the current entering the positive terminal of that load impedance can be represented by (2.6.9) and (2.6.10). Then (2.6.11) through (2.6.16) are valid for the power absorbed by the balanced-Y load.

For a balanced-Δ load, the line-to-line voltage across the phase a-b load impedance and the current into the positive terminal of that load impedance can be represented by

Copyright 2017 Cengage Learning. All Rights Reserved. May not be copied, scanned, or duplicated, in whole or in part. Due to electronic rights, some third party content may be suppressed from the eBook and/or eChapter(s). Editorial review has deemed that any suppressed content does not materially affect the overall learning experience. Cengage Learning reserves the right to remove additional content at any time if subsequent rights restrictions require it.

$$V_{ab} = \mathrm{V}_{\mathrm{LL}}\underline{/\delta} \quad \text{volts} \tag{2.6.17}$$

$$I_{ab} = \mathrm{I}_{\Delta}\underline{/\beta} \quad \mathrm{A} \tag{2.6.18}$$

where V_{LL} is the rms line-to-line voltage and I_{Δ} is the rms Δ-load current. The complex power S_{ab} absorbed by the phase $a-b$ load impedance is then

$$S_{ab} = V_{ab}I^{*}_{ab} = \mathrm{V}_{\mathrm{LL}}\mathrm{I}_{\Delta}\underline{/(\delta - \beta)} \tag{2.6.19}$$

The total complex power absorbed by the Δ load is

$$\begin{aligned} S_{3\phi} &= S_{ab} + S_{bc} + S_{ca} = 3S_{ab} \\ &= 3\mathrm{V}_{\mathrm{LL}}\mathrm{I}_{\Delta}\underline{/(\delta - \beta)} \\ &= 3\mathrm{V}_{\mathrm{LL}}\mathrm{I}_{\Delta}\cos(\delta - \beta) + j3\mathrm{V}_{\mathrm{LL}}\mathrm{I}_{\Delta}\sin(\delta - \beta) \end{aligned} \tag{2.6.20}$$

Rewriting (2.6.19) in terms of the total real and reactive power,

$$S_{3\phi} = \mathrm{P}_{3\phi} + j\mathrm{Q}_{3\phi} \tag{2.6.21}$$

$$\begin{aligned} \mathrm{P}_{3\phi} &= \mathrm{Re}(S_{3\phi}) = 3\mathrm{V}_{\mathrm{LL}}\mathrm{I}_{\Delta}\cos(\delta - \beta) \\ &= \sqrt{3}\mathrm{V}_{\mathrm{LL}}\mathrm{I}_{\mathrm{L}}\cos(\delta - \beta) \quad \mathrm{W} \end{aligned} \tag{2.6.22}$$

$$\begin{aligned} \mathrm{Q}_{3\phi} &= \mathrm{Im}(S_{3\phi}) = 3\mathrm{V}_{\mathrm{LL}}\mathrm{I}_{\Delta}\sin(\delta - \beta) \\ &= \sqrt{3}\mathrm{V}_{\mathrm{LL}}\mathrm{I}_{\mathrm{L}}\sin(\delta - \beta) \quad \text{var} \end{aligned} \tag{2.6.23}$$

where the Δ-load current I_{Δ} is expressed in terms of the line current $\mathrm{I}_{\mathrm{L}} = \sqrt{3}\mathrm{I}_{\Delta}$ in (2.6.22) and (2.6.23). Also, the total apparent power is

$$\mathrm{S}_{3\phi} = |S_{3\phi}| = 3\mathrm{V}_{\mathrm{LL}}\mathrm{I}_{\Delta} = \sqrt{3}\mathrm{V}_{\mathrm{LL}}\mathrm{I}_{\mathrm{L}} \quad \mathrm{VA} \tag{2.6.24}$$

Equations (2.6.21) through (2.6.24) developed for the balanced-Δ load are identical to (2.6.13) through (2.6.16).

EXAMPLE 2.5

Power in a balanced three-phase system

Two balanced three-phase motors in parallel, an induction motor drawing 400 kW at 0.8 power factor lagging and a synchronous motor drawing 150 kVA at 0.9 power factor leading, are supplied by a balanced, three-phase 4160-volt source. Cable impedances between the source and load are neglected. (a) Draw the power triangle for each motor and for the combined-motor load. (b) Determine the power factor of the combined-motor load. (c) Determine the magnitude of the line current delivered by the source. (d) A delta-connected capacitor bank is now installed in parallel with the combined-motor load. What value of capacitive reactance is required in each leg of the capacitor bank to make the source power factor unity? (e) Determine the magnitude of the line current delivered by the source with the capacitor bank installed.

Copyright 2017 Cengage Learning. All Rights Reserved. May not be copied, scanned, or duplicated, in whole or in part. Due to electronic rights, some third party content may be suppressed from the eBook and/or eChapter(s). Editorial review has deemed that any suppressed content does not materially affect the overall learning experience. Cengage Learning reserves the right to remove additional content at any time if subsequent rights restrictions require it.

SOLUTION

(a) For the induction motor, P = 400 kW and

$S = P/\text{p.f.} = 400/0.8 = 500\ \text{kVA}$

$Q = \sqrt{S^2 - P^2} = \sqrt{(500)^2 - (400)^2} = 300\ \text{kvar absorbed}$

For the synchronous motor, *S* = 150 kVA and

$P = S(\text{p.f.}) = 150(0.9) = 135\ \text{kW}$

$Q = \sqrt{S^2 - P^2} = \sqrt{(150)^2 - (135)^2} = 65.4\ \text{kvar delivered}$

For the combined-motor load,

$P = 400 + 135 = 535\ \text{kW}$

$Q = 300 - 65.4 = 234.6\ \text{kvar absorbed}$

$S = \sqrt{P^2 + Q^2} = \sqrt{(535)^2 + (234.6)^2} = 584.2\ \text{kVA}$

a. The power triangles for each motor and the combined-motor load are shown in Figure 2.20.

b. The power factor of the combined-motor load is p.f. = P/S = 535/584.2 = 0.916 lagging.

c. The line current delivered by the source is $I = S/(\sqrt{3}\,V)$, where S is the three-phase apparent power of the combined-motor load and V is the magnitude of the line-to-line load voltage, which is the same as the source voltage for this example. $I = 584.2/(\sqrt{3}\,4160\ \text{V}) = 0.0811\ \text{kA} = 81.1$ per phase.

d. For unity power factor, the three-phase reactive power supplied by the capacitor bank should equal the three-phase reactive power absorbed by the combined-motor load. That is, $Q_c = 234.6$ kvar. For a Δ-connected capacitor bank, $Q_c = 3V^2/X_\Delta$ where V is the line-to-line voltage across the bank and X_Δ the capacitive reactance of each leg of the bank. The capacitive reactance of each leg is

$$X_\Delta = 3V^2/Q_c = 3(4160^2)/234.6 \times 10^3 = 221.3\ \Omega.$$

FIGURE 2.20

Power triangles for Example 2.5

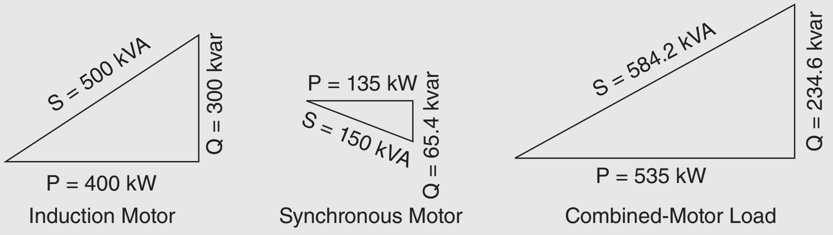

(Continued)

Copyright 2017 Cengage Learning. All Rights Reserved. May not be copied, scanned, or duplicated, in whole or in part. Due to electronic rights, some third party content may be suppressed from the eBook and/or eChapter(s). Editorial review has deemed that any suppressed content does not materially affect the overall learning experience. Cengage Learning reserves the right to remove additional content at any time if subsequent rights restrictions require it.

e. With the capacitor bank installed, the source power factor is unity, and the apparent power S delivered by the source is the same as the real power P delivered by the source. The line current magnitude is

$$I = S/(\sqrt{3}\,V) = P/(\sqrt{3}V) = 535/(\sqrt{3}\,4160) = 0.0743\text{kA} = 74.3 \text{ A per phase.}$$

In this example, the source voltage of 4160 V is not specified as a line-to-line voltage or line-to-neutral voltage, RMS or peak. Therefore, it is assumed to be an RMS line-to-line voltage, which is the convention throughout this text and a standard practice in the electric power industry. The combined-motor load absorbs 535 kW of real power. The induction motor, which operates at lagging power factor, absorbs reactive power (300 kvar) and the synchronous motor, which operates at leading power factor, delivers reactive power (65.4 kvar). The capacitor bank also delivers reactive power (234.6 kvar). Note that the line current delivered by the source is reduced from 81.1 A without the capacitor bank to 74.3 A with the capacitor bank. Any I^2R losses due to cable resistances and voltage drops due to cable reactances between the source and loads (not included in this example) would also be reduced.

2.7 ADVANTAGES OF BALANCED THREE-PHASE VERSUS SINGLE-PHASE SYSTEMS

Figure 2.21 shows three separate single-phase systems. Each single-phase system consists of the following identical components: (1) a generator represented by a voltage source and a generator impedance Z_g; (2) a forward and return conductor represented by two series line impedances Z_L; (3) a load represented by an impedance Z_Y. The three single-phase systems, although completely separated, are drawn in a Y configuration in the figure to illustrate two advantages of three-phase systems.

Each separate single-phase system requires that *both* the forward and return conductors have a current capacity (or *ampacity*) equal to or greater than the load current. However, if the source and load neutrals in Figure 2.21 are connected to form a three-phase system, and if the source voltages are balanced with equal magnitudes and with 120° displacement between phases, then the neutral current will be zero [see (2.5.10)] and the three neutral conductors can be removed. Thus, the balanced three-phase system, while delivering the same power to the three load impedances Z_Y, requires only half the number of conductors needed for the three separate single-phase systems. Also, the total I^2R line losses in the three-phase system are only half those of the three separate single-phase systems, and the line-voltage drop between the source and load in the three-phase system is half that of each single-phase system. Therefore, one advantage of balanced three-phase systems over separate single-phase systems is reduced capital and operating costs of transmission and distribution, as well as better voltage regulation.

Copyright 2017 Cengage Learning. All Rights Reserved. May not be copied, scanned, or duplicated, in whole or in part. Due to electronic rights, some third party content may be suppressed from the eBook and/or eChapter(s). Editorial review has deemed that any suppressed content does not materially affect the overall learning experience. Cengage Learning reserves the right to remove additional content at any time if subsequent rights restrictions require it.

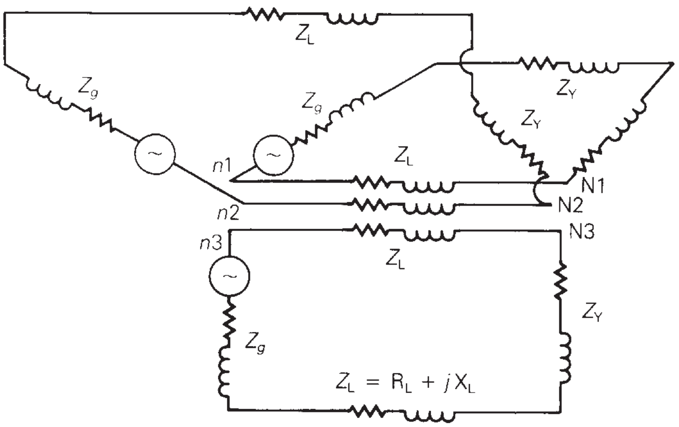

FIGURE 2.21

Three single-phase systems

Some three-phase systems such as Δ-connected systems and three-wire Y-connected systems do not have any neutral conductor. However, the majority of three-phase systems are four-wire Y-connected systems, where a grounded neutral conductor is used. Neutral conductors are used to reduce transient overvoltages, which can be caused by lightning strikes and by line-switching operations, and to carry unbalanced currents, which can occur during unsymmetrical short-circuit conditions. Neutral conductors for transmission lines are typically smaller in size and ampacity than the phase conductors because the neutral current is nearly zero under normal operating conditions. Thus, the cost of a neutral conductor is substantially less than that of a phase conductor. The capital and operating costs of three-phase transmission and distribution systems with or without neutral conductors are substantially less than those of separate single-phase systems.

A second advantage of three-phase systems is that the total instantaneous electric power delivered by a three-phase generator under balanced steady-state conditions is (nearly) constant, as shown in Section 2.6. A three-phase generator (constructed with its field winding on one shaft and with its three-phase windings equally displaced by 120° on the stator core) will also have a nearly constant mechanical input power under balanced steady-state conditions, since the mechanical input power equals the electrical output power plus the small generator losses. Furthermore, the mechanical shaft torque, which equals mechanical input power divided by mechanical radian frequency ($T_{\text{mech}} = P_{\text{mech}}/\omega_m$) is nearly constant.

On the other hand, the equation for the instantaneous electric power delivered by a single-phase generator under balanced steady-state conditions is the same as the instantaneous power delivered by one phase of a three-phase generator, given by $p_a(t)$ in (2.6.3). As shown in that equation, $p_a(t)$ has two components: a constant and a double-frequency sinusoid. Both the mechanical input power and the mechanical shaft torque of the single-phase generator will have corresponding double-frequency components that create shaft vibration and noise, which could cause shaft failure in large machines. Accordingly, most electric generators and motors rated 5 kVA and higher are constructed as three-phase machines in order to produce nearly constant torque and thereby minimize shaft vibration and noise.

Copyright 2017 Cengage Learning. All Rights Reserved. May not be copied, scanned, or duplicated, in whole or in part. Due to electronic rights, some third party content may be suppressed from the eBook and/or eChapter(s). Editorial review has deemed that any suppressed content does not materially affect the overall learning experience. Cengage Learning reserves the right to remove additional content at any time if subsequent rights restrictions require it.

MULTIPLE CHOICE QUESTIONS

SECTION 2.1

2.1 The rms value of $v(t) = V_{\max} \cos(\omega t + \delta)$ is given by
(a) $V_{\max}$ (b) $V_{\max}/\sqrt{2}$ (c) $2V_{\max}$ (d) $\sqrt{2}V_{\max}$

2.2 If the rms phasor of a voltage is given by $V = 120\underline{/60^\circ}$ volts, then the corresponding $v(t)$ is given by
(a) $120\sqrt{2}\cos(\omega t + 60^\circ)$
(b) $120\cos(\omega t + 60^\circ)$
(c) $120\sqrt{2}\sin(\omega r + 60^\circ)$

2.3 If a phasor representation of a current is given by $I = 70.7\underline{/45^\circ}$ A, it is equivalent to
(a) $100\, e^{j45^\circ}$ (b) $100 + j100$ (c) $50 + j50$

2.4 With sinusoidal-steady-state excitation, for a purely resistive circuit, the voltage and current phasors are
(a) In phase
(b) Perpendicular with each other with *V* leading *I*
(v) Perpendicular with each other with *I* leading *V*.

2.5 For a purely inductive circuit, with sinusoidal-steady-state excitation, the voltage and current phasors are
(a) In phase
(b) Perpendicular to each other with *V* leading *I*
(c) Perpendicular to each other with *I* leading *V*.

2.6 For a purely capacitive circuit, with sinusoidal-steady-state excitation, the voltage and current phasors are
(a) In phase
(b) Perpendicular to each other with *V* leading *I*
(c) Perpendicular to each other with *I* leading *V*.

SECTION 2.2

2.7 With sinusoidal-steady-state excitation, the average power in a single-phase ac circuit with a purely resistive load is given by
(a) $I_{\text{rms}}^2 R$ (b) $V_{\max}^2/R$ (c) Zero

2.8 The average power in a single-phase ac circuit with a purely inductive load, for sinusoidal-steady-state excitation, is
(a) $I^2\, X_L$ (b) $V_{\max}^2/X_L$ (c) Zero
[Note: $X_L = (\omega L)$ is the inductive reactance]

2.9 The average power in a single-phase ac circuit with a purely capacitive load, for sinusoidal-steady-state excitation, is
(a) Zero (b) $V_{\max}^2/X_C$ (c) $I_{\text{rms}}^2 X_C$
[Note: $X_C = 1/(\omega C)$ is the capacitive reactance]

Copyright 2017 Cengage Learning. All Rights Reserved. May not be copied, scanned, or duplicated, in whole or in part. Due to electronic rights, some third party content may be suppressed from the eBook and/or eChapter(s). Editorial review has deemed that any suppressed content does not materially affect the overall learning experience. Cengage Learning reserves the right to remove additional content at any time if subsequent rights restrictions require it.

2.10 The average value of a double-frequency sinusoid, sin $2(\omega t + \delta)$, is given by
(a) 1 (b) δ (c) Zero

2.11 The power factor for an inductive circuit (R-L load), in which the current lags the voltage, is said to be
(a) Lagging (b) Leading (c) Zero

2.12 The power factor for a capacitive circuit (R-C load), in which the current leads the voltage, is said to be
(a) Lagging (b) Leading (c) One

SECTION 2.3

2.13 In a single-phase ac circuit, for a general load composed of RLC elements under sinusoidal-steady-state excitation, the average reactive power is given by
(a) $V_{rms} I_{rms} \cos \phi$ (b) $V_{rms} I_{rms} \sin \phi$ (c) Zero
[Note: ϕ is the power-factor angle]

2.14 The instantaneous power absorbed by the load in a single-phase ac circuit, for a general RLC load under sinusoidal-steady-state excitation, is
(a) Nonzero constant (b) Zero
(c) Containing double-frequency components

2.15 With load convention, where the current enters the positive terminal of the circuit element, if Ω is positive then positive reactive power is absorbed.
(a) True (b) False

2.16 With generator convention, where the current leaves the positive terminal of the circuit element, if P is positive then positive real power is delivered.
(a) False (b) True

2.17 Consider the load convention that is used for the RLC elements shown in Figure 2.2 of the text.
A. If one says that an inductor absorbs zero real power and positive reactive power, is it
(a) True (b) False
B. If one says that a capacitor absorbs zero real power and negative reactive power (or delivers positive reactive power), is it
(a) False (b) True
C. If one says that a (positive-valued) resistor absorbs (positive) real power and zero reactive power, is it
(a) True (b) False

2.18 In an ac circuit, power factor improvement is achieved by
(a) Connecting a resistor in parallel with the inductive load.
(b) Connecting an inductor in parallel with the inductive load.
(c) Connecting a capacitor in parallel with the inductive load.

Copyright 2017 Cengage Learning. All Rights Reserved. May not be copied, scanned, or duplicated, in whole or in part. Due to electronic rights, some third party content may be suppressed from the eBook and/or eChapter(s). Editorial review has deemed that any suppressed content does not materially affect the overall learning experience. Cengage Learning reserves the right to remove additional content at any time if subsequent rights restrictions require it.

SECTION 2.4

2.19 The admittance of the impedance $-j\frac{1}{2}\,\Omega$ is given by

(a) $-j2S$ (b) $j2S^2$ (c) $-j4S$

2.20 Consider Figure 2.9 of the text. Let the nodal equations in matrix form be given by Eq. (2.4.1) of the text.

A. The element Y_{11} is given by

(a) 0 (b) $j13$ (c) $-j7$

B. The element Y_{31} is given by

(a) 0 (b) $-j5$ (c) $j1$

C. The admittance matrix is always symmetric square.

(a) False (b) True

SECTIONS 2.5 AND 2.6

2.21 The three-phase source line-to-neutral voltages are given by $E_{an} = 10\underline{/0^\circ}$, $E_{bn} = 10\underline{/+240^\circ}$, and $E_{cn} = 10\underline{/-240^\circ}$ volts.

Is the source balanced?

(a) Yes (b) No

2.22 In a balanced three-phase Y-connected system with a positive-sequence source, the line-to-line voltages are $\sqrt{3}$ times the line-to-neutral voltages and lend by 30°.

(a) True (b) False

2.23 In a balanced system, the phasor sum of the line-to-line voltages and the phasor sum of the line-to-neutral voltages are always equal to zero.

(a) False (b) True

2.24 Consider a three-phase Y-connected source feeding a balanced-Δ load. The phasor sum of the line currents as well as the neutral current are always zero.

(a) True (b) False

2.25 For a balanced-Δ load supplied by a balanced positive-sequence source, the line currents into the load are $\sqrt{3}$ times the Δ-load currents and lag by 30°.

(a) True (b) False

2.26 A balanced Δ-load can be converted to an equivalent balanced-Y load by dividing the Δ-load impedance by

(a) $\sqrt{3}$ (b) 3 (c) 1/3

2.27 When working with balanced three-phase circuits, per-phase analysis is commonly done after converting Δ loads to Y loads, thereby solving only one phase of the circuit.

(a) True (b) False

2.28 The total instantaneous power delivered by a three-phase generator under balanced operating conditions is

(a) A function of time (b) A constant

Copyright 2017 Cengage Learning. All Rights Reserved. May not be copied, scanned, or duplicated, in whole or in part. Due to electronic rights, some third party content may be suppressed from the eBook and/or eChapter(s). Editorial review has deemed that any suppressed content does not materially affect the overall learning experience. Cengage Learning reserves the right to remove additional content at any time if subsequent rights restrictions require it.

2.29 The total instantaneous power absorbed by a three-phase motor (under balanced steady-state conditions) as well as a balanced three-phase impedance load is

(a) A constant (b) A function of time

2.30 Under balanced operating conditions, consider the three-phase complex power delivered by the three-phase source to the three-phase load. Match the following expressions, those on the left to those on the right.

(i) Real power, $P_{3\phi}$	(a) $(\sqrt{3}\ V_{LL}\ I_L)$VA
(ii) Reactive power, $Q_{3\phi}$	(b) $(\sqrt{3}\ V_{LL}\ I_L \sin\phi)$ var
(iii) Total apparent power, $S_{3\phi}$	(c) $(\sqrt{3}\ V_{LL}\ I_L \cos\phi)$ W
(iv) Complex power, $S_{3\phi}$	(d) $P_{3\phi} + jQ_{3\phi}$

Note that V_{LL} is the rms line-to-line voltage, I_L is the rms line current, and ϕ is the power-factor angle.

2.31 One advantage of balanced three-phase systems over separate single-phase systems is reduced capital and operating costs of transmission and distribution.

(a) True (b) False

2.32 While the instantaneous electric power delivered by a single-phase generator under balanced steady-state conditions is a function of time having two components of a constant and a double-frequency sinusoid, the total instantaneous electric power delivered by a three-phase generator under balanced steady-state conditions is a constant.

(a) True (b) False

PROBLEMS

SECTION 2.1

2.1 Given the complex numbers $A_1 = 6\angle 30$ and $A_2 = 4 + j5$, (a) convert A_1 to rectangular form; (b) convert A_2 to polar and exponential form; (c) calculate $A_3 = (A_1 + A_2)$, giving your answer in polar form; (d) calculate $A_4 = A_1A_2$, giving your answer in rectangular form; (e) calculate $A_5 = A_1/(A_2^*)$, giving your answer in exponential form.

2.2 Convert the following instantaneous currents to phasors, using $\cos(\omega t)$ as the reference. Give your answers in both rectangular and polar form.

(a) $i(t) = 500\sqrt{2}\cos(\omega t - 30)$

(b) $i(t) = 4\sin(\omega t + 30)$

(c) $i(t) = 5\cos(\omega t - 15) + 4\sqrt{2}\sin(\omega t + 30)$

2.3 The instantaneous voltage across a circuit element is $v(t) = 400\sin(\omega t + 30°)$ volts, and the instantaneous current entering the

Copyright 2017 Cengage Learning. All Rights Reserved. May not be copied, scanned, or duplicated, in whole or in part. Due to electronic rights, some third party content may be suppressed from the eBook and/or eChapter(s). Editorial review has deemed that any suppressed content does not materially affect the overall learning experience. Cengage Learning reserves the right to remove additional content at any time if subsequent rights restrictions require it.

positive terminal of the circuit element is $i(t) = 100\cos(\omega t + 10°)$ A. For both the current and voltage, determine (a) the maximum value, (b) the rms value, and (c) the phasor expression, using $\cos(\omega t)$ as the reference.

2.4 For the single-phase circuit shown in Figure 2.22, $I = 10\underline{/0°}$A. (a) Compute the phasors I_1, I_2, and V. (b) Draw a phasor diagram showing I, I_1, I_2, and V.

FIGURE 2.22

Circuit for Problem 2.4

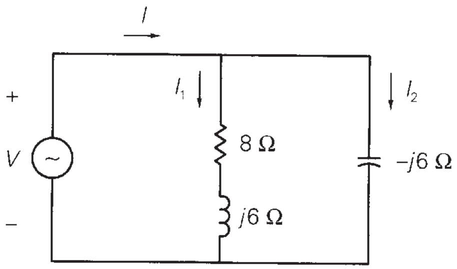

2.5 A 60-Hz, single-phase source with $V = 277\underline{/30°}$ volts is applied to a circuit element. (a) Determine the instantaneous source voltage. Also determine the phasor and instantaneous currents entering the positive terminal if the circuit element is (b) a 20-Ω resistor, (c) a 10-mH inductor, and (d) a capacitor with 25-Ω reactance.

2.6 (a) Transform $v(t) = 75\cos(377t - 15°)$ to phasor form. Comment on whether $\omega = 377$ appears in your answer. (b) Transform $V = 50\underline{/10°}$ to instantaneous form. Assume that $\omega = 377$. (c) Add the two sinusoidal functions $a(t)$ and $b(t)$ of the same frequency given as follows: $a(t) = A\sqrt{2}\cos(\omega t + \alpha)$ and $b(t) = B\sqrt{2}\cos(\omega t + \beta)$. Use phasor methods and obtain the resultant $c(t)$. Does the resultant have the same frequency?

2.7 Let a 100-V sinusoidal source be connected to a series combination of a 3-Ω resistor, an 8-Ω inductor, and a 4-Ω capacitor. (a) Draw the circuit diagram. (b) Compute the series impedance. (c) Determine the current I delivered by the source. Is the current lagging or leading the source voltage? What is the power factor of this circuit?

2.8 Consider the circuit shown in Figure 2.23 in time domain. Convert the entire circuit into phasor domain.

FIGURE 2.23

Circuit for Problem 2.8

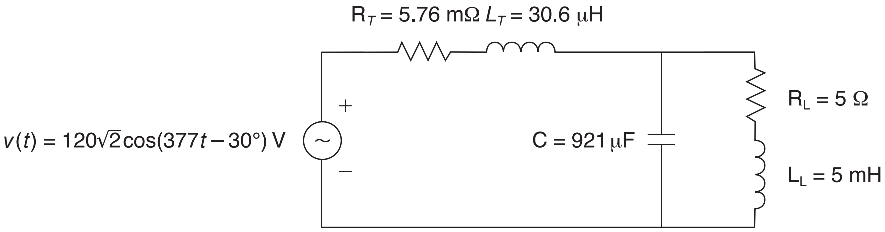

$R_T = 5.76$ mΩ $L_T = 30.6$ μH
+
–
$v(t) = 120\sqrt{2}\cos(377t - 30°)$ V
C = 921 μF
$R_L = 5$ Ω
$L_L = 5$ mH

Copyright 2017 Cengage Learning. All Rights Reserved. May not be copied, scanned, or duplicated, in whole or in part. Due to electronic rights, some third party content may be suppressed from the eBook and/or eChapter(s). Editorial review has deemed that any suppressed content does not materially affect the overall learning experience. Cengage Learning reserves the right to remove additional content at any time if subsequent rights restrictions require it.

2.9 For the circuit shown in Figure 2.24, compute the voltage across the load terminals.

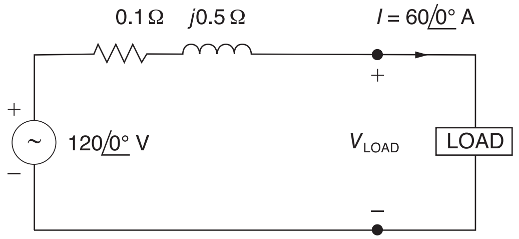

FIGURE 2.24

Circuit for Problem 2.9

SECTION 2.2

2.10 For the circuit element of Problem 2.3, calculate (a) the instantaneous power absorbed, (b) the real power (state whether it is delivered or absorbed), (c) the reactive power (state whether delivered or absorbed), (d) the power factor (state whether lagging or leading).
[*Note:* By convention the power factor $\cos(\delta - \beta)$ is positive. If $|\delta - \beta|$ is greater than 90°, then the reference direction for current may be reversed, resulting in a positive value of $\cos(\delta - \beta)$].

2.11 Referring to Problem 2.5, determine the instantaneous power, real power, and reactive power absorbed by (a) the 20-Ω resistor, (b) the 10-mH inductor, (c) the capacitor with 25-Ω reactance. Also determine the source power factor and state whether lagging or leading.

2.12 The voltage $v(t) = 359.3\cos(\omega t)$ volts is applied to a load consisting of a 10- resistor in parallel with a capacitive reactance $X_C = 25\ \Omega$. Calculate (a) the instantaneous power absorbed by the resistor, (b) the instantaneous power absorbed by the capacitor, (c) the real power absorbed by the resistor, (d) the reactive power delivered by the capacitor, and (e) the load power factor.

2.13 Repeat Problem 2.12 if the resistor and capacitor are connected in series.

2.14 A single-phase source is applied to a two-terminal, passive circuit with equivalent impedance $Z = 3.0\underline{/-45^\circ}\ \Omega$, measured from the terminals. The source current is $i(t) = 2\sqrt{2}\cos(\omega t)$ kA. Determine the (a) instantaneous power, (b) real power, (c) reactive power delivered by the source, and (d) source power factor.

2.15 Let a voltage source $v(t) = 4\cos(\omega t + 60^\circ)$ be connected to an impedance $Z = 2\underline{/30^\circ}\ \Omega$. (a) Given the operating frequency to be 60 Hz, determine the expressions for the current and instantaneous power delivered by the source as functions of time. (b) Plot these functions along with $v(t)$ on a single graph for comparison. (c) Find the frequency and average value of the instantaneous power.

Copyright 2017 Cengage Learning. All Rights Reserved. May not be copied, scanned, or duplicated, in whole or in part. Due to electronic rights, some third party content may be suppressed from the eBook and/or eChapter(s). Editorial review has deemed that any suppressed content does not materially affect the overall learning experience. Cengage Learning reserves the right to remove additional content at any time if subsequent rights restrictions require it.

2.16 A single-phase, 120-V (rms), 60-Hz source supplies power to a series R-L circuit consisting of R = 10 Ω and L = 40 mH. (a) Determine the power factor of the circuit and state whether it is lagging or leading. (b) Determine the real and reactive power absorbed by the load. (c) Calculate the peak magnetic energy W_{int} stored in the inductor by using the expression $W_{\text{int}} = L(I_{\text{rms}})^2$ and check whether the reactive power $Q = \omega W_{\text{int}}$ is satisfied. (*Note:* The instantaneous magnetic energy storage fluctuates between zero and the peak energy. This energy must be sent twice each cycle to the load from the source by means of reactive power flows.)

SECTION 2.3

2.17 Consider a load impedance of $Z = j\omega L$ connected to a voltage and V let the current drawn be I.

(a) Develop an expression for the reactive power Q in terms of ω, L, and I, from complex power considerations.

(b) Let the instantaneous current be $i(t) = \sqrt{2}I\cos(\omega t + \theta)$. Obtain an expression for the instantaneous power $p(t)$ into L, and then express it in terms of Q.

(c) Comment on the average real power P supplied to the inductor and the instantaneous power supplied.

2.18 Let a series RLC network be connected to a source voltage V, drawing a current I.

(a) In terms of the load impedance $Z = Z\,\underline{/Z}$, find expressions for P and Q, from complex power considerations.

(b) Express $p(t)$ in terms of P and Q, by choosing $i(t) = \sqrt{2}I\cos\omega t$.

(c) For the case of $Z = R + j\omega L + 1/j\omega C$, interpret the result of part (b) in terms of P, Q_L, and Q_C. In particular, if $\omega^2 LC = 1$, when the inductive and capacitive reactances cancel, comment on what happens.

2.19 Consider a single-phase load with an applied voltage $v(t) = 150\cos(\omega t + 10°)$ volts and load current $i(t) = 5\cos(\omega t - 50°)$ A. (a) Determine the power triangle. (b) Find the power factor and specify whether it is lagging or leading. (c) Calculate the reactive power supplied by capacitors in parallel with the load that correct the power factor to 0.9 lagging.

2.20 A circuit consists of two impedances, $Z_1 = 20\underline{/30°}\,\Omega$ and $Z_2 = 25\underline{/60°}\,\Omega$, in parallel, supplied by a source voltage $V = 100\underline{/60°}$ volts. Determine the power triangle for each of the impedances and for the source.

2.21 An industrial plant consisting primarily of induction motor loads absorbs 500 kW at 0.6 power factor lagging. (a) Compute the required kVA rating of a shunt capacitor to improve the power factor to 0.9 lagging. (b) Calculate the resulting power factor if a synchronous motor rated at 500 hp with 90% efficiency operating at rated load and at unity power

Copyright 2017 Cengage Learning. All Rights Reserved. May not be copied, scanned, or duplicated, in whole or in part. Due to electronic rights, some third party content may be suppressed from the eBook and/or eChapter(s). Editorial review has deemed that any suppressed content does not materially affect the overall learning experience. Cengage Learning reserves the right to remove additional content at any time if subsequent rights restrictions require it.

factor is added to the plant instead of the capacitor. Assume constant voltage (1 hp = 0.746 kW).

2.22 The real power delivered by a source to two impedances, $Z_1 = 4 + j5\ \Omega$ and $Z_2 = 10\ \Omega$, connected in parallel, is 1000 W. Determine (a) the real power absorbed by each of the impedances and (b) the source current.

2.23 A single-phase source has a terminal voltage $V = 120\angle 0°$ volts and a current $I = 15\angle 30°$ A, which leaves the positive terminal of the source. Determine the real and reactive power, and state whether the source is delivering or absorbing each.

2.24 A source supplies power to the following three loads connected in parallel: (1) a lighting load drawing 10 kW, (2) an induction motor drawing 10 kVA at 0.90 power factor lagging, and (3) a synchronous motor operating at 10 hp, 85% efficiency and 0.95 power factor leading (1 hp = 0.746 kW). Determine the real, reactive, and apparent power delivered by the source. Also, draw the source power triangle.

2.25 Consider the series RLC circuit of Problem 2.7 and calculate the complex power absorbed by each of the R, L, and C elements, as well as the complex power absorbed by the total load. Draw the resultant power triangle. Check whether the complex power delivered by the source equals the total complex power absorbed by the load.

2.26 A small manufacturing plant is located 2 km down a transmission line, which has a series reactance of 0.5 Ω/km. The line resistance is negligible. The line voltage at the plant is $480\angle 0°$ V (rms), and the plant consumes 120 kW at 0.85 power factor lagging. Determine the voltage and power factor at the sending end of the transmission line by using (a) a complex power approach and (b) a circuit analysis approach.

2.27 An industrial load consisting of a bank of induction motors consumes 50 kW at a power factor of 0.8 lagging from a 220-V, 60-Hz, single-phase source. By placing a bank of capacitors in parallel with the load, the resultant power factor is to be raised to 0.95 lagging. Find the net capacitance of the capacitor bank in μF that is required.

2.28 Three loads are connected in parallel across a single-phase source voltage of 240 V (RMS).
Load 1 absorbs 15 kW and 6.667 kvar;
Load 2 absorbs 3 kVA at 0.96PF leading;
Load 3 absorbs 15 kW at unity power factor.
Calculate the equivalent impedance, Z, for the three parallel loads, for two cases:
(i) Series combination of R and X, and (ii) parallel combination of R and X.

Copyright 2017 Cengage Learning. All Rights Reserved. May not be copied, scanned, or duplicated, in whole or in part. Due to electronic rights, some third party content may be suppressed from the eBook and/or eChapter(s). Editorial review has deemed that any suppressed content does not materially affect the overall learning experience. Cengage Learning reserves the right to remove additional content at any time if subsequent rights restrictions require it.

2.29 Modeling the transmission lines as inductors, with $S_{ij} = S_{ji}^*$, Compute S_{13}, S_{31}, S_{23}, S_{32}, and S_{G3} in Figure 2.25. (*Hint:* complex power balance holds good at each bus, satisfying KCL.)

FIGURE 2.25

System diagram for Problem 2.29

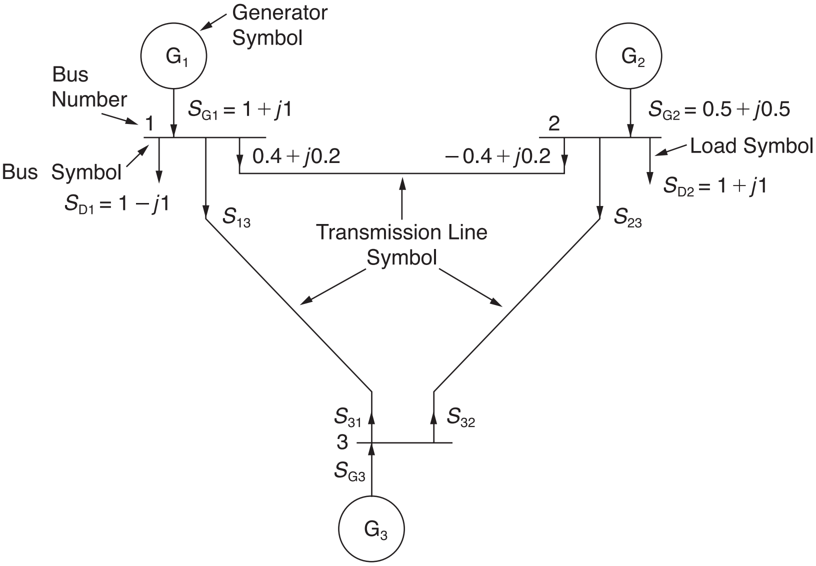
Generator Symbol
G₁
G₂
Bus Number
1
$S_{G1} = 1 + j1$
2
$S_{G2} = 0.5 + j0.5$
Load Symbol
Bus Symbol
$0.4 + j0.2$
$-0.4 + j0.2$
$S_{D1} = 1 - j1$
$S_{D2} = 1 + j1$
S_{13}
S_{23}
Transmission Line Symbol
S_{31}
S_{32}
3
S_{G3}
G₃

2.30 Figure 2.26 shows three loads connected in parallel across a 1000-V (RMS), 60-Hz single-phase source.

Load 1: Inductive load, 125 kVA, 0.28PF lagging.
Load 2: Capacitive load, 10 kW, 40 kvar.
Load 3: Resistive load, 15 kW.

(a) Determine the total kW, kvar, kva, and supply power factor.

(b) In order to improve the power factor to 0.8 lagging, a capacitor of negligible resistance is connected in parallel with the above loads. Find the kvar rating of that capacitor and the capacitance in μF.

Comment on the magnitude of the supply current after adding the capacitor.

FIGURE 2.26

Circuit for Problem 2.30

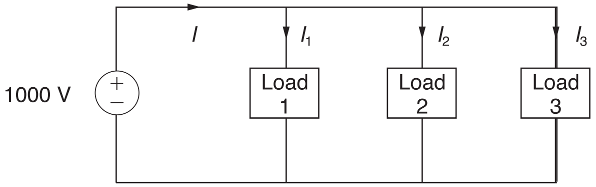
I
I_1
I_2
I_3
1000 V
+
−
Load 1
Load 2
Load 3

2.31 Consider two interconnected voltage sources connected by a line of impedance $Z = jX\ \Omega$, as shown in Figure 2.27.

(a) Obtain expressions for P_{12} and Q_{12}.

Copyright 2017 Cengage Learning. All Rights Reserved. May not be copied, scanned, or duplicated, in whole or in part. Due to electronic rights, some third party content may be suppressed from the eBook and/or eChapter(s). Editorial review has deemed that any suppressed content does not materially affect the overall learning experience. Cengage Learning reserves the right to remove additional content at any time if subsequent rights restrictions require it.

(b) Determine the maximum power transfer and the condition for it to occur.

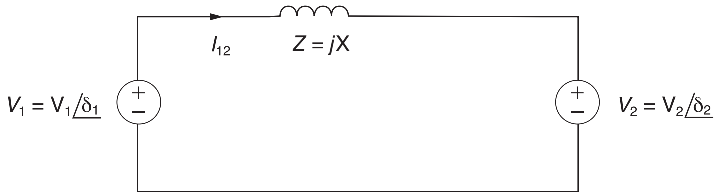
I_{12}
$Z = jX$
$V_1 = V_1\underline{/\delta_1}$
$V_2 = V_2\underline{/\delta_2}$
+
−
+
−

FIGURE 2.27

Circuit for Problem 2.31

2.32 In PowerWorld Simulator case Problem 2_32 (see Figure 2.28) a 8 MW and 4 Mvar load is supplied at 13.8 kV through a feeder with an impedance of $1 + j2\ \Omega$. The load is compensated with a capacitor whose output, Ω_{cap}, can be varied in 0.5 Mvar steps between 0 and 10.0 Mvars. What value of Ω_{cap} minimizes the real power line losses? What value of Ω_{cap} minimizes the MVA power flow into the feeder?

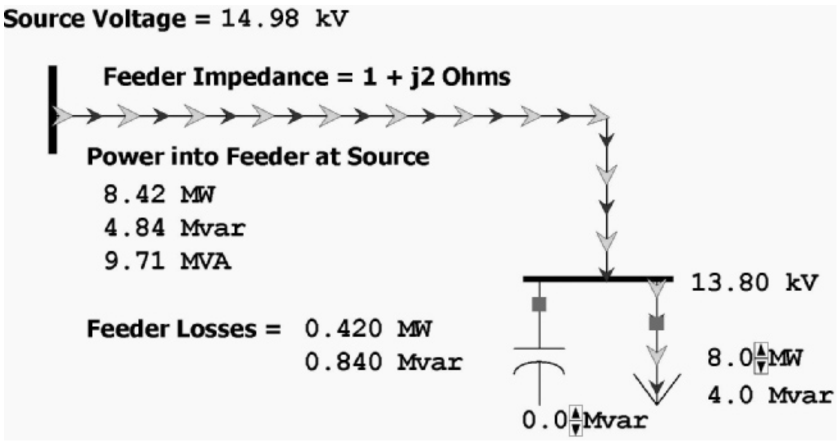

Source Voltage = 14.98 kV

Feeder Impedance = 1 + j2 Ohms

Power into Feeder at Source
8.42 MW
4.84 Mvar
9.71 MVA

13.80 kV

Feeder Losses = 0.420 MW
0.840 Mvar

8.0 MW
4.0 Mvar

0.0 Mvar

FIGURE 2.28

Screen for Problem 2.32

2.33 For the system from Problem 2.32, plot the real and reactive line losses as Ω_{cap} is varied between 0 and 10.0 Mvars.

2.34 For the system from Problem 2.32, assume that half the time the load is 10 MW and 5 Mvar, and for the other half it is 20 MW and 10 Mvar. What single value of Q_{cap} would minimize the average losses? Assume that Q_{cap} can only be varied in 0.5 Mvar steps.

Copyright 2017 Cengage Learning. All Rights Reserved. May not be copied, scanned, or duplicated, in whole or in part. Due to electronic rights, some third party content may be suppressed from the eBook and/or eChapter(s). Editorial review has deemed that any suppressed content does not materially affect the overall learning experience. Cengage Learning reserves the right to remove additional content at any time if subsequent rights restrictions require it.

SECTION 2.4

2.35 For the circuit shown in Figure 2.29, convert the voltage sources to equivalent current sources and write nodal equations in matrix format using bus 0 as the reference bus. Do not solve the equations.

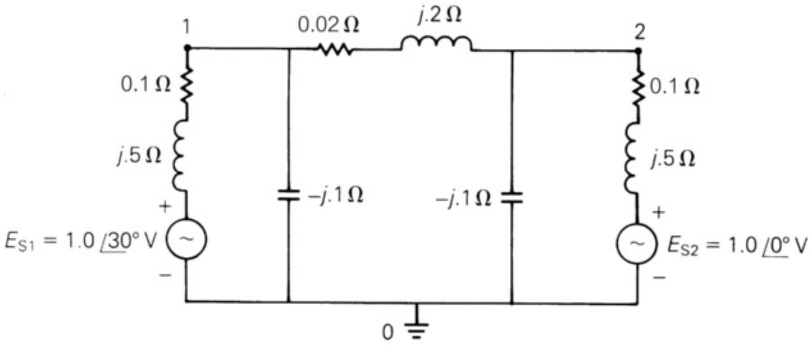

FIGURE 2.29

Circuit diagram for Problems 2.35 and 2.36

2.36 For the circuit shown in Figure 2.29, (a) determine the 2 × 2 bus admittance matrix $\boldsymbol{Y}_{\text{bus}}$, (b) convert the voltage sources to current sources and determine the vector of source currents into buses 1 and 2.

2.37 Determine the 4 × 4 bus admittance matrix $\boldsymbol{Y}_{\text{bus}}$ and write nodal equations in matrix format for the circuit shown in Figure 2.30. Do not solve the equations.

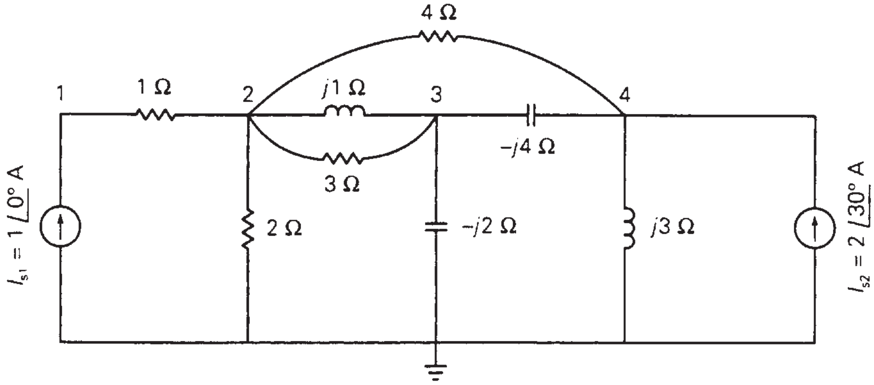

FIGURE 2.30

Circuit for Problem 2.37

2.38 Given the impedance diagram of a simple system as shown in Figure 2.31, draw the admittance diagram for the system and develop the 4 × 4 bus admittance matrix $\boldsymbol{Y}_{\text{bus}}$ by inspection.

Copyright 2017 Cengage Learning. All Rights Reserved. May not be copied, scanned, or duplicated, in whole or in part. Due to electronic rights, some third party content may be suppressed from the eBook and/or eChapter(s). Editorial review has deemed that any suppressed content does not materially affect the overall learning experience. Cengage Learning reserves the right to remove additional content at any time if subsequent rights restrictions require it.

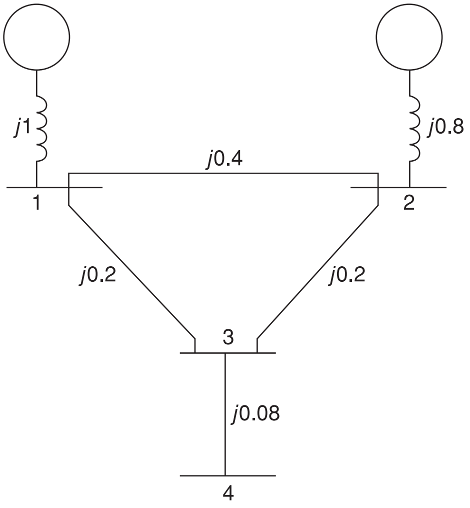

FIGURE 2.31

System diagram for Problem 2.38

2.39 (a) Given the circuit diagram in Figure 2.32 showing admittances and current sources at nodes 3 and 4, set up the nodal equations in matrix format. (b) If the parameters are given by: $Y_a = -j0.8$ S, $Y_b = -j4.0$ S, $Y_c = -j4.0$ S, $Y_d = -j8.0$ S, $Y_e = -j5.0$ S, $Y_f = -j2.5$ S, $Y_g = -j0.8$ S, $I_3 = 1.0\underline{/-90°}$ A, and $I_4 = 0.62\underline{/-135°}$ A, set up the nodal equations and suggest how you would go about solving for the voltages at the nodes.

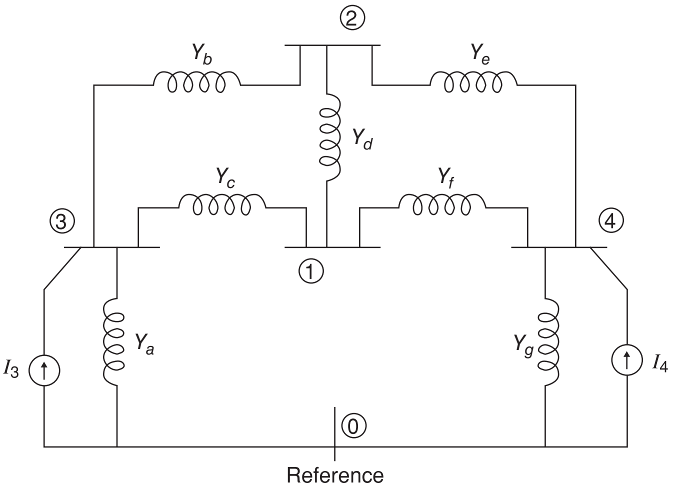

FIGURE 2.32

Circuit diagram for Problem 2.39

Copyright 2017 Cengage Learning. All Rights Reserved. May not be copied, scanned, or duplicated, in whole or in part. Due to electronic rights, some third party content may be suppressed from the eBook and/or eChapter(s). Editorial review has deemed that any suppressed content does not materially affect the overall learning experience. Cengage Learning reserves the right to remove additional content at any time if subsequent rights restrictions require it.

SECTIONS 2.5 AND 2.6

2.40 A balanced three-phase 240-V source supplies a balanced three-phase load. If the line current I_A is measured to be 15 A and is in phase with the line-to-line voltage, V_{BC}, find the per-phase load impedance if the load is (a) Y-connected, (b) Δ-connected.

2.41 A three-phase 25-kVA, 480-V, 60-Hz alternator, operating under balanced steady-state conditions, supplies a line current of 20 A per phase at a 0.8 lagging power factor and at rated voltage. Determine the power triangle for this operating condition.

2.42 A balanced Δ-connected impedance load with $(12 + j9)\ \Omega$ per phase is supplied by a balanced three-phase 60-Hz, 208-V source, (a) Calculate the line current, the total real and reactive power absorbed by the load, the load power factor, and the apparent load power, (b) Sketch a phasor diagram showing the line currents, the line-to-line source voltages, and the Δ-load currents. Use V_{ab} as the reference.

2.43 A three-phase line, which has an impedance of $(2 + j4)\ \Omega$ per phase, feeds two balanced three-phase loads that are connected in parallel. One of the loads is Y-connected with an impedance of $(30 + j40)\ \Omega$ per phase, and the other is Δ-connected with an impedance of $(60 - j45)\ \Omega$ per phase. The line is energized at the sending end from a 60-Hz, three-phase, balanced voltage source of $120\sqrt{3}$ V (rms, line-to-line). Determine (a) the current, real power, and reactive power delivered by the sending-end source; (b) the line-to-line voltage at the load; (c) the current per phase in each load; and (d) the total three-phase real and reactive powers absorbed by each load and by the line. Check that the total three-phase complex power delivered by the source equals the total three-phase power absorbed by the line and loads.

2.44 Two balanced three-phase loads that are connected in parallel are fed by a three-phase line having a series impedance of $(0.4 + j2.7)\ \Omega$ per phase. One of the loads absorbs 560 kVA at 0.707 power factor lagging, and the other 132 kW at unity power factor. The line-to-line voltage at the load end of the line is $2200\sqrt{3}$ V. Compute (a) the line-to-line voltage at the source end of the line, (b) the total real and reactive power losses in the three-phase line, and (c) the total three-phase real and reactive power supplied at the sending end of the line. Check that the total three-phase complex power delivered by the source equals the total three-phase complex power absorbed by the line and loads.

2.45 Two balanced Y-connected loads, one drawing 10 kW at 0.8 power factor lagging and the other 15 kW at 0.9 power factor leading, are connected in parallel and supplied by a balanced three-phase Y-connected, 480-V source. (a) Determine the source current. (b) If the load neutrals are connected to the source neutral by a zero-ohm neutral wire through an ammeter, what will the ammeter read?

2.46 Three identical impedances $Z_\Delta = 30\underline{/30^\circ}\Omega$ are connected in Δ to a balanced three-phase 208-V source by three identical line conductors with

Copyright 2017 Cengage Learning. All Rights Reserved. May not be copied, scanned, or duplicated, in whole or in part. Due to electronic rights, some third party content may be suppressed from the eBook and/or eChapter(s). Editorial review has deemed that any suppressed content does not materially affect the overall learning experience. Cengage Learning reserves the right to remove additional content at any time if subsequent rights restrictions require it.

impedance $Z_L = (0.8 + j0.6)\ \Omega$ per line. (a) Calculate the line-to-line voltage at the load terminals. (b) Repeat part (a) when a Δ-connected capacitor bank with reactance $(-j60)\ \Omega$ per phase is connected in parallel with the load.

2.47 Two three-phase generators supply a three-phase load through separate three-phase lines. The load absorbs 30 kW at 0.8 power factor lagging. The line impedance is $(1.4 + j1.6)\ \Omega$ per phase between generator G_1 and the load, and $(0.8 + j1)\ \Omega$ per phase between generator G_2 and the load. If generator G_1 supplies 15 kW at 0.8 power factor lagging, with a terminal voltage of 460 V line-to-line, determine (a) the voltage at the load terminals, (b) the voltage at the terminals of generator G_2, and (c) the real and reactive power supplied by generator G_2. Assume balanced operation.

2.48 Two balanced Y-connected loads in parallel, one drawing 15 kW at 0.6 power factor lagging and the other drawing 10 kVA at 0.8 power factor leading, are supplied by a balanced, three-phase, 480-volt source. (a) Draw the power triangle for each load and for the combined load. (b) Determine the power factor of the combined load and state whether lagging or leading. (c) Determine the magnitude of the line current from the source. (d) Δ-connected capacitors are now installed in parallel with the combined load. What value of capacitive reactance is needed in each leg of the A to make the source power factor unity? Give your answer in Ω. (e) Compute the magnitude of the current in each capacitor and the line current from the source.

2.49 Figure 2.33 gives the general Δ-Y transformation. (a) Show that the general transformation reduces to that given in Figure 2.16 for a balanced three-phase load. (b) Determine the impedances of the equivalent Y for the following Δ impedances: $Z_{AB} = j10$, $Z_{BC} = j20$, and $Z_{CA} = -j25\ \Omega$.

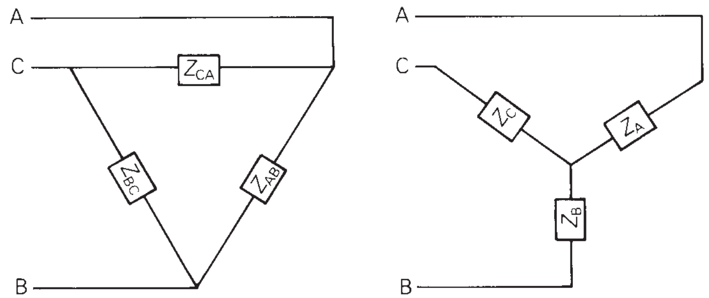

$$Z_{AB} = \frac{Z_A Z_B + Z_B Z_C + Z_C Z_A}{Z_C} \qquad Z_A = \frac{Z_{AB} Z_{CA}}{Z_{AB} + Z_{BC} + Z_{CA}}$$

$$Z_{BC} = \frac{Z_A Z_B + Z_B Z_C + Z_C Z_A}{Z_A} \qquad Z_B = \frac{Z_{AB} Z_{BC}}{Z_{AB} + Z_{BC} + Z_{CA}}$$

$$Z_{CA} = \frac{Z_A Z_B + Z_B Z_C + Z_C Z_A}{Z_B} \qquad Z_C = \frac{Z_{CA} Z_{BC}}{Z_{AB} + Z_{BC} + Z_{CA}}$$

FIGURE 2.33

General Δ-Y transformation

Copyright 2017 Cengage Learning. All Rights Reserved. May not be copied, scanned, or duplicated, in whole or in part. Due to electronic rights, some third party content may be suppressed from the eBook and/or eChapter(s). Editorial review has deemed that any suppressed content does not materially affect the overall learning experience. Cengage Learning reserves the right to remove additional content at any time if subsequent rights restrictions require it.

2.50 Consider the balanced three-phase system shown in Figure 2.34. Determine $v_1(t)$ and $i_2(t)$. Assume positive phase sequence.

FIGURE 2.34

Circuit for Problem 2.50

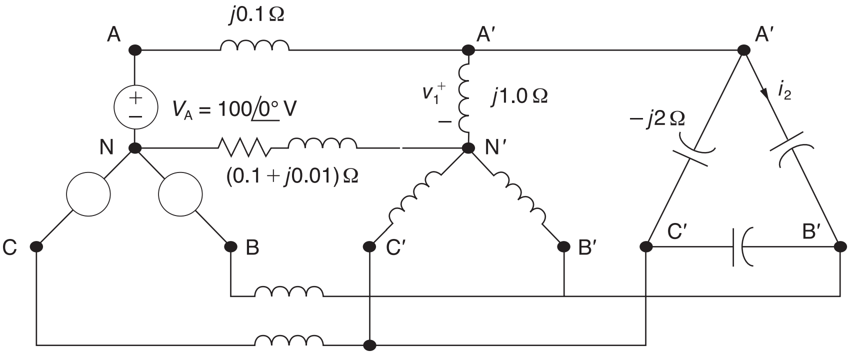

2.51 A three-phase line with an impedance of $(0.2 + j1.0)\ \Omega$ /phase feeds three balanced three-phase loads connected in parallel.

Load 1: Absorbs a total of 150 kW and 120 kvar.
Load 2: Delta connected with an impedance of $(150 - j48)\ \Omega$ /phase.
Load 3: 120 kVA at 0.6 PF leading.

If the line-to-neutral voltage at the load end of the line is 2000 v (rms), determine the magnitude of the line-to-line voltage at the source end of the line.

2.52 A balanced three-phase load is connected to a 4.16-kV, three-phase, four-wire, grounded-wye dedicated distribution feeder. The load can be modeled by an impedance of $Z_L = (4.7 + j9)\ \Omega$ /phase, wye-connected. The impedance of the phase conductors is $(0.3 + j1)\ \Omega$. Determine the following by using the phase A to neutral voltage as a reference and assume positive phase sequence:

(a) Line currents for phases A, B, and C.
(b) Line-to-neutral voltages for all three phases at the load.
(c) Apparent, active, and reactive power dissipated per phase, and for all three phases in the load.
(d) Active power losses per phase and for all three phases in the phase conductors.

CASE STUDY QUESTIONS

a. What is a microgrid?

b. What are the benefits of microgrids?

Copyright 2017 Cengage Learning. All Rights Reserved. May not be copied, scanned, or duplicated, in whole or in part. Due to electronic rights, some third party content may be suppressed from the eBook and/or eChapter(s). Editorial review has deemed that any suppressed content does not materially affect the overall learning experience. Cengage Learning reserves the right to remove additional content at any time if subsequent rights restrictions require it.

c. What are the two primary goals of the U.S. Department of Energy's Smart Grid Research & Development Program?

d. Can smart grids defer transmission and distribution investments? If so, how?

REFERENCES

1. W. H. Hayt, Jr. and J. E. Kemmerly, *Engineering Circuit Analysis*, 7th ed. (New York: McGraw-Hill, 2006).
2. W. A. Blackwell and L. L. Grigsby, *Introductory Network Theory* (Boston: PWS, 1985).
3. A. E. Fitzgerald, D. E. Higginbotham, and A. Grabel, *Basic Electrical Engineering* (New York: McGraw-Hill, 1981).
4. W. D. Stevenson, Jr., *Elements of Power System Analysis*, 4th ed. (New York: McGraw-Hill, 1982).
5. M. Smith and D. Tan, "Key Connections," *IEEE Power and Energy Magazine*, 11,4 (July/August 2013), pp. 22–27.

Copyright 2017 Cengage Learning. All Rights Reserved. May not be copied, scanned, or duplicated, in whole or in part. Due to electronic rights, some third party content may be suppressed from the eBook and/or eChapter(s). Editorial review has deemed that any suppressed content does not materially affect the overall learning experience. Cengage Learning reserves the right to remove additional content at any time if subsequent rights restrictions require it.

Copyright 2017 Cengage Learning. All Rights Reserved. May not be copied, scanned, or duplicated, in whole or in part. Due to electronic rights, some third party content may be suppressed from the eBook and/or eChapter(s). Editorial review has deemed that any suppressed content does not materially affect the overall learning experience. Cengage Learning reserves the right to remove additional content at any time if subsequent rights restrictions require it.

3

Power Transformers

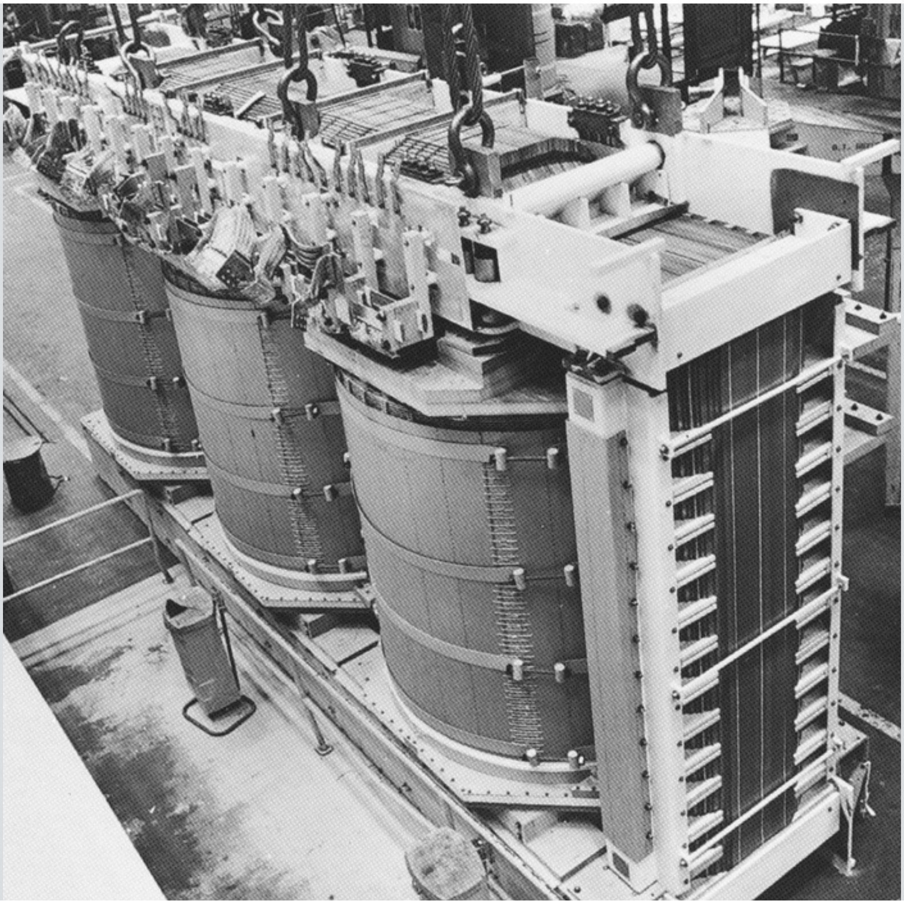

Core and coil assemblies of a three-phase 20.3 kVΔ/345kVY step-up transformer. This oil-immersed transformer is rated 325 MVA self-cooled (OA)/542 MVA forced oil, forced air-cooled (FOA)/607 MVA forced oil, forced air-cooled (FOA) (Courtesy of General Electric.)

The power transformer is a major power system component that permits economical power transmission with high efficiency and low series voltage drops. Since electric power is proportional to the product of voltage and current, low current levels (and therefore low I^2R losses and low IZ voltage drops) can be maintained for given power levels via high voltages. Power transformers transform ac voltage and current to optimum levels for generation, transmission, distribution, and utilization of electric power.

The development in 1885 by William Stanley of a commercially practical transformer was what made ac power systems more attractive than dc power systems.

Copyright 2017 Cengage Learning. All Rights Reserved. May not be copied, scanned, or duplicated, in whole or in part. Due to electronic rights, some third party content may be suppressed from the eBook and/or eChapter(s). Editorial review has deemed that any suppressed content does not materially affect the overall learning experience. Cengage Learning reserves the right to remove additional content at any time if subsequent rights restrictions require it.

The ac system with a transformer overcame voltage problems encountered in dc systems as load levels and transmission distances increased. Today's modern power transformers have nearly 100% efficiency, with ratings up to and beyond 1300 MVA.

In this chapter, basic transformer theory is reviewed and equivalent circuits for practical transformers operating under sinusoidal steady-state conditions are developed. Models of single-phase two-winding, three-phase two-winding, and three-phase three-winding transformers, as well as auto-transformers and regulating transformers are introduced. Also, the per-unit system, which simplifies power system analysis by eliminating the ideal transformer winding in transformer equivalent circuits, is introduced in this chapter and used throughout the remainder of the text.

CASE STUDY

The following article reviews methods of extending the life of a power transformer. Starting with specifying and purchasing; then manufacturing, installing, and commissioning; and finally operating and maintaining a transformer; options for extending life with the best cost-to-benefit ratio are explored [8].

POWER TRANSFORMERS
—*Life Management and Extension*

Carlos Gamez

TxMonitor

How Long is a Transformer Supposed to Last?

In this case study, the options to manage and, as far as possible, extend the life of these important assets in your system are explored. How long should a transformer last?

The life of a particular transformer depends on many factors, some of which are unpredictable in nature. In most circumstances there is not enough information to accurately predict the remaining life of a particular unit with any significant confidence. Current national and international standards and publications [1],[2],[3] and [4] favor the definition of life in "per unit" terms.

However, enough statistical data might be available in a particular system to be able to ascertain an estimated "average" life for a transformer in that system. An average life of 35 to 40 years is a reasonable number to be expected for transformers manufactured before the '90s and working under nominal conditions with some

Reprinted with permission from Carlos Gamez, "Power transformer life Part 3: Life management and extension," Transformers Magazine Vol. 1 Issue 3.

Copyright 2017 Cengage Learning. All Rights Reserved. May not be copied, scanned, or duplicated, in whole or in part. Due to electronic rights, some third party content may be suppressed from the eBook and/or eChapter(s). Editorial review has deemed that any suppressed content does not materially affect the overall learning experience. Cengage Learning reserves the right to remove additional content at any time if subsequent rights restrictions require it.

transformers, in very isolated cases, reaching into the 70 to 100 years of age mark [5].

So, if a transformer is to last 40 or more years of active service, what can you do to give it the best chances to do so?

The Life Cycle View of Life Extension

You might be tempted to think of the term life *extension* as something that is executed towards the end of the life of the asset in an attempt to extend its life. However, this would be a very shortsighted view of the topic. Life extension starts before the transformer is even manufactured. A holistic view of the complete life cycle of the unit will allow making the right decisions and putting the appropriate measures in place at every step of the way, from purchasing to disposal of the asset.

Just as with your own life and health, the most effective way of preventing a premature death is with prevention more than remediation. In the case of transformers this is not only logical, but considerably less costly. On a dollar per year of service of a particular asset, investing in prevention is almost always the wisest decision.

In this case study, the most important actions you can take to maximize the benefit that you get for your investment are laid out.

Specifying and Purchasing

A good start in life leads to a good-performing transformer during operation. By investing the time and resources in correctly specifying and sourcing the transformer most suitable for your application, you will save an incredible amount of money in the long run and a lot of headaches to your operations and maintenance team. A properly documented specification that adequately reflects your needs is essential to ensure that you are getting the right asset for the intended function. In many instances I have seen asset owners and buyers content with buying transformers that merely stick to the existing standards. While standards should be the starting point of any specification, they are certainly not sufficient in most cases. Standards are just the bare minimum that a transformer should comply with. By their very nature, standards cannot cater for the specific requirements that you might have in your specific operational context and circumstances.

Buying a transformer that simply meets the standards is like buying a car only specifying that you want it to have an engine, a body, and four wheels. The point is that you are likely to require certain characteristics in your transformers that are not listed or spelled out in the standards and that you will need to be explicit about when requesting a new unit. Things like specific types of bushing terminals, connection boxes, control wiring, and protective devices are but a few of the elements of your transformer design that you might want to stipulate to ensure compatibility with your environment. A well-crafted specification will also allow you to compare apples to apples when evaluating offers from various manufacturers. The best way to

Copyright 2017 Cengage Learning. All Rights Reserved. May not be copied, scanned, or duplicated, in whole or in part. Due to electronic rights, some third party content may be suppressed from the eBook and/or eChapter(s). Editorial review has deemed that any suppressed content does not materially affect the overall learning experience. Cengage Learning reserves the right to remove additional content at any time if subsequent rights restrictions require it.

avoid unexpected outcomes is to be explicit about what you want.

Manufacturing

You have now ordered a new unit with a proper specification and from a manufacturer you feel comfortable with. Well, the next step is building the transformer. A good manufacture is made up of many small details that add up to a properly built and good quality finished transformer. From the quality of the raw materials, to the expertise and skill of the people manufacturing these machines, to the attention to detail on every step of the manufacturing process, it all counts.

The process of building a transformer is complex and hand-labor intensive where a lot of things can go wrong. In fact, almost always something will not go exactly as planned. In essence you will want to associate with a manufacturer that is not shy in acknowledging and correcting the issues that will inevitably arise during the manufacturing process.

In the realm of client-to-manufacturer relations, each company will have its own preference in how these are handled. Some customers prefer a pre-approval process to select the manufacturer or manufacturers with whom they plan to establish a long-term relationship. Others prefer to witness key milestones at the factory during the manufacturing process like tanking or final testing. It is in your best interest to ensure that you have a mechanism to guarantee that the manufacturing quality of your transformer is adequate and the final product fulfills your expectations.

Installation and Commissioning

Most power transformers of a certain size and above are like flat-packed furniture—some assembly is required. The level of assembly required varies with the size and manufacturer of the transformer. In some cases it is only necessary to fit a few of the components like radiators and conservator tanks and then “top up” the oil. In other cases a full assembly is required that finishes with the vacuum dry-out and hot oil-fill process.

In any case, executing the assembly procedure according to the manufacturer’s recommendations will not only insure the unit is put together properly but also ensure your warranty is in full effect by the time the unit is placed in service. There are many factors that need to be taken care of during the final field assembly of the unit. You would want to ensure that a qualified team of technicians perform this assembly. Investing in the right service provider at this stage will increase your chances to avoid issues like oil leaks or any other type of assembly related malfunctions after energizing the transformer.

It is at this stage in the life of a transformer that the initial moisture level in the insulation system is established. It might be tempting to take shortcuts in this process. Sometimes the dry-out might take days to bring down the moisture to acceptable

Copyright 2017 Cengage Learning. All Rights Reserved. May not be copied, scanned, or duplicated, in whole or in part. Due to electronic rights, some third party content may be suppressed from the eBook and/or eChapter(s). Editorial review has deemed that any suppressed content does not materially affect the overall learning experience. Cengage Learning reserves the right to remove additional content at any time if subsequent rights restrictions require it.

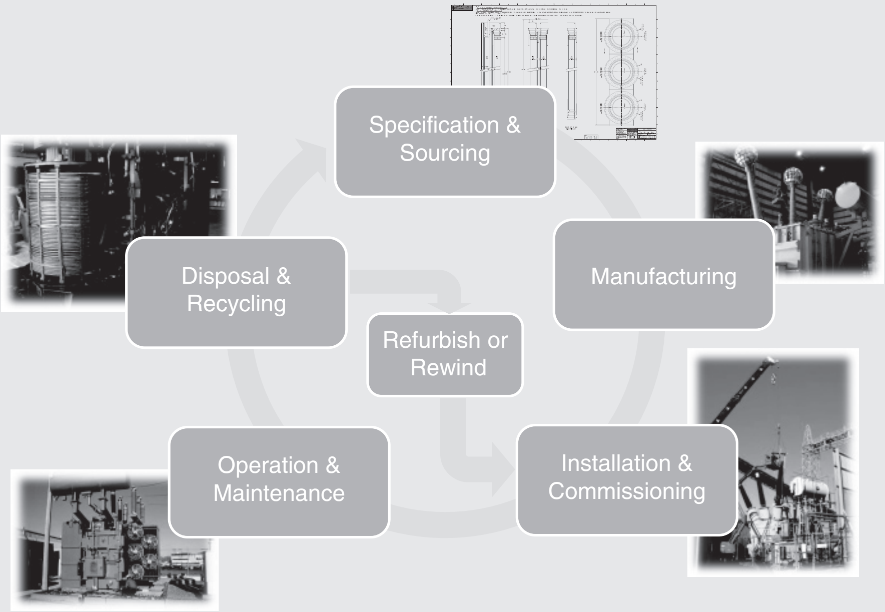
Specification & Sourcing
Manufacturing
Disposal & Recycling
Refurbish or Rewind
Operation & Maintenance
Installation & Commissioning

Figure 1 Typical transformer lifecycle

Figure 2 Good quality coils are essential to ensure the longevity of your transformer

Copyright 2017 Cengage Learning. All Rights Reserved. May not be copied, scanned, or duplicated, in whole or in part. Due to electronic rights, some third party content may be suppressed from the eBook and/or eChapter(s). Editorial review has deemed that any suppressed content does not materially affect the overall learning experience. Cengage Learning reserves the right to remove additional content at any time if subsequent rights restrictions require it.

levels (typically 0.5% by dry weight). But water is one of the main catalysts that accelerate the aging processes of the solid insulation of the transformer. Saving a few days or even a few hours of work at this stage has the potential to reduce the life by years in the long run. The economy is simply not there unless you want to operate your plant on a very short-term basis.

Operation and Maintenance

Since this stage in the life of a transformer is the longest (or at least it is supposed to be), much of your attention and day-to-day efforts will be spent in maintaining the unit in an adequate condition.

What you should focus your preventive maintenance efforts on during this period:

- Keep the transformer dry. Water is one of the main aging accelerating factors. In order to keep the transformer dry, you would want to ensure that there are no oil leaks (if oil can come out, moisture can come in). You will want to make sure that the oil preservation system is operating as the design intended. If silica gels are used, they should be dry and with enough capacity to dry the air that the transformer breathes. If diaphragms are used to separate the oil in the conservator tank from the ambient air, you want to make sure they are in good condition and free of ruptures. If automatic nitrogen equipment is used, it should be kept in good working order, with sufficient nitrogen in the

Figure 3 Different environments require different specifications

Copyright 2017 Cengage Learning. All Rights Reserved. May not be copied, scanned, or duplicated, in whole or in part. Due to electronic rights, some third party content may be suppressed from the eBook and/or eChapter(s). Editorial review has deemed that any suppressed content does not materially affect the overall learning experience. Cengage Learning reserves the right to remove additional content at any time if subsequent rights restrictions require it.

supply and that the regulating system always ensures adequate positive pressure in the nitrogen chamber. In summary, ensure that water does not find its way into the coils of the unit.

- Keep the oxygen to a minimum. Similar to the point above, you would want to minimize the exposure of the oil to oxygen, which obviously accelerates the oxidation processes in the transformer. The same recommendations given above to keep the water out of the unit are applicable to keep the oxygen out, although in some cases, like a conservator tank without diaphragm, it is not always possible.
- Ensure nominal operating conditions. Temperature plays a major role in the aging processes. The unit is designed to operate within a certain temperature range, and the more you can do to keep it within that range, the better chances you are giving the unit a long useful life. Situations like overloading are sometimes unavoidable, and in these cases, there are clear guidelines available in the technical literature to allow you to estimate the impact of overloading in the life of a particular transformer. On a maintenance basis, you can help by ensuring that the cooling system is operating adequately and that the top oil or winding hot-spot temperature has not reached alarm levels. If you find that this has happened, you need to investigate the root cause so you can address it as soon as possible.

Now, what if you are not the person who has watched the transformer its entire life, and you just got handed a fleet of old transformers to maintain? (Hard to imagine right?) In this case you are in corrective maintenance territory, where the best course of action would be:

- Establish the condition of each unit in your fleet. You have many tools at your disposal for this purpose. Try to gather as much information as possible on each unit, and establish an effective information storage and retrieval mechanism. Include oil-analysis history and any other test and inspection performed on each transformer. This information will allow you to establish a preliminary condition ranking for each asset in the fleet.
- Once the above has been established, you will have a clearer idea of which units are priorities and which units can wait.
- Depending on the state of each unit, a number of actions can be taken in order to ameliorate the current condition or remove some of the agents that might be causing the accelerated aging.

Copyright 2017 Cengage Learning. All Rights Reserved. May not be copied, scanned, or duplicated, in whole or in part. Due to electronic rights, some third party content may be suppressed from the eBook and/or eChapter(s). Editorial review has deemed that any suppressed content does not materially affect the overall learning experience. Cengage Learning reserves the right to remove additional content at any time if subsequent rights restrictions require it.

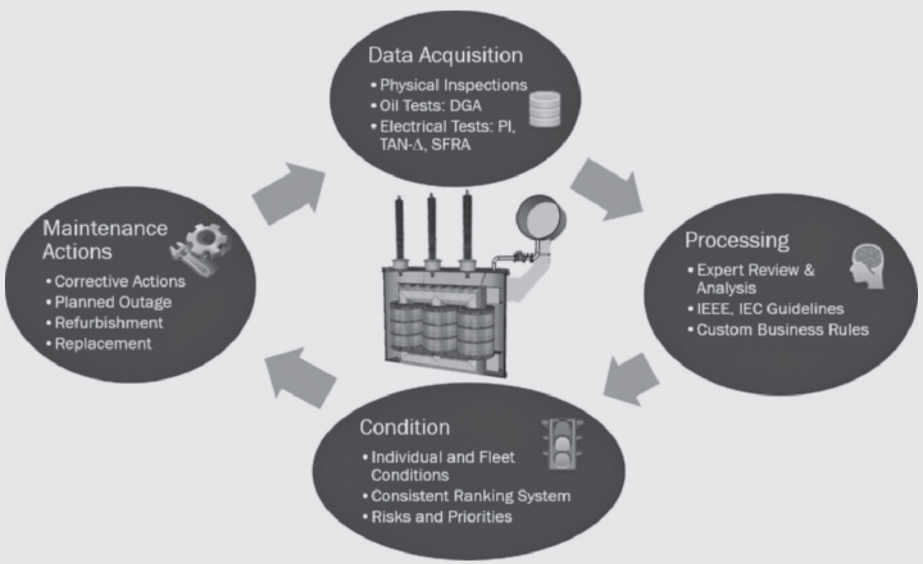
Data Acquisition
• Physical Inspections
• Oil Tests: DGA
• Electrical Tests: PI, TAN-Δ, SFRA
Processing
• Expert Review & Analysis
• IEEE, IEC Guidelines
• Custom Business Rules
Condition
• Individual and Fleet Conditions
• Consistent Ranking System
• Risks and Priorities
Maintenance Actions
• Corrective Actions
• Planned Outage
• Refurbishment
• Replacement

Figure 4 Example of a condition monitoring and maintenance program

- The oil can be processed to remove water and acids, which contribute to the aging processes.
- If any, more serious, failure modes are suspected, these need to be addressed on a case-by-case basis until you have satisfied the risk management policies of your company and you are aware of the condition of each unit.

Last but not least, an adequate condition monitoring program is essential to give you as much reaction time as possible if a failure mode starts to affect any particular transformer.

The condition monitoring method most commonly used is oil sampling and analysis. The analysis of the oil is a well-established technique that allows the early detection of incipient failures in the transformers. A suitable condition monitoring strategy will minimize the probability of unexpected failures and therefore minimize the overall operational risk of your transformer fleet.

References

[1] Institute of Electrical and Electronic Engineers (IEEE), C57.91-2011, *IEEE Guide for Loading Mineral-Oil-Immersed Transformers and Step-Voltage Regulators*. 2011. C57.91-2011.

[2] International Electrotechnical Commission (IEC), IEC 60076-7 ed1.0 - Power transformers—Part 7: *Loading guide for oil-immersed power transformers*. 2005. IEC 60076-7 ed1.0.

[3] Standards Australia, AS/NZS 60076.7: 2013 - *Power Transformers—Loading guide for oil-immersed power transformers*. s.l.: Standards Australia, Committee EL-008, 2013.

Copyright 2017 Cengage Learning. All Rights Reserved. May not be copied, scanned, or duplicated, in whole or in part. Due to electronic rights, some third party content may be suppressed from the eBook and/or eChapter(s). Editorial review has deemed that any suppressed content does not materially affect the overall learning experience. Cengage Learning reserves the right to remove additional content at any time if subsequent rights restrictions require it.

[4] CIGRE, *Cigré 227, guide for life management techniques for power transformer*. 2003. 227.
[5] ABB, Three workhorses retired after 100 years of active service in Australia! ABB, http://www.abbaustralia.com.au/cawp/seitp202/95613170ca5ec79dc1257cca001471b7.aspx., current 08.09.2014.

Author

After graduating in Electrical and Mechanical Engineering in 1996, Carlos started working as a Transformer Design Engineer at PROLEC-GE, the biggest transformer factory for General Electric on the American continent.

Over the course of the following years, he gained expertise working in various roles such as product development, manufacturing improvements, technology and software development, field engineering, and customer service.

In early 2007, Carlos was seconded by General Electric to move to Perth, WA, to start up the Transformer Division to provide field and workshop maintenance and repair services to customers across Australia.

Having fulfilled this mission, in early 2011, Carlos accepted a principal consultant position with Assetivity, a consultancy firm leader in asset management.

In early 2013, he moved to TxMonitor, part of MM Group Holdings, where he currently works as a principal consultant and product manager in developing innovative solutions for the electrical asset management industry using both his technical and business acumen. ■

3.1 THE IDEAL TRANSFORMER

Figure 3.1 shows a basic single-phase two-winding transformer, where the two windings are wrapped around a magnetic core [1, 2, 3]. It is assumed here that the transformer is operating under sinusoidal steady-state excitation. Shown in the figure are the phasor voltages E_1 and E_2 across the windings, and the phasor

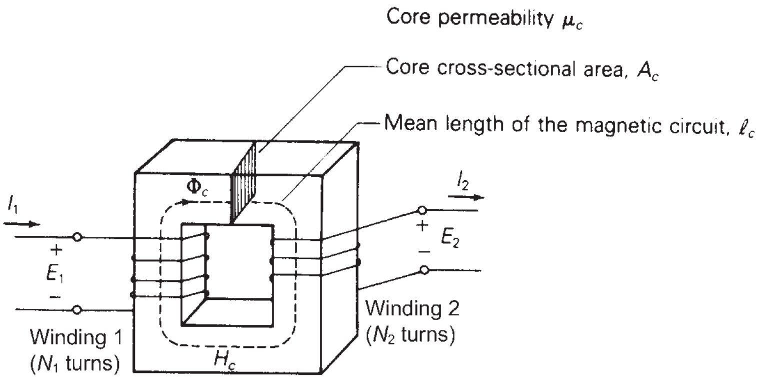
Core permeability μ_c
Core cross-sectional area, A_c
Mean length of the magnetic circuit, ℓ_c
Φ_c
I_1
I_2
+
E_1
−
+
E_2
−
Winding 1
(N_1 turns)
Winding 2
(N_2 turns)
H_c

FIGURE 3.1

Basic single-phase two-winding transformer

Copyright 2017 Cengage Learning. All Rights Reserved. May not be copied, scanned, or duplicated, in whole or in part. Due to electronic rights, some third party content may be suppressed from the eBook and/or eChapter(s). Editorial review has deemed that any suppressed content does not materially affect the overall learning experience. Cengage Learning reserves the right to remove additional content at any time if subsequent rights restrictions require it.

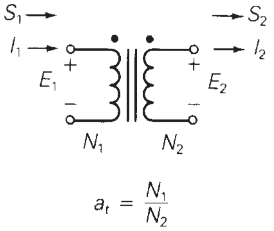

FIGURE 3.2 Schematic representation of a single-phase two-winding transformer

currents I_1 entering winding 1, which has N_1 turns, and I_2 leaving winding 2, which has N_2 turns. A phasor flux Φ_c set up in the core and a magnetic field intensity phasor H_c are also shown. The core has a cross-sectional area denoted A_c, a mean length of the magnetic circuit l_c, and a magnetic permeability μ_c, assumed constant.

For an ideal transformer, the following are assumed:

1. The windings have zero resistance; therefore, the I^2R losses in the windings are zero.
2. The core permeability μ_c is infinite, which corresponds to zero core reluctance.
3. There is no leakage flux; that is, the entire flux Φ_c is confined to the core and links both windings.
4. There are no core losses.

A schematic representation of a two-winding transformer is shown in Figure 3.2. Ampere's and Faraday's laws can be used along with the preceding assumptions to derive the ideal transformer relationships. *Ampere's law* states that the tangential component of the magnetic field intensity vector integrated along a closed path equals the net current enclosed by that path; that is,

$$\oint H_{\tan}\, dl = I_{\text{enclosed}} \tag{3.1.1}$$

If the core center line shown in Figure 3.1 is selected as the closed path, and if H_c is constant along the path as well as tangent to the path, then (3.1.1) becomes

$$H_c l_c = N_1 I_1 - N_2 I_2 \tag{3.1.2}$$

Note that the current I_1 is enclosed N_1 times and I_2 is enclosed N_2 times, one time for each turn of the coils. Also, using the right-hand rule*, current I_1 contributes to clockwise flux, but current I_2 contributes to counterclockwise flux. Thus, in (3.1.2)

---

*The right-hand rule for a coil is as follows: Wrap the fingers of your right hand around the coil in the direction of the current. Your right thumb then points in the direction of the flux.

Copyright 2017 Cengage Learning. All Rights Reserved. May not be copied, scanned, or duplicated, in whole or in part. Due to electronic rights, some third party content may be suppressed from the eBook and/or eChapter(s). Editorial review has deemed that any suppressed content does not materially affect the overall learning experience. Cengage Learning reserves the right to remove additional content at any time if subsequent rights restrictions require it.

the net current enclosed is $N_1I_1 - N_2I_2$. For constant core permeability μ_c, the magnetic flux density B_c within the core, also constant, is

$$B_c = \mu_c H_c \quad \text{Wb/m}^2 \tag{3.1.3}$$

and the core flux Φ_c is

$$\Phi_c = B_C \mathrm{A}_C \quad \text{Wb} \tag{3.1.4}$$

Using (3.1.3) and (3.1.4) in (3.1.2) yields

$$N_1I_1 - N_2I_2 = l_c B_c/\mu_c = \left(\frac{l_c}{\mu_c \mathrm{A}_c}\right)\Phi_c \tag{3.1.5}$$

Core reluctance R_c is defined as

$$\mathrm{R}_c = \frac{l_c}{\mu_c \mathrm{A}_c} \tag{3.1.6}$$

Then (3.1.5) becomes

$$N_1I_1 - N_2I_2 = \mathrm{R}_c\Phi_c \tag{3.1.7}$$

Equation (3.1.7) can be called *Ohm's law* for the magnetic circuit, wherein the net magnetomotive force mmf $= N_1I_1 - N_2I_2$ equals the product of the core reluctance R_c and the core flux Φ_c. Reluctance R_c, which impedes the establishment of flux in a magnetic circuit, is analogous to resistance in an electric circuit. For an ideal transformer, μ_c is assumed infinite, which from (3.1.6) means that R_c is 0, and (3.1.7) becomes

$$N_1I_1 = N_2I_2 \tag{3.1.8}$$

In practice, power transformer windings and cores are contained within enclosures, and the winding directions are not visible. One way of conveying winding information is to place a dot at one end of each winding such that when current enters a winding at the dot, it produces an mmf acting in the *same* direction. This dot convention is shown in the schematic of Figure 3.2. The dots are conventionally called *polarity marks.*

Equation (3.1.8) is written for current I_1 *entering* its dotted terminal and current I_2 *leaving* its dotted terminal. As such, I_1 and I_2 are *in phase,* since $I_1 = (N_2/N_1)I_2$, If the direction chosen for I_2 were reversed, such that both currents entered their dotted terminals, then I_1 would be 180° *out of phase* with I_2.

Faraday's law states that the voltage $e(t)$ induced across an N-turn winding by a time-varying flux $\phi(t)$ linking the winding is

$$e(t) = N\frac{d\phi(t)}{dt} \tag{3.1.9}$$

Assuming a sinusoidal steady-state flux with constant frequency ω, and representing $e(t)$ and $\phi(t)$ by their phasors E and Φ, (3.1.9) becomes

$$E = N(j\omega)\Phi \tag{3.1.10}$$

Copyright 2017 Cengage Learning. All Rights Reserved. May not be copied, scanned, or duplicated, in whole or in part. Due to electronic rights, some third party content may be suppressed from the eBook and/or eChapter(s). Editorial review has deemed that any suppressed content does not materially affect the overall learning experience. Cengage Learning reserves the right to remove additional content at any time if subsequent rights restrictions require it.

For an ideal transformer, the entire flux is assumed to be confined to the core, linking both windings. From Faraday's law, the induced voltages across the windings of Figure 3.1 are

$$E_1 = N_1(j\omega)\Phi_c \tag{3.1.11}$$

$$E_2 = N_2(j\omega)\Phi_c \tag{3.1.12}$$

Dividing (3.1.11) by (3.1.12) yields

$$\frac{E_1}{E_2} = \frac{N_1}{N_2} \tag{3.1.13}$$

or

$$\frac{E_1}{N_1} = \frac{E_2}{N_2} \tag{3.1.14}$$

The dots shown in Figure 3.2 indicate that the voltages E_1 and E_2, both of which have their + polarities at the dotted terminals, are in phase. If the polarity chosen for one of the voltages in Figure 3.1 were reversed, then E_1 would be 180° out of phase with E_2.

The turns ratio a_t is defined as follows:

$$a_t = \frac{N_1}{N_2} \tag{3.1.15}$$

Using a_t in (3.1.8) and (3.1.14), the basic relations for an ideal single-phase two-winding transformer are

$$E_1 = \left(\frac{N_1}{N_2}\right)E_2 = a_t E_2 \tag{3.1.16}$$

$$I_1 = \left(\frac{N_2}{N_1}\right)I_2 = \frac{I_2}{a_t} \tag{3.1.17}$$

Two additional relations concerning complex power and impedance can be derived from (3.1.16) and (3.1.17) as follows. The complex power entering winding 1 in Figure 3.2 is

$$S_1 = E_1 I_1^* \tag{3.1.18}$$

Using (3.1.16) and (3.1.17),

$$S_1 = E_1 I_1^* = (a_t E_2)\left(\frac{I_2}{a_t}\right)^* = E_2 I_2^* = S_2 \tag{3.1.19}$$

As shown by (3.1.19), the complex power S_1 entering winding 1 equals the complex power S_2 leaving winding 2. That is, an ideal transformer has no real or reactive power loss.

Copyright 2017 Cengage Learning. All Rights Reserved. May not be copied, scanned, or duplicated, in whole or in part. Due to electronic rights, some third party content may be suppressed from the eBook and/or eChapter(s). Editorial review has deemed that any suppressed content does not materially affect the overall learning experience. Cengage Learning reserves the right to remove additional content at any time if subsequent rights restrictions require it.

If an impedance Z_2 is connected across winding 2 of the ideal transformer in Figure 3.2, then

$$Z_2 = \frac{E_2}{I_2} \tag{3.1.20}$$

This impedance, when measured from winding 1, is

$$Z_2' = \frac{E_1}{I_1} = \frac{a_t E_2}{I_2/a_t} = a_t^2 Z_2 = \left(\frac{N_1}{N_2}\right)^2 Z_2 \tag{3.1.21}$$

Thus, the impedance Z_2 connected to winding 2 is referred to winding 1 by multiplying Z_2 by a_t^2, which is the square of the turns ratio.

EXAMPLE 3.1

Ideal, single-phase two-winding transformer

A single-phase two-winding transformer is rated 20 kVA, 480/120 V, and 60 Hz. A source connected to the 480-V winding supplies an impedance load connected to the 120-V winding. The load absorbs 15 kVA at 0.8 p.f. lagging when the load voltage is 118 V. Assume that the transformer is ideal and calculate the following:

a. The voltage across the 480-V winding.
b. The load impedance.
c. The load impedance referred to the 480-V winding.
d. The real and reactive power supplied to the 480-V winding.

SOLUTION

a. The circuit is shown in Figure 3.3, where winding 1 denotes the 480-V winding and winding 2 denotes the 120-V winding. Selecting the load voltage E_2 as the reference,

$$E_2 = 118\underline{/0°} \text{ V}$$

FIGURE 3.3

Circuit for Example 3.1

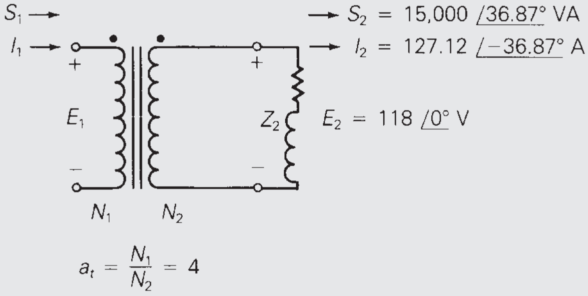
S_1
I_1
+
E_1
−
N_1
N_2
+
Z_2
−
$S_2 = 15{,}000\underline{/36.87°}$ VA
$I_2 = 127.12\underline{/-36.87°}$ A
$E_2 = 118\underline{/0°}$ V
$a_t = \frac{N_1}{N_2} = 4$

(*Continued*)

Copyright 2017 Cengage Learning. All Rights Reserved. May not be copied, scanned, or duplicated, in whole or in part. Due to electronic rights, some third party content may be suppressed from the eBook and/or eChapter(s). Editorial review has deemed that any suppressed content does not materially affect the overall learning experience. Cengage Learning reserves the right to remove additional content at any time if subsequent rights restrictions require it.

The turns ratio is, from (3.1.13),

$$a_t = \frac{N_1}{N_2} = \frac{E_{1\text{rated}}}{E_{2\text{rated}}} = \frac{480}{120} = 4$$

and the voltage across winding 1 is

$$E_1 = a_t E_2 = 4(118\underline{/0^\circ}) = 472\underline{/0^\circ} \quad \text{V}$$

b. The complex power S_2 absorbed by the load is

$$S_2 = E_2 I_2^* = 118 I_2^* = 15{,}000\underline{/\cos^{-1}}(0.8) = 15{,}000\underline{/36.87^\circ} \quad \text{VA}$$

Solving, the load current I_2 is

$$I_2 = 127.12\underline{/-36.87^\circ} \quad \text{A}$$

The load impedance Z_2 is

$$Z_2 = \frac{E_2}{I_2} = \frac{118\underline{/0^\circ}}{127.12\underline{/-36.87^\circ}} = 0.9283\underline{/36.87^\circ} \quad \Omega$$

c. From (3.1.21), the load impedance referred to the 480-V winding is

$$Z_2' = a_t^2 Z_2 = (4)^2(0.9283\underline{/36.87^\circ}) = 14.85\underline{/36.87^\circ} \quad \Omega$$

d. From (3.1.19)

$$S_1 = S_2 = 15{,}000\underline{/36.87^\circ} = 12{,}000 + j9000$$

Thus, the real and reactive powers supplied to the 480-V winding are

$$P_1 = \text{Re}\, S_1 = 12{,}000 \text{ W} = 12 \text{ kW}$$
$$Q_1 = \text{Im}\, S_1 = 9000 \text{ var} = 9 \text{ kvar}$$

Figure 3.4 shows a schematic of a conceptual single-phase, phase-shifting transformer. This transformer is not an idealization of an actual transformer since it is physically impossible to obtain a complex turns ratio. It is used later in this chapter as a mathematical model for representing phase shift of three-phase transformers. As shown in Figure 3.4, the complex turns ratio a_t is defined for the phase-shifting transformer as

$$a_t = \frac{e^{j\phi}}{1} = e^{j\phi} \tag{3.1.22}$$

where ϕ is the phase-shift angle. The transformer relations are then

$$E_1 = a_t E_2 = e^{j\phi} E_2 \tag{3.1.23}$$

Copyright 2017 Cengage Learning. All Rights Reserved. May not be copied, scanned, or duplicated, in whole or in part. Due to electronic rights, some third party content may be suppressed from the eBook and/or eChapter(s). Editorial review has deemed that any suppressed content does not materially affect the overall learning experience. Cengage Learning reserves the right to remove additional content at any time if subsequent rights restrictions require it.

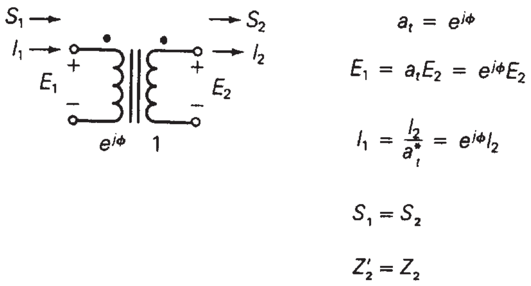

FIGURE 3.4

Schematic representation of a conceptual single-phase, phase-shifting transformer

$$I_1 = \frac{I_2}{a_t^*} = e^{j\phi} I_2 \tag{3.1.24}$$

Note that the phase angle of E_1 leads the phase angle of E_2 by ϕ. Similarly, I_1 leads I_2 by the angle ϕ. However, the magnitudes are unchanged; that is, $|E_1| = |E_2|$ and $|I_1| = |I_2|$.

From these two relations, the following two additional relations are derived:

$$S_1 = E_1 I_1^* = (a_t E_2)\left(\frac{I_2}{a_t^*}\right)^* = E_2 I_2^* = S_2 \tag{3.1.25}$$

$$Z_2' = \frac{E_1}{I_1} = \frac{a_t E_2}{\dfrac{1}{a_t^*} I_2} = |a_t|^2 Z_2 = Z_2 \tag{3.1.26}$$

Thus, impedance is unchanged when it is referred from one side of an ideal phase-shifting transformer to the other. Also, the ideal phase-shifting transformer has no real or reactive power losses since $S_1 = S_2$.

Note that (3.1.23) and (3.1.24) for the phase-shifting transformer are the same as (3.1.16) and (3.1.17) for the ideal physical transformer except for the complex conjugate (*) in (3.1.24). The complex conjugate for the phase-shifting transformer is required to make $S_1 = S_2$ (complex power into winding 1 equals complex power out of winding 2), as shown in (3.1.25).

3.2 EQUIVALENT CIRCUITS FOR PRACTICAL TRANSFORMERS

Figure 3.5 shows an equivalent circuit for a practical single-phase two-winding transformer, which differs from the ideal transformer as follows:

1. The windings have resistance.
2. The core permeability μ_c is finite.

Copyright 2017 Cengage Learning. All Rights Reserved. May not be copied, scanned, or duplicated, in whole or in part. Due to electronic rights, some third party content may be suppressed from the eBook and/or eChapter(s). Editorial review has deemed that any suppressed content does not materially affect the overall learning experience. Cengage Learning reserves the right to remove additional content at any time if subsequent rights restrictions require it.

FIGURE 3.5

Equivalent circuit of a practical single-phase two-winding transformer

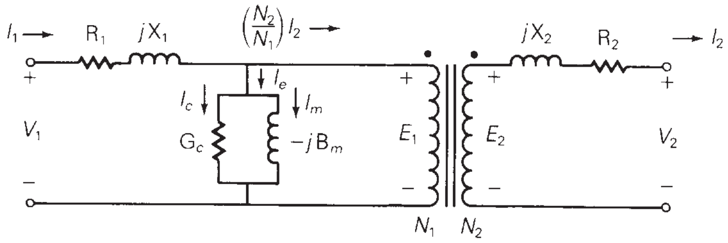

3. The magnetic flux is not entirely confined to the core.
4. There are real and reactive power losses in the core.

The resistance R_1 is included in series with winding 1 of the figure to account for I^2R losses in this winding. A reactance X_1, called the *leakage reactance* of winding 1, is also included in series with winding 1 to account for the leakage flux of winding 1. This leakage flux is the component of the flux that links winding 1 but does not link winding 2; it causes a voltage drop $I_1(jX_1)$, which is proportional to I_1 and leads I_1 by 90°. There is also a reactive power loss $I_1^2X_1$ associated with this leakage reactance. Similarly, there is a resistance R_2 and a leakage reactance X_2 in series with winding 2.

Equation (3.1.7) shows that for finite core permeability μ_c, the total mmf is not zero. Dividing (3.1.7) by N_1 and using (3.1.11), the result is

$$I_1 - \left(\frac{N_2}{N_1}\right)I_2 = \frac{R_c}{N_1}\Phi_c = \frac{R_c}{N_1}\left(\frac{E_1}{j\omega N_1}\right) = -j\left(\frac{R_c}{\omega N_1^2}\right)E_1 \tag{3.2.1}$$

Defining the term on the right-hand side of (3.2.1) to be I_m, called *magnetizing* current, it is evident that I_m lags E_1 by 90°, and can be represented by a shunt inductor with susceptance $B_m = \left(\frac{R_c}{\omega N_1^2}\right)$ mhos.* However, in reality, there is an additional shunt branch, represented by a resistor with conductance G_c mhos, which carries a current I_c, called the *core loss* current. I_c is in phase with E_1. When the core loss current I_c is included, (3.2.1) becomes

$$I_1 - \left(\frac{N_2}{N_1}\right)I_2 = I_c + I_m = (G_c - jB_m)E_1 \tag{3.2.2}$$

The equivalent circuit of Figure 3.5, which includes the shunt branch with admittance $(G_c - jB_m)$ mhos, satisfies the KCL equation (3.2.2). Note that when winding 2 is open ($I_2 = 0$) and when a sinusoidal voltage V_1 is applied to winding 1, then (3.2.2) indicates that the current I_1 will have two components: the core loss current I_c and the magnetizing current I_m. Associated with I_c is a real power loss $I_c^2/G_c = E_1^2G_c$ W. This real power loss accounts for both hysteresis and eddy current losses within the core. Hysteresis loss occurs because a cyclic variation of flux within the core requires

---

*The units of admittance, conductance, and susceptance, which in the SI system are siemens (with symbol S), are also called mhos (with symbol ℧) or ohms^{-1} (with symbol Ω^{-1}).

Copyright 2017 Cengage Learning. All Rights Reserved. May not be copied, scanned, or duplicated, in whole or in part. Due to electronic rights, some third party content may be suppressed from the eBook and/or eChapter(s). Editorial review has deemed that any suppressed content does not materially affect the overall learning experience. Cengage Learning reserves the right to remove additional content at any time if subsequent rights restrictions require it.

energy dissipated as heat. As such, hysteresis loss can be reduced by the use of special high grades of alloy steel as core material. Eddy current loss occurs because induced currents called eddy currents flow within the magnetic core perpendicular to the flux. As such, eddy current loss can be reduced by constructing the core with laminated sheets of alloy steel. Associated with I_m is a reactive power loss $I_m^2/B_m = E_1^2 B_m$ var. This reactive power is required to magnetize the core. The phasor sum $(I_c + I_m)$ is called the *exciting* current I_e.

Figure 3.6 shows three alternative equivalent circuits for a practical single-phase two-winding transformer. In Figure 3.6(a), the resistance R_2 and leakage reactance X_2 of winding 2 are referred to winding 1 via (3.1.21).

In Figure 3.6(b), the shunt branch is omitted, which corresponds to neglecting the exciting current. Since the exciting current is usually less than 5% of rated current, neglecting it in power system studies is often valid unless transformer efficiency or exciting current phenomena are of particular concern. For large power transformers rated more than 500 kVA, the winding resistances, which are small compared to the leakage reactances, often can be neglected, as shown in Figure 3.6(c).

Thus, a practical transformer operating in sinusoidal steady state is equivalent to an ideal transformer with external impedance and admittance branches, as shown in Figure 3.6. The external branches can be evaluated from short-circuit and open-circuit tests, as illustrated by the following example.

FIGURE 3.6

Equivalent circuits for a practical single-phase two-winding transformer

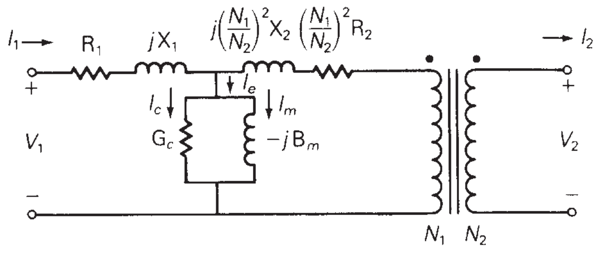
I_1
R_1
jX_1
$j\left(\frac{N_1}{N_2}\right)^2 X_2$
$\left(\frac{N_1}{N_2}\right)^2 R_2$
I_2
+
I_e
I_c
I_m
V_1
G_c
$-jB_m$
V_2
–
N_1 N_2

(a) R_2 and X_2 are referred to winding 1

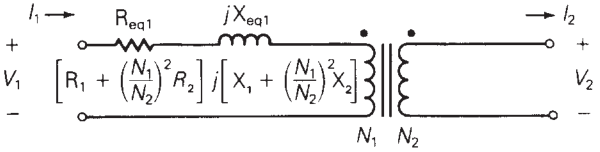
I_1
R_{eq1}
jX_{eq1}
I_2
+
V_1
$\left[R_1 + \left(\frac{N_1}{N_2}\right)^2 R_2\right]$
$j\left[X_1 + \left(\frac{N_1}{N_2}\right)^2 X_2\right]$
V_2
–
N_1 N_2

(b) Neglecting exciting current

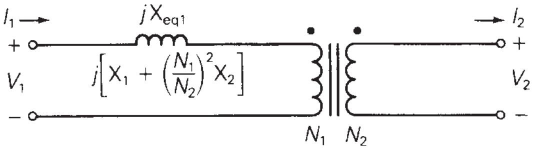

(c) Neglecting exciting current and I^2R winding loss

Copyright 2017 Cengage Learning. All Rights Reserved. May not be copied, scanned, or duplicated, in whole or in part. Due to electronic rights, some third party content may be suppressed from the eBook and/or eChapter(s). Editorial review has deemed that any suppressed content does not materially affect the overall learning experience. Cengage Learning reserves the right to remove additional content at any time if subsequent rights restrictions require it.

EXAMPLE 3.2

Transformer short-circuit and open-circuit tests

A single-phase two-winding transformer is rated 20 kVA, 480/120 volts, and 60 Hz. During a short-circuit test, where rated current at rated frequency is applied to the 480-volt winding (denoted winding 1), with the 120-volt winding (winding 2) shorted, the following readings are obtained: $V_1 = 35$ volts, $P_1 = 300$ W. During an open-circuit test, where rated voltage is applied to winding 2, with winding 1 open, the following readings are obtained: $I_2 = 12$ A, $P_2 = 200$ W.

a. From the short-circuit test, determine the equivalent series impedance $Z_{eq1} = R_{eq1} + jX_{eq1}$ referred to winding 1. Neglect the shunt admittance.

b. From the open-circuit test, determine the shunt admittance $Y_m = G_c - jB_m$ referred to winding 1. Neglect the series impedance.

SOLUTION

a. The equivalent circuit for the short-circuit test is shown in Figure 3.7(a), where the shunt admittance branch is neglected. Rated current for winding 1 is

$$I_{1\text{rated}} = \frac{S_{\text{rated}}}{V_{1\text{rated}}} = \frac{20 \times 10^3}{480} = 41.667 \quad \text{A}$$

R_{eq1}, Z_{eq1}, and X_{eq1} are then determined as follows:

$$R_{eq1} = \frac{P_1}{I_{1\text{rated}}^2} = \frac{300}{(41.667)^2} = 0.1728 \quad \Omega$$

$$|Z_{eq1}| = \frac{V_1}{I_{1\text{rated}}} = \frac{35}{41.667} = 0.8400 \quad \Omega$$

$$X_{eq1} = \sqrt{Z_{eq1}^2 - R_{eq1}^2} = 0.8220 \quad \Omega$$

$$Z_{eq1} = R_{eq1} + jX_{eq1} + 0.1728 + j0.8220 = 0.8400\underline{/78.13^\circ} \quad \Omega$$

b. The equivalent circuit for the open-circuit test is shown in Figure 3.7(b), where the series impedance is neglected. From (3.1.16),

$$V_1 = E_1 = a_t E_2 = \frac{N_1}{N_2} V_{2\text{rated}} = \frac{480}{120}(120) = 480 \quad \text{volts}$$

G_c, Y_m, and B_m are then determined as follows:

$$G_c = \frac{P_2}{V_1^2} = \frac{200}{(480)^2} = 0.000868 \quad \text{S}$$

$$|Y_m| = \frac{\left(\frac{N_2}{N_1}\right) I_2}{V_1} = \frac{\left(\frac{120}{480}\right)(12)}{480} = 0.00625 \quad \text{S}$$

Copyright 2017 Cengage Learning. All Rights Reserved. May not be copied, scanned, or duplicated, in whole or in part. Due to electronic rights, some third party content may be suppressed from the eBook and/or eChapter(s). Editorial review has deemed that any suppressed content does not materially affect the overall learning experience. Cengage Learning reserves the right to remove additional content at any time if subsequent rights restrictions require it.

FIGURE 3.7

Circuits for Example 3.2

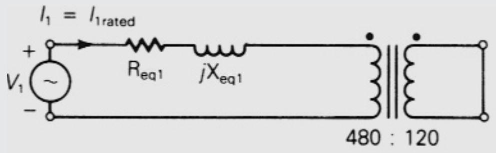

(a) Short-circuit test (neglecting shunt admittance)

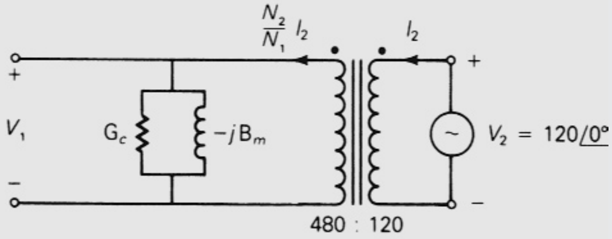

(b) Open-circuit test (neglecting series impedance)

$$B_m = \sqrt{Y_m^2 - G_c^2} = \sqrt{(0.00625)^2 - (0.000868)^2} = 0.00619 \quad \text{S}$$

$$Y_m = G_c - jB_m = 0.000868 - j0.00619 = 0.00625\underline{/-82.02°} \quad \text{S}$$

Note that the equivalent series impedance is usually evaluated at rated current from a short-circuit test, and the shunt admittance is evaluated at rated voltage from an open-circuit test. For small variations in transformer operation near rated conditions, the impedance and admittance values are often assumed constant.

The following are not represented by the equivalent circuit of Figure 3.5:

1. Saturation
2. Inrush current
3. Nonsinusoidal exciting current
4. Surge phenomena

They are briefly discussed in the following sections.

SATURATION

In deriving the equivalent circuit of the ideal and practical transformers, constant core permeability μ_c and the linear relationship $B_c = \mu_c H_c$ of (3.1.3) were assumed. However, the relationship between B and H for ferromagnetic materials used for transformer cores is nonlinear and multivalued. Figure 3.8 shows a set of B–H curves for a grain-oriented electrical steel typically used in transformers. As shown, each curve is multivalued, which is caused by hysteresis. For many engineering applications, the

Copyright 2017 Cengage Learning. All Rights Reserved. May not be copied, scanned, or duplicated, in whole or in part. Due to electronic rights, some third party content may be suppressed from the eBook and/or eChapter(s). Editorial review has deemed that any suppressed content does not materially affect the overall learning experience. Cengage Learning reserves the right to remove additional content at any time if subsequent rights restrictions require it.

FIGURE 3.8

B–H curves for M-5 grain-oriented electrical steel 0.012 in. thick (Reprinted with permission of AK Steel Corporation.)

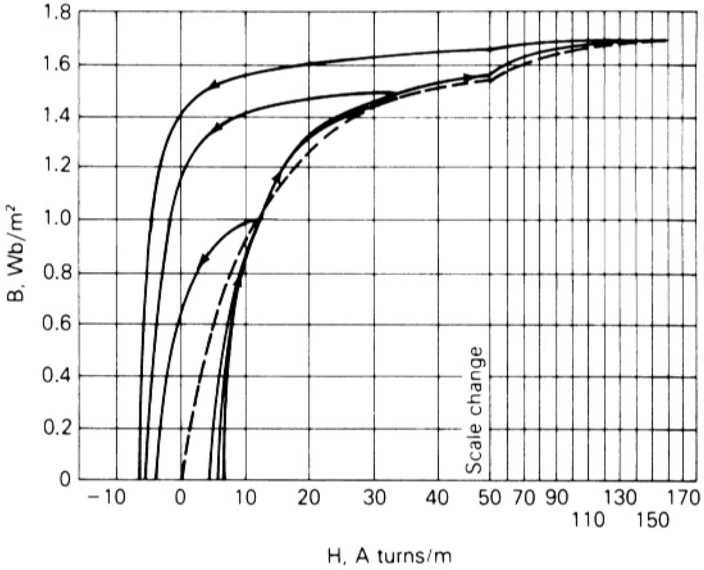

B–H curves can be adequately described by the dashed line drawn through the curves in Figure 3.8. Note that as H increases, the core becomes saturated; that is, the curves flatten out as B increases above 1 Wb/m^2. If the magnitude of the voltage applied to a transformer is too large, the core will saturate and a high magnetizing current will flow. In a well-designed transformer, the applied peak voltage causes the peak flux density in steady state to occur at the knee of the B–H curve, with a corresponding low value of magnetizing current.

INRUSH CURRENT

When a transformer is first energized, a transient current much larger than rated transformer current can flow for several cycles. This current, called *inrush current,* is nonsinusoidal and has a large dc component. To understand the cause of inrush, assume that before energization, the transformer core is magnetized with a residual flux density B(0) = 1.5 Wb/m^2 (near the knee of the dotted curve in Figure 3.8). If the transformer is then energized when the source voltage is positive and increasing, Faraday's law, (3.1.9), will cause the flux density B(t) to increase further, since

$$\mathrm{B}(t) = \frac{\phi(t)}{\mathrm{A}} = \frac{1}{\mathrm{NA}}\int_0^t e(t)\,dt + \mathrm{B}(0)$$

As B(t) moves into the saturation region of the B–H curve, large values of H(t) will occur, and, from Ampere's law, (3.1.1), corresponding large values of current $i(t)$ will flow for several cycles until it has dissipated. Since normal inrush currents can be as large as abnormal short-circuit currents in transformers, transformer protection schemes must be able to distinguish between these two types of currents.

Copyright 2017 Cengage Learning. All Rights Reserved. May not be copied, scanned, or duplicated, in whole or in part. Due to electronic rights, some third party content may be suppressed from the eBook and/or eChapter(s). Editorial review has deemed that any suppressed content does not materially affect the overall learning experience. Cengage Learning reserves the right to remove additional content at any time if subsequent rights restrictions require it.

NONSINUSOIDAL EXCITING CURRENT

When a sinusoidal voltage is applied to one winding of a transformer with the other winding open, the flux $\phi(t)$ and flux density B(t) will, from Faraday's law, (3.1.9), be very nearly sinusoidal in steady state. However, the magnetic field intensity H(t) and the resulting exciting current is not sinusoidal in steady state, due to the nonlinear B–H curve. If the exciting current is measured and analyzed by Fourier analysis techniques, one finds that it has a fundamental component and a set of odd harmonics. The principal harmonic is the third, whose rms value is typically about 40% of the total rms exciting current. However, the nonsinusoidal nature of exciting current is usually neglected unless harmonic effects are of direct concern, because the exciting current itself is usually less than 5% of rated current for power transformers.

SURGE PHENOMENA

When power transformers are subjected to transient overvoltages caused by lightning or switching surges, the capacitances of the transformer windings have important effects on transient response. Transformer winding capacitances and response to surges are discussed in Chapter 13.

3.3 THE PER-UNIT SYSTEM

Power-system quantities such as voltage, current, power, and impedance are often expressed in per-unit or percent of specified base values. For example, if a base voltage of 20 kV is specified, then the voltage 18 kV is (18/20) = 0.9 per unit or 90%. Calculations then can be made with per-unit quantities rather than with the actual quantities.

One advantage of the per-unit system is that by properly specifying base quantities, the transformer equivalent circuit can be simplified. The ideal transformer winding can be eliminated, such that voltages, currents, and external impedances and admittances expressed in per-unit do not change when they are referred from one side of a transformer to the other. This can be a significant advantage even in a power system of moderate size, where hundreds of transformers may be encountered. Using the per-unit system avoids the possibility of making serious calculation errors when referring quantities from one side of a transformer to the other. Another advantage of the per-unit system is that the per-unit impedances of electrical equipment of similar type usually lie within a narrow numerical range when the equipment ratings are used as base values. Because of this, per-unit impedance data can be checked rapidly for gross errors by someone familiar with per-unit quantities. In addition, manufacturers usually specify the impedances of machines and transformers in per-unit or percent of nameplate rating.

Per-unit quantities are calculated as follows:

$$\text{per-unit quantity} = \frac{\text{actual quantity}}{\text{base value of quantity}} \tag{3.3.1}$$

Copyright 2017 Cengage Learning. All Rights Reserved. May not be copied, scanned, or duplicated, in whole or in part. Due to electronic rights, some third party content may be suppressed from the eBook and/or eChapter(s). Editorial review has deemed that any suppressed content does not materially affect the overall learning experience. Cengage Learning reserves the right to remove additional content at any time if subsequent rights restrictions require it.

where *actual quantity* is the value of the quantity in the actual units. The base value has the same units as the actual quantity, thus making the per-unit quantity dimensionless. Also, the base value is always a real number. Therefore, the angle of the per-unit quantity is the same as the angle of the actual quantity.

Two independent base values can be arbitrarily selected at one point in a power system. Usually the base voltage V_{baseLN} and base complex power $S_{\text{base}1\phi}$ are selected for either a single-phase circuit or for one phase of a three-phase circuit. Then, in order for electrical laws to be valid in the per-unit system, the following relations must be used for other base values:

$$P_{\text{base}1\phi} = Q_{\text{base}1\phi} = S_{\text{base}1\phi} \tag{3.3.2}$$

$$I_{\text{base}} = \frac{S_{\text{base}1\phi}}{V_{\text{baseLN}}} \tag{3.3.3}$$

$$Z_{\text{base}} = R_{\text{base}} = X_{\text{base}} = \frac{V_{\text{baseLN}}}{I_{\text{base}}} = \frac{V^2_{\text{baseLN}}}{S_{\text{base}1\phi}} \tag{3.3.4}$$

$$Y_{\text{base}} = G_{\text{base}} = B_{\text{base}} = \frac{1}{Z_{\text{base}}} \tag{3.3.5}$$

In (3.3.2) through (3.3.5), the subscripts LN and 1ϕ denote "line-to-neutral" and "per-phase," respectively, for three-phase circuits. These equations are also valid for single-phase circuits, where subscripts can be omitted.

Convention requires adoption of the following two rules for base quantities:

1. The value of $S_{\text{base}1\phi}$ is the same for the entire power system of concern.
2. The ratio of the voltage bases on either side of a transformer is selected to be the same as the ratio of the transformer voltage ratings.

With these two rules, a per-unit impedance remains unchanged when referred from one side of a transformer to the other.

EXAMPLE 3.3

Per-unit impedance: single-phase transformer

A single-phase two-winding transformer is rated 20 kVA, 480/120 volts, and 60 Hz. The equivalent leakage impedance of the transformer referred to the 120-volt winding, denoted winding 2, is $Z_{\text{eq}2} = 0.0525\underline{/78.13^\circ}\ \Omega$. Using the transformer ratings as base values, determine the per-unit leakage impedance referred to winding 2 and referred to winding 1.

SOLUTION

The values of S_{base}, $V_{\text{base}1}$, and $V_{\text{base}2}$ are, from the transformer ratings,

$$S_{\text{base}} = 20 \text{ kVA}, \quad V_{\text{base}1} = 480 \text{ volts}, \quad V_{\text{base}2} = 120 \text{ volts}$$

Copyright 2017 Cengage Learning. All Rights Reserved. May not be copied, scanned, or duplicated, in whole or in part. Due to electronic rights, some third party content may be suppressed from the eBook and/or eChapter(s). Editorial review has deemed that any suppressed content does not materially affect the overall learning experience. Cengage Learning reserves the right to remove additional content at any time if subsequent rights restrictions require it.

Using (3.3.4), the base impedance on the 120-volt side of the transformer is

$$Z_{\text{base2}} = \frac{V^2_{\text{base2}}}{S_{\text{base}}} = \frac{(120)^2}{20{,}000} = 0.72 \quad \Omega$$

Then, using (3.3.1), the per-unit leakage impedance referred to winding 2 is

$$Z_{\text{eq2p.u.}} = \frac{Z_{\text{eq2}}}{Z_{\text{base2}}} = \frac{0.0525\underline{/78.13^\circ}}{0.72} = 0.0729\underline{/78.13^\circ} \quad \text{per unit}$$

If Z_{eq2} is referred to winding 1,

$$Z_{\text{eq1}} = a_t^2 Z_{\text{eq2}} = \left(\frac{N_1}{N_2}\right)^2 Z_{\text{eq2}} = \left(\frac{480}{120}\right)^2 (0.0525\underline{/78.13^\circ})$$

$$= 0.84\underline{/78.13^\circ} \quad \Omega$$

The base impedance on the 480 volt side of the transformer is

$$Z_{\text{base1}} = \frac{V^2_{\text{base1}}}{S_{\text{base}}} = \frac{(480)^2}{20{,}000} = 11.52 \quad \Omega$$

and the per-unit leakage reactance referred to winding 1 is

$$Z_{\text{eq1p.u.}} = \frac{Z_{\text{eq1}}}{Z_{\text{base1}}} = \frac{0.84\underline{/78.13^\circ}}{11.52} = 0.0729 \ \underline{/78.13^\circ} \text{ per unit} = Z_{\text{eq2p.u.}}$$

Thus, the *per-unit* leakage impedance remains unchanged when referred from winding 2 to winding 1. This has been achieved by specifying

$$\frac{V_{\text{base1}}}{V_{\text{base2}}} = \frac{V_{\text{rated1}}}{V_{\text{rated2}}} = \left(\frac{480}{120}\right)$$

Figure 3.9 shows three per-unit circuits of a single-phase two-winding transformer. The ideal transformer, shown in Figure 3.9(a), satisfies the per-unit relations $E_{1\text{p.u.}} = E_{2\text{p.u.}}$ and $I_{1\text{p.u.}} = I_{2\text{p.u.}}$, which can be derived as follows. First divide (3.1.16) by V_{base1}:

$$E_{1\text{p.u.}} = \frac{E_1}{V_{\text{base1}}} = \frac{N_1}{N_2} \times \frac{E_2}{V_{\text{base1}}} \tag{3.3.6}$$

Then, using $V_{\text{base1}}/V_{\text{base2}} = V_{\text{rated1}}/V_{\text{rated2}} = N_1/N_2$,

$$E_{1\text{p.u.}} = \frac{N_1}{N_2} \frac{E_2}{\left(\frac{N_1}{N_2}\right) V_{\text{base2}}} = \frac{E_2}{V_{\text{base2}}} = E_{2\text{p.u.}} \tag{3.3.7}$$

Copyright 2017 Cengage Learning. All Rights Reserved. May not be copied, scanned, or duplicated, in whole or in part. Due to electronic rights, some third party content may be suppressed from the eBook and/or eChapter(s). Editorial review has deemed that any suppressed content does not materially affect the overall learning experience. Cengage Learning reserves the right to remove additional content at any time if subsequent rights restrictions require it.

FIGURE 3.9

Per-unit equivalent circuits of a single-phase two-winding transformer

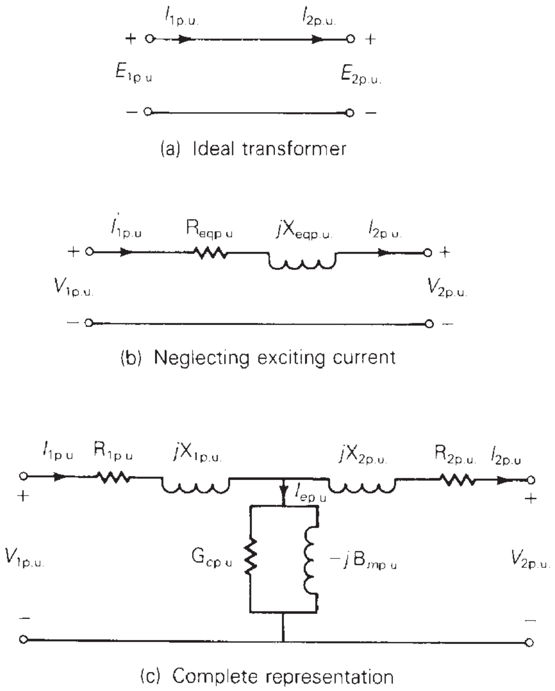

$I_{1\text{p.u.}}$
$I_{2\text{p.u.}}$
$E_{1\text{p.u.}}$
$E_{2\text{p.u.}}$
+
−
(a) Ideal transformer
$I_{1\text{p.u.}}$
$R_{\text{eqp.u.}}$
$jX_{\text{eqp.u.}}$
$I_{2\text{p.u.}}$
$V_{1\text{p.u.}}$
$V_{2\text{p.u.}}$
(b) Neglecting exciting current
$I_{1\text{p.u.}}$
$R_{1\text{p.u.}}$
$jX_{1\text{p.u.}}$
$jX_{2\text{p.u.}}$
$R_{2\text{p.u.}}$
$I_{2\text{p.u.}}$
$I_{e\text{p.u.}}$
$G_{c\text{p.u.}}$
$-jB_{m\text{p.u.}}$
$V_{1\text{p.u.}}$
$V_{2\text{p.u.}}$
(c) Complete representation

Similarly, divide (3.1.17) by I_{base1}:

$$I_{1\text{p.u.}} = \frac{I_1}{I_{\text{base1}}} = \frac{N_2}{N_1}\frac{I_2}{I_{\text{base1}}} \tag{3.3.8}$$

Then, using $I_{\text{base1}} = S_{\text{base}}/V_{\text{base1}} = S_{\text{base}}/[(N_1/N_2)V_{\text{base2}}] = (N_2/N_1)I_{\text{base2}}$

$$I_{1\text{p.u.}} = \frac{N_2}{N_1}\frac{I_2}{\left(\frac{N_2}{N_1}\right)I_{\text{base2}}} = \frac{I_2}{I_{\text{base2}}} = I_{2\text{p.u.}} \tag{3.3.9}$$

Thus, the ideal transformer winding in Figure 3.2 is eliminated from the per-unit circuit in Figure 3.9(a). The per-unit leakage impedance is included in Figure 3.9(b), and the per-unit shunt admittance branch is added in Figure 3.9(c) to obtain the complete representation.

When only one component, such as a transformer, is considered, the nameplate ratings of that component are usually selected as base values. When several components are involved, however, the system base values may be different from the nameplate ratings of any particular device. It is then necessary to convert the per-unit impedance of a device from its nameplate ratings to the system base values. To convert a per-unit impedance from “old” to “new” base values, use

$$Z_{\text{p.u.new}} = \frac{Z_{\text{actual}}}{Z_{\text{basenew}}} = \frac{Z_{\text{p.u.old}}Z_{\text{baseold}}}{Z_{\text{basenew}}} \tag{3.3.10}$$

Copyright 2017 Cengage Learning. All Rights Reserved. May not be copied, scanned, or duplicated, in whole or in part. Due to electronic rights, some third party content may be suppressed from the eBook and/or eChapter(s). Editorial review has deemed that any suppressed content does not materially affect the overall learning experience. Cengage Learning reserves the right to remove additional content at any time if subsequent rights restrictions require it.

or, from (3.3.4),

$$Z_{\text{p.u.new}} = Z_{\text{p.u.old}}\left(\frac{V_{\text{baseold}}}{V_{\text{basenew}}}\right)^2\left(\frac{S_{\text{basenew}}}{S_{\text{baseold}}}\right) \tag{3.3.11}$$

EXAMPLE 3.4

Per-unit circuit: three-zone single-phase network

Three zones of a single-phase circuit are identified in Figure 3.10(a). The zones are connected by transformers T_1 and T_2, whose ratings are also shown. Using base values of 30 kVA and 240 volts in zone 1, draw the per-unit circuit and determine the per-unit impedances and the per-unit source voltage. Then calculate the load current both in per-unit and in amperes. Transformer winding resistances and shunt admittance branches are neglected.

FIGURE 3.10

Circuit for Example 3.4

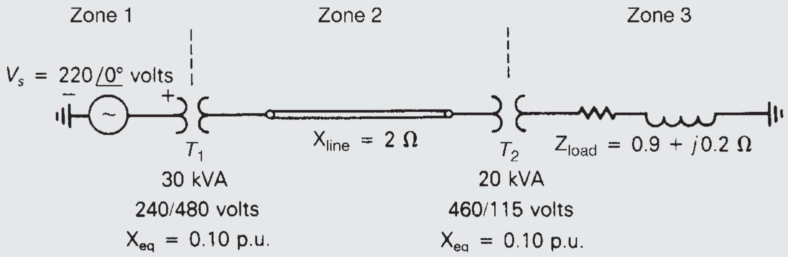
Zone 1
Zone 2
Zone 3
V_s = 220/0° volts
−
+
T_1
30 kVA
240/480 volts
X_{eq} = 0.10 p.u.
X_{line} = 2 Ω
T_2
20 kVA
460/115 volts
X_{eq} = 0.10 p.u.
Z_{load} = 0.9 + j0.2 Ω

(a) Single-phase circuit

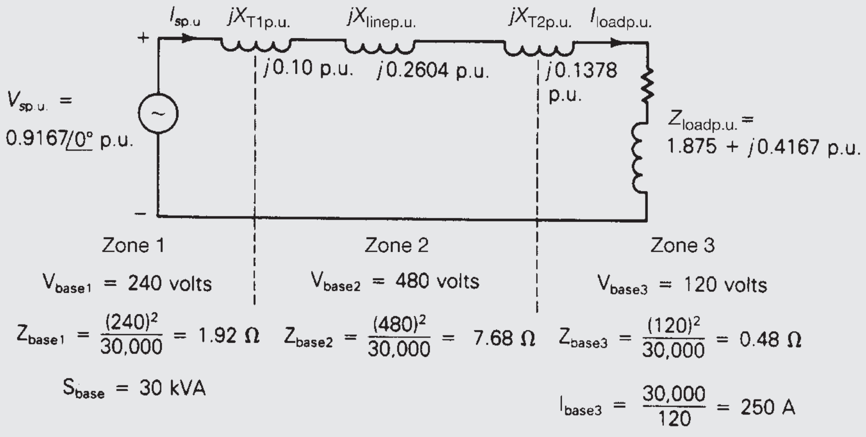
$I_{sp.u}$
$jX_{T1p.u.}$
$jX_{linep.u.}$
$jX_{T2p.u.}$
$I_{loadp.u.}$
+
−
j0.10 p.u.
j0.2604 p.u.
j0.1378 p.u.
$V_{sp.u.}$ = 0.9167/0° p.u.
$Z_{loadp.u.}$ = 1.875 + j0.4167 p.u.
Zone 1
Zone 2
Zone 3
V_{base1} = 240 volts
V_{base2} = 480 volts
V_{base3} = 120 volts
$Z_{base1} = \frac{(240)^2}{30,000} = 1.92\ \Omega$
$Z_{base2} = \frac{(480)^2}{30,000} = 7.68\ \Omega$
$Z_{base3} = \frac{(120)^2}{30,000} = 0.48\ \Omega$
S_{base} = 30 kVA
$I_{base3} = \frac{30,000}{120} = 250$ A

(b) Per-unit circuit

(*Continued*)

Copyright 2017 Cengage Learning. All Rights Reserved. May not be copied, scanned, or duplicated, in whole or in part. Due to electronic rights, some third party content may be suppressed from the eBook and/or eChapter(s). Editorial review has deemed that any suppressed content does not materially affect the overall learning experience. Cengage Learning reserves the right to remove additional content at any time if subsequent rights restrictions require it.

SOLUTION

First the base values in each zone are determined. $S_{base} = 30$ kVA is the same for the entire network. Also, $V_{base1} = 240$ volts, as specified for zone 1. When moving across a transformer, the voltage base is changed in proportion to the transformer voltage ratings. Thus,

$$V_{base2} = \left(\frac{480}{240}\right)(240) = 480 \quad \text{volts}$$

and

$$V_{base3} = \left(\frac{115}{460}\right)(480) = 120 \quad \text{volts}$$

The base impedances in zones 2 and 3 are

$$Z_{base2} = \frac{V_{base2}^2}{S_{base}} = \frac{480^2}{30{,}000} = 7.86 \quad \Omega$$

and

$$Z_{base3} = \frac{V_{base3}^2}{S_{base}} = \frac{120^2}{30{,}000} = 0.48 \quad \Omega$$

and the base current in zone 3 is

$$I_{base3} = \frac{S_{base}}{V_{base3}} = \frac{30{,}000}{120} = 250 \quad \text{A}$$

Next, the per-unit circuit impedances are calculated using the system base values. Since $S_{base} = 30$ kVA is the same as the kVA rating of transformer T_1, and $V_{base1} = 240$ volts is the same as the voltage rating of the zone 1 side of transformer T_1, the per-unit leakage reactance of T_1 is the same as its nameplate value, $X_{T1p.u.} = 0.1$ per unit. However, the per-unit leakage reactance of transformer T_2 must be converted from its nameplate rating to the system base. Using (3.3.11) and $V_{base2} = 480$ volts,

$$X_{T2p.u.} = (0.10)\left(\frac{460}{480}\right)^2\left(\frac{30{,}000}{20{,}000}\right) = 0.1378 \quad \text{per unit}$$

Alternatively, using $V_{base3} = 120$ volts,

$$X_{T2p.u.} = (0.10)\left(\frac{115}{120}\right)^2\left(\frac{30{,}000}{20{,}000}\right) = 0.1378 \quad \text{per unit}$$

which gives the same result. The line, which is located in zone 2, has a per-unit reactance

$$X_{linep.u.} = \frac{X_{line}}{Z_{base2}} = \frac{2}{7.68} = 0.2604 \quad \text{per unit}$$

Copyright 2017 Cengage Learning. All Rights Reserved. May not be copied, scanned, or duplicated, in whole or in part. Due to electronic rights, some third party content may be suppressed from the eBook and/or eChapter(s). Editorial review has deemed that any suppressed content does not materially affect the overall learning experience. Cengage Learning reserves the right to remove additional content at any time if subsequent rights restrictions require it.

and the load, which is located in zone 3, has a per-unit impedance

$$Z_{\text{loadp.u.}} = \frac{Z_{\text{load}}}{Z_{\text{base3}}} = \frac{0.9 + j0.2}{0.48} = 1.875 + j0.4167 \quad \text{per unit}$$

The per-unit circuit is shown in Figure 3.10(b), where the base values for each zone, per-unit impedances, and the per-unit source voltage are shown. The per-unit load current is then easily calculated from Figure 3.10(b) as follows:

$$\begin{aligned} I_{\text{loadp.u.}} = I_{\text{sp.u.}} &= \frac{V_{\text{sp.u.}}}{j(X_{\text{T1p.u.}} + X_{\text{linep.u.}} + X_{\text{T2p.u.}}) + Z_{\text{loadp.u.}}} \\ &= \frac{0.9167\underline{/0^\circ}}{j(0.10 + 0.2604 + 0.1378) + (1.875 + j0.4167)} \\ &= \frac{0.9167\underline{/0^\circ}}{1.875 + j0.9149} = \frac{0.9167\underline{/0^\circ}}{2.086\underline{/26.01^\circ}} \\ &= 0.4395\underline{/-26.01^\circ} \quad \text{per unit} \end{aligned}$$

The actual load current is

$$I_{\text{load}} = (I_{\text{loadp.u.}})\text{I}_{\text{base3}} = (0.4395\underline{/-26.01^\circ})\,(250) = 109.9\underline{/-26.01^\circ} \quad \text{A}$$

Note that the per-unit equivalent circuit of Figure 3.10(b) is relatively easy to analyze, since ideal transformer windings have been eliminated by proper selection of base values.

Balanced three-phase circuits can be solved in per-unit on a per-phase basis after converting Δ-load impedances to equivalent Y impedances. Base values can be selected either on a per-phase basis or on a three-phase basis. Equations (3.3.1) through (3.3.5) remain valid for three-phase circuits on a per-phase basis. Usually $\text{S}_{\text{base}3\phi}$ and V_{baseLL} are selected, where the subscripts 3ϕ and LL denote "three-phase" and "line-to-line," respectively. Then the following relations must be used for other base values:

$$\text{S}_{\text{base}1\phi} = \frac{\text{S}_{\text{base}3\phi}}{3} \tag{3.3.12}$$

$$\text{V}_{\text{baseLN}} = \frac{\text{V}_{\text{baseLL}}}{\sqrt{3}} \tag{3.3.13}$$

$$\text{S}_{\text{base}3\phi} = \text{P}_{\text{base}3\phi} = \text{Q}_{\text{base}3\phi} \tag{3.3.14}$$

$$\text{I}_{\text{base}} = \frac{\text{S}_{\text{base}1\phi}}{\text{V}_{\text{baseLN}}} = \frac{\text{S}_{\text{base}3\phi}}{\sqrt{3}\text{V}_{\text{baseLL}}} \tag{3.3.15}$$

$$Z_{\text{base}} = \frac{\text{V}_{\text{baseLN}}}{\text{I}_{\text{base}}} = \frac{\text{V}^2_{\text{baseLN}}}{\text{S}_{\text{base}1\phi}} = \frac{\text{V}^2_{\text{baseLL}}}{\text{S}_{\text{base}3\phi}} \tag{3.3.16}$$

$$\text{R}_{\text{base}} = X_{\text{base}} = Z_{\text{base}} = \frac{1}{Y_{\text{base}}} \tag{3.3.17}$$

Copyright 2017 Cengage Learning. All Rights Reserved. May not be copied, scanned, or duplicated, in whole or in part. Due to electronic rights, some third party content may be suppressed from the eBook and/or eChapter(s). Editorial review has deemed that any suppressed content does not materially affect the overall learning experience. Cengage Learning reserves the right to remove additional content at any time if subsequent rights restrictions require it.

EXAMPLE 3.5

Per-unit and actual currents in balanced three-phase networks

As in Example 2.5, a balanced-Y-connected voltage source with $E_{ab} = 480\underline{/0°}$ volts is applied to a balanced-Δ load with $Z_\Delta = 30\underline{/40°}\ \Omega$. The line impedance between the source and load is $Z_L = 1\underline{/85°}\ \Omega$ for each phase. Calculate the per-unit and actual current in phase *a* of the line using $S_{\text{base}3\phi} = 10$ kVA and $V_{\text{baseLL}} = 480$ volts.

SOLUTION

First, convert Z_Δ to an equivalent Z_Y; the equivalent line-to-neutral diagram is shown in Figure 2.17. The base impedance is, from (3.3.16),

$$Z_{\text{base}} = \frac{V^2_{\text{baseLL}}}{S_{\text{base}3\phi}} = \frac{(480)^2}{10{,}000} = 23.04 \quad \Omega$$

The per-unit line and load impedances are

$$Z_{\text{Lp.u.}} = \frac{Z_L}{Z_{\text{base}}} = \frac{10\underline{/85°}}{23.04} = 0.04340\underline{/85°} \quad \text{per unit}$$

and

$$Z_{\text{Yp.u.}} = \frac{Z_Y}{Z_{\text{base}}} = \frac{10\underline{/40°}}{23.04} = 0.4340\underline{/40°} \quad \text{per unit}$$

Also,

$$V_{\text{baseLN}} = \frac{V_{\text{baseLL}}}{\sqrt{3}} = \frac{480}{\sqrt{3}} = 277 \quad \text{volts}$$

and

$$E_{an\text{p.u.}} = \frac{E_{an}}{V_{\text{baseLN}}} = \frac{277\underline{/-30°}}{277} = 1.0\underline{/-30°} \quad \text{per unit}$$

The per-unit equivalent circuit is shown in Figure 3.11. The per-unit line current in phase *a* is then

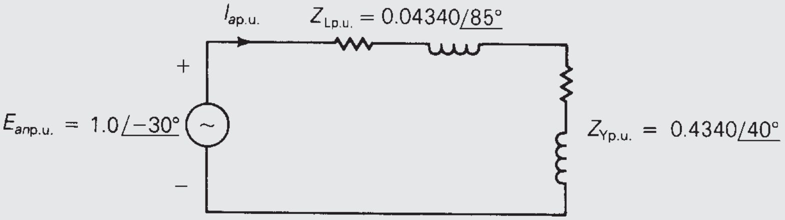
$I_{a\text{p.u.}}$
$Z_{\text{Lp.u.}} = 0.04340\underline{/85°}$
+
−
$E_{an\text{p.u.}} = 1.0\underline{/-30°}$
$Z_{\text{Yp.u.}} = 0.4340\underline{/40°}$

FIGURE 3.11

Circuit for Example 3.5

Copyright 2017 Cengage Learning. All Rights Reserved. May not be copied, scanned, or duplicated, in whole or in part. Due to electronic rights, some third party content may be suppressed from the eBook and/or eChapter(s). Editorial review has deemed that any suppressed content does not materially affect the overall learning experience. Cengage Learning reserves the right to remove additional content at any time if subsequent rights restrictions require it.

$$
\begin{aligned}
I_{a\text{p.u.}} = \frac{E_{an\text{p.u.}}}{Z_{\text{Lp.u.}} + Z_{\text{Yp.u.}}} &= \frac{1.0\underline{/-30^\circ}}{0.04340\underline{/85^\circ} + 0.4340\underline{/40^\circ}} \\
&= \frac{1.0\underline{/-30^\circ}}{(0.00378 + j0.04323) + (0.3325 + j0.2790)} \\
&= \frac{1.0\underline{/-30^\circ}}{0.3362 + j0.3222} = \frac{1.0\underline{/-30^\circ}}{0.4657\underline{/43.78^\circ}} \\
&= 2.147\underline{/-73.78^\circ} \quad \text{per unit}
\end{aligned}
$$

The base current is

$$
\text{I}_{\text{base}} = \frac{\text{S}_{\text{base}3\phi} =}{\sqrt{3}\text{V}_{\text{baseLL}}} = \frac{10{,}000}{\sqrt{3}(480)} = 12.03 \quad \text{A}
$$

and the actual phase *a* line current is

$$
I_a = (2.147\underline{/-73.78^\circ})(12.03) = 25.83\underline{/-73.78^\circ} \quad \text{A}
$$

3.4 THREE-PHASE TRANSFORMER CONNECTIONS AND PHASE SHIFT

Three identical single-phase two-winding transformers may be connected to form a three-phase bank. Four ways to connect the windings are Y–Y, Y–Δ, Δ–Y, and Δ–Δ. For example, Figure 3.12 shows a three-phase Y–Y bank. Figure 3.12(a) shows the core and coil arrangements. The American standard for marking three-phase transformers substitutes H1, H2, and H3 on the high-voltage terminals and X1, X2, and X3 on the low-voltage terminals in place of the polarity dots. Also, this text uses uppercase letters *ABC* to identify phases on the high-voltage side of the transformer and lowercase letters *abc* to identify phases on the low-voltage side of the transformer. In Figure 3.12(a), the transformer high-voltage terminals H1, H2, and H3 are connected to phases *A, B,* and *C*, and the low-voltage terminals X1, X2, and X3 are connected to phases *a, b,* and c, respectively.

Figure 3.12(b) shows a schematic representation of the three-phase Y–Y transformer. Windings on the same core are drawn in parallel, and the phasor relationship for balanced positive-sequence operation is shown. For example, high-voltage winding Hl–*N* is on the same magnetic core as low-voltage winding Xl–*n* in Figure 3.12(b). Also, V_{AN} is in phase with V_{an}. Figure 3.12(c) shows a single-line diagram of a Y–Y transformer. A single-line diagram shows one phase of a three-phase network with the neutral wire omitted and with components represented by symbols rather than equivalent circuits.

Copyright 2017 Cengage Learning. All Rights Reserved. May not be copied, scanned, or duplicated, in whole or in part. Due to electronic rights, some third party content may be suppressed from the eBook and/or eChapter(s). Editorial review has deemed that any suppressed content does not materially affect the overall learning experience. Cengage Learning reserves the right to remove additional content at any time if subsequent rights restrictions require it.

FIGURE 3.12

Three-phase two-winding Y–Y transformer bank

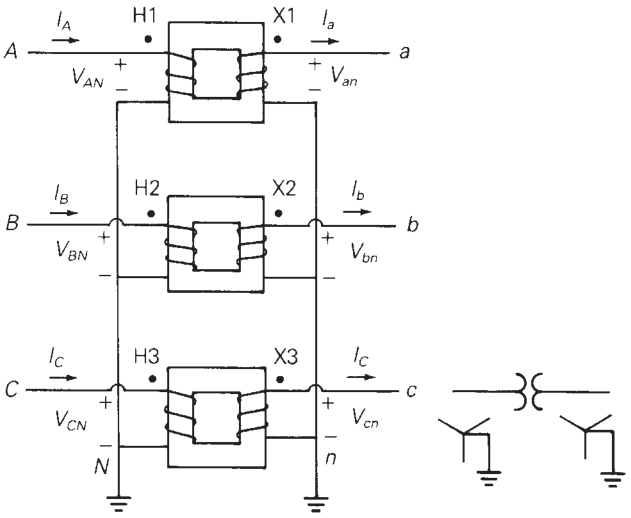

(a) Core and coil arrangements (c) Single-line diagram

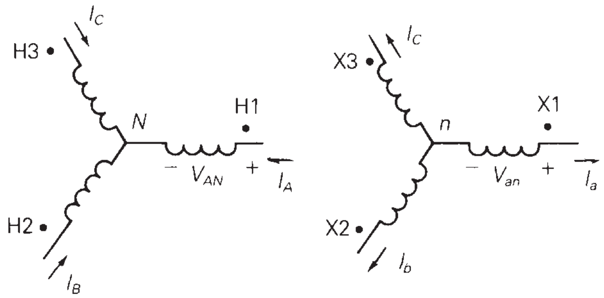

(b) Schematic representation showing phasor relationship for positive sequence operation

The phases of a Y–Y or a Δ–Δ transformer can be labeled so there is no phase shift between corresponding quantities on the low- and high-voltage windings. However, for Y–Δ and Δ–Y transformers, there is always a phase shift. Figure 3.13 shows a Y–Δ transformer. The labeling of the windings and the schematic representation are in accordance with the American standard, which is as follows:

> In either a Y–Δ or Δ–Y transformer, positive-sequence quantities on the high-voltage side shall lead their corresponding quantities on the low-voltage side by 30°.

As shown in Figure 3.13(b), V_{AN} leads V_{an} by 30°.

The positive-sequence phasor diagram shown in Figure 3.13(b) can be constructed via the following five steps, which are also indicated in Figure 3.13.

Copyright 2017 Cengage Learning. All Rights Reserved. May not be copied, scanned, or duplicated, in whole or in part. Due to electronic rights, some third party content may be suppressed from the eBook and/or eChapter(s). Editorial review has deemed that any suppressed content does not materially affect the overall learning experience. Cengage Learning reserves the right to remove additional content at any time if subsequent rights restrictions require it.

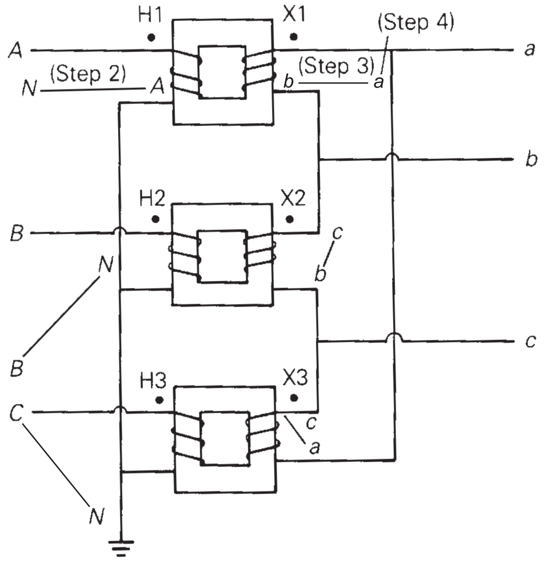

(a) Core and coil arrangement

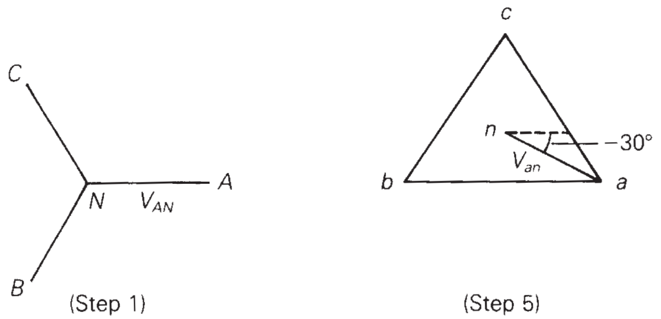

(Step 1)

(Step 5)

(b) Positive-sequence phasor diagram

FIGURE 3.13

Three-phase two-winding Y–Δ transformer bank

STEP 1 Assume that balanced positive-sequence voltages are applied to the Y winding. Draw the positive-sequence phasor diagram for these voltages.

STEP 2 Move phasor *A*–*N* next to terminals *A*–*N* in Figure 3.13(a). Identify the ends of this line in the same manner as in the phasor diagram. Similarly, move phasors *B*–*N* and *C*–*N* next to terminals *B*–*N* and *C*–*N* in Figure 3.13(a).

STEP 3 For each single-phase transformer, the voltage across the low-voltage winding must be in phase with the voltage across the high-voltage winding, assuming an ideal transformer. Therefore, draw a line

Copyright 2017 Cengage Learning. All Rights Reserved. May not be copied, scanned, or duplicated, in whole or in part. Due to electronic rights, some third party content may be suppressed from the eBook and/or eChapter(s). Editorial review has deemed that any suppressed content does not materially affect the overall learning experience. Cengage Learning reserves the right to remove additional content at any time if subsequent rights restrictions require it.

next to each low-voltage winding parallel to the corresponding line already drawn next to the high-voltage winding.

STEP 4 Label the ends of the lines drawn in Step 3 by inspecting the polarity marks. For example, phase A is connected to dotted terminal H1, and A appears on the *right* side of line A–N. Therefore, phase a, which is connected to dotted terminal X1, must be on the *right* side, and b on the left side of line a–b. Similarly, phase B is connected to dotted terminal H2, and B is *down* on line B–N. Therefore, phase b, connected to dotted terminal X2, must be *down* on line b–c. Similarly, c is *up* on line c–a.

STEP 5 Bring the three lines labeled in Step 4 together to complete the phasor diagram for the low-voltage A winding. Note that V_{AN} leads V_{an} by 30° in accordance with the American standard.

EXAMPLE 3.6

Phase shift in Δ–Y transformers

Assume that balanced negative-sequence voltages are applied to the high-voltage windings of the Y–Δ transformer shown in Figure 3.13. Determine the negative-sequence phase shift of this transformer.

SOLUTION

The negative-sequence diagram, shown in Figure 3.14, is constructed from the following five steps, as outlined previously:

STEP 1 Draw the phasor diagram of balanced negative-sequence voltages, which are applied to the Y winding.

STEP 2 Move the phasors A–N, B–N, and C–N next to the high-voltage Y windings.

STEP 3 For each single-phase transformer, draw a line next to the low-voltage winding that is parallel to the line drawn in Step 2 next to the high-voltage winding.

STEP 4 Label the lines drawn in Step 3. For example, phase B, which is connected to dotted terminal H2, is shown *up* on line B–N; therefore phase b, which is connected to dotted terminal X2, must be *up* on line b–c.

STEP 5 Bring the lines drawn in Step 4 together to form the negative-sequence phasor diagram for the low-voltage Δ winding.

As shown in Figure 3.14, the high-voltage phasors *lag* the low-voltage phasors by 30°. Thus the negative-sequence phase shift is the reverse of the positive-sequence phase shift.

Copyright 2017 Cengage Learning. All Rights Reserved. May not be copied, scanned, or duplicated, in whole or in part. Due to electronic rights, some third party content may be suppressed from the eBook and/or eChapter(s). Editorial review has deemed that any suppressed content does not materially affect the overall learning experience. Cengage Learning reserves the right to remove additional content at any time if subsequent rights restrictions require it.

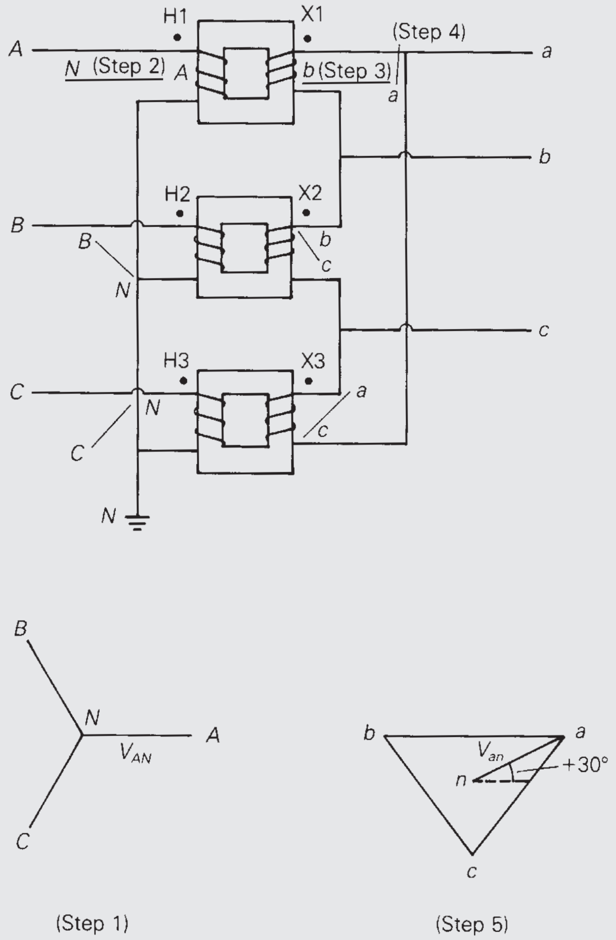

FIGURE 3.14

Example 3.6—Construction of negative-sequence phasor diagram for Y–Δ transformer bank

The Δ–Y transformer is commonly used as a generator step-up transformer, where the Δ winding is connected to the generator terminals and the Y winding is connected to a transmission line. One advantage of a high-voltage Y winding is that a neutral point *N* is provided for grounding on the high-voltage side. With a permanently grounded neutral, the insulation requirements for the high-voltage transformer windings are reduced. The high-voltage insulation can be graded or tapered from maximum insulation at terminals *ABC* to minimum insulation at grounded terminal *N*. One advantage of the Δ winding is that the undesirable third harmonic magnetizing current, caused by the nonlinear core *B*–*H* characteristic, remains trapped inside the Δ winding. Third harmonic currents are (triple-frequency) zero-sequence currents, which cannot enter or leave a Δ connection, but can flow within the Δ. The Y–Y transformer is seldom used because of difficulties with third harmonic exciting current.

Copyright 2017 Cengage Learning. All Rights Reserved. May not be copied, scanned, or duplicated, in whole or in part. Due to electronic rights, some third party content may be suppressed from the eBook and/or eChapter(s). Editorial review has deemed that any suppressed content does not materially affect the overall learning experience. Cengage Learning reserves the right to remove additional content at any time if subsequent rights restrictions require it.

FIGURE 3.15

Transformer core configurations

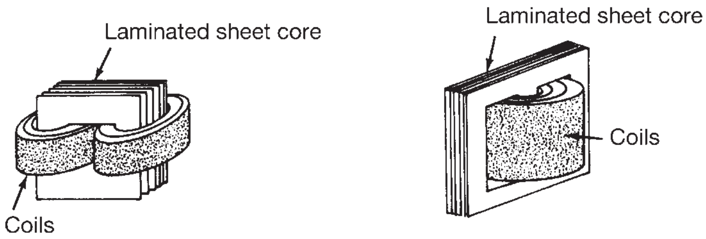

(a) Single-phase core type

(b) Single-phase shell type

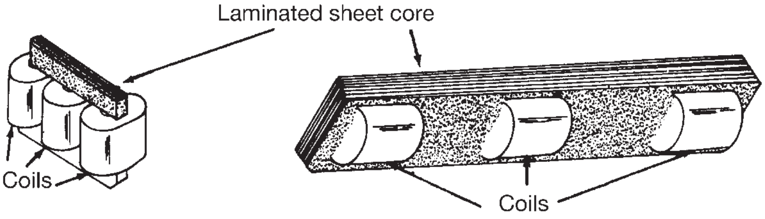

(c) Three-phase, three-legged core type

(d) Three-phase shell type

The Δ–Δ transformer has the advantage that one phase can be removed for repair or maintenance while the remaining phases continue to operate as a three-phase bank. This *open*-Δ connection permits balanced three-phase operation with the kVA rating reduced to 58% of the original bank (see Problem 3.36).

Instead of a bank of three single-phase transformers, all six windings may be placed on a common three-phase core to form a three-phase transformer, as shown in Figure 3.15. The three-phase core contains less iron than the three single-phase units; therefore it costs less, weighs less, requires less floor space, and has a slightly higher efficiency. However, a winding failure would require replacement of an entire three-phase transformer, compared to replacement of only one phase of a three-phase bank.

3.5 PER-UNIT EQUIVALENT CIRCUITS OF BALANCED THREE-PHASE TWO-WINDING TRANSFORMERS

Figure 3.16(a) is a schematic representation of an ideal Y–Y transformer grounded through neutral impedances Z_N and Z_n. Figure 3.16(b) shows the per-unit equivalent circuit of this ideal transformer for balanced three-phase operation. Throughout the remainder of this text, per-unit quantities are used unless otherwise indicated. Also, the subscript "p.u.," used to indicate a per-unit quantity, is omitted in most cases.

Copyright 2017 Cengage Learning. All Rights Reserved. May not be copied, scanned, or duplicated, in whole or in part. Due to electronic rights, some third party content may be suppressed from the eBook and/or eChapter(s). Editorial review has deemed that any suppressed content does not materially affect the overall learning experience. Cengage Learning reserves the right to remove additional content at any time if subsequent rights restrictions require it.

FIGURE 3.16

Ideal Y–Y transformer

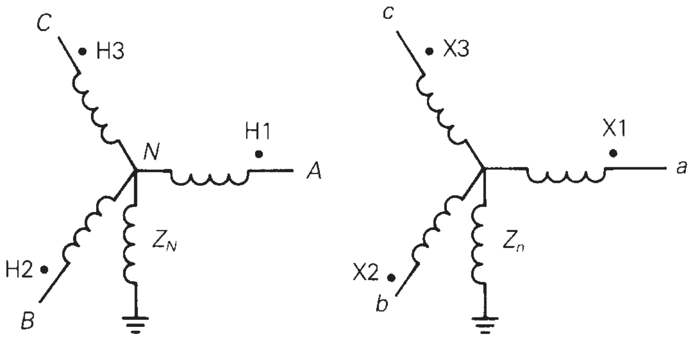

(a) Schematic representation

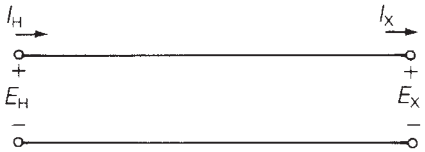

(b) Per-unit equivalent circuit for balanced three-phase operation

The following are two conventional rules for selecting base quantities:

1. A common S_{base} is selected for both the H and X terminals.
2. The ratio of the voltage bases V_{baseH}/V_{baseX} is selected to be equal to the ratio of the rated line-to-line voltages $V_{ratedHLL}/V_{ratedXLL}$.

When balanced three-phase currents are applied to the transformer, the neutral currents are zero, and there are no voltage drops across the neutral impedances. Therefore, the per-unit equivalent circuit of the ideal Y–Y transformer, Figure 3.16(b), is the same as the per-unit single-phase ideal transformer, Figure 3.9(a).

The per-unit equivalent circuit of a practical Y–Y transformer is shown in Figure 3.17(a). This network is obtained by adding external impedances to the equivalent circuit of the ideal transformer, as in Figure 3.9(c).

The per-unit equivalent circuit of the Y–Δ transformer, shown in Figure 3.17(b), includes a phase shift. For the American standard, the positive-sequence voltages and currents on the high-voltage side of the Y–Δ transformer lead the corresponding quantities on the low-voltage side by 30°. The phase shift in the equivalent circuit of Figure 3.17(b) is represented by the phase-shifting transformer of Figure 3.4.

The per-unit equivalent circuit of the Δ–Δ transformer, shown in Figure 3.17(c), is the same as that of the Y–Y transformer. It is assumed that the windings are labeled so there is no phase shift. Also, the per-unit impedances do not depend on the winding connections, but the base voltages do.

Copyright 2017 Cengage Learning. All Rights Reserved. May not be copied, scanned, or duplicated, in whole or in part. Due to electronic rights, some third party content may be suppressed from the eBook and/or eChapter(s). Editorial review has deemed that any suppressed content does not materially affect the overall learning experience. Cengage Learning reserves the right to remove additional content at any time if subsequent rights restrictions require it.

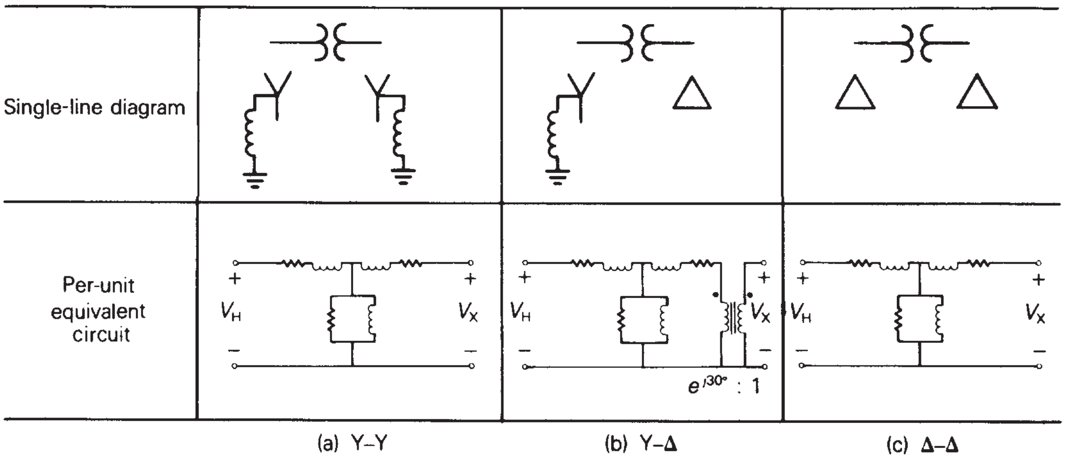

FIGURE 3.17

Per-unit equivalent circuits of practical Y–Y, Y–Δ, and Δ–Δ transformers for balanced three-phase operation

EXAMPLE 3.7

Voltage calculations: balanced Y–Y and Δ–Y transformers

Three single-phase two-winding transformers, each rated 400 MVA, 13.8/199.2 kV, with leakage reactance $X_{eq} = 0.10$ per unit, are connected to form a three-phase bank. Winding resistances and exciting current are neglected. The high-voltage windings are connected in Y. A three-phase load operating under balanced positive-sequence conditions on the high-voltage side absorbs 1000 MVA at 0.90 p.f. lagging, with $V_{AN} = 199.2\underline{/0°}$ kV. Determine the voltage V_{an} at the low-voltage bus if the low-voltage windings are connected (a) in Y and (b) in Δ.

SOLUTION

The per-unit network is shown in Figure 3.18. Using the transformer bank ratings as base quantities, $S_{base3\phi} = 1200$ MVA, $V_{baseHLL} = 345$ kV, and $I_{baseH} = 1200/(345\sqrt{3}) = 2.008$ kA. The per-unit load voltage and load current are then

$$V_{AN} = 1.0\underline{/0°} \quad \text{per unit}$$

$$I_A = \frac{1000/(345\sqrt{3})}{2.008}\underline{/-\cos^{-1}0.9} = 0.8333\underline{/-25.84°} \quad \text{per unit}$$

a. For the Y–Y transformer, Figure 3.18(a),

$$I_a = I_A = 0.8333\underline{/-25.84°} \quad \text{per unit}$$

Copyright 2017 Cengage Learning. All Rights Reserved. May not be copied, scanned, or duplicated, in whole or in part. Due to electronic rights, some third party content may be suppressed from the eBook and/or eChapter(s). Editorial review has deemed that any suppressed content does not materially affect the overall learning experience. Cengage Learning reserves the right to remove additional content at any time if subsequent rights restrictions require it.

FIGURE 3.18

Per-unit network for Example 3.7

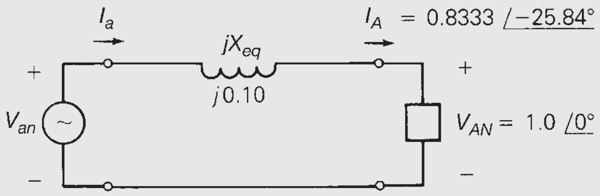

I_a
$I_A = 0.8333\underline{/-25.84^\circ}$
jX_{eq}
$j0.10$
+
V_{an}
~
+
$V_{AN} = 1.0\underline{/0^\circ}$
−
−

(a) Y-connected low-voltage windings

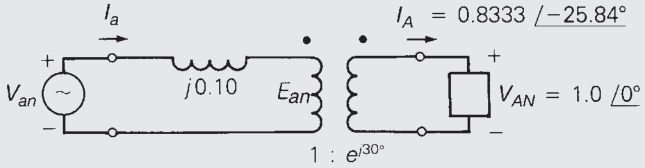

I_a
$I_A = 0.8333\underline{/-25.84^\circ}$
+
V_{an}
~
−
$j0.10$
E_{an}
+
$V_{AN} = 1.0\underline{/0^\circ}$
−
$1 : e^{j30^\circ}$

(b) Δ-connected low-voltage windings

$$\begin{aligned} V_{an} &= V_{AN} + (j\mathrm{X}_{\mathrm{eq}})I_A \\ &= 1.0\underline{/0^\circ} + (j0.10)(0.8333\underline{/-25.84^\circ}) \\ &= 1.0 + 0.08333\underline{/64.16^\circ} = 1.0363 + j0.0750 = 1.039\underline{/4.139^\circ} \\ &= 1.039\underline{/4.139^\circ} \text{ per unit} \end{aligned}$$

Further, since $V_{\mathrm{base}XLN} = 13.8$ kV for the low-voltage Y windings, $\mathrm{V}_{an} = 1.039(13.8) = 14.34$ kV, and

$$V_{an} = 14.34\underline{/4.139^\circ} \text{ kV}$$

b. For the Δ–Y transformer, Figure 3.18(b),

$$E_{an} = e^{-j30^\circ}V_{AN} = 1.0\underline{/-30^\circ} \text{ per unit}$$

$$I_a = e^{-j30^\circ}I_A = 0.8333\underline{/-25.84^\circ - 30^\circ} = 0.8333\underline{/-55.84^\circ} \text{ per unit}$$

$$V_{an} = E_{an} + (j\mathrm{X}_{\mathrm{eq}})I_a = 1.0\underline{/-30^\circ} + (j0.10)(0.8333\underline{/-55.84^\circ})$$

$$V_{an} = 1.039\underline{/-25.861^\circ} \text{ per unit}$$

Further, since $\mathrm{V}_{\mathrm{baseXLN}} = 13.8/\sqrt{3} = 7.967$ kV for the low-voltage Δ windings, $V_{an} = (1.039)(7.967) = 8.278$ kV, and

$$V_{an} = 8.278\underline{/-25.861^\circ} \text{ kV}$$

Copyright 2017 Cengage Learning. All Rights Reserved. May not be copied, scanned, or duplicated, in whole or in part. Due to electronic rights, some third party content may be suppressed from the eBook and/or eChapter(s). Editorial review has deemed that any suppressed content does not materially affect the overall learning experience. Cengage Learning reserves the right to remove additional content at any time if subsequent rights restrictions require it.

EXAMPLE 3.8

Per-unit voltage drop and per-unit fault current: balanced three-phase transformer

A 200-MVA, 345-kVΔ/34.5-kV Y substation transformer has an 8% leakage reactance. The transformer acts as a connecting link between 345-kV transmission and 34.5-kV distribution. Transformer winding resistances and exciting current are neglected. The high-voltage bus connected to the transformer is assumed to be an ideal 345-kV positive-sequence source with negligible source impedance. Using the transformer ratings as base values, determine:

a. The per-unit magnitudes of transformer voltage drop and voltage at the low-voltage terminals when rated transformer current at 0.8 p.f. lagging enters the high-voltage terminals.

b. The per-unit magnitude of the fault current when a three-phase-to-ground bolted short circuit occurs at the low-voltage terminals.

SOLUTION

In both parts (a) and (b), only balanced positive-sequence current will flow, since there are no imbalances. Because the only interest is in voltage and current magnitudes, the Δ–Y transformer phase shift can be omitted.

a. As shown in Figure 3.19(a),

$$V_{\text{drop}} = I_{\text{rated}}X_{\text{eq}} = (1.0)(0.08) = 0.08 \quad \text{per unit and}$$

$$\begin{aligned} V_{an} &= V_{AN} - (jX_{\text{eq}})I_{\text{rated}} \\ &= 1.0\underline{/0^\circ} - (j0.08)(1.0\underline{/-36.87^\circ}) \\ &= 1.0 - (j0.08)(0.8 - j0.6) = 0.952 - j0.064 \\ &= 0.954\underline{/-3.85^\circ} \quad \text{per unit} \end{aligned}$$

b. As shown in Figure 3.19(b),

$$I_{\text{SC}} = \frac{V_{AN}}{X_{\text{eq}}} = \frac{1.0}{0.08} = 12.5 \quad \text{per unit}$$

Under rated current conditions [part (a)], the 0.08 per-unit voltage drop across the transformer leakage reactance causes the voltage at the low-voltage terminals to be 0.954 per unit. Also, under three-phase short-circuit conditions [part (b)], the fault current is 12.5 times the rated transformer current. This example illustrates a compromise in the design or specification of transformer leakage reactance. A low value is desired to minimize voltage drops, but a high value is desired to limit fault currents. Typical transformer leakage reactances are given in Table A.2 in the Appendix.

Copyright 2017 Cengage Learning. All Rights Reserved. May not be copied, scanned, or duplicated, in whole or in part. Due to electronic rights, some third party content may be suppressed from the eBook and/or eChapter(s). Editorial review has deemed that any suppressed content does not materially affect the overall learning experience. Cengage Learning reserves the right to remove additional content at any time if subsequent rights restrictions require it.

FIGURE 3.19

Circuits for Example 3.8

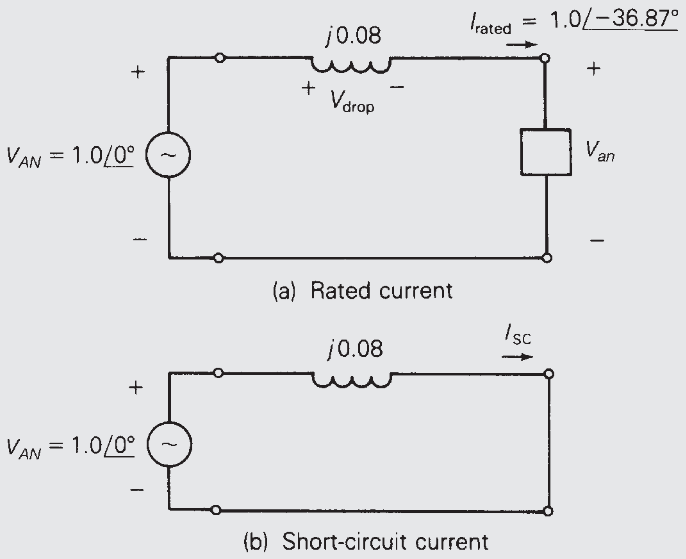

3.6 THREE-WINDING TRANSFORMERS

Figure 3.20(a) shows a basic single-phase three-winding transformer. The ideal transformer relations for a two-winding transformer, (3.1.8) and (3.1.14), easily can be extended to obtain corresponding relations for an ideal three-winding transformer. In actual units, these relations are

$$N_1 I_1 = N_2 I_2 + N_3 I_3 \tag{3.6.1}$$

$$\frac{E_1}{N_1} = \frac{E_2}{N_2} = \frac{E_3}{N_3} \tag{3.6.2}$$

where I_1 enters the dotted terminal, I_2 and I_3 leave dotted terminals, and E_1, E_2, and E_3 have their + polarities at dotted terminals. In per-unit, (3.6.1) and (3.6.2) are

$$I_{1\text{p.u.}} = I_{2\text{p.u.}} + I_{3\text{p.u.}} \tag{3.6.3}$$

$$E_{1\text{p.u.}} = E_{2\text{p.u.}} = E_{3\text{p.u.}} \tag{3.6.4}$$

where a common S_{base} is selected for all three windings, and voltage bases are selected in proportion to the rated voltages of the windings. These two per-unit relations are satisfied by the per-unit equivalent circuit shown in Figure 3.20(b). Also, external series impedance and shunt admittance branches are included in the practical three-winding transformer circuit shown in Figure 3.20(c). The shunt

Copyright 2017 Cengage Learning. All Rights Reserved. May not be copied, scanned, or duplicated, in whole or in part. Due to electronic rights, some third party content may be suppressed from the eBook and/or eChapter(s). Editorial review has deemed that any suppressed content does not materially affect the overall learning experience. Cengage Learning reserves the right to remove additional content at any time if subsequent rights restrictions require it.

FIGURE 3.20

Single-phase three-winding transformer

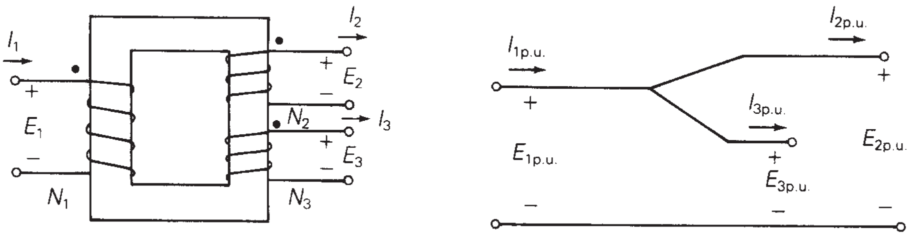

(a) Basic core and coil configuration (b) Per-unit equivalent circuit—ideal transformer

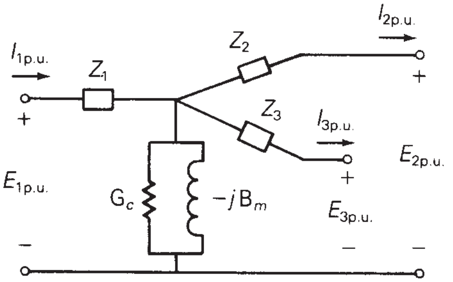

(c) Per-unit equivalent circuit—practical transformer

admittance branch, a core loss resistor in parallel with a magnetizing inductor, can be evaluated from an open-circuit test. Also, when one winding is left open, the three-winding transformer behaves as a two-winding transformer, and standard short-circuit tests can be used to evaluate per-unit leakage impedances, which are defined as follows:

Z_{12} = per-unit leakage impedance measured from winding 1, with winding 2 shorted and winding 3 open
Z_{13} = per-unit leakage impedance measured from winding 1, with winding 3 shorted and winding 2 open
Z_{23} = per-unit leakage impedance measured from winding 2, with winding 3 shorted and winding 1 open

From Figure 3.20(c), with winding 2 shorted and winding 3 open, the leakage impedance measured from winding 1 is, neglecting the shunt admittance branch,

$$Z_{12} = Z_1 + Z_2 \tag{3.6.5}$$

Similarly,

$$Z_{13} = Z_1 + Z_3 \tag{3.6.6}$$

and

$$Z_{23} = Z_2 + Z_3 \tag{3.6.7}$$

Copyright 2017 Cengage Learning. All Rights Reserved. May not be copied, scanned, or duplicated, in whole or in part. Due to electronic rights, some third party content may be suppressed from the eBook and/or eChapter(s). Editorial review has deemed that any suppressed content does not materially affect the overall learning experience. Cengage Learning reserves the right to remove additional content at any time if subsequent rights restrictions require it.

Solving (3.6.5) through (3.6.7),

$$Z_1 = \tfrac{1}{2}(Z_{12} + Z_{13} - Z_{23}) \tag{3.6.8}$$

$$Z_2 = \tfrac{1}{2}(Z_{12} + Z_{23} - Z_{13}) \tag{3.6.9}$$

$$Z_3 = \tfrac{1}{2}(Z_{13} + Z_{23} - Z_{12}) \tag{3.6.10}$$

Equations (3.6.8) through (3.6.10) can be used to evaluate the per-unit series impedances Z_1, Z_2, and Z_3 of the three-winding transformer equivalent circuit from the per-unit leakage impedances Z_{12}, Z_{13}, and Z_{23}, which, in turn, are determined from short-circuit tests.

Note that each of the windings on a three-winding transformer may have a *different* kVA rating. If the leakage impedances from short-circuit tests are expressed in per-unit based on winding ratings, they must first be converted to per-unit on a common S_{base} *before* they are used in (3.6.8) through (3.6.10).

EXAMPLE 3.9

Three-winding single-phase transformer: per-unit impedances

The ratings of a single-phase three-winding transformer are

winding 1: 300 MVA, 13.8 kV
winding 2: 300 MVA, 199.2 kV
winding 3: 50 MVA, 19.92 kV

The leakage reactances, from short-circuit tests, are

$X_{12} = 0.10$ per unit on a 300-MVA, 13.8-kV base
$X_{13} = 0.16$ per unit on a 50-MVA, 13.8-kV base
$X_{23} = 0.14$ per unit on a 50-MVA, 199.2-kV base

Winding resistances and exciting current are neglected. Calculate the impedances of the per-unit equivalent circuit using a base of 300 MVA and 13.8 kV for terminal 1.

SOLUTION

$S_{\text{base}} = 300$ MVA is the same for all three terminals. Also, the specified voltage base for terminal 1 is $V_{\text{base1}} = 13.8$ kV. The base voltages for terminals 2 and 3 are then $V_{\text{base2}} = 199.2$ kV and $V_{\text{base3}} = 19.92$ kV, which are the rated voltages of these windings. From the data given, $X_{12} = 0.10$ per unit was measured from terminal 1 using the same base values as those specified for the circuit. However, $X_{13} = 0.16$ and $X_{23} = 0.14$ per unit on a 50-MVA base are first converted to the 300-MVA circuit base.

(*Continued*)

Copyright 2017 Cengage Learning. All Rights Reserved. May not be copied, scanned, or duplicated, in whole or in part. Due to electronic rights, some third party content may be suppressed from the eBook and/or eChapter(s). Editorial review has deemed that any suppressed content does not materially affect the overall learning experience. Cengage Learning reserves the right to remove additional content at any time if subsequent rights restrictions require it.

FIGURE 3.21

Circuit for Example 3.9

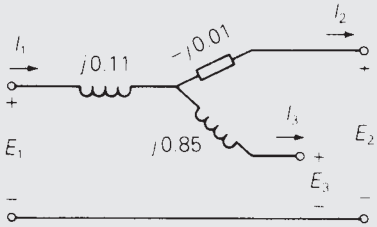

$$X_{13} = (0.16)\left(\frac{300}{50}\right) = 0.96 \quad \text{per unit}$$

$$X_{23} = (0.14)\left(\frac{300}{50}\right) = 0.84 \quad \text{per unit}$$

Then, from (3.6.8) through (3.6.10),

$$X_1 = \tfrac{1}{2}(0.10 + 0.96 - 0.84) = 0.11 \quad \text{per unit}$$

$$X_2 = \tfrac{1}{2}(0.10 + 0.84 - 0.96) = -0.01 \quad \text{per unit}$$

$$X_3 = \tfrac{1}{2}(0.84 + 0.96 - 0.10) = 0.85 \quad \text{per unit}$$

The per-unit equivalent circuit of this three-winding transformer is shown in Figure 3.21. Note that X_2 is negative. This illustrates the fact that X_1, X_2, and X_3 are *not* leakage reactances, but instead are equivalent reactances derived from the leakage reactances. Leakage reactances are always positive.

Note also that the node where the three equivalent circuit reactances are connected does not correspond to any physical location within the transformer. Rather, it is simply part of the equivalent circuit representation.

EXAMPLE 3.10

Three-winding three-phase transformer: balanced operation

Three transformers, each identical to that described in Example 3.9, are connected as a three-phase bank in order to feed power from a 900-MVA, 13.8-kV generator to a 345-kV transmission line and to a 34.5-kV distribution line. The transformer windings are connected as follows:

13.8-kV windings (X): Δ, to generator
199.2-kV windings (H): solidly grounded Y, to 345-kV line
19.92-kV windings (M): grounded Y through $Z_n = j0.10\ \Omega$, to 34.5-kV line

Copyright 2017 Cengage Learning. All Rights Reserved. May not be copied, scanned, or duplicated, in whole or in part. Due to electronic rights, some third party content may be suppressed from the eBook and/or eChapter(s). Editorial review has deemed that any suppressed content does not materially affect the overall learning experience. Cengage Learning reserves the right to remove additional content at any time if subsequent rights restrictions require it.

FIGURE 3.22

Per-unit network for Example 3.10

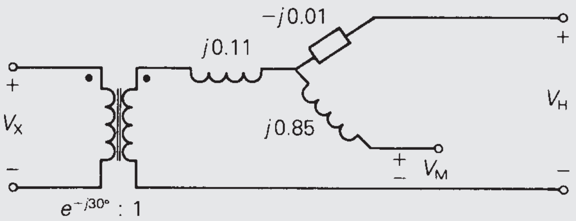

The positive-sequence voltages and currents of the high- and medium-voltage Y windings lead the corresponding quantities of the low-voltage Δ winding by 30°. Draw the per-unit network, using a three-phase base of 900 MVA and 13.8 kV for terminal X. Assume balanced positive-sequence operation.

SOLUTION

The per-unit network is shown in Figure 3.22. $V_{baseX} = 13.8$ kV, which is the rated line-to-line voltage of terminal X. Since the M and H windings are Y-connected, $V_{baseM} = \sqrt{3}(19.92) = 34.5$ kV, and $V_{baseH} = \sqrt{3}(199.2) = 345$ kV, which are the rated line-to-line voltages of the M and H windings. Also, a phase-shifting transformer is included in the network. The neutral impedance is not included in the network, since there is no neutral current under balanced operation.

3.7 AUTOTRANSFORMERS

A single-phase two-winding transformer is shown in Figure 3.23(a) with two separate windings, which is the usual two-winding transformer; the same transformer is shown in Figure 3.23(b) with the two windings connected in series, which is called an *autotransformer*. For the usual transformer [Figure 3.23(a)], the two windings are coupled magnetically via the mutual core flux. For the autotransformer [Figure 3.23(b)], the windings are both electrically and magnetically coupled. The autotransformer has smaller per-unit leakage impedances than the usual transformer; this results in both smaller series-voltage drops (an advantage) and higher short-circuit currents

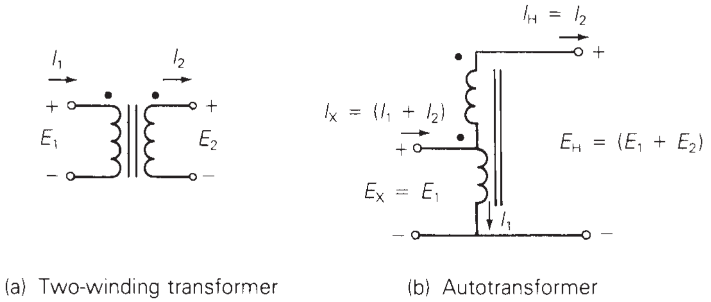

(a) Two-winding transformer (b) Autotransformer

FIGURE 3.23

Ideal single-phase transformers

Copyright 2017 Cengage Learning. All Rights Reserved. May not be copied, scanned, or duplicated, in whole or in part. Due to electronic rights, some third party content may be suppressed from the eBook and/or eChapter(s). Editorial review has deemed that any suppressed content does not materially affect the overall learning experience. Cengage Learning reserves the right to remove additional content at any time if subsequent rights restrictions require it.

(a disadvantage). The autotransformer also has lower per-unit losses (higher efficiency), lower exciting current, and lower cost if the turns ratio is not too large. The electrical connection of the windings, however, allows transient overvoltages to pass through the autotransformer more easily.

EXAMPLE 3.11

Autotransformer: single-phase

The single-phase two-winding 20-kVA, 480/120-volt transformer of Example 3.3 is connected as an autotransformer, as in Figure 3.23(b), where winding 1 is the 120-volt winding. For this autotransformer, determine (a) the voltage ratings E_X and E_H of the low- and high-voltage terminals, (b) the kVA rating, and (c) the per-unit leakage impedance.

SOLUTION

a. Since the 120-volt winding is connected to the low-voltage terminal, $E_X =$ 120 volts. When $E_X = E_1 = 120$ volts is applied to the low-voltage terminal, $E_2 =$ 480 volts is induced across the 480-volt winding, neglecting the voltage drop across the leakage impedance. Therefore, $E_H = E_1 + E_2 = 120 + 480 = 600$ volts.

b. As a normal two-winding transformer rated 20 kVA, the rated current of the 480-volt winding is $I_2 = I_H = 20{,}000/480 = 41.667$ A. As an autotransformer, the 480-volt winding can carry the same current. Therefore, the kVA rating $S_H = E_H I_H = (600)\,(41.667) = 25$ kVA. Note also that when $I_H = I_2 = 41.667$ A, a current $I_1 = (480/120)(41.667) = 166.7$ A is induced in the 120-volt winding. Therefore, $I_x = I_1 + I_2 = 208.3$ A (neglecting exciting current) and $S_X = E_X I_X =$ (120)(208.3) = 25 kVA, which is the same rating as calculated for the high-voltage terminal.

c. From Example 3.3, the leakage impedance is $0.0729/\underline{78.13^\circ}$ per unit as a normal, two-winding transformer. As an autotransformer, the leakage impedance *in ohms* is the same as for the normal transformer, since the core and windings are the same for both (only the external winding connections are different). However, the base impedances are different. For the high-voltage terminal, using (3.3.4),

$$Z_{\text{baseHold}} = \frac{(480)^2}{20{,}000} = 11.52\ \Omega \quad \text{as a normal transformer}$$

$$Z_{\text{baseHnew}} = \frac{(600)^2}{25{,}000} = 14.4\quad \Omega \quad \text{as an autotransformer}$$

Therefore, using (3.3.10),

$$Z_{\text{p.u.new}} = (0.0729\,\underline{/78.13^\circ})\left(\frac{11.52}{14.4}\right) = 0.05832\,\underline{/78.13^\circ} \quad \text{per unit}$$

Copyright 2017 Cengage Learning. All Rights Reserved. May not be copied, scanned, or duplicated, in whole or in part. Due to electronic rights, some third party content may be suppressed from the eBook and/or eChapter(s). Editorial review has deemed that any suppressed content does not materially affect the overall learning experience. Cengage Learning reserves the right to remove additional content at any time if subsequent rights restrictions require it.

For this example, the rating is 25 kVA, 120/600 volts as an autotransformer versus 20 kVA, 120/480 volts as a normal transformer. The autotransformer has both a larger kVA rating and a larger voltage ratio for the same cost. Also, the per-unit leakage impedance of the autotransformer is smaller. However, the increased high-voltage rating as well as the electrical connection of the windings may require more insulation for both windings.

3.8 TRANSFORMERS WITH OFF-NOMINAL TURNS RATIOS

It has been shown that models of transformers that use per-unit quantities are simpler than those that use actual quantities. The ideal transformer winding is eliminated when the ratio of the selected voltage bases equals the ratio of the voltage ratings of the windings. In some cases, however, it is impossible to select voltage bases in this manner. For example, consider the two transformers connected in parallel in Figure 3.24. Transformer T_1 is rated 13.8/345 kV and T_2 is rated 13.2/345 kV. If $\text{V}_{\text{baseH}} = 345$ kV is selected, then transformer T_1 requires $\text{V}_{\text{baseX}} = 13.8$ kV and T_2 requires $\text{V}_{\text{baseX}} = 13.2$ kV. It is clearly impossible to select the appropriate voltage bases for both transformers.

To accommodate this situation, develop a per-unit model of a transformer whose voltage ratings are not in proportion to the selected base voltages. Such a transformer is said to have an off-nominal turns ratio. Figure 3.25(a) shows a transformer with rated voltages $V_{1\text{rated}}$ and $V_{2\text{rated}}$, which satisfy

$$V_{1\text{rated}} = a_t V_{2\text{rated}} \tag{3.8.1}$$

where a_t is assumed, in general, to be either real or complex. Suppose the selected voltage bases satisfy

$$\text{V}_{\text{base1}} = b\text{V}_{\text{base2}} \tag{3.8.2}$$

Defining $c = \frac{a_t}{b}$, (3.8.1) can be rewritten as

$$V_{1\text{rated}} = b\left(\frac{a_t}{b}\right) V_{2\text{rated}} = bc\ V_{2\text{rated}} \tag{3.8.3}$$

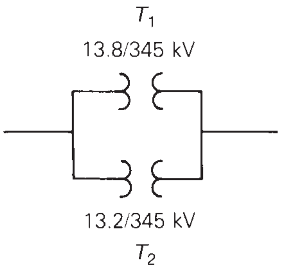

FIGURE 3.24

Two transformers connected in parallel

Copyright 2017 Cengage Learning. All Rights Reserved. May not be copied, scanned, or duplicated, in whole or in part. Due to electronic rights, some third party content may be suppressed from the eBook and/or eChapter(s). Editorial review has deemed that any suppressed content does not materially affect the overall learning experience. Cengage Learning reserves the right to remove additional content at any time if subsequent rights restrictions require it.

FIGURE 3.25

Transformer with off-nominal turns ratio

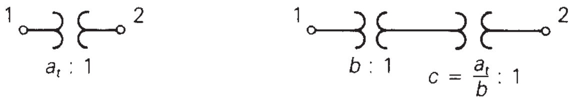

(a) Single-line diagram

(b) Represented as two transformers in series

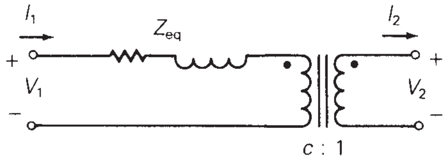

(c) Per-unit equivalent circuit
(Per-unit impedance is shown)

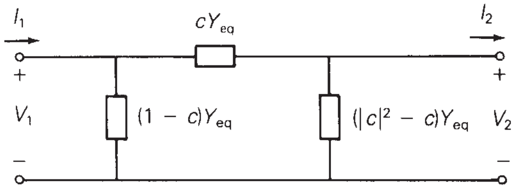

(d) π circuit representation for real c
$\left(\text{Per-unit admittances are shown; } Y_{eq} = \frac{1}{Z_{eq}}\right)$

Equation (3.8.3) can be represented by two transformers in series, as shown in Figure 3.25(b). The first transformer has the same ratio of rated winding voltages as the ratio of the selected base voltages, b. Therefore, this transformer has a standard per-unit model, as shown in Figure 3.9 or 3.17. Assume that the second transformer is ideal, and all real and reactive losses are associated with the first transformer. The resulting per-unit model is shown in Figure 3.25(c), where, for simplicity, the shunt-exciting branch is neglected. Note that if $a_t = b$, then the ideal transformer winding shown in this figure can be eliminated, since its turns ratio $c = (a_t/b) = 1$.

The per-unit model shown in Figure 3.25(c) is perfectly valid, but it is not suitable for some of the computer programs presented in later chapters because these programs do not accommodate ideal transformer windings. An alternative representation can be developed, however, by writing nodal equations for this figure as follows:

$$\begin{bmatrix} I_1 \\ -I_2 \end{bmatrix} = \begin{bmatrix} Y_{11} & Y_{12} \\ Y_{21} & Y_{22} \end{bmatrix} \begin{bmatrix} V_1 \\ V_2 \end{bmatrix} \tag{3.8.4}$$

where both I_1 and $-I_2$ are referenced *into* their nodes in accordance with the nodal equation method (Section 2.4). Recalling two-port network theory, the admittance parameters of (3.8.4) are, from Figure 3.23(c)

Copyright 2017 Cengage Learning. All Rights Reserved. May not be copied, scanned, or duplicated, in whole or in part. Due to electronic rights, some third party content may be suppressed from the eBook and/or eChapter(s). Editorial review has deemed that any suppressed content does not materially affect the overall learning experience. Cengage Learning reserves the right to remove additional content at any time if subsequent rights restrictions require it.

$$Y_{11} = \frac{I_1}{V_1}\bigg|_{V_2 = 0} = \frac{1}{Z_{\text{eq}}} = Y_{\text{eq}} \tag{3.8.5}$$

$$Y_{22} = \frac{-I_2}{V_2}\bigg|_{V_1 = 0} = \frac{1}{Z_{\text{eq}}/|c|^2} = |c|^2 Y_{\text{eq}} \tag{3.8.6}$$

$$Y_{12} = \frac{I_1}{V_2}\bigg|_{V_1 = 0} = \frac{-cV_2/Z_{\text{eq}}}{V_2} = -cY_{\text{eq}} \tag{3.8.7}$$

$$Y_{21} = \frac{-I_2}{V_1}\bigg|_{V_2 = 0} = \frac{-c^*I_1}{V_1} = -c^*Y_{\text{eq}} \tag{3.8.8}$$

Equations (3.8.4) through (3.8.8) with real or complex c are convenient for representing transformers with off-nominal turns ratios in the computer programs presented later. Note that when c is complex, Y_{12} is not equal to Y_{21}, and the preceding admittance parameters cannot be synthesized with a passive RLC circuit. However, the π network shown in Figure 3.25(d), which has the same admittance parameters as (3.8.4) through (3.8.8), can be synthesized for real c. Note also that when $c = 1$, the shunt branches in this figure become open circuits (zero per unit mhos), and the series branch becomes Y_{eq} per unit mhos (or Z_{eq} per unit ohms).

EXAMPLE 3.12

Tap-changing three-phase transformer: per-unit positive-sequence network

A three-phase generator step-up transformer is rated 1000 MVA, 13.8 kV Δ/345 kV Y with $Z_{\text{eq}} = j0.10$ per unit. The transformer high-voltage winding has ±10% taps. The system base quantities are

$$S_{\text{base}3\phi} = 500 \quad \text{MVA}$$

$$V_{\text{baseXLL}} = 13.8 \quad \text{kV}$$

$$V_{\text{baseHLL}} = 345 \quad \text{kV}$$

Determine the per-unit equivalent circuit for the following tap settings:

a. Rated tap

b. –10% tap (providing a 10% voltage decrease for the high-voltage winding)

Assume balanced positive-sequence operation. Neglect transformer winding resistance, exciting current, and phase shift.

(*Continued*)

Copyright 2017 Cengage Learning. All Rights Reserved. May not be copied, scanned, or duplicated, in whole or in part. Due to electronic rights, some third party content may be suppressed from the eBook and/or eChapter(s). Editorial review has deemed that any suppressed content does not materially affect the overall learning experience. Cengage Learning reserves the right to remove additional content at any time if subsequent rights restrictions require it.

SOLUTION

a. Using (3.8.1) and (3.8.2) with the low-voltage winding denoted winding 1,

$$a_t = \frac{13.8}{345} = 0.04 \qquad b = \frac{\mathrm{V}_{\mathrm{baseXLL}}}{\mathrm{V}_{\mathrm{baseHLL}}} = \frac{13.8}{345} = a_t \qquad c = 1$$

From (3.3.11),

$$Z_{\text{p.u.new}} = (j0.10)\left(\frac{500}{1000}\right) = j0.05 \quad \text{per unit}$$

The per-unit equivalent circuit, not including winding resistance, exciting current, and phase shift is

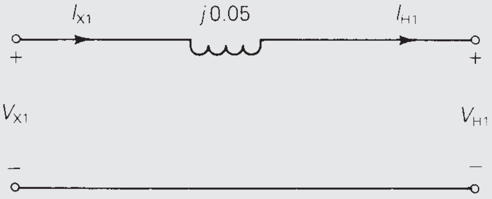

(Per-unit impedance is shown)

b. Using (3.8.1) and (3.8.2),

$$a_t = \frac{13.8}{345(0.9)} = 0.04444 \qquad b = \frac{13.8}{345} = 0.04$$

$$c = \frac{a_t}{b} = \frac{0.04444}{0.04} = 1.1111$$

From Figure 3.23(d),

$$c\,Y_{\text{eq}} = 1.1111\left(\frac{1}{j0.05}\right) = -j22.22 \quad \text{per unit}$$

$$(1 - c)\,Y_{\text{eq}} = (-0.11111)(-j20) = +j2.222 \quad \text{per unit}$$

$$(|c|^2 - c)\,Y_{\text{eq}} = (1.2346 - 1.1)(-j20) = -j2.469 \quad \text{per unit}$$

The per-unit positive-sequence network is

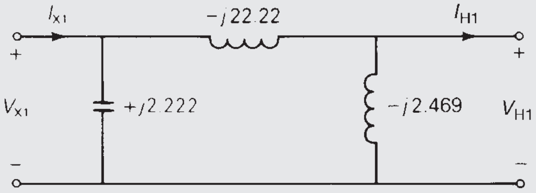

(Per-unit admittances are shown)

Copyright 2017 Cengage Learning. All Rights Reserved. May not be copied, scanned, or duplicated, in whole or in part. Due to electronic rights, some third party content may be suppressed from the eBook and/or eChapter(s). Editorial review has deemed that any suppressed content does not materially affect the overall learning experience. Cengage Learning reserves the right to remove additional content at any time if subsequent rights restrictions require it.

Open PowerWorld Simulator case Example 3_12 (see Figure 3.26) and select **Tools, Play** to see an animated view of this LTC transformer example. Initially the generator/step-up transformer feeds a 500 MW/100 Mvar load. As is typical in practice, the transformer's taps are adjusted in discrete steps, with each step changing the tap ratio by 0.625% (hence a 10% change requires 16 steps). Click on arrows next to the transformer's tap to manually adjust the tap by one step. Note that changing the tap directly changes the load voltage.

Because of the varying voltage drops caused by changing loads, LTCs are often operated to automatically regulate a bus voltage. This is particularly true when they are used as step-down transformers. To place the example transformer on automatic control, click on the LTC Control Status "No" field. This toggles the transformer control mode to automatic. Now the transformer manually changes its tap ratio to maintain the load voltage within a specified voltage range, between 0.995 and 1.005 per unit (343.3 to 346.7 kV) in this case. To see the LTC in automatic operation, use the load arrows to vary the load, particularly the Mvar field, noting that the LTC changes to keep the load's voltage within the specified deadband.

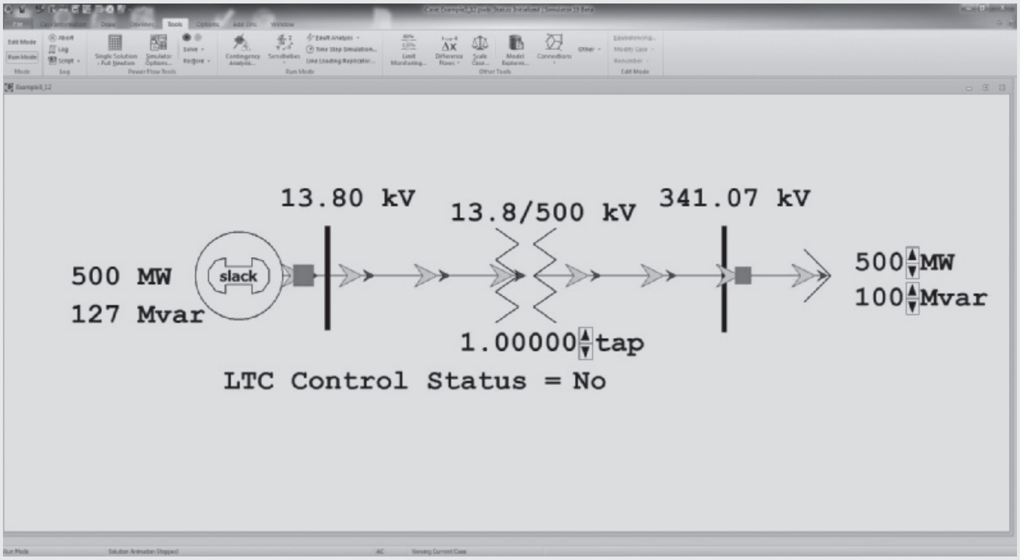

FIGURE 3.26

Screen for Example 3.12

Copyright 2017 Cengage Learning. All Rights Reserved. May not be copied, scanned, or duplicated, in whole or in part. Due to electronic rights, some third party content may be suppressed from the eBook and/or eChapter(s). Editorial review has deemed that any suppressed content does not materially affect the overall learning experience. Cengage Learning reserves the right to remove additional content at any time if subsequent rights restrictions require it.

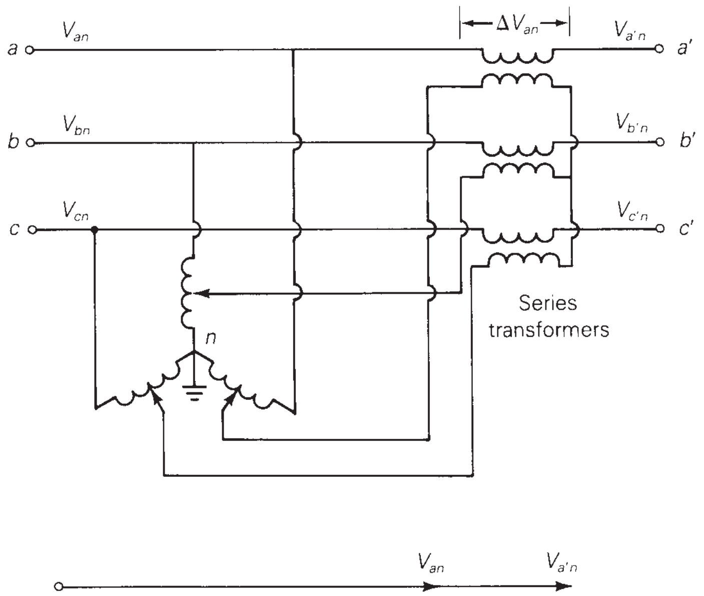
a
V_{an}
ΔV_{an}
$V_{a'n}$
a'
b
V_{bn}
$V_{b'n}$
b'
c
V_{cn}
$V_{c'n}$
c'
n
Series transformers
V_{an}
$V_{a'n}$

FIGURE 3.27

An example of a voltage-magnitude-regulating transformer

The three-phase regulating transformers shown in Figures 3.27 and 3.28 can be modeled as transformers with off-nominal turns ratios. For the voltage-magnitude-regulating transformer shown in Figure 3.27, adjustable voltages ΔV_{an}, ΔV_{bn}, and ΔV_{cn} which have equal magnitudes ΔV and which are in phase with the phase voltages V_{an}, V_{bn}, and V_{cn} are placed in the series link between buses *a–a′*, *b–b′*, and *c–c′*. Modeled as a transformer with an off-nominal turns ratio (see Figure 3.25), $c = (1 + \Delta V)$ for a voltage-magnitude increase toward bus *abc*, or $c = (1 + \Delta V)^{-1}$ for an increase toward bus *a′b′c′*.

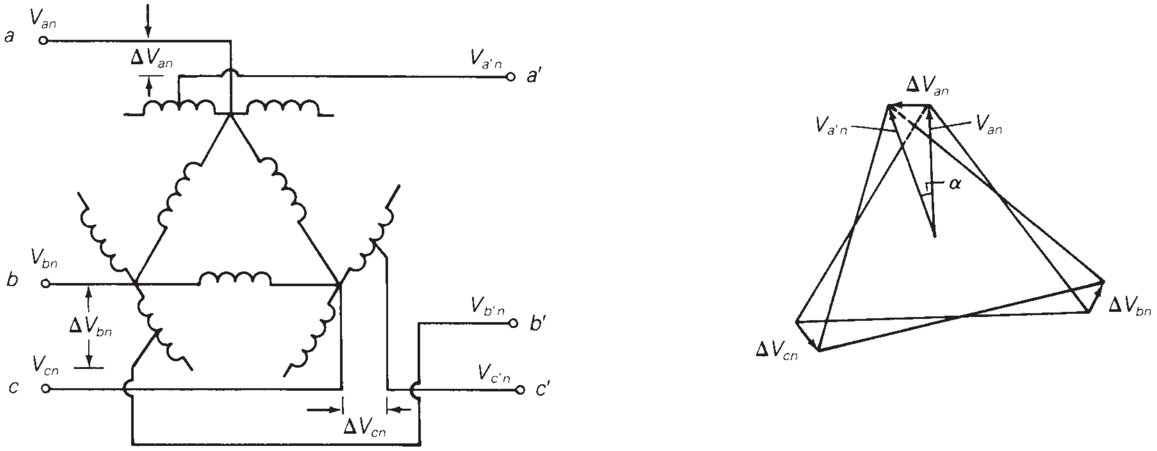
a
V_{an}
ΔV_{an}
$V_{a'n}$
a'
b
V_{bn}
ΔV_{bn}
$V_{b'n}$
b'
c
V_{cn}
$V_{c'n}$
c'
ΔV_{cn}
ΔV_{an}
$V_{a'n}$
V_{an}
α
ΔV_{bn}
ΔV_{cn}

FIGURE 3.28

An example of a phase-angle-regulating transformer. Windings drawn in parallel are on the same core

Copyright 2017 Cengage Learning. All Rights Reserved. May not be copied, scanned, or duplicated, in whole or in part. Due to electronic rights, some third party content may be suppressed from the eBook and/or eChapter(s). Editorial review has deemed that any suppressed content does not materially affect the overall learning experience. Cengage Learning reserves the right to remove additional content at any time if subsequent rights restrictions require it.

For the phase-angle-regulating transformer in Figure 3.28, the series voltages ΔV_{an}, ΔV_{bn}, and ΔV_{cn}, are ±90° out of phase with the phase voltages ΔV_{an}, V_{bn}, and V_{cn}. The phasor diagram in Figure 3.28 indicates that each of the bus voltages $V_{a'n}$, $V_{b'n}$, and $V_{c'n}$, has a phase shift that is approximately proportional to the magnitude of the added series voltage. Modeled as a transformer with an off-nominal turns ratio (see Figure 3.25), $c \approx 1\underline{/\alpha}$ for a phase increase toward bus *abc* or $c \approx 1\underline{/-\alpha}$ for a phase increase toward bus $a'b'c'$.

EXAMPLE 3.13

Voltage-regulating and phase-shifting three-phase transformers

Two buses *abc* and $a'b'c'$ are connected by two parallel lines L1 and L2 with positive-sequence series reactances $X_{L1} = 0.25$ and $X_{L2} = 0.20$ per unit. A regulating transformer is placed in series with line L1 at bus $a'b'c'$. Determine the 2 × 2 bus admittance matrix when the regulating transformer (a) provides a 0.05 per-unit increase in voltage magnitude toward bus $a'b'c'$ and (b) advances the phase 3° toward bus $a'b'c'$. Assume that the regulating transformer is ideal. Also, the series resistance and shunt admittance of the lines are neglected.

SOLUTION

The circuit is shown in Figure 3.29.

a. For the voltage-magnitude-regulating transformer, $c = (1 + \Delta V)^{-1} = (1.05)^{-1} = 0.9524$ per unit. From (3.8.5) through (3.8.8), the admittance parameters of the regulating transformer in series with line L1 are

$$Y_{11L1} = \frac{1}{j0.25} = -j4.0$$

$$Y_{22L1} = (0.9524)^2(-j4.0) = -j3.628$$

$$Y_{12L1} = Y_{21L1} = (-0.9524)(-j4.0) = j3.810$$

For line L2 alone,

$$Y_{11L2} = Y_{22L2} = \frac{1}{j0.20} = -j5.0$$

$$Y_{12L2} = Y_{21L2} = -(-j5.0) = j5.0$$

Combining the above admittances in parallel,

$$Y_{11} = Y_{11L1} + Y_{11L2} = -j4.0 - j5.0 = -j9.0$$

$$Y_{22} = Y_{22L1} + Y_{22L2} = -j3.628 - j5.0 = -j8.628$$

$$Y_{12} = Y_{21} = Y_{12L1} + Y_{12L2} = j3.810 + j5.0 = j8.810 \quad \text{per unit}$$

(Continued)

Copyright 2017 Cengage Learning. All Rights Reserved. May not be copied, scanned, or duplicated, in whole or in part. Due to electronic rights, some third party content may be suppressed from the eBook and/or eChapter(s). Editorial review has deemed that any suppressed content does not materially affect the overall learning experience. Cengage Learning reserves the right to remove additional content at any time if subsequent rights restrictions require it.

FIGURE 3.29

Positive-sequence circuit for Example 3.13

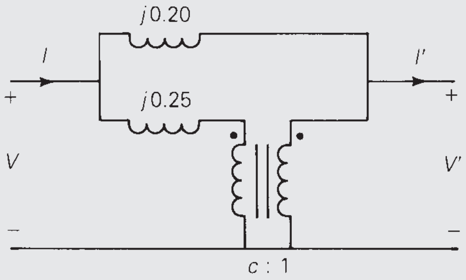

b. For the phase-angle-regulating transformer, $c = 1\underline{/-\alpha} = 1\underline{/-3°}$. Then, for this regulating transformer in series with line L1,

$$Y_{11L1} = \frac{1}{j0.25} = -j4.0$$

$$Y_{22L1} = |1.0\underline{/-3°}|^2(-j4.0) = -j4.0$$

$$Y_{12L1} = -(1.0\underline{/-3°})(-j4.0) = 4.0\underline{/87°} = 0.2093 + j3.9945$$

$$Y_{21L1} = -(1.0\underline{/-3°})^*(-j4.0) = 4.0\underline{/93°} = -0.2093 + j3.9945$$

The admittance parameters for line L2 alone are given in part (a). Combining the admittances in parallel,

$$Y_{11} = Y_{22} = -j4.0 - j5.0 = -j9.0$$

$$Y_{12} = 0.2093 + j3.9945 + j5.0 = 0.2093 + j8.9945$$

$$Y_{21} = -0.2093 + j3.9945 + j5.0 = -0.2093 + j8.9945 \quad \text{per unit}$$

To see this example in the PowerWorld Simulator, open case Example 3_13 (see Figure 3.30). In this case, the transformer and a parallel transmission line are assumed to be supplying power from a 345-kV generator to a 345-kV load. Initially, the off-nominal turns ratio is set to the value in part (a) of the example (PowerWorld has the off-nominal turns ratio on the load side [right-hand] so its tap value of 1.05 = c^{-1}). To view the PowerWorld Simulator bus admittance matrix, select the **Case Information** ribbon, then **Solution Details**, **Ybus**. To see how the system flows vary with changes to the tap, select **Tools**, **Play**, and then click on the arrows next to the tap field to change the LTC tap in 0.625% steps. Next, to verify the results from part (b), change the tap

Copyright 2017 Cengage Learning. All Rights Reserved. May not be copied, scanned, or duplicated, in whole or in part. Due to electronic rights, some third party content may be suppressed from the eBook and/or eChapter(s). Editorial review has deemed that any suppressed content does not materially affect the overall learning experience. Cengage Learning reserves the right to remove additional content at any time if subsequent rights restrictions require it.

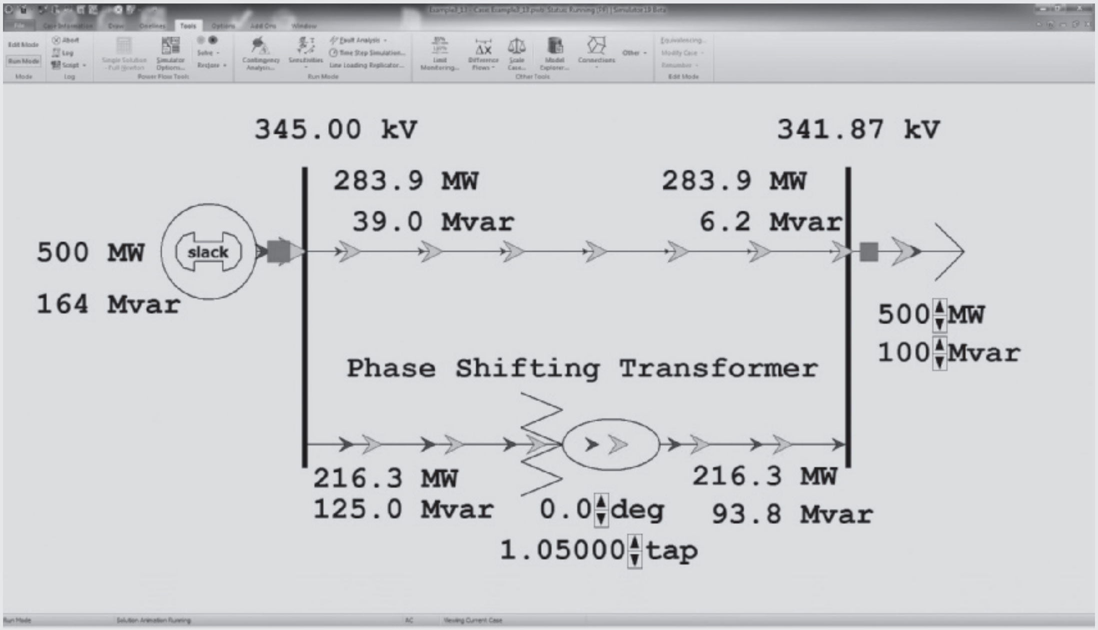

FIGURE 3.30

Screen for Example 3.13

field to 1.0 and the deg field to 3.0 degrees, and then again look at the bus admittance matrix. Click on the deg field arrow to vary the phase shift angle in one-degree steps. Notice that changing the phase angle primarily changes the real power flow, whereas changing the LTC tap changes the reactive power flow. In this example, the line flow fields show the absolute value of the real or reactive power flow; the direction of the flow is indicated with arrows. Traditional power flow programs usually indicate power flow direction using a convention that flow into a transmission line or transformer is assumed to be positive. You can display results in PowerWorld Simulator using this convention by first clicking on the **Onelines** ribbon and then selecting **Oneline Options**. Then on the **Display Options** tab uncheck the Use Absolute Values for MW/Mvar Line Flows fields.

Note that a voltage-magnitude-regulating transformer controls the *reactive* power flow in the series link in which it is installed, whereas a phase-angle-regulating transformer controls the *real* power flow (see Problem 3.59).

Copyright 2017 Cengage Learning. All Rights Reserved. May not be copied, scanned, or duplicated, in whole or in part. Due to electronic rights, some third party content may be suppressed from the eBook and/or eChapter(s). Editorial review has deemed that any suppressed content does not materially affect the overall learning experience. Cengage Learning reserves the right to remove additional content at any time if subsequent rights restrictions require it.

MULTIPLE CHOICE QUESTIONS

SECTION 3.1

3.1 The "Ohm's law" for the magnetic circuit states that the net magnetomotive force (mmf) equals the product of the core reluctance and the core flux.
(a) True (b) False

3.2 For an ideal transformer, the efficiency is
(a) 0% (b) 100% (c) 50%

3.3 For an ideal 2-winding transformer, the ampere-turns of the primary winding, $N_1 I_1$, is equal to the ampere-turns of the secondary winding, $N_2 I_2$
(a) True (b) False

3.4 An ideal transformer has no real or reactive power loss.
(a) True (b) False

3.5 For an ideal 2-winding transformer, an impedance Z_2 connected across winding 2 (secondary) is referred to winding 1 (primary) by multiplying Z_2 by
(a) The turns ratio (N_1/N_2)
(b) The square of the turns ratio $(N_1/N_2)^2$
(c) The cubed turns ratio $(N_1/N_2)^3$

3.6 Consider Figure 3.4. For an ideal phase-shifting transformer, the impedance is unchanged when it is referred from one side to the other.
(a) True (b) False

SECTION 3.2

3.7 Consider Figure 3.5. Match the following, those on the left to those on the right.

(i) I_m	(a) Exciting current
(ii) I_c	(b) Magnetizing current
(iii) I_e	(c) Core loss current

3.8 The units of admittance, conductance, and susceptance are siemens.
(a) True (b) False

3.9 Match the following:

(i) Hysteresis loss	(a) Can be reduced by constructing the core with laminated sheets of alloy steel
(ii) Eddy current loss	(b) Can be reduced by the use of special high grades of alloy steel as core material.

3.10 For large power transformers rated more than 500 kVA, the winding resistances, which are small compared with the leakage reactances, can often be neglected.
(a) True (b) False

Copyright 2017 Cengage Learning. All Rights Reserved. May not be copied, scanned, or duplicated, in whole or in part. Due to electronic rights, some third party content may be suppressed from the eBook and/or eChapter(s). Editorial review has deemed that any suppressed content does not materially affect the overall learning experience. Cengage Learning reserves the right to remove additional content at any time if subsequent rights restrictions require it.

3.11 For a short-circuit test on a 2-winding transformer, with one winding shorted, can you apply the rated voltage on the other winding?
(a) Yes (b) No

SECTION 3.3

3.12 The per-unit quantity is always dimensionless.
(a) True (b) False

3.13 Consider the adopted per-unit system for the transformers. Specify true or false for each of the following statements:

(a) For the entire power system of concern, the value of S_{base} is not the same.
(b) The ratio of the voltage bases on either side of a transformer is selected to be the same as the ratio of the transformer voltage ratings.
(c) Per-unit impedance remains unchanged when referred from one side of a transformer to the other.

3.14 The ideal transformer windings are eliminated from the per-unit equivalent circuit of a transformer.

(a) True (b) False

3.15 To convert a per-unit impedance from "old" to "new" base values, the equation to be used is

(a) $Z_{\text{p.u.new}} = Z_{\text{p.u.old}}\left(\dfrac{V_{\text{baseold}}}{V_{\text{basenew}}}\right)^2\left(\dfrac{S_{\text{basenew}}}{S_{\text{baseold}}}\right)$

(b) $Z_{\text{p.u.new}} = Z_{\text{p.u.old}}\left(\dfrac{V_{\text{baseold}}}{V_{\text{basenew}}}\right)^2\left(\dfrac{S_{\text{basenew}}}{S_{\text{baseold}}}\right)$

(c) $Z_{\text{p.u.new}} = Z_{\text{p.u.old}}\left(\dfrac{V_{\text{baseold}}}{V_{\text{basenew}}}\right)^2\left(\dfrac{S_{\text{baseold}}}{S_{\text{basenew}}}\right)$

3.16 In developing per-unit circuits of systems such as the one shown in Figure 3.10, when moving across a transformer, the voltage base is changed in proportion to the transformer voltage ratings.
(a) True (b) False

3.17 Consider Figure 3.10 of the text. The per-unit leakage reactance of transformer T_1, given as 0.1 p.u., is based on the name plate ratings of transformer T_1.
(a) True (b) False

3.18 For balanced three-phase systems, Z_{base} is given by

$$Z_{\text{base}} = \frac{V^2_{\text{baseLL}}}{S_{\text{base3}}}$$

(a) True (b) False

Copyright 2017 Cengage Learning. All Rights Reserved. May not be copied, scanned, or duplicated, in whole or in part. Due to electronic rights, some third party content may be suppressed from the eBook and/or eChapter(s). Editorial review has deemed that any suppressed content does not materially affect the overall learning experience. Cengage Learning reserves the right to remove additional content at any time if subsequent rights restrictions require it.

SECTION 3.4

3.19 With the American Standard notation, in either a Y–Δ or Δ–Y transformer, positive- sequence quantities on the high-voltage side shall lead their corresponding quantities on the low-voltage side by 30°.
(a) True (b) False

3.20 In either a Y–Δ or Δ–Y transformer, as per the American Standard notation, the negative-sequence phase shift is the reverse of the positive-sequence phase shift.
(a) True (b) False

3.21 In order to avoid difficulties with third-harmonic exciting current, which three-phase transformer connection is seldom used for step-up transformers between a generator and a transmission line in power systems.
(a) Y–Δ (b) Δ–Y (c) Y–Y

3.22 Does an open-Δ connection permit balanced three-phase operation?
(a) Yes (b) No

3.23 Does an open-Δ operation, the kVA rating compared to that of the original three-phase bank is
(a) 2/3 (b) 58% (c) 1

SECTION 3.5

3.24 It is stated that
(i) balanced three-phase circuits can be solved in per unit on a per-phase basis after converting Δ-load impedances to equivalent Y impedances.
(ii) Base values can be selected either on a per-phase basis or on a three-phase basis.
(a) Both statements are true.
(b) Neither is true.
(c) Only one of the above is true.

3.25 In developing per-unit equivalent circuits for three-phase transformers, under balanced three-phase operation.
(i) A common S_{base} is selected for both the H and X terminals.
(ii) The ratio of the voltage bases V_{baseH}/V_{baseX} is selected to be equal to the ratio of the rated line-to-line voltages $V_{ratedHLL}/V_{ratedXLL}$.
(a) Only one of the above is true.
(b) Neither is true.
(c) Both statements are true.

3.26 In per-unit equivalent circuits of practical three-phase transformers, under balanced three-phase operation, in which of the following connections would a phase-shifting transformer come up?
(a) Y–Y (b) Y–Δ (c) Δ–Δ

3.27 A low value of transformer leakage reactance is desired to minimize the voltage drop, but a high value is desired to limit the fault current, thereby leading to a compromise in the design specification.
(a) True (b) False

Copyright 2017 Cengage Learning. All Rights Reserved. May not be copied, scanned, or duplicated, in whole or in part. Due to electronic rights, some third party content may be suppressed from the eBook and/or eChapter(s). Editorial review has deemed that any suppressed content does not materially affect the overall learning experience. Cengage Learning reserves the right to remove additional content at any time if subsequent rights restrictions require it.

SECTION 3.6

3.28 Consider a single-phase three-winding transformer with the primary excited winding of N_1 turns carrying a current I_1 and two secondary windings of N_2 and N_3 turns, delivering currents of I_2 and I_3 respectively. For an ideal case, how are the ampere-turns balanced?

(a) $N_1 I_1 = N_2 I_2 - N_3 I_3$ (b) $N_1 I_1 = N_2 I_2 + N_3 I_3$

(c) $N_1 I_1 = -(N_2 I_2 - N_3 I_3)$

3.29 For developing per-unit equivalent circuits of single-phase three-winding transformer, a common S_{base} is selected for all three windings, and voltage bases are selected in proportion to the rated voltage of the windings.

(a) True (b) False

3.30 Consider the equivalent circuit of Figure 3.20(c) in the text. After neglecting the winding resistances and exciting current, could X_1, X_2, or X_3 become negative, even though the leakage reactance are always positive?

(a) Yes (b) No

SECTION 3.7

3.31 Consider an ideal single-phase 2-winding transformer of turns ratio $N_1/N_2 = a$. If it is converted to an autotransformer arrangement with a transformation ratio of $V_H/V_X = 1 + a$, (the autotransformer rating/two-winding transformer rating) would then be

(a) $1 + a$ (b) $1 + \frac{1}{a}$ (c) a

3.32 For the same output, the autotransformer (with not too large a turns ratio) is smaller in size than a two-winding transformer and has high efficiency as well as superior voltage regulation.

(a) True (b) False

3.33 The direct electrical connection of the windings allows transient over voltages to pass through the autotransformer more easily, and that is an important disadvantage of the autotransformer.

(a) True (b) False

SECTION 3.8

3.34 Consider Figure 3.25 of the text for a transformer with off-nominal turns ratio.

(i) The per-unit equivalent circuit shown in part (c) contains an ideal transformer which cannot be accommodated by some computer programs.

(a) True (b) False

(ii) In the π-circuit representation for real c in part (d), the admittance parameters Y_{11} and Y_{12} would be unequal.

(a) True (b) False

(iii) For complex c, can the admittance parameters be synthesized with a passive RLC circuit?

(a) Yes (b) No

Copyright 2017 Cengage Learning. All Rights Reserved. May not be copied, scanned, or duplicated, in whole or in part. Due to electronic rights, some third party content may be suppressed from the eBook and/or eChapter(s). Editorial review has deemed that any suppressed content does not materially affect the overall learning experience. Cengage Learning reserves the right to remove additional content at any time if subsequent rights restrictions require it.

PROBLEMS

SECTION 3.1

3.1 (a) An ideal single-phase two-winding transformer with turns ratio $a_t = N_1/N_2$ is connected with a series impedance Z_2 across winding 2. If one wants to replace Z_2, with a series impedance Z_1 across winding 1 and keep the terminal behavior of the two circuits to be identical, find Z_1 in terms of Z_2.

(b) Would the above result be true if instead of a series impedance there is a shunt impedance?

(c) Can one refer a ladder network on the secondary (2) side to the primary (1) side simply by multiplying every impendance bya_t^2?

3.2 An ideal transformer with $N_1 = 1000$ and $N_2 = 250$ is connected with an impedance Z_{22} across winding 2. If $V_1 = 1000 \underline{/0°}$ V and $I_1 = 5 \underline{/-30°}$ A, determine V_2, I_2, Z_2, and the impedance Z'_2, which is the value of Z_2 referred to the primary side of the transformer.

3.3 Consider an ideal transformer with $N_1 = 3000$ and $N_2 = 1000$ turns. Let winding 1 be connected to a source whose voltage is $e_1(t) = 100(1 - |t|)$ volts for $-1 \le t \le 1$ and $e_1(t) = 0$ for $|t| > 1$ second. A 2-farad capacitor is connected across winding 2. Sketch $e_1(t)$, $e_2(t)$, $i_1(t)$, and $i_2(t)$ versus time t.

3.4 A single-phase 100-kVA, 2400/240-volt, 60-Hz distribution transformer is used as a step-down transformer. The load, which is connected to the 240-volt secondary winding, absorbs 60 kVA at 0.8 power factor lagging and is at 230 volts. Assuming an ideal transformer, calculate the following: (a) primary voltage, (b) load impedance, (c) load impedance referred to the primary, and (d) the real and reactive power supplied to the primary winding.

3.5 Rework Problem 3.4 if the load connected to the 240-V secondary winding absorbs 110 kVA under short-term overload conditions at an 0.8 power factor leading and at 230 volts.

3.6 For a conceptual single-phase phase-shifting transformer, the primary voltage leads the secondary voltage by 30°. A load connected to the secondary winding absorbs 110 kVA at an 0.8 power factor leading and at a voltage $E_2 = 277\underline{/0°}$ volts. Determine (a) the primary voltage, (b) primary and secondary currents, (c) load impedance referred to the primary winding, and (d) complex power supplied to the primary winding.

3.7 Consider a source of voltage $v(t) = 10\sqrt{2}\,\sin(2t)$V, with an internal resistance of 1800 Ω. A transformer that can be considered as ideal is used to couple a 50-Ω resistive load to the source. (a) Determine the transformer primary-to-secondary turns ratio required to ensure maximum power transfer by matching the load and source resistances. (b) Find the average power delivered to the load, assuming maximum power transfer.

Copyright 2017 Cengage Learning. All Rights Reserved. May not be copied, scanned, or duplicated, in whole or in part. Due to electronic rights, some third party content may be suppressed from the eBook and/or eChapter(s). Editorial review has deemed that any suppressed content does not materially affect the overall learning experience. Cengage Learning reserves the right to remove additional content at any time if subsequent rights restrictions require it.

3.8 For the circuit shown in Figure 3.31, determine $v_{out}(t)$

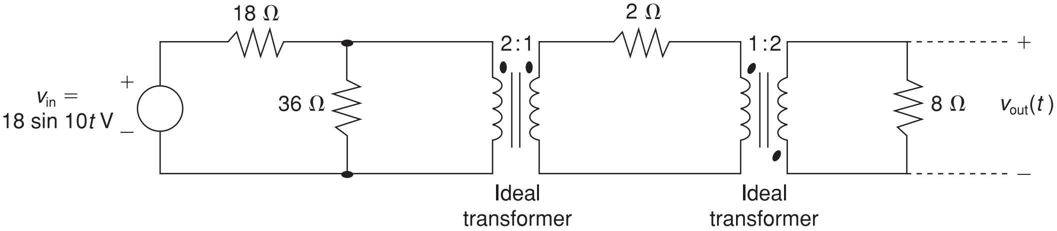

FIGURE 3.31

Problem 3.8

SECTION 3.2

3.9 A single-phase transformer has 2000 turns on the primary winding and 500 turns on the secondary. Winding resistances are $R_1 = 2\ \Omega$, and $R_2 = 0.125\ \Omega$; leakage reactances are $X_1 = 8\ \Omega$ and $X_2 = 0.5\ \Omega$. The resistance load on the secondary is 12 Ω.

(a) If the applied voltage at the terminals of the primary is 1000 V, determine V_2 at the load terminals of the transformer, neglecting magnetizing current.

(b) If the voltage regulation is defined as the difference between the voltage magnitude at the load terminals of the transformer at full load and at no load in percent of full-load voltage with input voltage held constant, compute the percent voltage regulation.

3.10 A single-phase step-down transformer is rated 13 MVA, 66 kV/11.5 kV. With the 11.5 kV winding short-circuited, rated current flows when the voltage applied to the primary is 5.5 kV. The power input is read as 100 kW. Determine R_{eq1} and X_{eq1} in ohms referred to the high-voltage winding.

3.11 For the transformer in Problem 3.10, the open-circuit test with 11.5 kV applied results in a power input of 65 kW and a current of 30 A. Compute the values for G_c and B_m in siemens referred to the high-voltage winding. Compute the efficiency of the transformer for a load of 10 MW at 0.8 p.f. lagging at rated voltage.

3.12 The following data are obtained when open-circuit and short-circuit tests are performed on a single-phase, 50-kVA, 2400/240-volt, 60-Hz distribution transformer.

	VOLTAGE (volts)	CURRENT (amperes)	POWER (watts)
Measurements on low-voltage side with high-voltage winding open	240	4.85	173
Measurements on high-voltage side with low-voltage winding shorted	52.0	20.8	650

Copyright 2017 Cengage Learning. All Rights Reserved. May not be copied, scanned, or duplicated, in whole or in part. Due to electronic rights, some third party content may be suppressed from the eBook and/or eChapter(s). Editorial review has deemed that any suppressed content does not materially affect the overall learning experience. Cengage Learning reserves the right to remove additional content at any time if subsequent rights restrictions require it.

(a) Neglecting the series impedance, determine the exciting admittance referred to the high-voltage side. (b) Neglecting the exciting admittance, determine the equivalent series impedance referred to the high-voltage side. (c) Assuming equal series impedances for the primary and referred secondary, obtain an equivalent T-circuit referred to the high-voltage side.

3.13 A single-phase 50-kVA, 2400/240-volt, 60-Hz distribution transformer has a 1-ohm equivalent leakage reactance and a 5000-ohm magnetizing reactance referred to the high-voltage side. If rated voltage is applied to the high-voltage winding, calculate the open-circuit secondary voltage. Neglect I^2R and G_c^2V losses. Assume equal series leakage reactances for the primary and the referred secondary.

3.14 A single-phase 50-kVA, 2400/240-volt, 60-Hz distribution transformer is used as a step-down transformer at the load end of a 2400-volt feeder whose series impedance is $(1.0 + j2.0)$ ohms. The equivalent series impedance of the transformer is $(1.0 + j2.5)$ ohms referred to the high-voltage (primary) side. The transformer is delivering rated load at a 0.8 power factor lagging and at a rated secondary voltage. Neglecting the transformer exciting current, determine (a) the voltage at the transformer primary terminals, (b) the voltage at the sending end of the feeder, and (c) the real and reactive power delivered to the sending end of the feeder.

3.15 Rework Problem 3.14 if the transformer is delivering rated load at rated secondary voltage and at (a) unity power factor, (b) 0.8 power factor leading. Compare the results with those of Problem 3.14.

3.16 A single-phase, 50-kVA, 2400/240-V, 60-Hz distribution transformer has the following parameters:

Resistance of the 2400-V winding: $R_1 = 0.75\ \Omega$
Resistance of the 240-V winding: $R_2 = 0.0075\ \Omega$
Leakage reactance of the 2400-V winding: $X_1 = 1.0\ \Omega$
Leakage reactance of the 240-V winding: $X_2 = 0.01\ \Omega$
Exciting admittance on the 240-V side $= 0.003 - j0.02$ S

(a) Draw the equivalent circuit referred to the high-voltage side of the transformer.
(b) Draw the equivalent circuit referred to the low-voltage side of the transformer. Show the numerical values of impedances on the equivalent circuits.

3.17 The transformer of Problem 3.16 is supplying a rated load of 50 kVA at a rated sec ondary voltage of 240 V and at 0.8 power factor lagging. Neglect the transformer exciting current. (a) Determine the input terminal voltage of the transformer on the high-voltage side. (b) Sketch the corresponding phasor diagram. (c) If the transformer is used as a step-down transformer at the load end of a feeder whose impedance is $0.5 + j2.0\ \Omega$, find the voltage V_S and the power factor at the sending end of the feeder.

Copyright 2017 Cengage Learning. All Rights Reserved. May not be copied, scanned, or duplicated, in whole or in part. Due to electronic rights, some third party content may be suppressed from the eBook and/or eChapter(s). Editorial review has deemed that any suppressed content does not materially affect the overall learning experience. Cengage Learning reserves the right to remove additional content at any time if subsequent rights restrictions require it.

SECTION 3.3

3.18 Using the transformer ratings as base quantities, work Problem 3.13 in per-unit.

3.19 Using the transformer ratings as base quantities, work Problem 3.14 in per-unit.

3.20 Using base values of 20 kVA and 115 volts in zone 3, rework Example 3.4.

3.21 Rework Example 3.5; using $S_{base3\phi} = 100$ kVA and $V_{baseLL} = 600$ volts.

3.22 A balanced Y-connected voltage source with $E_{ag} = 277\underline{/0^\circ}$ volts is applied to a balanced-Y load in parallel with a balanced-Δ load where $Z_Y = 20 + j10$ and $Z\Delta = 30 - j15$ ohms. The Y load is solidly grounded. Using base values of $S_{base1\phi} = 10$ kVA and $V_{baseLN} = 277$ volts, calculate the source current I_a in per-unit and in amperes.

3.23 Figure 3.32 shows the oneline diagram of a three-phase power system. By selecting a common base of 100 MVA and 22 kV on the generator side, draw an impedance diagram showing all impedances including the load impedance in per-unit. The data are given as follows:

G:	90 MVA	22 kV	x = 0.18 per unit
T_1:	50 MVA	22/220 kV	x = 0.10 per unit
T_2:	40 MVA	220/11 kV	x = 0.06 per unit
T_3:	40 MVA	22/110 kV	x = 0.064 per unit
T_4:	40 MVA	110/11 kV	x = 0.08 per unit
M:	66.5 MVA	10.45 kV	x = 0.185 per unit

Lines 1 and 2 have series reactances of 48.4 and 65.43 Ω, respectively. At bus 4, the three-phase load absorbs 57 MVA at 10.45 kV and 0.6 power factor lagging.

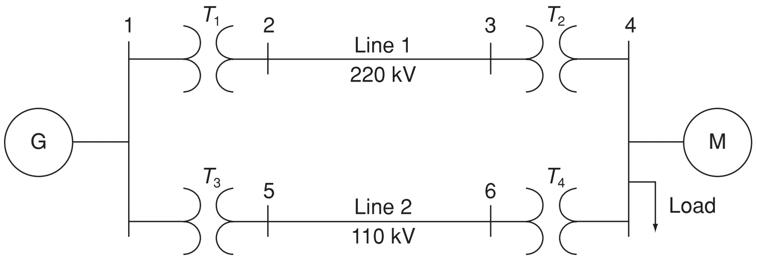

FIGURE 3.32

Problem 3.23

3.24 For Problem 3.18, the motor operates at full load, at 0.8 power factor leading, and at a terminal voltage of 10.45 kV. Determine (a) the voltage at bus 1, which is the generator bus, and (b) the generator and motor internal EMFs.

Copyright 2017 Cengage Learning. All Rights Reserved. May not be copied, scanned, or duplicated, in whole or in part. Due to electronic rights, some third party content may be suppressed from the eBook and/or eChapter(s). Editorial review has deemed that any suppressed content does not materially affect the overall learning experience. Cengage Learning reserves the right to remove additional content at any time if subsequent rights restrictions require it.

3.25 Consider a single-phase electric system shown in Figure 3.33. Transformers are rated as follows:

X–Y 15 MVA, 13.8/138 kV, leakage reactance 10%
Y–Z 15 MVA, 138/69 kV, leakage reactance 8%

With the base in circuit Y chosen as 15 MVA, 138 kV, determine the per-unit impedance of the 500 Ω resistive load in circuit Z, referred to circuits Z, Y, and X. Neglecting magnetizing currents, transformer resistances, and line impedances, draw the impedance diagram in per unit.

FIGURE 3.33

Single-phase electric system for Problem 3.25

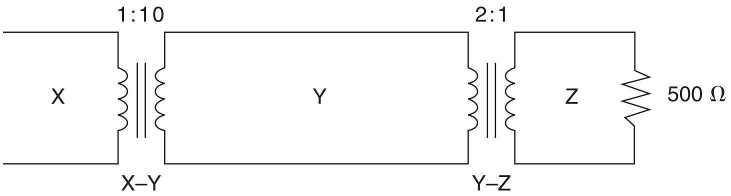

3.26 A bank of three single-phase transformers, each rated 30 MVA, 38.1/3.81 kV, are connected in Y–Δ with a balanced load of three 1 Ω, Y-connected resistors. Choosing a base of 90 MVA, 66 kV for the high-voltage side of the three-phase transformer, specify the base for the low-voltage side. Compute the per-unit resistance of the load on the base for the low-voltage side. Also, determine the load resistance in ohms referred to the high-voltage side and the per-unit value on the chosen base.

3.27 A three-phase transformer is rated 1000 MVA, 220 Y/22 Δ kV. The Y-equivalent short-circuit impedance, considered equal to the leakage reactance, measured on the low-voltage side is 0.1 Ω. Compute the per-unit reactance of the transformer. In a system in which the base on the high-voltage side of the transformer is 100 MVA, 230 kV, what value of the per-unit reactance should be used to represent this transformer?

3.28 For the system shown in Figure 3.34, draw an impedance diagram in per unit by choosing 100 kVA to be the base kVA and 2400 V as the base voltage for the generators.

FIGURE 3.34

System for Problem 3.28

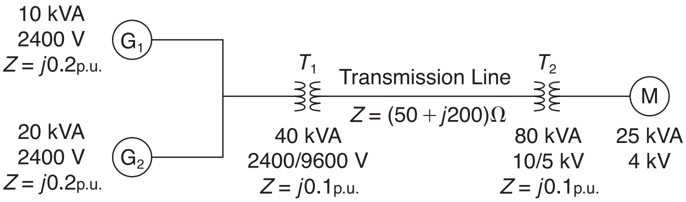

Copyright 2017 Cengage Learning. All Rights Reserved. May not be copied, scanned, or duplicated, in whole or in part. Due to electronic rights, some third party content may be suppressed from the eBook and/or eChapter(s). Editorial review has deemed that any suppressed content does not materially affect the overall learning experience. Cengage Learning reserves the right to remove additional content at any time if subsequent rights restrictions require it.

3.29 Consider three ideal single-phase transformers (with a voltage gain of η) put together as a Δ–Ω three-phase bank as shown in Figure 3.35. Assuming positive-sequence voltages for V_{an}, V_{bn}, and V_{cn}, find $V_{a'n'}$, $V_{b'n'}$, and $V_{C'n'}$ in terms of V_{an}, V_{bn}, and V_{cn}, respectively.

(a) Would such relationships hold for the line voltages as well?

(b) Looking into the current relationships, express I'_a, I'_b, and I'_c in terms of I_a, I_b, and I_c, respectively.

(c) Let S' and S be the per-phase complex power output and input, respectively. Find S′ in terms of S.

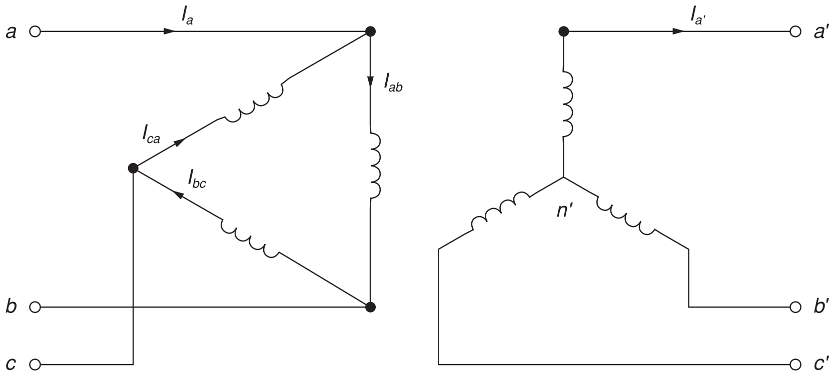

FIGURE 3.35

$\Delta-$Y connection for Problem 3.29

3.30 Reconsider Problem 3.29. If V_{an}, V_{bn}, and V_{cn} are a negative-sequence set, how would the voltage and current relationships change?

(a) If C_1 is the complex positive-sequence voltage gain in Problem 3.29 and (b) if C_2 is the negative sequence complex voltage gain, express the relationship between C_1 and C_2

3.31 If positive-sequence voltages are assumed and the Y-Δ connection is considered, again with ideal transformers as in Problem 3.29, find the complex voltage gain C_3.

(a) What would the gain be for a negative-sequence set?

(b) Comment on the complex power gain.

(c) When terminated in a symmetric Y-connected load, find the referred impedance Z'_L, the secondary impedance Z_L referred to primary (i.e., the per-phase driving-point impedance on the primary side), in terms of Z_L and the complex voltage gain C.

SECTION 3.4

3.32 Determine the positive- and negative-sequence phase shifts for the three-phase transformers shown in Figure 3.36.

3.33 Consider the three single-phase two-winding transformers shown in Figure 3.37. The high-voltage windings are connected in Y. (a) For the

Copyright 2017 Cengage Learning. All Rights Reserved. May not be copied, scanned, or duplicated, in whole or in part. Due to electronic rights, some third party content may be suppressed from the eBook and/or eChapter(s). Editorial review has deemed that any suppressed content does not materially affect the overall learning experience. Cengage Learning reserves the right to remove additional content at any time if subsequent rights restrictions require it.

low-voltage side, connect the windings in Δ, place the polarity marks, and label the terminals *a, b,* and *c* in accordance with the American standard. (b) Relabel the terminals a', b', and c' such that V_{AN} is 90° out of phase with $V_{a'n}$ for positive sequence.

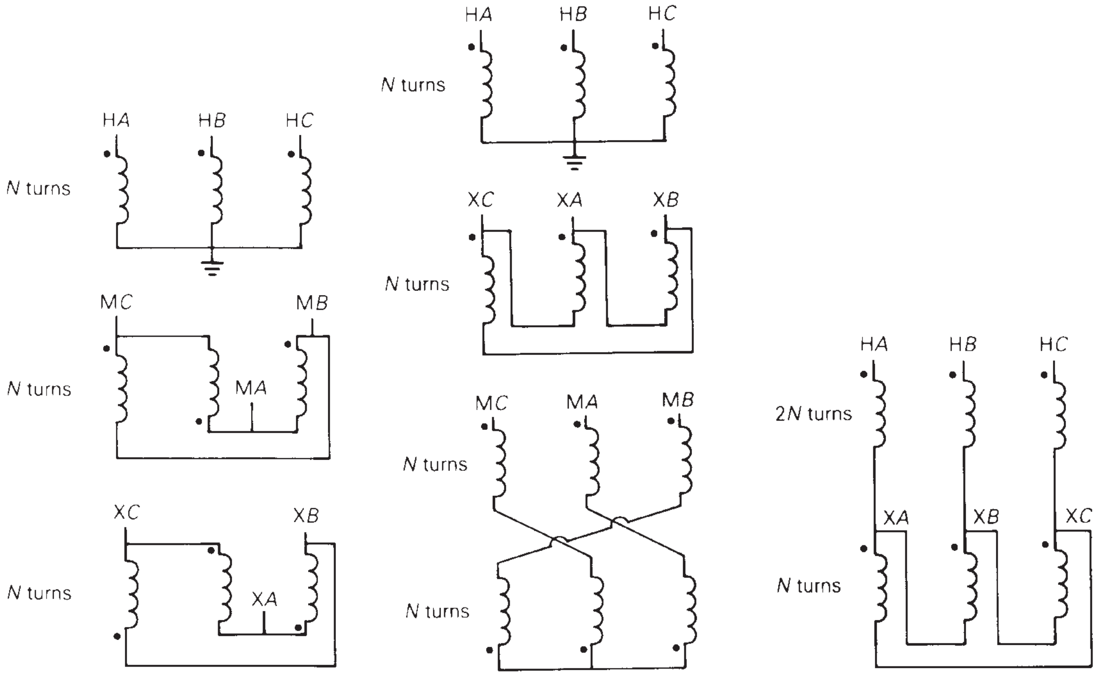
HA
HB
HC
N turns
MC
MB
MA
N turns
XC
XB
XA
N turns
HA
HB
HC
N turns
XC
XA
XB
N turns
MC
MA
MB
N turns
N turns
HA
HB
HC
2N turns
XA
XB
XC
N turns

(a) Y–Δ–Δ transformer

(b) Y–Δ–zig-zag transformer

(c) Extended Δ autotransformer

FIGURE 3.36

Problems 3.32 and 3.52 (Coils drawn on the same vertical line are on the same core)

FIGURE 3.37

Problem 3.33

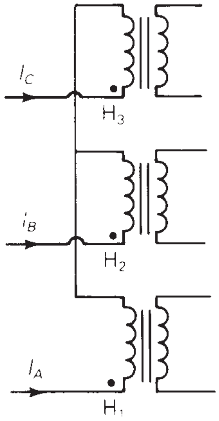
I_C
H_3
I_B
H_2
I_A
H_1

Copyright 2017 Cengage Learning. All Rights Reserved. May not be copied, scanned, or duplicated, in whole or in part. Due to electronic rights, some third party content may be suppressed from the eBook and/or eChapter(s). Editorial review has deemed that any suppressed content does not materially affect the overall learning experience. Cengage Learning reserves the right to remove additional content at any time if subsequent rights restrictions require it.

3.34 Three single-phase, two-winding transformers, each rated 450 MVA, 20 kV/288.7 kV, with leakage reactance $X_{eq} = 0.10$ per unit, are connected to form a three-phase bank. The high-voltage windings are connected in Y with a solidly grounded neutral. Draw the per-unit equivalent circuit if the low-voltage windings are connected (a) in Δ with American standard phase shift or (b) in Y with an open neutral. Use the transformer ratings as base quantities. Winding resistances and exciting current are neglected.

3.35 Consider a bank of three single-phase two-winding transformers whose high-voltage terminals are connected to a three-phase, 13.8-kV feeder. The low-voltage terminals are connected to a three-phase substation load rated 2.0 MVA and 2.5 kV. Determine the required voltage, current, and MVA ratings of both windings of each transformer, when the high-voltage/low-voltage windings are connected (a) Y–Δ, (b) Δ–Y, (c) Y–Y, and (d) Δ–Δ.

3.36 Three single-phase two-winding transformers, each rated 25 MVA, 34.5/13.8 kV, are connected to form a three-phase Δ–Δ bank. Balanced positive-sequence voltages are applied to the high-voltage terminals, and a balanced, resistive Y load connected to the low-voltage terminals absorbs 75 MW at 13.8 kV. If one of the single-phase transformers is removed (resulting in an open-Δ connection) and the balanced load is simultaneously reduced to 43.3 MW (57.7% of the original value), determine (a) the load voltages V_{an}, V_{bn}, and V_{cn}; (b) load currents I_a, I_b, and I_c; and (c) the MVA supplied by each of the remaining two transformers. Are balanced voltages still applied to the load? Is the open-Δ transformer overloaded?

3.37 Three single-phase two-winding transformers, each rated 25 MVA, 54.2/5.42 kV, are connected to form a three-phase Y–Δ bank with a balanced Y-connected resistive load of 0.6 Ω per phase on the low-voltage side. By choosing a base of 75 MVA (three phase) and 94 kV (line-to-line) for the high-voltage side of the transformer bank, specify the base quantities for the low-voltage side. Determine the per-unit resistance of the load on the base for the low-voltage side. Then determine the load resistance R_L in ohms referred to the high-voltage side and the per-unit value of this load resistance on the chosen base.

3.38 Consider a three-phase generator rated 300 MVA, 23 kV, supplying a system load of 240 MVA and 0.9 power factor lagging at 230 kV through a 330 MVA, 23 Δ/ 230 Y-kV step-up transformer with a leakage reactance of 0.11 per unit. (a) Neglecting the exciting current and choosing base values at the load of 100 MVA and 230 kV, find the phasor currents I_A, I_B, and I_C supplied to the load in per unit. (b) By choosing the load terminal voltage V_A as reference, specify the proper base for the generator circuit and determine the generator voltage V as well as the phasor currents I_A, I_B, and I_C, from the generator. (*Note:* Take into account the phase shift of the transformer.) (c) Find the generator terminal voltage in kV and the real power supplied by the generator in MW. (d) By omitting the transformer phase shift altogether, check to see whether you get the same magnitude of generator terminal voltage and real power delivered by the generator.

Copyright 2017 Cengage Learning. All Rights Reserved. May not be copied, scanned, or duplicated, in whole or in part. Due to electronic rights, some third party content may be suppressed from the eBook and/or eChapter(s). Editorial review has deemed that any suppressed content does not materially affect the overall learning experience. Cengage Learning reserves the right to remove additional content at any time if subsequent rights restrictions require it.

SECTION 3.5

3.39 The leakage reactance of a three-phase, 300-MVA, 230 Y/23 Δ-kV transformer is 0.06 per unit based on its own ratings. The Y winding has a solidly grounded neutral. Draw the per-unit equivalent circuit. Neglect the exciting admittance and assume the American Standard phase shift.

3.40 Choosing system bases to be 240/24 kV and 100 MVA, redraw the per-unit equivalent circuit for Problem 3.39.

3.41 Consider the single-line diagram of the power system shown in Figure 3.38. Equipment ratings are

Generator 1:	1000 MVA, 18 kV, X” = 0.2 per unit
Generator 2:	1000 MVA, 18 kV, X” = 0.2 p.u.
Synchronous motor 3:	1500 MVA, 20 kV, X” = 0.2 p.u.
Three-phase Δ–Y transformers T_1,T_2, T_3, T_4:	1000 MVA, 500 kV Y/20 kV Δ, X = 0.1 p.u.
Three-phase Y–Y transformer T_5:	1500 MVA, 500 kV Y/20 kV Y, X = 0.1 p.u.

Neglecting resistance, transformer phase shift, and magnetizing reactance, draw the equivalent reactance diagram. Use a base of 100 MVA and 500 kV for the 50-ohm line. Determine the per-unit reactances.

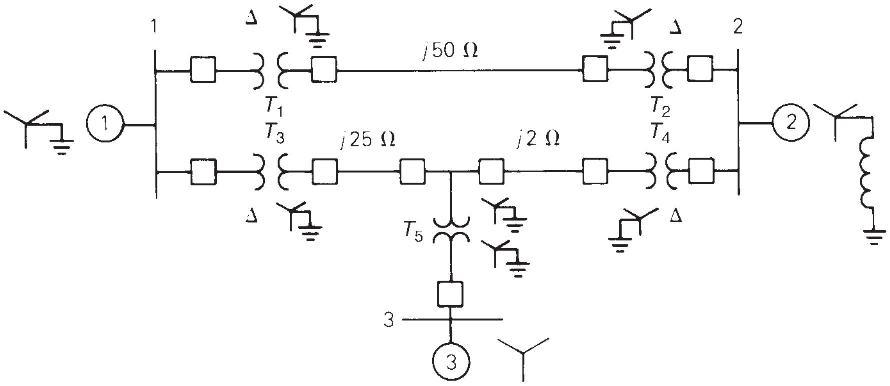

FIGURE 3.38

Problems 3.41 and 3.42

3.42 For the power system in Problem 3.41, the synchronous motor absorbs 1500 MW at 0.8 power factor leading with the bus 3 voltage at 18 kV. Determine the bus 1 and bus 2 voltages in kV. Assume that generators 1 and 2 deliver equal real powers and equal reactive powers. Also assume a balanced three-phase system with positive-sequence sources.

Copyright 2017 Cengage Learning. All Rights Reserved. May not be copied, scanned, or duplicated, in whole or in part. Due to electronic rights, some third party content may be suppressed from the eBook and/or eChapter(s). Editorial review has deemed that any suppressed content does not materially affect the overall learning experience. Cengage Learning reserves the right to remove additional content at any time if subsequent rights restrictions require it.

3.43 Three single-phase transformers, each rated 10 MVA, 66.4/12.5 kV, 60 Hz, with an equivalent series reactance of 0.1 per unit divided equally between primary and secondary, are connected in a three-phase bank. The high-voltage windings are Y-connected and their terminals are directly connected to a 115-kV three-phase bus. The secondary terminals are all shorted together. Find the currents entering the high-voltage terminals and leaving the low-voltage terminals if the low-voltage windings are (a) Y-connected and (b) Δ-connected.

3.44 A 130-MVA, 13.2-kV three-phase generator, which has a positive-sequence reactance of 1.5 per unit on the generator base, is connected to a 135-MVA, 13.2 Δ/115 Y-kV step-up transformer with a series impedance of $(0.005+j0.1)$ per unit on its own base. (a) Calculate the per-unit generator reactance on the transformer base. (b) The load at the transformer terminals is 15 MW at unity power factor and at 115 kV. Choosing the transformer high-side voltage as the reference phasor, draw a phasor diagram for this condition. (c) For the condition of part (b), find the transformer low-side voltage and the generator internal voltage behind its reactance. Also compute the generator output power and power factor.

3.45 Figure 3.39 shows a oneline diagram of a system in which the three-phase generator is rated 300 MVA, 20 kV with a subtransient reactance of 0.2 per unit and with its neutral grounded through a 0.4-Ω reactor. The transmission line is 64 km long with a series reactance of 0.5 Ω/km. The three-phase transformer T_1 is rated 350 MVA, 230/ 20 kV with a leakage reactance of 0.1 per unit. Transformer T_2 is composed of three single-phase transformers, each rated 100 MVA, 127/13.2 kV with a leakage reactance of 0.1 per unit. Two 13.2-kV motors M_1 and M_2 with a subtransient reactance of 0.2 per unit for each motor represent the load. M_1 has a rated input of 200 MVA with its neutral grounded through a 0.4-Ω current-limiting reactor. M_2 has a rated input of 100 MVA with its neutral not connected to ground. Neglect phase shifts associated with the transformers. Choose the generator rating as base in the generator circuit and draw the positive-sequence reactance diagram showing all reactances in per unit.

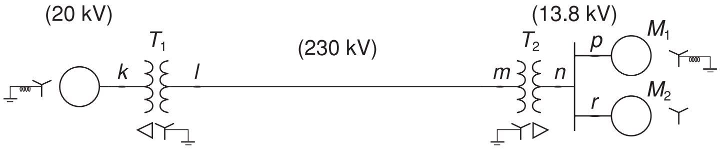

FIGURE 3.39

Problems 3.45 and 3.46

3.46 The motors M_1 and M_2 of Problem 3.45 have inputs of 120 and 60 MW, respectively, at 13.2 kV, and both operate at unity power factor. Determine the generator terminal voltage and voltage regulation of the line. Neglect transformer phase shifts.

3.47 Consider the oneline diagram shown in Figure 3.40. The three-phase transformer bank is made up of three identical single-phase transformers,

Copyright 2017 Cengage Learning. All Rights Reserved. May not be copied, scanned, or duplicated, in whole or in part. Due to electronic rights, some third party content may be suppressed from the eBook and/or eChapter(s). Editorial review has deemed that any suppressed content does not materially affect the overall learning experience. Cengage Learning reserves the right to remove additional content at any time if subsequent rights restrictions require it.

each specified by $X_1 = 0.24\ \Omega$ (on the low-voltage side), negligible resistance and magnetizing current, and turns ratio $\eta = N_2/N_1 = 10$. The transformer bank is delivering 100 MW at 0.8 p.f. lagging to a substation bus whose voltage is 230 kV.

(a) Determine the primary current magnitude, primary voltage (line-to-line) magnitude, and the three-phase complex power supplied by the generator. Choose the line-to-neutral voltage at the bus, $V_{a'n'}$ as the reference. Account for the phase shift, and assume positive-sequence operation.

(b) Find the phase shift between the primary and secondary voltages.

FIGURE 3.40

Oneline diagram for Problem 3.47

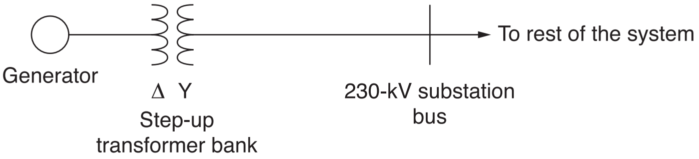

3.48 With the same transformer banks as in Problem 3.47, Figure 3.41 shows the oneline diagram of a generator, a step-up transformer bank, a transmission line, a step-down transformer bank, and an impedance load. The generator terminal voltage is 15 kV (line-to-line).

FIGURE 3.41

Oneline diagram for Problem 3.48

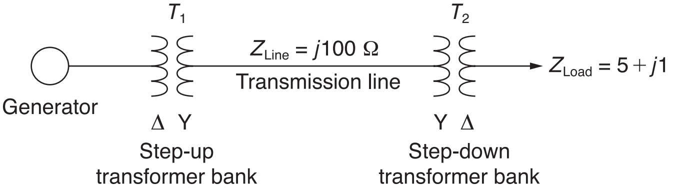
T_1
T_2
$Z_{\text{Line}} = j100\ \Omega$
Transmission line
$Z_{\text{Load}} = 5 + j1$
Generator
Δ Y
Step-up transformer bank
Y Δ
Step-down transformer bank

(a) Draw the per-phase equivalent circuit, accounting for phase shifts for positive-sequence operation.

(b) By choosing the line-to-neutral generator terminal voltage as the reference, determine the magnitudes of the generator current, transmission-line current, load current, and line-to-line load voltage. Also, find the three-phase complex power delivered to the load.

3.49 Consider the single-line diagram of a power system shown in Figure 3.42 with equipment ratings given:

Generator G_1:	50 MVA, 13.2 kV, $x = 0.15$ p.u.
Generator G_2:	20 MVA, 13.8 kV, $x = 0.15$ p.u.
Three-phase Δ–Y transformer T_1:	80MVA,13.2Δ/165YkV,X=0.1p.u.
Three-phase Y–Δ transformer T_2:	40MVA,165Y/13.8ΔkV,X=0.1p.u.
Load:	40 MVA, 0.8 PF lagging, operating at 150 kV

Copyright 2017 Cengage Learning. All Rights Reserved. May not be copied, scanned, or duplicated, in whole or in part. Due to electronic rights, some third party content may be suppressed from the eBook and/or eChapter(s). Editorial review has deemed that any suppressed content does not materially affect the overall learning experience. Cengage Learning reserves the right to remove additional content at any time if subsequent rights restrictions require it.

Choose a base of 100 MVA for the system and 132-kV base in the transmission-line circuit. Let the load be modeled as a parallel combination of resistance and inductance. Neglect transformer phase shifts. Draw a per-phase equivalent circuit of the system showing all impedances in per unit.

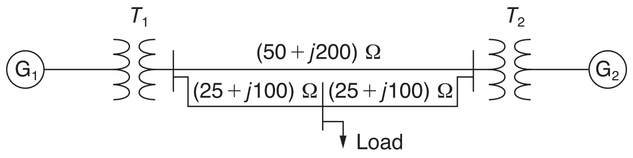

FIGURE 3.42 Oneline diagram for Problem 3.49

SECTION 3.6

3.50 A single-phase three-winding transformer has the following parameters: $Z_1 = Z_2 = Z_3 = 0 + j0.05$, $G_C = 0$, and $B_M = 0.2$ per unit. Three identical transformers, as described, are connected with their primaries in Y (solidly grounded neutral) and with their secondaries and tertiaries in Δ. Draw the per-unit sequence networks of this transformer bank.

3.51 The ratings of a three-phase three-winding transformer are

Primary (1): Y connected, 66 kV, 15 MVA

Secondary (2): Y connected, 13.2 kV, 10 MVA

Tertiary (3): A connected, 2.3 kV, 5 MVA

Neglecting winding resistances and exciting current, the per-unit leakage reactances are

$X_{12} = 0.08$ on a 15-MVA,66-kV base

$X_{13} = 0.10$ on a 15-MVA,66-kV base

$X_{23} = 0.09$ on a 10-MVA, 13.2-kV base

(a) Determine the per-unit reactances X_1, X_2, X_3 of the equivalent circuit on a 15-MVA, 66-kV base at the primary terminals. (b) Purely resistive loads of 7.5 MW at 13.2 kV and 5 MW at 2.3 kV are connected to the secondary and tertiary sides of the transformer, respectively. Draw the per-unit impedance diagram, showing the per-unit impedances on a 15-MVA, 66-kV base at the primary terminals.

3.52 Draw the per-unit equivalent circuit for the transformers shown in Figure 3.34. Include ideal phase-shifting transformers showing phase shifts determined in Problem 3.32. Assume that all windings have the same kVA rating and that the equivalent leakage reactance of any two windings with the third winding open is 0.10 per unit. Neglect the exciting admittance.

Copyright 2017 Cengage Learning. All Rights Reserved. May not be copied, scanned, or duplicated, in whole or in part. Due to electronic rights, some third party content may be suppressed from the eBook and/or eChapter(s). Editorial review has deemed that any suppressed content does not materially affect the overall learning experience. Cengage Learning reserves the right to remove additional content at any time if subsequent rights restrictions require it.

3.53 The ratings of a three-phase, three-winding transformer are

Primary: Y connected, 66 kV, 15 MVA
Secondary: Y connected, 13.2 kV, 10 MVA
Tertiary: Δ connected, 2.3 kV, 5 MVA

Neglecting resistances and exciting current, the leakage reactances are:

$X_{PS} = 0.09$ per unit on a 15-MVA, 66-kV base
$X_{PT} = 0.08$ per unit on a 15-MVA, 66-kV base
$X_{ST} = 0.05$ per unit on a 10-MVA, 13.2-kV base

Determine the per-unit reactances of the per-phase equivalent circuit using a base of 15 MVA and 66 kV for the primary.

3.54 An infinite bus, which is a constant voltage source, is connected to the primary of the three-winding transformer of Problem 3.53. A 7.5-MVA, 13.2-kV synchronous motor with a subtransient reactance of 0.2 per unit is connected to the transformer secondary. A 5-MW, 2.3-kV three-phase resistive load is connected to the tertiary. Choosing a base of 66 kV and 15 MVA in the primary, draw the impedance diagram of the system showing per-unit impedances. Neglect transformer exciting current, phase shifts, and all resistances except the resistive load.

SECTION 3.7

3.55 A single-phase 10-kVA, 2300/230-volt, 60-Hz two-winding distribution transformer is connected as an autotransformer to step up the voltage from 2300 to 2530 volts. (a) Draw a schematic diagram of this arrangement, showing all voltages and currents when delivering full load at rated voltage. (b) Find the permissible kVA rating of the autotransformer if the winding currents and voltages are not to exceed the rated values as a two-winding transformer. How much of this kVA rating is transformed by magnetic induction? (c) The following data are obtained from tests carried out on the transformer when it is connected as a two-winding transformer:

Open-circuit test with the low-voltage terminals excited:
Applied voltage = 230 V, input current = 0.45 A, input power = 70 W.

Short-circuit test with the high-voltage terminals excited:
Applied voltage = 120 V, input current = 4.5 A, input power = 240 W.

Based on the data, compute the efficiency of the autotransformer corresponding to full load, rated voltage, and 0.8 power factor lagging. Comment on why the efficiency is higher as an autotransformer than as a two-winding transformer.

Copyright 2017 Cengage Learning. All Rights Reserved. May not be copied, scanned, or duplicated, in whole or in part. Due to electronic rights, some third party content may be suppressed from the eBook and/or eChapter(s). Editorial review has deemed that any suppressed content does not materially affect the overall learning experience. Cengage Learning reserves the right to remove additional content at any time if subsequent rights restrictions require it.

3.56 Three single-phase two-winding transformers, each rated 3 kVA, 220/110 volts, 60 Hz, with a 0.10 per-unit leakage reactance, are connected as a three-phase extended Δ autotransformer bank, as shown in Figure 3.36 (c). The low-voltage Δ winding has a 110 volt rating. (a) Draw the positive-sequence phasor diagram and show that the high-voltage winding has a 479.5 volt rating. (b) A three-phase load connected to the low-voltage terminals absorbs 6 kW at 110 volts and at 0.8 power factor lagging. Draw the per-unit impedance diagram and calculate the voltage and current at the high-voltage terminals. Assume positive-sequence operation.

3.57 A two-winding single-phase transformer rated 60 kVA, 240/1200 V, 60 Hz, has an efficiency of 0.96 when operated at rated load, 0.8 power factor lagging. This transformer is to be utilized as a 1440/1200-V step-down autotransformer in a power distribution system. (a) Find the permissible kVA rating of the autotransformer if the winding currents and voltages are not to exceed the ratings as a two-winding transformer. Assume an ideal transformer. (b) Determine the efficiency of the autotransformer with the kVA loading of part (a) and 0.8 power factor leading.

3.58 A single-phase two-winding transformer rated 90 MVA, 80/120 kV is to be connected as an autotransformer rated 80/200 kV. Assume that the transformer is ideal. (a) Draw a schematic diagram of the ideal transformer connected as an autotransformer, showing the voltages, currents, and dot notation for polarity. (b) Determine the permissible kVA rating of the autotransformer if the winding currents and voltages are not to exceed the rated values as a two-winding transformer. How much of the kVA rating is transferred by magnetic induction?

SECTION 3.8

3.59 The two parallel lines in Example 3.13 supply a balanced load with a load current of $1.0\underline{/-30^\circ}$ per unit. Determine the real and reactive power supplied to the load bus from each parallel line with (a) no regulating transformer, (b) the voltage-magnitude-regulating transformer in Example 3.13(a), and (c) the phase-angle-regulating transformer in Example 3.13(b). Assume that the voltage at bus *abc* is adjusted so that the voltage at bus $a'b'c'$ remains constant at $1.0\underline{/0^\circ}$ per unit. Also assume positive sequence. Comment on the effects of the regulating transformers.

PW **3.60** PowerWorld Simulator case Problem 3_60 duplicates Example 3.13 except that a resistance term of 0.06 per unit has been added to the transformer and 0.05 per unit to the transmission line. Since the system is no longer lossless, a field showing the real power losses has also been added to the oneline. With the LTC tap fixed at 1.05, plot the real power losses as the phase shift angle is varied from −10 to +10 degrees. What value of phase shift minimizes the system losses?

PW **3.61** Repeat Problem 3.60, except keep the phase-shift angle fixed at 3.0 degrees while varying the LTC tap between 0.9 and 1.1. What tap value minimizes the real power losses?

Copyright 2017 Cengage Learning. All Rights Reserved. May not be copied, scanned, or duplicated, in whole or in part. Due to electronic rights, some third party content may be suppressed from the eBook and/or eChapter(s). Editorial review has deemed that any suppressed content does not materially affect the overall learning experience. Cengage Learning reserves the right to remove additional content at any time if subsequent rights restrictions require it.

3.62 Rework Example 3.12 for a +10% tap, providing a 10% increase for the high-voltage winding.

3.63 A 23/230-kV step-up transformer feeds a three-phase transmission line, which in turn supplies a 150-MVA, 0.8 lagging power factor load through a step-down 230/23-kV transformer. The impedance of the line and transformers at 230 kV is $18 + j60\ \Omega$. Determine the tap setting for each transformer to maintain the voltage at the load at 23 kV.

3.64 The per-unit equivalent circuit of two transformers T_a and T_b connected in parallel, with the same nominal voltage ratio and the same reactance of 0.1 per unit on the same base, is shown in Figure 3.43. Transformer T_b has a voltage-magnitude step-up toward the load of 1.05 times that of T_a (that is, the tap on the secondary winding of T_b is set to 1.05). The load is represented by $0.8 + j0.6$ per unit at a voltage $V_2 = 1.0\angle 0°$ per unit. Determine the complex power in per unit transmitted to the load through each transformer. Comment on how the transformers share the real and reactive powers.

FIGURE 3.43

Problem 3.64

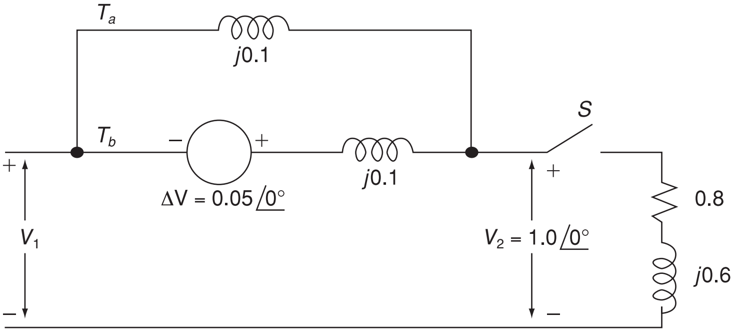

3.65 Reconsider Problem 3.64 with the change that now T_b includes both a transformer of the same turns ratio as T_a and a regulating transformer with a 4° phase shift. On the base of T_a, the impedance of the two components of T_b is $j0.1$ per unit. Determine the complex power in per unit transmitted to the load through each transformer. Comment on how the transformers share the real and reactive powers.

CASE STUDY QUESTIONS

a. What are the advantages of correctly specifying a transformer most suitable for its application?

b. Why is it important to reduce the moisture within a transformer to acceptable levels during transformer installation?

c. What should be the focus of transformer preventive maintenance efforts?

Copyright 2017 Cengage Learning. All Rights Reserved. May not be copied, scanned, or duplicated, in whole or in part. Due to electronic rights, some third party content may be suppressed from the eBook and/or eChapter(s). Editorial review has deemed that any suppressed content does not materially affect the overall learning experience. Cengage Learning reserves the right to remove additional content at any time if subsequent rights restrictions require it.

REFERENCES

1. R. Feinberg, *Modern Power Transformer Practice* (New York: Wiley, 1979).
2. A. C. Franklin and D. P. Franklin, *The J & P Transformer Book,* 11th ed. (London: Butterworths, 1983).
3. W. D. Stevenson, Jr., *Elements of Power System Analysis,* 4th ed. (New York: McGraw-Hill, 1982).
4. J. R. Neuenswander, *Modern Power Systems* (Scranton, PA: International Textbook Company, 1971).
5. M. S. Sarma, *Electric Machines* (Dubuque, IA: Brown, 1985).
6. A. E. Fitzgerald, C. Kingsley, and S. Umans, *Electric Machinery,* 4th ed. (New York: McGraw-Hill, 1983).
7. O. I. Elgerd, *Electric Energy Systems: An Introduction* (New York: McGraw-Hill, 1982).
8. C. Gamez, "Power Transformer–Part 3: Life Management and Extension," *Transformers Magazine*, 1, 3, October 2014, pp. 10–15 (www.transformers-magazine.com).

Copyright 2017 Cengage Learning. All Rights Reserved. May not be copied, scanned, or duplicated, in whole or in part. Due to electronic rights, some third party content may be suppressed from the eBook and/or eChapter(s). Editorial review has deemed that any suppressed content does not materially affect the overall learning experience. Cengage Learning reserves the right to remove additional content at any time if subsequent rights restrictions require it.

Copyright 2017 Cengage Learning. All Rights Reserved. May not be copied, scanned, or duplicated, in whole or in part. Due to electronic rights, some third party content may be suppressed from the eBook and/or eChapter(s). Editorial review has deemed that any suppressed content does not materially affect the overall learning experience. Cengage Learning reserves the right to remove additional content at any time if subsequent rights restrictions require it.

4 Transmission Line Parameters

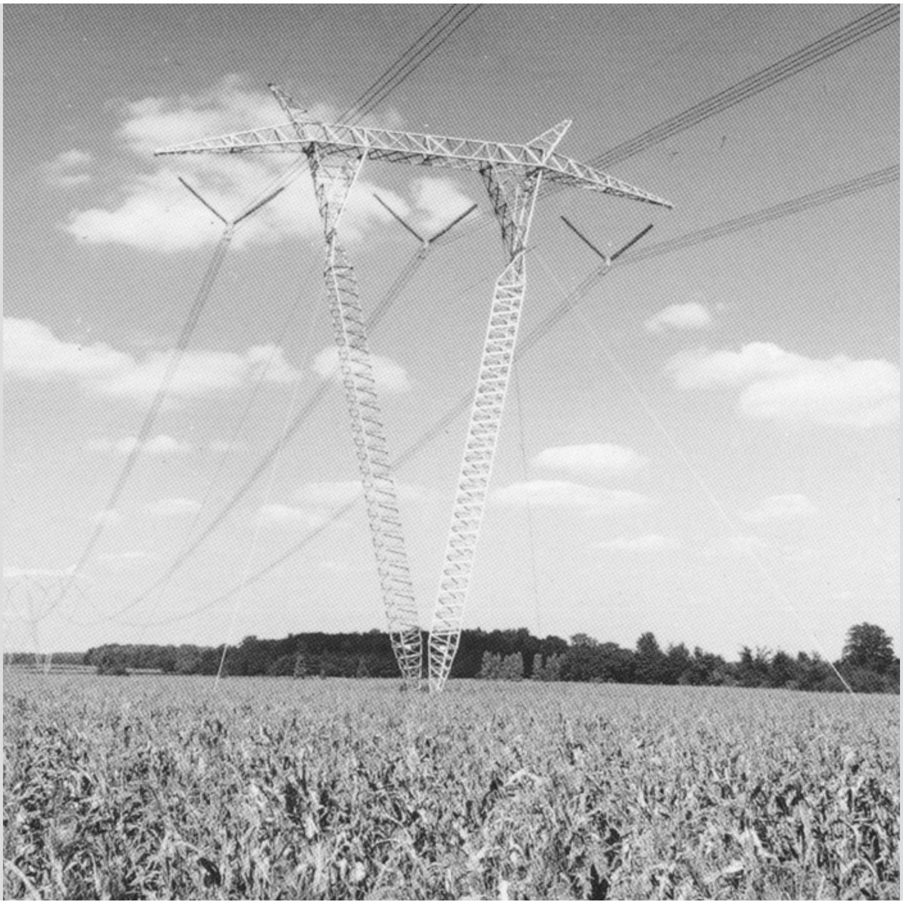

765-kV transmission line with aluminum guyed-V towers (Courtesy of American Electric Power Company.)

This chapter discusses the four basic transmission-line parameters: series resistance, series inductance, shunt capacitance, and shunt conductance and investigates transmission-line electric and magnetic fields.

Series resistance accounts for ohmic (I^2R) line losses. Series impedance, including resistance and inductive reactance, gives rise to series-voltage drops along the line. Shunt capacitance gives rise to line-charging currents. Shunt conductance accounts for V^2G line losses due to leakage currents between conductors or between conductors and ground. Shunt conductance of overhead lines is usually neglected.

Copyright 2017 Cengage Learning. All Rights Reserved. May not be copied, scanned, or duplicated, in whole or in part. Due to electronic rights, some third party content may be suppressed from the eBook and/or eChapter(s). Editorial review has deemed that any suppressed content does not materially affect the overall learning experience. Cengage Learning reserves the right to remove additional content at any time if subsequent rights restrictions require it.

Although the ideas developed in this chapter can be applied to underground transmission and distribution, the primary focus here is on overhead lines. Underground transmission in the United States presently accounts for less than 1% of total transmission and is found mostly in large cities or under waterways. There is, however, a large application for underground cable in distribution systems.

CASE STUDY

Two transmission articles are presented here. The first article describes the integrated nature of the Canada-United States transmission grid and highlights its mutual benefits. The article identifies four strategic goals to further strengthen the bilateral electricity relationship [10]. The second article describes the ongoing congestion of the North American transmission grid, including its impacts on reliability, efficiency, and costs. The article emphasizes the need to upgrade and modernize the grid while leveraging new technologies [12].

Integrating North America's Power Grid

Patrick Brown

Canadian Electricity Association (CEA)

How the U.S. and Canada Maximize Their Working Relationship

North America is shifting towards a new energy paradigm. Where it was once viewed through the prism of scarcity, some are now beginning to speak of energy in the language of abundance.

The grounds for optimism are understandable. For instance, technological breakthroughs on the production side are unlocking previously inaccessible deposits of oil and natural gas, while advances in conservation and efficiency practices are affording customers greater control over their energy use.

Still, the achievement of North American independence from volatile global energy markets is by no means a foregone conclusion. Economic recovery efforts remain fragile. The supply and delivery infrastructure for our resources is in urgent need of upgrade while an evolving landscape of risks poses significant threats to its security. And perhaps most importantly, transformative events in the market—such as the North American boom in natural gas production—have overtaken many of the policy structures in place across Canada and the United States.

Too much of the framework shaping governments' approach on energy issues is therefore not optimally suited to addressing the opportunities and challenges at hand. The backbone of any strategy to confront and leverage the new energy landscape

"Integrating North America's Power Grid", by Patrick Brown, *Electricity Today T & D Magazine* (June 2013) Reprinted with Permission.

Copyright 2017 Cengage Learning. All Rights Reserved. May not be copied, scanned, or duplicated, in whole or in part. Due to electronic rights, some third party content may be suppressed from the eBook and/or eChapter(s). Editorial review has deemed that any suppressed content does not materially affect the overall learning experience. Cengage Learning reserves the right to remove additional content at any time if subsequent rights restrictions require it.

must be an enhanced North American electricity system.

Electricity plays an integral role in the robust Canada-U.S. relationship on energy, which itself is a fundamental pillar of the broader flow of two-way trade that is without compare anywhere in the world. The linkages between the Canadian and U.S. grids—more than three dozen in total—offer several advantages to both countries, such as higher reliability and expanded access to low-emitting resources. These physical interconnections have facilitated steady growth in what has become a continent-wide marketplace for electricity, with supply fulfilling demand in an efficient, cost-effective manner across North America.

From the vantage point of the voice of the Canadian electricity sector, CEA views our vibrant, bilateral electricity relationship—which has long served as a central instrument for economic vitality in both countries—as being an ideal platform from which to launch a renewed push towards a more secure, prosperous, and autonomous continental energy posture.

This case study is intended to help guide such efforts. In order to set a proper context, the first section provides an overview of the interconnected and integrated nature of the Canada-U.S. relationship on electricity and highlights the mutual benefits thereof. The second section identifies four strategic goals to further strengthen the relationship.

The U.S.-Canada Electricity Relationship

The trading relationship enjoyed by Canada and the U.S. is a model of bilateral cooperation. According to the government of Canada, approximately 300,000 individuals and $1.6 billion (CAD) worth of goods and services move freely across the U.S.-Canada border daily, making each country the other's most important trading partner. The scope and scale of this two-way trading flow is without compare anywhere in the world. An integral part of this relationship is energy.

Energy serves as the main engine fueling economic activity and prosperity across North America, delivering a wealth of societal benefits and enabling a high quality of life on both sides of the border. The two countries have long acted as each other's best customers when it comes to the buying and selling of energy commodities. For example, research from the report, "*U.S. Natural Gas Exports by Country*," published by the United States Energy Information Administration, reveals that Canada receives the greatest share of U.S. natural gas exports (with volumes nearly tripling between 2006 and 2012). Also, the Embassy of Canada in the United States reports that Canada provides the United States with more crude oil and petroleum products, coal, uranium, and natural gas than any other foreign source.

Canada is the largest supplier to the U.S. of another vital commodity—electricity. Crucial in the day-to-day lives of North Americans, it is so reliable as to be taken for granted. In our homes, offices, factories, ports, and stock exchanges, it is instinctively assumed that the lights will turn on with a simple flick of the switch. Likewise, the origin of the electrons being used is rarely considered. The

Copyright 2017 Cengage Learning. All Rights Reserved. May not be copied, scanned, or duplicated, in whole or in part. Due to electronic rights, some third party content may be suppressed from the eBook and/or eChapter(s). Editorial review has deemed that any suppressed content does not materially affect the overall learning experience. Cengage Learning reserves the right to remove additional content at any time if subsequent rights restrictions require it.

crowds cheering on the Vancouver Canucks might never contemplate that electricity generated in the United States could be illuminating the arena. And the car manufacturer in Michigan may be unaware that electricity from Canadian generators is powering its assembly line (see Figure 1).

The movement of electricity between Canada and the United States may go unnoticed by the public. However, this should not be viewed as a cause for concern. Instead, it reflects how routine and reliable a transaction the cross-border exchange of electricity has become in North America. The integration of electricity markets in Canada and the United States means supply can fulfill demand in an efficient, cost-effective manner across the continent.

North Americans benefit from a shared system which can generate and transmit electrons across vast distances to ensure a reliable, secure, and competitively priced supply of electricity, 24 hours a day, seven days a week. Figures 1 and 2 offer a clear visual indicator of the extent of the current integration of the electricity systems in Canada and the United States. By interconnecting into each other's networks at over 35 points, the two countries benefit from numerous advantages: a higher level of

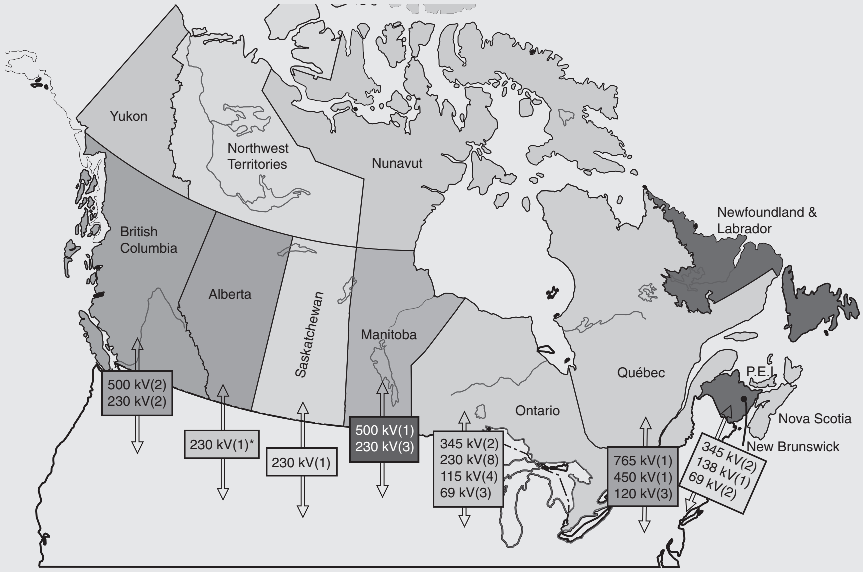
Yukon
Northwest Territories
Nunavut
British Columbia
Alberta
Saskatchewan
Manitoba
Ontario
Québec
Newfoundland & Labrador
P.E.I.
Nova Scotia
New Brunswick
500 kV(2)
230 kV(2)
230 kV(1)*
230 kV(1)
500 kV(1)
230 kV(3)
345 kV(2)
230 kV(8)
115 kV(4)
69 kV(3)
765 kV(1)
450 kV(1)
120 kV(3)
345 kV(2)
138 kV(1)
69 kV(2)

* According to the National Energy Board, construction scheduled for completion in summer 2013.

Figure 1 Major Transmission Interconnections
The physical linkages between the Canadian and U.S. grids have likewise enabled steady growth in what has become a robust, continent-wide marketplace for electricity. Electricity trade occurs at a range of points across and beyond the international border, reflecting the largely north–south nature of the networks in Canadian provinces, as they seamlessly tie into the denser web of transmission infrastructure in the United States.

Copyright 2017 Cengage Learning. All Rights Reserved. May not be copied, scanned, or duplicated, in whole or in part. Due to electronic rights, some third party content may be suppressed from the eBook and/or eChapter(s). Editorial review has deemed that any suppressed content does not materially affect the overall learning experience. Cengage Learning reserves the right to remove additional content at any time if subsequent rights restrictions require it.

reliable service for customers through enhanced system stability; efficiencies in system operation; efficiencies in fuel management; opportunities to use power from nearby markets to address local contingencies; and expanded access to low emitting and competitively priced resources.

Maximizing The Benefits of Grid Integration

Four Strategic Goals for Canada and The U.S. to Further Strengthen their Relationship

1. **Plugging the electric infrastructure gap**
   - Coordinate and cooperate on identifying new infrastructure needs and addressing aging infrastructure on the North American grid and effectively communicate such needs to the general public.
   - Remove regulatory impediments to much-needed electric infrastructure investments.
   - Update and enhance the efficiency of permitting procedures for international power line projects.
2. **Maximizing environmental sustainability**
   - Ensure that any market-based solution to combat climate change that incorporates the electricity sector recognizes the integrated nature of the North American electricity market, encourages the continued two-way flow in cross-border electricity trade, and contains credit provisions for early action taken to reduce emissions.
   - Support existing measures that are proven to cost-effectively deliver emission reductions and help enable intermittent renewable technologies.
   - Recognize hydropower as a clean, renewable resource across policy programs.
   - Maintain support for fostering cleaner ways to use North America's plentiful supplies of natural gas and coal for power generation, including the deployment of carbon capture and storage technology.
3. **Maintaining vigilance on reliability and security**
   - Support the existing framework in place at the North American Electric Reliability Corporation to develop reliability standards (including for cyber security protection) for the North American transmission grid.
   - Enhance public-private sector, as well as government-to-government coordination and sharing of timely and actionable threat information.
   - Address cyber and other security threats in a comprehensive manner across all industry sectors, with a focus on securing the most critical assets from the most urgent challenges.
   - Standardize and streamline border-crossing procedures for crews providing assistance to utilities in the other country.

Copyright 2017 Cengage Learning. All Rights Reserved. May not be copied, scanned, or duplicated, in whole or in part. Due to electronic rights, some third party content may be suppressed from the eBook and/or eChapter(s). Editorial review has deemed that any suppressed content does not materially affect the overall learning experience. Cengage Learning reserves the right to remove additional content at any time if subsequent rights restrictions require it.

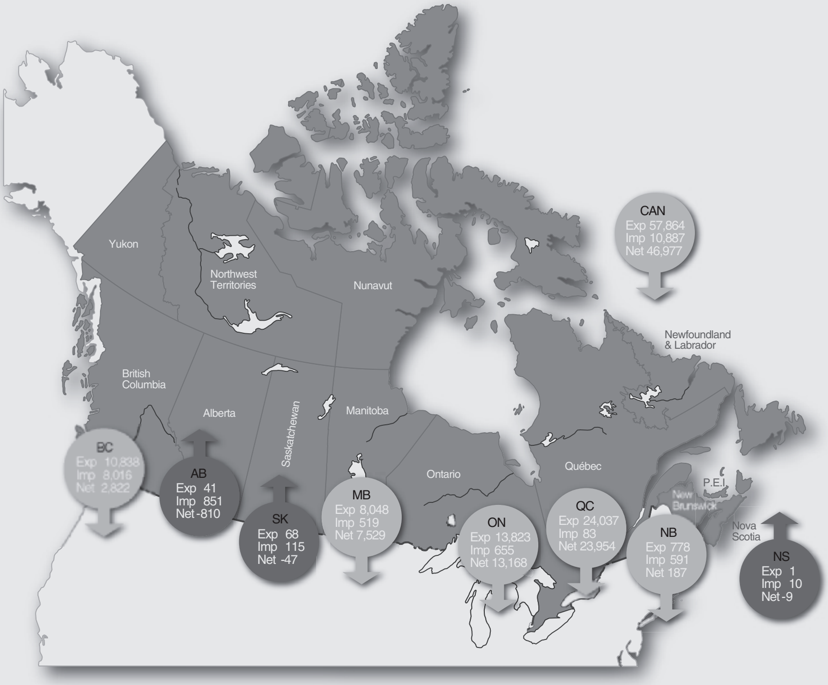
Yukon
Northwest Territories
Nunavut
British Columbia
Alberta
Saskatchewan
Manitoba
Ontario
Québec
Newfoundland & Labrador
P.E.I.
New Brunswick
Nova Scotia
CAN
Exp 57,864
Imp 10,887
Net 46,977
BC
Exp 10,838
Imp 8,016
Net 2,822
AB
Exp 41
Imp 851
Net -810
SK
Exp 68
Imp 115
Net -47
MB
Exp 8,048
Imp 519
Net 7,529
ON
Exp 13,823
Imp 655
Net 13,168
QC
Exp 24,037
Imp 83
Net 23,954
NB
Exp 778
Imp 591
Net 187
NS
Exp 1
Imp 10
Net -9

Figure 2 Electricity Exports and Imports Between Canada and the U.S. (2012)

Source: National Energy Board, Electricity Exports and Imports, 2012. Retrieved February 21, 2013

4. **Ensuring free, fair, and fluid inter-jurisdictional trade**
    - Remain vigilant in avoiding erecting barriers that may inhibit inter-jurisdictional electricity trade.
    - Refrain from imposing unnecessarily burdensome over-the-counter derivatives of regulatory requirements on energy endusers which pose no systemic risk to the marketplace.
    - Update and enhance the efficiency of administrative procedures for authorizing exports of electricity across the international border.

Last Look

Against the backdrop of transformation and transition in the North American energy landscape, CEA believes that there are numerous opportunities for leveraging the legacy of cooperation and achievement in operating the world's largest integrated power grid, and expanding the suite of benefits which such integration offers to consumers in Canada and the United States.

Electricity Imports & Exports

Historically, electricity exports to the United States have represented

Copyright 2017 Cengage Learning. All Rights Reserved. May not be copied, scanned, or duplicated, in whole or in part. Due to electronic rights, some third party content may be suppressed from the eBook and/or eChapter(s). Editorial review has deemed that any suppressed content does not materially affect the overall learning experience. Cengage Learning reserves the right to remove additional content at any time if subsequent rights restrictions require it.

anywhere from 5 to 10 percent of Canada's total production. The bulk of these exports involve the sale of surplus generation from major hydropower producing provinces such as Québec, British Columbia, and Manitoba. More recently, export volumes from Ontario have also risen, making the province the second largest exporter (on both a gross and net basis) for several consecutive years. While hydro enjoys a sizeable share of Ontario's supply mix, nuclear energy comprises approximately half of the province's portfolio.

Overall, the vast majority of electrons delivered across the border from Canadian generators to U.S. customers are derived from clean, non-emitting sources.

Patrick Brown is the director of U.S. Affairs for the Canadian Electricity Association. ■

Grid Congestion

Dave Bryant
CTC Global Corporation

Unclogging the Arteries of North America's Power Grid

Without access to affordable and reliable electricity, no society in today's world can possibly flourish. Canada and the United States rely heavily on electricity to pump water to grow crops, manufacture products competitively, and power North America's information-based infrastructure, wide-screen televisions, iPhones, and air conditioning. In many ways, the electric infrastructure could be considered society's most important artery.

Sadly, however, the American Society of Civil Engineers (ASCE) gave the U.S. energy infrastructure and electric artery a D+ rating in 2013. According to ASCE, the primary reason the United States received such a low grade is the fact that the country's electrical infrastructure is substantially aged and congested. The low rating is also a function of how difficult it will be for the United States to improve the power grid in light of its complexities, regulatory challenges, and implementation hurdles.

What is Grid Congestion?

Grid congestion is a situation wherein the existing transmission and/or distribution lines are unable to accommodate all required load during periods of high demand or during emergency load conditions, such as when an adjacent line is taken out of service or damaged by a storm, commonly referred to as an "N minus 1" or "N minus 2" condition—or worse. Grid congestion not only impacts reliability, it also reflects a decrease

"Grid Congestion", by Dave Bryant, *Electricity Today T & D Magazine* (July/August 2013) Reprinted with Permission.

Copyright 2017 Cengage Learning. All Rights Reserved. May not be copied, scanned, or duplicated, in whole or in part. Due to electronic rights, some third party content may be suppressed from the eBook and/or eChapter(s). Editorial review has deemed that any suppressed content does not materially affect the overall learning experience. Cengage Learning reserves the right to remove additional content at any time if subsequent rights restrictions require it.

in efficiency. Under high load conditions, line losses escalate exponentially. If lines are congested and operating at or near their thermal limits, they would also be exhibiting significant line losses during high load conditions. Another significant problem with grid congestion is that during periods of high demand, electric retailers may not have access to the least expensive source of electricity which can "artificially" drive consumer prices to very high levels.

As North America has learned in the wake of several major blackouts, not unlike clogged arteries in the human body, a weak or congested transmission grid can lead to very unfavorable consequences.

Back Story

The Energy Policy Act of 1992 mandated that the Federal Energy Regulatory Commission (FERC) open up the national grid on a nondiscriminatory, non-preferential basis for the wholesale delivery of electric power. In April of 1996, FERC issued Orders 888 and 889 that encouraged wholesale competition. The primary objective of these orders was the elimination of the monopoly over the transmission of electricity. To achieve this objective, FERC required all public utilities that own, control, or operate facilities used for transmitting electric energy in interstate commerce to separate transmission from generation and marketing functions. FERC also required that these entities file open-access nondiscriminatory transmission tariffs.

In September, 1996, the State of California also put into law *The Electric Utility Industry Restructuring Act* (AB 1890) in an effort to make the generation of electricity more competitive. In 1999, FERC issued Order 2000 which asked all transmission-owning utilities, including non-public utilities, to place their transmission facilities under the control of an appropriate Regional Transmission Organization (RTO). This was done in an effort to better manage transmission congestion, oversee tariff management, and support the regional planning of system upgrades, among other objectives.

During the transition or "decoupling," as FERC later described in their staff report of March 26, 2003 (Docket No PA02-2-000), a supply-demand imbalance, flawed market design, and inconsistent rules made significant wholesale market manipulation possible. These, and several other factors, set the stage for the *Western energy crisis of 2000 to 2001*.

According to a report released by the Federal Energy Regulatory Commission, California's retail rate freeze (a component of new U.S. bill AB 1890 instituted by the California Legislature) and the inability to pass along price increases to customers not only bankrupted Pacific Gas & Electric (and nearly bankrupted Southern California Edison), the conditions also caused widespread rolling outages with an economic impact estimated at 40 to 45 billion dollars. In 1999, the retail rate freeze imposed on San Diego Gas & Electric (SDG&E) was temporarily lifted so retail customers in Southern California felt the brunt of cost increases immediately.

According to the final FERC report released in late March 2003,

Copyright 2017 Cengage Learning. All Rights Reserved. May not be copied, scanned, or duplicated, in whole or in part. Due to electronic rights, some third party content may be suppressed from the eBook and/or eChapter(s). Editorial review has deemed that any suppressed content does not materially affect the overall learning experience. Cengage Learning reserves the right to remove additional content at any time if subsequent rights restrictions require it.

a number of factors contributed to the Western energy crisis of 2000 and 2001. While strong economic growth at that time led to increased demand for electricity, environmental concerns limited, prevented, or delayed new generation from being built locally.

Drought conditions in the Northwestern United States also resulted in reduced hydropower generation for the country while a ruptured natural gas line feeding California led to further generation constraints in a state that was highly dependent upon gas-fired generation. Unusually high temperatures, unplanned—or intentional—plant outages of older plants, and transmission capacity constraints also contributed to the crisis.

Congestion Costs

On the east coast, in 2002, the newly-established PJM Interconnection (a regional transmission organization) assessed the costs of congestion associated with individual transmission and distribution lines within their jurisdiction. PJM Interconnection reported that in several cases, over a period of several months, the combined costs of congestion of many transmission lines were measured to be over a billion dollars per year. This value doesn't include the costs of congestion from other regional transmission organizations.

The aforementioned costs were primarily a function of the difference in cost between a potentially available energy resource versus the cost paid for energy delivered from a more expensive but deliverable source (and/or as a function of market driven "supply and demand" pricing).

Impact of Congestion

On August 14, 2003, the Northeast United States and Ontario, Canada experienced the second most widespread blackout on record at that time (after Brazil in 1999), affecting 55 million people. Six weeks later, on September 28, 2003, a similar outage occurred in Europe that affected 56 million people.

According to the final report released by the North American Electric Reliability Corporation (NERC), the organization responsible for the adequacy and reliability of the bulk power transmission in North America, the U.S./Canada blackout of August 2003 was caused by a number of factors. The report stated that the causes of the blackout included inaccurate telemetry data used to operate the Midwest Independent Transmission System Operator (MISO) "State Estimator" (and a subsequent computer re-boot failure); a "race condition" computer bug in FirstEnergy's Energy Management System; and three 345 kilovolt (kV) transmission line trips (outages) due to excessive conductor sag, which led to a cascading of similar sag-trip outages on their 138-kV system.

These events and lack of effective communication between other utilities ultimately shut down 508 generating units at 265 power plants. According to the final NERC Report "*Technical Analysis of the August 14, 2003, Blackout: What Happened, Why, and What Did We Learn?*," the economic impact was estimated to approach 10 billion dollars. On July 30 and 31 of 2012, a similar series of cascading outages in India affected more than 670 million people. The Indian Government Ministry

Copyright 2017 Cengage Learning. All Rights Reserved. May not be copied, scanned, or duplicated, in whole or in part. Due to electronic rights, some third party content may be suppressed from the eBook and/or eChapter(s). Editorial review has deemed that any suppressed content does not materially affect the overall learning experience. Cengage Learning reserves the right to remove additional content at any time if subsequent rights restrictions require it.

of Power also reported that substantial grid limitations and line tripping also played major roles in this event.

Steps Forward

Following the blackout of 2003, the Energy Policy Act of 2005 was established as a mechanism to help improve the efficiency, reliability, and capacity of the grid by creating incentives for utilities to invest in grid improvements and leverage new technologies including high-capacity low-sag conductors.

In 2009, the American Clean Energy and Security Act was approved by the House of Representatives but defeated in the Senate. While much of this bill was focused on climate change issues, many of its components also supported the modernization of the grid, primarily to enable the addition of new alternative "clean" sources of generation and develop and leverage new technology. Though the bill didn't pass, the message was clear and new cleaner sources of generation continue to be brought online.

The Challenges Continue

The addition of new sources of generation is further adding to the challenge of alleviating grid congestion. While new transmission lines are being proposed and/or built to link new generation, existing transmission and distribution lines may not be robust enough to handle additional load, especially during peak or emergency conditions, depending on where and how the new lines are integrated into the existing grid.

The Worst May Be Yet to Come

In the coming years, as outlined in the North American Reliability Corporation (NERC) "2012 Long-Term Reliability Assessment" report, the problem of congested transmission lines may become exacerbated not only by the increase in renewable resources that need to be integrated onto the grid, but with potentially greater impact, by the fact that the renewables may, under certain conditions, be unavailable at the same time.

The retirement of larger and/or strategically situated generation units will also impact the grid. Changes in generation type and location will require enhancements to the grid to provide reactive and voltage support, and address thermal (conductor sag) constraints, in order to insure system stability. This will be particularly challenging considering the timeframes required to make grid changes and the fact that, in many of the deregulated market areas, the system operator (performing the planning function) may have little insight into the retirement decisions of generation, which can be shut down with only a 90-day notice.

As the electric industry moves from conventional base load generation to various renewables that are dependent upon ambient conditions to perform (or not), and, if transmission enhancements are not implemented to accommodate the somewhat unpredictable changes, overall system reliability could be adversely affected.

Smart Grid Strategy Flaws

While utilities will continue to face significant challenges in securing permits to build new transmission lines, and incentives for utilities to invest in upgrading existing lines are not completely clear, another concern

Copyright 2017 Cengage Learning. All Rights Reserved. May not be copied, scanned, or duplicated, in whole or in part. Due to electronic rights, some third party content may be suppressed from the eBook and/or eChapter(s). Editorial review has deemed that any suppressed content does not materially affect the overall learning experience. Cengage Learning reserves the right to remove additional content at any time if subsequent rights restrictions require it.

is the scope of the new Smart Grid policy enacted by the U.S. federal government.

The U.S. Department of Energy (DOE) defines Smart Grid "as an electrical grid that uses information and communications technology to gather and act on information, such as information about the behaviors of suppliers and consumers, in an automated fashion to improve the efficiency, reliability, economics, and sustainability of the production and distribution of electricity."

Surprisingly absent from the U.S. DOE definition is the word "capacity." The Energy Policy Act of 2005 clearly called for and provided a framework for incentives to leverage technology to "improve the efficiency, reliability and capacity of the grid." Capacity is not only a key element in mitigating congestion costs (which is a nice way of saying 'giving' the consumer access to the least expensive source of electricity—without artificial market manipulation), capacity is also extremely critical to grid reliability, not to mention North America's national security and financial wellbeing.

Lessons Learned

The key point in this feature is that utilities, consumers and regulatory bodies need to recognize the limitations of data and computers if they are serious about grid efficiency, capacity, and reliability—especially in this era of increasing cyber security risks. When telemetry devices and computers fail, thus leading to blackouts and outages, remember that the power grid is fundamentally a function of conductor capacity and thermal sag.

Figure 3 High-capacity low-sag conductor.

Modern Conductors

As increasingly higher levels of current are carried by overhead conductors, the electrical resistance of the wires causes them to heat up. Their coefficient of thermal expansion can then increase the conductor's sag, which can lead to short-circuit events and outages. While smart meters and other electronic devices may help utilities identify areas impacted by outages, strategies that outline prevention should become the priority.

The use of high-capacity, low-sag conductors (Figure 3) can alleviate grid congestion and serve to improve the efficiency, capacity, and reliability of the grid while also enabling utilities to more flexibly handle new sources of generation and storage technologies as they emerge and are integrated into the grid in varied locations.

Leveraging Technology

Today, a number of utilities such as American Electric Power (AEP), NV Energy, OG&E Energy Corporation, and others are discovering how to leverage new technologies including high-capacity, low-sag conductors.

Copyright 2017 Cengage Learning. All Rights Reserved. May not be copied, scanned, or duplicated, in whole or in part. Due to electronic rights, some third party content may be suppressed from the eBook and/or eChapter(s). Editorial review has deemed that any suppressed content does not materially affect the overall learning experience. Cengage Learning reserves the right to remove additional content at any time if subsequent rights restrictions require it.

These modern conductors use aerospace-derived technology to reduce conductor sag, increase line capacity, and reduce line losses.

The reduction of line losses has the same impact as building new generation. Thus, the economics of incorporating these technologies into the grid are very favorable—especially because existing structures rarely require modifications to accommodate the new wire. AEP is currently using a new high-capacity, low-sag conductor to increase the capacity of 240 circuit miles of a 345kV line near Corpus Christi, Texas, to accommodate new generation and growing demand (Figure 4). More than 100 other utilities in more than 25 countries have also deployed the technology for similar reasons at over 250 projects so far.

Role of Efficiency

For more than 100 years, utilities and their suppliers spent billions of dollars improving the efficiency of generators in an effort to squeak more out of less and improve economics. In the last 30 years, the push for improved efficiency has trickled downstream to the consumer where they too have discovered the benefits of using energy-efficient appliances to reduce their monthly bills. This effort has not only benefited consumers; it has also enabled utilities to postpone the development of new generation resources or retire old ones. As the saying goes, "it is cheaper to save a 'Negawatt' than it is to create a Megawatt."

Having spent billions of dollars improving the efficiency of generation and demand side appliances, perhaps it's time to focus on building more

Altec
NATIONAL CRANE

Figure 4 Re-conductoring a 345-kV line.

Copyright 2017 Cengage Learning. All Rights Reserved. May not be copied, scanned, or duplicated, in whole or in part. Due to electronic rights, some third party content may be suppressed from the eBook and/or eChapter(s). Editorial review has deemed that any suppressed content does not materially affect the overall learning experience. Cengage Learning reserves the right to remove additional content at any time if subsequent rights restrictions require it.

efficiency into the grid itself where, in the United States, according to Jim Rogers, Chairman of Duke Energy, eight to 10 percent of all energy generated is lost during transmission and distribution.

Famous Last Words

What began as a function of old age—and continued growth in demand for affordable and reliable electricity—is now known as grid congestion. Congestion not only reflects capacity constraints, it also reflects substantial inefficiencies and decreased reliability. While electronics, smart meters and other technologies are certainly playing a role in decreasing stress on the grid and generation resources, to truly resolve the problem and prepare for a somewhat unknown future, the physical grid needs to be upgraded to combat grid congestion. The cost of upgrades will pale in comparison with the cost of ignoring this physical reality.

Later this year, the U.S. Department of Energy will be releasing its “2012 National Electric Transmission Congestion Study.” It will be interesting to see how this report will impact the future of transmission congestion in North America. ■

4.1 TRANSMISSION LINE DESIGN CONSIDERATIONS

An overhead transmission line consists of conductors, insulators, support structures, and, in most cases, shield wires.

CONDUCTORS

Aluminum has replaced copper as the most common conductor metal for overhead transmission. Although a larger aluminum cross-sectional area is required to obtain the same loss as in a copper conductor, aluminum has a lower cost and lighter weight. Also, the supply of aluminum is abundant, whereas that of copper is limited.

One of the most common conductor types is aluminum conductor, steel-reinforced (ACSR), which consists of layers of aluminum strands surrounding a central core of steel strands (Figure 4.1). Stranded conductors are easier to manufacture, since larger conductor sizes can be obtained by simply adding successive layers of strands. Stranded conductors are also easier to handle and more flexible than solid conductors, especially in larger sizes. The use of steel strands gives ACSR conductors a high strength-to-weight ratio. For purposes of heat dissipation, overhead transmission-line conductors are bare (no insulating cover).

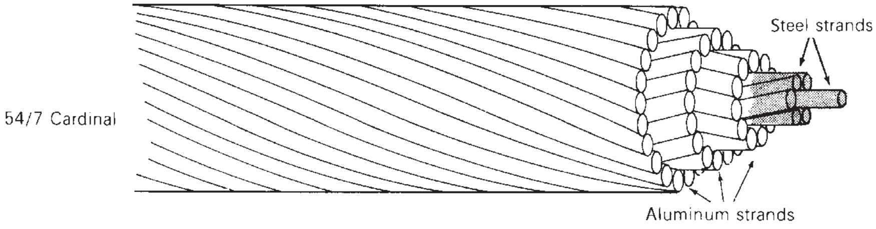

FIGURE 4.1

Typical ACSR conductor

Copyright 2017 Cengage Learning. All Rights Reserved. May not be copied, scanned, or duplicated, in whole or in part. Due to electronic rights, some third party content may be suppressed from the eBook and/or eChapter(s). Editorial review has deemed that any suppressed content does not materially affect the overall learning experience. Cengage Learning reserves the right to remove additional content at any time if subsequent rights restrictions require it.

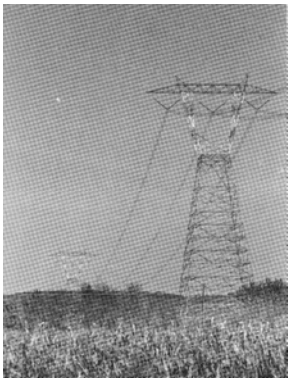

FIGURE 4.2

A 765-kV transmission line with self-supporting lattice steel towers (Courtesy of the American Electric Power Company)

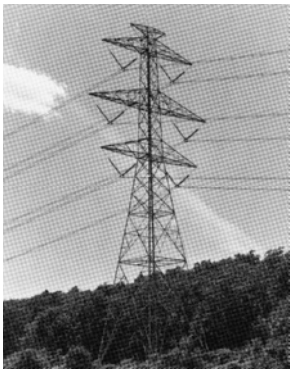

FIGURE 4.3

A 345-kV double-circuit transmission line with self-supporting lattice steel towers (Courtesy of NSTAR, formerly Boston Edison Company)

Other conductor types include the all-aluminum conductor (AAC), all-aluminum-alloy conductor (AAAC), aluminum conductor alloy-reinforced (ACAR), and aluminum-clad steel conductor (Alumoweld). Higher-temperature conductors capable of operation in excess of 150°C include the aluminum conductor steel supported (ACSS) that uses fully annealed aluminum around a steel core, and the gap-type ZT-aluminum conductor (GTZACSR) that uses heat-resistant aluminum over a steel core with a small annular gap between the steel and first layer of aluminum strands. Emerging technologies use composite materials, including the aluminum conductor carbon reinforced (ACFR), whose core is a resinmatrix composite containing carbon fiber, and the aluminum conductor composite reinforced (ACCR), whose core is an aluminum-matrix containing aluminum fibers [10].

EHV lines often have more than one conductor per phase; these conductors are called a *bundle.* The 765-kV line in Figure 4.2 has four conductors per phase, and the 345-kV double-circuit line in Figure 4.3 has two conductors per phase. Bundle conductors have a lower electric field strength at the conductor surfaces, thereby controlling corona. They also have a smaller series reactance.

INSULATORS

Insulators for transmission lines above 69 kV are typically suspension-type insulators, that consist of a string of discs constructed of porcelain, toughened glass, or polymer. The standard disc (Figure 4.4) has a 10-in. (0.254-m) diameter, $5\frac{3}{4}$-in. (0.146-m) spacing between centers of adjacent discs, and a mechanical strength of 7500 kg. The 765-kV line in Figure 4.2 has two strings per phase in a V-shaped arrangement, which helps to restrain conductor swings. The 345-kV line in Figure 4.5 has one vertical string per phase. The number of insulator discs in a string increases

Copyright 2017 Cengage Learning. All Rights Reserved. May not be copied, scanned, or duplicated, in whole or in part. Due to electronic rights, some third party content may be suppressed from the eBook and/or eChapter(s). Editorial review has deemed that any suppressed content does not materially affect the overall learning experience. Cengage Learning reserves the right to remove additional content at any time if subsequent rights restrictions require it.

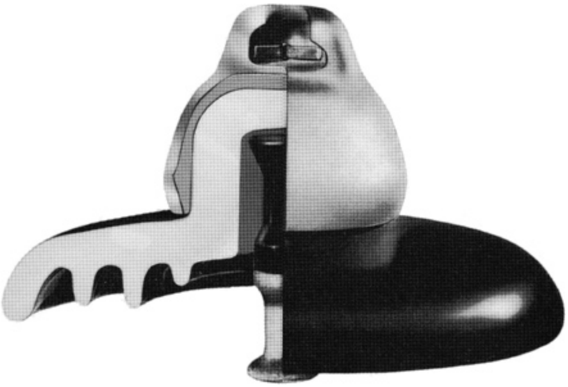

FIGURE 4.4

Cut-away view of a standard porcelain insulator disc for suspension insulator strings (Courtesy of Ohio Brass)

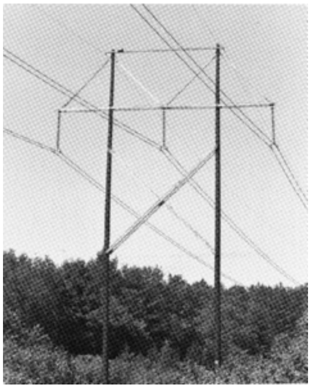

FIGURE 4.5

Wood frame structure for a 345-kV line (Courtesy of NSTAR, formerly Boston Edison Company)

with line voltage (Table 4.1). Other types of discs include larger units with higher mechanical strength and fog insulators for use in contaminated areas.

SUPPORT STRUCTURES

Transmission lines employ a variety of support structures. Figure 4.2 shows a self-supporting, lattice steel tower typically used for 500- and 765-kV lines. Double-circuit 345-kV lines usually have self-supporting steel towers with the phases arranged either in a triangular configuration to reduce tower height or in a vertical configuration to reduce tower width (Figure 4.3). Wood frame configurations are commonly used for voltages of 345 kV and below (Figure 4.5).

SHIELD WIRES

Shield wires located above the phase conductors protect the phase conductors against lightning. They are usually high- or extra-high-strength steel, Alumoweld, or ACSR with much smaller cross section than the phase conductors. The number and location of the shield wires are selected so that almost all lightning strokes terminate on the shield wires rather than on the phase conductors. Figures 4.2, 4.3, and 4.5 have two shield wires. Shield wires are grounded to the tower. As such, when lightning strikes a shield wire, it flows harmlessly to ground, provided the tower impedance and tower footing resistance are small.

The decision to build new transmission is based on power-system planning studies to meet future system requirements of load growth and new generation. The points of interconnection of each new line to the system, as well as the power and voltage ratings of each, are selected based on these studies. Thereafter, transmission-line design is based on optimization of electrical, mechanical, environmental, and economic factors.

Copyright 2017 Cengage Learning. All Rights Reserved. May not be copied, scanned, or duplicated, in whole or in part. Due to electronic rights, some third party content may be suppressed from the eBook and/or eChapter(s). Editorial review has deemed that any suppressed content does not materially affect the overall learning experience. Cengage Learning reserves the right to remove additional content at any time if subsequent rights restrictions require it.

Nominal Voltage	Phase Conductors				
				Minimum Clearances	
(kV)	Number of Conductors per Bundle	Aluminum Cross-Section Area per Conductor (ACSR) (kcmil)	Bundle Spacing (cm)	Phase-to-Phase (m)	Phase-to-Ground (m)
69	1	—	—	—	—
138	1	300—700	—	4 to 5	—
230	1	400—1000	—	6 to 9	—
345	1	2000—2500	—	6 to 9	7.6 to 11
345	2	800—2200	45.7	6 to 9	7.6 to 11
500	2	2000—2500	45.7	9 to 11	9 to 14
500	3	900—1500	45.7	9 to 11	9 to 14
765	4	900—1300	45.7	13.7	12.2

Nominal Voltage	Suspension Insulator String		Shield Wires		
(kV)	Number of Strings per Phase	Number of Standard Insulator Discs per Suspension String	Type	Number	Diameter (cm)
69	1	4 to 6	Steel	0, 1 or 2	—
138	1	8 to 11	Steel	0, 1 or 2	—
230	1	12 to 21	Steel or ACSR	1 or 2	1.1 to 1.5
345	1	18 to 21	Alumoweld	2	0.87 to 1.5
345	1 and 2	18 to 21	Alumoweld	2	0.87 to 1.5
500	2 and 4	24 to 27	Alumoweld	2	0.98 to 1.5
500	2 and 4	24 to 27	Alumoweld	2	0.98 to 1.5
765	2 and 4	30 to 35	Alumoweld	2	0.98

TABLE 4.1

Typical transmission-line characteristics [1, 2] (Electric Power Research Institute (EPRI), EPRI AC Transmission Line Reference Book—200 kV and Above (Palo Alto, CA: EPRI, www.epri.com, December 2005); Westinghouse Electric Corporation, Electrical Transmission and Distribution Reference Book, 4th ed. (East Pittsburgh, PA, 1964).)

Copyright 2017 Cengage Learning. All Rights Reserved. May not be copied, scanned, or duplicated, in whole or in part. Due to electronic rights, some third party content may be suppressed from the eBook and/or eChapter(s). Editorial review has deemed that any suppressed content does not materially affect the overall learning experience. Cengage Learning reserves the right to remove additional content at any time if subsequent rights restrictions require it.

ELECTRICAL FACTORS

Electrical design dictates the type, size, and number of bundle conductors per phase. Phase conductors are selected to have sufficient thermal capacity to meet continuous, emergency overload, and short-circuit current ratings. For EHV lines, the number of bundle conductors per phase is selected to control the voltage gradient at conductor surfaces, thereby reducing or eliminating corona.

Electrical design also dictates the number of insulator discs, vertical or V-shaped string arrangement, phase-to-phase clearance, and phase-to-tower clearance, all selected to provide adequate line insulation. Line insulation must withstand transient overvoltages due to lightning and switching surges, even when insulators are contaminated by fog, salt, or industrial pollution. Reduced clearances due to conductor swings during winds must also be accounted for.

The number, type, and location of shield wires are selected to intercept lightning strikes that would otherwise hit the phase conductors. Also, tower footing resistance can be reduced by using driven ground rods or a buried conductor (called *counterpoise*) running parallel to the line. Line height is selected to satisfy prescribed conductor-to-ground clearances and to control ground-level electric field and its potential shock hazard.

Conductor spacings, types, and sizes also determine the series impedance and shunt admittance. Series impedance affects line-voltage drops, I^2R losses, and stability limits (Chapters 5, 13). Shunt admittance, primarily capacitive, affects line-charging currents, which inject reactive power into the power system. Shunt reactors (inductors) are often installed on lightly loaded EHV lines to absorb part of this reactive power, thereby reducing overvoltages.

MECHANICAL FACTORS

Mechanical design focuses on the strength of the conductors, insulator strings, and support structures. Conductors must be strong enough to support a specified thickness of ice and a specified wind in addition to their own weight. Suspension insulator strings must be strong enough to support the phase conductors with ice and wind loadings from tower to tower (span length). Towers that satisfy minimum strength requirements, called suspension towers, are designed to support the phase conductors and shield wires with ice and wind loadings, and, in some cases, the unbalanced pull due to breakage of one or two conductors. Dead-end towers located every mile or so satisfy the maximum strength requirement of breakage of all conductors on one side of the tower. Angles in the line employ angle towers with intermediate strength. Conductor vibrations, which can cause conductor fatigue failure and damage to towers, are also of concern. Vibrations are controlled by adjustment of conductor tensions, use of vibration dampers, and—for bundle conductors—large bundle spacing and frequent use of bundle spacers.

ENVIRONMENTAL FACTORS

Environmental factors include land usage and visual impact. When a line route is selected, the effect on local communities and population centers, land values, access to property, wildlife, and use of public parks and facilities must all be considered. Reduction in visual impact is obtained by aesthetic tower design and by blending the line with the countryside. Also, the biological effects of prolonged exposure to electric and magnetic fields near transmission lines is of concern. Extensive research has been and continues to be done in this area.

Copyright 2017 Cengage Learning. All Rights Reserved. May not be copied, scanned, or duplicated, in whole or in part. Due to electronic rights, some third party content may be suppressed from the eBook and/or eChapter(s). Editorial review has deemed that any suppressed content does not materially affect the overall learning experience. Cengage Learning reserves the right to remove additional content at any time if subsequent rights restrictions require it.

ECONOMIC FACTORS

The optimum line design meets all the technical design criteria at lowest overall cost, which includes the total installed cost of the line as well as the cost of line losses over the operating life of the line. Many design factors affect cost. Utilities and consulting organizations use digital computer programs combined with specialized knowledge and physical experience to achieve optimum line design.

4.2 RESISTANCE

The dc resistance of a conductor at a specified temperature T is

$$R_{dc,T} = \frac{\rho_T l}{A} \quad \Omega \tag{4.2.1}$$

where ρ_T = conductor resistivity at temperature T
l = conductor length
A = conductor cross-sectional area

Two sets of units commonly used for calculating resistance, SI and English units, are summarized in Table 4.2. In English units, conductor cross-sectional area is expressed in circular mils (cmil). One inch equals 1000 mils, and 1 cmil equals $\pi/4$ sq mil. A circle with diameter D in., or (D in.) (1000 mil/in.) = 1000 D mil = d mil, has an area

$$A = \left(\frac{\pi}{4} D^2 \text{ in.}^2\right)\left(1000 \frac{\text{mil}}{\text{in.}}\right)^2 = \frac{\pi}{4}(1000\,D)^2 = \frac{\pi}{4} d^2 \quad \text{sq mil}$$

or

$$A = \left(\frac{\pi}{4} d^2 \text{ sq mil}\right)\left(\frac{1 \text{ cmil}}{\pi/4 \text{ sq mil}}\right) = d^2 \quad \text{cmil} \tag{4.2.2}$$

Resistivity depends on the conductor metal. Annealed copper is the international standard for measuring resistivity ρ (or conductivity σ, where $\sigma = 1/\rho$). Resistivity of conductor metals is listed in Table 4.3. As shown, hard-drawn aluminum, which has 61% of the conductivity of the international standard, has a resistivity at 20 °C of 17.00 Ω-cmil/ft or 2.83×10^{-8} Ωm.

Quantity	Symbol	SI Units	English Units
Resistivity	ρ	Ωm	Ω-cmil/ft
Length	ℓ	m	ft
Cross-sectional area	A	m^2	cmil
dc resistance	$R_{dc} = \frac{\rho\ell}{A}$	Ω	Ω

TABLE 4.2

Comparison of SI and English units for calculating conductor resistance

Copyright 2017 Cengage Learning. All Rights Reserved. May not be copied, scanned, or duplicated, in whole or in part. Due to electronic rights, some third party content may be suppressed from the eBook and/or eChapter(s). Editorial review has deemed that any suppressed content does not materially affect the overall learning experience. Cengage Learning reserves the right to remove additional content at any time if subsequent rights restrictions require it.

		$\rho_{20°\text{C}}$		T
		Resistivity at 20°C		Temperature Constant
Material	% Conductivity	$\Omega\text{m} \times 10^{-8}$	Ω-cmil/ft	°C
Copper:				
Annealed	100%	1.72	10.37	234.5
Hard-drawn	97.3%	1.77	10.66	241.5
Aluminum				
Hard-drawn	61%	2.83	17.00	228.1
Brass	20–27%	6.4–8.4	38–51	480
Iron	17.2%	10	60	180
Silver	108%	1.59	9.6	243
Sodium	40%	4.3	26	207
Steel	2–14%	12–88	72–530	180–980

TABLE 4.3

% Conductivity, resistivity, and temperature constant of conductor metals

Conductor resistance depends on the following factors:

1. Spiraling
2. Temperature
3. Frequency ("skin effect")
4. Current magnitude—magnetic conductors

These are described in the following paragraphs.

For stranded conductors, alternate layers of strands are spiraled in opposite directions to hold the strands together. Spiraling makes the strands 1 or 2% longer than the actual conductor length. As a result, the dc resistance of a stranded conductor is 1 or 2% larger than that calculated from (4.2.1) for a specified conductor length.

Resistivity of conductor metals varies linearly over normal operating temperatures according to

$$\rho_{T2} = \rho_{T1}\left(\frac{T_2 + T}{T_1 + T}\right) \tag{4.2.3}$$

where ρ_{T2} and ρ_{T1} are resistivities at temperatures T_2 and T_1°C, respectively. T is a temperature constant that depends on the conductor material and is listed in Table 4.3.

The ac resistance or *effective* resistance of a conductor is

$$R_{ac} = \frac{P_{loss}}{|I|^2} \quad \Omega \tag{4.2.4}$$

where P_{loss} is the conductor real power loss in watts and I is the rms conductor current. For dc, the current distribution is uniform throughout the conductor cross section, and (4.2.1) is valid. However, for ac, the current distribution is nonuniform.

Copyright 2017 Cengage Learning. All Rights Reserved. May not be copied, scanned, or duplicated, in whole or in part. Due to electronic rights, some third party content may be suppressed from the eBook and/or eChapter(s). Editorial review has deemed that any suppressed content does not materially affect the overall learning experience. Cengage Learning reserves the right to remove additional content at any time if subsequent rights restrictions require it.

As frequency increases, the current in a solid cylindrical conductor tends to crowd toward the conductor surface with smaller current density at the conductor center. This phenomenon is called *skin effect.* A conductor with a large radius can even have an oscillatory current density versus the radial distance from the conductor center.

With increasing frequency, conductor loss increases, which, from (4.2.4), causes the ac resistance to increase. At power frequencies (60 Hz), the ac resistance is at most a few percent higher than the dc resistance. Conductor manufacturers normally provide dc, 50-Hz, and 60-Hz conductor resistance based on test data (see Appendix Tables A.3 and A.4).

For magnetic conductors, such as steel conductors used for shield wires, resistance depends on current magnitude. The internal flux linkages, and therefore the iron or magnetic losses, depend on the current magnitude. For ACSR conductors, the steel core has a relatively high resistivity compared to the aluminum strands, and therefore the effect of current magnitude on ACSR conductor resistance is small. Tables on magnetic conductors list resistance at two current levels (see Table A.4).

EXAMPLE 4.1

Stranded conductor: dc and ac resistance

Table A.3 lists a 4/0 copper conductor with 12 strands. Strand diameter is 0.1328 in. For this conductor:

a. Verify the total copper cross-sectional area of 211,600 cmil.

b. Verify the dc resistance at 50°C of 0.302 Ω/mi. Assume a 2% increase in resistance due to spiraling.

c. From Table A.3, determine the percent increase in resistance at 60 Hz versus dc.

SOLUTION

a. The strand diameter is $d = (0.1328 \text{ in.})\,(1000 \text{ mil/in.}) = 132.8$ mil, and, from (4.2.2), the strand area is d^2 cmil. Using four significant figures, the cross-sectional area of the 12-strand conductor is

$$A = 12d^2 = 12(132.8)^2 = 211{,}600 \quad \text{cmil}$$

which agrees with the value given in Table A.3.

b. Using (4.2.3) and hard-drawn copper data from Table 4.3,

$$\rho_{50^\circ\text{C}} = 10.66\left(\frac{50 + 241.5}{20 + 241.5}\right) = 11.88 \quad \Omega\text{-cmil/ft}$$

From (4.2.1), the dc resistance at 50°C for a conductor length of 1 mile (5280 ft) is

$$R_{\text{dc, }50^\circ\text{C}} = \frac{(11.88)(5280 \times 1.02)}{211{,}600} = 0.302 \quad \Omega/\text{mi}$$

Copyright 2017 Cengage Learning. All Rights Reserved. May not be copied, scanned, or duplicated, in whole or in part. Due to electronic rights, some third party content may be suppressed from the eBook and/or eChapter(s). Editorial review has deemed that any suppressed content does not materially affect the overall learning experience. Cengage Learning reserves the right to remove additional content at any time if subsequent rights restrictions require it.

which agrees with the value listed in Table A.3.

c. From Table A.3,

$$\frac{R_{60\text{ Hz}, 50^\circ\text{C}}}{R_{\text{dc}, 50^\circ\text{C}}} = \frac{0.303}{0.302} = 1.003 \qquad \frac{R_{60\text{ Hz}, 25^\circ\text{C}}}{R_{\text{dc}, 25^\circ\text{C}}} = \frac{0.278}{0.276} = 1.007$$

Thus, the 60-Hz resistance of this conductor is about 0.3 to 0.7% higher than the dc resistance. The variation of these two ratios is due to the fact that resistance in Table A.3 is given to only three significant figures.

4.3 CONDUCTANCE

Conductance accounts for real power loss between conductors or between conductors and ground. For overhead lines, this power loss is due to leakage currents at insulators and to corona. Insulator leakage current depends on the amount of dirt, salt, and other contaminants that have accumulated on insulators, as well as on meteorological factors, particularly the presence of moisture. Corona occurs when a high value of electric field strength at a conductor surface causes the air to become electrically ionized and to conduct. The real power loss due to corona, called *corona loss*, depends on meteorological conditions, particularly rain, and on conductor surface irregularities. Losses due to insulator leakage and corona are usually small compared to conductor I^2R loss. Conductance is usually neglected in power system studies because it is a very small component of the shunt admittance.

4.4 INDUCTANCE: SOLID CYLINDRICAL CONDUCTOR

The inductance of a magnetic circuit that has a constant permeability μ can be obtained by determining the following:

1. Magnetic field intensity H, from Ampere's law
2. Magnetic flux density B ($B = \mu H$)
3. Flux linkages λ
4. Inductance from flux linkages per ampere ($L = \lambda/I$)

As a step toward computing the inductances of more general conductors and conductor configurations, first compute the internal, external, and total inductance of a solid cylindrical conductor. Also compute the flux linking one conductor in an array of current-carrying conductors.

Figure 4.6 shows a 1-meter section of a solid cylindrical conductor with radius r, carrying current I. For simplicity, assume that the conductor (1) is sufficiently long that end effects are neglected, (2) is nonmagnetic ($\mu = \mu_0 = 4\pi \times 10^{-7}$ H/m), and (3) has a uniform current density (skin effect is neglected). From (3.1.1), Ampere's law states that

Copyright 2017 Cengage Learning. All Rights Reserved. May not be copied, scanned, or duplicated, in whole or in part. Due to electronic rights, some third party content may be suppressed from the eBook and/or eChapter(s). Editorial review has deemed that any suppressed content does not materially affect the overall learning experience. Cengage Learning reserves the right to remove additional content at any time if subsequent rights restrictions require it.

FIGURE 4.6

Internal magnetic field of a solid cylindrical conductor

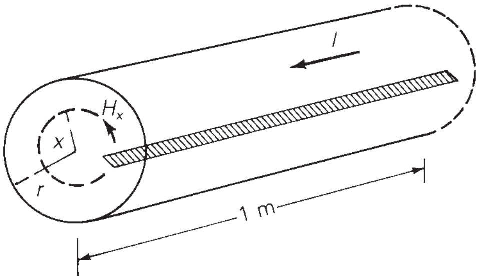

$$\oint H_{\tan}\, dl = I_{\text{enclosed}} \tag{4.4.1}$$

To determine the magnetic field inside the conductor, select the dashed circle of radius $x < r$ shown in Figure 4.6 as the closed contour for Ampere's law. Due to symmetry, H_x is constant along the contour. Also, there is no radial component of H_x, so H_x is tangent to the contour. That is, the conductor has a concentric magnetic field. From (4.4.1), the integral of H_x around the selected contour is

$$H_x(2\pi x) = I_x \qquad \text{for } x < r \tag{4.4.2}$$

where I_x is the portion of the total current enclosed by the contour. Solving (4.4.2),

$$H_x = \frac{I_x}{2\pi x} \quad \text{A/m} \tag{4.4.3}$$

Now assume a uniform current distribution within the conductor, that is

$$I_x = \left(\frac{x}{r}\right)^2 I \qquad \text{for } x < r \tag{4.4.4}$$

Using (4.4.4) in (4.4.3)

$$H_x = \frac{xI}{2\pi r^2} \quad \text{A/m} \tag{4.4.5}$$

For a nonmagnetic conductor, the magnetic flux density B_x is

$$B_x = \mu_0 H_x = \frac{\mu_0 x I}{2\pi r^2} \quad \text{Wb/m}^2 \tag{4.4.6}$$

The differential flux $d\Phi$ per-unit length of conductor in the cross-hatched rectangle of width dx shown in Figure 4.6 is

$$d\Phi = B_x\, dx \quad \text{Wb/m} \tag{4.4.7}$$

Computation of the differential flux linkage $d\lambda$ in the rectangle is tricky since only the fraction $(x/r)^2$ of the total current I is linked by the flux. That is,

$$d\lambda = \left(\frac{x}{r}\right)^2 d\Phi = \frac{\mu_0 I}{2\pi r^4} x^3\, dx \quad \text{Wb-t/m} \tag{4.4.8}$$

Copyright 2017 Cengage Learning. All Rights Reserved. May not be copied, scanned, or duplicated, in whole or in part. Due to electronic rights, some third party content may be suppressed from the eBook and/or eChapter(s). Editorial review has deemed that any suppressed content does not materially affect the overall learning experience. Cengage Learning reserves the right to remove additional content at any time if subsequent rights restrictions require it.

Integrating (4.4.8) from $x = 0$ to $x = r$ determines the total flux linkages λ_{int} inside the conductor

$$\lambda_{\text{int}} = \int_0^r d\lambda = \frac{\mu_0 I}{2\pi r^4}\int_0^r x^3\,dx = \frac{\mu_0 I}{8\pi} = \frac{1}{2}\times 10^{-7} I \quad \text{Wb-t/m} \tag{4.4.9}$$

The internal inductance L_{int} per-unit length of conductor due to this flux linkage is then

$$L_{\text{int}} = \frac{\lambda_{\text{int}}}{I} = \frac{\mu_0}{8\pi} = \frac{1}{2}\times 10^{-7} \quad \text{H/m} \tag{4.4.10}$$

Next, in order to determine the magnetic field outside the conductor, select the dashed circle of radius $x > r$ shown in Figure 4.7 as the closed contour for Ampere's law. Noting that this contour encloses the entire current I, integration of (4.4.1) yields

$$H_x(2\pi x) = I \tag{4.4.11}$$

which gives

$$H_x = \frac{I}{2\pi x} \quad \text{A/m} \quad x > r \tag{4.4.12}$$

Outside the conductor, $\mu = \mu_0$ and

$$B_x = \mu_0 H_x = (4\pi \times 10^{-7})\frac{I}{2\pi x} = 2\times 10^{-7}\frac{I}{x} \quad \text{Wb/m}^2 \tag{4.4.13}$$

$$d\Phi = B_x\,dx = 2\times 10^{-7}\frac{I}{x}\,dx \quad \text{Wb/m} \tag{4.4.14}$$

Since the entire current I is linked by the flux outside the conductor,

$$d\lambda = d\Phi = 2\times 10^{-7}\frac{I}{x}\,dx \quad \text{Wb-t/m} \tag{4.4.15}$$

Integrating (4.4.15) between two external points at distances D_1 and D_2 from the conductor center gives the external flux linkage λ_{12} between D_1 and D_2:

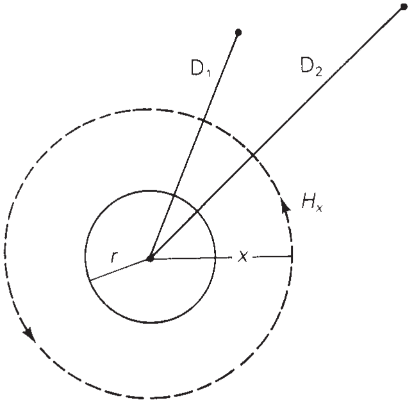

FIGURE 4.7

External magnetic field of a solid cylindrical conductor

Copyright 2017 Cengage Learning. All Rights Reserved. May not be copied, scanned, or duplicated, in whole or in part. Due to electronic rights, some third party content may be suppressed from the eBook and/or eChapter(s). Editorial review has deemed that any suppressed content does not materially affect the overall learning experience. Cengage Learning reserves the right to remove additional content at any time if subsequent rights restrictions require it.

$$\lambda_{12} = \int_{D_1}^{D_2} d\lambda = 2 \times 10^{-7} I \int_{D_1}^{D_2} \frac{dx}{x}$$

$$= 2 \times 10^{-7} I \ln\left(\frac{D_2}{D_1}\right) \quad \text{Wb-t/m} \tag{4.4.16}$$

The external inductance L_{12} per-unit length due to the flux linkages between D_1 and D_2 is then

$$L_{12} = \frac{\lambda_{12}}{I} = 2 \times 10^{-7} \ln\left(\frac{D_2}{D_1}\right) \quad \text{H/m} \tag{4.4.17}$$

The total flux λ_P linking the conductor out to external point P at distance D is the sum of the internal flux linkage, (4.4.9), and the external flux linkage, (4.4.16) from $D_1 = r$ to $D_2 = D$. That is

$$\lambda_P = \frac{1}{2} \times 10^{-7} I + 2 \times 10^{-7} I \ln \frac{D}{r} \tag{4.4.18}$$

Using the identity $\frac{1}{2} = 2 \ln e^{1/4}$ in (4.4.18), a more convenient expression for λ_P is obtained:

$$\lambda_p = 2 \times 10^{-7} I \left(\ln e^{1/4} + \ln \frac{D}{r}\right)$$

$$= 2 \times 10^{-7} I \ln \frac{D}{e^{-1/4} r}$$

$$= 2 \times 10^{-7} I \ln \frac{D}{r'} \quad \text{Wb-t/m} \tag{4.4.19}$$

where

$$r' = e^{-1/4} r = 0.7788 r \tag{4.4.20}$$

Also, the total inductance L_P due to both internal and external flux linkages out to distance D is

$$L_P = \frac{\lambda_P}{I} = 2 \times 10^{-7} \ln\left(\frac{D}{r'}\right) \quad \text{H/m} \tag{4.4.21}$$

Finally, consider the array of M solid cylindrical conductors shown in Figure 4.8. Assume that each conductor m carries current I_m referenced out of the page. Also assume that the sum of the conductor currents is zero—that is,

$$I_1 + I_2 + \cdots + I_M = \sum_{m=1}^{M} I_m = 0 \tag{4..4.22}$$

The flux linkage λ_{kPk}, which links conductor k out to point P due to current I_k, is, from (4.4.19),

$$\lambda_{kPk} = 2 \times 10^{-7} I_k \ln \frac{D_{Pk}}{r'_k} \tag{4.4.23}$$

Note that λ_{kPk} includes both internal and external flux linkages due to I_k. The flux linkage λ_{kPm}, which links conductor k out to P due to I_m, is, from (4.4.16),

Copyright 2017 Cengage Learning. All Rights Reserved. May not be copied, scanned, or duplicated, in whole or in part. Due to electronic rights, some third party content may be suppressed from the eBook and/or eChapter(s). Editorial review has deemed that any suppressed content does not materially affect the overall learning experience. Cengage Learning reserves the right to remove additional content at any time if subsequent rights restrictions require it.

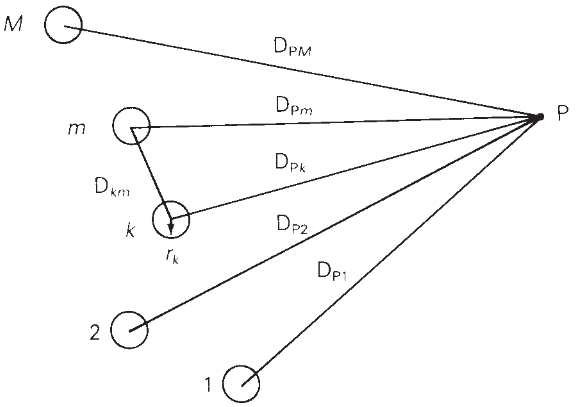

FIGURE 4.8

Array of *M* solid cylindrical conductors

$$\lambda_{k\mathrm{P}m} = 2 \times 10^{-7} I_m \ln \frac{\mathrm{D}_{\mathrm{P}m}}{\mathrm{D}_{km}} \tag{4.4.24}$$

Equation (4.4.24) uses D_{km} instead of $(\mathrm{D}_{km} - r_k)$ or $(\mathrm{D}_{km} + r_k)$, which is a valid approximation when D_{km} is much greater than r_k. It can also be shown that this is a good approximation even when D_{km} is small. Using superposition, the total flux linkage $\lambda_{k\mathrm{p}}$, which links conductor k out to P due to all the currents, is

$$\begin{aligned}\lambda_{k\mathrm{P}} &= \lambda_{k\mathrm{P}1} + \lambda_{k\mathrm{P}2} + \cdots + \lambda_{k\mathrm{P}M} \\ &= 2 \times 10^{-7} \sum_{m=1}^{M} I_m \ln \frac{\mathrm{D}_{\mathrm{P}m}}{\mathrm{D}_{km}} \end{aligned} \tag{4.4.25}$$

where $D_{kk} = r'_k = e^{-1/4} r_k$ is defined when $m = k$ in the above summation. Equation (4.4.25) is separated into two summations:

$$\lambda_{k\mathrm{P}} = 2 \times 10^{-7} \sum_{m=1}^{M} I_m \ln \frac{1}{\mathrm{D}_{km}} + 2 \times 10^{-7} \sum_{m=1}^{M} I_m \ln \mathrm{D}_{\mathrm{P}m} \tag{4.4.26}$$

Removing the last term from the second summation results in

$$\lambda_{k\mathrm{P}} = 2 \times 10^{-7} \left[\sum_{m=1}^{M} I_m \ln \frac{1}{\mathrm{D}_{km}} + \sum_{m=1}^{M-1} I_m \ln \mathrm{D}_{\mathrm{P}m} + I_M \ln \mathrm{D}_{\mathrm{P}M} \right] \tag{4.4.27}$$

From (4.4.22),

$$I_M = -(I_1 + I_2 + \cdots + I_{M-1}) = -\sum_{m=1}^{M-1} I_m \tag{4.4.28}$$

Using (4.4.28) in (4.4.27)

$$\begin{aligned}\lambda_{k\mathrm{P}} &= 2 \times 10^{-7} \left[\sum_{m=1}^{M} I_m \ln \frac{1}{\mathrm{D}_{km}} + \sum_{m=1}^{M-1} I_m \ln \mathrm{D}_{\mathrm{P}m} - \sum_{m=1}^{M-1} I_m \ln \mathrm{D}_{\mathrm{P}M} \right] \\ &= 2 \times 10^{-7} \left[\sum_{m=1}^{M} I_m \ln \frac{1}{\mathrm{D}_{km}} + \sum_{m=1}^{M-1} I_m \ln \frac{\mathrm{D}_{\mathrm{P}m}}{\mathrm{D}_{\mathrm{P}M}} \right] \end{aligned} \tag{4.4.29}$$

Copyright 2017 Cengage Learning. All Rights Reserved. May not be copied, scanned, or duplicated, in whole or in part. Due to electronic rights, some third party content may be suppressed from the eBook and/or eChapter(s). Editorial review has deemed that any suppressed content does not materially affect the overall learning experience. Cengage Learning reserves the right to remove additional content at any time if subsequent rights restrictions require it.

Now, let λ_k equal the total flux linking conductor k out to infinity. That is, $\lambda_k = \lim_{P \to \infty} \lambda_{kP}$. As $P \to \infty$, all the distances D_{Pm} become equal, the ratios D_{Pm}/D_{PM} become unity, and $\ln(D_{Pm}/D_{PM}) \to 0$. Therefore, the second summation in (4.4.29) becomes zero as $P \to \infty$, and

$$\lambda_k = 2 \times 10^{-7} \sum_{m=1}^{M} I_m \ln \frac{1}{D_{km}} \quad \text{Wb-t/m} \tag{4.4.30}$$

Equation (4.4.30) gives the total flux linking conductor k in an array of M conductors carrying currents $I_1, I_2, \ldots, I_M$, whose sum is zero. This equation is valid for either dc or ac currents. λ_k is a dc flux linkage when the currents are dc, and λ_k is a phasor flux linkage when the currents are phasor representations of sinusoids.

4.5 INDUCTANCE: SINGLE-PHASE TWO-WIRE LINE AND THREE-PHASE THREE-WIRE LINE WITH EQUAL PHASE SPACING

The results of the previous section are used here to determine the inductances of two relatively simple transmission lines: a single-phase two-wire line and a three-phase three-wire line with equal phase spacing.

Figure 4.9(a) shows a single-phase two-wire line consisting of two solid cylindrical conductors x and y. Conductor x with radius r_x carries phasor current $I_x = I$ referenced out of the page. Conductor y with radius r_y carries return current $I_y = -I$. Since the sum of the two currents is zero, (4.4.30) is valid, from which the total flux linking conductor x is

$$\begin{aligned}\lambda_x &= 2 \times 10^{-7}\left(I_x \ln \frac{1}{D_{xx}} + I_y \ln \frac{1}{D_{xy}}\right)\\ &= 2 \times 10^{-7}\left(I \ln \frac{1}{r'_x} - I \ln \frac{1}{D}\right)\\ &= 2 \times 10^{-7} I \ln \frac{D}{r'_x} \quad \text{Wb-t/m}\end{aligned} \tag{4.5.1}$$

FIGURE 4.9

Single-phase two-wire line

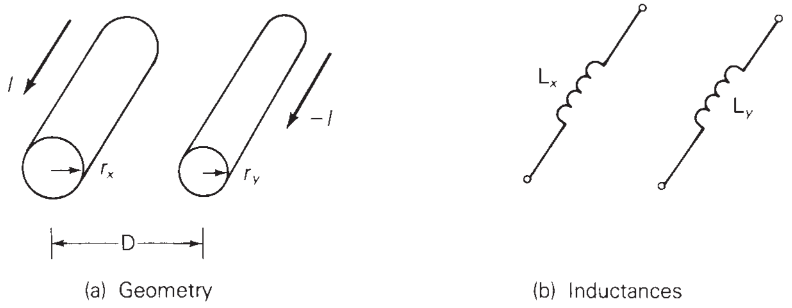

(a) Geometry (b) Inductances

Copyright 2017 Cengage Learning. All Rights Reserved. May not be copied, scanned, or duplicated, in whole or in part. Due to electronic rights, some third party content may be suppressed from the eBook and/or eChapter(s). Editorial review has deemed that any suppressed content does not materially affect the overall learning experience. Cengage Learning reserves the right to remove additional content at any time if subsequent rights restrictions require it.

Where $r_x' = e^{-1/4} r_x = 0.7788 r_x$.

The inductance of conductor x is then

$$L_x = \frac{\lambda_x}{I_x} = \frac{\lambda_x}{I} = 2 \times 10^{-7} \ln \frac{D}{r_x'} \quad \text{H/m per conductor} \tag{4.5.2}$$

Similarly, the total flux linking conductor y is

$$\begin{aligned} \lambda_y &= 2 \times 10^{-7} \left(I_x \ln \frac{1}{D_{yx}} + I_y \ln \frac{1}{D_{yy}} \right) \\ &= 2 \times 10^{-7} \left(I \ln \frac{1}{D} - I \ln \frac{1}{r_y'} \right) \\ &= -2 \times 10^{-7}\, I \ln \frac{D}{r_y'} \end{aligned} \tag{4.5.3}$$

and

$$L_y = \frac{\lambda_y}{I_y} = \frac{\lambda_y}{-I} = 2 \times 10^{-7} \ln \frac{D}{r_y'} \quad \text{H/m per conductor} \tag{4.5.4}$$

The total inductance of the single-phase circuit, also called *loop inductance,* is

$$\begin{aligned} L = L_x + L_y &= 2 \times 10^{-7} \left(\ln \frac{D}{r_x'} + \ln \frac{D}{r_y'} \right) \\ &= 2 \times 10^{-7} \ln \frac{D^2}{r_x' r_y'} \\ &= 4 \times 10^{-7} \ln \frac{D}{\sqrt{r_x' r_y'}} \quad \text{H/m per circuit} \end{aligned} \tag{4.5.5}$$

Also, if $r_x' = r_y' = r'$, the total circuit inductance is

$$L = 4 \times 10^{-7} \ln \frac{D}{r'} \quad \text{H/m per circuit} \tag{4.5.6}$$

The inductances of the single-phase two-wire line are shown in Figure 4.9(b).

Figure 4.10(a) shows a three-phase three-wire line consisting of three solid cylindrical conductors a, b, c, each with radius r, and with equal phase spacing D between any two conductors. To determine inductance, assume balanced positive-sequence currents I_a, I_b, I_c that satisfy $I_a + I_b + I_c = 0$. Then (4.4.30) is valid and the total flux linking the phase a conductor is

$$\begin{aligned} \lambda_a &= 2 \times 10^{-7} \left(I_a \ln \frac{1}{r'} + I_b \ln \frac{1}{D} + I_c \ln \frac{1}{D} \right) \\ &= 2 \times 10^{-7} \left[I_a \ln \frac{1}{r'} + (I_b + I_c) \ln \frac{1}{D} \right] \end{aligned} \tag{4.5.7}$$

Copyright 2017 Cengage Learning. All Rights Reserved. May not be copied, scanned, or duplicated, in whole or in part. Due to electronic rights, some third party content may be suppressed from the eBook and/or eChapter(s). Editorial review has deemed that any suppressed content does not materially affect the overall learning experience. Cengage Learning reserves the right to remove additional content at any time if subsequent rights restrictions require it.

FIGURE 4.10

Three-phase three-wire line with equal phase spacing

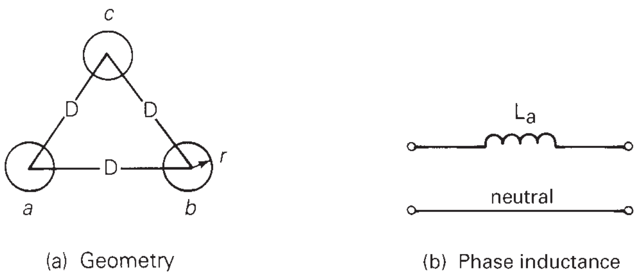

(a) Geometry (b) Phase inductance

Using $(I_b + I_c) = -I_a$,

$$\lambda_a = 2 \times 10^{-7}\left(I_a \ln \frac{1}{r'} - I_a \ln \frac{1}{\mathrm{D}}\right)$$

$$= 2 \times 10^{-7}\, I_a \ln \frac{\mathrm{D}}{r'} \quad \text{Wb-t/m} \tag{4.5.8}$$

The inductance of phase *a* is then

$$\mathrm{L}_a = \frac{\lambda_a}{I_a} = 2 \times 10^{-7} \ln \frac{\mathrm{D}}{r'} \quad \text{H/m per phase} \tag{4.5.9}$$

Due to symmetry, the same result is obtained for $\mathrm{L}_b = \lambda_b/I_b$ and for $\mathrm{L}_c = \lambda_c/I_c$. However, only one phase need be considered for balanced three-phase operation of this line, since the flux linkages of each phase have equal magnitudes and 120° displacement. The phase inductance is shown in Figure 4.10(b).

4.6 INDUCTANCE: COMPOSITE CONDUCTORS, UNEQUAL PHASE SPACING, BUNDLED CONDUCTORS

The results of Section 4.5 are extended here to include composite conductors, which consist of two or more solid cylindrical subconductors in parallel. A stranded conductor is one example of a composite conductor. For simplicity assume that for each conductor, the subconductors are identical and share the conductor current equally.

Figure 4.11 shows a single-phase two-conductor line consisting of two composite conductors *x* and *y*. Conductor *x* has *N* identical subconductors, each with radius r_x and with current (I/N) referenced out of the page. Similarly, conductor *y* consists of *M* identical subconductors, each with radius r_y and with return current $(-I/M)$. Since the sum of all the currents is zero, (4.4.30) is valid and the total flux Φ_k linking subconductor *k* of conductor *x* is

$$\Phi_k = 2 \times 10^{-7}\left[\frac{I}{N}\sum_{m=1}^{N} \ln \frac{1}{\mathrm{D}_{km}} - \frac{1}{M}\sum_{m=1'}^{M} \ln \frac{1}{\mathrm{D}_{km}}\right] \tag{4.6.1}$$

Copyright 2017 Cengage Learning. All Rights Reserved. May not be copied, scanned, or duplicated, in whole or in part. Due to electronic rights, some third party content may be suppressed from the eBook and/or eChapter(s). Editorial review has deemed that any suppressed content does not materially affect the overall learning experience. Cengage Learning reserves the right to remove additional content at any time if subsequent rights restrictions require it.

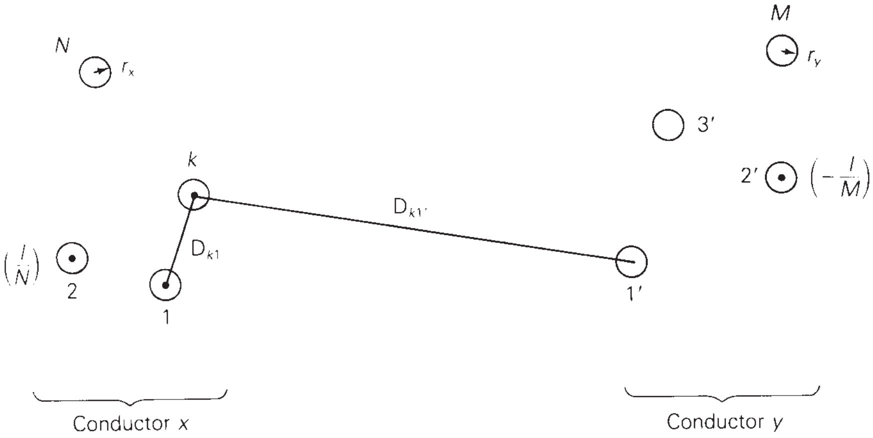

FIGURE 4.11 Single-phase two-conductor line with composite conductors

Since only the fraction ($1/N$) of the total conductor current I is linked by this flux, the flux linkage λ_k of (the current in) subconductor k is

$$\lambda_k = \frac{\Phi_k}{N} = 2 \times 10^{-7} I \left[\frac{1}{N^2}\sum_{m=1}^{N} \ln\frac{1}{D_{km}} - \frac{1}{NM}\sum_{m=1'}^{M} \ln\frac{1}{D_{km}}\right] \tag{4.6.2}$$

The total flux linkage of conductor x is

$$\lambda_x = \sum_{k=1}^{N}\lambda_k = 2 \times 10^{-7} I \sum_{k=1}^{N}\left[\frac{1}{N^2}\sum_{m=1}^{N} \ln\frac{1}{D_{km}} - \frac{1}{NM}\sum_{m=1'}^{M} \ln\frac{1}{D_{km}}\right] \tag{4.6.3}$$

Using $\ln A^{\alpha} = \alpha \ln A$ and $\sum \ln A_k = \ln \prod A_k$ (sum of ln s = ln of products), (4.6.3) can be rewritten in the following form:

$$\lambda_x = 2 \times 10^{-7}\, I \ln \prod_{k=1}^{N} \frac{\left(\prod_{m=1'}^{M} D_{km}\right)^{1/NM}}{\left(\prod_{m=1}^{N} D_{km}\right)^{1/N^2}} \tag{4.6.4}$$

and the inductance of conductor x, $L_x = \dfrac{\lambda_x}{I}$, can be written as

$$L_x = 2 \times 10^{-7} \ln \frac{D_{xy}}{D_{xx}} \quad \text{H/m per conductor} \tag{4.6.5}$$

where

$$D_{xy} = \sqrt[MN]{\prod_{k=1}^{N}\prod_{m=1'}^{M} D_{km}} \tag{4.6.6}$$

$$D_{xx} = \sqrt[N^2]{\prod_{k=1}^{N}\prod_{m=1}^{N} D_{km}} \tag{4.6.7}$$

Copyright 2017 Cengage Learning. All Rights Reserved. May not be copied, scanned, or duplicated, in whole or in part. Due to electronic rights, some third party content may be suppressed from the eBook and/or eChapter(s). Editorial review has deemed that any suppressed content does not materially affect the overall learning experience. Cengage Learning reserves the right to remove additional content at any time if subsequent rights restrictions require it.

D_{xy}, given by (4.6.6), is the MNth root of the product of the MN distances from the subconductors of conductor x to the subconductors of conductor y. Associated with each subconductor k of conductor x are the M distances $D_{k1'}$, $D_{k2'}$, …, D_{kM} to the subconductors of conductor y. For N subconductors in conductor x, there are therefore MN of these distances. D_{xy} is called the *geometric mean distance* or GMD between conductors x and y.

Also, D_{xx}, given by (4.6.7), is the N^2 root of the product of the N^2 distances between the subconductors of conductor x. Associated with each subconductor k are the N distances D_{k1}, D_{k2}, …, $D_{kk} = r'$, …, D_{kN}. For N subconductors in conductor x, there are therefore N^2 of these distances. D_{xx} is called the *geometric mean radius* or GMR of conductor x.

Similarly, for conductor y,

$$L_y = 2 \times 10^{-7} \ln \frac{D_{xy}}{D_{yy}} \quad \text{H/m per conductor} \tag{4.6.8}$$

where

$$D_{yy} = \sqrt[M^2]{\prod_{k=1'}^{M} \prod_{m=1'}^{M} D_{km}} \tag{4.6.9}$$

D_{yy}, the GMR of conductor y, is the M^2 root of the product of the M^2 distances between the subconductors of conductor y. The total inductance L of the single-phase circuit is

$$L = L_x + L_y \quad \text{H/m per circuit} \tag{4.6.10}$$

EXAMPLE 4.2

GMR, GMD, and inductance: single-phase two-conductor line

Expand (4.6.6), (4.6.7), and (4.6.9) for $N = 3$ and $M = 2'$. Then evaluate L_x, L_y, and L in H/m for the single-phase two-conductor line shown in Figure 4.12.

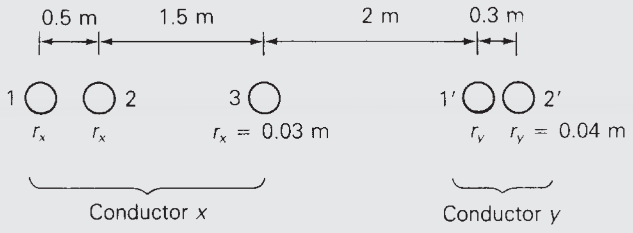

FIGURE 4.12 Single-phase two-conductor line for Example 4.2

Copyright 2017 Cengage Learning. All Rights Reserved. May not be copied, scanned, or duplicated, in whole or in part. Due to electronic rights, some third party content may be suppressed from the eBook and/or eChapter(s). Editorial review has deemed that any suppressed content does not materially affect the overall learning experience. Cengage Learning reserves the right to remove additional content at any time if subsequent rights restrictions require it.

SOLUTION

For $N = 3$ and $M = 2'$, (4.6.6) becomes

$$D_{xy} = \sqrt[6]{\prod_{k=1}^{3}\prod_{m=1'}^{2'} D_{km}}$$

$$= \sqrt[6]{\prod_{k=1}^{3} D_{k1'}D_{k2'}}$$

$$= \sqrt[6]{(D_{11'}D_{12'})(D_{21'}D_{22'})(D_{31'}D_{32'})}$$

Similarly, (4.6.7) becomes

$$D_{xx} = \sqrt[9]{\prod_{k=1}^{3}\prod_{m=1}^{3} D_{km}}$$

$$= \sqrt[9]{\prod_{k=1}^{3} D_{k1}D_{k2}D_{k3}}$$

$$= \sqrt[9]{(D_{11}D_{12}D_{13})(D_{21}D_{22}D_{23})(D_{31}D_{32}D_{33})}$$

and (4.6.9) becomes

$$D_{yy} = \sqrt[4]{\prod_{k=1'}^{2'}\prod_{m=1'}^{2'} D_{km}}$$

$$= \sqrt[4]{\prod_{k=1'}^{2'} D_{k1'}D_{k2'}}$$

$$= \sqrt[4]{(D_{1'1'}D_{1'2'})(D_{2'1'}D_{2'2'})}$$

Evaluating D_{xy}, D_{xx}, and D_{yy} for the single-phase two-conductor line shown in Figure 4.12,

$D_{11'} = 4$ m $\quad D_{12'} = 4.3$ m $\quad D_{21'} = 3.5$ m

$D_{22'} = 3.8$ m $\quad D_{31'} = 2$ m $\quad D_{32'} = 2.3$ m

$D_{xy} = \sqrt[6]{(4)(4.3)(3.5)(3.8)(2)(2.3)} = 3.189$ m

$D_{11} = D_{22} = D_{33} = r'_x = e^{-1/4}r_x = (0.7788)(0.03) = 0.02336$ m

$D_{21} = D_{12} = 0.5$ m

$D_{23} = D_{32} = 1.5$ m

$D_{31} = D_{13} = 2.0$ m

(Continued)

Copyright 2017 Cengage Learning. All Rights Reserved. May not be copied, scanned, or duplicated, in whole or in part. Due to electronic rights, some third party content may be suppressed from the eBook and/or eChapter(s). Editorial review has deemed that any suppressed content does not materially affect the overall learning experience. Cengage Learning reserves the right to remove additional content at any time if subsequent rights restrictions require it.

$$D_{xx} = \sqrt[9]{(0.02336)^3(0.5)^2(1.5)^2(2.0)^2} = 0.3128 \text{ m}$$

$$D_{1'1'} = D_{2'2'} = r'_y = e^{-1/4}r_y = (0.7788)(0.4) = 0.03115 \text{ m}$$

$$D_{1'2'} = D_{2'1'} = 0.3 \text{ m}$$

$$D_{yy} = \sqrt[4]{(0.03115)^2(0.3)^2} = 0.09667 \text{ m}$$

Then, from (4.6.5), (4.6.8), and (4.6.10):

$$L_x = 2 \times 10^{-7} \ln\left(\frac{3.189}{0.3128}\right) = 4.644 \times 10^{-7} \quad \text{H/m per conductor}$$

$$L_y = 2 \times 10^{-7} \ln\left(\frac{3.189}{0.09667}\right) = 6.992 \times 10^{-7} \quad \text{H/m per conductor}$$

$$L = L_x + L_y = 1.164 \times 10^{-6} \quad \text{H/m per circuit}$$

It is seldom necessary to calculate GMR or GMD for standard lines. The GMR of standard conductors is provided by conductor manufacturers and can be found in various handbooks (see Appendix Tables A.3 and A.4). Also, if the distances between conductors are large compared to the distances between subconductors of each conductor, then the GMD between conductors is approximately equal to the distance between conductor centers.

EXAMPLE 4.3

Inductance and inductive reactance: single-phase line

A single-phase line operating at 60 Hz consists of two 4/0 12-strand copper conductors with 5 ft spacing between conductor centers. The line length is 20 miles. Determine the total inductance in H and the total inductive reactance in Ω.

SOLUTION

The GMD between conductor centers is $D_{xy} = 5$ ft. Also, from Table A.3, the GMR of a 4/0 12-strand copper conductor is $D_{xx} = D_{yy} = 0.01750$ ft. From (4.6.5) and (4.6.8),

$$L_x = L_y = 2 \times 10^{-7} \ln\left(\frac{5}{0.01750}\right)\frac{\text{H}}{\text{m}} \times 1609\frac{\text{m}}{\text{mi}} \times 20 \text{ mi}$$

$$= 0.03639 \quad \text{H per conductor}$$

The total inductance is

$$L = L_x + L_y = 2 \times 0.03639 = 0.07279 \quad \text{H per circuit}$$

and the total inductive reactance is

$$X_L = 2\pi f L = (2\pi)(60)(0.07279) = 27.44 \quad \Omega \text{ per circuit}$$

Copyright 2017 Cengage Learning. All Rights Reserved. May not be copied, scanned, or duplicated, in whole or in part. Due to electronic rights, some third party content may be suppressed from the eBook and/or eChapter(s). Editorial review has deemed that any suppressed content does not materially affect the overall learning experience. Cengage Learning reserves the right to remove additional content at any time if subsequent rights restrictions require it.

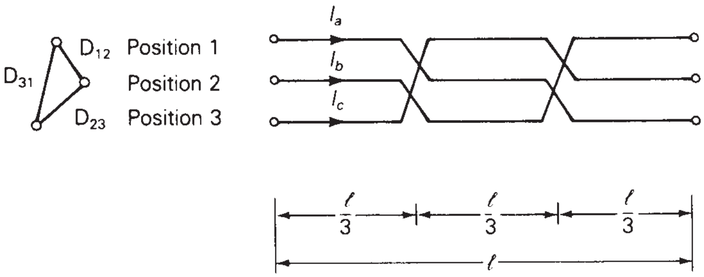

FIGURE 4.13

Completely transposed three-phase line

To calculate inductance for three-phase lines with stranded conductors and equal phase spacing, r' is replaced by the conductor GMR in (4.5.9). If the spacings between phases are unequal, then balanced positive-sequence flux linkages are not obtained from balanced positive-sequence currents. Instead, unbalanced flux linkages occur, and the phase inductances are unequal. However, balance can be restored by exchanging the conductor positions along the line, which is a technique called *transposition.*

Figure 4.13 shows a completely transposed three-phase line. The line is transposed at two locations such that each phase occupies each position for one-third of the line length. Conductor positions are denoted 1, 2, 3 with distances D_{12}, D_{23}, D_{31} between positions. The conductors are identical, each with GMR denoted D_S. To calculate inductance of this line, assume balanced positive-sequence currents I_a, I_b, I_c, for which $I_a + I_b + I_c = 0$. Again, (4.4.30) is valid, and the total flux linking the phase a conductor while it is in position 1 is

$$\lambda_{a1} = 2 \times 10^{-7}\left[I_a \ln\frac{1}{D_S} + I_b \ln\frac{1}{D_{12}} + I_c \ln\frac{1}{D_{31}}\right] \quad \text{Wb-t/m} \tag{4.6.11}$$

Similarly, the total flux linkage of this conductor while it is in positions 2 and 3 is

$$\lambda_{a2} = 2 \times 10^{-7}\left[I_a \ln\frac{1}{D_S} + I_b \ln\frac{1}{D_{23}} + I_c \ln\frac{1}{D_{12}}\right] \quad \text{Wb-t/m} \tag{4.6.12}$$

$$\lambda_{a3} = 2 \times 10^{-7}\left[I_a \ln\frac{1}{D_S} + I_b \ln\frac{1}{D_{31}} + I_c \ln\frac{1}{D_{23}}\right] \quad \text{Wb-t/m} \tag{4.6.13}$$

The average of the above flux linkages is

$$\lambda_a = \frac{\lambda_{a1}\left(\frac{l}{3}\right) + \lambda_{a2}\left(\frac{l}{3}\right) + \lambda_{a3}\left(\frac{l}{3}\right)}{l} = \frac{\lambda_{a1} + \lambda_{a2} + \lambda_{a3}}{3}$$

$$= \frac{2 \times 10^{-7}}{3}\left[3I_a \ln\frac{1}{D_S} + I_b \ln\frac{1}{D_{12}D_{23}D_{31}} + I_c \ln\frac{1}{D_{12}D_{23}D_{31}}\right] \tag{4.6.14}$$

Using $(I_b + I_c) = -I_a$ in (4.6.14),

$$\lambda_a = \frac{2 \times 10^{-7}}{3}\left[3I_a \ln\frac{1}{D_S} - I_a \ln\frac{1}{D_{12}D_{23}D_{31}}\right]$$

$$= 2 \times 10^{-7} I_a \ln\frac{\sqrt[3]{D_{12}D_{23}D_{31}}}{D_S} \quad \text{Wb-t/m} \tag{4.6.15}$$

Copyright 2017 Cengage Learning. All Rights Reserved. May not be copied, scanned, or duplicated, in whole or in part. Due to electronic rights, some third party content may be suppressed from the eBook and/or eChapter(s). Editorial review has deemed that any suppressed content does not materially affect the overall learning experience. Cengage Learning reserves the right to remove additional content at any time if subsequent rights restrictions require it.

and the average inductance of phase *a* is

$$L_a = \frac{\lambda_a}{I_a} = 2 \times 10^{-7} \ln \frac{\sqrt[3]{D_{12}D_{23}D_{31}}}{D_S} \quad \text{H/m per phase} \tag{4.6.16}$$

The same result is obtained for $L_b = \lambda_b/I_b$ and for $L_c = \lambda_c/I_c$. However, only one phase need be considered for balanced three-phase operation of a completely transposed three-phase line. Defining

$$D_{eq} = \sqrt[3]{D_{12}D_{23}D_{31}} \tag{4.6.17}$$

results in

$$L_a = 2 \times 10^{-7} \ln \frac{D_{eq}}{D_S} \quad \text{H/m} \tag{4.6.18}$$

D_{eq}, the cube root of the product of the three-phase spacings, is the geometric mean distance between phases. Also, D_S is the conductor GMR for stranded conductors, or r' for solid cylindrical conductors.

EXAMPLE 4.4

Inductance and inductive reactance: three-phase line

A completely transposed 60-Hz three-phase line has flat horizontal phase spacing with 10 m between adjacent conductors. The conductors are 1,590,000 cmil ACSR with 54/3 stranding. Line length is 200 km. Determine the inductance in H and the inductive reactance in Ω.

SOLUTION

From Table A.4, the GMR of a 1,590,000 cmil 54/3 ACSR conductor is

$$D_S = 0.0520 \text{ ft} \frac{1 \text{ m}}{3.28 \text{ ft}} = 0.0159 \text{ m}$$

Also, from (4.6.17) and (4.6.18),

$$D_{eq} = \sqrt[3]{(10)(10)(20)} = 12.6 \text{ m}$$

$$L_a = 2 \times 10^{-7} \ln \left(\frac{12.6}{0.0159}\right) \frac{\text{H}}{\text{m}} \times \frac{1000 \text{ m}}{\text{km}} \times 200 \text{ km}$$

$$= 0.267 \text{ H}$$

The inductive reactance of phase *a* is

$$X_a = 2\pi f L_a = 2\pi(60)(0.267) = 101 \quad \Omega$$

Copyright 2017 Cengage Learning. All Rights Reserved. May not be copied, scanned, or duplicated, in whole or in part. Due to electronic rights, some third party content may be suppressed from the eBook and/or eChapter(s). Editorial review has deemed that any suppressed content does not materially affect the overall learning experience. Cengage Learning reserves the right to remove additional content at any time if subsequent rights restrictions require it.

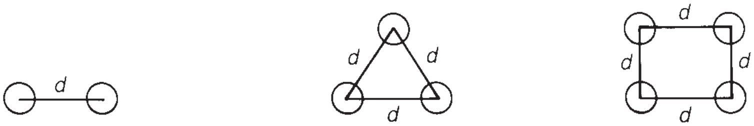

FIGURE 4.14

Bundle conductor configurations

It is common practice for EHV lines to use more than one conductor per phase, a practice called *bundling*. Bundling reduces the electric field strength at the conductor surfaces, which in turn reduces or eliminates corona and its results: undesirable power loss, communications interference, and audible noise. Bundling also reduces the series reactance of the line by increasing the GMR of the bundle.

Figure 4.14 shows common EHV bundles consisting of two, three, or four conductors. The three-conductor bundle has its conductors on the vertices of an equilateral triangle, and the four-conductor bundle has its conductors on the corners of a square. To calculate inductance, D_S in (4.6.18) is replaced by the GMR of the bundle. Since the bundle constitutes a composite conductor, calculation of bundle GMR is, in general, given by (4.6.7). If the conductors are stranded and the bundle spacing d is large compared to the conductor outside radius, each stranded conductor is first replaced by an equivalent solid cylindrical conductor with GMR $= D_S$. Then the bundle is replaced by one equivalent conductor with GMR $= D_{SL}$, given by (4.6.7) with $n = 2, 3$, or 4 as follows:

Two-conductor bundle:

$$D_{SL} = \sqrt[4]{(D_S \times d)^2} = \sqrt{D_S d} \tag{4.6.19}$$

Three-conductor bundle:

$$D_{SL} = \sqrt[9]{(D_S \times d \times d)^3} = \sqrt[3]{D_S d^2} \tag{4.6.20}$$

Four-conductor bundle:

$$D_{SL} = \sqrt[16]{(D_S \times d \times d \times d\sqrt{2})^4} = 1.091\sqrt[4]{D_S d^3} \tag{4.6.21}$$

The inductance is then

$$L_a = 2 \times 10^{-7} \ln \frac{D_{eq}}{D_{SL}} \quad \text{H/m} \tag{4.6.22}$$

If the phase spacings are large compared to the bundle spacing, then sufficient accuracy for D_{eq} is obtained by using the distances between bundle centers.

EXAMPLE 4.5

Inductive reactance: three-phase line with bundled conductors

Each of the 1,590,000 cmil conductors in Example 4.4 is replaced by two 795,000 cmil ACSR 26/2 conductors, as shown in Figure 4.15. Bundle spacing is

(*Continued*)

Copyright 2017 Cengage Learning. All Rights Reserved. May not be copied, scanned, or duplicated, in whole or in part. Due to electronic rights, some third party content may be suppressed from the eBook and/or eChapter(s). Editorial review has deemed that any suppressed content does not materially affect the overall learning experience. Cengage Learning reserves the right to remove additional content at any time if subsequent rights restrictions require it.

FIGURE 4.15

Three-phase bundled conductor line for Example 4.5

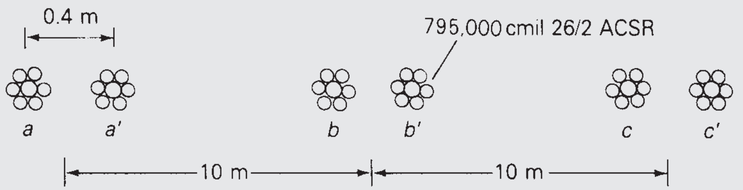

0.40 m. Flat horizontal spacing is retained, with 10 m between adjacent bundle centers. Calculate the inductive reactance of the line and compare it with that of Example 4.4.

SOLUTION

From Table A.4, the GMR of a 795,000 cmil 26/2 ACSR conductor is

$$D_S = 0.0375 \text{ ft} \times \frac{1 \text{ m}}{3.28 \text{ ft}} = 0.0114 \text{ m}$$

From (4.6.19), the two-conductor bundle GMR is

$$D_{SL} = \sqrt{(0.0114)(0.40)} = 0.0676 \quad \text{m}$$

Since $D_{eq} = 12.6$ m is the same as in Example 4.4,

$$L_a = 2 \times 10^{-7} \ln\left(\frac{12.6}{0.0676}\right)(1000)\,(200) = 0.209 \text{ H}$$

$$X_a = 2\pi f L_1 = (2\pi)(60)(0.209) = 78.8 \quad \Omega$$

The reactance of the bundled line, 78.8 Ω, is 22% less than that of Example 4.4, even though the two-conductor bundle has the same amount of conductor material (that is, the same cmil per phase). One advantage of reduced series line reactance is smaller line-voltage drops. Also, the loadability of medium and long EHV lines is increased (see Chapter 5).

4.7 SERIES IMPEDANCES: THREE-PHASE LINE WITH NEUTRAL CONDUCTORS AND EARTH RETURN

This section develops equations suitable for computer calculation of the series impedances, including resistances and inductive reactances, for the three-phase overhead line shown in Figure 4.16. This line has three phase conductors *a*, *b*, and c, where bundled conductors, if any, have already been replaced by equivalent conductors, as described in Section 4.6. The line also has *N* neutral conductors denoted *n*1, *n*2, ..., *nN*.* All the neutral conductors are connected in parallel and are grounded

---

* Instead of *shield wire,* the term *neutral conductor* is used. It applies to distribution as well as transmission lines.

Copyright 2017 Cengage Learning. All Rights Reserved. May not be copied, scanned, or duplicated, in whole or in part. Due to electronic rights, some third party content may be suppressed from the eBook and/or eChapter(s). Editorial review has deemed that any suppressed content does not materially affect the overall learning experience. Cengage Learning reserves the right to remove additional content at any time if subsequent rights restrictions require it.

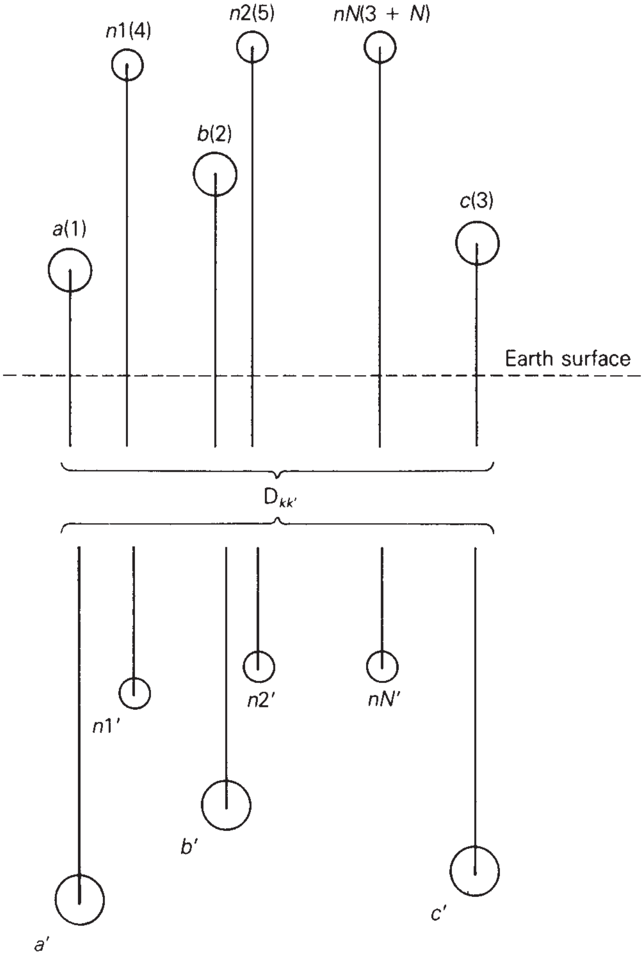

FIGURE 4.16

Three-phase transmission line with earth replaced by earth return conductors

to the earth at regular intervals along the line. Any isolated neutral conductors that carry no current are omitted. The phase conductors are insulated from each other and from the earth.

If the phase currents are not balanced, there may be a return current in the grounded neutral wires and in the earth. The earth return current will spread out under the line, seeking the lowest impedance return path. A classic paper by Carson [4], later modified by others [5, 6], shows that the earth can be replaced by a set of "earth return" conductors located directly under the overhead conductors, as shown in Figure 4.16. Each earth return conductor carries the negative of its overhead conductor current, has a GMR denoted $D_{k'k'}$, distance $D_{kk'}$ from its overhead conductor, and resistance $R_{k'}$ given by:

$$D_{k'k'} = D_{kk} \quad \text{m} \tag{4.7.1}$$

$$D_{kk'} = 658.5\sqrt{\rho/f} \quad \text{m} \tag{4.7.2}$$

$$R_{k'} = 9.869 \times 10^{-7} f \quad \Omega/\text{m} \tag{4.7.3}$$

Copyright 2017 Cengage Learning. All Rights Reserved. May not be copied, scanned, or duplicated, in whole or in part. Due to electronic rights, some third party content may be suppressed from the eBook and/or eChapter(s). Editorial review has deemed that any suppressed content does not materially affect the overall learning experience. Cengage Learning reserves the right to remove additional content at any time if subsequent rights restrictions require it.

TABLE 4.4

Earth resistivities and 60-Hz equivalent conductor distances

Type of Earth	Resistivity (Ωm)	$D_{kk'}$ (m)
Sea water	0.01–1.0	8.50–85.0
Swampy ground	10–100	269–850
Average damp earth	100	850
Dry earth	1000	2690
Pure slate	10^7	269,000
Sandstone	10^9	2,690,000

where ρ is the earth resistivity in ohm-meters and f is frequency in hertz. Table 4.4 lists earth resistivities and 60-Hz equivalent conductor distances for various types of earth. It is common practice to select $\rho = 100$ Ωm when actual data are unavailable.

Note that the GMR of each earth return conductor, $D_{k'k'}$, is the same as the GMR of its corresponding overhead conductor, D_{kk}. Also, all the earth return conductors have the same distance $D_{kk'}$ from their overhead conductors and the same resistance $R_{k'}$.

For simplicity, renumber the overhead conductors from 1 to $(3 + N)$, beginning with the phase conductors, then overhead neutral conductors, as shown in Figure 4.16. Operating as a transmission line, the sum of the currents in all the conductors is zero. That is,

$$\sum_{k=1}^{(6+2N)} I_k = 0 \tag{4.7.4}$$

Equation (4.4.30) is therefore valid, and the flux linking overhead conductor k is

$$\lambda_k = 2 \times 10^{-7} \sum_{m=1}^{(3+N)} I_m \ln \frac{D_{km'}}{D_{km'}} \quad \text{Wb-t/m} \tag{4.7.5}$$

In matrix format, (4.7.5) becomes

$$\boldsymbol{\lambda} = \mathbf{L}\boldsymbol{I} \tag{4.7.6}$$

where

$\boldsymbol{\lambda}$ is a $(3 + N)$ vector

$\boldsymbol{I}$ is a $(3 + N)$ vector

$\mathbf{L}$ is a $(3 + N) \times (3 + N)$ matrix whose elements are

$$L_{km} = 2 \times 10^{-7} \ln \frac{D_{km'}}{D_{km}} \tag{4.7.7}$$

When $k = m$, D_{kk} in (4.7.7) is the GMR of (bundled) conductor k. When $k \neq m$, D_{km} is the distance between conductors k and m.

Copyright 2017 Cengage Learning. All Rights Reserved. May not be copied, scanned, or duplicated, in whole or in part. Due to electronic rights, some third party content may be suppressed from the eBook and/or eChapter(s). Editorial review has deemed that any suppressed content does not materially affect the overall learning experience. Cengage Learning reserves the right to remove additional content at any time if subsequent rights restrictions require it.

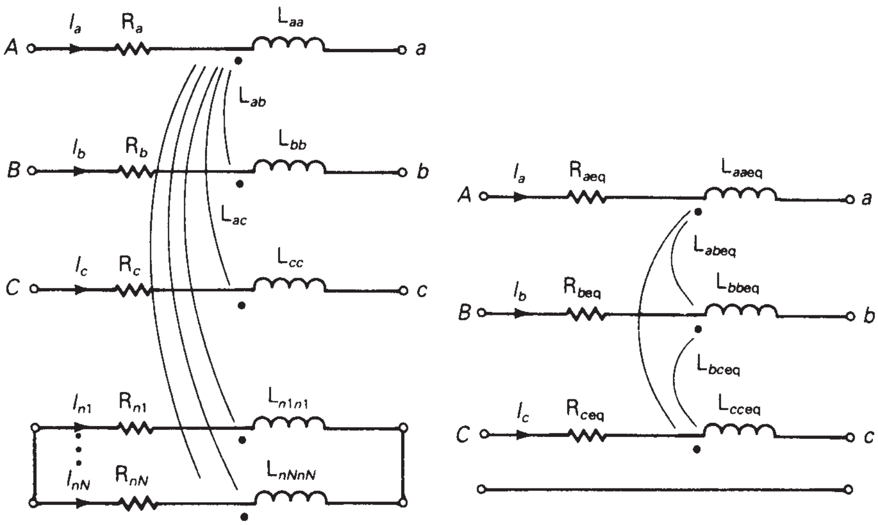

(a) Complete circuit (b) Simplified circuit

FIGURE 4.17

Circuit representation of series-phase impedances

A circuit representation of a 1-meter section of the line is shown in Figure 4.17(a). Using this circuit, the vector of voltage drops across the conductors is

$$\begin{bmatrix} E_{Aa} \\ E_{Bb} \\ E_{Cc} \\ 0 \\ 0 \\ \vdots \\ 0 \end{bmatrix} = (\mathbf{R} + j\omega\mathbf{L}) \begin{bmatrix} I_a \\ I_b \\ I_c \\ I_{n1} \\ \vdots \\ I_{nN} \end{bmatrix} \tag{4.7.8}$$

where **L** is given by (4.7.7) and **R** is a $(3 + N) \times (3 + N)$ matrix of conductor resistances.

$$\mathbf{R} = \begin{bmatrix} (\mathrm{R}_a+\mathrm{R}_{k'})\mathrm{R}_{k'}\ldots & & \mathrm{R}_{k'} \\ \mathrm{R}_{k'}(\mathrm{R}_b+\mathrm{R}_{k'})\mathrm{R}_{k'}\cdots & & \vdots \\ (\mathrm{R}_c+\mathrm{R}_{k'})\mathrm{R}_{k'}\cdots & & \\ (\mathrm{R}_{n1}+\mathrm{R}_{k'})\mathrm{R}_{k'}\cdots & & \\ \ddots & & \\ \mathrm{R}_{k'} & & (R_{nN}+R_{K'}) \end{bmatrix} \Omega/\mathrm{m} \tag{4.7.9}$$

The resistance matrix of (4.7.9) includes the resistance R_k of each overhead conductor and a mutual resistance $R_{k'}$ due to the image conductors. R_k of each overhead conductor is obtained from conductor tables such as Appendix Table A.3 or A.4, for a specified frequency, temperature, and current. $R_{k'}$ of all the image conductors is the same, as given by (4.7.3).

Copyright 2017 Cengage Learning. All Rights Reserved. May not be copied, scanned, or duplicated, in whole or in part. Due to electronic rights, some third party content may be suppressed from the eBook and/or eChapter(s). Editorial review has deemed that any suppressed content does not materially affect the overall learning experience. Cengage Learning reserves the right to remove additional content at any time if subsequent rights restrictions require it.

Our objective now is to reduce the $(3 + N)$ equations in (4.7.8) to three equations, thereby obtaining the simplified circuit representations shown in Figure 4.17(b). We partition (4.7.8) as follows:

$$\left[\begin{array}{c} E_{Aa}\\ E_{Bb}\\ E_{Cc}\\ \hdashline 0\\ \cdots\\ 0 \end{array}\right]
\left[\;\overbrace{\underbrace{\begin{array}{ccc} Z_{11} & Z_{12} & Z_{13}\\ Z_{21} & Z_{22} & Z_{23}\\ Z_{31} & Z_{32} & Z_{33}\\ \hdashline Z_{41} & Z_{42} & Z_{43}\\ & & \\ Z_{(3+N)1} & Z_{(3+N)2} & Z_{(3+N)3} \end{array}}_{Z_C}}^{Z_A}
\;\vdots\;
\overbrace{\underbrace{\begin{array}{ccc} Z_{14} & \cdots & Z_{1(3+N)}\\ Z_{24} & \cdots & Z_{2(3+N)}\\ Z_{34} & \cdots & Z_{3(3+N)}\\ \hdashline Z_{44} & \cdots & Z_{4(3+N)}\\ & & \\ Z_{(3+N)4} & \cdots & Z_{(3+N)(3+N)} \end{array}}_{Z_D}}^{Z_B}\;\right]
\left[\begin{array}{c} I_a\\ I_b\\ I_c\\ \hdashline I_{n1}\\ I_{nN}\\ \vdots \end{array}\right] \tag{4.7.10}$$

The diagonal elements of this matrix are

$$Z_{kk} = \text{R}_k + \text{R}_{k'} + j\omega 2 \times 10^{-7} \ln \frac{\text{D}_{kk'}}{\text{D}_{kk}} \quad \Omega/\text{m} \tag{4.7.11}$$

And the off-diagonal elements, for $k \neq m$, are

$$Z_{km} = \text{R}_{k'} + j\omega 2 \times 10^{-7} \ln \frac{\text{D}_{km'}}{\text{D}_{km}} \quad \Omega/\text{m} \tag{4.7.12}$$

Next, (4.7.10) is partitioned as shown above to obtain

$$\left[\begin{array}{c} \boldsymbol{E}_{\text{P}}\\ \hline 0 \end{array}\right] = \left[\begin{array}{c|c} \boldsymbol{Z}_A & \boldsymbol{Z}_B\\ \hline \boldsymbol{Z}_C & \boldsymbol{Z}_D \end{array}\right] \left[\begin{array}{c} \boldsymbol{I}_{\text{P}}\\ \hline \boldsymbol{I}_n \end{array}\right] \tag{4.7.13}$$

where

$$\boldsymbol{E}_{\text{P}} = \begin{bmatrix} E_{Aa}\\ E_{Bb}\\ E_{Cc} \end{bmatrix}; \quad \boldsymbol{I}_{\text{P}} = \begin{bmatrix} I_a\\ I_b\\ I_c \end{bmatrix}; \quad \boldsymbol{I}_n = \begin{bmatrix} I_{n1}\\ \vdots\\ I_{nN} \end{bmatrix}$$

$\boldsymbol{E}_{\text{P}}$ is the three-dimensional vector of voltage drops across the phase conductors (including the neutral voltage drop), $\boldsymbol{I}_{\text{P}}$ is the three-dimensional vector of phase currents and $\boldsymbol{I}_n$ is the N vector of neutral currents. Also, the $(3 + N) \times (3 + N)$ matrix in (4.7.10) is partitioned to obtain the following matrices:

$\boldsymbol{Z}_A$ with dimension 3×3

$\boldsymbol{Z}_B$ with dimension $3 \times N$

$\boldsymbol{Z}_C$ with dimension $N \times 3$

$\boldsymbol{Z}_D$ with dimension $N \times N$

Copyright 2017 Cengage Learning. All Rights Reserved. May not be copied, scanned, or duplicated, in whole or in part. Due to electronic rights, some third party content may be suppressed from the eBook and/or eChapter(s). Editorial review has deemed that any suppressed content does not materially affect the overall learning experience. Cengage Learning reserves the right to remove additional content at any time if subsequent rights restrictions require it.

Equation (4.7.13) is rewritten as two separate matrix equations:

$$\boldsymbol{E}_{\mathrm{P}} = \boldsymbol{Z}_A\boldsymbol{I}_{\mathrm{P}} + \boldsymbol{Z}_B\boldsymbol{I}_n \tag{4.7.14}$$

$$\boldsymbol{0} = \boldsymbol{Z}_C\boldsymbol{I}_{\mathrm{P}} + \boldsymbol{Z}_D\boldsymbol{I}_n \tag{4.7.15}$$

Solving (4.7.15) for $\boldsymbol{I}_n$,

$$\boldsymbol{I}_n = -\boldsymbol{Z}_D^{-1}\boldsymbol{Z}_C\,\boldsymbol{I}_{\mathrm{P}} \tag{4.7.16}$$

Using (4.7.16) in (4.7.14),

$$\boldsymbol{E}_{\mathrm{P}} = [\boldsymbol{Z}_A - \boldsymbol{Z}_B\boldsymbol{Z}_D^{-1}\boldsymbol{Z}_C]\boldsymbol{I}_{\mathrm{P}} \tag{4.7.17}$$

or

$$\boldsymbol{E}_{\mathrm{P}} = \boldsymbol{Z}_{\mathrm{P}}\boldsymbol{I}_{\mathrm{P}} \tag{4.7.18}$$

where

$$\boldsymbol{Z}_{\mathrm{P}} = [\boldsymbol{Z}_A - \boldsymbol{Z}_B\boldsymbol{Z}_D^{-1}\boldsymbol{Z}_C] \tag{4.7.19}$$

Equation (4.7.17), the desired result, relates the phase-conductor voltage drops (including neutral voltage drop) to the phase currents. $\boldsymbol{Z}_{\mathrm{P}}$ given by (4.7.19) is the 3 × 3 series-phase impedance matrix, whose elements are denoted

$$\boldsymbol{Z}_{\mathrm{p}} = \begin{bmatrix} Z_{aa\mathrm{eq}} & Z_{ab\mathrm{eq}} & Z_{ac\mathrm{eq}} \\ Z_{ab\mathrm{eq}} & Z_{bb\mathrm{eq}} & Z_{bc\mathrm{eq}} \\ Z_{ac\mathrm{eq}} & Z_{bc\mathrm{eq}} & Z_{cc\mathrm{eq}} \end{bmatrix} \quad \Omega/\mathrm{m} \tag{4.7.20}$$

If the line is completely transposed, the diagonal and off-diagonal elements are averaged to obtain

$$\hat{\boldsymbol{Z}}_{\mathrm{P}} = \begin{bmatrix} \hat{Z}_{aa\mathrm{eq}} & \hat{Z}_{ab\mathrm{eq}} & \hat{Z}_{ab\mathrm{eq}} \\ \hat{Z}_{ab\mathrm{eq}} & \hat{Z}_{aa\mathrm{eq}} & \hat{Z}_{ab\mathrm{eq}} \\ \hat{Z}_{ab\mathrm{eq}} & \hat{Z}_{ab\mathrm{eq}} & \hat{Z}_{aa\mathrm{eq}} \end{bmatrix} \quad \Omega/\mathrm{m} \tag{4.7.21}$$

where

$$\hat{Z}_{aa\mathrm{eq}} = \tfrac{1}{3}(Z_{aa\mathrm{eq}} + Z_{bb\mathrm{eq}} + Z_{cc\mathrm{eq}}) \tag{4.7.22}$$

$$\hat{Z}_{ab\mathrm{eq}} = \tfrac{1}{3}(Z_{ab\mathrm{eq}} + Z_{ac\mathrm{eq}} + Z_{bc\mathrm{eq}}) \tag{4.7.23}$$

4.8 ELECTRIC FIELD AND VOLTAGE: SOLID CYLINDRICAL CONDUCTOR

The capacitance between conductors in a medium with constant permittivity ε can be obtained by determining the following properties.

Copyright 2017 Cengage Learning. All Rights Reserved. May not be copied, scanned, or duplicated, in whole or in part. Due to electronic rights, some third party content may be suppressed from the eBook and/or eChapter(s). Editorial review has deemed that any suppressed content does not materially affect the overall learning experience. Cengage Learning reserves the right to remove additional content at any time if subsequent rights restrictions require it.

1. Electric field strength E, from Gauss's law
2. Voltage between conductors
3. Capacitance from charge per unit volt ($C = q/V$)

As a step toward computing capacitances of general conductor configurations, first compute the electric field of a uniformly charged, solid cylindrical conductor and the voltage between two points outside the conductor. Also compute the voltage between two conductors in an array of charged conductors.

Gauss's law states that the total electric flux leaving a closed surface equals the total charge within the volume enclosed by the surface. That is, the normal component of electric flux density integrated over a closed surface equals the charge enclosed:

$$\oiint D_{\perp}\, ds = \oiint \varepsilon E_{\perp}\, ds = Q_{\text{enclosed}} \tag{4.8.1}$$

where $D_{\perp}$ denotes the normal component of electric flux density, $E_{\perp}$ denotes the normal component of electric field strength, and ds denotes the differential surface area. From Gauss's law, electric charge is a source of electric fields. Electric field lines originate from positive charges and terminate at negative charges.

Figure 4.18 shows a solid cylindrical conductor with radius r and with charge q coulombs per meter (assumed positive in the figure), uniformly distributed on the conductor surface. For simplicity, assume that the conductor is (1) sufficiently long that end effects are negligible, and (2) a perfect conductor (that is, zero resistivity, $\rho = 0$).

Inside the perfect conductor, Ohm's law gives $E_{\text{int}} = \rho J = 0$. That is, the internal electric field E_{int} is zero. To determine the electric field outside the conductor, select the cylinder with radius $x > r$ and with 1-meter length, shown in Figure 4.18, as the closed surface for Gauss's law. Due to the uniform charge distribution, the

FIGURE 4.18

Perfectly conducting solid cylindrical conductor with uniform charge distribution

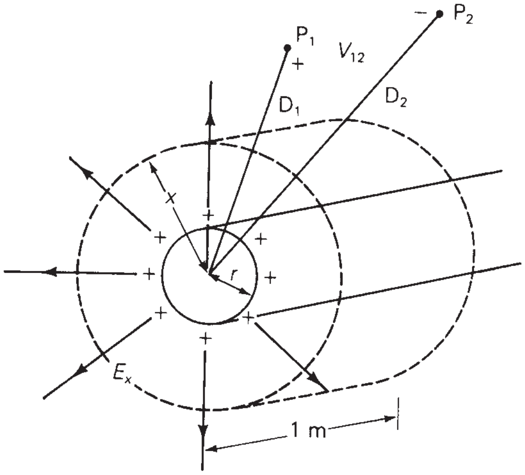

Copyright 2017 Cengage Learning. All Rights Reserved. May not be copied, scanned, or duplicated, in whole or in part. Due to electronic rights, some third party content may be suppressed from the eBook and/or eChapter(s). Editorial review has deemed that any suppressed content does not materially affect the overall learning experience. Cengage Learning reserves the right to remove additional content at any time if subsequent rights restrictions require it.

electric field strength E_x is constant on the cylinder. Also, there is no tangential component of E_x, so the electric field is radial to the conductor. Then, integration of (4.8.1) yields

$$\varepsilon E_x(2\pi x)(1) = q(1)$$

$$E_x = \frac{q}{2\pi\varepsilon x} \quad \text{V/m} \tag{4.8.2}$$

where, for a conductor in free space, $\varepsilon = \varepsilon_0 = 8.854 \times 10^{-12}$ F/m.

A plot of the electric field lines is also shown in Figure 4.18. The direction of the field lines, denoted by the arrows, is from the positive charges where the field originates, to the negative charges, which in this case are at infinity. If the charge on the conductor surface were negative, then the direction of the field lines would be reversed.

Concentric cylinders surrounding the conductor are constant potential surfaces. The potential difference between two concentric cylinders at distances D_1 and D_2 from the conductor center is

$$V_{12} = \int_{D_1}^{D_2} E_x dx \tag{4.8.3}$$

Using (4.8.2) in (4.8.1),

$$V_{12} = \int_{D_1}^{D_2} \frac{q}{2\pi\varepsilon x} dx = \frac{q}{2\pi\varepsilon} \ln\frac{D_2}{D_1} \quad \text{volts} \tag{4.8.4}$$

Equation (4.8.4) gives the voltage V_{12} between two points, P_1 and P_2, at distances D_1 and D_2 from the conductor center, as shown in Figure 4.18. Also, in accordance with the notation, V_{12} is the voltage at P_1 with respect to P_2. If q is positive and D_2 is greater than D_1, as shown in the figure, then V_{12} is positive; that is, P_1 is at a higher potential than P_2. Equation (4.8.4) is also valid for either dc or ac. For ac, V_{12} is a phasor voltage and q is a phasor representation of a sinusoidal charge.

Now apply (4.8.4) to the array of M solid cylindrical conductors shown in Figure 4.19. Assume that each conductor m has an ac charge q_m C/m uniformly

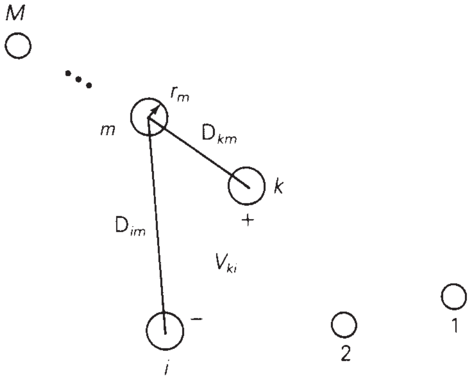

FIGURE 4.19

Array of *M* solid cylindrical conductors

Copyright 2017 Cengage Learning. All Rights Reserved. May not be copied, scanned, or duplicated, in whole or in part. Due to electronic rights, some third party content may be suppressed from the eBook and/or eChapter(s). Editorial review has deemed that any suppressed content does not materially affect the overall learning experience. Cengage Learning reserves the right to remove additional content at any time if subsequent rights restrictions require it.

distributed along the conductor. The voltage V_{ki} between conductors k and i due to the charge q_m acting alone is

$$V_{ki} = \frac{q_m}{2\pi\varepsilon} \ln \frac{\mathrm{D}_{im}}{\mathrm{D}_{km}} \quad \text{volts} \tag{4.8.5}$$

where $\mathrm{D}_{mm} = r_m$ when $k = m$ or $i = m$. In (4.8.5), neglected is the distortion of the electric field in the vicinity of the other conductors, caused by the fact that the other conductors themselves are constant potential surfaces. V_{kim} can be thought of as the voltage between cylinders with radii D_{km} and D_{im} concentric to conductor m at points on the cylinders remote from conductors, where there is no distortion.

Using superposition, the voltage V_{ki} between conductors k and i due to all the changes is

$$V_{ki} = \frac{1}{2\pi\varepsilon} \sum_{m=1}^{M} q_m \ln \frac{\mathrm{D}_{im}}{\mathrm{D}_{km}} \quad \text{volts} \tag{4.8.6}$$

4.9 CAPACITANCE: SINGLE-PHASE TWO-WIRE LINE AND THREE-PHASE THREE-WIRE LINE WITH EQUAL PHASE SPACING

The results of the previous section are used here to determine the capacitances of the two relatively simple transmission lines considered in Section 4.5, a single-phase two-wire line and a three-phase three-wire line with equal phase spacing.

First consider the single-phase two-wire line shown in Figure 4.9. Assume that the conductors are energized by a voltage source such that conductor x has a uniform charge q C/m and, assuming conservation of charge, conductor y has an equal quantity of negative charge $-q$. Using (4.8.6) with $k = x$, $i = y$, and $m = x, y$,

$$\begin{aligned} V_{xy} &= \frac{1}{2\pi\varepsilon}\left[q \ln \frac{\mathrm{D}_{yx}}{\mathrm{D}_{xx}} - q \ln \frac{\mathrm{D}_{yy}}{\mathrm{D}_{xy}}\right] \\ &= \frac{q}{2\pi\varepsilon} \ln \frac{\mathrm{D}_{yx}\mathrm{D}_{xy}}{\mathrm{D}_{xx}\mathrm{D}_{yy}} \end{aligned} \tag{4.9.1}$$

Using $\mathrm{D}_{xy} = \mathrm{D}_{yx} = \mathrm{D}$, $\mathrm{D}_{xx} = r_x$, and $\mathrm{D}_{yy} = r_y$, (4.9.1) becomes

$$V_{xy} = \frac{q}{\pi\varepsilon} \ln \frac{\mathrm{D}}{\sqrt{r_x r_y}} \quad \text{volts} \tag{4.9.2}$$

For a 1-meter line length, the capacitance between conductors is

$$\mathrm{C}_{xy} = \frac{q}{V_{xy}} = \frac{\pi\varepsilon}{\ln\left(\dfrac{\mathrm{D}}{\sqrt{r_x r_y}}\right)} \quad \text{F/m line-to-line} \tag{4.9.3}$$

Copyright 2017 Cengage Learning. All Rights Reserved. May not be copied, scanned, or duplicated, in whole or in part. Due to electronic rights, some third party content may be suppressed from the eBook and/or eChapter(s). Editorial review has deemed that any suppressed content does not materially affect the overall learning experience. Cengage Learning reserves the right to remove additional content at any time if subsequent rights restrictions require it.

and if $r_x = r_y = r$,

$$C_{xy} = \frac{\pi\varepsilon}{\ln(D/r)} \quad \text{F/m line-to-line} \tag{4.9.4}$$

If the two-wire line is supplied by a transformer with a grounded center tap, then the voltage between each conductor and ground is one-half that given by (4.9.2). That is,

$$V_{xn} = V_{yn} = \frac{V_{xy}}{2} \tag{4.9.5}$$

and the capacitance from either line to the grounded neutral is

$$\begin{aligned} C_n = C_{xn} = C_{yn} &= \frac{q}{V_{xn}} = 2C_{xy} \\ &= \frac{2\pi\varepsilon}{\ln(D/r)} \quad \text{F/m line-to-neutral} \end{aligned} \tag{4.9.6}$$

Circuit representations of the line-to-line and line-to-neutral capacitances are shown in Figure 4.20. Note that if the neutral is open in Figure 4.20(b), the two line-to-neutral capacitances combine in series to give the line-to-line capacitance.

Next consider the three-phase line with equal phase spacing shown in Figure 4.10. Neglect the effect of earth and neutral conductors here. To determine the positive-sequence capacitance, assume positive-sequence charges q_a, q_b, q_c such that $q_a + q_b + q_c = 0$. Using (4.8.6) with $k = a$, $i = b$, and $m = a, b, c$, the voltage V_{ab} between conductors a and b is

$$V_{ab} = \frac{1}{2\pi\varepsilon}\left[q_a \ln\frac{D_{ba}}{D_{aa}} + q_b \ln\frac{D_{bb}}{D_{ab}} + q_c \ln\frac{D_{bc}}{D_{ac}}\right] \tag{4.9.7}$$

Using $D_{aa} = D_{bb} = r$, and $D_{ab} = D_{ba} = D_{ca} = D_{cb} = D$, (4.9.7) becomes

$$\begin{aligned} V_{ab} &= \frac{1}{2\pi\varepsilon}\left[q_a \ln\frac{D}{r} + q_b \ln\frac{r}{D} + q_c \ln\frac{D}{D}\right] \\ &= \frac{1}{2\pi\varepsilon}\left[q_a \ln\frac{D}{r} + q_b \ln\frac{r}{D}\right] \quad \text{volts} \end{aligned} \tag{4.9.8}$$

Note that the third term in (4.9.8) is zero because conductors a and b are equidistant from conductor c. Thus, conductors a and b lie on a constant potential cylinder for the electric field due to q_c.

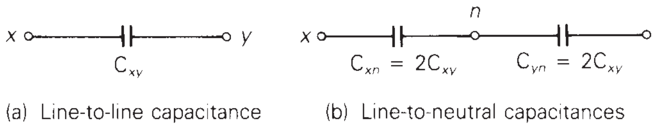
x
y
C_{xy}
(a) Line-to-line capacitance
x
n
y
$C_{xn} = 2C_{xy}$
$C_{yn} = 2C_{xy}$
(b) Line-to-neutral capacitances

FIGURE 4.20

Circuit representation of capacitances for a single-phase two-wire line

Copyright 2017 Cengage Learning. All Rights Reserved. May not be copied, scanned, or duplicated, in whole or in part. Due to electronic rights, some third party content may be suppressed from the eBook and/or eChapter(s). Editorial review has deemed that any suppressed content does not materially affect the overall learning experience. Cengage Learning reserves the right to remove additional content at any time if subsequent rights restrictions require it.

Similarly, using (4.8.6) with $k = a$, $i = c$, and $m = a,b,c$, the voltage V_{ac} is

$$\begin{aligned} V_{ab} &= \frac{1}{2\pi\varepsilon}\left[q_a \ln\frac{D_{ca}}{D_{aa}} + q_b \ln\frac{D_{cb}}{D_{ab}} + q_c \ln\frac{D_{cc}}{D_{ac}}\right] \\ &= \frac{1}{2\pi\varepsilon}\left[q_a \ln\frac{D}{r} + q_b \ln\frac{D}{D} + q_c \ln\frac{r}{D}\right] \\ &= \frac{1}{2\pi\varepsilon}\left[q_a \ln\frac{D}{r} + q_c \ln\frac{r}{D}\right] \quad \text{volts} \end{aligned} \tag{4.9.9}$$

Recall that for balanced positive-sequence voltages,

$$V_{ab} = \sqrt{3}V_{an}\underline{/+30^\circ} = \sqrt{3}V_{an}\left[\frac{\sqrt{3}}{2} + j\frac{1}{2}\right] \tag{4.9.10}$$

$$V_{ac} = -V_{ca} = \sqrt{3}V_{an}\underline{/-30^\circ} = \sqrt{3}V_{an}\left[\frac{\sqrt{3}}{2} - j\frac{1}{2}\right] \tag{4.9.11}$$

Adding (4.9.10) and (4.9.11) yields

$$V_{ab} + V_{ac} = 3V_{an} \tag{4.9.12}$$

Using (4.9.8) and (4.9.9) in (4.9.12),

$$V_{an} = \frac{1}{3}\left(\frac{1}{2\pi\varepsilon}\right)\left[2q_a \ln\frac{D}{r} + (q_b + q_c)\ln\frac{r}{D}\right] \tag{4.9.13}$$

and with $q_b + q_c = -q_a$,

$$V_{an} = \frac{1}{2\pi\varepsilon} q_a \ln\frac{D}{r} \quad \text{volts} \tag{4.9.14}$$

The capacitance-to-neutral per line length is

$$C_{an} = \frac{q_a}{V_{an}} = \frac{2\pi\varepsilon}{\ln\left(\dfrac{D}{r}\right)} \quad \text{F/m line-to-neutral} \tag{4.9.15}$$

Due to symmetry, the same result is obtained for $C_{bn} = qb/V_{bn}$ and $C_{cn} = qc/V_{cn}$. For balanced three-phase operation, however, only one phase need be considered. A circuit representation of the capacitance-to-neutral is shown in Figure 4.21.

FIGURE 4.21

Circuit representation of the capacitance-to-neutral of a three-phase line with equal phase spacing

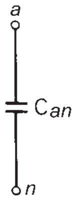

4.10 CAPACITANCE: STRANDED CONDUCTORS, UNEQUAL PHASE SPACING, BUNDLED CONDUCTORS

Equations (4.9.6) and (4.9.15) are based on the assumption that the conductors are solid cylindrical conductors with zero resistivity. The electric field inside these conductors is zero, and the external electric field is perpendicular to the conductor surfaces. Practical conductors with resistivities similar to those listed in Table 4.3 have a small

Copyright 2017 Cengage Learning. All Rights Reserved. May not be copied, scanned, or duplicated, in whole or in part. Due to electronic rights, some third party content may be suppressed from the eBook and/or eChapter(s). Editorial review has deemed that any suppressed content does not materially affect the overall learning experience. Cengage Learning reserves the right to remove additional content at any time if subsequent rights restrictions require it.

internal electric field. As a result, the external electric field is slightly altered near the conductor surfaces. Also, the electric field near the surface of a stranded conductor is not the same as that of a solid cylindrical conductor. However, it is normal practice when calculating line capacitance to replace a stranded conductor by a perfectly conducting solid cylindrical conductor whose radius equals the outside radius of the stranded conductor. The resulting error in capacitance is small, since only the electric field near the conductor surfaces is affected.

Also, (4.8.2) is based on the assumption that there is uniform charge distribution. But conductor charge distribution is nonuniform in the presence of other charged conductors. Therefore (4.9.6) and (4.9.15), which are derived from (4.8.2), are not exact. However, the nonuniformity of conductor charge distribution can be shown to have a negligible effect on line capacitance.

For three-phase lines with unequal phase spacing, balanced positive-sequence voltages are not obtained with balanced positive-sequence charges. Instead, unbalanced line-to-neutral voltages occur, and the phase-to-neutral capacitances are unequal. Balance can be restored by transposing the line such that each phase occupies each position for one-third of the line length. If equations similar to (4.9.7) for V_{ab} as well as for V_{ac} are written for each position in the transposition cycle, and are then averaged and used in (4.9.12) through (4.9.14), the resulting capacitance becomes

$$C_{an} = \frac{2\pi\varepsilon}{\ln(D_{eq}/r)} \quad \text{F/m} \tag{4.10.1}$$

where

$$D_{eq} = \sqrt[3]{D_{ab}D_{bc}D_{ac}} \tag{4.10.2}$$

Figure 4.22 shows a bundled conductor line with two conductors per bundle. To determine the capacitance of this line, assume balanced positive-sequence charges q_a, q_b, q_c for each phase such that $q_a + q_b + q_c = 0$. Assume that the conductors in each bundle, which are in parallel, share the charges equally. Thus conductors a and a' each have the charge $q_a/2$. Also assume that the phase spacings are much larger than the bundle spacings so that D_{ab} may be used instead of $(D_{ab} - d)$ or $(D_{ab} + d)$. Then, using (4.8.6) with $k = a$, $i = b$, $m = a, a', b, b', c, c'$,

$$\begin{aligned} V_{ab} &= \frac{1}{2\pi\varepsilon}\left[\frac{q_a}{2}\ln\frac{D_{ba}}{D_{aa}} + \frac{q_a}{2}\ln\frac{D_{ba'}}{D_{aa'}} + \frac{q_b}{2}\ln\frac{D_{bb}}{D_{ab}} \right.\\ &\qquad \left. + \frac{q_b}{2}\ln\frac{D_{bb'}}{D_{ab'}} + \frac{q_c}{2}\ln\frac{D_{bc}}{D_{ac}} + \frac{q_c}{2}\ln\frac{D_{bc'}}{D_{ac'}}\right] \\ &= \frac{1}{2\pi\varepsilon}\left[\frac{q_a}{2}\left(\ln\frac{D_{ab}}{r} + \ln\frac{D_{ab}}{d}\right) + \frac{q_b}{2}\left(\ln\frac{r}{D_{ab}} + \ln\frac{d}{D_{ab}}\right)\right. \\ &\qquad \left. + \frac{q_c}{2}\left(\ln\frac{D_{bc}}{D_{ac}} + \ln\frac{D_{bc}}{D_{ac}}\right)\right] \\ &= \frac{1}{2\pi\varepsilon}\left[q_a\ln\frac{D_{ab}}{\sqrt{rd}} + q_b\ln\frac{\sqrt{rd}}{D_{ab}} + q_c\ln\frac{D_{bc}}{D_{ac}}\right] \end{aligned} \tag{4.10.3}$$

Copyright 2017 Cengage Learning. All Rights Reserved. May not be copied, scanned, or duplicated, in whole or in part. Due to electronic rights, some third party content may be suppressed from the eBook and/or eChapter(s). Editorial review has deemed that any suppressed content does not materially affect the overall learning experience. Cengage Learning reserves the right to remove additional content at any time if subsequent rights restrictions require it.

FIGURE 4.22

Three-phase line with two conductors per bundle

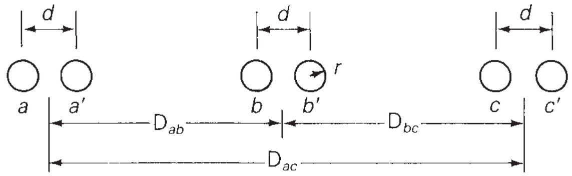

Equation (4.10.3) is the same as (4.9.7), except that D_{aa} and D_{bb}, in (4.9.7) are replaced by $\sqrt{rd}$ in this equation. Therefore, for a transposed line, derivation of the capacitance would yield

$$C_{an} = \frac{2\pi\varepsilon}{\ln(D_{eq}/D_{SC})} \quad \text{F/m} \tag{4.10.4}$$

where

$$D_{SC} = \sqrt{rd} \quad \text{for a two-conductor bundle} \tag{4.10.5}$$

Similarly,

$$D_{SC} = \sqrt[3]{rd^2} \quad \text{for a three-conductor bundle} \tag{4.10.6}$$

$$D_{SC} = 1.091\sqrt[4]{rd^3} \quad \text{for a four-conductor bundle} \tag{4.10.7}$$

Equation (4.10.4) for capacitance is analogous to (4.6.22) for inductance. In both cases D_{eq}, given by (4.6.17) or (4.10.2), is the geometric mean of the distances between phases. Also, (4.10.5)–(4.10.7) for D_{SC} are analogous to (4.6.19)−(4.6.21) for D_{SL}, except that the conductor outside radius r replaces the conductor GMR D_S.

The current supplied to the transmission-line capacitance is called *charging current*. For a single-phase circuit operating at line-to-line voltage $V_{xy} = V_{xy}\underline{/0°}$, the charging current is

$$I_{chg} = Y_{xy}V_{xy} = j\omega C_{xy}V_{xy} \quad \text{A} \tag{4.10.8}$$

As shown in Chapter 2, a capacitor delivers reactive power. From (2.3.5), the reactive power delivered by the line-to-line capacitance is

$$Q_C = \frac{V_{xy}^2}{X_c} = Y_{xy}V_{xy}^2 = \omega C_{xy}V_{xy}^2 \quad \text{var} \tag{4.10.9}$$

For a completely transposed three-phase line that has balanced positive-sequence voltages with $V_{an} = V_{LN}\underline{/0°}$, the phase a charging current is

$$I_{chg} = YV_{an} = j\omega C_{an}V_{LN} \quad \text{A} \tag{4.10.10}$$

and the reactive power delivered by phase a is

$$Q_{C1\phi} = YV_{an}^2 = \omega C_{an}V_{LN}^2 \quad \text{var} \tag{4.10.11}$$

The total reactive power supplied by the three-phase line is

$$Q_{C3\phi} = 3Q_{C1\phi} = 3\omega C_{an}V_{LN}^2 = \omega C_{an}V_{LL}^2 \quad \text{var} \tag{4.10.12}$$

Copyright 2017 Cengage Learning. All Rights Reserved. May not be copied, scanned, or duplicated, in whole or in part. Due to electronic rights, some third party content may be suppressed from the eBook and/or eChapter(s). Editorial review has deemed that any suppressed content does not materially affect the overall learning experience. Cengage Learning reserves the right to remove additional content at any time if subsequent rights restrictions require it.

EXAMPLE 4.6

Capacitance, admittance, and reactive power supplied: single-phase line

For the single-phase line in Example 4.3, determine the line-to-line capacitance in F and the line-to-line admittance in S. If the line voltage is 20 kV, determine the reactive power in kvar supplied by this capacitance.

SOLUTION

From Table A.3, the outside radius of a 4/0 12-strand copper conductor is

$$r = \frac{0.552}{2}\text{ in.} \times \frac{1\text{ ft}}{12\text{ in.}} = 0.023\text{ ft}$$

and from (4.9.4),

$$C_{xy} = \frac{\pi(8.854 \times 10^{-12})}{\ln\left(\dfrac{5}{0.023}\right)} = 5.169 \times 10^{-12} \quad \text{F/m}$$

or

$$C_{xy} = 5.169 \times 10^{-12}\frac{\text{F}}{\text{m}} \times 1609\frac{\text{m}}{\text{mi}} \times 20\text{ mi} = 1.66 \times 10^{-7} \quad \text{F}$$

and the shunt admittance is

$$Y_{xy} = j\omega C_{xy} = j(2\pi 60)(1.66 \times 10^{-7})$$

$$= j6.27 \times 10^{-5} \quad \text{S line-to-line}$$

From (4.10.9),

$$Q_C = (6.27 \times 10^{-5})(20 \times 10^3)^2 = 25.1 \quad \text{kvar}$$

EXAMPLE 4.7

Capacitance and shunt admittance; charging current and reactive power supplied: three-phase line

For the three-phase line in Example 4.5, determine the capacitance-to-neutral in F and the shunt admittance-to-neutral in S. If the line voltage is 345 kV, determine the charging current in kA per phase and the total reactive power in Mvar supplied by the line capacitance. Assume balanced positive-sequence voltages.

SOLUTION

From Table A.4, the outside radius of a 795,000 cmil 26/2 ACSR conductor is

$$r = \frac{1.108}{2}\text{ in.} \times 0.0254\frac{\text{m}}{\text{in.}} = 0.0141 \quad \text{m}$$

(*Continued*)

Copyright 2017 Cengage Learning. All Rights Reserved. May not be copied, scanned, or duplicated, in whole or in part. Due to electronic rights, some third party content may be suppressed from the eBook and/or eChapter(s). Editorial review has deemed that any suppressed content does not materially affect the overall learning experience. Cengage Learning reserves the right to remove additional content at any time if subsequent rights restrictions require it.

From (4.10.5), the equivalent radius of the two-conductor bundle is

$$D_{SC} = \sqrt{(0.0141)(0.40)} = 0.0750 \quad \text{m}$$

$D_{eq} = 12.6$ m is the same as in Example 4.5. Therefore, from (4.10.4),

$$C_{an} = \frac{(2\pi)(8.854 \times 10^{-12})}{\ln\left(\dfrac{12.6}{0.0750}\right)} \frac{\text{F}}{\text{m}} \times 1000 \frac{\text{m}}{\text{km}} \times 200 \text{ km}$$

$$= 2.17 \times 10^{-6} \quad \text{F}$$

The shunt admittance-to-neutral is

$$Y_{an} = j\omega C_{an} = j\,(2\pi 60)(2.17 \times 10^{-6})$$

$$= j8.19 \times 10^{-4} \quad \text{S}$$

From (4.10.10),

$$I_{chg} = |I_{chg}| = (8.19 \times 10^{-4})\left(\frac{345}{\sqrt{3}}\right) = 0.163 \text{ kA/phase}$$

and from (4.10.12),

$$Q_{C3\phi} = (8.19 \times 10^{-4})(345)^2 = 97.5 \quad \text{Mvar}$$

4.11 SHUNT ADMITTANCES: LINES WITH NEUTRAL CONDUCTORS AND EARTH RETURN

This section covers equations suitable for computer calculation of the shunt admittances for the three-phase overhead line shown in Figure 4.16. Approximate the earth's surface as a perfectly conducting horizontal plane, even though the earth under the line may have irregular terrain and resistivities as shown in Table 4.4.

The *method of images* accounts for the effect of the earth plane, described as follows. Consider a single conductor with uniform charge distribution and with height H above a perfectly conducting earth plane, as shown in Figure 4.23(a). When the conductor has a positive charge, an equal quantity of negative charge is induced on the earth. The electric field lines originate from the positive charges on the conductor and terminate at the negative charges on the earth. Also, the electric field lines are perpendicular to the surfaces of the conductor and earth.

Now replace the earth by the image conductor shown in Figure 4.23(b), which has the same radius as the original conductor, lies directly below the original conductor with conductor separation $H_{11} = 2H$, and has an equal quantity of negative charge. The electric field above the dashed line representing the location of the

Copyright 2017 Cengage Learning. All Rights Reserved. May not be copied, scanned, or duplicated, in whole or in part. Due to electronic rights, some third party content may be suppressed from the eBook and/or eChapter(s). Editorial review has deemed that any suppressed content does not materially affect the overall learning experience. Cengage Learning reserves the right to remove additional content at any time if subsequent rights restrictions require it.

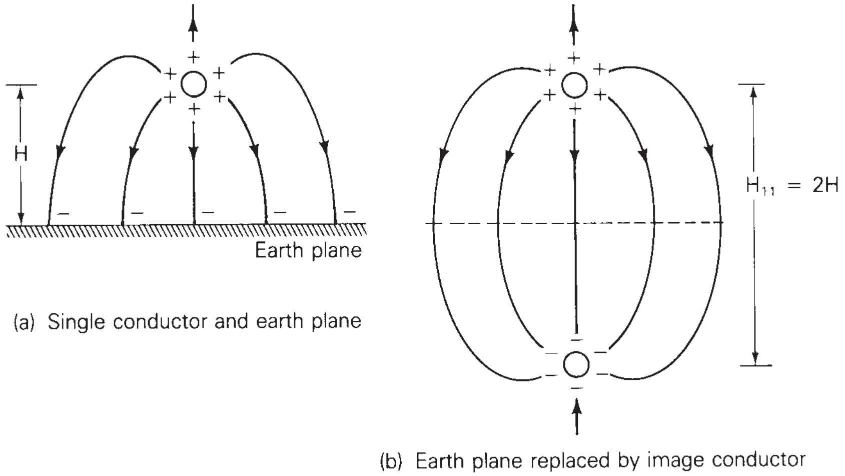

(a) Single conductor and earth plane

(b) Earth plane replaced by image conductor

FIGURE 4.23

Method of images

removed earth plane in Figure 4.23(b) is identical to the electric field above the earth plane in Figure 4.23(a). Therefore, the voltage between any two points above the earth is the same in both figures.

EXAMPLE 4.8

Effect of earth on capacitance: single-phase line

If the single-phase line in Example 4.6 has flat horizontal spacing with 18-ft average line height, determine the effect of the earth on capacitance. Assume a perfectly conducting earth plane.

SOLUTION

The earth plane is replaced by a separate image conductor for each overhead conductor, and the conductors are charged as shown in Figure 4.24. From (4.8.6), the voltage between conductors x and y is

FIGURE 4.24

Single-phase line for Example 4.8

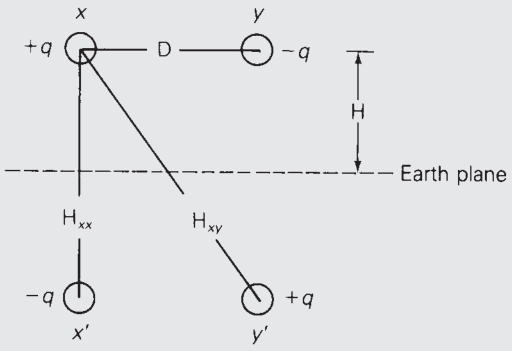

(*Continued*)

Copyright 2017 Cengage Learning. All Rights Reserved. May not be copied, scanned, or duplicated, in whole or in part. Due to electronic rights, some third party content may be suppressed from the eBook and/or eChapter(s). Editorial review has deemed that any suppressed content does not materially affect the overall learning experience. Cengage Learning reserves the right to remove additional content at any time if subsequent rights restrictions require it.

$$V_{xy} = \frac{q}{2\pi\varepsilon}\left[\ln\frac{D_{yx}}{D_{xx}} - \ln\frac{D_{yy}}{D_{xy}} - \ln\frac{H_{yx}}{H_{xx}} + \ln\frac{H_{yy}}{H_{xy}}\right]$$

$$= \frac{q}{2\pi\varepsilon}\left[\ln\frac{D_{yx}D_{xy}}{D_{xx}D_{yy}} - \ln\frac{H_{yx}H_{xy}}{H_{xx}H_{yy}}\right]$$

$$= \frac{q}{\pi\varepsilon}\left[\ln\frac{D}{r} - \ln\frac{H_{xy}}{H_{xx}}\right]$$

The line-to-line capacitance is

$$C_{xy} = \frac{q}{V_{xy}} = \frac{\pi\varepsilon}{\ln\frac{D}{r} - \ln\frac{H_{xy}}{H_{xx}}} \quad \text{F/m}$$

Using $D = 5\,\text{ft}$, $r = 0.023\,\text{ft}$, $H_{xx} = 2H = 36$ ft, and $H_{xy} = \sqrt{(36)^2 + (5)^2} = 36.346$ ft,

$$C_{xy} = \frac{\pi(8.854 \times 10^{-12})}{\ln\frac{5}{0.023} - \ln\frac{36.346}{36}} = 5.178 \times 10^{-12} \quad \text{F/m}$$

compared with 5.169×10^{-12} F/m in Example 4.6. The effect of the earth plane is to slightly increase the capacitance. Note that as the line height H increases, the ratio H_{xy}/H_{xx} approaches 1, $\ln(H_{xy}/H_{xx}) \to 0$, and the effect of the earth becomes negligible.

For the three-phase line with N neutral conductors shown in Figure 4.25, the perfectly conducting earth plane is replaced by a separate image conductor for each overhead conductor. The overhead conductors $a, b, c, n1, n2, \ldots, nN$ carry charges $q_a, q_b, q_c, q_{n1}, \ldots, q_{nN}$, and the image conductors $a', b', c', n1', \ldots, nN'$ carry charges $-q_a, -qb, -qc, -qn_1, \ldots, -q_{nN}$. Applying (4.8.6) to determine the voltage $V_{kk'}$ between any conductor k and its image conductor k',

$$V_{kk'} = \frac{1}{2\pi\varepsilon}\left[\sum_{m=a}^{nN} q_m \ln\frac{H_{km}}{D_{km}} - \sum_{m=a}^{nN} q_m \ln\frac{D_{km}}{H_{km}}\right]$$

$$= \frac{2}{2\pi\varepsilon}\sum_{m=a}^{nN} q_m \ln\frac{H_{km}}{D_{km}} \tag{4.11.1}$$

where $D_{kk} = r_k$ and D_{km} is the distance between overhead conductors k and m. H_{km} is the distance between overhead conductor k and image conductor m. By symmetry, the voltage V_{kn} between conductor k and the earth is one-half of $V_{kk'}$.

$$V_{kn} = \frac{1}{2}V_{kk'} = \frac{1}{2\pi\varepsilon}\sum_{m=a}^{nN} q_m \ln\frac{H_{km}}{D_{km}} \tag{4.11.2}$$

Copyright 2017 Cengage Learning. All Rights Reserved. May not be copied, scanned, or duplicated, in whole or in part. Due to electronic rights, some third party content may be suppressed from the eBook and/or eChapter(s). Editorial review has deemed that any suppressed content does not materially affect the overall learning experience. Cengage Learning reserves the right to remove additional content at any time if subsequent rights restrictions require it.

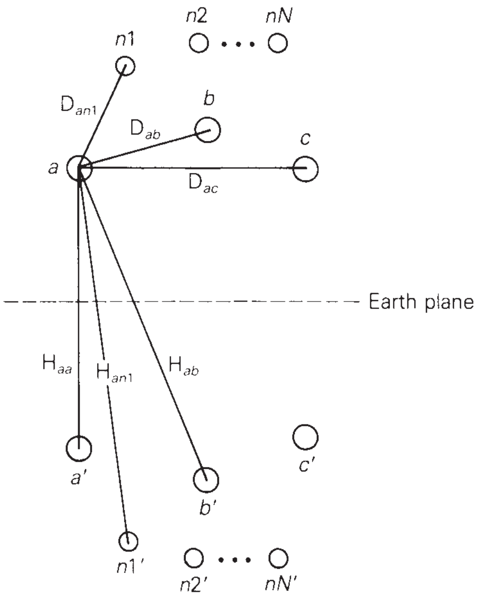

FIGURE 4.25

Three-phase line with neutral conductors and with earth plane replaced by image conductors

where

$$k = a, b, c, n1, n2, \ldots, nN$$
$$m = a, b, c, n1, n2, \ldots, nN$$

Since all the neutral conductors are grounded to the earth.

$$V_{kn} = 0 \qquad \text{for } k = n1, n2, \ldots, nN \tag{4.11.3}$$

In matrix format, (4.11.2) and (4.11.3) are

$$\left[\begin{array}{c} V_{an}\\ V_{bn}\\ V_{cn}\\ \hline 0\\ \vdots\\ 0 \end{array}\right] = \left[\begin{array}{c|c} \overbrace{\begin{matrix} P_{aa} & P_{ab} & P_{ac}\\ P_{ba} & P_{bb} & P_{bc}\\ P_{ca} & P_{cb} & P_{cc} \end{matrix}}^{\mathbf{P}_A} & \overbrace{\begin{matrix} P_{an1} & \cdots & P_{anN}\\ P_{bn1} & \cdots & P_{bnN}\\ P_{cn1} & \cdots & P_{cnN} \end{matrix}}^{\mathbf{P}_B} \\ \hline \underbrace{\begin{matrix} P_{n1a} & P_{n1b} & P_{n1c}\\ \vdots & & \\ P_{nNa} & P_{nNb} & P_{nNc} \end{matrix}}_{\mathbf{P}_C} & \underbrace{\begin{matrix} P_{n1n1} & \cdots & P_{n1nN}\\ & & \\ P_{nNn1} & \cdots & P_{nNnN} \end{matrix}}_{\mathbf{P}_D} \end{array}\right] \left[\begin{array}{c} q_a\\ q_b\\ q_c\\ \hline q_{n1}\\ \vdots\\ q_{nN} \end{array}\right] \tag{4.11.4}$$

The elements of the $(3 + N) \times (3 + N)$ matrix $\mathbf{P}$ are

$$P_{km} = \frac{1}{2\pi\varepsilon} \ln \frac{H_{km}}{D_{km}} \quad \text{m/F} \tag{4.11.5}$$

where

$$k = a, b, c, n1, \ldots, nN$$
$$m = a, b, c, n1, \ldots, nN$$

Copyright 2017 Cengage Learning. All Rights Reserved. May not be copied, scanned, or duplicated, in whole or in part. Due to electronic rights, some third party content may be suppressed from the eBook and/or eChapter(s). Editorial review has deemed that any suppressed content does not materially affect the overall learning experience. Cengage Learning reserves the right to remove additional content at any time if subsequent rights restrictions require it.

Equation (4.11.4) is now partitioned as shown to obtain

$$\left[\begin{array}{c} V_{\mathrm{P}} \\ \hline \mathbf{0} \end{array}\right] = \left[\begin{array}{c|c} \mathbf{P}_A & \mathbf{P}_B \\ \hline \mathbf{P}_C & \mathbf{P}_D \end{array}\right] \left[\begin{array}{c} q_{\mathrm{P}} \\ \hline q_n \end{array}\right] \tag{4.11.6}$$

V_{P} is the three-dimensional vector of phase-to-neutral voltages. q_{P} is the three-dimensional vector of phase-conductor charges and q_n is the N vector of neutral conductor charges. The $(3 + N) \times (3 + N)$**P** matrix is partitioned as shown in (4.11.4) to obtain:

$\mathbf{P}_A$ with dimension 3×3

$\mathbf{P}_B$ with dimension $3 \times N$

$\mathbf{P}_C$ with dimension $N \times 3$

$\mathbf{P}_D$ with dimension $N \times N$

Equation (4.11.6) is rewritten as two separate equations:

$$V_{\mathrm{P}} = \mathbf{P}_A q_{\mathrm{P}} + \mathbf{P}_B q_n \tag{4.11.7}$$

$$\mathbf{0} = \mathbf{P}_C q_P + \mathbf{P}_D q_n \tag{4.11.8}$$

Then (4.11.8) is solved for q_n, which is used in (4.11.7) to obtain

$$V_{\mathrm{P}} = (\mathbf{P}_A - \mathbf{P}_B \mathbf{P}_D^{-1} \mathbf{P}_C) q_{\mathrm{P}} \tag{4.11.9}$$

or

$$q_{\mathrm{P}} = \mathbf{C}_{\mathrm{P}} \mathbf{V}_{\mathrm{P}} \tag{4.11.10}$$

where

$$\mathbf{C}_{\mathrm{P}} = (\mathbf{P}_A - \mathbf{P}_B \mathbf{P}_D^{-1} \mathbf{P}_C)^{-1} \quad \mathrm{F/m} \tag{4.11.11}$$

Equation (4.11.10), the desired result, relates the phase-conductor charges to the phase-to-neutral voltages. $\mathbf{C}_{\mathrm{P}}$ is the 3×3 matrix of phase capacitances whose elements are denoted

$$\mathbf{C}_{\mathrm{P}} = \begin{bmatrix} C_{aa} & C_{ab} & C_{ac} \\ C_{ab} & C_{bb} & C_{bc} \\ C_{ac} & C_{bc} & C_{cc} \end{bmatrix} \quad \mathrm{F/m} \tag{4.11.12}$$

It can be shown that $\mathbf{C}_{\mathrm{P}}$ is a symmetric matrix whose diagonal terms C_{aa}, C_{bb}, C_{cc} are positive, and whose off-diagonal terms C_{ab}, C_{bc}, C_{ac} are negative. This indicates that when a positive line-to-neutral voltage is applied to one phase, a positive charge is induced on that phase and negative charges are induced on the other phases, which is physically correct.

If the line is completely transposed, the diagonal and off-diagonal elements of $\mathbf{C}_{\mathrm{P}}$ are averaged to obtain

Copyright 2017 Cengage Learning. All Rights Reserved. May not be copied, scanned, or duplicated, in whole or in part. Due to electronic rights, some third party content may be suppressed from the eBook and/or eChapter(s). Editorial review has deemed that any suppressed content does not materially affect the overall learning experience. Cengage Learning reserves the right to remove additional content at any time if subsequent rights restrictions require it.

$$\hat{\mathbf{C}}_{\mathrm{P}} = \begin{bmatrix} \hat{C}_{aa} & \hat{C}_{ab} & \hat{C}_{ab} \\ \hat{C}_{ab} & \hat{C}_{aa} & \hat{C}_{ab} \\ \hat{C}_{ab} & \hat{C}_{ab} & \hat{C}_{aa} \end{bmatrix} \quad \mathrm{F/m} \tag{4.11.13}$$

where

$$\hat{C}_{aa} = \tfrac{1}{3}\,(C_{aa} + C_{bb} + C_{cc}) \quad \mathrm{F/m} \tag{4.11.14}$$

$$\hat{C}_{ab} = \tfrac{1}{3}\,(C_{ab} + C_{bc} + C_{ac}) \quad \mathrm{F/m} \tag{4.11.15}$$

$\hat{\mathbf{C}}_{\mathrm{P}}$ is a symmetrical capacitance matrix.

The shunt phase admittance matrix is given by

$$\boldsymbol{Y}_{\mathrm{P}} = j\omega\mathbf{C}_{\mathrm{P}} = j(2\pi f)\mathbf{C}_{\mathrm{P}} \quad \mathrm{S/m} \tag{4.11.16}$$

or, for a completely transposed line,

$$\hat{\boldsymbol{Y}}_{\mathrm{P}} = j\omega\hat{\mathbf{C}}_{\mathrm{P}} = j(2\pi f)\hat{\mathbf{C}}_{\mathrm{P}} \quad \mathrm{S/m} \tag{4.11.17}$$

4.12 ELECTRIC FIELD STRENGTH AT CONDUCTOR SURFACES AND AT GROUND LEVEL

When the electric field strength at a conductor surface exceeds the breakdown strength of air, current discharges occur. This phenomenon, called *corona*, causes additional line losses (corona loss), communications interference, and audible noise. Although breakdown strength depends on many factors, a rough value is 30 kV/cm in a uniform electric field for dry air at atmospheric pressure. The presence of water droplets or rain can lower this value significantly. To control corona, transmission lines are usually designed to maintain calculated values of conductor surface electric field strength below 20 $\mathrm{kV_{rms}}$/cm.

When line capacitances are determined and conductor voltages are known, the conductor charges can be calculated from (4.9.3) for a single-phase line or from (4.11.10) for a three-phase line. Then the electric field strength at the surface of one phase conductor, neglecting the electric fields due to charges on other phase conductors and neutral wires, is, from (4.8.2),

$$E_r = \frac{q}{2\pi\varepsilon r} \quad \mathrm{V/m} \tag{4.12.1}$$

where r is the conductor outside radius.

For bundled conductors with N_b conductors per bundle and with charge q C/m per phase, the charge per conductor is q/N_b and

$$E_{\mathrm{rave}} = \frac{q/N_b}{2\pi\varepsilon r} \quad \mathrm{V/m} \tag{4.12.2}$$

Copyright 2017 Cengage Learning. All Rights Reserved. May not be copied, scanned, or duplicated, in whole or in part. Due to electronic rights, some third party content may be suppressed from the eBook and/or eChapter(s). Editorial review has deemed that any suppressed content does not materially affect the overall learning experience. Cengage Learning reserves the right to remove additional content at any time if subsequent rights restrictions require it.

FIGURE 4.26

Vector addition of electric fields at the surface of one conductor in a bundle

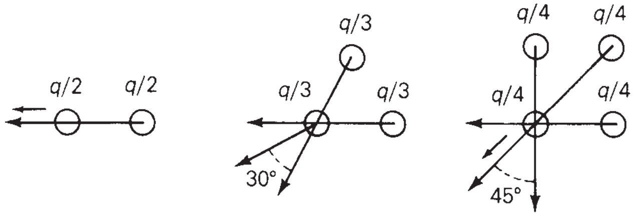

Equation (4.12.2) represents an average value for an individual conductor in a bundle. The maximum electric field strength at the surface of one conductor due to all charges in a bundle, obtained by the vector addition of electric fields (as shown in Figure 4.26), is as follows:

Two-conductor bundle ($N_b = 2$):

$$E_{r\max} = \frac{q/2}{2\pi\varepsilon r} + \frac{q/2}{2\pi\varepsilon d} = \frac{q/2}{2\pi\varepsilon r}\left(1 + \frac{r}{d}\right)$$

$$= E_{\text{rave}}\left(1 + \frac{r}{d}\right) \tag{4.12.3}$$

Three-conductor bundle ($N_b = 3$):

$$E_{r\max} = \frac{q/3}{2\pi\varepsilon}\left(\frac{1}{r} + \frac{2\cos 30°}{d}\right) = E_{\text{rave}}\left(1 + \frac{r\sqrt{3}}{d}\right) \tag{4.12.4}$$

Four-conductor bundle ($N_b = 4$):

$$E_{r\max} = \frac{q/4}{2\pi\epsilon}\left(\frac{1}{r} + \frac{1}{d\sqrt{2}} + \frac{2\cos 45°}{d}\right) = E_{\text{rave}}\left[1 + \frac{r}{d}(2.1213)\right] \tag{4.12.5}$$

Although the electric field strength at ground level is much less than at conductor surfaces where corona occurs, there are still capacitive coupling effects. Charges are induced on ungrounded equipment, such as vehicles with rubber tires located near a line. If a person contacts the vehicle and ground, a discharge current will flow to ground. Transmission-line heights are designed to maintain discharge currents below prescribed levels for any equipment that may be on the right-of-way. Table 4.5 shows examples of maximum ground-level electric field strength.

As shown in Figure 4.27, the ground-level electric field strength due to charged conductor k and its image conductor is perpendicular to the earth plane has a value of

$$E_k(w) = \left(\frac{q_k}{2\pi\varepsilon}\right)\frac{2\cos\theta}{\sqrt{y_k^2 + (w - x_k)^2}}$$

$$= \left(\frac{q_k}{2\pi\varepsilon}\right)\frac{2y_k}{y_k^2 + (w - x_k)^2} \quad \text{V/m} \tag{4.12.6}$$

where (x_k, y_k) are the horizontal and vertical coordinates of conductor k with respect to reference point R, w is the horizontal coordinate of the ground-level point where the electric field strength is to be determined, and q_k is the charge on conductor k.

Copyright 2017 Cengage Learning. All Rights Reserved. May not be copied, scanned, or duplicated, in whole or in part. Due to electronic rights, some third party content may be suppressed from the eBook and/or eChapter(s). Editorial review has deemed that any suppressed content does not materially affect the overall learning experience. Cengage Learning reserves the right to remove additional content at any time if subsequent rights restrictions require it.

Line Voltage (kV_{rms})	Maximum Ground-Level Electric Field Strength (kV_{rms}/m)
23 (1ϕ)	0.01–0.025
23 (3ϕ)	0.01–0.05
115	0.1–0.2
345	2.3–5.0
345 (double circuit)	5.6
500	8.0
765	10.0

TABLE 4.5

Examples of maximum ground-level electric field strength versus transmission-line voltage [1] (©Copyright 1987. Electric Power Research Institute (EPRI), Publication Number EL-2500. *Transmission Line Reference Book, 345-kV and Above, Second Edition, Revised*. Reprinted with permission.)

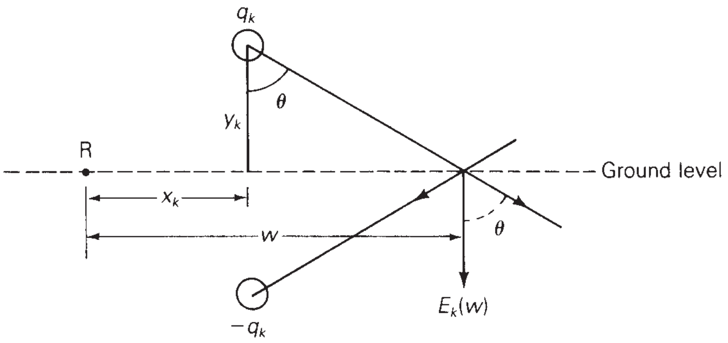

FIGURE 4.27

Ground-level electric field strength due to an overhead conductor and its image

The total ground-level electric field is the phasor sum of terms $E_k(w)$ for all overhead conductors. A lateral profile of ground-level electric field strength is obtained by varying w from the center of the line to the edge of the right-of-way.

EXAMPLE 4.9

Conductor surface and ground-level electric field strengths: single-phase line

For the single-phase line of Example 4.8, calculate the conductor surface electric field strength in kV_{rms}/cm. Also calculate the ground-level electric field in kV_{rms}/m directly under conductor x. The line voltage is 20 kV.

SOLUTION

From Example 4.8, $C_{xy} = 5.178 \times 10^{-12}$ F/m. Using (4.9.3) with $V_{xy} = 20\underline{/0°}$ kV,

$$q_x = -q_y = (5.178 \times 10^{-12})(20 \times 10^3\underline{/0°}) = 1.036 \times 10^{-7}\underline{/0°} \quad \text{C/m}$$

(*Continued*)

Copyright 2017 Cengage Learning. All Rights Reserved. May not be copied, scanned, or duplicated, in whole or in part. Due to electronic rights, some third party content may be suppressed from the eBook and/or eChapter(s). Editorial review has deemed that any suppressed content does not materially affect the overall learning experience. Cengage Learning reserves the right to remove additional content at any time if subsequent rights restrictions require it.

From (4.12.1), the conductor surface electric field strength is, with $r = 0.023$ ft $=$ 0.00701 m,

$$E_r = \frac{1.036 \times 10^{-7}}{(2\pi)(8.854 \times 10^{-12})(0.00701)} \frac{\text{V}}{\text{m}} \times \frac{\text{kV}}{1000\ \text{V}} \times \frac{\text{m}}{100\ \text{cm}}$$

$$= 2.66\ \text{kV}_{\text{rms}}/\text{cm}$$

Selecting the center of the line as the reference point R, the coordinates (x_x, y_x) for conductor x are (-2.5 ft, 18 ft) or (-0.762 m, 5.49 m) and ($+0.762$ m, 5.49 m) for conductor y. The ground-level electric field directly under conductor x, where $w = -0.762$ m, is, from (4.12.6),

$$E(-0.762) = E_x(-0.762) + E_y(-0.762)$$

$$= \frac{1.036 \times 10^{-7}}{(2\pi)(8.85 \times 10^{-12})} \left[\frac{(2)(5.49)}{(5.49)^2} - \frac{(2)(5.49)}{(5.49)^2 + (0.762 + 0.762)^2} \right]$$

$$= 1.862 \times 10^3 (0.364 - 0.338) = 48.5\underline{/0^\circ}\ \text{V/m} = 0.0485\ \text{kV/m}$$

For this 20-kV line, the electric field strengths at the conductor surface and at ground level are low enough to be of relatively small concern. For EHV lines, electric field strengths and the possibility of corona and shock hazard are of more concern.

4.13 PARALLEL CIRCUIT THREE-PHASE LINES

If two parallel three-phase circuits are close together, either on the same tower as in Figure 4.3, or on the same right-of-way, there are mutual inductive and capacitive couplings between the two circuits. When calculating the equivalent series impedance and shunt admittance matrices, these couplings should not be neglected unless the spacing between the circuits is large.

Consider the double-circuit line shown in Figure 4.28. For simplicity, assume that the lines are not transposed. Since both are connected in parallel. they have the same series-voltage drop for each phase. Following the same procedure as in Section 4.7, write $2(6 + N)$ equations similar to (4.7.6) through (4.7.9): six equations for the overhead phase conductors, N equations for the overhead neutral conductors,

FIGURE 4.28

Single-line diagram of a double-circuit line

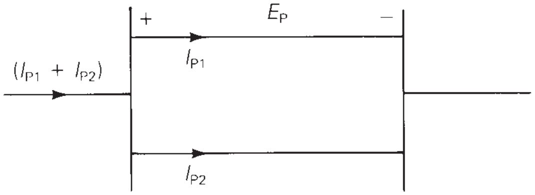

Copyright 2017 Cengage Learning. All Rights Reserved. May not be copied, scanned, or duplicated, in whole or in part. Due to electronic rights, some third party content may be suppressed from the eBook and/or eChapter(s). Editorial review has deemed that any suppressed content does not materially affect the overall learning experience. Cengage Learning reserves the right to remove additional content at any time if subsequent rights restrictions require it.

and (6 + N) equations for the earth return conductors. After lumping the neutral voltage drop into the voltage drops across the phase conductors, and eliminating the neutral and earth return currents, resulting in

$$\begin{bmatrix} \boldsymbol{E}_{\mathrm{P}} \\ \boldsymbol{E}_{\mathrm{P}} \end{bmatrix} = \boldsymbol{Z}_{\mathrm{P}} \begin{bmatrix} \boldsymbol{I}_{\mathrm{P1}} \\ \boldsymbol{I}_{\mathrm{P2}} \end{bmatrix} \tag{4.13.1}$$

where $\boldsymbol{E}_{\mathrm{P}}$ is the vector of phase-conductor voltage drops (including the neutral voltage drop), and $\boldsymbol{I}_{\mathrm{P1}}$ and $\boldsymbol{I}_{\mathrm{P2}}$ are the vectors of phase currents for lines 1 and 2. $\boldsymbol{Z}_{\mathrm{p}}$ is a 6 × 6 impedance matrix. Solving (4.13.1),

$$\left[\begin{array}{c} \boldsymbol{I}_{\mathrm{P1}} \\ \hline \boldsymbol{I}_{\mathrm{P2}} \end{array}\right] = \boldsymbol{Z}_{\mathrm{P}}^{-1} \left[\begin{array}{c} \boldsymbol{E}_{\mathrm{P}} \\ \hline \boldsymbol{E}_{\mathrm{P}} \end{array}\right] = \left[\begin{array}{c|c} \boldsymbol{Y}_A & \boldsymbol{Y}_B \\ \hline \boldsymbol{Y}_C & \boldsymbol{Y}_D \end{array}\right] \left[\begin{array}{c} \boldsymbol{E}_{\mathrm{P}} \\ \hline \boldsymbol{E}_{\mathrm{P}} \end{array}\right] = \begin{bmatrix} (\boldsymbol{Y}_A + \boldsymbol{Y}_B) \\ (\boldsymbol{Y}_C + \boldsymbol{Y}_D) \end{bmatrix} \boldsymbol{E}_{\mathrm{P}} \tag{4.13.2}$$

where $\boldsymbol{Y}_A$, $\boldsymbol{Y}_B$, $\boldsymbol{Y}_C$, and $\boldsymbol{Y}_D$ are obtained by partitioning $\boldsymbol{Z}_{\mathrm{P}}^{-1}$ into four 3 × 3 matrices. Adding $\boldsymbol{I}_{\mathrm{P1}}$ and $\boldsymbol{I}_{\mathrm{P2}}$,

$$(\boldsymbol{I}_{\mathrm{P1}} + \boldsymbol{I}_{\mathrm{P2}}) = (\boldsymbol{Y}_A + \boldsymbol{Y}_B + \boldsymbol{Y}_C + \boldsymbol{Y}_D)\boldsymbol{E}_{\mathrm{P}} \tag{4.13.3}$$

and solving for $\boldsymbol{E}_{\mathrm{P}}$,

$$\boldsymbol{E}_{\mathrm{P}} = \boldsymbol{Z}_{\mathrm{Peq}}(\boldsymbol{I}_{\mathrm{P1}} + \boldsymbol{I}_{\mathrm{P2}}) \tag{4.13.4}$$

where

$$\boldsymbol{Z}_{\mathrm{Peq}} = (\boldsymbol{Y}_A + \boldsymbol{Y}_B + \boldsymbol{Y}_c + \boldsymbol{Y}_D)^{-1} \tag{4.13.5}$$

$\boldsymbol{Z}_{\mathrm{Peq}}$ is the equivalent 3 × 3 series phase impedance matrix of the double-circuit line. Note that in (4.13.5) the matrices $\boldsymbol{Y}_B$ and $\boldsymbol{Y}_C$ account for the inductive coupling between the two circuits.

An analogous procedure can be used to obtain the shunt admittance matrix. Following the ideas of Section 4.11, write (6 + N) equations similar to (4.11.4). After eliminating the neutral wire charges, the result is

$$\left[\begin{array}{c} \boldsymbol{q}_{\mathrm{P1}} \\ \hline \boldsymbol{q}_{\mathrm{P2}} \end{array}\right] = \mathbf{C}_{\mathrm{P}} \left[\begin{array}{c} \boldsymbol{V}_{\mathrm{P}} \\ \hline \boldsymbol{V}_{\mathrm{P}} \end{array}\right] = \left[\begin{array}{c|c} \mathbf{C}_A & \mathbf{C}_B \\ \hline \mathbf{C}_C & \mathbf{C}_D \end{array}\right] \left[\begin{array}{c} \boldsymbol{V}_{\mathrm{P}} \\ \hline \boldsymbol{V}_{\mathrm{P}} \end{array}\right] = \begin{bmatrix} (\mathbf{C}_A + \mathbf{C}_B) \\ (\mathbf{C}_C + \mathbf{C}_D) \end{bmatrix} \boldsymbol{V}_{\mathrm{P}} \tag{4.13.6}$$

where $\boldsymbol{V}_{\mathrm{p}}$ is the vector of phase-to-neutral voltages, and $\boldsymbol{q}_{\mathrm{P1}}$ and $\boldsymbol{q}_{\mathrm{P2}}$ are the vectors of phase-conductor charges for lines 1 and 2. $\mathbf{C}_{\mathrm{p}}$ is a 6 × 6 capacitance matrix that is partitioned into four 3 × 3 matrices $\mathbf{C}_A$, $\mathbf{C}_B$, $\mathbf{C}_C$, and $\mathbf{C}_D$. Adding $\boldsymbol{q}_{\mathrm{P1}}$ and $\boldsymbol{q}_{\mathrm{P2}}$

$$(\boldsymbol{q}_{\mathrm{P1}} + \boldsymbol{q}_{\mathrm{P2}}) = \mathbf{C}_{\mathrm{Peq}}\boldsymbol{V}_{\mathrm{P}} \tag{4.13.7}$$

where

$$\mathbf{C}_{\mathrm{Peq}} = (\mathbf{C}_A + \mathbf{C}_B + \mathbf{C}_C + \mathbf{C}_D) \tag{4.13.8}$$

Also,

$$\boldsymbol{Y}_{\mathrm{Peq}} = j\omega\mathbf{C}_{\mathrm{Peq}} \tag{4.13.9}$$

$\boldsymbol{Y}_{\mathrm{peq}}$ is the equivalent 3 × 3 shunt admittance matrix of the double-circuit line. The matrices $\mathbf{C}_B$ and $\mathbf{C}_C$ in (4.13.8) account for the capacitive coupling between the two circuits.

Copyright 2017 Cengage Learning. All Rights Reserved. May not be copied, scanned, or duplicated, in whole or in part. Due to electronic rights, some third party content may be suppressed from the eBook and/or eChapter(s). Editorial review has deemed that any suppressed content does not materially affect the overall learning experience. Cengage Learning reserves the right to remove additional content at any time if subsequent rights restrictions require it.

These ideas can be extended in a straightforward fashion to more than two parallel circuits.

MULTIPLE CHOICE QUESTIONS

SECTION 4.1

4.1 ACSR stands for
(a) Aluminum-clad steel conductor
(b) Aluminum conductor steel supported
(c) Aluminum conductor steel reinforced

4.2 Overhead transmission-line conductors are bare with no insulating cover.
(a) True (b) False

4.3 Alumoweld is an aluminum-clad steel conductor.
(a) True (b) False

4.4 EHV lines often have more than one conductor per phase; these conductors are called a _______.

4.5 Shield wires located above the phase conductors protect the phase conductors against lightning.
(a) True (b) False

4.6 Conductor spacings, types, and sizes do have an impact on the series impedance and shunt admittance.
(a) True (b) False

SECTION 4.2

4.7 A circle with diameter D in. = 1000 D mil = d mil has an area of _______ c mil.

4.8 An ac resistance is higher than a dc resistance.
(a) True (b) False

4.9 Match the following for the current distribution throughout the conductor cross section:

(i) For dc	(a) uniform
(ii) For ac	(b) nonuniform

SECTION 4.3

4.10 Transmission line conductance is usually neglected in power system studies.
(a) True (b) False

SECTION 4.4

4.11 The internal inductance L_{int} per unit-length of a solid cylindrical conductor is a constant, given by $\frac{1}{2} \times 10^{-7}$H/m in SI system of units.
(a) True (b) False

Copyright 2017 Cengage Learning. All Rights Reserved. May not be copied, scanned, or duplicated, in whole or in part. Due to electronic rights, some third party content may be suppressed from the eBook and/or eChapter(s). Editorial review has deemed that any suppressed content does not materially affect the overall learning experience. Cengage Learning reserves the right to remove additional content at any time if subsequent rights restrictions require it.

4.12 The total inductance L_P of a solid cylindrical conductor (of radius r) due to both internal and external flux linkages out of distance D is given by (in H/m)

(a) 2×10^{-7} (b) $4 \times 10^{-7}\ln\left(\frac{D}{r}\right)$

(c) $2 \times 10^{-7}\ln\left(\frac{D}{r}\right)$

where $r' = e^{-\frac{1}{4}}r = 0.778r$.

SECTION 4.5

4.13 For a single-phase, two-wire line consisting of two solid cylindrical conductors of same radius, r, the total circuit inductance, also called loop inductance, is given by (in H/m)

(a) $2 \times 10^{-7}\ln\left(\frac{D}{r'}\right)$ (b) $4 \times 10^{-7}\ln\left(\frac{D}{r'}\right)$

where $r' = e^{-\frac{1}{4}}r = 0.778r$

4.14 For a three-phase three-wire line consisting of three solid cylindrical conductors, each with radius r and with equal phase spacing D between any two conductors, the inductance in H/m per phase is given by

(a) $2 \times 10^{-7}\ln\left(\frac{D}{r'}\right)$ (b) $4 \times 10^{-7}\ln\left(\frac{D}{r'}\right)$

(c) $6 \times 10^{-7}\ln\left(\frac{D}{r'}\right)$

where $r' = e^{-\frac{1}{4}}r = 0.778\,r$

4.15 For a balanced three-phase positive-sequence currents I_a, I_b, I_c, does the equation $I_a + I_b + I_c = 0$ hold good?

SECTION 4.6

4.16 A stranded conductor is an example of a composite conductor.

(a) True (b) False

4.17 $\Sigma \ln A_k = \ln \Pi\, A_k$

(a) True (b) False

4.18 Is Geometric Mean Distance (GMD) the same as Geometric Mean Radius (GMR)?

(a) Yes (b) No

4.19 Expand $6\sqrt{\Pi_{k=1}^{3}\,\Pi_{m=1'}^{2'}\,D_{km}}$.

4.20 If the distance between conductors are large compared to the distances between subconductors of each conductor, then the GMD between conductors is approximately equal to the distance between conductor centers.

(a) True (b) False

4.21 For a single-phase two-conductor line with composite conductors x and y, express the inductance of conductor x in terms of GMD and its GMR.

4.22 In a three-phase line, in order to avoid unequal phase inductances due to unbalanced flux linkages, what technique is used?

Copyright 2017 Cengage Learning. All Rights Reserved. May not be copied, scanned, or duplicated, in whole or in part. Due to electronic rights, some third party content may be suppressed from the eBook and/or eChapter(s). Editorial review has deemed that any suppressed content does not materially affect the overall learning experience. Cengage Learning reserves the right to remove additional content at any time if subsequent rights restrictions require it.

4.23 For a completely transposed three-phase line identical conductors, each with GMR denoted D_S with conductor distance D_{12}, D_{23}, and D_{31} give expressions for GMD between phases and the average per-phase inductance.

4.24 For EHV lines, a common practice of conductor bundling is used. Why?

4.25 Does bundling reduce the series reactance of the line?
(a) Yes (b) No

4.26 Does $r' = e^{-\frac{1}{4}} r = 0.788r$, which comes in calculation of inductance, play a role in capacitance computations?
(a) Yes (b) No

4.27 In terms of line-to-line capacitance, the line-to-neutral capacitance of a single-phase transmission line is
(a) Same (b) Twice (c) One-half

4.28 For either single-phase two-wire line or balanced three-phase three-wire line with equal phase spacing D and with conductor radius r, the capacitance (line-to-neutral) in F/m is given by $C_{an} =$ ____.

4.29 In deriving expressions for capacitance for a balanced three-phase three-wire line with equal phase spacing, the following relationships may have been used.
(i) Sum of positive-sequence charges, $q_a + q_b + q_c = 0$
(ii) The sum of the two line-to-line voltages $V_{ab} + V_{ac}$ is equal to three-times the line-to-neutral voltage V_{an}.

Which of the following is true?
(a) Both (b) Only (i) (c) Only (ii) (d) None

SECTION 4.10

4.30 When calculating line capacitance, it is normal practice to replace a stranded conductor by a perfectly conducting solid cylindrical conductor whose radius equals the out side radius of the stranded conductor.
(a) True (b) False

4.31 For bundled-conductor configurations, the expressions for calculating D_{SL} in inductance calculations and D_{SC} in capacitance calculations are analogous, except that the conductor outside radius r replaces the conductor GMR, D_S.
(a) True (b) False

4.32 The current supplied to the transmission-line capacitance is called ____.

4.33 For a completely transposed three-phase line that has balanced positive-sequence voltages, the total reactive power supplied by the three-phase line, in var, is given by $Q_{C3} =$ ______ in terms of frequency ω, line-to-neutral capacitance C_{an}, and line-to-line voltage V_{LL}.

Copyright 2017 Cengage Learning. All Rights Reserved. May not be copied, scanned, or duplicated, in whole or in part. Due to electronic rights, some third party content may be suppressed from the eBook and/or eChapter(s). Editorial review has deemed that any suppressed content does not materially affect the overall learning experience. Cengage Learning reserves the right to remove additional content at any time if subsequent rights restrictions require it.

SECTION 4.11

4.34 Considering lines with neutral conductors and earth return, the effect of earth plane is accounted for by the method of _______ with a perfectly conducting earth plane.

4.35 The affect of the earth plane is to slightly increase the capacitance, and as the line height increases, the effect of earth becomes negligible.
(a) True (b) False

SECTION 4.12

4.36 When the electric field strength at a conductor surface exceeds the breakdown strength of air, current discharges occur. This phenomenon is called ______.

4.37 To control corona, transmission lines are usually designed to maintain the calculated conductor surface electric field strength below _______ $\mathrm{kV_{rms}/cm}$.

4.38 Along with limiting corona and its effects, particularly for EHV lines, the maximum ground-level electric field strength needs to be controlled to avoid the shock hazard.
(a) True (b) False

SECTION 4.13

4.39 Considering two parallel three-phase circuits that are close together, when calculating the equivalent series-impedance and shunt-admittance matrices, mutual inductive and capacitive couplings between the two circuits can be neglected.
(a) True (b) False

PROBLEMS

SECTION 4.2

4.1 The *Aluminum Electrical Conductor Handbook* lists a dc resistance of 0.01558 ohm per 1000 ft at 20°C and a 60-Hz resistance of 0.0956 ohm per mile at 50°C for the all-aluminum Marigold conductor, which has 61 strands and whose size is 1113 kcmil. Assuming an increase in resistance of 2% for spiraling, calculate and verify the dc resistance. Then calculate the dc resistance at 50°C, and determine the percentage increase due to skin effect.

4.2 The temperature dependence of resistance is also quantified by the relation $R_2 = R_1[1 + \alpha(T_2 - T_1)]$ where R_1 and R_2 are the resistances at temperatures T_1 and T_2, respectively, and α is known as the temperature coefficient of resistance. If a copper wire has a resistance of 55 Ω at 20°C, find the maximum permissible operating temperature of the wire if its

Copyright 2017 Cengage Learning. All Rights Reserved. May not be copied, scanned, or duplicated, in whole or in part. Due to electronic rights, some third party content may be suppressed from the eBook and/or eChapter(s). Editorial review has deemed that any suppressed content does not materially affect the overall learning experience. Cengage Learning reserves the right to remove additional content at any time if subsequent rights restrictions require it.

resistance is to increase by at most 20%. Take the temperature coefficient at 20°C to be $\alpha = 0.00382$.

4.3 A transmission-line cable with a length of 2 km consists of 19 strands of identical copper conductors, each 1.5 mm in diameter. Because of the twist of the strands, the actual length of each conductor is increased by 5%. Determine the resistance of the cable if the resistivity of copper is 1.72 $\mu\Omega$-cm at 20°C.

4.4 One thousand circular mils or 1 kcmil is sometimes designated by the abbreviation MCM. Data for commercial bare-aluminum electrical conductors lists a 60 Hz resistance of 0.0080 ohm per kilometer at 75°C for a 793-MCM AAC conductor.

(a) Determine the cross-sectional conducting area of this conductor in square meters.

(b) Find the 60 Hz resistance of this conductor in ohms per kilometer at 50°C.

4.5 A 60-Hz, 765-kV, three-phase overhead transmission line has four ACSR 900 kcmil 54/3 conductors per phase. Determine the 60 Hz resistance of this line in ohms per kilometer per phase at 50°C.

4.6 A three-phase overhead transmission line is designed to deliver 190.5 MVA at 220 kV over a distance of 63 km, such that the total transmission line loss is not to exceed 2.5% of the rated line MVA. Given the resistivity of the conductor material to be 2.84×10^{-8} Ω-m, determine the required conductor diameter and the conductor size in circular mils. Neglect power losses due to insulator leakage currents and corona.

4.7 If the per-phase line loss in a 70-km-long transmission line is not to exceed 65 kW while it is delivering 100 A per phase, compute the required conductor diameter if the resistivity of the conductor material is 1.72×10^{-8} Ω-m.

SECTIONS 4.4 AND 4.5

4.8 A 60-Hz, single-phase two-wire overhead line has solid cylindrical copper conductors with a 1.5 cm diameter. The conductors are arranged in a horizontal configuration with 0.5 m spacing. Calculate in mH/km (a) the inductance of each conductor due to internal flux linkages only, (b) the inductance of each conductor due to both internal and external flux linkages, and (c) the total inductance of the line.

4.9 Rework Problem 4.8 if the diameter of each conductor is (a) increased by 20% to 1.8 cm or (b) decreased by 20% to 1.2 cm without changing the phase spacing. Compare the results with those of Problem 4.8.

4.10 A 60-Hz, three-phase three-wire overhead line has solid cylindrical conductors arranged in the form of an equilateral triangle with 4-ft conductor spacing. The conductor diameter is 0.5 in. Calculate the positive-sequence inductance in H/m and the positive-sequence inductive reactance in Ω/km.

Copyright 2017 Cengage Learning. All Rights Reserved. May not be copied, scanned, or duplicated, in whole or in part. Due to electronic rights, some third party content may be suppressed from the eBook and/or eChapter(s). Editorial review has deemed that any suppressed content does not materially affect the overall learning experience. Cengage Learning reserves the right to remove additional content at any time if subsequent rights restrictions require it.

4.11 Rework Problem 4.10 if the phase spacing is (a) increased by 20% to 4.8 ft or (b) decreased by 20% to 3.2 ft. Compare the results with those of Problem 4.10.

4.12 Find the inductive reactance per mile of a single-phase overhead transmission line operating at 60 Hz given the conductors to be *Partridge* and the spacing between centers to be 30 ft.

4.13 A single-phase overhead transmission line consists of two solid aluminum conductors having a radius of 3 cm with a spacing 3.5 m between centers. (a) Determine the total line inductance in mH/m. (b) Given the operating frequency to be 60 Hz, find the total inductive reactance of the line in Ω/km and in Ω/mi. (c) If the spacing is doubled to 7 m, how does the reactance change?

4.14 (a) In practice, one deals with the inductive reactance of the line per phase per mile and use the logarithm to the base 10. Show that Eq. (4.5.9) of the text can be rewritten as

$$\begin{aligned} x &= k \log \frac{D}{r'} \text{ ohms per mile per phase} \\ &= x_d + x_a \end{aligned}$$

where $x_d = k \log D$ is the inductive reactance spacing factor in ohms per mile

$x_a = k \log \frac{1}{r'}$ is the inductive reactance at 1-ft spacing in ohms per mile

$k = 4.657 \times 10^{-3} f = 0.2794$ at 60 Hz

(b) Determine the inductive reactance per mile per phase at 60 Hz for a single-phase line with phase separation of 10 ft and conductor radius of 0.06677 ft. If the spacing is doubled, how does the reactance change?

SECTION 4.6

4.15 Find the GMR of a stranded conductor consisting of six outer strands surrounding and touching one central strand, all strands having the same radius r.

4.16 A bundle configuration for UHV lines (above 1000 kV) has identical conductors equally spaced around a circle, as shown in Figure 4.29. N_b is the number of conductors in the bundle, A is the circle radius, and D_S is the conductor GMR. Using the distance D_{1n} between conductors 1 and n given by $D_{1n} = 2A \sin[(n-1)\pi/N_b]$ for $n = 1, 2, \ldots, N_b$, and the following trigonometric identity:

$$[2\sin(\pi/N_b)][2\sin(2\pi/N_b)][2\sin(3\pi/N_b)]\cdots[2\sin\{(N_b-1)\pi/N_b\}] = N_b$$

show that the bundle GMR, denoted D_{SL}, is

$$D_{SL} = [N_b D_S A^{(N_b-1)}]^{(1/N_b)}$$

Also show that the above formula agrees with (4.6.19) through (4.6.21) for EHV lines with $N_b = 2$, 3, and 4.

Copyright 2017 Cengage Learning. All Rights Reserved. May not be copied, scanned, or duplicated, in whole or in part. Due to electronic rights, some third party content may be suppressed from the eBook and/or eChapter(s). Editorial review has deemed that any suppressed content does not materially affect the overall learning experience. Cengage Learning reserves the right to remove additional content at any time if subsequent rights restrictions require it.

FIGURE 4.29

Bundle configuration for Problem 4.16

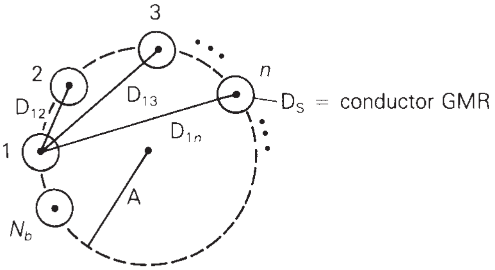

4.17 Determine the GMR of each of the unconventional stranded conductors shown in Figure 4.30. All strands have the same radius r.

FIGURE 4.30

Unconventional stranded conductors for Problem 4.17

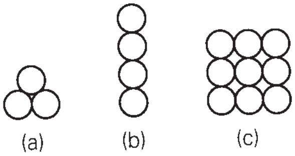
(a) (b) (c)

4.18 A 230-kV, 60-Hz, three-phase completely transposed overhead line has one ACSR 954 kcmil conductor per phase and flat horizontal phase spacing, with 7 m between adjacent conductors. Determine the inductance in H/m and the inductive reactance in Ω/km.

4.19 Rework Problem 4.18 if the phase spacing between adjacent conductors is (a) increased by 10% to 7.7 m or (b) decreased by 10% to 6.3 m. Compare the results with those of Problem 4.18.

4.20 Calculate the inductive reactance in Ω/km of a bundled 500-kV, 60-Hz, three-phase completely transposed overhead line having three ACSR 1113 kcmil conductors per bundle, with 0.5 m between conductors in the bundle. The horizontal phase spacings between bundle centers are 10, 10, and 20 m.

4.21 Rework Problem 4.20 if the bundled line has (a) three ACSR, 1351 kcmil conductors per phase or (b) three ACSR, 900 kcmil conductors per phase, without changing the bundle spacing or the phase spacings between bundle centers. Compare the results with those of Problem 4.20.

4.22 The conductor configuration of a bundled single-phase overhead transmission line is shown in Figure 4.31. Line X has its three conductors situated at the corners of an equilateral triangle with 10 cm spacing. Line Y has its three conductors arranged in a horizontal configuration with 10 cm spacing. All conductors are identical, solid-cylindrical conductors each with a radius of 2 cm. Find the equivalent representation in terms of the geometric mean radius of each bundle and a separation that is the geometric mean distance.

Copyright 2017 Cengage Learning. All Rights Reserved. May not be copied, scanned, or duplicated, in whole or in part. Due to electronic rights, some third party content may be suppressed from the eBook and/or eChapter(s). Editorial review has deemed that any suppressed content does not materially affect the overall learning experience. Cengage Learning reserves the right to remove additional content at any time if subsequent rights restrictions require it.

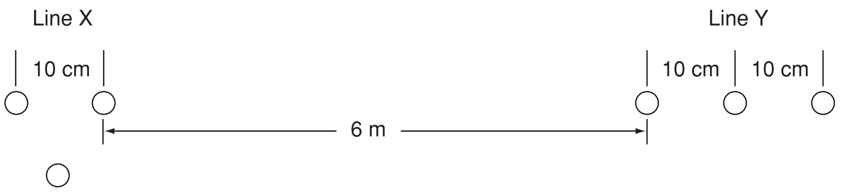

FIGURE 4.31

Problem 4.22

4.23 Figure 4.32 shows the conductor configuration of a completely transposed three-phase overhead transmission line with bundled phase conductors. All conductors have a radius of 0.74 cm with a 30-cm bundle spacing. (a) Determine the inductance per phase in mH/km and in mH/mi. (b) Find the inductive line reactance per phase in Ω/mi at 60 Hz.

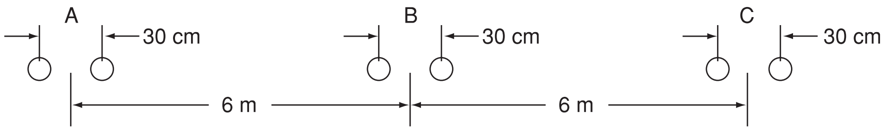

FIGURE 4.32

Problem 4.23

4.24 Consider a three-phase overhead line made up of three phase conductors: Linnet, 336.4 kcmil, and ACSR 26/7. The line configuration is such that the horizontal separation between center of C and that of A is 40", and between that of A and B is also 40" in the same line; the vertical separation of A from the line of C–B is 16". If the line is operated at 60 Hz at a conductor temperature of 75°C, determine the inductive reactance per phase in Ω/mi,

(a) by using the formula given in Problem 4.14 (a), and
(b) by using (4.6.18) from the text.

4.25 For the overhead line of configuration shown in Figure 4.33 operating at 60 Hz and a conductor temperature of 70°C, determine the resistance per phase, inductive reactance in ohms/mile/phase, and the current-carrying capacity of the overhead line. Each conductor is ACSR Cardinal of Table A.4.

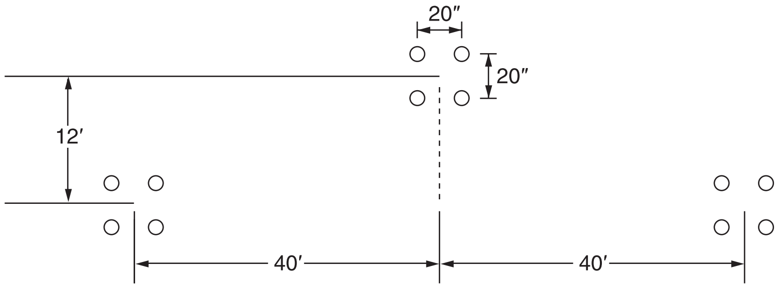

FIGURE 4.33

Line configuration for Problem 4.25

Copyright 2017 Cengage Learning. All Rights Reserved. May not be copied, scanned, or duplicated, in whole or in part. Due to electronic rights, some third party content may be suppressed from the eBook and/or eChapter(s). Editorial review has deemed that any suppressed content does not materially affect the overall learning experience. Cengage Learning reserves the right to remove additional content at any time if subsequent rights restrictions require it.

4.26 Consider a symmetrical bundle with N subconductors arranged in a circle of radius A. The inductance of a single-phase symmetrical bundle-conductor line is given by

$$L = 2 \times 10^{-7} \ln \frac{\text{GMD}}{\text{GMR}} \text{ H/m}$$

Where GMR is given by $[Nr'(A)^{N-1}]^{1/N}$ $r' = (e^{-1/4}r)$, r being the subconductor radius, and GMD is approximately the distance D between the bundle centers. Note that A is related to the subconductor spacing S in the bundle circle by $S = 2A\sin(\Pi/N)$

Now consider a 965-kV, single-phase, bundle-conductor line with eight subconductors per phase, phase spacing D = 20 m, and the subconductor spacing S = 45.72 cm. Each subconductor has a diameter of 4.572 cm. Determine the line inductance in H/m.

4.27 Figure 4.34 shows double-circuit conductors' relative positions in segment 1 of transposition of a completely transposed three-phase overhead transmission line. The inductance is given by

$$L = 2 \times 10^{-7} \ln \frac{\text{GMD}}{\text{GMR}} \text{ H/m/phase}$$

Where $\text{GMD} = (D_{AB_{eq}} D_{BC_{eq}} D_{AC_{eq}})^{1/3}$

With mean distances defined by equivalent spacings

FIGURE 4.34

For Problem 4.27 (Double-circuit conductor configuration)

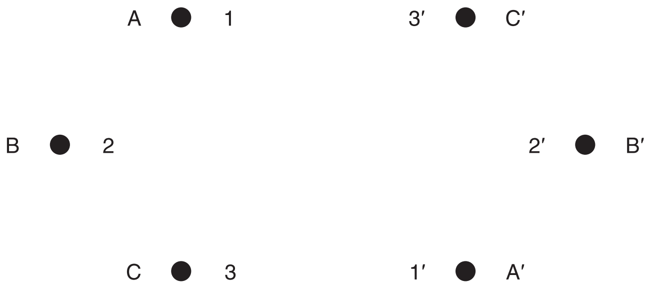

$$D_{AB_{eq}} = (D_{12}D_{1'2'}D_{12'}D_{1'2})^{1/4}$$

$$D_{BC_{eq}} = (D_{23}D_{2'3'}D_{2'3}D_{23'})^{1/4}$$

$$D_{AC_{eq}} = (D_{13}D_{1'3'}D_{13'}D_{1'3})^{1/4}$$

And $\text{GMR} = [(\text{GMR})_A(\text{GMR})_B(\text{GMR})_C]^{1/3}$ with phase GMRs defined by

$$(\text{GMR})_A = [r'D_{11'}]^{1/2};\ (\text{GMR})_B = [r'D_{22'}]^{1/2};\ (\text{GMR})_C = [r'D_{33'}]^{1/2}$$

and r' is the GMR of phase conductors.

Now consider a 345-kV, three-phase, double-circuit line with phase-conductor's GMR of 0.0588 ft and the horizontal conductor configuration shown in Figure 4.35.

Copyright 2017 Cengage Learning. All Rights Reserved. May not be copied, scanned, or duplicated, in whole or in part. Due to electronic rights, some third party content may be suppressed from the eBook and/or eChapter(s). Editorial review has deemed that any suppressed content does not materially affect the overall learning experience. Cengage Learning reserves the right to remove additional content at any time if subsequent rights restrictions require it.

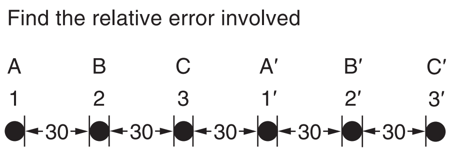

FIGURE 4.35

For Problem 4.27

(a) Determine the inductance per meter per phase in Henries (H).

(b) Calculate the inductance of just one circuit and then divide by 2 to obtain the inductance of the double circuit.

4.28 For the case of double-circuit, bundle-conductor lines, the same method indicated in Problem 4.27 applies with r' replaced by the bundle's GMR in the calculation of the overall GMR.

Now consider a double-circuit configuration shown in Figure 4.36 that belongs to a 500-kV, three-phase line with bundle conductors of three subconductors at 21 in. spacing. The GMR of each subconductor is given to be 0.0485 ft.

Determine the inductive reactance of the line in ohms per mile per phase. You may use

$$X_L = 0.2794 \log \frac{\text{GMD}}{\text{GMR}} \ \Omega/\text{mi/phase}$$

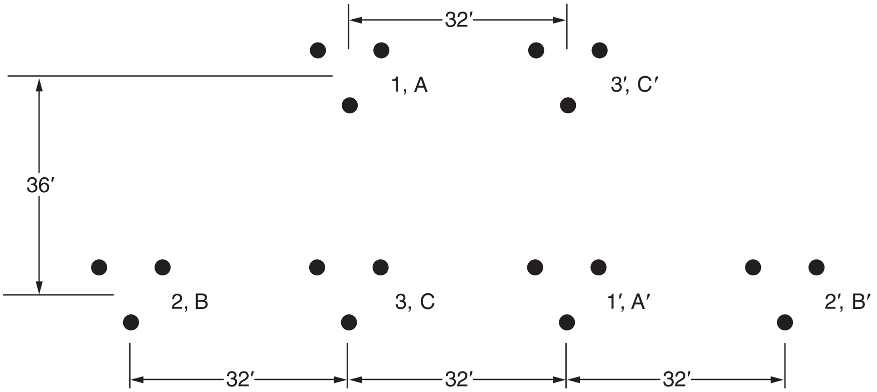

FIGURE 4.36

Configuration for Problem 4.28

4.29 Reconsider Problem 4.28 with an alternate phase placement given below:

	Physical Position					
	1	2	3	1′	2′	3′
Phase Placement	A	B	B′	C	C′	A′

Calculate the inductive reactance of the line in Ω/mi/phase.

Copyright 2017 Cengage Learning. All Rights Reserved. May not be copied, scanned, or duplicated, in whole or in part. Due to electronic rights, some third party content may be suppressed from the eBook and/or eChapter(s). Editorial review has deemed that any suppressed content does not materially affect the overall learning experience. Cengage Learning reserves the right to remove additional content at any time if subsequent rights restrictions require it.

4.30 Reconsider Problem 4.28 with still another alternate phase placement shown below.

	Physical Position					
	1	2	3	1′	2′	3′
Phase Placement	C	A	B	B	A	C

Find the inductive reactance of the line in Ω/mi/phase.

4.31 Figure 4.37 shows the conductor configuration of a three-phase transmission line and a telephone line supported on the same towers. The power line carries a balanced current of 250 A/phase at 60 Hz, while the telephone line is directly located below phase b. Assume balanced three-phase currents in the power line. Calculate the voltage per kilometer induced in the telephone line.

FIGURE 4.37

Conductor layout for Problem 4.31

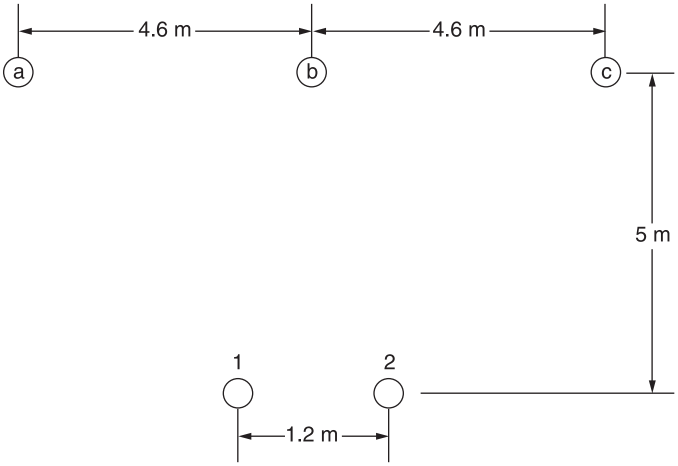

SECTION 4.9

4.32 Calculate the capacitance-to-neutral in F/m and the admittance-to-neutral in S/km for the single-phase line in Problem 4.8. Neglect the effect of the earth plane.

4.33 Rework Problem 4.32 if the diameter of each conductor is (a) increased by 20% to 1.8 cm or (b) decreased by 20% to 1.2 cm. Compare the results with those of Problem 4.32.

4.34 Calculate the capacitance-to-neutral in F/m and the admittance-to-neutral in S/km for the three-phase line in Problem 4.10. Neglect the effect of the earth plane.

Copyright 2017 Cengage Learning. All Rights Reserved. May not be copied, scanned, or duplicated, in whole or in part. Due to electronic rights, some third party content may be suppressed from the eBook and/or eChapter(s). Editorial review has deemed that any suppressed content does not materially affect the overall learning experience. Cengage Learning reserves the right to remove additional content at any time if subsequent rights restrictions require it.

4.35 Rework Problem 4.34 if the phase spacing is (a) increased by 20% to 4.8 ft or (b) decreased by 20% to 3.2 ft. Compare the results with those of Problem 4.34.

4.36 The line of Problem 4.23 as shown in Figure 4.32 is operating at 60 Hz. Determine (a) the line-to-neutral capacitance in nF/km per phase and in nF/mi per phase; (b) the capacitive reactance in Ω-km per phase and in Ω-mi per phase; and (c) the capacitive reactance in Ω per phase for a line length of 100 mi.

4.37 (a) In practice, one deals with the capacitive reactance of the line in ohms · mi to neutral. Show that Eq. (4.9.15) of the text can be rewritten as

$$\begin{aligned} X_C &= k' \log \frac{D}{r} \quad \text{ohms} \cdot \text{mi to netural} \\ &= x_d' + x_a' \end{aligned}$$

where $x_d' = k' \log D$ is the capacitive reactance spacing factor
$x_a' = k' \log \frac{1}{r}$ is the capacitive reactance at 1-ft spacing
$k' = (4.1 \times 10^6)/f = 0.06833 \times 10^6$ at $f = 60$ Hz

(b) Determine the capacitive reactance in Ω · mi. for a single-phase line of Problem 4.14. If the spacing is doubled, how does the reactance change?

4.38 The capacitance per phase of a balanced three-phase overhead line is given by

$$C = \frac{0.0389}{\log(\text{GMD}/r)} \, \mu f/\text{mi}/\text{phase}$$

For the line of Problem 4.24, determine the capacitive reactance per phase in Ω · mi.

SECTION 4.10

4.39 Calculate the capacitance-to-neutral in F/m and the admittance-to-neutral in S/km for the three-phase line in Problem 4.18. Also calculate the line-charging current in kA/phase if the line is 110 km in length and is operated at 230 kV. Neglect the effect of the earth plane.

4.40 Rework Problem 4.39 if the phase spacing between adjacent conductors is (a) increased by 10% to 7.7 m or (b) decreased by 10% to 6.3 m. Compare the results with those of Problem 4.39.

4.41 Calculate the capacitance-to-neutral in F/m and the admittance-to-neutral in S/km for the line in Problem 4.20. Also calculate the total reactive power in Mvar/km supplied by the line capacitance when it is operated at 500 kV. Neglect the effect of the earth plane.

Copyright 2017 Cengage Learning. All Rights Reserved. May not be copied, scanned, or duplicated, in whole or in part. Due to electronic rights, some third party content may be suppressed from the eBook and/or eChapter(s). Editorial review has deemed that any suppressed content does not materially affect the overall learning experience. Cengage Learning reserves the right to remove additional content at any time if subsequent rights restrictions require it.

4.42 Rework Problem 4.41 if the bundled line has (a) three ACSR, 1351-kcmil conductors per phase or (b) three ACSR, 900 kcmil conductors per phase without changing the bundle spacing or the phase spacings between bundle centers.

4.43 Three ACSR *Drake* conductors are used for a three-phase overhead transmission line operating at 60 Hz. The conductor configuration is in the form of an isosceles triangle with sides of 20, 20, and 38 ft. (a) Find the capacitance-to-neutral and capacitive reactance-to-neutral for each 1-mile length of line. (b) For a line length of 175 mi and a normal operating voltage of 220 kV, determine the capacitive reactance-to-neutral for the entire line length as well as the charging current per mile and total three-phase reactive power supplied by the line capacitance.

4.44 Consider the line of Problem 4.25. Calculate the capacitive reactance per phase in $\Omega \cdot$ mi.

SECTION 4.11

4.45 For an average line height of 10 m, determine the effect of the earth on capacitance for the single-phase line in Problem 4.32. Assume a perfectly conducting earth plane.

4.46 A three-phase 60-Hz, 125-km overhead transmission line has flat horizontal spacing with three identical conductors. The conductors have an outside diameter of 3.28 cm with 12 m between adjacent conductors. (a) Determine the capacitive reactance-to-neutral in Ω-m per phase and the capacitive reactance of the line in Ω per phase. Neglect the effect of the earth plane. (b) Assuming that the conductors are horizontally placed 20 m above ground, repeat part (a) while taking into account the effect of ground. Consider the earth plane to be a perfect conductor.

4.47 For the single-phase line of Problem 4.14 (b), if the height of the conductor above ground is 80 ft., determine the line-to-line capacitance in F/m. Neglecting earth effect, evaluate the relative error involved. If the phase separation is doubled, repeat the calculations.

4.48 The capacitance of a single-circuit, three-phase transposed line with the configuration shown in Figure 4.38, including ground effect, and with conductors not equilaterally spaced is given by

$$C_{a\eta}\frac{2\pi\varepsilon_0}{\ln\dfrac{D_{eq}}{r} - \ln\dfrac{H_m}{H_s}} \text{ F/m line-to-neutral}$$

where $D_{eq} = \sqrt[3]{D_{12}D_{23}D_{13}} = \text{GMD}$

r = conductor's outside radius

$$H_m = (H_{12}H_{23}H_{13})^{1/3}$$

$$H_s = (H_1H_2H_3)^{1/3}$$

Copyright 2017 Cengage Learning. All Rights Reserved. May not be copied, scanned, or duplicated, in whole or in part. Due to electronic rights, some third party content may be suppressed from the eBook and/or eChapter(s). Editorial review has deemed that any suppressed content does not materially affect the overall learning experience. Cengage Learning reserves the right to remove additional content at any time if subsequent rights restrictions require it.

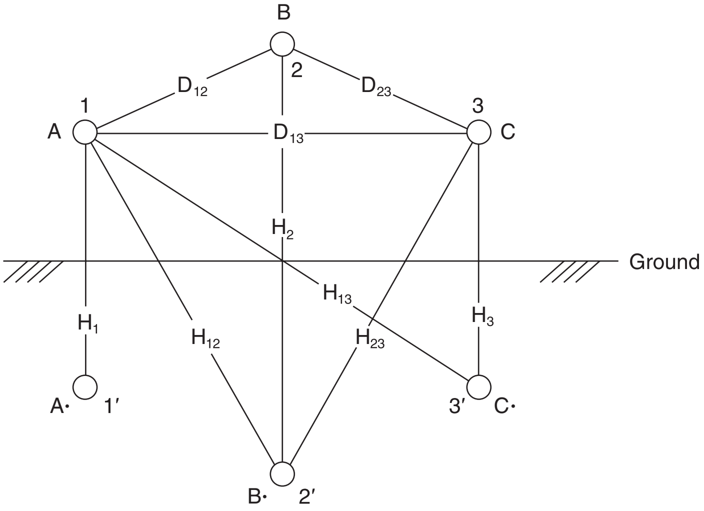

FIGURE 4.38

Three-phase single-circuit line configuration including ground effect for Problem 4.48

(a) Now consider Figure 4.39 in which the configuration of a three-phase, single circuit, 345-kV line with conductors having an outside diameter of 1.065 in. is shown. Determine the capacitance to neutral in F/m, including the ground effect.

(b) Next, neglecting the effect of ground, see how the value changes.

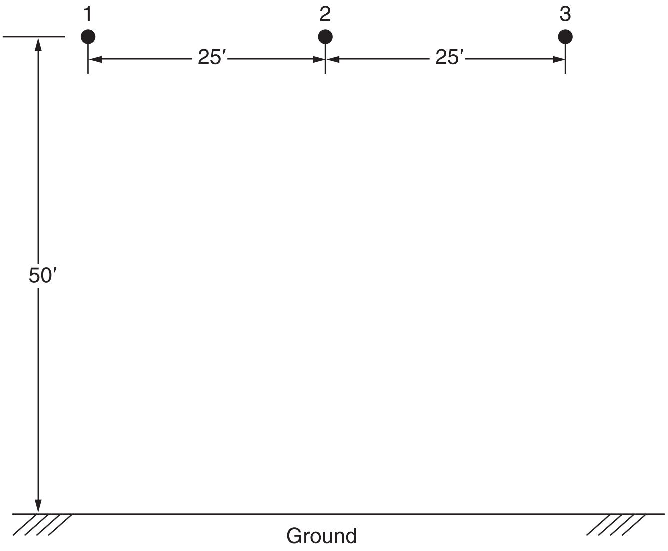

FIGURE 4.39

Configuration for Problem 4.48 (a)

4.49 The capacitance-to-neutral, neglecting the ground effect, for the three-phase, single-circuit, bundle-conductor line is given by

Copyright 2017 Cengage Learning. All Rights Reserved. May not be copied, scanned, or duplicated, in whole or in part. Due to electronic rights, some third party content may be suppressed from the eBook and/or eChapter(s). Editorial review has deemed that any suppressed content does not materially affect the overall learning experience. Cengage Learning reserves the right to remove additional content at any time if subsequent rights restrictions require it.

$$C_{a\eta} = \frac{2\pi\varepsilon_0}{\ell\eta\left(\dfrac{\text{GMD}}{\text{GMR}}\right)} \text{ F/m line-to-neutral}$$

$$\text{Where GMD} = (D_{AB}D_{BC}D_{AC})^{1/3}$$
$$\text{GMR} = [rN(\text{A})^{N-1}]^{1/N}$$

in which N is the number of subconductors of the bundle conductor on a circle of radius A, and each subconductor has an outside radius of r. The capacitive reactance in mega-ohms for 1 mi of line at 60 Hz can be shown to be

$$X_C = 0.0683 \log\left(\frac{\text{GMD}}{\text{GMR}}\right) = X'_a + X'_d$$

where $X'_a = 0.0683 \log\left(\dfrac{1}{\text{GMR}}\right)$ and $X'_d = 0.0683 \log(\text{GMD})$.

Note that A is related to the bundle spacing S given by

$$\text{A} = \frac{S}{2\sin\left(\dfrac{\pi}{N}\right)} \quad \text{for } N > 1$$

Using the above information for the configuration shown in Figure 4.40, compute the capacitance-to-neutral in F/m and the capacitive reactance in Ω · mi to neutral for the three-phase, 765-kV, 60-Hz, single-circuit, bundle-conductor line ($N = 4$) with subconductor's outside diameter of 1.16 in. and subconductor spacing (S) of 18 in.

FIGURE 4.40

Configuration for Problem 4.49

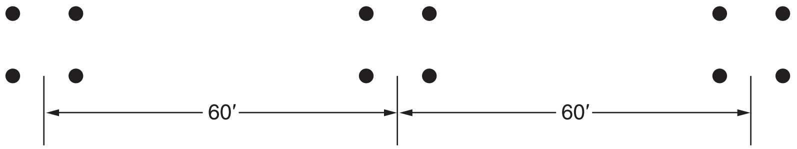

SECTION 4.12

4.50 Calculate the conductor surface electric field strength in kVrms/cm for the single-phase line in Problem 4.32 when the line is operating at 20 kV. Also calculate the ground-level electric field strength in kVrms/m directly under one conductor. Assume a line height of 10 m.

Copyright 2017 Cengage Learning. All Rights Reserved. May not be copied, scanned, or duplicated, in whole or in part. Due to electronic rights, some third party content may be suppressed from the eBook and/or eChapter(s). Editorial review has deemed that any suppressed content does not materially affect the overall learning experience. Cengage Learning reserves the right to remove additional content at any time if subsequent rights restrictions require it.

4.51 Rework Problem 4.50 if the diameter of each conductor is (a) increased by 25% to 1.875 cm or (b) decreased by 25% to 1.125 cm without changing the phase spacings. Compare the results with those of Problem 4.50.

CASE STUDY QUESTIONS

a. Approximately how many physical transmission interconnections are there between the United States and Canada? Across which states and provinces are the interconnections located?

b. How many kWhs of electrical energy was exported from Canada to the United States in 2012? Was the majority of that energy export derived from clean, non-emitting sources of electrical power?

c. What caused the August 2003 blackout in the United States and Canada? How many generating units were forced to shut down during that blackout?

d. What are the advantages of high-capacity, low-sag conductors? As of 2013, how many electric utilities in the world had deployed high-capacity, low-sag conductor technology?

REFERENCES

1. Electric Power Research Institute (EPRI), *EPRI AC Transmission Line Reference Book—200 kV and Above* (Palo Alto, CA: EPRI, www.epri.com, December 2005).
2. Westinghouse Electric Corporation, *Electrical Transmission and Distribution Reference Book*, 4th ed. (East Pittsburgh, PA, 1964).
3. General Electric Company, *Electric Utility Systems and Practices*, 4th ed. (New York: Wiley, 1983).
4. John R. Carson, "Wave Propagation in Overhead Wires with Ground Return," *Bell System Tech. J.* 5 (1926): 539–554.
5. C. F. Wagner and R. D. Evans, *Symmetrical Components* (New York: McGraw-Hill, 1933).
6. Paul M. Anderson, *Analysis of Faulted Power Systems* (Ames, IA: Iowa State Press, 1973).
7. M. H. Hesse, "Electromagnetic and Electrostatic Transmission Line Parameters by Digital Computer," *Trans. IEEE* PAS-82 (1963): 282–291.
8. W. D. Stevenson, Jr., *Elements of Power System Analysis,* 4th ed. (New York: McGraw-Hill, 1982).

Copyright 2017 Cengage Learning. All Rights Reserved. May not be copied, scanned, or duplicated, in whole or in part. Due to electronic rights, some third party content may be suppressed from the eBook and/or eChapter(s). Editorial review has deemed that any suppressed content does not materially affect the overall learning experience. Cengage Learning reserves the right to remove additional content at any time if subsequent rights restrictions require it.

9. C. A. Gross, *Power System Analysis* (New York: Wiley, 1979).

10. P. Brown, "Integrating North America's Power Grid," *Electricity Today T & D Magazine*, 26, 5, (June 2013), pp. 8–11 (www.electricity-today.com).

11. IEEE ANCI C2. *National Electrical Safety Code*, 2007 edition (New York: Institute of Electrical and Electronics Engineers).

12. D. Bryant, "Grid Congestion," *Electricity Today T & D Magazine*, 26, 6 (July/August 2013), pp. 58–60 (www.electricity-today.com).

Copyright 2017 Cengage Learning. All Rights Reserved. May not be copied, scanned, or duplicated, in whole or in part. Due to electronic rights, some third party content may be suppressed from the eBook and/or eChapter(s). Editorial review has deemed that any suppressed content does not materially affect the overall learning experience. Cengage Learning reserves the right to remove additional content at any time if subsequent rights restrictions require it.

5 Transmission Lines: Steady-State Operation

Series capacitor installation at Goshen Substation, Goshen, Idaho, USA rated at 395 kV, 965 Mvar (Courtesy of PacifiCorp.)

This chapter analyzes the performance of single-phase and balanced three-phase transmission lines under normal steady-state operating conditions. Expressions for voltage and current at any point along a line are developed where the distributed nature of the series impedance and shunt admittance is taken into account. A line is treated here as a two-port network for which the *ABCD* parameters and an equivalent π circuit are derived. Also, approximations are given for a medium-length line lumping the shunt admittance, for a short line neglecting the shunt admittance, and for a lossless line assuming zero series resistance and shunt conductance.

Copyright 2017 Cengage Learning. All Rights Reserved. May not be copied, scanned, or duplicated, in whole or in part. Due to electronic rights, some third party content may be suppressed from the eBook and/or eChapter(s). Editorial review has deemed that any suppressed content does not materially affect the overall learning experience. Cengage Learning reserves the right to remove additional content at any time if subsequent rights restrictions require it.

The concepts of *surge impedance loading* and transmission-line *wavelength* are also presented.

An important issue discussed in this chapter is *voltage regulation*. Transmission-line voltages are generally high during light load periods and low during heavy load periods. Voltage regulation, defined in Section 5.1, refers to the change in line voltage as line loading varies from no-load to full load.

Another important issue discussed here is line loadability. Three major line-loading limits are (1) the thermal limit, (2) the voltage-drop limit, and (3) the steady-state stability limit. Thermal and voltage-drop limits are discussed in Section 5.1. The theoretical steady-state stability limit, discussed in Section 5.4 for lossless lines and in Section 5.5 for lossy lines, refers to the ability of synchronous machines at the ends of a line to remain in synchronism. Practical line loadability is discussed in Section 5.6.

Section 5.7 covers line compensation techniques for improving voltage regulation and for raising line loadings closer to the thermal limit.

CASE STUDY

High voltage direct current (HVDC) applications embedded within ac power system grids have many benefits. A bipolar HVDC transmission line has only two insulated sets of conductors versus three for an ac transmission line. As such, HVDC transmission lines have smaller transmission towers, narrower rights-of-way, and lower line losses compared to ac lines with similar capacity. The resulting cost savings can offset the higher converter station costs of HVDC. Further, HVDC may be the only feasible method to (1) interconnect two asynchronous ac networks; (2) utilize long underground or underwater cable circuits; (3) bypass network congestion; (4) reduce fault currents; (5) share utility rights-of-way without degrading reliability; and (6) mitigate environmental concerns. The following article provides an overview of HVDC along with HVDC applications [6].

The ABCs of HVDC Transmission Technologies: An Overview of High Voltage Direct Current Systems and Applications

By Michael P. Bahrman and Brian K. Johnson

High voltage direct current (HVDC) technology has characteristics that make it especially attractive for certain transmission applications. HVDC transmission is widely recognized as being advantageous for long-distance bulk-power delivery, asynchronous interconnections, and long submarine cable crossings. The number of HVDC projects committed

Copyright 2017 Cengage Learning. All Rights Reserved. May not be copied, scanned, or duplicated, in whole or in part. Due to electronic rights, some third party content may be suppressed from the eBook and/or eChapter(s). Editorial review has deemed that any suppressed content does not materially affect the overall learning experience. Cengage Learning reserves the right to remove additional content at any time if subsequent rights restrictions require it.

or under consideration globally has increased in recent years, reflecting a renewed interest in this mature technology. New converter designs have broadened the potential range of HVDC transmission to include applications for underground, offshore, economic replacement of reliability-must-run generation, and voltage stabilization. This broader range of applications has contributed to the recent growth of HVDC transmission. There are approximately ten new HVDC projects under construction or active consideration in North America along with many more projects underway globally. Figure 1 shows the Danish terminal for Skagerrak's pole 3, which is rated 440 MW. Figure 2 shows the ±500-kV HVDC transmission line for the 2000 MW Intermountain Power Project between Utah and California. This article discusses HVDC technologies, application areas where HVDC is favorable compared to ac transmission, system configuration, station design, and operating principles.

Core HVDC Technologies

Two basic converter technologies are used in modem HVDC transmission systems. These are conventional line-commutated current source converters (CSCs) and self-commutated voltage source converters (VSCs). Figure 3 shows a conventional HVDC converter station with CSCs while Figure 4 shows a HVDC converter station with VSCs.

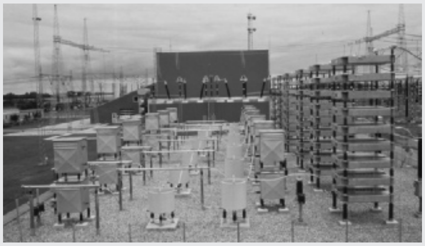

Figure 1 HVDC converter station with ac filters in the foreground and valve hall in the background

Figure 2 A ±500-kV HVDC transmission line

Line-Commutated Current Source Converter

Conventional HVDC transmission employs line-commutated CSCs with thyristor valves. Such converters require a synchronous voltage source in order to operate. The basic building block used for HVDC conversion is the three-phase, full-wave bridge referred to as a six-pulse or Graetz bridge. The term six-pulse is due to six commutations or switching operations per period resulting in a characteristic harmonic ripple of six times the fundamental frequency in the dc output voltage. Each six-pulse bridge is comprised of six controlled switching elements or thyristor

(“The ABCs of HVDC Transmission Technologies” by Michael P. Bahrman and Brian K. Johnson. © 2007 *IEEE*. Reprinted, I with permission, from *IEEE Power & Energy Magazine*, March/April 2007)

Copyright 2017 Cengage Learning. All Rights Reserved. May not be copied, scanned, or duplicated, in whole or in part. Due to electronic rights, some third party content may be suppressed from the eBook and/or eChapter(s). Editorial review has deemed that any suppressed content does not materially affect the overall learning experience. Cengage Learning reserves the right to remove additional content at any time if subsequent rights restrictions require it.

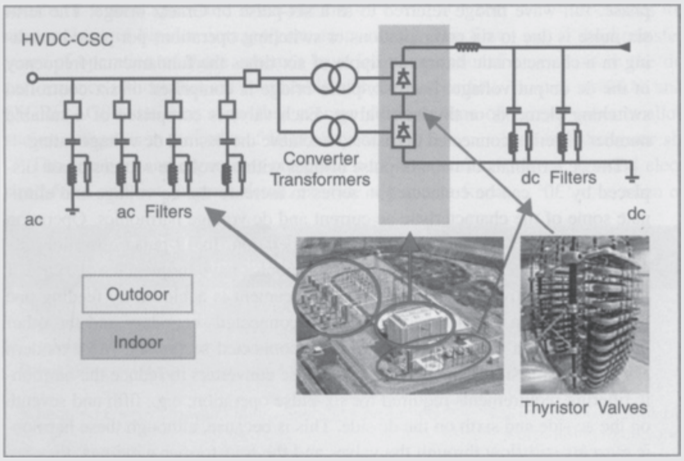

Figure 3 Conventional HVDC with current source converters

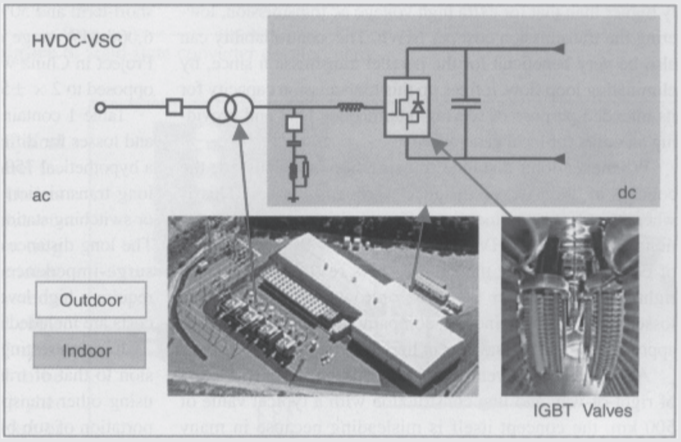

Figure 4 HVDC with voltage source converters

valves. Each valve is comprised of a suitable number of series-connected thyristors to achieve the desired dc voltage rating.

The dc terminals of two six-pulse bridges with ac voltage sources phase displaced by 30° can be connected in series to increase the dc voltage and eliminate some of the characteristic ac current and dc voltage harmonics. Operation in this manner is referred to as 12-pulse operation. In 12-pulse operation, the characteristic ac current and dc voltage harmonics have frequencies of $12n \pm 1$ and $12n$, respectively. The 30° phase displacement is achieved by feeding one bridge through a transformer with a wye-connected secondary and the other bridge through a transformer with a delta-connected secondary. Most modern HVDC transmission

Copyright 2017 Cengage Learning. All Rights Reserved. May not be copied, scanned, or duplicated, in whole or in part. Due to electronic rights, some third party content may be suppressed from the eBook and/or eChapter(s). Editorial review has deemed that any suppressed content does not materially affect the overall learning experience. Cengage Learning reserves the right to remove additional content at any time if subsequent rights restrictions require it.

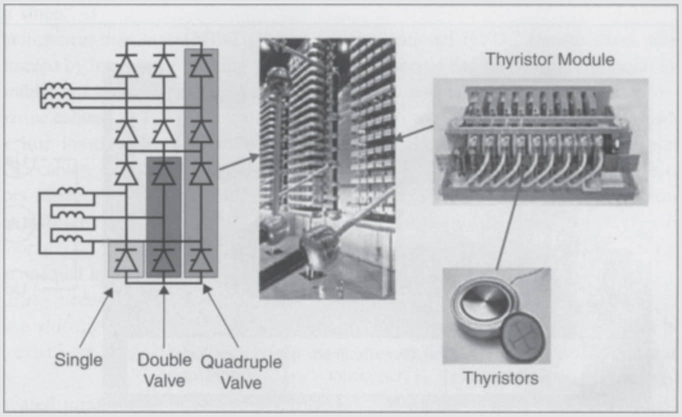

Figure 5 Thyristor valve arrangement for a 12-pulse converter with three quadruple valves, one for each phase

schemes utilize 12-pulse converters to reduce the harmonic filtering requirements required for six-pulse operation; for example, fifth and seventh on the ac side and sixth on the dc side. This is because, although these harmonic currents still flow through the valves and the transformer windings, they are 180° out of phase and cancel out on the primary side of the converter transformer. Figure 5 shows the thyristor valve arrangement for a 12-pulse converter with three quadruple valves, one for each phase. Each thyristor valve is built up with series-connected thyristor modules.

Line-commutated converters require a relatively strong synchronous voltage source in order to commutate. Commutation is the transfer of current from one phase to another in a synchronized firing sequence of the thyristor valves. The three-phase symmetrical short-circuit capacity available from the network at the converter connection point should be at least twice the converter rating for converter operation. Line-commutated CSCs can only operate with the ac current lagging the voltage, so the conversion process demands reactive power. Reactive power is supplied from the ac filters, which look capacitive at the fundamental frequency, shunt banks, or series capacitors that are an integral part of the converter station. Any surplus or deficit in reactive power from these local sources must be accommodated by the ac system. This difference in reactive power needs to be kept within a given band to keep the ac voltage within the desired tolerance. The weaker the ac system or the further the converter is away from generation, the tighter the reactive power exchange must be to stay within the desired voltage tolerance. Figure 6 illustrates the reactive power demand, reactive power compensation, and reactive power exchange with the ac network as a function of dc load current.

Copyright 2017 Cengage Learning. All Rights Reserved. May not be copied, scanned, or duplicated, in whole or in part. Due to electronic rights, some third party content may be suppressed from the eBook and/or eChapter(s). Editorial review has deemed that any suppressed content does not materially affect the overall learning experience. Cengage Learning reserves the right to remove additional content at any time if subsequent rights restrictions require it.

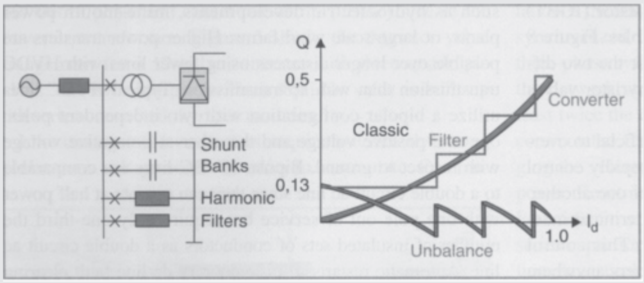

Figure 6 Reactive power compensation for conventional HVDC converter station

Converters with series capacitors connected between the valves and the transformers were introduced in the late 1990s for weak-system, back-to-back applications. These converters are referred to as capacitor-commutated converters (CCCs). The series capacitor provides some of the converter reactive power compensation requirements automatically with load current and provides part of the commutation voltage, improving voltage stability. The overvoltage protection of the series capacitors is simple since the capacitor is not exposed to line faults, and the fault current for internal converter faults is limited by the impedance of the converter transformers. The CCC configuration allows higher power ratings in areas were the ac network is close to its voltage stability limit. The asynchronous Garabi interconnection between Brazil and Argentina consists of four × 550 MW parallel CCC links. The Rapid City Tie between the Eastern and Western interconnected systems consists of 2 × 10 MW parallel CCC links (Figure 7). Both installations use a modular design with converter valves located within prefabricated electrical enclosures rather than a conventional valve hall.

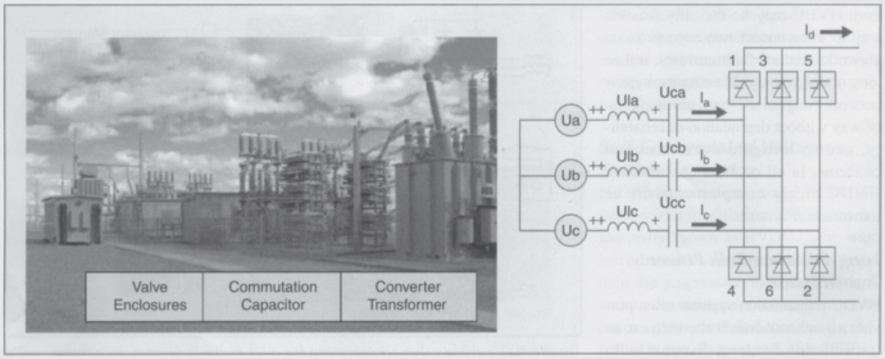

Figure 7 Asynchronous back-to-back tie with capacitor-commutated converter near Rapid City, South Dakota

Copyright 2017 Cengage Learning. All Rights Reserved. May not be copied, scanned, or duplicated, in whole or in part. Due to electronic rights, some third party content may be suppressed from the eBook and/or eChapter(s). Editorial review has deemed that any suppressed content does not materially affect the overall learning experience. Cengage Learning reserves the right to remove additional content at any time if subsequent rights restrictions require it.

Self-Commutated Voltage Source Converter

HVDC transmission using VSCs with pulse-width modulation (PWM), commercially known as HVDC Light, was introduced in the late 1990s. Since then, the progression to higher voltage and power ratings for these converters has roughly paralleled that for thyristor valve converters in the 1970s. These VSC-based systems are self-commutated with insulated-gate bipolar transistor (IGBT) valves and solid-dielectric extruded HVDC cables. Figure 8 illustrates solid-state converter development for the two different types of converter technologies using thyristor valves and IGBT valves.

HVDC transmission with VSCs can be beneficial to overall system performance. VSC technology can rapidly control both active and reactive power independently of one another. Reactive power can also be controlled at each terminal independent of the dc transmission voltage level. This control capability gives total flexibility to place converters anywhere in the ac network because there is no restriction on minimum network short-circuit capacity. Self-commutation with VSC even permits black start; that is, the converter can be used to synthesize a balanced set of three-phase voltages like a virtual synchronous generator. The dynamic support of the ac voltage at each converter terminal improves the voltage stability and can increase the transfer capability of the sending- and receiving-end ac systems, thereby leveraging the transfer capability of the dc link. Figure 9 shows the IGBT converter valve arrangement for a VSC station. Figure 10 shows the active and reactive power operating range for a converter station with a VSC. Unlike conventional HVDC transmission, the converters themselves have

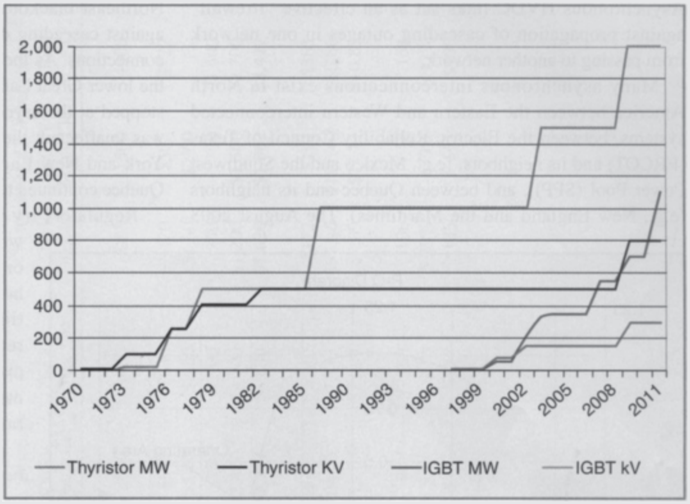

Figure 8 Solid-state converter development

Copyright 2017 Cengage Learning. All Rights Reserved. May not be copied, scanned, or duplicated, in whole or in part. Due to electronic rights, some third party content may be suppressed from the eBook and/or eChapter(s). Editorial review has deemed that any suppressed content does not materially affect the overall learning experience. Cengage Learning reserves the right to remove additional content at any time if subsequent rights restrictions require it.

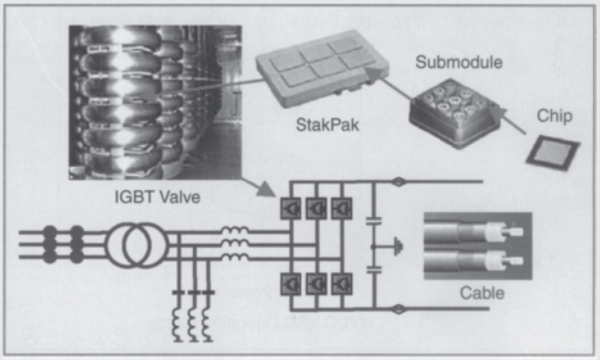

Figure 9 HVDC IGBT valve converter arrangement

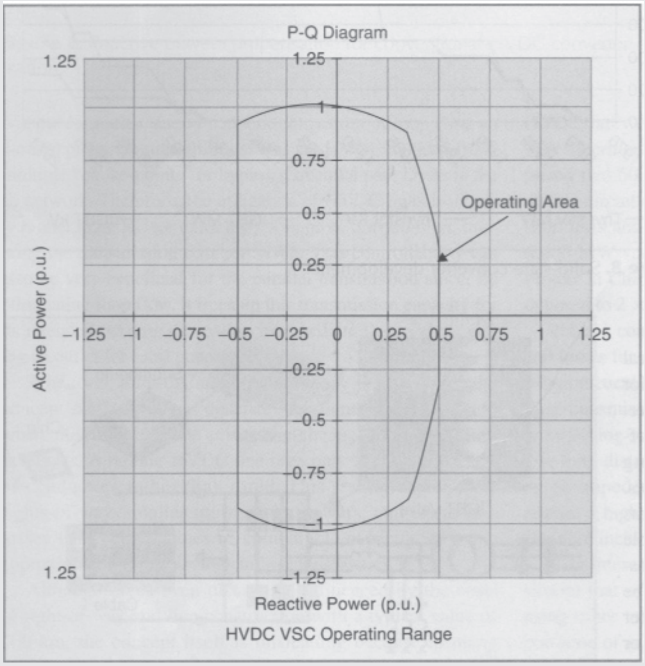

Figure 10 Operating range for voltage source converter HVDC transmission

no reactive power demand and can actually control their reactive power to regulate ac system voltage, just like a generator.

HVDC Applications

HVDC transmission applications can be broken down into different basic categories. Although the rationale

Copyright 2017 Cengage Learning. All Rights Reserved. May not be copied, scanned, or duplicated, in whole or in part. Due to electronic rights, some third party content may be suppressed from the eBook and/or eChapter(s). Editorial review has deemed that any suppressed content does not materially affect the overall learning experience. Cengage Learning reserves the right to remove additional content at any time if subsequent rights restrictions require it.

for selection of HVDC is often economic, there may be other reasons for its selection. HVDC may be the only feasible way to interconnect two asynchronous networks, reduce fault currents, utilize long underground cable circuits, bypass network congestion, share utility rights-of-way without degradation of reliability, and to mitigate environmental concerns. In all of these applications, HVDC nicely complements the ac transmission system.

Long-Distance Bulk Power Transmission

HVDC transmission systems often provide a more economical alternative to ac transmission for long-distance bulk-power delivery from remote resources such as hydroelectric developments, mine-mouth power plants, or large-scale wind farms. Higher power transfers are possible over longer distances using fewer lines with HVDC transmission than with ac transmission. Typical HVDC lines utilize a bipolar configuration with two independent poles, one at a positive voltage and the other at a negative voltage with respect to ground. Bipolar HVDC lines are comparable to a double-circuit ac line since they can operate at half power with one pole out of service while requiring only one-third the number of insulated sets of conductors as a double circuit ac line. Automatic restarts from temporary dc line fault clearing sequences are routine, even for generator outlet transmission. No synchro-checking is required as for automatic reclosures following ac line faults since the dc restarts do not expose turbine generator units to high risk of transient torque amplification from closing into faults or across high phase angles. The controllability of HVDC links offer firm transmission capacity without limitation due to network congestion or loop flow on parallel paths. Controllability allows the HVDC to “leap-frog” multiple “choke-points” or bypass sequential path limits in the ac network. Therefore, the utilization of HVDC links is usually higher than that for extra high voltage ac transmission, lowering the transmission cost per MWh. This controllability can also be very beneficial for the parallel transmission since, by eliminating loop flow, it frees up this transmission capacity for its intended purpose of serving intermediate load and providing an outlet for local generation.

Whenever long-distance transmission is discussed, the concept of “break-even distance” frequently arises. This is where the savings in line costs offset the higher converter station costs. A bipolar HVDC line uses only two insulated sets of conductors rather than three. This results in narrower rights-of-way, smaller transmission towers, and lower line losses than with ac lines of comparable capacity. A rough approximation of the savings in line construction is 30%.

Although break-even distance is influenced by the costs of right-of-way and line construction with a typical value of 500 km, the concept itself is misleading because in many cases more ac lines are needed to deliver the same power over the same distance due to system stability limitations.

Copyright 2017 Cengage Learning. All Rights Reserved. May not be copied, scanned, or duplicated, in whole or in part. Due to electronic rights, some third party content may be suppressed from the eBook and/or eChapter(s). Editorial review has deemed that any suppressed content does not materially affect the overall learning experience. Cengage Learning reserves the right to remove additional content at any time if subsequent rights restrictions require it.

Furthermore, the long-distance ac lines usually require intermediate switching stations and reactive power compensation. This can increase the substation costs for ac transmission to the point where it is comparable to that for HVDC transmission.

For example, the generator outlet transmission alternative for the ±250-kV, 500-MW Square Butte project was two 345-kV series-compensated ac transmission lines. The 12,600-MW Itaipu project has half its power delivered on three 800-kV series-compensated ac lines (three circuits) and the other half delivered on two ±600-kV bipolar HVDC lines (four circuits). Similarly, the ±500-kV, 1600-MW Intermountain Power Project (IPP) ac alternative comprised two 500-kV ac lines. The IPP takes advantage of the double-circuit nature of the bipolar line and includes a 100% short-term and 50% continuous monopolar overload. The first 6000-MW stage of the transmission for the Three Gorges project in China would have required 5 × 500-kV ac lines as opposed to 2 × ±500-kV, 3000-MW bipolar HVDC lines.

Table 1 contains an economic comparison of capital costs and losses for different ac and dc transmission alternatives for a hypothetical 750-mile, 3000-MW transmission system. The long transmission distance requires intermediate substations or switching stations and shunt reactors for the ac alternatives. The long distance and heavy power transfer, nearly twice the surge-impedance loading on the 500-kV ac alternatives, require a high level of series compensation. These ac station costs are included in the cost estimates for the ac alternatives.

It is interesting to compare the economics for transmission to that of transporting an equivalent amount of energy using other transport methods, in this case using rail transportation of sub-bituminous western coal with a heat content of 8500 Btu/lb to support a 3000-MW base load power plant with heat rate of 8500 Btu/kWh operating at an 85% load factor. The rail route is assumed to be longer than the more direct transmission route—900 miles. Each unit train is comprised of 100 cars each carrying 100 tons of coal. The plant requires three unit trains per day. The annual coal transportation costs are about US$560 million per year at an assumed rate of US$50/ton. This works out to be US$186 kW/year and US$25 per MWh. The annual diesel fuel consumed in the process is in excess of 20 million gallons at 500 net ton-miles per gallon. The rail transportation costs are subject to escalation and congestion whereas the transmission costs are fixed. Furthermore, transmission is the only way to deliver remote renewable resources.

Underground and Submarine Cable Transmission

Unlike the case for ac cables, there is no physical restriction limiting the distance or power level for HVDC underground or submarine cables. Underground cables can be used on shared rights-of-way with other utilities without impacting reliability concerns over use of common corridors.

Copyright 2017 Cengage Learning. All Rights Reserved. May not be copied, scanned, or duplicated, in whole or in part. Due to electronic rights, some third party content may be suppressed from the eBook and/or eChapter(s). Editorial review has deemed that any suppressed content does not materially affect the overall learning experience. Cengage Learning reserves the right to remove additional content at any time if subsequent rights restrictions require it.

	DC Alternatives				AC Alternatives			Hybrid AC/DC Alternative		
Alternative Capital Cost	+ 500 kV Bipole	2 × +500 kV 2 bipoles	+ 600 kV Bipole	+800 kV Bipole	500 kV 2 Single Ckt	500 kV Double Ckt	765 kV 2 Single Ckt	+500 kV Bipole	500 kV Single Ckt	Total AC + DC
Rated power (MW)	3000	4000	3000	3000	3000	3000	3000	3000	1500	4500
Station costs including reactive compensation (M$)	$420	$680	$465	$510	$542	$542	$630	$420	$302	$722
Transmission line cost (M$/mile)	$1.60	$1.60	$1.80	$1.95	$2.00	$3.20	$2.80	$1.60	$2.00	
Distance in miles	750	1500	750	750	1500	750	1500	750	750	1500
Transmission Line Cost (M$)	$1200	$2400	$1350	$1463	$3000	$2400	$4200	$1200	$1500	$2700
Total Cost (M$)	**$1620**	**$3080**	**$1815**	**$1973**	**$3542**	**$2942**	**$4830**	**$1620**	**$1802**	**$3422**
Annual Payment, 30 years @ 10%	$172	$327	$193	$209	$376	$312	$512	$172	$191	$363
Cost per kW-Yr	$57.28	$81.68	$64.18	$69.75	$125.24	$104.03	$170.77	$57.28	$127.40	$80.66
Cost per MWh @ 85%										
Utilization Factor	$7.69	$10.97	$8.62	$9.37	$16.82	$13.97	$22.93	$7.69	$17.11	$10.83
Losses @ full load	193	134	148	103	208	208	139	106	48	154
Losses at full load in %	6.44%	3.35%	4.93%	3.43%	6.93%	6.93%	4.62%	5.29%	4.79%	5.12%
Capitalized cost of losses @$1500kW(M$)	$246	$171	$188	$131	$265	$265	$177	$135	$61	$196
Parameters:										
Interest rate %	10%									
Capitalized cost of losses	$1500 $/kW									

Note:
AC current assumes 94% p.f.

Full load converter station losses = 0.75% per station

Total substation losses (transformers, reactors) assumed = 0.5% of rated power

TABLE 1

Comparative costs of HVDC and EHV AC transmission alternatives

Copyright 2017 Cengage Learning. All Rights Reserved. May not be copied, scanned, or duplicated, in whole or in part. Due to electronic rights, some third party content may be suppressed from the eBook and/or eChapter(s). Editorial review has deemed that any suppressed content does not materially affect the overall learning experience. Cengage Learning reserves the right to remove additional content at any time if subsequent rights restrictions require it.

For underground or submarine cable systems, there is considerable savings in installed cable costs and cost of losses when using HVDC transmission. Depending on the power level to be transmitted, these savings can offset the higher converter station costs at distances of 40 km or more. Furthermore, there is a drop-off in cable capacity with ac transmission over distance due to its reactive component of charging current since cables have higher capacitances and lower inductances than ac overhead lines. Although this can be compensated by intermediate shunt compensation for underground cables at increased expense, it is not practical to do so for submarine cables.

For a given cable conductor area, the line losses with HVDC cables can be about half those of ac cables. This is due to ac cables requiring more conductors (three phases), carrying the reactive component of current, skin-effect, and induced currents in the cable sheath and armor.

With a cable system, the need to balance unequal loadings or the risk of postcontingency overloads often necessitates use of series-connected reactors or phase-shifting transformers. These potential problems do not exist with a controlled HVDC cable system.

Extruded HVDC cables with prefabricated joints used with VSC-based transmission are lighter, more flexible, and easier to splice than the mass-impregnated oil-paper cables (MINDs) used for conventional HVDC transmission, thus making them more conducive for land cable applications where transport limitations and extra splicing costs can drive up installation costs. The lower-cost cable installations made possible by the extruded HVDC cables and prefabricated joints makes long-distance underground transmission economically feasible for use in areas with rights-of-way constraints or subject to permitting difficulties or delays with overhead lines.

Asynchronous Ties

With HVDC transmission systems, interconnections can be made between asynchronous networks for more economic or reliable system operation. The asynchronous interconnection allows interconnections of mutual benefit while providing a buffer between the two systems. Often these interconnections use back-to-back converters with no transmission line. Asynchronous HVDC links act as an effective “firewall” against propagation of cascading outages in one network from passing to another network.

Many asynchronous interconnections exist in North America between the Eastern and Western interconnected systems, between the Electric Reliability Council of Texas (ERCOT) and its neighbors, [e.g., Mexico and the Southwest Power Pool (SPP)], and between Quebec and its neighbors (e.g., New England and the Maritimes). The August 2003 Northeast blackout provides an example of the “firewall” against cascading outages provided by asynchronous interconnections. As the outage expanded and propagated around the lower Great Lakes and through Ontario and New York, it stopped at the

Copyright 2017 Cengage Learning. All Rights Reserved. May not be copied, scanned, or duplicated, in whole or in part. Due to electronic rights, some third party content may be suppressed from the eBook and/or eChapter(s). Editorial review has deemed that any suppressed content does not materially affect the overall learning experience. Cengage Learning reserves the right to remove additional content at any time if subsequent rights restrictions require it.

asynchronous interface with Quebec. Quebec was unaffected; the weak ac interconnections between New York and New England tripped, but the HVDC links from Quebec continued to deliver power to New England.

Regulators try to eliminate "seams" in electrical networks because of their potential restriction on power markets. Electrical seams, however, serve as natural points of separation by acting as "shearpins," thereby reducing the impact of large-scale system disturbances. Asynchronous ties can eliminate market seams while retaining natural points of separation.

Interconnections between asynchronous networks are often at the periphery of the respective systems where the networks tend to be weak relative to the desired power transfer. Higher power transfers can be achieved with improved voltage stability in weak system applications using CCCs. The dynamic voltage support and improved voltage stability offered by VSC-based converters permits even higher power transfers without as much need for ac system reinforcement. VSCs do not suffer commutation failures, allowing fast recoveries from nearby ac faults. Economic power schedules that reverse power direction can be made without any restrictions since there is no minimum power or current restrictions.

Offshore Transmission

Self-commutation, dynamic voltage control, and black-start capability allow compact VSC HVDC transmission to serve isolated loads on islands or offshore production platforms over long-distance submarine cables. This capability can eliminate the need for running expensive local generation or provide an outlet for offshore generation such as that from wind. The VSCs can operate at variable frequency to more efficiently drive large compressor or pumping loads using high-voltage motors. Figure 11 shows the Troll A production platform in the North Sea where power to drive compressors is delivered from shore

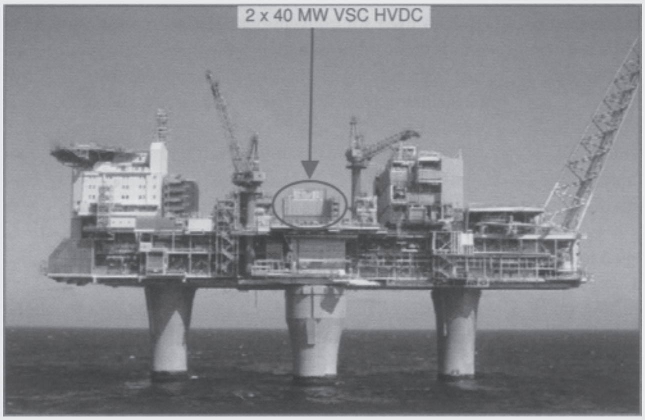

Figure 11 VSC power supply to Troll A production platform

Copyright 2017 Cengage Learning. All Rights Reserved. May not be copied, scanned, or duplicated, in whole or in part. Due to electronic rights, some third party content may be suppressed from the eBook and/or eChapter(s). Editorial review has deemed that any suppressed content does not materially affect the overall learning experience. Cengage Learning reserves the right to remove additional content at any time if subsequent rights restrictions require it.

to reduce the higher carbon emissions and higher O&M costs associated with less efficient platform-based generation.

Large remote wind generation arrays require a collector system, reactive power support, and outlet transmission. Transmission for wind generation must often traverse scenic or environmentally sensitive areas or bodies of water. Many of the better wind sites with higher capacity factors are located offshore. VSC-based HVDC transmission allows efficient use of long-distance land or submarine cables and provides reactive support to the wind-generation complex. Figure 12 shows a design for an offshore converter station designed to transmit power from offshore wind generation.

Multiterminal Systems

Most HVDC systems are for point-to-point transmission with a converter station at each end. The use of intermediate taps is rare. Conventional HVDC transmission uses voltage polarity reversal to reverse the power direction. Polarity reversal requires no special switching arrangement for a two-terminal system where both terminals reverse polarity by control action with no switching to reverse power direction. Special dc-side switching arrangements are needed for polarity reversal in a multiterminal system, however, where it may be desired to reverse the power direction at a tap while maintaining the same power direction on the remaining terminals. For a bipolar system, this can be done by connecting the converter to the opposite pole. VSC HVDC transmission, however, reverses power through reversal of the current direction rather than voltage polarity. Thus, power can be reversed at an intermediate tap independently of the main power flow direction without switching to reverse voltage polarity.

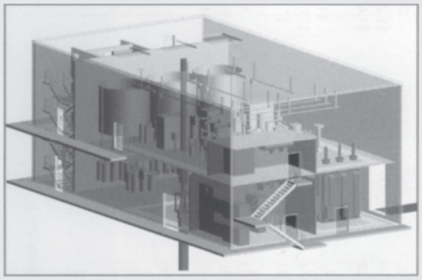

Figure 12 VSC converter for offshore wind generation

Power Delivery to Large Urban Areas

Power supply for large cities depends on local generation and power import capability. Local generation is often older and less efficient than newer units located remotely. Often, however, the older, less-efficient units located near the city center must be dispatched out-of-merit because they must be run for voltage support or reliability due to inadequate transmission. Air-quality regulations may limit the availability of these units. New transmission into large cities is difficult to site due to right-of-way limitations and land-use constraints.

Compact VSC-based underground transmission circuits can be placed on existing dual-use rights-of-way to bring in power as well as to provide voltage support, allowing a more economical power supply

Copyright 2017 Cengage Learning. All Rights Reserved. May not be copied, scanned, or duplicated, in whole or in part. Due to electronic rights, some third party content may be suppressed from the eBook and/or eChapter(s). Editorial review has deemed that any suppressed content does not materially affect the overall learning experience. Cengage Learning reserves the right to remove additional content at any time if subsequent rights restrictions require it.

without compromising reliability. The receiving terminal acts like a virtual generator, delivering power and supplying voltage regulation and dynamic reactive power reserve. Stations are compact and housed mainly indoors, making siting in urban areas somewhat easier. Furthermore, the dynamic voltage support offered by the VSC can often increase the capability of the adjacent ac transmission.

System Configurations and Operating Modes

Figure 13 shows the different common system configurations and operating modes used for HVDC transmission. Monopolar systems are the simplest and least expensive systems for moderate power transfers since only two converters and one high-voltage insulated cable or line conductor are required. Such systems have been used with low-voltage electrode lines and sea electrodes to carry the return current in submarine cable crossings.

In some areas, conditions are not conducive to monopolar earth or sea return. This could be the case in heavily congested areas, fresh-water cable crossings, or areas with high earth resistivity. In such cases a metallic neutral- or low-voltage cable is used for the return path, and the dc circuit uses a simple local ground connection for potential reference only. Back-to-back stations are used for interconnection of asynchronous networks and use ac lines to connect

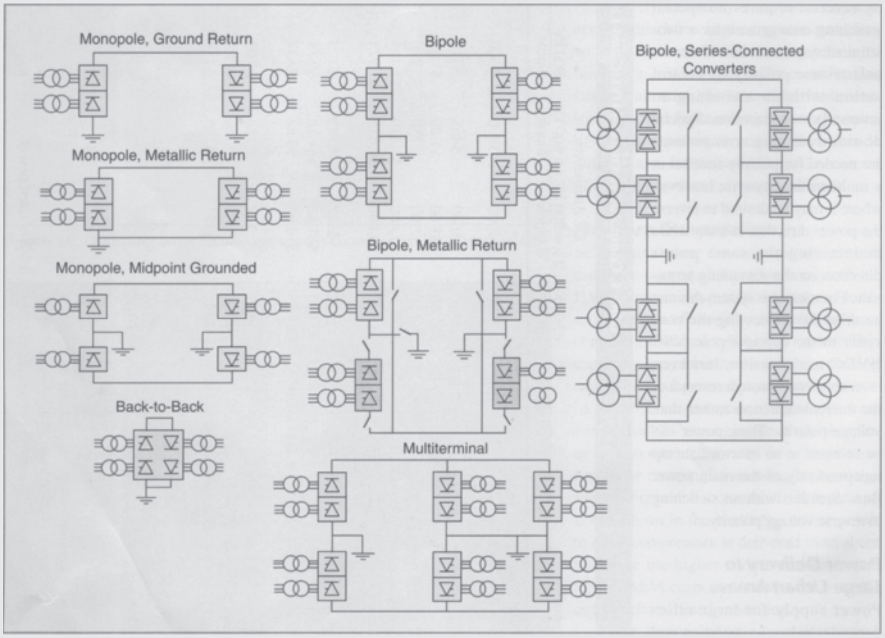
Monopole, Ground Return
Bipole
Bipole, Series-Connected Converters
Monopole, Metallic Return
Monopole, Midpoint Grounded
Bipole, Metallic Return
Back-to-Back
Multiterminal

Figure 13 HVDC configurations and operating modes

Copyright 2017 Cengage Learning. All Rights Reserved. May not be copied, scanned, or duplicated, in whole or in part. Due to electronic rights, some third party content may be suppressed from the eBook and/or eChapter(s). Editorial review has deemed that any suppressed content does not materially affect the overall learning experience. Cengage Learning reserves the right to remove additional content at any time if subsequent rights restrictions require it.

on either side. In such systems, power transfer is limited by the relative capacities of the adjacent ac systems at the point of connection.

As an economic alternative to a monopolar system with metallic return, the midpoint of a 12-pulse converter can be connected to earth directly or through an impedance and two half-voltage cables or line conductors can be used. The converter is only operated in 12-pulse mode so there is never any stray earth current.

VSC-based HVDC transmission is usually arranged with a single converter connected pole-to-pole rather than pole-to-ground. The center point of the converter is connected to ground through a high impedance to provide a reference for the dc voltage. Thus, half the converter dc voltage appears across the insulation on each of the two dc cables, one positive and the other negative.

The most common configuration for modern overhead HVDC transmission lines is bipolar with a single 12-pulse converter for each pole at each terminal. This gives two independent dc circuits with each capable of half capacity. For normal balanced operation there is no earth current. Monopolar earth return operation, often with overload capacity, can be used during outages of the opposite pole.

Earth return operation can be minimized during monopolar outages by using the opposite pole line for metallic return via pole/converter bypass switches at each end. This requires a metallic-return transfer breaker in the ground electrode line at one of the dc terminals to commutate the current from the relatively low resistance of the earth into that of the dc line conductor. Metallic return operation capability is provided for most dc transmission systems. This not only is effective during converter outages but also during line insulation failures where the remaining insulation strength is adequate to withstand the low resistive voltage drop in the metallic return path.

For very-high-power HVDC transmission, especially at dc voltages above ±500 kV (i.e., ±600 kV or ±800 kV), series-connected converters can be used to reduce the energy unavailability for individual converter outages or partial line insulation failure. By using two series-connected converters per pole in a bipolar system, only one quarter of the transmission capacity is lost for a converter outage or if the line insulation for the affected pole is degraded to where it can only support half the rated dc line voltage. Operating in this mode also avoids the need to transfer to monopolar metallic return to limit the duration of emergency earth return.

Station Design and Layout

Conventional HVDC

The converter station layout depends on a number of factors such as the dc system configuration (i.e., monopolar, bipolar, or back-to-back), ac filtering, and reactive power compensation requirements. The thyristor valves are air-insulated, water-cooled, and enclosed in a converter building often referred to as a valve hall. For back-to-back ties with their

Copyright 2017 Cengage Learning. All Rights Reserved. May not be copied, scanned, or duplicated, in whole or in part. Due to electronic rights, some third party content may be suppressed from the eBook and/or eChapter(s). Editorial review has deemed that any suppressed content does not materially affect the overall learning experience. Cengage Learning reserves the right to remove additional content at any time if subsequent rights restrictions require it.

characteristically low dc voltage, thyristor valves can be housed in prefabricated electrical enclosures, in which case a valve hall is not required.

To obtain a more compact station design and reduce the number of insulated high-voltage wall bushings, converter transformers are often placed adjacent to the valve hall with valve winding bushings protruding through the building walls for connection to the valves. Double or quadruple valve structures, housing valve modules, are used within the valve hall. Valve arresters are located immediately adjacent to the valves. Indoor motor-operated grounding switches are used for personnel safety during maintenance. Closed-loop valve cooling systems are used to circulate the cooling medium of deionized water or water-glycol mix through the indoor thyristor valves with heat transfer to dry coolers located outdoors. Area requirements for conventional HVDC converter stations are influenced by the ac system voltage and reactive power compensation requirements where each individual bank rating may be limited by such system requirements as reactive power exchange and maximum voltage step on bank switching. The ac yard with filters and shunt compensation can take up as much as three quarters of the total area requirements of the converter station. Figure 14 shows a typical arrangement for an HVDC converter station.

VSC-Based HVDC

The transmission circuit consists of a bipolar two-wire HVDC system with converters connected pole-to-pole. DC capacitors are used to provide a

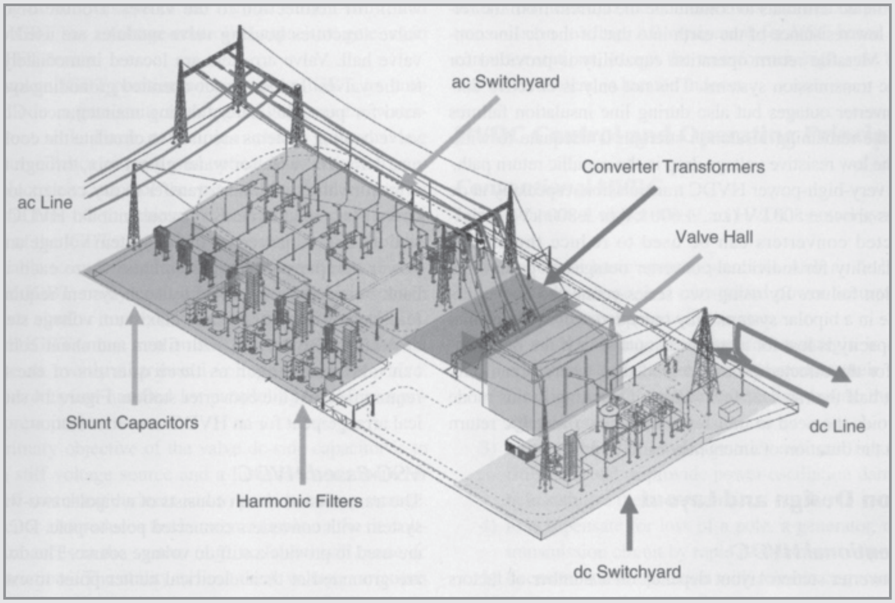

Figure 14 Monopolar HVDC converter station

Copyright 2017 Cengage Learning. All Rights Reserved. May not be copied, scanned, or duplicated, in whole or in part. Due to electronic rights, some third party content may be suppressed from the eBook and/or eChapter(s). Editorial review has deemed that any suppressed content does not materially affect the overall learning experience. Cengage Learning reserves the right to remove additional content at any time if subsequent rights restrictions require it.

stiff dc voltage source. The dc capacitors are grounded at their electrical center point to establish the earth reference potential for the transmission system. There is no earth return operation. The converters are coupled to the ac system through ac phase reactors and power transformers. Unlike most conventional HVDC systems, harmonic filters are located between the phase reactors and power transformers. Therefore, the transformers are exposed to no dc voltage stresses or harmonic loading, allowing use of ordinary power transformers. Figure 15 shows the station arrangement for a ±150-kV, 350 to 550-MW VSC converter station.

The IGBT valves used in VSC converters are comprised of series-connected IGBT positions. The IGBT is a hybrid device exhibiting the low forward drop of a bipolar transistor as a conducting device. Instead of the regular current-controlled base, the IGBT has a voltage-controlled capacitive gate, as in the MOSFET device.

A complete IGBT position consists of an IGBT, an anti-parallel diode, a gate unit, a voltage divider, and a water-cooled heat sink. Each gate unit includes gate-driving circuits, surveillance circuits, and optical interface. The gate-driving electronics control the gate voltage and current at turn-on and turn-off to achieve optimal turn-on and turn-off processes of the IGBTs.

To be able to switch voltages higher than the rated voltage of one IGBT, many positions are connected in series in each valve similar to thyristors in conventional HVDC valves. All IGBTs must turn on and off at the same moment to achieve an evenly distributed voltage across the valve. Higher currents are handled by paralleling IGBT components or press packs.

The primary objective of the valve dc-side capacitor is to provide a stiff voltage source and a low-inductance path for the turn-off switching currents and to provide

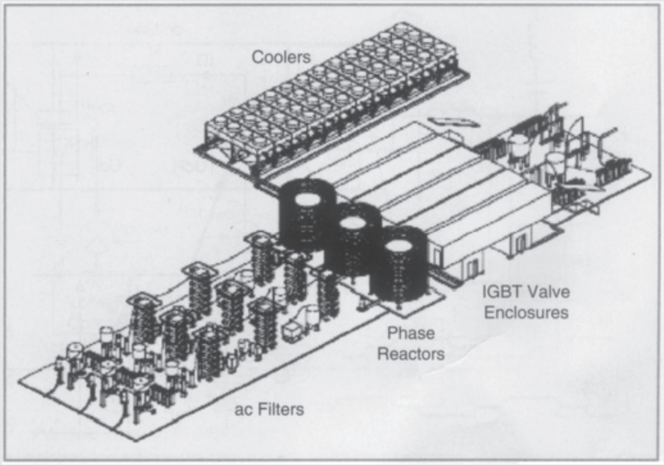

Figure 15 VSC HVDC converter station

Copyright 2017 Cengage Learning. All Rights Reserved. May not be copied, scanned, or duplicated, in whole or in part. Due to electronic rights, some third party content may be suppressed from the eBook and/or eChapter(s). Editorial review has deemed that any suppressed content does not materially affect the overall learning experience. Cengage Learning reserves the right to remove additional content at any time if subsequent rights restrictions require it.

energy storage. The capacitor also reduces the harmonic ripple on the dc voltage. Disturbances in the system (e.g., ac faults) cause dc voltage variations. The ability to limit these voltage variations depends on the size of the dc-side capacitor. Since the dc capacitors are used indoors, dry capacitors are used.

AC filters for VSC HVDC converters have smaller ratings than those for conventional converters and are not required for reactive power compensation. Therefore, these filters are always connected to the converter bus and not switched with transmission loading. All equipment for VSC-based HVDC converter stations, except the transformer, high-side breaker, and valve coolers, is located indoors.

HVDC Control and Operating Principles

Conventional HVDC

The fundamental objectives of an HVDC control system are as follows:

1. to control basic system quantities such as dc line current, dc voltage, and transmitted power accurately and with sufficient speed of response;
2. to maintain adequate commutation margin in inverter operation so that the valves can recover their forward blocking capability after conduction before their voltage polarity reverses;
3. to control higher-level quantities such as frequency in isolated mode or provide power oscillation damping to help stabilize the ac network;
4. to compensate for loss of a pole, a generator, or an ac transmission circuit by rapid readjustment of power;
5. to ensure stable operation with reliable commutation in the presence of system disturbances;
6. to minimize system losses and converter reactive power consumption; and
7. to ensure proper operation with fast and stable recoveries during ac system faults and disturbances.

For conventional HVDC transmission, one terminal sets the dc voltage level while the other terminal(s) regulates the (its) dc current by controlling its output voltage relative to that maintained by the voltage-setting terminal. Since the dc line resistance is low, large changes in current and hence power can be made with relatively small changes in firing angle (alpha). Two independent methods exist for controlling the converter dc output voltage. These are (1) by changing the ratio between the direct voltage and the ac voltage by varying the delay angle or (2) by changing the converter ac voltage via load tap changers (LTCs) on the converter transformer. Whereas the former method is rapid, the latter method is slow due to the limited speed of response of the LTC. Use of high-delay angles to achieve a larger dynamic range, however, increases the converter reactive power consumption.

Copyright 2017 Cengage Learning. All Rights Reserved. May not be copied, scanned, or duplicated, in whole or in part. Due to electronic rights, some third party content may be suppressed from the eBook and/or eChapter(s). Editorial review has deemed that any suppressed content does not materially affect the overall learning experience. Cengage Learning reserves the right to remove additional content at any time if subsequent rights restrictions require it.

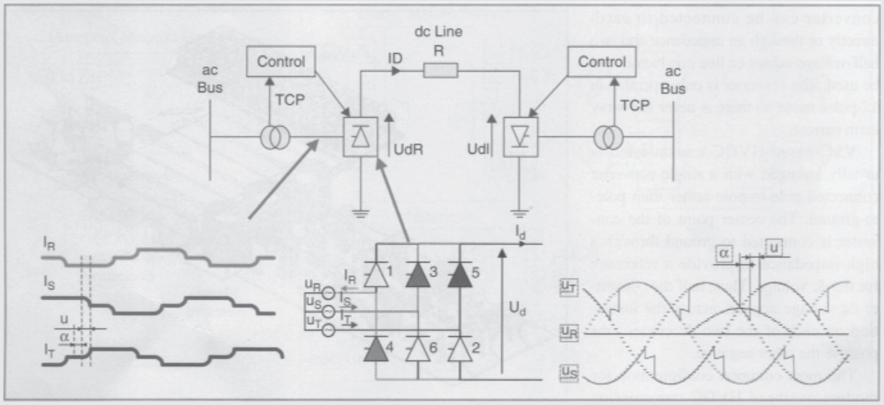

Figure 16 Conventional HVDC control

To minimize the reactive power demand while still providing adequate dynamic control range and commutation margin, the LTC is used at the rectifier terminal to keep the delay angle within its desired steady-state range (e.g., 13–18°) and at the inverter to keep the extinction angle within its desired range (e.g., 17–20°) if the angle is used for dc voltage control or to maintain rated dc voltage if operating in minimum commutation margin control mode. Figure 16 shows the characteristic transformer current and dc bridge voltage waveforms along with the controlled items Ud, Id, and tap changer position (TCP).

VSC-Based HVDC

Power can be controlled by changing the phase angle of the converter ac voltage with respect to the filter bus voltage, whereas the reactive power can be controlled by changing the magnitude of the fundamental component of the converter ac voltage with respect to the filter bus voltage. By controlling these two aspects of the converter voltage, operation in all four quadrants is possible. This means that the converter can be operated in the middle of its reactive power range near unity power factor to maintain dynamic reactive power reserve for contingency voltage support similar to a static var compensator. It also means that the real power transfer can be changed rapidly without altering the reactive power exchange with the ac network or waiting for switching of shunt compensation.

Being able to independently control ac voltage magnitude and phase relative to the system voltage allows use of separate active and reactive power control loops for HVDC system regulation. The active power control loop can be set to control either the active power or the dc-side voltage. In a dc link, one station is then selected to control the active power while the other must be set to control the dc-side voltage. The reactive power control loop can be set to control either the reactive power or the ac-side voltage. Either of these two modes can be selected independently at either end of the dc link.

Copyright 2017 Cengage Learning. All Rights Reserved. May not be copied, scanned, or duplicated, in whole or in part. Due to electronic rights, some third party content may be suppressed from the eBook and/or eChapter(s). Editorial review has deemed that any suppressed content does not materially affect the overall learning experience. Cengage Learning reserves the right to remove additional content at any time if subsequent rights restrictions require it.

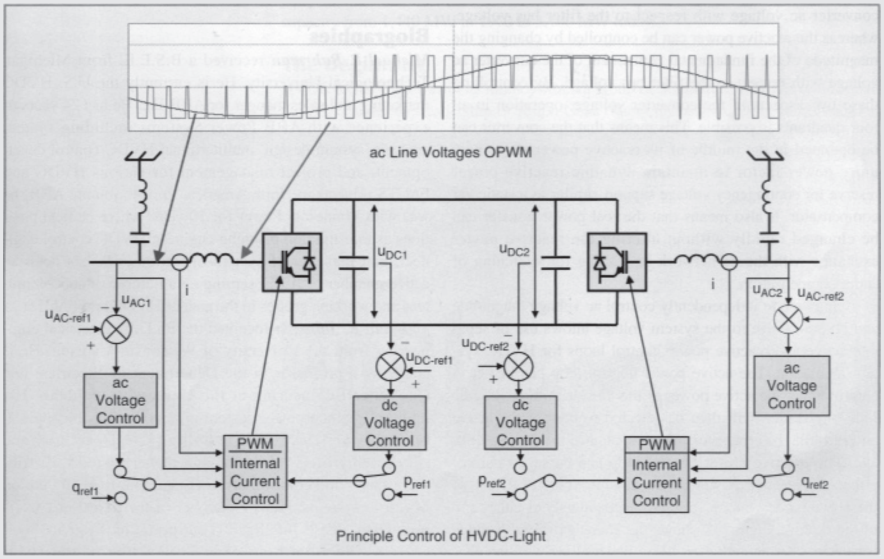
ac Line Voltages OPWM
u_{DC1}
u_{DC2}
i
i
u_{AC1}
$u_{AC\text{-}ref1}$
u_{AC2}
$u_{AC\text{-}ref2}$
$u_{DC\text{-}ref1}$
$u_{DC\text{-}ref2}$
ac Voltage Control
dc Voltage Control
dc Voltage Control
ac Voltage Control
PWM Internal Current Control
PWM Internal Current Control
q_{ref1}
P_{ref1}
P_{ref2}
q_{ref2}
Principle Control of HVDC-Light

Figure 17 Control of VSC HVDC transmission

Figure 17 shows the characteristic ac voltage waveforms before and after the ac filters along with the controlled items Ud, Id, Q, and Uac.

Conclusions

The favorable economics of long-distance bulk-power transmission with HVDC together with its controllability make it an interesting alternative or complement to ac transmission. The higher voltage levels, mature technology, and new converter designs have significantly increased the interest in HVDC transmission and expanded the range of applications.

For Further Reading

B. Jacobson, Y. Jiang-Hafner, R. Rey, and G. Asplund, "HVDC with voltage source converters and extruded cables for up to ±300 kV and 1000 MW," in Proc. *CIGRE 2006*, Paris, France, pp. B4–105.

L. Ronstrom, B.D. Railing, J.J. Miller, R. Steckley, G. Moreau, R. Bard, and J. Lindberg, "Cross sound cable project second generation VSC technology for HVDC," *Proc. CIGRE 2006*, Paris, France, pp. B4–102.

M. Bahrman, D. Dickinson, P. Fisher, and M. Stoltz, "The Rapid City Tie—New Technology Tames the East-West Interconnection," in *Proc. Minnesota Power Systems Conf.*, St. Paul, MN, Nov. 2004.

D. McCallum, G. Moreau, J. Primeau, D. Soulier, M. Bahrman, and B. Ekehov, "Multiterminal Integration of the Nicolet Converter Station into the Quebec-New England Phase II Transmission System," in *Proc. CIGRE* 1994, Paris, France.

A. Ekstrom and G. Liss, "A refined HVDC control system," *IEEE Trans. Power Systems*, vol. PAS-89, pp. 723–732, May–June 1970.

Copyright 2017 Cengage Learning. All Rights Reserved. May not be copied, scanned, or duplicated, in whole or in part. Due to electronic rights, some third party content may be suppressed from the eBook and/or eChapter(s). Editorial review has deemed that any suppressed content does not materially affect the overall learning experience. Cengage Learning reserves the right to remove additional content at any time if subsequent rights restrictions require it.

Biographies

Michael P. Bahrman received a B.S.E.E. from Michigan Technological University. He is currently the U.S. HVDC marketing and sales manager for ABB Inc. He has 24 years of experience with ABB Power Systems, including system analysis, system design, multiterminal HVDC control development, and project management for various HVDC and FACTS projects in North America. Prior to joining ABB, he was with Minnesota Power for ten years where he held positions as transmission planning engineer, HVDC control engineer, and manager of system operations. He has been an active member of IEEE, serving on a number of subcommittees and working groups in the area of HVDC and FACTS.

Brian K. Johnson received the PhD in electrical engineering from the University of Wisconsin-Madison. He is currently a professor in the Department of Electrical and Computer Engineering at the University of Idaho. His interests include power system protection and the application of power electronics to utility systems, security, and survivability of ITS systems and power systems, distributed sensor and control networks, and real-time simulation of traffic systems. He is a member of the Board of Governors of the IEEE Intelligent Transportation Systems Society and the Administrative Committee of the IEEE Council on Superconductivity. ■

5.1 MEDIUM AND SHORT LINE APPROXIMATIONS

In this section, short and medium-length transmission-line approximations as a means of introducing *ABCD* parameters are presented. Some readers may prefer to start in Section 5.2, which presents the exact transmission-line equations.

It is convenient to represent a transmission line by the two-port network shown in Figure 5.1, where V_S and I_S are the sending-end voltage and current, and V_R and I_R are the receiving-end voltage and current.

The relation between the sending-end and receiving-end quantities can be written as

$$V_S = AV_R + BI_R \quad \text{volts} \tag{5.1.1}$$

$$I_S = CV_R + DI_R \quad \text{A} \tag{5.1.2}$$

FIGURE 5.1

Representation of two-port network

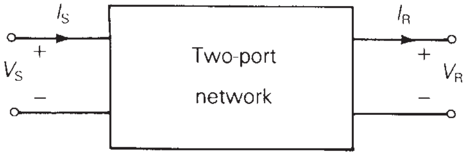

Copyright 2017 Cengage Learning. All Rights Reserved. May not be copied, scanned, or duplicated, in whole or in part. Due to electronic rights, some third party content may be suppressed from the eBook and/or eChapter(s). Editorial review has deemed that any suppressed content does not materially affect the overall learning experience. Cengage Learning reserves the right to remove additional content at any time if subsequent rights restrictions require it.

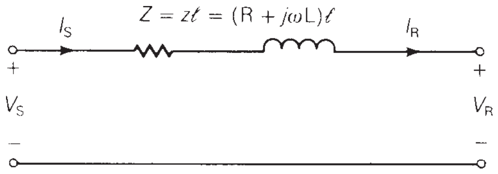

FIGURE 5.2

Short transmission line

or, in matrix format,

$$\begin{bmatrix} V_S \\ I_S \end{bmatrix} = \left[\begin{array}{c|c} A & B \\ \hline C & D \end{array}\right] \begin{bmatrix} V_R \\ I_R \end{bmatrix} \tag{5.1.3}$$

where A, B, C, and D are parameters that depend on the transmission-line constants R, L, C, and G. The $ABCD$ parameters are, in general, complex numbers. A and D are dimensionless. B has units of ohms, and C has units of siemens. Network theory texts [5] show that $ABCD$ parameters apply to linear, passive, bilateral two-port networks, with the following general relation:

$$AD - BC = 1 \tag{5.1.4}$$

The circuit in Figure 5.2 represents a short transmission line, usually applied to overhead 60-Hz lines less than 25 km in length. Only the series resistance and reactance are included. The shunt admittance is neglected. The circuit applies to either single-phase or completely transposed three-phase lines operating under balanced conditions. For a completely transposed three-phase line, Z is the series impedance, V_S and I_R are positive-sequence line-to-neutral voltages, and I_S and I_R are positive-sequence line currents.

To avoid confusion between total series impedance and series impedance per unit length, use the following notation:

$z = \mathrm{R} + j\omega\mathrm{L} \quad \Omega/\mathrm{m}$, series impedance per unit length
$y = \mathrm{G} + j\omega\mathrm{C} \quad \mathrm{S/m}$, shunt admittance per unit length
$Z = zl \quad \Omega$, total series impedance
$Y = yl \quad \mathrm{S}$, total shunt admittance
l = line length m

Recall that shunt conductance G is usually neglected for overhead transmission.

The $ABCD$ parameters for the short line in Figure 5.2 are easily obtained by writing a KVL and KCL equation as

$$V_S = V_R + ZI_R \tag{5.1.5}$$

$$I_S = I_R \tag{5.1.6}$$

or, in matrix format,

$$\begin{bmatrix} V_S \\ I_S \end{bmatrix} = \left[\begin{array}{c|c} 1 & Z \\ \hline 0 & 1 \end{array}\right] \begin{bmatrix} V_R \\ I_R \end{bmatrix} \tag{5.1.7}$$

Copyright 2017 Cengage Learning. All Rights Reserved. May not be copied, scanned, or duplicated, in whole or in part. Due to electronic rights, some third party content may be suppressed from the eBook and/or eChapter(s). Editorial review has deemed that any suppressed content does not materially affect the overall learning experience. Cengage Learning reserves the right to remove additional content at any time if subsequent rights restrictions require it.

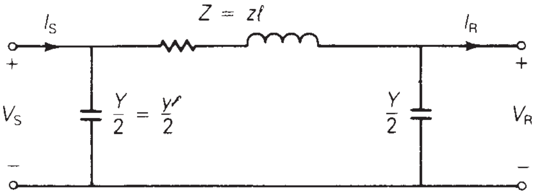

FIGURE 5.3 Medium-length transmission line—nominal π circuit

Comparing (5.1.7) and (5.1.3), the *ABCD* parameters for a short line are

$$A = D = 1 \text{ per unit} \tag{5.1.8}$$
$$B = Z\ \Omega \tag{5.1.9}$$
$$C = 0\ \text{S} \tag{5.1.10}$$

For medium-length lines, typically ranging from 25 to 250 km at 60 Hz, it is common to lump the total shunt capacitance and locate half at each end of the line. Such a circuit, called a *nominal π circuit*, is shown in Figure 5.3.

To obtain the *ABCD* parameters of the nominal π circuit, note first that the current in the series branch in Figure 5.3 equals $I_R + \frac{V_R Y}{2}$. Then, writing a KVL equation,

$$\begin{aligned} V_S &= V_R + Z\left(I_R + \frac{V_R Y}{2}\right) \\ &= \left(1 + \frac{YZ}{2}\right) V_R + Z I_R \end{aligned} \tag{5.1.11}$$

Also, writing a KCL equation at the sending end,

$$I_S = I_R + \frac{V_R Y}{2} + \frac{V_S Y}{2} \tag{5.1.12}$$

Using (5.1.11) in (5.1.12),

$$\begin{aligned} I_S &= I_R + \frac{V_R Y}{2} + \left[\left(1 + \frac{YZ}{2}\right) V_R + Z I_R\right] \frac{Y}{2} \\ &= Y\left(1 + \frac{YZ}{4}\right) V_R + \left(1 + \frac{YZ}{2}\right) I_R \end{aligned} \tag{5.1.13}$$

Writing (5.1.11) and (5.1.13) in matrix format,

$$\begin{bmatrix} V_S \\ \\ I_S \end{bmatrix} = \left[\begin{array}{c|c} \left(1 + \frac{YZ}{2}\right) & Z \\ \hline Y\left(1 + \frac{YZ}{4}\right) & \left(1 + \frac{YZ}{2}\right) \end{array}\right] \begin{bmatrix} V_R \\ \\ I_R \end{bmatrix} \tag{5.1.14}$$

Copyright 2017 Cengage Learning. All Rights Reserved. May not be copied, scanned, or duplicated, in whole or in part. Due to electronic rights, some third party content may be suppressed from the eBook and/or eChapter(s). Editorial review has deemed that any suppressed content does not materially affect the overall learning experience. Cengage Learning reserves the right to remove additional content at any time if subsequent rights restrictions require it.

Thus, comparing (5.1.14) and (5.1.3)

$$A = D = 1 + \frac{YZ}{2} \quad \text{per unit} \tag{5.1.15}$$

$$B = Z \quad \Omega \tag{5.1.16}$$

$$C = Y\left(1 + \frac{YZ}{4}\right) \quad \text{S} \tag{5.1.17}$$

Note that for both the short and medium-length lines, the relation $AD - BC = 1$ is verified. Note also that since the line is the same when viewed from either end, $A = D$.

Figure 5.4 gives the *ABCD* parameters for some common networks, including a series impedance network that approximates a short line and a π circuit that approximates a medium-length line. A medium-length line could also be approximated by the T circuit shown in Figure 5.4, lumping half of the series impedance at each end

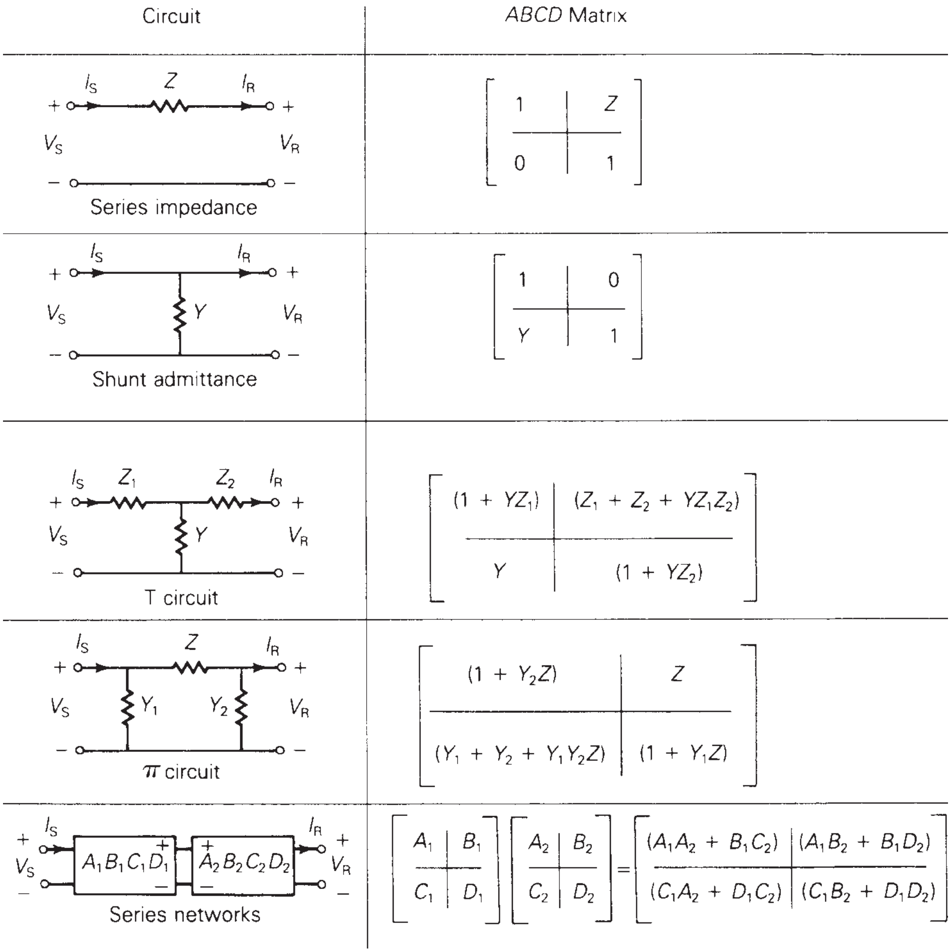
Circuit
ABCD Matrix
I_S Z I_R
V_S V_R
Series impedance
$\begin{bmatrix} 1 & Z \\ 0 & 1 \end{bmatrix}$
Shunt admittance
Y
$\begin{bmatrix} 1 & 0 \\ Y & 1 \end{bmatrix}$
T circuit
Z_1 Z_2 Y
$\begin{bmatrix} (1 + YZ_1) & (Z_1 + Z_2 + YZ_1Z_2) \\ Y & (1 + YZ_2) \end{bmatrix}$
π circuit
Z Y_1 Y_2
$\begin{bmatrix} (1 + Y_2Z) & Z \\ (Y_1 + Y_2 + Y_1Y_2Z) & (1 + Y_1Z) \end{bmatrix}$
Series networks
$A_1B_1C_1D_1$ $A_2B_2C_2D_2$
$\begin{bmatrix} A_1 & B_1 \\ C_1 & D_1 \end{bmatrix}\begin{bmatrix} A_2 & B_2 \\ C_2 & D_2 \end{bmatrix} = \begin{bmatrix} (A_1A_2 + B_1C_2) & (A_1B_2 + B_1D_2) \\ (C_1A_2 + D_1C_2) & (C_1B_2 + D_1D_2) \end{bmatrix}$

FIGURE 5.4

ABCD parameters of common networks

Copyright 2017 Cengage Learning. All Rights Reserved. May not be copied, scanned, or duplicated, in whole or in part. Due to electronic rights, some third party content may be suppressed from the eBook and/or eChapter(s). Editorial review has deemed that any suppressed content does not materially affect the overall learning experience. Cengage Learning reserves the right to remove additional content at any time if subsequent rights restrictions require it.

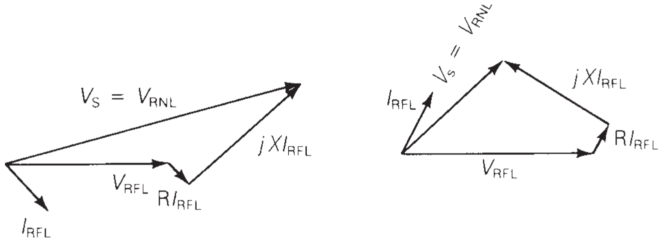

(a) Lagging p.f. load (b) Leading p.f. load

FIGURE 5.5

Phasor diagrams for a short transmission line

of the line. Also given are the *ABCD* parameters for networks in series, which are conveniently obtained by multiplying the *ABCD* matrices of the individual networks.

ABCD parameters can be used to describe the variation of line voltage with line loading. *Voltage regulation* is the change in voltage at the receiving end of the line when the load varies from no-load to a specified full load at a specified power factor, while the sending-end voltage is held constant. Expressed in percent of full-load voltage,

$$\text{percent VR} = \frac{|V_{RNL}| - |V_{RFL}|}{|V_{RFL}|} \times 100 \tag{5.1.18}$$

where percent VR is the percent voltage regulation, $|V_{RNL}|$ is the magnitude of the no-load receiving-end voltage, and $|V_{RFL}|$ is the magnitude of the full-load receiving-end voltage.

The effect of load power factor on voltage regulation is illustrated by the phasor diagrams in Figure 5.5 for short lines. The phasor diagrams are graphical representations of (5.1.5) for lagging and leading power factor loads. Note that, from (5.1.5) at no-load, $I_{RNL} = 0$ and $V_S = V_{RNL}$ for a short line. As shown, the higher (worse) voltage regulation occurs for the lagging p.f. load, where V_{RNL} exceeds V_{RFL} by the larger amount. A smaller or even negative voltage regulation occurs for the leading p.f. load. In general, the no-load voltage is, from (5.1.1) with $I_{RNL} = 0$,

$$V_{RNL} = \frac{V_S}{A} \tag{5.1.19}$$

which can be used in (5.1.18) to determine voltage regulation.

In practice, transmission-line voltages decrease when heavily loaded and increase when lightly loaded. When voltages on EHV lines are maintained within +5% of rated voltage, corresponding to about 10% voltage regulation, unusual operating problems are not encountered. Ten percent voltage regulation for lower voltage lines including transformer-voltage drops is also considered good operating practice.

In addition to voltage regulation, line loadability is an important issue. Three major line-loading limits are (1) the thermal limit, (2) the voltage-drop limit, and (3) the steady-state stability limit.

The maximum temperature of a conductor determines its thermal limit. Conductor temperature affects the conductor sag between towers and the loss of

Copyright 2017 Cengage Learning. All Rights Reserved. May not be copied, scanned, or duplicated, in whole or in part. Due to electronic rights, some third party content may be suppressed from the eBook and/or eChapter(s). Editorial review has deemed that any suppressed content does not materially affect the overall learning experience. Cengage Learning reserves the right to remove additional content at any time if subsequent rights restrictions require it.

conductor tensile strength due to annealing. If the temperature is too high, prescribed conductor-to-ground clearances may not be met, or the elastic limit of the conductor may be exceeded such that it cannot shrink to its original length when cooled. Conductor temperature depends on the current magnitude and its time duration, as well as on ambient temperature, wind velocity, and conductor surface conditions. Appendix Tables A.3 and A.4 give approximate current-carrying capacities of copper and ACSR conductors. The loadability of short transmission lines (less than 25 km in length for 60-Hz overhead lines) is usually determined by the conductor thermal limit or by ratings of line terminal equipment such as circuit breakers.

For longer line lengths (up to 300 km), line loadability is often determined by the voltage-drop limit. Although more severe voltage drops may be tolerated in some cases, a heavily loaded line with $V_R/V_S \geq 0.95$ is usually considered safe operating practice. For line lengths over 300 km, steady-state stability becomes a limiting factor. Stability, discussed in Section 5.4, refers to the ability of synchronous machines on either end of a line to remain in synchronism.

EXAMPLE 5.1

ABCD parameters and the nominal π circuit: medium-length line

A three-phase, 60-Hz, completely transposed 345-kV, 200-km line has two 795,000-cmil 26/2 ACSR conductors per bundle and the following positive-sequence line constants:

$$z = 0.032 + j0.35 \quad \Omega/\text{km}$$
$$y = j4.2 \times 10^{-6} \quad \text{S/km}$$

Full load at the receiving end of the line is 700 MW at 0.99 p.f. leading and at 95% of rated voltage. Assuming a medium-length line, determine the following:

a. *ABCD* parameters of the nominal π circuit

b. Sending-end voltage V_S, current I_S, and real power P_S

c. Percent voltage regulation

d. Thermal limit, based on the approximate current-carrying capacity listed in Table A.4

e. Transmission-line efficiency at full load

SOLUTION

a. The total series impedance and shunt admittance values are

$$Z = zl = (0.032 + j0.35)(200) = 6.4 + j70 = 70.29\underline{/84.78^\circ} \quad \Omega$$
$$Y = yl = (j4.2 \times 10^{-6})(200) = 8.4 \times 10^{-4}\underline{/90^\circ} \quad \text{S}$$

(*Continued*)

Copyright 2017 Cengage Learning. All Rights Reserved. May not be copied, scanned, or duplicated, in whole or in part. Due to electronic rights, some third party content may be suppressed from the eBook and/or eChapter(s). Editorial review has deemed that any suppressed content does not materially affect the overall learning experience. Cengage Learning reserves the right to remove additional content at any time if subsequent rights restrictions require it.

From (5.1.15) through (5.1.17),

$$\begin{aligned} A = D &= 1 + (8.4 \times 10^{-4}\underline{/90°})(70.29\underline{/84.78°})\left(\tfrac{1}{2}\right) \\ &= 1 + 0.02952\underline{/174.78°} \\ &= 0.9706 + j0.00269 = 0.9706\underline{/0.159°} \quad \text{per unit} \end{aligned}$$

$$B = Z = 70.29\underline{/84.78°} \quad \Omega$$

$$\begin{aligned} C &= (8.4 \times 10^{-4}\underline{/90°})(1 + 0.01476\underline{/174.78°}) \\ &= (8.4 \times 10^{-4}\underline{/90°})(0.9853 + j0.00134) \\ &= 8.277 \times 10^{-4}\underline{/90.08°} \quad \text{S} \end{aligned}$$

b. The receiving-end voltage and current quantities are

$$\text{V}_\text{R} = (0.95)(345) = 327.8 \text{ kV}_\text{LL}$$

$$V_\text{R} = \frac{327.8}{\sqrt{3}}\underline{/0°} = 189.2\underline{/0°} \quad \text{kV}_\text{LN}$$

$$I_\text{R} = \frac{700\underline{/\cos^{-1}0.99}}{(\sqrt{3})(0.95 \times 345)(0.99)} = 1.246\underline{/8.11°} \quad \text{kA}$$

From (5.1.1) and (5.1.2), the sending-end quantities are

$$\begin{aligned} V_\text{S} &= (0.9706\underline{/0.159°})(189.2\underline{/0°}) + (70.29\underline{/84.78})(1.246\underline{/8.11°}) \\ &= 183.6\underline{/0.159°} + 87.55\underline{/92.89°} \\ &= 179.2 + j87.95 = 199.6\underline{/26.14°} \quad \text{kV}_\text{LN} \end{aligned}$$

$$\text{V}_\text{S} = 199.6\sqrt{3} = 345.8 \text{ kV}_\text{LL} \approx 1.00 \quad \text{per unit}$$

$$\begin{aligned} I_\text{S} &= (8.277 \times 10^{-4}\underline{/90.08°})(189.2\underline{/0°}) + (0.9706\underline{/0.159°})(1.246\underline{/8.11°}) \\ &= 0.1566\underline{/90.08°} + 1.209\underline{/8.27°} \\ &= 1.196 + j0.331 = 1.241\underline{/15.5°} \quad \text{kA} \end{aligned}$$

and the real power delivered to the sending end is

$$\begin{aligned} \text{P}_\text{S} &= (\sqrt{3})(345.8)(1.241)\cos(26.14° - 15.5°) \\ &= 730.5 \quad \text{MW} \end{aligned}$$

c. From (5.1.19), the no-load receiving-end voltage is

$$\text{V}_\text{RNL} = \frac{\text{V}_\text{S}}{\text{A}} = \frac{345.8}{0.9706} = 356.3 \quad \text{kV}_\text{LL}$$

and, from (5.1.18),

$$\text{percent VR} = \frac{356.3 - 327.8}{327.8} \times 100 = 8.7\%$$

Copyright 2017 Cengage Learning. All Rights Reserved. May not be copied, scanned, or duplicated, in whole or in part. Due to electronic rights, some third party content may be suppressed from the eBook and/or eChapter(s). Editorial review has deemed that any suppressed content does not materially affect the overall learning experience. Cengage Learning reserves the right to remove additional content at any time if subsequent rights restrictions require it.

d. From Table A.4, the approximate current-carrying capacity of two 795,000-cmil 26/2 ACSR conductors is 2 × 0.9 = 1.8 kA.

e. The full-load line losses are $P_S - P_R = 730.5 - 700 = 30.5$ MW and the full-load transmission efficiency is

$$\text{percent EFF} = \frac{P_R}{P_S} \times 100 = \frac{700}{730.5} \times 100 = 95.8\%$$

Since $V_S = 1.00$ per unit, the full-load receiving-end voltage of 0.95 per unit corresponds to $V_R/V_S = 0.95$, considered in practice to be about the lowest operating voltage possible without encountering operating problems. Thus, for this 345-kV 200-km uncompensated line, voltage drop limits the full-load current to 1.246 kA at 0.99 p.f. leading, which is well below the thermal limit of 1.8 kA.

5.2 TRANSMISSION-LINE DIFFERENTIAL EQUATIONS

The line constants R, L, and C are derived in Chapter 4 as per-length values having units of Ω/m, H/m, and F/m. They are not lumped, but rather are uniformly distributed along the length of the line. In order to account for the distributed nature of transmission-line constants, consider the circuit shown in Figure 5.6, which represents a line section of length Δx. $V(x)$ and $I(x)$ denote the voltage and current at position x, which is measured in meters from the right, or receiving end of the line. Similarly, $V(x + \Delta x)$ and $I(x + \Delta x)$ denote the voltage and current at position $(x + \Delta x)$. The circuit constants are

$$z = R + j\omega L \quad \Omega/\text{m} \tag{5.2.1}$$

$$y = G + j\omega C \quad \text{S/m} \tag{5.2.2}$$

where G is usually neglected for overhead 60-Hz lines. Writing a KVL equation for the circuit

$$V(x + \Delta x) = V(x) + (z\Delta x)I(x) \quad \text{volts} \tag{5.2.3}$$

Rearranging (5.2.3),

$$\frac{V(x + \Delta x) - V(x)}{\Delta x} = zI(x) \tag{5.2.4}$$

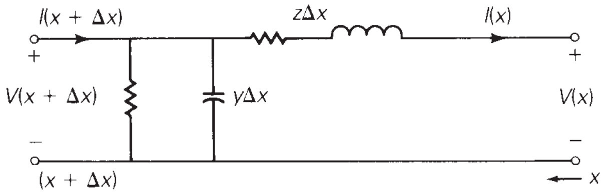

FIGURE 5.6 Transmission-line section of length Δx

Copyright 2017 Cengage Learning. All Rights Reserved. May not be copied, scanned, or duplicated, in whole or in part. Due to electronic rights, some third party content may be suppressed from the eBook and/or eChapter(s). Editorial review has deemed that any suppressed content does not materially affect the overall learning experience. Cengage Learning reserves the right to remove additional content at any time if subsequent rights restrictions require it.

and taking the limit as Δx approaches zero,

$$\frac{dV(x)}{dx} = zI(x) \tag{5.2.5}$$

Similarly, writing a KCL equation for the circuit,

$$I(x + \Delta x) = I(x) + (y\Delta x)V(x + \Delta x) \quad \text{A} \tag{5.2.6}$$

Rearranging,

$$\frac{I(x + \Delta x) - I(x)}{\Delta x} = yV(x) \tag{5.2.7}$$

and taking the limit as Δx approaches zero,

$$\frac{dI(x)}{dx} = yV(x) \tag{5.2.8}$$

Equations (5.2.5) and (5.2.8) are two linear, first-order, homogeneous differential equations with two unknowns, $V(x)$ and $I(x)$. Eliminate $I(x)$ by differentiating (5.2.5) and using (5.2.8) as follows:

$$\frac{d^2V(x)}{dx^2} = z\frac{dI(x)}{dx} = zyV(x) \tag{5.2.9}$$

or

$$\frac{d^2V(x)}{dx^2} - zyV(x) = 0 \tag{5.2.10}$$

Equation (5.2.10) is a linear, second-order, homogeneous differential equation with one unknown, $V(x)$. By inspection, its solution is

$$V(x) = A_1e^{\gamma x} + A_2e^{-\gamma x} \quad \text{volts} \tag{5.2.11}$$

where A_1 and A_2 are integration constants and

$$\gamma = \sqrt{zy} \quad \text{m}^{-1} \tag{5.2.12}$$

γ, whose units are m^{-1}, is called the *propagation constant*. By inserting (5.2.11) and (5.2.12) into (5.2.10), the solution to the differential equation can be verified.

Next, using (5.2.11) in (5.2.5),

$$\frac{dV(x)}{dx} = \gamma A_1e^{\gamma x} - \gamma A_2e^{-\gamma x} = zI(x) \tag{5.2.13}$$

Solving for $I(x)$,

$$I(x) = \frac{A_1e^{\gamma x} - A_2e^{-\gamma x}}{z/\gamma} \tag{5.2.14}$$

Copyright 2017 Cengage Learning. All Rights Reserved. May not be copied, scanned, or duplicated, in whole or in part. Due to electronic rights, some third party content may be suppressed from the eBook and/or eChapter(s). Editorial review has deemed that any suppressed content does not materially affect the overall learning experience. Cengage Learning reserves the right to remove additional content at any time if subsequent rights restrictions require it.

Using (5.2.12), $z/\gamma = z/\sqrt{zy} = \sqrt{z/y}$, (5.2.14) becomes

$$I(x) = \frac{A_1 e^{\gamma x} - A_2 e^{-\gamma x}}{Z_c} \tag{5.2.15}$$

where

$$Z_c = \sqrt{\frac{z}{y}} \quad \Omega \tag{5.2.16}$$

Z_c, whose units are ohms, is called the *characteristic impedance*.

Next, the integration constants A_1 and A_2 are evaluated from the boundary conditions. At $x = 0$, which is the receiving end of the line, the receiving-end voltage and current are

$$V_R = V(0) \tag{5.2.17}$$

$$I_R = I(0) \tag{5.2.18}$$

Also, at $x = 0$, (5.2.11) and (5.2.15) become

$$V_R = A_1 + A_2 \tag{5.2.19}$$

$$I_R = \frac{A_1 - A_2}{Z_c} \tag{5.2.20}$$

Solving for A_1 and A_2,

$$A_1 = \frac{V_R + Z_c I_R}{2} \tag{5.2.21}$$

$$A_2 = \frac{V_R - Z_c I_R}{2} \tag{5.2.22}$$

Substituting A_1 and A_2 into (5.2.11) and (5.2.15),

$$V(x) = \left(\frac{V_R + Z_c I_R}{2}\right)e^{\gamma x} + \left(\frac{V_R - Z_c I_R}{2}\right)e^{-\gamma x} \tag{5.2.23}$$

$$I(x) = \left(\frac{V_R + Z_c I_R}{2Z_c}\right)e^{\gamma x} - \left(\frac{V_R - Z_c I_R}{2Z_c}\right)e^{-\gamma x} \tag{5.2.24}$$

Rearranging (5.2.23) and (5.2.24),

$$V(x) = \left(\frac{e^{\gamma x} + e^{-\gamma x}}{2}\right)V_R + Z_c\left(\frac{e^{\gamma x} - e^{-\gamma x}}{2}\right)I_R \tag{5.2.25}$$

$$I(x) = \frac{1}{Z_c}\left(\frac{e^{\gamma x} - e^{-\gamma x}}{2}\right)V_R + \left(\frac{e^{\gamma x} + e^{-\gamma x}}{2}\right)I_R \tag{5.2.26}$$

Copyright 2017 Cengage Learning. All Rights Reserved. May not be copied, scanned, or duplicated, in whole or in part. Due to electronic rights, some third party content may be suppressed from the eBook and/or eChapter(s). Editorial review has deemed that any suppressed content does not materially affect the overall learning experience. Cengage Learning reserves the right to remove additional content at any time if subsequent rights restrictions require it.

Recognizing the hyperbolic functions cosh and sinh,

$$V(x) = \cosh(\gamma x)V_{\text{R}} + Z_c \sinh(\gamma x)I_{\text{R}} \tag{5.2.27}$$

$$I(x) = \frac{1}{Z_c}\sinh(\gamma x)\; V_{\text{R}} + \cosh(\gamma x)I_{\text{R}} \tag{5.2.28}$$

Equations (5.2.27) and (5.2.28) give the *ABCD* parameters of the distributed line. In matrix format,

$$\begin{bmatrix} V(x) \\ I(x) \end{bmatrix} = \left[\begin{array}{c|c} A(x) & B(x) \\ \hline C(x) & D(x) \end{array}\right] \begin{bmatrix} V_{\text{R}} \\ I_{\text{R}} \end{bmatrix} \tag{5.2.29}$$

where

$$A(x) = D(x) = \cosh(\gamma x) \text{ per unit} \tag{5.2.30}$$

$$B(x) = Z_c \sinh(\gamma x) \quad \Omega \tag{5.2.31}$$

$$C(x) = \frac{1}{Z_c}\sinh(\gamma x) \quad \text{S} \tag{5.2.32}$$

Equation (5.2.29) gives the current and voltage at any point x along the line in terms of the receiving-end voltage and current. At the sending end, where $x = l$, $V(l) = V_{\text{S}}$ and $I(l) = I_{\text{S}}$. That is,

$$\begin{bmatrix} V_{\text{S}} \\ I_{\text{S}} \end{bmatrix} = \left[\begin{array}{c|c} A & B \\ \hline C & D \end{array}\right] \begin{bmatrix} V_{\text{R}} \\ I_{\text{R}} \end{bmatrix} \tag{5.2.33}$$

where

$$A = D = \cosh(\gamma l) \text{ per unit} \tag{5.2.34}$$

$$B = Z_c \sinh(\gamma l) \quad \Omega \tag{5.2.35}$$

$$C = \frac{1}{Z_c}\sinh(\gamma l) \quad \text{S} \tag{5.2.36}$$

Equations (5.2.34) through (5.2.36) give the *ABCD* parameters of the distributed line. In these equations, the propagation constant γ is a complex quantity with real and imaginary parts denoted α and β. That is,

$$\gamma = \alpha + j\beta \quad \text{m}^{-1} \tag{5.2.37}$$

The quantity γl is dimensionless. Also

$$e^{\gamma l} = e^{(\alpha l + j\beta l)} = e^{\alpha l}e^{j\beta l} = e^{\alpha l}\underline{/\beta l} \tag{5.2.38}$$

Using (5.2.38), the hyperbolic functions cosh and sinh can be evaluated as follows:

$$\cosh(\gamma l) = \frac{e^{\gamma l} + e^{-\gamma l}}{2} = \frac{1}{2}\left(e^{\alpha l}\underline{/\beta l} + e^{-\alpha l}\underline{/-\beta l}\right) \tag{5.2.39}$$

Copyright 2017 Cengage Learning. All Rights Reserved. May not be copied, scanned, or duplicated, in whole or in part. Due to electronic rights, some third party content may be suppressed from the eBook and/or eChapter(s). Editorial review has deemed that any suppressed content does not materially affect the overall learning experience. Cengage Learning reserves the right to remove additional content at any time if subsequent rights restrictions require it.

Parameter	$A = D$	B	C
Units	per Unit	Ω	S
Short line (less than 25 km)	1	Z	0
Medium line—nominal π circuit (25 to 250 km)	$1 + \frac{YZ}{2}$	Z	$Y\left(1 + \frac{YZ}{4}\right)$
Long line—equivalent π circuit (more than 250 km)	$\cosh(\gamma\ell) = 1 + \frac{Y'Z'}{2}$	$Z_c \sinh(\gamma\ell) = Z'$	$(1/Z_c)\sinh(\gamma\ell)$ $= Y'\left(1 + \frac{Y'Z'}{4}\right)$
Lossless line (R = G = 0)	$\cos(\beta\ell)$	$jZ_c \sin(\beta\ell)$	$\frac{j\sin(\beta\ell)}{Z_c}$

TABLE 5.1

Summary: Transmission-line *ABCD* parameters

and

$$\sinh(\gamma l) = \frac{e^{\gamma l} - e^{-\gamma l}}{2} = \frac{1}{2}\left(e^{\alpha l}\underline{/\beta l} - e^{-\alpha l}\underline{/-\beta l}\right) \tag{5.2.40}$$

Alternatively, the following identities can be used:

$$\cosh(\alpha l + j\beta l) = \cosh(\alpha l)\cos(\beta l) + j\sinh(\alpha l)\sin(\beta l) \tag{5.2.41}$$

$$\sinh(\alpha l + j\beta l) = \sinh(\alpha l)\cos(\beta l) + j\cosh(\alpha l)\sin(\beta l) \tag{5.2.42}$$

Note that in (5.2.39) through (5.2.42), the dimensionless quantity βl is in radians, not degrees.

The *ABCD* parameters given by (5.2.34) through (5.2.36) are exact parameters valid for any line length. For accurate calculations, these equations must be used for overhead 60-Hz lines longer than 250 km. The *ABCD* parameters derived in Section 5.1 are approximate parameters that are more conveniently used for hand calculations involving short- and medium-length lines. Table 5.1 summarizes the *ABCD* parameters for short, medium, long, and lossless (see Section 5.4) lines.

EXAMPLE 5.2

Exact *ABCD* parameters: long line

A three-phase 765-kV, 60-Hz, 300-km, completely transposed line has the following positive-sequence impedance and admittance:

$$z = 0.0165 + j0.3306 = 0.3310\underline{/87.14^\circ} \quad \Omega/\text{km}$$

$$y = j4.674 \times 10^{-6} \text{ S/km}$$

(*Continued*)

Copyright 2017 Cengage Learning. All Rights Reserved. May not be copied, scanned, or duplicated, in whole or in part. Due to electronic rights, some third party content may be suppressed from the eBook and/or eChapter(s). Editorial review has deemed that any suppressed content does not materially affect the overall learning experience. Cengage Learning reserves the right to remove additional content at any time if subsequent rights restrictions require it.

Assuming positive-sequence operation, calculate the exact *ABCD* parameters of the line. Compare the exact *B* parameter with that of the nominal π circuit.

SOLUTION

From (5.2.12) and (5.2.16),

$$Z_c = \sqrt{\frac{0.3310\underline{/87.14^\circ}}{4.674\times 10^{-6}\underline{/90^\circ}}} = \sqrt{7.082\times 10^{4}\underline{/-2.86^\circ}}$$
$$= 266.1\underline{/-1.43^\circ}\quad \Omega$$

and

$$\gamma l = \sqrt{(0.3310\underline{/87.14^\circ})(4.674\times 10^{-6}\underline{/90^\circ})}\times(300)$$
$$= \sqrt{1.547\times 10^{-6}\underline{/177.14^\circ}}\times(300)$$
$$= 0.3731\underline{/88.57^\circ} = 0.00931 + j0.3730 \quad \text{per unit}$$

From (5.2.38),

$$e^{\gamma l} = e^{0.00931}e^{+j0.3730} = 1.0094\underline{/0.3730}\quad \text{radians}$$
$$= 0.9400 + j0.3678$$

and

$$e^{-\gamma l} = e^{-0.00931}e^{-j0.3730} = 0.9907\underline{/-0.3730}\quad \text{radians}$$
$$= 0.9226 - j0.3610$$

Then, from (5.2.39) and (5.2.40),

$$\cosh(\gamma l) = \frac{(0.9400 + j0.3678) + (0.9226 - j0.3610)}{2}$$
$$= 0.9313 + j0.0034 = 0.9313\underline{/0.209^\circ}$$
$$\sinh(\gamma l) = \frac{(0.9400 + j0.3678) - (0.9226 - j0.3610)}{2}$$
$$= 0.0087 + j0.3644 = 0.3645\underline{/88.63^\circ}$$

Finally, from (5.2.34) through (5.2.36),

$$A = D = \cosh(\gamma l) = 0.9313\underline{/0.209^\circ}\quad \text{per unit}$$

$$B = (266.1\underline{/-1.43^\circ})(0.3645\underline{/88.63^\circ}) = 97.0\underline{/87.2^\circ}\quad \Omega$$

$$C = \frac{0.3645\underline{/88.63^\circ}}{266.1\underline{/-1.43^\circ}} = 1.37\times 10^{-3}\underline{/90.06^\circ}\quad \text{S}$$

Copyright 2017 Cengage Learning. All Rights Reserved. May not be copied, scanned, or duplicated, in whole or in part. Due to electronic rights, some third party content may be suppressed from the eBook and/or eChapter(s). Editorial review has deemed that any suppressed content does not materially affect the overall learning experience. Cengage Learning reserves the right to remove additional content at any time if subsequent rights restrictions require it.

Using (5.1.16), the B parameter for the nominal π circuit is

$$B_{\text{nominal } \pi} = Z = (0.3310\underline{/87.14^\circ})(300) = 99.3\underline{/87.14^\circ} \quad \Omega$$

which is 2% larger than the exact value.

5.3 EQUIVALENT π CIRCUIT

Many computer programs used in power system analysis and design assume circuit representations of components such as transmission lines and transformers. It is therefore convenient to represent the terminal characteristics of a transmission line by an equivalent circuit instead of its *ABCD* parameters.

The circuit shown in Figure 5.7 is called an *equivalent π circuit*. It is identical in structure to the nominal π circuit of Figure 5.3, except that Z' and Y' are used instead of Z and Y. The objective is to determine Z' and Y' such that the equivalent π circuit has the same *ABCD* parameters as those of the distributed line, (5.2.34) through (5.2.36). The *ABCD* parameters of the equivalent π circuit, which has the same structure as the nominal π, are

$$A = D = 1 + \frac{Y'Z'}{2} \quad \text{per unit} \tag{5.3.1}$$

$$B = Z' \quad \Omega \tag{5.3.2}$$

$$C = Y'\left(1 + \frac{Y'Z'}{4}\right) \quad \text{S} \tag{5.3.3}$$

where Z and Y in (5.1.15) through (5.1.17) have been replaced with Z' and Y' in (5.3.1) through (5.3.3). Equating (5.3.2) to (5.2.35),

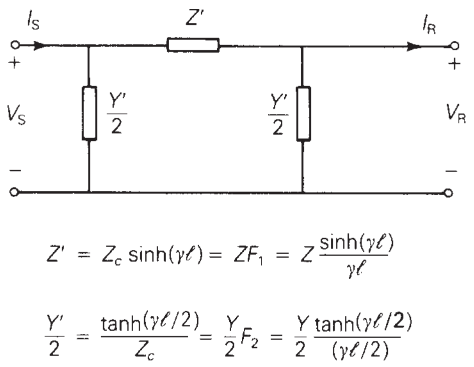
I_S
Z'
I_R
+
V_S
−
$\frac{Y'}{2}$
$\frac{Y'}{2}$
+
V_R
−
$Z' = Z_c \sinh(\gamma\ell) = ZF_1 = Z\frac{\sinh(\gamma\ell)}{\gamma\ell}$
$\frac{Y'}{2} = \frac{\tanh(\gamma\ell/2)}{Z_c} = \frac{Y}{2}F_2 = \frac{Y}{2}\frac{\tanh(\gamma\ell/2)}{(\gamma\ell/2)}$

FIGURE 5.7

Transmission-line equivalent π circuit

Copyright 2017 Cengage Learning. All Rights Reserved. May not be copied, scanned, or duplicated, in whole or in part. Due to electronic rights, some third party content may be suppressed from the eBook and/or eChapter(s). Editorial review has deemed that any suppressed content does not materially affect the overall learning experience. Cengage Learning reserves the right to remove additional content at any time if subsequent rights restrictions require it.

$$Z' = Z_c \sinh(\gamma l) = \sqrt{\frac{z}{y}} \sinh(\gamma l) \tag{5.3.4}$$

Rewriting (5.3.4) in terms of the nominal π circuit impedance $Z = zl$,

$$\begin{aligned} Z' &= zl\left[\sqrt{\frac{z}{y}}\,\frac{\sinh(\gamma l)}{zl}\right] = zl\left[\frac{\sinh(\gamma l)}{\sqrt{zy}\,l}\right] \\ &= ZF_1 \quad \Omega \end{aligned} \tag{5.3.5}$$

where

$$F_1 = \frac{\sinh(\gamma l)}{\gamma l} \quad \text{per unit} \tag{5.3.6}$$

Similarly, equating (5.3.1) to (5.2.34),

$$\begin{aligned} 1 + \frac{Y'Z'}{2} &= \cosh(\gamma l) \\ \frac{Y'}{2} &= \frac{\cosh(\gamma l) - 1}{Z'} \end{aligned} \tag{5.3.7}$$

Using (5.3.4) and the identity $\tanh\left(\frac{\gamma l}{2}\right) = \frac{\cosh(\gamma l) - 1}{\sinh(\gamma l)}$, (5.3.7) becomes

$$\frac{Y'}{2} = \frac{\cosh(\gamma l) - 1}{Z_c \sinh(\gamma l)} = \frac{\tanh(\gamma l/2)}{Z_c} = \frac{\tanh(\gamma l/2)}{\sqrt{\dfrac{z}{y}}} \tag{5.3.8}$$

Rewriting (5.3.8) in terms of the nominal π circuit admittance $Y = yl$,

$$\begin{aligned} \frac{Y'}{2} &= \frac{yl}{2}\left[\frac{\tanh(\gamma l/2)}{\sqrt{\dfrac{z}{y}}\,\dfrac{yl}{2}}\right] = \frac{yl}{2}\left[\frac{\tanh(\gamma l/2)}{\sqrt{zy}\,l/2}\right] \\ &= \frac{Y}{2}F_2 \quad \text{S} \end{aligned} \tag{5.3.9}$$

where

$$F_2 = \frac{\tanh(\gamma l/2)}{\gamma l/2} \quad \text{per unit} \tag{5.3.10}$$

Equations (5.3.6) and (5.3.10) give the correction factors F_1 and F_2 to convert Z and Y for the nominal π circuit to Z' and Y' for the equivalent π circuit.

Copyright 2017 Cengage Learning. All Rights Reserved. May not be copied, scanned, or duplicated, in whole or in part. Due to electronic rights, some third party content may be suppressed from the eBook and/or eChapter(s). Editorial review has deemed that any suppressed content does not materially affect the overall learning experience. Cengage Learning reserves the right to remove additional content at any time if subsequent rights restrictions require it.

EXAMPLE 5.3

Equivalent π circuit: long line

Compare the equivalent and nominal π circuits for the line in Example 5.2.

SOLUTION

For the nominal π circuit,

$$Z = zl = (0.3310\,\underline{/87.14^\circ})(300) = 99.3\,\underline{/87.14^\circ} \quad \Omega$$

$$\frac{Y}{2} = \frac{yl}{2} = \left(\frac{j4.674 \times 10^{-6}}{2}\right)(300) = 7.011 \times 10^{-4}\,\underline{/90^\circ} \quad \text{S}$$

From (5.3.6) and (5.3.10), the correction factors are

$$F_1 = \frac{0.3645\,\underline{/88.63^\circ}}{0.3731\,\underline{/88.57^\circ}} = 0.9769\,\underline{/0.06^\circ} \quad \text{per unit}$$

$$\begin{aligned} F_2 &= \frac{\tanh(\gamma l/2)}{\gamma l/2} = \frac{\cosh(\gamma l) - 1}{(\gamma l/2)\sinh(\gamma l)} \\ &= \frac{0.9313 + j0.0034 - 1}{\left(\frac{0.3731}{2}\,\underline{/88.57^\circ}\right)(0.3645\,\underline{/88.63^\circ})} \\ &= \frac{-0.0687 + j0.0034}{0.06800\,\underline{/177.20^\circ}} \\ &= \frac{0.06878\,\underline{/177.17^\circ}}{0.06800\,\underline{/177.20^\circ}} = 1.012\,\underline{/-0.03^\circ} \quad \text{per unit} \end{aligned}$$

Then, from (5.3.5) and (5.3.9), for the equivalent π circuit,

$$Z' = (99.3\,\underline{/87.14^\circ})(0.9769\,\underline{/0.06^\circ}) = 97.0\,\underline{/87.2^\circ} \quad \Omega$$

$$\begin{aligned} \frac{Y'}{2} &= (7.011 \times 10^{-4}\,\underline{/90^\circ})(1.012\,\underline{/-0.03^\circ}) = 7.095 \times 10^{-4}\,\underline{/89.97^\circ} \quad \text{S} \\ &= 3.7 \times 10^{-7} + j7.095 \times 10^{-4} \quad \text{S} \end{aligned}$$

Comparing these nominal and equivalent π circuit values, Z' is about 2% smaller than Z, and $Y'/2$ is about 1% larger than $Y/2$. Although the circuit values are approximately the same for this line, the equivalent π circuit should be used for accurate calculations involving long lines. Note the small shunt conductance, $G' = 3.7 \times 10^{-7}$ S, introduced in the equivalent π circuit. G' is often neglected.

Copyright 2017 Cengage Learning. All Rights Reserved. May not be copied, scanned, or duplicated, in whole or in part. Due to electronic rights, some third party content may be suppressed from the eBook and/or eChapter(s). Editorial review has deemed that any suppressed content does not materially affect the overall learning experience. Cengage Learning reserves the right to remove additional content at any time if subsequent rights restrictions require it.

5.4 LOSSLESS LINES

This section discusses the following concepts for lossless lines: surge impedance, *ABCD* parameters, equivalent π circuit, wavelength, surge impedance loading, voltage profiles, and steady-state stability limit.

When line losses are neglected, simpler expressions for the line parameters are obtained and the above concepts are more easily understood. Since transmission and distribution lines for power transfer generally are designed to have low losses, the equations and concepts developed here can be used for quick and reasonably accurate hand calculations leading to seat-of-the-pants analyses and to initial designs. More accurate calculations then can be made with computer programs for follow-up analysis and design.

SURGE IMPEDANCE

For a lossless line, $\mathrm{R} = \mathrm{G} = 0$, and

$$z = j\omega\mathrm{L} \quad \Omega/\mathrm{m} \tag{5.4.1}$$

$$y = j\omega\mathrm{C} \quad \mathrm{S/m} \tag{5.4.2}$$

From (5.2.12) and (5.2.16),

$$Z_c = \sqrt{\frac{z}{y}} = \sqrt{\frac{j\omega\mathrm{L}}{j\omega\mathrm{C}}} = \sqrt{\frac{\mathrm{L}}{\mathrm{C}}} \quad \Omega \tag{5.4.3}$$

and

$$\gamma = \sqrt{zy} = \sqrt{(j\omega\mathrm{L})(j\omega\mathrm{C})} = j\omega\sqrt{\mathrm{LC}} = j\beta \quad \mathrm{m}^{-1} \tag{5.4.4}$$

where

$$\beta = \omega\sqrt{\mathrm{LC}} \quad \mathrm{m}^{-1} \tag{5.4.5}$$

The characteristic impedance $Z_c = \sqrt{\mathrm{L}/\mathrm{C}}$, commonly called the *surge impedance* for a lossless line, is pure real—that is, resistive. The propagation constant $\gamma = j\beta$ is pure imaginary.

ABCD PARAMETERS

The *ABCD* parameters are, from (5.2.30) through (5.2.32),

$$\begin{aligned} \mathrm{A}(x) = \mathrm{D}(x) &= \cosh(\gamma x) = \cosh(j\beta x) \\ &= \frac{e^{j\beta x} + e^{-j\beta x}}{2} = \cos(\beta x) \quad \text{per unit} \end{aligned} \tag{5.4.6}$$

Copyright 2017 Cengage Learning. All Rights Reserved. May not be copied, scanned, or duplicated, in whole or in part. Due to electronic rights, some third party content may be suppressed from the eBook and/or eChapter(s). Editorial review has deemed that any suppressed content does not materially affect the overall learning experience. Cengage Learning reserves the right to remove additional content at any time if subsequent rights restrictions require it.

$$\sinh(\gamma x) = \sinh(j\beta x) = \frac{e^{j\beta x} - e^{-j\beta x}}{2} = j\sin(\beta x) \quad \text{per unit} \tag{5.4.7}$$

$$B(x) = Z_c \sinh(\gamma x) = jZ_c \sin(\beta x) = j\sqrt{\frac{\mathrm{L}}{\mathrm{C}}}\sin(\beta x) \quad \Omega \tag{5.4.8}$$

$$C(x) = \frac{\sinh(\gamma x)}{Z_c} = \frac{j\sin(\beta x)}{\sqrt{\dfrac{\mathrm{L}}{\mathrm{C}}}} \quad \mathrm{S} \tag{5.4.9}$$

EQUIVALENT π CIRCUIT

For the equivalent π circuit, using (5.3.4).

$$Z' = jZ_c \sin(\beta l) = j\mathrm{X}' \quad \Omega \tag{5.4.10}$$

or, from (5.3.5) and (5.3.6),

$$Z' = (j\omega \mathrm{L}l)\left(\frac{\sin(\beta l)}{\beta l}\right) = j\mathrm{X}' \quad \Omega \tag{5.4.11}$$

Also, from (5.3.9) and (5.3.10),

$$\begin{aligned}\frac{Y'}{2} &= \frac{Y}{2}\frac{\tanh(j\beta l/2)}{j\beta l/2} = \frac{Y}{2}\frac{\sinh(j\beta l/2)}{(j\beta l/2)\cosh(j\beta l/2)}\\ &= \left(\frac{j\omega Cl}{2}\right)\frac{j\sin(\beta l/2)}{(j\beta l/2)\cos(\beta l/2)} = \left(\frac{j\omega Cl}{2}\right)\frac{\tan(\beta l/2)}{\beta l/2}\\ &= \left(\frac{j\omega C'l}{2}\right) \quad \mathrm{S}\end{aligned} \tag{5.4.12}$$

Z' and Y' are both pure imaginary. Also, for βl less than π radians, Z' is pure inductive and Y' is pure capacitive. Thus the equivalent π circuit for a lossless line, shown in Figure 5.8, is also lossless.

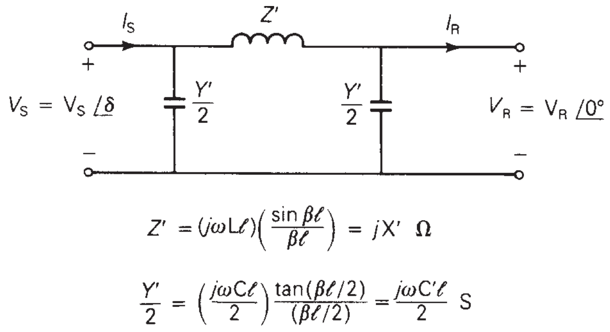
I_S
Z'
I_R
+
+
$V_S = V_S \angle\delta$
$\frac{Y'}{2}$
$\frac{Y'}{2}$
$V_R = V_R \angle 0°$
–
–
$Z' = (j\omega \mathrm{L}\ell)\left(\frac{\sin\beta\ell}{\beta\ell}\right) = j\mathrm{X}' \quad \Omega$
$\frac{Y'}{2} = \left(\frac{j\omega C\ell}{2}\right)\frac{\tan(\beta\ell/2)}{(\beta\ell/2)} = \frac{j\omega C'\ell}{2} \quad \mathrm{S}$

FIGURE 5.8

Equivalent π circuit for a lossless line ($\beta\ell$ less than π)

Copyright 2017 Cengage Learning. All Rights Reserved. May not be copied, scanned, or duplicated, in whole or in part. Due to electronic rights, some third party content may be suppressed from the eBook and/or eChapter(s). Editorial review has deemed that any suppressed content does not materially affect the overall learning experience. Cengage Learning reserves the right to remove additional content at any time if subsequent rights restrictions require it.

WAVELENGTH

A *wavelength* is the distance required to change the phase of the voltage or current by 2π radians or 360°. For a lossless line, using (5.2.29),

$$\begin{aligned} V(x) &= \mathrm{A}(x)V_\mathrm{R} + B(x)I_\mathrm{R} \\ &= \cos(\beta x)\, V_\mathrm{R} + jZ_c \sin(\beta x) I_\mathrm{R} \end{aligned} \tag{5.4.13}$$

and

$$\begin{aligned} I(x) &= C(x)V_\mathrm{R} + \mathrm{D}(x)I_\mathrm{R} \\ &= \frac{j\sin(\beta x)}{Z}V_\mathrm{R} + \cos(\beta x)I_\mathrm{R} \end{aligned} \tag{5.4.14}$$

From (5.4.13) and (5.4.14), $V(x)$ and $I(x)$ change phase by 2π radians when $x = 2\pi/\beta$. Denoting wavelength by λ, and using (5.4.5),

$$\lambda = \frac{2\pi}{\beta} = \frac{2\pi}{\omega\sqrt{\mathrm{LC}}} = \frac{1}{f\sqrt{\mathrm{LC}}} \quad \mathrm{m} \tag{5.4.15}$$

or

$$f\lambda = \frac{1}{\sqrt{\mathrm{LC}}} \tag{5.4.16}$$

The term $(1/\sqrt{\mathrm{LC}})$ in (5.4.16) is the velocity of propagation of voltage and current waves along a lossless line, as shown in Chapter 13. For overhead lines, $(1/\sqrt{\mathrm{LC}}) \approx 3 \times 10^8$ m/s, and for $f = 60$ Hz, (5.4.14) gives

$$\lambda \approx \frac{3 \times 10^8}{60} = 5 \times 10^6\,\mathrm{m} = 5000\ \mathrm{km} = 3100\ \mathrm{mi}$$

Typical power-line lengths are only a small fraction of the above 60-Hz wavelength.

SURGE IMPEDANCE LOADING

Surge impedance loading (SIL) is the power delivered by a lossless line to a load resistance equal to the surge impedance $Z_c = \sqrt{\mathrm{L}/\mathrm{C}}$. Figure 5.9 shows a lossless line terminated by a resistance equal to its surge impedance. This line represents either

FIGURE 5.9

Lossless line terminated by its surge impedance

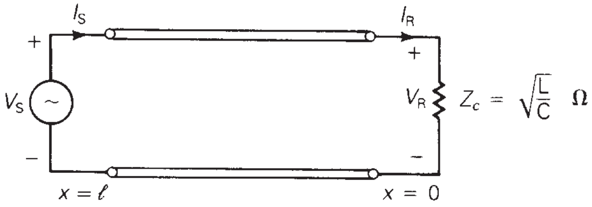

Copyright 2017 Cengage Learning. All Rights Reserved. May not be copied, scanned, or duplicated, in whole or in part. Due to electronic rights, some third party content may be suppressed from the eBook and/or eChapter(s). Editorial review has deemed that any suppressed content does not materially affect the overall learning experience. Cengage Learning reserves the right to remove additional content at any time if subsequent rights restrictions require it.

a single-phase line or one phase-to-neutral of a balanced three-phase line. At SIL, from (5.4.13),

$$\begin{aligned} V(x) &= \cos(\beta x)\,V_R + jZ_c\sin(\beta x)I_R \\ &= \cos(\beta x)V_R + jZ_c\sin(\beta x)\left(\frac{V_R}{Z_c}\right) \\ &= (\cos\beta x + j\sin\beta x)\,V_R \\ &= e^{j\beta x}V_R \quad \text{volts} \qquad (5.4.17) \end{aligned}$$

$$|V(x)| = |V_R| \quad \text{volts} \qquad (5.4.18)$$

Thus, at SIL, the voltage profile is flat. That is, the voltage magnitude at any point x along a lossless line at SIL is constant. Also from (5.4.14) at SIL,

$$\begin{aligned} I(x) &= \frac{j\sin(\beta x)}{Z_c}V_R + (\cos\beta x)\frac{V_R}{Z_c} \\ &= (\cos\beta x + j\sin\beta x)\frac{V_R}{Z_c} \\ &= (e^{j\beta x})\frac{V_R}{Z_c} \quad \text{A} \qquad (5.4.19) \end{aligned}$$

Using (5.4.17) and (5.4.19), the complex power flowing at any point x along the line is

$$\begin{aligned} S(x) &= \mathrm{P}(x) + j\mathrm{Q}(x) = V(x)I^*(x) \\ &= (e^{j\beta x}V_R)\left(\frac{e^{j\beta x}V_R}{Z_c}\right)^* \\ &= \frac{|V_R|^2}{Z_c} \qquad (5.4.20) \end{aligned}$$

Thus the real power flow along a lossless line at SIL remains constant from the sending end to the receiving end. The reactive power flow is zero.

At rated line voltage, the real power delivered, or SIL, from (5.4.20), is

$$\text{SIL} = \frac{\mathrm{V}^2_{\text{rated}}}{Z_c} \qquad (5.4.21)$$

where rated voltage is used for a single-phase line and rated line-to-line voltage is used for the total real power delivered by a three-phase line. Table 5.2 lists surge impedance and SIL values for typical overhead 60-Hz three-phase lines.

VOLTAGE PROFILES

In practice, power lines are not terminated by their surge impedance. Instead, loadings can vary from a small fraction of SIL during light load conditions up to multiples of SIL, depending on line length and line compensation, during heavy load conditions. If a line is not terminated by its surge impedance, then the voltage profile is not flat.

Copyright 2017 Cengage Learning. All Rights Reserved. May not be copied, scanned, or duplicated, in whole or in part. Due to electronic rights, some third party content may be suppressed from the eBook and/or eChapter(s). Editorial review has deemed that any suppressed content does not materially affect the overall learning experience. Cengage Learning reserves the right to remove additional content at any time if subsequent rights restrictions require it.

V_{rated} (kV)	$Z_C = \sqrt{L/C}$ (Ω)	$\text{SIL} = V_{\text{rated}}^2/Z_C$ (MW)
69	366–400	12–13
138	366–405	47–52
230	365–395	134–145
345	280–366	325–425
500	233–294	850–1075
765	254–266	2200–2300

TABLE 5.2

Surge impedance and SIL values for typical 60-Hz overhead lines [1, 2]
(Source: Electric Power Research Institute (EPRI), EPRI AC Transmission Line Reference Book—200 kV and Above (Palo Alto, CA: EPRI, *www.epri.com*. December 2005); Westinghouse Electric Corporation, *Electrical Transmission and Distribution Reference Book*, 4th ed. (East Pittsburgh, PA, 1964).)

Figure 5.10 shows voltage profiles of lines with a fixed sending-end voltage magnitude V_S for line lengths l up to a quarter wavelength. This figure shows four loading conditions: (1) no-load. (2) SIL, (3) short circuit, and (4) full load, which are described as follows:

1. At no-load, $I_{RNL} = 0$ and (5.4.13) yields

$$V_{NL}(x) = (\cos \beta x)V_{RNL} \tag{5.4.22}$$

The no-load voltage increases from $V_S = (\cos \beta l)V_{RNL}$ at the sending end to V_{RNL} at the receiving end (where $x = 0$).

2. From (5.4.18), the voltage profile at SIL is flat.
3. For a short circuit at the load, $V_{RSC} = 0$ and (5.4.13) yields

$$V_{SC}(x) = (Z_c \sin \beta x)I_{RSC} \tag{5.4.23}$$

FIGURE 5.10

Voltage profiles of an uncompensated lossless line with fixed sending-end voltage for line lengths up to a quarter wavelength

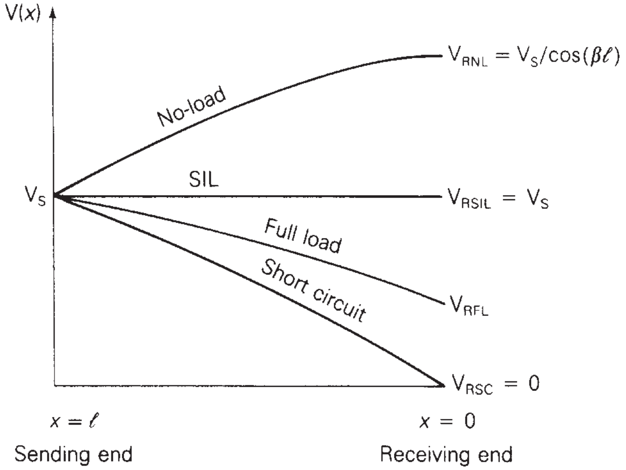

Copyright 2017 Cengage Learning. All Rights Reserved. May not be copied, scanned, or duplicated, in whole or in part. Due to electronic rights, some third party content may be suppressed from the eBook and/or eChapter(s). Editorial review has deemed that any suppressed content does not materially affect the overall learning experience. Cengage Learning reserves the right to remove additional content at any time if subsequent rights restrictions require it.

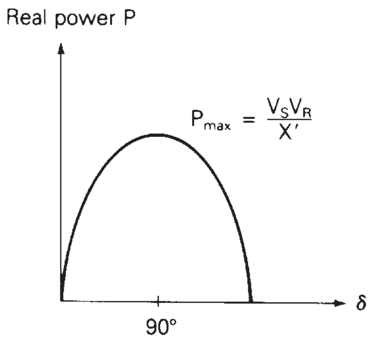

FIGURE 5.11

Real power delivered by a lossless line versus voltage angle across the line

The voltage decreases from $V_S = (\sin \beta l)(Z_c I_{RSC})$ at the sending end to $V_{RSC} = 0$ at the receiving end.

4. The full-load voltage profile, which depends on the specification of full-load current, lies above the short-circuit voltage profile.

Figure 5.10 summarizes these results, showing a high receiving-end voltage at no-load and a low receiving-end voltage at full load. This voltage regulation problem becomes more severe as the line length increases. In Section 5.6, shunt compensation methods to reduce voltage fluctuations are presented.

STEADY-STATE STABILITY LIMIT

The equivalent π circuit of Figure 5.8 can be used to obtain an equation for the real power delivered by a lossless line. Assume that the voltage magnitudes V_S and V_R at the ends of the line are held constant. Also, let δ denote the voltage-phase angle at the sending end with respect to the receiving end. From KVL, the receiving-end current I_R is

$$\begin{aligned} I_R &= \frac{V_S - V_R}{Z'} - \frac{Y'}{2} V_R \\ &= \frac{V_S e^{j\delta} - V_R}{jX'} - \frac{j\omega C' l}{2} V_R \end{aligned} \tag{5.4.24}$$

and the complex power S_R delivered to the receiving end is

$$\begin{aligned} S_R = V_R I_R^* &= V_R \left(\frac{V_S e^{j\delta} - V_R}{jX'} \right)^* + \frac{j\omega C' l}{2} V_R^2 \\ &= V_R \left(\frac{V_S e^{-j\delta} - V_R}{-jX'} \right) + \frac{j\omega C l}{2} V_R^2 \\ &= \frac{jV_R V_S \cos\delta + V_R V_S \sin\delta - jV_R^2}{X'} + \frac{j\omega C l}{2} V_R^2 \end{aligned} \tag{5.4.25}$$

Copyright 2017 Cengage Learning. All Rights Reserved. May not be copied, scanned, or duplicated, in whole or in part. Due to electronic rights, some third party content may be suppressed from the eBook and/or eChapter(s). Editorial review has deemed that any suppressed content does not materially affect the overall learning experience. Cengage Learning reserves the right to remove additional content at any time if subsequent rights restrictions require it.

FIGURE 5.12

Transmission-line loadability curve for 60-Hz overhead lines—no series or shunt compensation

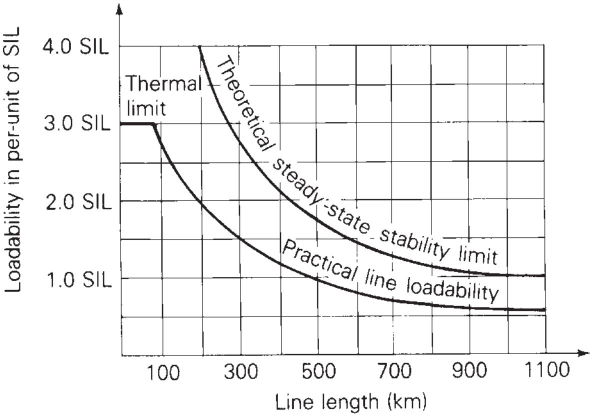

The real power delivered is

$$P = P_S = P_R = \mathrm{Re}(S_R) = \frac{V_R V_S}{X'}\sin\delta \quad \mathrm{W} \tag{5.4.26}$$

Note that since the line is lossless, $P_S = P_R$.

Equation (5.4.26) is plotted in Figure 5.11. For fixed voltage magnitudes V_S and V_R, the phase angle δ increases from 0 to 90° as the real power delivered increases. The maximum power that the line can deliver, which occurs when $\delta = 90°$, is given by

$$P_{\max} = \frac{V_S V_R}{X'} \quad \mathrm{W} \tag{5.4.27}$$

$P_{\max}$ represents the theoretical *steady-state stability* limit of a lossless line. If an attempt were made to exceed this steady-state stability limit, then synchronous machines at the sending end would lose synchronism with those at the receiving end. Stability is further discussed in Chapter 11.

It is convenient to express the steady-state stability limit in terms of SIL. Using (5.4.10) in (5.4.26),

$$P = \frac{V_S V_R \sin\delta}{Z_c \sin\beta l} = \left(\frac{V_S V_R}{Z_c}\right)\frac{\sin\delta}{\sin\left(\frac{2\pi l}{\lambda}\right)} \tag{5.4.28}$$

Expressing V_S and V_R in per-unit of rated line voltage,

$$P = \left(\frac{V_S}{V_{\text{rated}}}\right)\left(\frac{V_R}{V_{\text{rated}}}\right)\left(\frac{V^2_{\text{rated}}}{Z_c}\right)\frac{\sin\delta}{\sin\left(\frac{2\pi l}{\lambda}\right)}$$

$$= V_{S\text{p.u.}} V_{R\text{p.u.}} (\mathrm{SIL}) \frac{\sin\delta}{\sin\left(\frac{2\pi l}{\lambda}\right)} \quad \mathrm{W} \tag{5.4.29}$$

Copyright 2017 Cengage Learning. All Rights Reserved. May not be copied, scanned, or duplicated, in whole or in part. Due to electronic rights, some third party content may be suppressed from the eBook and/or eChapter(s). Editorial review has deemed that any suppressed content does not materially affect the overall learning experience. Cengage Learning reserves the right to remove additional content at any time if subsequent rights restrictions require it.

And for $\delta = 90°$, the theoretical steady-state stability limit is

$$P_{\max} = \frac{V_{\text{Sp.u.}} V_{\text{Rp.u.}} (\text{SIL})}{\sin\left(\frac{2\pi l}{\lambda}\right)} \quad \text{W} \tag{5.4.30}$$

Equations (5.4.27) through (5.4.30) reveal two important factors affecting the steady-state stability limit. First, from (5.4.27), it increases with the square of the line voltage. For example, a doubling of line voltage enables a fourfold increase in maximum power flow. Second, it decreases with line length. Equation (5.4.30) is plotted in Figure 5.12 for $V_{\text{Sp.u.}} = V_{\text{Rp.u.}} = 1$, $\lambda = 5000$ km, and line lengths up to 1100 km. As shown, the theoretical steady-state stability limit decreases from 4(SIL) for a 200 km line to about 2(SIL) for a 400 km line.

EXAMPLE 5.4

Theoretical steady-state stability limit: long line

Neglecting line losses, find the theoretical steady-state stability limit for the 300-km line in Example 5.2. Assume a 266.1-Ω surge impedance, a 5000 km wavelength, and $V_S = V_R = 765$ kV.

SOLUTION

From (5.4.21),

$$\text{SIL} = \frac{(765)^2}{266.1} = 2199 \quad \text{MW}$$

From (5.4.30) with $l = 300$ km and $\lambda = 5000$ km,

$$P_{\max} = \frac{(1)(1)(2199)}{\sin\left(\frac{2\pi \times 300}{5000}\right)} = (2.716)(2199) = 5974 \quad \text{MW}$$

Alternatively, from Figure 5.12, for a 300 km line, the theoretical steady-state stability limit is (2.72)SIL = (2.72)(2199) = 5980 MW, which is about the same as the previous result (see Figure 5.13).

Open PowerWorld Simulator case Example 5_4 and select **Tools**, **Play** to see this example. When the load on a line is equal to the SIL, the voltage profile across the line is flat, and the line's net reactive power losses are zero. For loads above the SIL, the line consumes reactive power, and the load's voltage magnitude is below the sending-end value. Conversely, for loads below the SIL, the line actually generates reactive power, and the load's voltage magnitude is above the

(*Continued*)

Copyright 2017 Cengage Learning. All Rights Reserved. May not be copied, scanned, or duplicated, in whole or in part. Due to electronic rights, some third party content may be suppressed from the eBook and/or eChapter(s). Editorial review has deemed that any suppressed content does not materially affect the overall learning experience. Cengage Learning reserves the right to remove additional content at any time if subsequent rights restrictions require it.

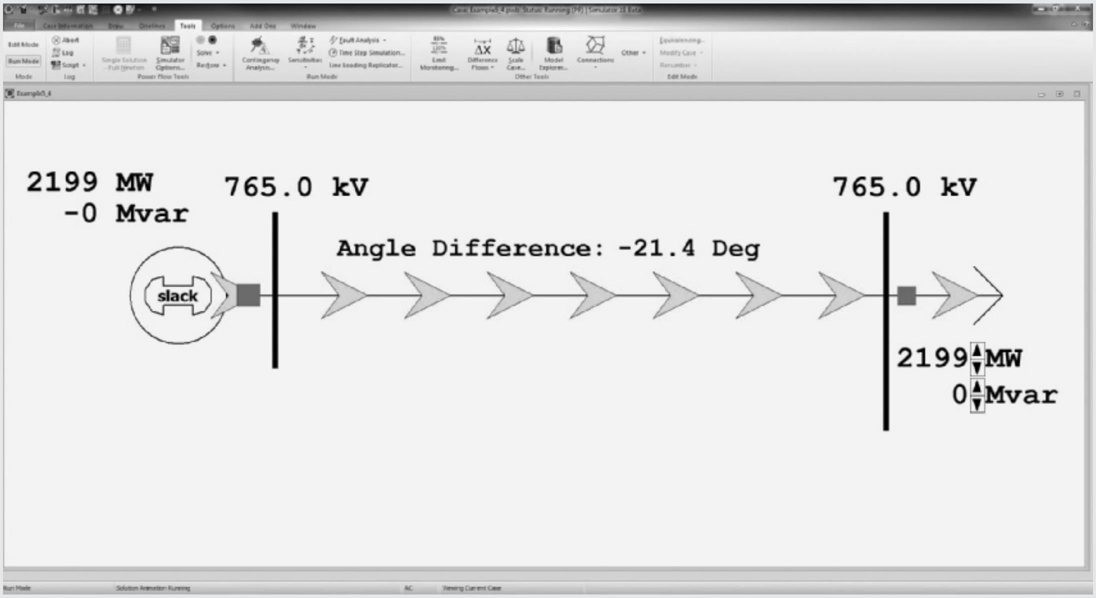

FIGURE 5.13

Screen for Example 5.4

sending-end value. Use the load arrow button to vary the load to see the changes in the receiving-end voltage and the line's reactive power consumption (indicated by the reactive power supplied by the generator).

5.5 MAXIMUM POWER FLOW

Maximum power flow, discussed in Section 5.4 for lossless lines, is derived here in terms of the *ABCD* parameters for lossy lines. The following notation is used:

$$A = \cosh(\gamma\ell) = \mathrm{A}\underline{/\theta_{\mathrm{A}}}$$
$$B = Z' = Z'\underline{/\theta_Z}$$
$$V_{\mathrm{S}} = \mathrm{V}_{\mathrm{S}}\underline{/\delta} \qquad V_{\mathrm{R}} = \mathrm{V}_{\mathrm{R}}\underline{/0^\circ}$$

Solving (5.2.33) for the receiving-end current,

$$I_{\mathrm{R}} = \frac{V_{\mathrm{S}} - AV_{\mathrm{R}}}{B} = \frac{\mathrm{V}_{\mathrm{S}}e^{j\delta} - \mathrm{A}\mathrm{V}_{\mathrm{R}}e^{j\theta_{\mathrm{A}}}}{Z'e^{j\theta_Z}} \tag{5.5.1}$$

The complex power delivered to the receiving end is

Copyright 2017 Cengage Learning. All Rights Reserved. May not be copied, scanned, or duplicated, in whole or in part. Due to electronic rights, some third party content may be suppressed from the eBook and/or eChapter(s). Editorial review has deemed that any suppressed content does not materially affect the overall learning experience. Cengage Learning reserves the right to remove additional content at any time if subsequent rights restrictions require it.

$$S_R = P_R + jQ_R = V_R I_R^* = V_R \left[\frac{V_S e^{j(\delta-\theta_Z)} - AV_R e^{j(\theta_A-\theta_Z)}}{Z'} \right]^*$$

$$= \frac{V_R V_S}{Z'} e^{j(\theta_Z-\delta)} - \frac{AV_R^2}{Z'} e^{j(\theta_Z-\theta_A)} \tag{5.5.2}$$

The real and reactive power delivered to the receiving end are thus

$$P_R = \text{Re}(S_R) = \frac{V_R V_S}{Z'} \cos(\theta_Z - \delta) - \frac{AV_R^2}{Z'} \cos(\theta_Z - \theta_A) \tag{5.5.3}$$

$$Q_R = \text{Im}(S_R) = \frac{V_R V_S}{Z'} \sin(\theta_Z - \delta) - \frac{AV_R^2}{Z'} \sin(\theta_Z - \theta_A) \tag{5.5.4}$$

Note that for a lossless line, $\theta_A = 0°$, $B = Z' = jX'$, $Z' = X'$, $\theta_Z = 90°$, and (5.5.3) reduces to

$$P_R = \frac{V_R V_S}{X'} \cos(90 - \delta) - \frac{AV_R^2}{X'} \cos(90°)$$

$$= \frac{V_R V_S}{X'} \sin\delta \tag{5.5.5}$$

which is the same as (5.4.26).

The theoretical maximum real power delivered (or steady-state stability limit) occurs when $\delta = \theta z$ in (5.5.3):

$$P_{R\max} = \frac{V_R V_S}{Z'} - \frac{AV_R^2}{Z'} \cos(\theta_Z - \theta_A) \tag{5.5.6}$$

The second term in (5.5.6), and the fact that Z' is larger than X', reduce $P_{R\max}$ to a value somewhat less than that given by (5.4.27) for a lossless line.

EXAMPLE 5.5

Theoretical maximum power delivered: long line

Determine the theoretical maximum power, in MW and in per-unit of SIL, that the line in Example 5.2 can deliver. Assume $V_S = V_R = 765$ kV.

SOLUTION

From Example 5.2,

$A = 0.9313$ per unit; $\theta_A = 0.209°$

$B = Z' = 97.0\ \Omega$ $\theta_Z = 87.2$

$Z_c = 266.1\ \Omega$

(*Continued*)

Copyright 2017 Cengage Learning. All Rights Reserved. May not be copied, scanned, or duplicated, in whole or in part. Due to electronic rights, some third party content may be suppressed from the eBook and/or eChapter(s). Editorial review has deemed that any suppressed content does not materially affect the overall learning experience. Cengage Learning reserves the right to remove additional content at any time if subsequent rights restrictions require it.

From (5.5.6) with $V_S = V_R = 765$ kV,

$$P_{R\max} = \frac{(765)^2}{97} - \frac{(0.9313)(765)^2}{97}\cos(87.2^\circ - 0.209^\circ)$$

From (5.4.20),

$$\text{SIL} = \frac{(765)^2}{266.1} = 2199 \quad \text{MW}$$

Thus

$$P_{R\max} = \frac{5738}{2199} = 2.61 \quad \text{per unit}$$

This value is about 4% less than that found in Example 5.4, where losses were neglected.

5.6 LINE LOADABILITY

In practice, power lines are not operated to deliver their theoretical maximum power, which is based on rated terminal voltages and an angular displacement $\delta = 90^\circ$ across the line. Figure 5.12 shows a practical line loadability curve plotted below the theoretical steady-state stability limit. This curve is based on the voltage-drop limit $V_R/V_S \geq 0.95$ and on a maximum angular displacement of 30 to 35° across the line (or about 45° across the line and equivalent system reactances) in order to maintain stability during transient disturbances [1, 3]. The curve is valid for typical overhead 60-Hz lines with no compensation. Note that for short lines less than 25 km long, loadability is limited by the thermal rating of the conductors or by terminal equipment ratings, not by voltage drop or stability considerations. Section 5.7 investigates series and shunt compensation techniques to increase the loadability of longer lines toward their thermal limit.

EXAMPLE 5.6

Practical line loadability and percent voltage regulation: long line

The 300-km uncompensated line in Example 5.2 has four 1,272,000 cmil 54/3 ACSR conductors per bundle. The sending-end voltage is held constant at 1.0 per-unit of rated line voltage. Determine the following:

a. The practical line loadability. (Assume an approximate receiving-end voltage $V_R = 0.95$ per unit and $\delta = 35^\circ$ maximum angle across the line.)

Copyright 2017 Cengage Learning. All Rights Reserved. May not be copied, scanned, or duplicated, in whole or in part. Due to electronic rights, some third party content may be suppressed from the eBook and/or eChapter(s). Editorial review has deemed that any suppressed content does not materially affect the overall learning experience. Cengage Learning reserves the right to remove additional content at any time if subsequent rights restrictions require it.

b. The full-load current at 0.986 p.f. leading based on the above practical line loadability

c. The exact receiving-end voltage for the full-load current found in part (b)

d. Percent voltage regulation for the above full-load current

e. Thermal limit of the line, based on the approximate current-carrying capacity given in Table A.4

SOLUTION

a. From (5.5.3), with $V_S = 765$, $V_R = 0.95 \times 765$ kV, and $\delta = 35°$, using the values of Z', θ_z, A, and θ_A from Example 5.5,

$$\begin{aligned} P_R &= \frac{(765)(0.95\times765)}{97.0}\cos(87.2° - 35°) \\ &\quad - \frac{(0.9313)(0.95\times765)^2}{97.0}\cos(87.2° - 0.209°) \\ &= 3513 - 266 = 3247 \quad \text{MW} \end{aligned}$$

$P_R = 3247$ MW is the practical line loadability, provided the thermal and voltage-drop limits are not exceeded. Alternatively, from Figure 5.12 for a 300 km line, the practical line loadability is (1.49)SIL= (1.49)(2199) = 3277 MW, which is about the same as the previous result.

b. For the loading at 0.986 p.f. leading and at 0.95 × 765 kV, the full-load receiving-end current is

$$I_{RFL} = \frac{P_R}{\sqrt{3}V_R(\text{p.f.})} = \frac{3247}{(\sqrt{3})(0.95\times765)(0.986)} = 2.616 \quad \text{kA}$$

c. From (5.1.1) with $I_{RFL} = 2.616\underline{/\cos^{-1} 0.986} = 2.616\underline{/9.599°}$ kA, using the A and B parameters from Example 5.2,

$$V_S = AV_{RFL} + BI_{RFL}$$

$$\frac{765}{\sqrt{3}}\underline{/\delta} = (0.9313\underline{/0.209°})\,(V_{RFL}\underline{/0°}) + (97.0\underline{/87.2°})\,(2.616\underline{/9.599°})$$

$$441.7\underline{/\delta} = (0.9313\,V_{RFL} - 30.04) + j(0.0034V_{RFL} + 251.97)$$

Taking the squared magnitude of the above equation,

$$(441.7)^2 = 0.8673V_{RFL}^2 - 54.24V_{RFL} + 64{,}391$$

Solving,

$$\begin{aligned} V_{RFL} &= 420.7 \text{ kV}_{LN} \\ &= 420.7\sqrt{3} = 728.7 \text{ kV}_{LL} = 0.953 \text{ per unit} \end{aligned}$$

(*Continued*)

Copyright 2017 Cengage Learning. All Rights Reserved. May not be copied, scanned, or duplicated, in whole or in part. Due to electronic rights, some third party content may be suppressed from the eBook and/or eChapter(s). Editorial review has deemed that any suppressed content does not materially affect the overall learning experience. Cengage Learning reserves the right to remove additional content at any time if subsequent rights restrictions require it.

d. From (5.1.19), the receiving-end no-load voltage is

$$V_{RNL} = \frac{V_S}{A} = \frac{765}{0.9313} = 821.4 \quad kV_{LL}$$

And from (5.1.18),

$$\text{percent VR} = \frac{821.4 - 728.7}{728.7} \times 100 = 12.72\%$$

e. From Table A.4, the approximate current-carrying capacity of four 1,272,000-cmil 54/3 ACSR conductors is $4 \times 1.2 = 4.8$ kA.

Since the voltages $V_S = 1.0$ and $V_{RFL} = 0.953$ per unit satisfy the voltage-drop limit $V_R/V_S \geq 0.95$, the factor that limits line loadability is steady-state stability for this 300-km uncompensated line. The full-load current of 2.616 kA corresponding to loadability is also well below the thermal limit of 4.8 kA. The 12.7% voltage regulation is too high because the no-load voltage is too high. Compensation techniques to reduce no-load voltages are discussed in Section 5.7.

EXAMPLE 5.7

Selection of transmission line voltage and number of lines for power transfer

From a hydroelectric power plant, 9000 MW are to be transmitted to a load center located 500 km from the plant. Based on practical line loadability criteria, determine the number of three-phase, 60 Hz lines required to transmit this power, with one line out of service, for the following cases: (a) 345 kV lines with $Z_c = 297\ \Omega$; (b) 500-kV lines with $Z_c = 277\ \Omega$; and (c) 765-kV lines with $Z_c = 266\ \Omega$. Assume $V_S = 1.0$ per unit, $V_R = 0.95$ per unit, and $\delta = 35°$. Also assume that the lines are uncompensated and widely separated such that there is negligible mutual coupling between them.

SOLUTION

a. For 345 kV lines, (5.4.21) yields

$$\text{SIL} = \frac{(345)^2}{297} = 401 \quad \text{MW}$$

Neglecting losses, from (5.4.29), with $\ell = 500$ km and $\delta = 35°$,

$$P = \frac{(1.0)(0.95)(401)\sin(35°)}{\sin\left(\dfrac{2\pi \times 500}{5000}\right)} = (401)\,(0.927) = 372 \quad \text{MW/line}$$

Copyright 2017 Cengage Learning. All Rights Reserved. May not be copied, scanned, or duplicated, in whole or in part. Due to electronic rights, some third party content may be suppressed from the eBook and/or eChapter(s). Editorial review has deemed that any suppressed content does not materially affect the overall learning experience. Cengage Learning reserves the right to remove additional content at any time if subsequent rights restrictions require it.

Alternatively, the practical line loadability curve in Figure 5.12 can be used to obtain P = (0.93)SIL for typical 500-km overhead 60-Hz uncompensated lines.

In order to transmit 9000 MW with one line out of service,

$$\#345\text{ kV lines} = \frac{9000\text{ MW}}{372\text{ MW/line}} + 1 = 24.2 + 1 \approx 26$$

b. For 500 kV lines,

$$\text{SIL} = \frac{(500)^2}{277} = 903 \quad \text{MW}$$

$$\text{P} = (903)(0.927) = 837 \quad \text{MW/line}$$

$$\#500\text{ kV lines} = \frac{9000}{837} + 1 = 10.8 + 1 \approx 12$$

c. For 765 kV lines,

$$\text{SIL} = \frac{(765)^2}{266} = 2200 \quad \text{MW}$$

$$\text{P} = (2200)(0.927) = 2039 \quad \text{MW/line}$$

$$\#765\text{ kV lines} = \frac{9000}{2039} + 1 = 4.4 + 1 \approx 6$$

Increasing the line voltage from 345 to 765 kV, which is a factor of 2.2, reduces the required number of lines from 26 to 6, which is a factor of 4.3.

EXAMPLE 5.8

Effect of intermediate substations on number of lines required for power transfer

Can five instead of six 765 kV lines transmit the required power in Example 5.7 if there are two intermediate substations that divide each line into three 167-km line sections, and if only one line section is out of service?

SOLUTION

The lines are shown in Figure 5.14. For simplicity, neglect line losses. The equivalent π circuit of one 500 km, 765 kV line has a series reactance from (5.4.10) and (5.4.15),

$$X' = (266)\sin\left(\frac{2\pi \times 500}{5000}\right) = 156.35 \quad \Omega$$

(*Continued*)

Copyright 2017 Cengage Learning. All Rights Reserved. May not be copied, scanned, or duplicated, in whole or in part. Due to electronic rights, some third party content may be suppressed from the eBook and/or eChapter(s). Editorial review has deemed that any suppressed content does not materially affect the overall learning experience. Cengage Learning reserves the right to remove additional content at any time if subsequent rights restrictions require it.

FIGURE 5.14

Transmission-line configuration for Example 5.8

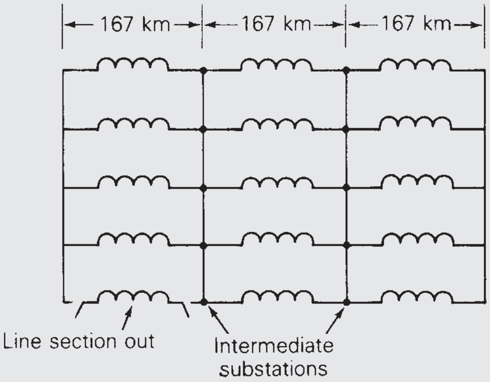

Combining series/parallel reactances in Figure 5.14, the equivalent reactance of five lines with one line section out of service is

$$X_{eq} = \frac{1}{5}\left(\frac{2}{3}X'\right) + \frac{1}{4}\left(\frac{X'}{3}\right) = 0.2167X' = 33.88 \quad \Omega$$

Then, from (5.4.26) with $\delta = 35°$,

$$P = \frac{(765)(765 \times 0.95)\sin(35°)}{33.88} = 9412 \quad \text{MW}$$

Inclusion of line losses would reduce the above value by 3 or 4% to about 9100 MW. Therefore, the answer is yes. Five 765-kV, 500-km uncompensated lines with two intermediate substations and with one line section out of service transmits 9000 MW. Intermediate substations are often economical if their costs do not outweigh the reduction in line costs.

This example is modeled in PowerWorld Simulator case Example 5_8 (see Figure 5.15). Each line segment is represented with the lossless line model from Example 5.4 with the π circuit parameters modified to exactly match those for a 167-km distributed line. The pie charts on each line segment show the percentage loading of the line, assuming a rating of 3500 MVA. The solid red squares on the lines represent closed circuit breakers, and the green squares correspond to open circuit breakers. Clicking on a circuit breaker toggles its status. The simulation results differ slightly from the simplified analysis done earlier in the example because the PowerWorld simulation includes the charging capacitance of the transmission lines. With all line segments in-service, use the load's arrow to verify that the SIL for this system is 11,000 MW, which is five times that of the single circuit line in Example 5.4.

Copyright 2017 Cengage Learning. All Rights Reserved. May not be copied, scanned, or duplicated, in whole or in part. Due to electronic rights, some third party content may be suppressed from the eBook and/or eChapter(s). Editorial review has deemed that any suppressed content does not materially affect the overall learning experience. Cengage Learning reserves the right to remove additional content at any time if subsequent rights restrictions require it.

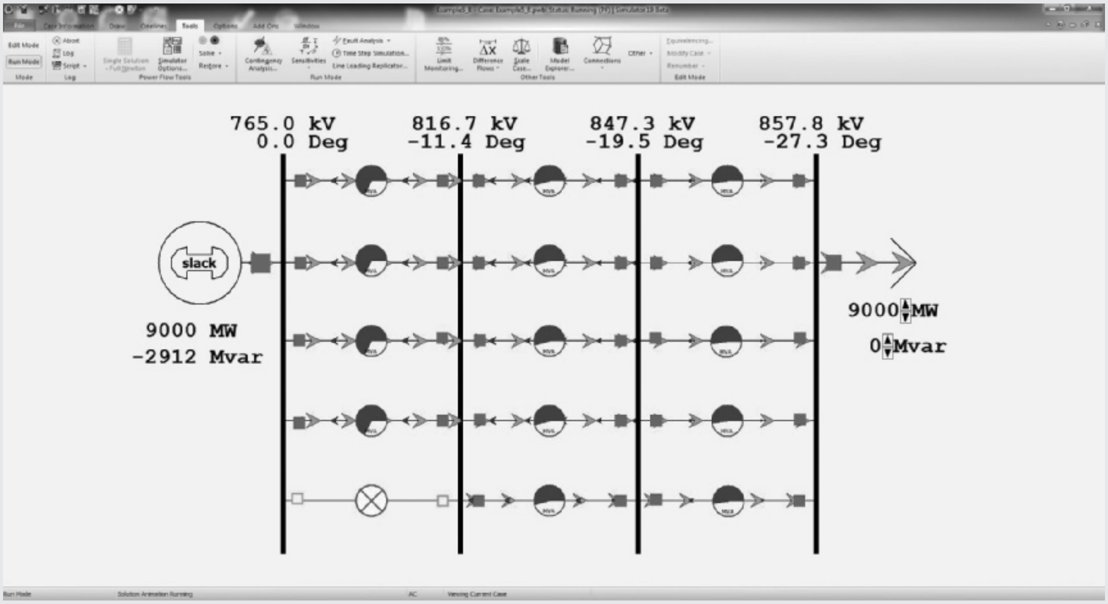

FIGURE 5.15

Screen for Example 5.8

5.7 REACTIVE COMPENSATION TECHNIQUES

Inductors and capacitors are used on medium-length and long transmission lines to increase line loadability and to maintain voltages near rated values.

Shunt reactors (inductors) are commonly installed at selected points along EHV lines from each phase to neutral. The inductors absorb reactive power and reduce overvoltages during light load conditions. They also reduce transient overvoltages due to switching and lightning surges. However, shunt reactors can reduce line loadability if they are not removed under full-load conditions.

In addition to shunt reactors, shunt capacitors are sometimes used to deliver reactive power and increase transmission voltages during heavy load conditions. Another type of shunt compensation includes thyristor-switched reactors in parallel with capacitors. These devices, called *static var compensators*, can absorb reactive power during light loads and deliver reactive power during heavy loads. Through automatic control of the thyristor switches, voltage fluctuations are minimized and line loadability is increased. Synchronous condensors (synchronous motors with no mechanical load) can also control their reactive power output, although more slowly than static var compensators.

Series capacitors are sometimes used on long lines to increase line loadability. Capacitor banks are installed in series with each phase conductor at selected points

Copyright 2017 Cengage Learning. All Rights Reserved. May not be copied, scanned, or duplicated, in whole or in part. Due to electronic rights, some third party content may be suppressed from the eBook and/or eChapter(s). Editorial review has deemed that any suppressed content does not materially affect the overall learning experience. Cengage Learning reserves the right to remove additional content at any time if subsequent rights restrictions require it.

FIGURE 5.16

Compensated transmission-line section

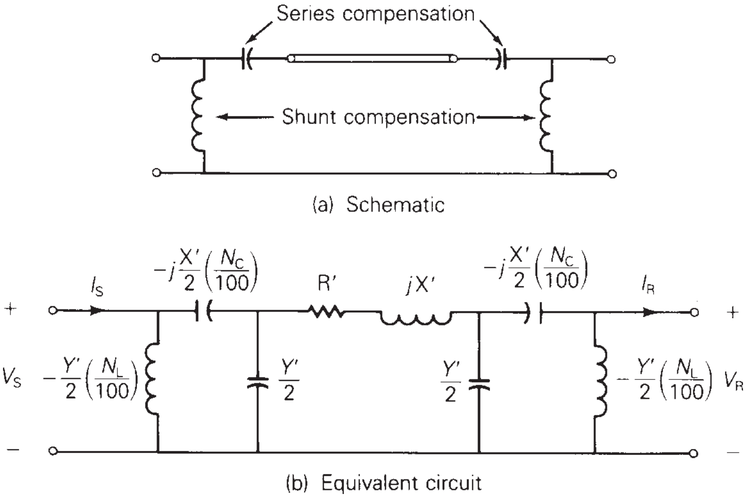
Series compensation
Shunt compensation
(a) Schematic
I_S
$-j\frac{X'}{2}\left(\frac{N_C}{100}\right)$
R′
jX'
$-j\frac{X'}{2}\left(\frac{N_C}{100}\right)$
I_R
+
V_S
$-\frac{Y'}{2}\left(\frac{N_L}{100}\right)$
$\frac{Y'}{2}$
$\frac{Y'}{2}$
$-\frac{Y'}{2}\left(\frac{N_L}{100}\right)$
V_R
−
(b) Equivalent circuit

along a line. Their effect is to reduce the net series impedance of the line in series with the capacitor banks, thereby reducing line-voltage drops and increasing the steady-state stability limit. A disadvantage of series capacitor banks is that automatic protection devices must be installed to bypass high currents during faults and to reinsert the capacitor banks after fault clearing. Also, the addition of series capacitors can excite low-frequency oscillations, a phenomenon called *subsynchronous resonance*, which may damage turbine-generator shafts. Studies have shown, however, that series capacitive compensation can increase the loadability of long lines at only a fraction of the cost of new transmission [1].

Figure 5.16 shows a schematic and an equivalent circuit for a compensated line section, where N_C is the amount of series capacitive compensation expressed in percent of the positive-sequence line impedance and N_L is the amount of shunt reactive compensation in percent of the positive-sequence line admittance. It is assumed in Figure 5.16 that half of the compensation is installed at each end of the line section. The following two examples illustrate the effect of compensation.

EXAMPLE 5.9

Shunt reactive compensation to improve transmission-line voltage regulation

Identical shunt reactors (inductors) are connected from each phase conductor to neutral at both ends of the 300 km line in Example 5.2 during light load conditions, providing 75% compensation. The reactors are removed during heavy load conditions. Full load is 1.90 kA at unity p.f. and at 730 kV. Assuming that the sending-end voltage is constant, determine the following properties.

Copyright 2017 Cengage Learning. All Rights Reserved. May not be copied, scanned, or duplicated, in whole or in part. Due to electronic rights, some third party content may be suppressed from the eBook and/or eChapter(s). Editorial review has deemed that any suppressed content does not materially affect the overall learning experience. Cengage Learning reserves the right to remove additional content at any time if subsequent rights restrictions require it.

a. Percent voltage regulation of the uncompensated line
b. The equivalent shunt admittance and series impedance of the compensated line
c. Percent voltage regulation of the compensated line

SOLUTION

a. From (5.1.1) with $I_{RFL} = 1.9\underline{/0°}$ kA, using the A and B parameters from Example 5.2,

$$\begin{aligned} V_S &= AV_{RFL} + BI_{RFL} \\ &= (0.9313\underline{/0.209°})\left(\frac{730}{\sqrt{3}}\underline{/0°}\right) + (97.0\underline{/87.2°})(1.9\underline{/0°}) \\ &= 392.5\underline{/0.209°} + 184.3\underline{/87.2°} \\ &= 401.5 + j185.5 \\ &= 442.3\underline{/24.8°} \quad \text{kV}_{LN} \end{aligned}$$

$$\text{V}_S = 442.3\sqrt{3} = 766.0 \quad \text{kV}_{LL}$$

The no-load receiving-end voltage is, from (5.1.19),

$$\text{V}_{RNL} = \frac{766.0}{0.9313} = 822.6 \quad \text{kV}_{LL}$$

and the percent voltage regulation for the uncompensated line is, from (5.1.18),

$$\text{percent VR} = \frac{822.6 - 730}{730} \times 100 = 12.68\%$$

b. From Example 5.3, the shunt admittance of the equivalent π circuit without compensation is

$$\begin{aligned} Y' &= 2(3.7 \times 10^{-7} + j7.094 \times 10^{-4}) \\ &= 7.4 \times 10^{-7} + j14.188 \times 10^{-4} \quad \text{S} \end{aligned}$$

With 75% shunt compensation, the equivalent shunt admittance is

$$\begin{aligned} Y_{eq} &= 7.4 \times 10^{-7} + j14.188 \times 10^{-4}\left(1 - \tfrac{75}{100}\right) \\ &= 3.547 \times 10^{-4}\underline{/89.88°} \quad \text{S} \end{aligned}$$

Since there is no series compensation, the equivalent series impedance is the same as without compensation:

$$Z_{eq} = Z' = 97.0\underline{/87.2°} \quad \Omega$$

(*Continued*)

Copyright 2017 Cengage Learning. All Rights Reserved. May not be copied, scanned, or duplicated, in whole or in part. Due to electronic rights, some third party content may be suppressed from the eBook and/or eChapter(s). Editorial review has deemed that any suppressed content does not materially affect the overall learning experience. Cengage Learning reserves the right to remove additional content at any time if subsequent rights restrictions require it.

c. The equivalent A parameter for the compensated line is

$$\begin{aligned} A_{\text{eq}} &= 1 + \frac{Y_{\text{eq}} Z_{\text{eq}}}{2} \\ &= 1 + \frac{(3.547 \times 10^{-4} \underline{/89.88°})(97.0 \underline{/87.2°})}{2} \\ &= 1 + 0.0172 \underline{/177.1°} \\ &= 0.9828 \underline{/0.05°} \quad \text{per unit} \end{aligned}$$

Then, from (5.1.19),

$$V_{\text{RNL}} = \frac{766}{0.9828} = 779.4 \quad \text{kV}_{\text{LL}}$$

Since the shunt reactors are removed during heavy load conditions, $V_{\text{RFL}} = 730$ kV is the same as without compensation. Therefore

$$\text{percent VR} = \frac{779.4 - 730}{730} \times 100 = 6.77\%$$

The use of shunt reactors at light loads improves the voltage regulation from 12.68% to 6.77% for this line.

EXAMPLE 5.10

Series capacitive compensation to increase transmission-line loadability

Identical series capacitors are installed in each phase at both ends of the line in Example 5.2, providing 30% compensation. Determine the theoretical maximum power that this compensated line can deliver and compare with that of the uncompensated line. Assume $V_S = V_R = 765$ kV.

SOLUTION

From Example 5.3, the equivalent series reactance without compensation is

$$X' = 97.0 \sin 87.2° = 96.88 \quad \Omega$$

Based on 30% series compensation, half at each end of the line, the impedance of each series capacitor is

$$Z_{\text{cap}} = -jX_{\text{cap}} = -j\left(\tfrac{1}{2}\right)(0.30)(96.88) = -j14.53 \quad \Omega$$

Copyright 2017 Cengage Learning. All Rights Reserved. May not be copied, scanned, or duplicated, in whole or in part. Due to electronic rights, some third party content may be suppressed from the eBook and/or eChapter(s). Editorial review has deemed that any suppressed content does not materially affect the overall learning experience. Cengage Learning reserves the right to remove additional content at any time if subsequent rights restrictions require it.

From Figure 5.4, the *ABCD* matrix of this series impedance is

$$\left[\begin{array}{c|c} 1 & -j14.53 \\ \hline 0 & 1 \end{array}\right]$$

As also shown in Figure 5.4, the equivalent *ABCD* matrix of networks in series is obtained by multiplying the *ABCD* matrices of the individual networks. For this example there are three networks: the series capacitors at the sending end, the line, and the series capacitors at the receiving end. Therefore the equivalent *ABCD* matrix of the compensated line is, using the *ABCD* parameters, from Example 5.2,

$$\left[\begin{array}{c|c} 1 & -j14.53 \\ \hline 0 & 1 \end{array}\right]\left[\begin{array}{c|c} 0.9313\angle 0.209^\circ & 97.0\angle 87.2^\circ \\ \hline 1.37\times 10^{-3}\angle 90.06^\circ & 0.9313\angle 0.209^\circ \end{array}\right]\left[\begin{array}{c|c} 1 & -j14.53 \\ \hline 0 & 1 \end{array}\right]$$

After performing these matrix multiplications, results in

$$\left[\begin{array}{c|c} A_{\text{eq}} & B_{\text{eq}} \\ \hline C_{\text{eq}} & D_{\text{eq}} \end{array}\right] = \left[\begin{array}{c|c} 0.9512\angle 0.205^\circ & 69.70\angle 86.02^\circ \\ \hline 1.37\times 10^{-3}\angle 90.06^\circ & 0.9512\angle 0.205^\circ \end{array}\right]$$

Therefore

$$A_{\text{eq}} = 0.9512 \quad \text{per unit} \qquad \theta_{\text{Aeq}} = 0.205^\circ$$

$$B_{\text{eq}} = Z'_{\text{eq}} = 69.70 \quad \Omega \qquad \theta_{\text{Zeq}} = 86.02^\circ$$

From (5.5.6) with $V_S = V_R = 765$ kV,

$$P_{\text{Rmax}} = \frac{(765)^2}{69.70} - \frac{(0.9512)(765)^2}{69.70}\cos(86.02^\circ - 0.205^\circ)$$

$$= 8396 - 583 = 7813 \quad \text{MW}$$

which is 36.2% larger than the value of 5738 MW found in Example 5.5 without compensation. Note that the practical line loadability of this series compensated line is also about 35% larger than the value of 3247 MW found in Example 5.6 without compensation.

This example is modeled in PowerWorld Simulator case Example 5_10 (see Figure 5.17). When opened, both of the series capacitors are bypassed (i.e., they are modeled as short circuits), meaning this case is initially identical to the Example 5.4 case. Click on the blue Bypassed field to place each of the series capacitors into the circuit. This decreases the angle across the line, resulting in more net power transfer.

(*Continued*)

Copyright 2017 Cengage Learning. All Rights Reserved. May not be copied, scanned, or duplicated, in whole or in part. Due to electronic rights, some third party content may be suppressed from the eBook and/or eChapter(s). Editorial review has deemed that any suppressed content does not materially affect the overall learning experience. Cengage Learning reserves the right to remove additional content at any time if subsequent rights restrictions require it.

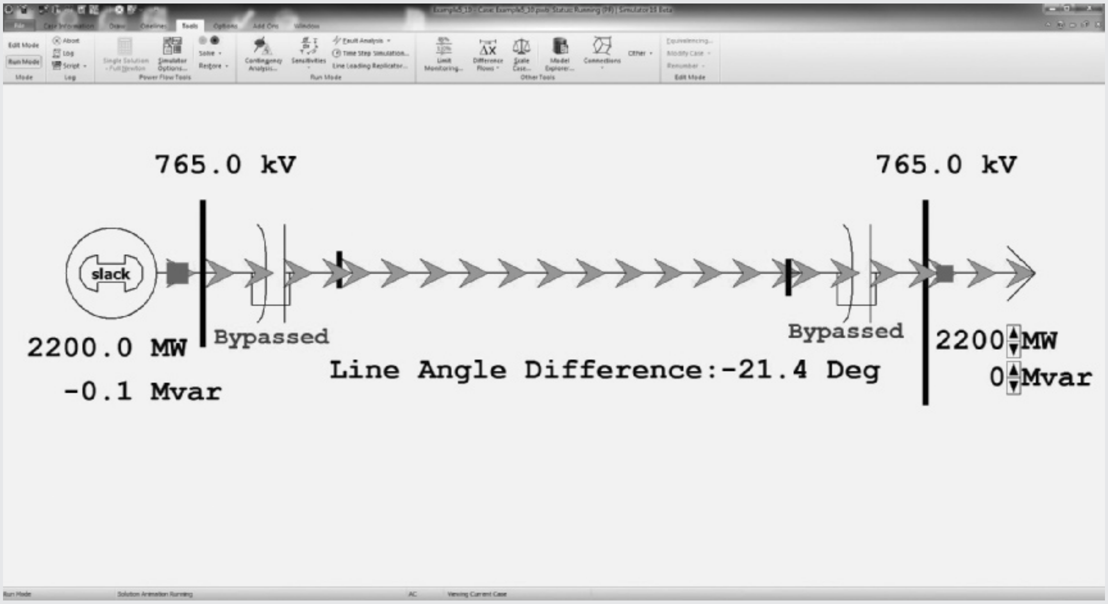

FIGURE 5.17

Screen for Example 5.10

MULTIPLE CHOICE QUESTIONS

SECTION 5.1

5.1 Representing a transmission line by the two-port network, in terms of *ABCD* parameters, (a) express V_S, which is the sending-end voltage, in terms of V_R, which is the receiving-end voltage, and I_R, the receiving-end current, and (b) express I_S, which is the sending-end current, in terms of V_R and I_R.
(a) $V_S =$ __________ (b) $I_S =$ __________

5.2 As applied to linear, passive, bilateral two-port networks, the *ABCD* parameters satisfy $AD - BC = 1$.
(a) True (b) False

5.3 Express the no-load receiving-end voltage V_{RNL} in terms of the sending-end voltage, V_S, and the *ABCD* parameters.

5.4 The *ABCD* parameters, which are in general complex numbers, have units of __________, __________, __________, and __________, respectively.

5.5 The loadability of short transmission lines (less than 25 km, represented by including only series resistance and reactance) is determined

Copyright 2017 Cengage Learning. All Rights Reserved. May not be copied, scanned, or duplicated, in whole or in part. Due to electronic rights, some third party content may be suppressed from the eBook and/or eChapter(s). Editorial review has deemed that any suppressed content does not materially affect the overall learning experience. Cengage Learning reserves the right to remove additional content at any time if subsequent rights restrictions require it.

by __________; that of medium lines (less than 250 km, represented by nominal π circuit) is determined by __________; and that of long lines (more than 250 km, represented by equivalent π circuit) is determined by __________.

5.6 Can the voltage regulation, which is proportional to $(V_{\text{RNL}} - V_{\text{RFL}})$, be negative?
(a) Yes (b) No

SECTION 5.2

5.7 The propagation constant, which is a complex quantity in general, has units of ______, and the characteristic impedance has units of ______.

5.8 Express hyperbolic functions cosh $\sqrt{x}$ and sinh $\sqrt{x}$ in terms of exponential functions.

5.9 e^{γ}, where $\gamma = \alpha + j\beta$, can be expressed as $e^{\alpha l} \underline{/\beta l}$, in which αl is dimensionless and βl is in radians (also dimensionless).
(a) True (b) False

SECTION 5.3

5.10 The equivalent π circuit is identical in structure to the nominal π circuit.
(a) True (b) False

5.11 The correction factors $F_1 = \sinh(\gamma l)\, \gamma l$ and $F_2 = \tanh(\gamma l/2)/(\gamma l/2)$, which are complex numbers, have the units of ______.

SECTION 5.4

5.12 For a lossless line, the surge impedance is purely resistive and the propagation constant is pure imaginary.
(a) True (b) False

5.13 For equivalent π circuits of lossless lines, the A and D parameters are pure _______, whereas B and C parameters are pure _______.

5.14 In equivalent π circuits of lossless lines, Z' is pure __________, and Y' is pure __________.

5.15 Typical power-line lengths are only a small fraction of the 60-Hz wavelength.
(a) True (b) False

5.16 The velocity of propagation of voltage and current waves along a lossless overhead line is the same as speed of light.
(a) True (b) False

5.17 Surge Impedance Loading (SIL) is the power delivered by a lossless line to a load resistance equal to __________.

5.18 For a lossless line, at SIL, the voltage profile is __________, and the real power delivered, in terms of rated line voltage V and surge impedance Z_c, is given by __________.

Copyright 2017 Cengage Learning. All Rights Reserved. May not be copied, scanned, or duplicated, in whole or in part. Due to electronic rights, some third party content may be suppressed from the eBook and/or eChapter(s). Editorial review has deemed that any suppressed content does not materially affect the overall learning experience. Cengage Learning reserves the right to remove additional content at any time if subsequent rights restrictions require it.

5.19 The maximum power that a lossless line can deliver, in terms of the voltage magnitudes V_S and V_R (in volts) at the ends of the line held constant, and the series reactance X' of the corresponding equivalent π circuit, is given by __________, in watts.

SECTION 5.5

5.20 The maximum power flow for a lossy line is somewhat less than that for a lossless line.
(a) True (b) False

SECTION 5.6

5.21 For short lines less than 25 km long, loadability is limited by the thermal rating of the conductors or by terminal equipment ratings, not by voltage drop or stability considerations.
(a) True (b) False

5.22 Increasing the transmission line voltage reduces the required number of lines for the same power transfer.
(a) True (b) False

5.23 Intermediate substations are often economical from the viewpoint of the number of lines required for power transfer if their costs do not outweigh the reduction in line costs.
(a) True (b) False

SECTION 5.7

5.24 Shunt reactive compensation improves transmission-line ______, whereas series capacitive compensation increases transmission-line ______.

5.25 Static-var-compensators can absorb reactive power during light loads and deliver reactive power during heavy loads.
(a) True (b) False

PROBLEMS

SECTION 5.1

5.1 A 30-km, 34.5-kV, 60-Hz, three-phase line has a positive-sequence series impedance $z = 0.19 + j0.34\ \Omega/\text{km}$. The load at the receiving end absorbs 10 MVA at 33 kV. Assuming a short line, calculate: (a) the *ABCD* parameters, (b) the sending-end voltage for a load power factor of 0.9 lagging, and (c) the sending-end voltage for a load power factor of 0.9 leading.

5.2 A 200-km, 230-kV, 60-Hz, three-phase line has a positive-sequence series impedance $z = 0.08 + j0.48\ \Omega/\text{km}$ and a positive-sequence shunt admittance $y = j3.33 \times 10^{-6}$ S/km. At full load, the line delivers 250 MW at

Copyright 2017 Cengage Learning. All Rights Reserved. May not be copied, scanned, or duplicated, in whole or in part. Due to electronic rights, some third party content may be suppressed from the eBook and/or eChapter(s). Editorial review has deemed that any suppressed content does not materially affect the overall learning experience. Cengage Learning reserves the right to remove additional content at any time if subsequent rights restrictions require it.

0.99 p.f. lagging and at 220 kV. Using the nominal π circuit, calculate: (a) the *ABCD* parameters, (b) the sending-end voltage and current, and (c) the percent voltage regulation.

5.3 Rework Problem 5.2 in per unit using 1000-MVA (three-phase) and 230-kV (line-to-line) base values. Calculate: (a) the per-unit *ABCD* parameters, (b) the per-unit sending-end voltage and current, and (c) the percent voltage regulation.

5.4 Derive the *ABCD* parameters for the two networks in series, as shown in Figure 5.4.

5.5 Derive the *ABCD* parameters for the T circuit shown in Figure 5.4.

5.6 (a) Consider a medium-length transmission line represented by a nominal π circuit shown in Figure 5.3 of the text. Draw a phasor diagram for lagging power-factor condition at the load (receiving end).

(b) Now consider a nominal T circuit of the medium-length transmission line shown in Figure 5.18.

First draw the corresponding phasor diagram for lagging power-factor load condition.

Then determine the *ABCD* parameters in terms of Y and Z for the nominal T circuit and for the nominal π circuit of part (a).

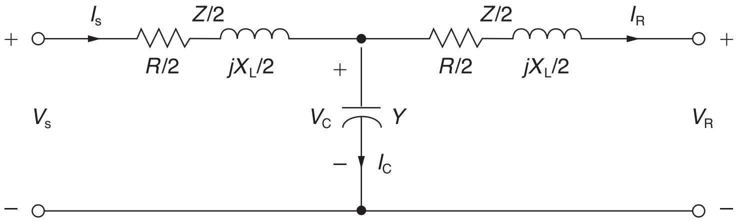

FIGURE 5.18

Nominal T-circuit for Problem 5.6

5.7 The per-phase impedance of a short three-phase transmission line is $0.5\underline{/53.15^\circ}\ \Omega$. The three-phase load at the receiving end is 1200 kW at 0.8 p.f. lagging. If the line-to-line sending-end voltage is 3.3 kV, determine (a) the receiving-end line-to-line voltage in kV and (b) the line current. Draw the phasor diagram with the line current I, as reference.

5.8 Reconsider Problem 5.7 and find the following: (a) sending-end power factor, (b) sending-end three-phase power, and (c) the three-phase line loss.

5.9 The 100-km, 230-kV, 60-Hz, three-phase line in Problems 4.18 and 4.39 delivers 300 MVA at 218 kV to the receiving end at full load. Using the nominal π circuit, calculate the *ABCD* parameters, sending-end voltage, and percent voltage regulation when the receiving-end power factor is (a) 0.9 lagging, (b) unity, and (c) 0.9 leading. Assume a 50°C conductor temperature to determine the resistance of this line.

Copyright 2017 Cengage Learning. All Rights Reserved. May not be copied, scanned, or duplicated, in whole or in part. Due to electronic rights, some third party content may be suppressed from the eBook and/or eChapter(s). Editorial review has deemed that any suppressed content does not materially affect the overall learning experience. Cengage Learning reserves the right to remove additional content at any time if subsequent rights restrictions require it.

5.10 The 500-kV, 60-Hz, three-phase line in Problems 4.20 and 4.41 has a 180-km length and delivers 1600 MW at 475 kV and at 0.95 power factor leading to the receiving end at full load. Using the nominal π circuit, calculate the (a) *ABCD* parameters, (b) sending-end voltage and current, (c) sending-end power and power factor, (d) full-load line losses and efficiency, and (e) percent voltage regulation. Assume a 50°C conductor temperature to determine the resistance of this line.

5.11 A 40-km, 220-kV, 60-Hz, three-phase overhead transmission line has a per-phase resistance of 0.15 Ω/km, a per-phase inductance of 1.3263 mH/km, and negligible shunt capacitance. Using the short line model, find the sending-end voltage, voltage regulation, sending-end power, and transmission line efficiency when the line is supplying a three-phase load of (a) 381 MVA at 0.8 power factor lagging and at 220 kV and (b) 381 MVA at 0.8 power factor leading and at 220 kV.

5.12 A 60-Hz, 100-mile, three-phase overhead transmission line, constructed of ACSR conductors, has a series impedance of $(0.1826 + j0.784)$ Ω/mi per phase and a shunt capacitive reactance-to-neutral of $185.5 \times 10^3 \underline{/-90^\circ}$ Ω-mi per phase. Using the nominal π circuit for a medium-length transmission line, (a) determine the total series impedance and shunt admittance of the line; (b) compute the voltage, the current, and the real and reactive power at the sending end if the load at the receiving end draws 200 MVA at unity power factor and at a line-to-line voltage of 230 kV; and (c) find the percent voltage regulation of the line.

SECTION 5.2

5.13 Evaluate $\cosh(\gamma l)$ and $\tanh(\gamma l/2)$ for $\gamma l = 0.40\underline{/85^\circ}$ per unit.

5.14 A 500-km, 500-kV, 60-Hz, uncompensated three-phase line has a positive-sequence series impedance $z = 0.03 + j0.35$ Ω/km and a positive-sequence shunt admittance $y = j4.4 \times 10^{-6}$ S/km. Calculate: (a) Z_c, (b) (γl), and (c) the exact *ABCD* parameters for this line.

5.15 At full load, the line in Problem 5.14 delivers 900 MW at unity power factor and at 475 kV. Calculate: (a) the sending-end voltage, (b) the sending-end current, (c) the sending-end power factor, (d) the full-load line losses, and (e) the percent voltage regulation.

5.16 The 500-kV, 60-Hz, three-phase line in Problems 4.20 and 4.41 has a 300-km length. Calculate: (a) Z_c, (b) (γl), and (c) the exact *ABCD* parameters for this line. Assume a 50°C conductor temperature.

5.17 At full load, the line in Problem 5.16 delivers 1500 MVA at 480 kV to the receiving-end load. Calculate the sending-end voltage and percent voltage regulation when the receiving-end power factor is (a) 0.9 lagging, (b) unity, and (c) 0.9 leading.

5.18 A 60-Hz, 230-mile, three-phase overhead transmission line has a series impedance $z = 0.8431\underline{/79.04^\circ}$ Ω/mi and a shunt admittance $\gamma = 5.105 \times 10^{-6}\underline{/90^\circ}$ S/mi. The load at the receiving end is 125 MW at unity power

Copyright 2017 Cengage Learning. All Rights Reserved. May not be copied, scanned, or duplicated, in whole or in part. Due to electronic rights, some third party content may be suppressed from the eBook and/or eChapter(s). Editorial review has deemed that any suppressed content does not materially affect the overall learning experience. Cengage Learning reserves the right to remove additional content at any time if subsequent rights restrictions require it.

factor and at 215 kV. Determine the voltage, current, and both real and reactive power at the sending end and the percent voltage regulation of the line. Also find the wavelength and velocity of propagation of the line.

5.19 Using per-unit calculations, rework Problem 5.18 to determine the sending-end voltage and current.

5.20 (a) The series expansions of the hyperbolic functions are given by

$$\cosh\theta = 1 + \frac{\theta^2}{2} + \frac{\theta^4}{24} + \frac{\theta^6}{720} + \cdots$$

$$\sinh\theta = 1 + \frac{\theta^2}{6} + \frac{\theta^4}{120} + \frac{\theta^6}{5040} + \cdots$$

For the *ABCD* parameters of a long transmission line represented by an equivalent π circuit, apply the above expansion considering only the first two terms, and express the result in terms of Y and Z.

(b) For the nominal π and equivalent π circuits shown in Figures 5.3 and 5.7 of the text, show that

$$\frac{A-1}{B} = \frac{Y}{2} \quad \text{and} \quad \frac{A-1}{B} = \frac{Y'}{2}$$

hold good, respectively.

5.21 Starting with (5.1.1) of the text, show that

$$A = \frac{V_S I_S + V_R I_R}{V_R I_S + V_S I_R} \quad \text{and} \quad B = \frac{V_S^2 - V_R^2}{V_R I_S + V_S I_R}$$

5.22 Consider the A parameter of the long line given by $\cosh\theta$, where $\theta = \sqrt{ZY}$. With $x = e^{-\theta} = x_1 + jx_2$ and $A = \mathrm{A}_1 + j\mathrm{A}_2$, show that x_1 and x_2 satisfy the following:

$$x_1^2 - x_2^2 - 2(\mathrm{A}_1 x_1 - \mathrm{A}_2 x_2) + 1 = 0$$

$$\text{and} \quad x_1 x_2 - (\mathrm{A}_2 x_1 + \mathrm{A}_1 x_2) = 0.$$

SECTION 5.3

5.23 Determine the equivalent π circuit for the line in Problem 5.14 and compare it with the nominal π circuit.

5.24 Determine the equivalent π circuit for the line in Problem 5.16. Compare the equivalent π circuit with the nominal π circuit.

5.25 Let the transmission line of Problem 5.12 be extended to cover a distance of 200 miles. Assume conditions at the load to be the same as in Problem 5.12. Determine the (a) sending-end voltage, (b) sending-end current, (c) sending-end real and reactive powers, and (d) percent voltage regulation.

Copyright 2017 Cengage Learning. All Rights Reserved. May not be copied, scanned, or duplicated, in whole or in part. Due to electronic rights, some third party content may be suppressed from the eBook and/or eChapter(s). Editorial review has deemed that any suppressed content does not materially affect the overall learning experience. Cengage Learning reserves the right to remove additional content at any time if subsequent rights restrictions require it.

SECTION 5.4

5.26 A 350-km, 500-kV, 60-Hz, three-phase uncompensated line has a positive-sequence series reactance $x = 0.34\ \Omega/\text{km}$ and a positive-sequence shunt admittance $y = j4.5 \times 10^{-6}$ S/km. Neglecting losses, calculate: (a) Z_c, (b) γl, (c) the *ABCD* parameters, (d) the wavelength λ of the line in kilometers, and (e) the surge impedance loading in MW.

5.27 Determine the equivalent π circuit for the line in Problem 5.26.

5.28 Rated line voltage is applied to the sending end of the line in Problem 5.26. Calculate the receiving-end voltage when the receiving end is terminated by (a) an open circuit, (b) the surge impedance of the line, and (c) one-half of the surge impedance. (d) Also calculate the theoretical maximum real power that the line can deliver when rated voltage is applied to both ends of the line.

5.29 Rework Problems 5.9 and 5.16, neglecting the conductor resistance. Compare the results with and without losses.

5.30 From (4.6.22) and (4.10.4), the series inductance and shunt capacitance of a three-phase overhead line are

$$L_a = 2 \times 10^{-7} \ln(D_{eq}/D_{SL}) = \frac{\mu_0}{2\pi} \ln(D_{eq}/D_{SL}) \quad \text{H/m}$$

$$C_{an} = \frac{2\pi\varepsilon_0}{\ln(D_{eq}/D_{SC})} \quad \text{F/m}$$

where $\mu_0 = 4\pi \times 10^{-7}$H/m and $\varepsilon_0 = \left(\frac{1}{36\pi}\right) \times 10^{-9}$F/m.

Using these equations, determine formulas for surge impedance and velocity of propagation of an overhead lossless line. Then determine the surge impedance and velocity of propagation for the three-phase line given in Example 4.5. Assume positive-sequence operation. Neglect line losses as well as the effects of the overhead neutral wires and the earth plane.

5.31 A 500-kV, 300-km, 60-Hz, three-phase overhead transmission line, assumed to be lossless, has a series inductance of 0.97 mH/km per phase and a shunt capacitance of 0.0115 μF/km per phase. (a) Determine the phase constant β, the surge impedance Z_c, velocity of propagation v, and the wavelength λ of the line. (b) Determine the voltage, current, real and reactive power at the sending end, and the percent voltage regulation of the line if the receiving-end load is 800 MW at 0.8 power factor lagging and at 500 kV.

5.32 The following parameters are based on a preliminary line design: $V_S = 1.0$ per unit, $V_R = 0.9$ per unit, $\lambda = 5000$ km, $Z_c = 320\ \Omega$, $\delta = 36.8°$.

Copyright 2017 Cengage Learning. All Rights Reserved. May not be copied, scanned, or duplicated, in whole or in part. Due to electronic rights, some third party content may be suppressed from the eBook and/or eChapter(s). Editorial review has deemed that any suppressed content does not materially affect the overall learning experience. Cengage Learning reserves the right to remove additional content at any time if subsequent rights restrictions require it.

A three-phase power of 700 MW is to be transmitted to a substation located 315 km from the source of power. (a) Determine a nominal voltage level for the three-phase transmission line, based on the practical line-loadability equation. (b) For the voltage level obtained in part (a), determine the theoretical maximum power that can be transferred by the line.

5.33 Consider a long radial line terminated in its characteristic impedance Z_c. Determine the following:

(a) V_1/I_1, known as the driving point impedance.

(b) $|V_2|/V_1|$, known as the voltage gain, in terms of $\alpha\ell$.

(c) $|I_2|/|I_1|$, known as the current gain, in terms of $\alpha\ell$.

(d) The complex power gain, $-S_{21}/S_{12}$, in terms of $\alpha\ell$.

(e) The real power efficiency, $(-P_{21}/P_{12}) = \eta$, terms of $\alpha\ell$.

Note: 1 refers to sending end and 2 refers to receiving end. (S_{21}) is the complex power received at 2; S_{12} is sent from 1.

5.34 For the case of a lossless line, how would the results of Problem 5.33 change?

In terms of Z_c, which is a real quantity for this case, express P_{12} in terms $|I_1|$ and $|V_1|$.

5.35 For a lossless open-circuited line, express the sending-end voltage, V_1, in terms of the receiving-end voltage, V_2, for the three cases of short-line model, medium-length line model, and long-line model. Is it true that the voltage at the open receiving end of a long line is higher than that at the sending end, for small βl?

5.36 For a short transmission line of impedance $(R + jX)$ ohms per phase, show that the maximum power that can be transmitted over the line is

$$P_{\max} = \frac{V_R^2}{Z^2}\left(\frac{ZV_S}{V_R} - R\right) \quad \text{where } Z = \sqrt{R^2 + X^2}$$

when the sending-end and receiving-end voltages are fixed, and for the condition

$$Q = \frac{-V_R^2 X}{R^2 + X^2} \quad \text{when } dP/dQ = 0$$

5.37 (a) Consider complex power transmission via the three-phase short line for which the per-phase circuit is shown in Figure 5.19. Express S_{12}, the complex power sent by bus 1 (or V_1), and $(-S_{21})$, the complex power received by bus 2 (or V_2), in terms of V_1, V_2, Z, $\angle Z$, and $\theta_{12} = \theta_1 - \theta_2$, which is the power angle.

(b) For a balanced three-phase transmission line in per-unit notation with $Z = 1\angle 85°$, $\theta_{12} = 10°$, determine S_{12} and $(-S_{21})$ for

Copyright 2017 Cengage Learning. All Rights Reserved. May not be copied, scanned, or duplicated, in whole or in part. Due to electronic rights, some third party content may be suppressed from the eBook and/or eChapter(s). Editorial review has deemed that any suppressed content does not materially affect the overall learning experience. Cengage Learning reserves the right to remove additional content at any time if subsequent rights restrictions require it.

(i) $V_1 = V_2 = 1.0$
(ii) $V_1 = 1.1$ and $V_2 = 0.9$
Comment on the changes of real and reactive powers from parts (i) to (ii).

FIGURE 5.19

Per-phase circuit for Problem 5.37

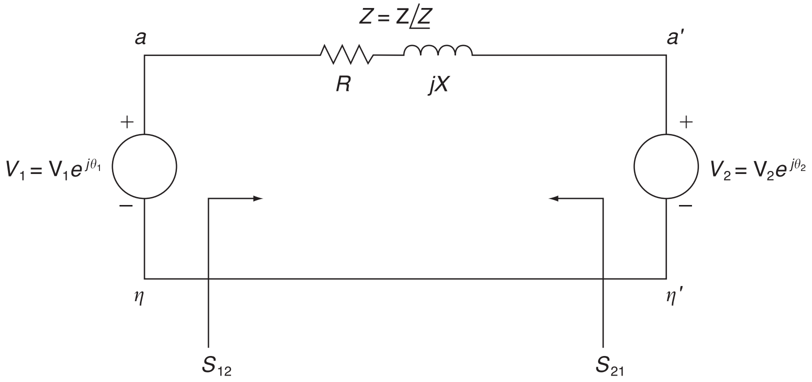

SECTION 5.5

5.38 The line in Problem 5.14 has three ACSR 1113 kcmil conductors per phase. Calculate the theoretical maximum real power that this line can deliver and compare with the thermal limit of the line. Assume $V_S = V_R = 1.0$ per unit and unity power factor at the receiving end.

5.39 Repeat Problems 5.14 and 5.38 if the line length is (a) 200 km or (b) 600 km.

5.40 For the 500 kV line given in Problem 5.16, (a) calculate the theoretical maximum real power that the line can deliver to the receiving end when rated voltage is applied to both ends; (b) calculate the receiving-end reactive power and power factor at this theoretical loading.

5.41 A 230-kV, 100-km, 60-Hz, three-phase overhead transmission line with a rated current of 900 A/phase has a series impedance $z = 0.088 + j0.465$ Ω/km and a shunt admittance $y = j3.524$ μS/km. (a) Obtain the nominal π equivalent circuit in normal units and in per unit on a base of 100 MVA (three phase) and 230 kV (line-to-line). (b) Determine the three-phase rated MVA of the line. (c) Compute the *ABCD* parameters. (d) Calculate the SIL.

5.42 A three-phase power of 460 MW is transmitted to a substation located 500 km from the source of power. With $V_S = 1$ per unit, $V_R = 0.9$ per unit, $\lambda = 5000$ km, $Z_c = 500$ Ω, and $\delta = 36.87°$, determine a nominal voltage level for the lossless transmission line based on Eq. (5.4.29) of the text.

Using this result, find the theoretical three-phase maximum power that can be transferred by the lossless transmission line.

PW **5.43** Open PowerWorld Simulator case Example 5_4 and graph the load bus voltage as a function of load real power (assuming unity power factor at the load). What is the maximum amount of real power that can be

Copyright 2017 Cengage Learning. All Rights Reserved. May not be copied, scanned, or duplicated, in whole or in part. Due to electronic rights, some third party content may be suppressed from the eBook and/or eChapter(s). Editorial review has deemed that any suppressed content does not materially affect the overall learning experience. Cengage Learning reserves the right to remove additional content at any time if subsequent rights restrictions require it.

transferred to the load at unity power factor if the load voltage always must be greater than 0.9 per unit?

PW **5.44** Repeat Problem 5.43, but now vary the load reactive power, assuming the load real power is fixed at 1499 MW.

SECTION 5.6

5.45 For the line in Problems 5.14 and 5.38, determine (a) the practical line loadability in MW, assuming $V_S = 1.0$ per unit, $V_R \approx 0.95$ per unit, and $\delta_{max} = 35°$; part (b) the full-load current at 0.99 p.f. leading, based on the above practical line loadability; (c) the exact receiving-end voltage for the full-load current in part (b); and (d) the percent voltage regulation. For this line, is loadability determined by the thermal limit, the voltage-drop limit, or steady-state stability?

5.46 Repeat Problem 5.45 for the 500 kV line given in Problem 5.10.

5.47 Determine the practical line loadability in MW and in per-unit of SIL for the line in Problem 5.14 if the line length is (a) 200 km or (b) 600 km. Assume $V_S = 1.0$ per unit, $V_R = 0.95$ per unit, $\delta_{max} = 35°$, and 0.99 leading power factor at the receiving end.

5.48 It is desired to transmit 2000 MW from a power plant to a load center located 300 km from the plant. Determine the number of 60 Hz, three-phase, uncompensated transmission lines required to transmit this power with one line out of service for the following cases: (a) 345 kV lines, $Z_c = 300\ \Omega$, (b) 500 kV lines, $Z_c = 275\ \Omega$, (c) 765 kV lines, $Z_c = 260\ \Omega$. Assume that $V_S = 1.0$ per unit, $V_R = 0.95$ per unit, and $\delta_{max} = 35°$.

5.49 Repeat Problem 5.48 if it is desired to transmit: (a) 3200 MW to a load center located 300 km from the plant or (b) 2000 MW to a load center located 400 km from the plant.

5.50 A three-phase power of 4000 MW is to be transmitted through four identical 60-Hz overhead transmission lines over a distance of 300 km. Based on a preliminary design, the phase constant and surge impedance of the line are $\beta = 9.46 \times 10^{-4}$ rad/km and $Z_c = 343\ \Omega$, respectively. Assuming $V_S = 1.0$ per unit, $V_R = 0.9$ per unit, and a power angle $\delta = 36.87°$, determine a suitable nominal voltage level in kV based on the practical line-loadability criteria.

5.51 The power flow at any point on a transmission line can be calculated in terms of the *ABCD* parameters. By letting $A = |A|\underline{/\alpha}$, $B = |B|\underline{/\beta}$, $V_R = |V_R|\underline{/0°}$, and $V_S = |V_S|\underline{/\delta}$, the complex power at the receiving end can be shown to be

$$P_R + jQ_R = \frac{|V_R||V_s|\underline{/\beta - \alpha}}{|B|} - \frac{|\delta||V_R^2|\underline{/\beta - \alpha}}{|B|}$$

(a) Draw a phasor diagram corresponding to the above equation. Let it be represented by a triangle O′OA with O′ as the origin and OA representing $P_R + jQ_R$.

Copyright 2017 Cengage Learning. All Rights Reserved. May not be copied, scanned, or duplicated, in whole or in part. Due to electronic rights, some third party content may be suppressed from the eBook and/or eChapter(s). Editorial review has deemed that any suppressed content does not materially affect the overall learning experience. Cengage Learning reserves the right to remove additional content at any time if subsequent rights restrictions require it.

(b) By shifting the origin from O′ to O, turn the result of part (a) into a power diagram, redrawing the phasor diagram. For a given fixed value of $|V_R|$ and a set of values for $|V_S|$, draw the loci of point A, thereby showing the so-called receiving-end circles.

(c) From the result of part (b) for a given load with a lagging power factor angle θ_R, determine the amount of reactive power that must be supplied to the receiving end to maintain a constant receiving-end voltage if the sending-end voltage magnitude decreases from $|V_{S1}|$ to $|V_{S2}|$

5.52 (a) Consider complex power transmission via the three-phase long line for which the per-phase circuit is shown in Figure 5.20. See Problem 5.37 in which the short-line case was considered. Show that

$$\text{sending-end power} = S_{12} = \frac{Y'^*}{2}V_1^2 + \frac{V_1^2}{Z'^*} - \frac{V_1V_2}{Z'^*}e^{j\theta_{12}}$$

$$\text{received power} = -S_{21} = -\frac{Y'^*}{2}V_2^2 - \frac{V_2^2}{Z'^*} + \frac{V_1V_2}{Z'^*}e^{-j\theta_{12}}$$

where $\theta_{12} = \theta_1 - \theta_2$.

(b) For a lossless line with equal voltage magnitudes at each end, show that

$$P_{12} = -P_{21} = \frac{V_1^2 \sin\theta_{12}}{Z_c \sin\beta\ell} = P_{SIL}\frac{\sin\theta_{12}}{\sin\beta\ell}$$

(c) For $\theta_{12} = 45°$ and $\beta = 0.002$ rad/km, find (P_{12}/P_{SIL}) as a function of line length in km, and sketch it.

(d) If a thermal limit of $(P_{12}/P_{SIL}) = 2$ is set, which limit governs for short lines and long lines?

FIGURE 5.20

Per-phase circuit for Problem 5.52

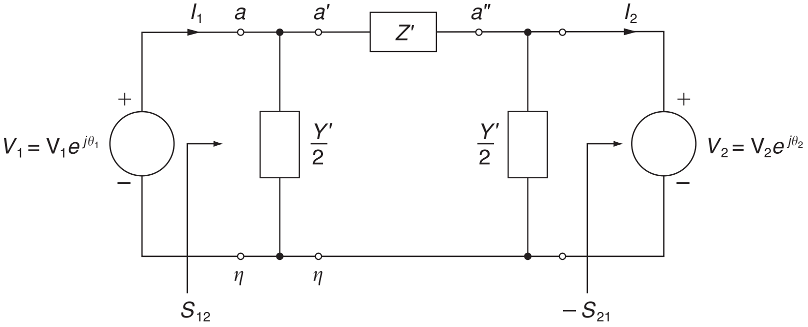

PW **5.53** Open PowerWorld Simulator case Example 5_8. If the load bus voltage is greater than or equal to 730 kV even with any line segment out of service, what is the maximum amount of real power that can be delivered to the load?

PW **5.54** Repeat Problem 5.53, but now assume any two line segments may be out of service.

Copyright 2017 Cengage Learning. All Rights Reserved. May not be copied, scanned, or duplicated, in whole or in part. Due to electronic rights, some third party content may be suppressed from the eBook and/or eChapter(s). Editorial review has deemed that any suppressed content does not materially affect the overall learning experience. Cengage Learning reserves the right to remove additional content at any time if subsequent rights restrictions require it.

SECTION 5.7

5.55 Recalculate the percent voltage regulation in Problem 5.15 when identical shunt reactors are installed at both ends of the line during light loads, providing 65% total shunt compensation. The reactors are removed at full load. Also calculate the impedance of each shunt reactor.

5.56 Rework Problem 5.17 when identical shunt reactors are installed at both ends of the line, providing 50% total shunt compensation. The reactors are removed at full load.

5.57 Identical series capacitors are installed at both ends of the line in Problem 5.14, providing 40% total series compensation. Determine the equivalent *ABCD* parameters of this compensated line. Also calculate the impedance of each series capacitor.

5.58 Identical series capacitors are installed at both ends of the line in Problem 5.16, providing 30% total series compensation. (a) Determine the equivalent *ABCD* parameters for this compensated line. (b) Determine the theoretical maximum real power that this series-compensated line can deliver when $V_S = V_R = 1.0$ per unit. Compare your result with that of Problem 5.40.

5.59 Determine the theoretical maximum real power that the series-compensated line in Problem 5.57 can deliver when $V_S = V_R = 1.0$ per unit. Compare your result with that of Problem 5.38.

5.60 What is the minimum amount of series capacitive compensation N_C in percent of the positive-sequence line reactance needed to reduce the number of 765-kV lines in Example 5.8 from five to four? Assume two intermediate substations with one line section out of service. Also, neglect line losses and assume that the series compensation is sufficiently distributed along the line so as to effectively reduce the series reactance of the equivalent π circuit to $X'(1-N_C/100)$.

5.61 Determine the equivalent *ABCD* parameters for the line in Problem 5.14 if it has 70% shunt reactive (inductors) compensation and 40% series capacitive compensation. Half of this compensation is installed at each end of the line, as in Figure 5.14.

5.62 Consider the transmission line of Problem 5.18. (a) Find the *ABCD* parameters of the line when uncompensated. (b) For a series capacitive compensation of 70% (35% at the sending end and 35% at the receiving end), determine the *ABCD* parameters. Comment on the relative change in the magnitude of the *B* parameter with respect to the relative changes in the magnitudes of the *A*, *C*, and *D* parameters. Also comment on the maximum power that can be transmitted when series compensated.

5.63 Given the uncompensated line of Problem 5.18, let a three-phase shunt reactor (inductor) that compensates for 70% of the total shunt admittance of the line be connected at the receiving end of the line during no-load conditions. Determine the effect of voltage regulation with the

Copyright 2017 Cengage Learning. All Rights Reserved. May not be copied, scanned, or duplicated, in whole or in part. Due to electronic rights, some third party content may be suppressed from the eBook and/or eChapter(s). Editorial review has deemed that any suppressed content does not materially affect the overall learning experience. Cengage Learning reserves the right to remove additional content at any time if subsequent rights restrictions require it.

reactor connected at no load. Assume that the reactor is removed under full-load conditions.

5.64 Let the three-phase lossless transmission line of Problem 5.31 supply a load of 1000 MVA at 0.8 power factor lagging and at 500 kV. (a) Determine the capacitance/phase and total three-phase Mvars supplied by a three-phase, Δ-connected shunt-capacitor bank at the receiving end to maintain the receiving-end voltage at 500 kV when the sending end of the line is energized at 500 kV. (b) If series capacitive compensation of 40% is installed at the midpoint of the line, without the shunt capacitor bank at the receiving end, compute the sending-end voltage and percent voltage regulation.

PW **5.65** Open PowerWorld Simulator case Example 5_10 with the series capacitive compensation at both ends of the line in service. Graph the load bus voltage as a function of load real power (assuming unity power factor at the load). What is the maximum amount of real power that can be transferred to the load at unity power factor if the load voltage is always greater than 0.85 per unit?

PW **5.66** Open PowerWorld Simulator case Example 5_10 with the series capacitive compensation at both ends of the line in service. With the reactive power load fixed at 400 Mvar, graph the load bus voltage as the MW load is varied between 0 and 2600 MW in 200 MW increments. Then repeat with both of the series compensation elements out of service.

CASE STUDY QUESTIONS

a. For underground and underwater transmission, why are line losses for HVDC cables lower than those of ac cables with similar capacity?

b. Where are back-to-back HVDC converters (back-to-back HVDC links) currently located in North America? What are the characteristics of those locations that prompted the installation of back-to-back HVDC links?

c. Which HVDC technology can independently control both active (real) power flow and reactive power flow to and from the interconnected ac system?

REFERENCES

1. Electric Power Research Institute (EPRI), *EPRI AC Transmission Line Reference Book—200 kV and Above* (Palo Alto, CA: EPRI, *www.epri.com*, December 2005).

2. Westinghouse Electric Corporation, *Electrical Transmission and Distribution Reference Book*, 4th ed. (East Pittsburgh, PA, 1964).

Copyright 2017 Cengage Learning. All Rights Reserved. May not be copied, scanned, or duplicated, in whole or in part. Due to electronic rights, some third party content may be suppressed from the eBook and/or eChapter(s). Editorial review has deemed that any suppressed content does not materially affect the overall learning experience. Cengage Learning reserves the right to remove additional content at any time if subsequent rights restrictions require it.

3. R. D. Dunlop, R. Gutman, and P. P. Marchenko, "Analytical Development of Load-ability Characteristics for EHV and UHV Lines," *IEEE Trans. PAS*, Vol. PAS-98, No. 2 (March/April 1979): pp. 606−607.

4. W. D. Stevenson, Jr. *Elements of Power System Analysis*, 4th ed. (New York: McGraw-Hill, 1982).

5. W. H. Hayt, Jr. and J. E. Kemmerly, *Engineering Circuit Analysis*, 7th ed. (New York: McGraw-Hill, 2006).

6. M. P. Bahrman and B. K. Johnson, "The ABCs of HVDC Transmission Technologies," *IEEE Power & Energy Magazine*, 5, 2 (March/April 2007): pp. 32–44.

Copyright 2017 Cengage Learning. All Rights Reserved. May not be copied, scanned, or duplicated, in whole or in part. Due to electronic rights, some third party content may be suppressed from the eBook and/or eChapter(s). Editorial review has deemed that any suppressed content does not materially affect the overall learning experience. Cengage Learning reserves the right to remove additional content at any time if subsequent rights restrictions require it.

Copyright 2017 Cengage Learning. All Rights Reserved. May not be copied, scanned, or duplicated, in whole or in part. Due to electronic rights, some third party content may be suppressed from the eBook and/or eChapter(s). Editorial review has deemed that any suppressed content does not materially affect the overall learning experience. Cengage Learning reserves the right to remove additional content at any time if subsequent rights restrictions require it.

6 Power Flows

Tennessee
Valley Authority
(TVA) Regional
Operations Center
(Courtesy of TVA.)

Successful power system operation under normal balanced three-phase steady-state conditions requires the following:

1. Generation supplies the demand (load) plus losses.
2. Bus voltage magnitudes remain close to rated values.
3. Generators operate within specified real and reactive power limits.
4. Transmission lines and transformers are not overloaded.

Copyright 2017 Cengage Learning. All Rights Reserved. May not be copied, scanned, or duplicated, in whole or in part. Due to electronic rights, some third party content may be suppressed from the eBook and/or eChapter(s). Editorial review has deemed that any suppressed content does not materially affect the overall learning experience. Cengage Learning reserves the right to remove additional content at any time if subsequent rights restrictions require it.

The power flow (sometimes also called the *load flow*) is the basic tool for investigating these requirements. The power flow determines the voltage magnitude and angle at each bus in a power system under balanced three-phase steady-state conditions. It also computes real and reactive power flows for all equipment interconnecting the buses, as well as equipment losses.

Both existing power systems and proposed changes, including new generation and transmission, are of interest.

Conventional nodal or loop analysis is not suitable for power flow studies because the input data for loads are normally given in terms of power, not impedance. Also, generators are considered to be power sources, not voltage or current sources. The power flow problem is therefore formulated as a set of nonlinear algebraic equations suitable for computer solution.

Sections 6.1 through 6.3 review some basic methods, including direct and iterative techniques for solving algebraic equations. Then Sections 6.4 through 6.6 formulate the power flow problem, specify input data, and present two solution methods: Gauss-Seidel and Newton-Raphson. Means for controlling power flows are discussed in Section 6.7. Sections 6.8 and 6.9 introduce sparsity techniques and a fast decoupled power flow method, while Section 6.10 discusses the dc power flow, and Section 6.11 considers the power flow representation of wind turbine generators. Formulations for economic dispatch and optimal power flow are given in Sections 6.12 and 6.13

Since balanced three-phase steady-state conditions are assumed, this chapter uses only positive-sequence networks. Also, all power flow equations and input/output data are given in per unit (p.u.).

CASE STUDY

During this century, renewable energy sources, including solar and wind generation, are projected to substantially increase in the United States and worldwide. High penetrations of wind and solar generation can induce increased cycling of fossil-fueled power plants. The following case study examines the operational impacts of up to 35% wind and solar penetrations in the western United States. The primary impact of displacing fuel, as well as displacing fuel costs and emissions associated with fossil-fueled power plants, and the secondary impact of increased cycling, including costs and emissions associated with cycling of fossil-fueled power plants, are analyzed.

Finding Flexibility: Cycling the Conventional Fleet

By Debra Lew, Greg Brinkman, Nikhil Kumar,
Steve Lefton, Gary Jordan, and Sundar Venkataraman

Adding new generation, load, or transmission to the grid changes the operation of the incumbent power system. Wind and solar generation plants are no different, but their impact on the rest

Copyright 2017 Cengage Learning. All Rights Reserved. May not be copied, scanned, or duplicated, in whole or in part. Due to electronic rights, some third party content may be suppressed from the eBook and/or eChapter(s). Editorial review has deemed that any suppressed content does not materially affect the overall learning experience. Cengage Learning reserves the right to remove additional content at any time if subsequent rights restrictions require it.

of the grid is exacerbated by the facts that wind and solar energy is nondispatchable and such generators produce variable output. And because wind and solar effectively bid into the market at very low or negative cost, they are preferred resources in the dispatch stack. They are used by system operators whenever possible, unless there are generator operating limits or transmission constraints.

At low wind and solar penetrations or with low-variability resources (e.g., from high geographic diversity), the impact on the rest of the system may be small. But at high penetrations or with high-variability resources, wind and solar can induce increased cycling of the fossil-fueled fleet. This means that coal and gas generators may be asked to start up and shut down, ramp up and down, or operate at minimum generation levels more frequently. Cycling has impacts on emissions and on the wear-and-tear costs of the fossil-fueled fleet.

Coal and gas generators tend to have additional emissions at startup and possibly also during ramps. Emissions are also affected by the output level of the generator. For example, units tend to be less efficient at partial load, thus increasing the carbon dioxide (CO_2) rates at minimum generation levels.

Starts and ramps also lead to increased wear and tear on the unit components and systems. Temperature and pressure changes lead to stresses that can result in premature component failure, an increased need for maintenance and overhauls, and more frequent repairs.

The primary impact of a MWh of wind or solar energy is to displace a MWh of other generation, typically fossil-fueled generation. Displacing a MWh of fossil-fueled generation displaces the costs and emissions associated with that fuel. But a secondary impact of this wind and solar energy can be to increase cycling of the fossil-fueled generators. As we have said, there are wear-and-tear costs and emissions impacts associated with cycling. This raises two questions: how big are those secondary impacts, and do they significantly negate the primary impacts that wind and solar energy bring to the table? Some recent analyses have claimed that wind actually increases overall emissions or that the avoided emissions from wind have been significantly overestimated.

Many integration studies have examined the impacts of high penetrations of wind power on particular systems and on the operation of the conventional fleet. Very few have considered cycling impacts in detail, partly because of the lack of data on cycling costs and emissions. This article describes the first study that combines detailed data on wear-and-tear costs and the emissions impacts of cycling with operational simulations of the entire western U.S. grid with high penetrations of wind and solar to determine these impacts.

© 2013 IEEE. Reprinted, with permission, from Debra Lew, Greg Brinkman, Nikhil Kumar, Steve Lefton, Gary Jordan, and Sundar Venkataraman, “Finding Flexibility: Cycling the Conventional Fleet,” *IEEE Power and Energy Magazine*, November/December 2013, pp. 20–32.

Copyright 2017 Cengage Learning. All Rights Reserved. May not be copied, scanned, or duplicated, in whole or in part. Due to electronic rights, some third party content may be suppressed from the eBook and/or eChapter(s). Editorial review has deemed that any suppressed content does not materially affect the overall learning experience. Cengage Learning reserves the right to remove additional content at any time if subsequent rights restrictions require it.

The Western Wind and Solar Integration Study: Phase 2

In 2011, GE Energy, Intertek AIM, the National Renewable Energy Laboratory (NREL), and RePPAE began the Western Wind and Solar Integration Study Phase 2 (WWSIS-2). This study built on the Phase 1 effort, which had examined up to 35% wind and solar penetrations in subregions in the Western Interconnection and mitigation options for integrating those resources. The conclusion of Phase 1 was that several changes in operating practices would be needed to integrate the wind and solar energy. The two most important of these were increased balancing area coordination and intrahour scheduling. There are many efforts being considered now in the western United States to implement these changes, including the creation of an energy imbalance market.

The goal of WWSIS-2 was to investigate the cycling impacts on the fossil-fueled fleet in detail and to determine if the wear-and-tear costs and the impacts on emissions significantly reduced the benefits of wind and solar power. The point of this study was not to determine whether wind and solar plants should be built, but rather to understand what the impacts on the fossil-fueled fleet would be if wind and solar were built to a high penetration—especially the impacts on costs and emissions.

To do this, we simulated future power system operations under varying levels of wind and solar penetration. Any simulation of the grid requires simplifying assumptions in order to develop a model that can be run with a reasonable amount of computing power and time. Power system operation in a future scenario with high penetrations of wind and solar is likely to be different from today. Additionally, we did not have access to confidential information such as bilateral contracts for power or transmission flows. The key differences between our model and today's operation are:

- We assumed a natural gas price that varied subregionally but averaged US$4.60/million Btu across the interconnection. We did not model a carbon tax or any renewable energy incentive, such as the production tax credit.
- We did not model bilateral contracts for power or transmission flows but assumed a least-cost unit commitment and economic dispatch.
- We modeled the nearly 40 standalone balancing authorities as 20 zones, each holding its own contingency and flexibility reserves, with no hurdle rates between them.

New Data Sets

NREL analyzed measured emissions from every power plant in the United States (using the Environmental Protection Agency's continuous emissions-monitoring data) to determine incremental emissions due to a start or ramp as well as emissions rates from part loading. This analysis

Copyright 2017 Cengage Learning. All Rights Reserved. May not be copied, scanned, or duplicated, in whole or in part. Due to electronic rights, some third party content may be suppressed from the eBook and/or eChapter(s). Editorial review has deemed that any suppressed content does not materially affect the overall learning experience. Cengage Learning reserves the right to remove additional content at any time if subsequent rights restrictions require it.

was used to create a unit-specific emissions data set for cycling and noncyclic operation. These unit-specific emissions were used in the detailed operational simulations. For display purposes, however, we have averaged the data by unit type to show high-level results.

Heat rates as a function of load were examined for combined cycle (CC), combustion turbine (CT), coal, and gas steam units. Table 1 shows the resulting penalties for operating at part load. This penalty is defined as the percentage increase in emissions rate (lb/MWh) when the average unit is operating at 50% of maximum capacity. CC units are the most efficient at full load and part load; CC and CT units have the most significant emissions penalties for operating at 50% compared with 100% of maximum generation, however.

NO_x emissions as a function of load were analyzed similarly and are shown in Table 1. Steam units (coal and gas) emit approximately an order of magnitude more NO_x per MWh than gas CC units and CT units. Although part-load operation leads to an NO_x penalty for the CC and CT units, such operation was found to benefit the coal-fired steam units. For example, coal units operating at 50% were found to emit 14% less NO_x per MWh compared with full-loading operation; gas CC units were found to emit 22% more NO_x per MWh at 50% load compared with full load. Most of the NO_x from all units is created from nitrogen in the combustion air ("thermal" NO_x), as opposed to in the fuel, so flame temperature is likely a primary driver of NO_x emissions.

Type of Unit	CO_2 (%)	NO_x (%)
Coal	5	−14
Gas CC	9	22
Gas CT	18	15
Gas steam	6	−14

TABLE 1

Emissions penalty for part-load operation

Because of the significant part-time usage of pollution control equipment for SO_2, it was impossible to create part-load emission curves.

Starting an off-line, fossil-fueled unit increases emissions for two reasons. First, it takes fuel to bring the unit online, and that fuel adds emissions without adding energy to the grid. Second, starts can increase emissions rates because most pollution-control equipment does not become fully effective until flame and flue gas temperatures are in the proper range. Table 2 shows the start penalties for different types of units and different emissions. For example, a coal unit emits 1.98 lb/MW of capacity of excess NO_x during start-up. This is equivalent to operating the unit at full load for approximately 30 minutes.

Ramping, or load-following, emissions were estimated in a similar way to the start-up emissions. A ramp was defined as an increase of output of 30% of maximum capacity (e.g., from 70% to 100% of maximum

Copyright 2017 Cengage Learning. All Rights Reserved. May not be copied, scanned, or duplicated, in whole or in part. Due to electronic rights, some third party content may be suppressed from the eBook and/or eChapter(s). Editorial review has deemed that any suppressed content does not materially affect the overall learning experience. Cengage Learning reserves the right to remove additional content at any time if subsequent rights restrictions require it.

Type of Unit	Heat Input per Start (Millions Btu/MW)	NO_x per Start (lb/MW)	SO_2 per Start (lb/MW)
Coal	16.5	1.98	3.9
Gas CC	2.0	0.53	n/a
Gas CT	3.5	0.79	n/a
Gas steam	13.7	0.84	n/a

TABLE 2

Start-up emissions per MW of capacity

capacity). Table 3 presents generation-weighted averages. Ramping emissions are much lower than start-up emissions. The most significant ramping emission impact is the NO_x emissions from coal units (equivalent to 10–15 minutes of full-load operation).

While emissions at various operating levels are reasonably well understood, many utilities in the western United States do not know the wear-and-tear costs of cycling their fossil-fueled units. First, they have not needed to know these costs because until very recently, many of these plants, which were designed as base load plants, were not cycled. Second, determining these costs is complex because cycling operation today may not have cost implications until several years in the future.

Intertek AIM studied wear-and-tear costs from cycling for hundreds of fossil-fueled units around the world. For each unit, Intertek AIM had determined a best fit and a lower-bound and upper-bound fit for cycling costs, where the bounds reflected the uncertainty range for that plant. While specific data from those studies were confidential, aggregated data from those studies could be used as generic wear-and-tear costs for similar units that have not been studied. In this way, we were able to define variable operations and maintenance (VOM) costs for a hot, warm, and cold start; a ramp (typical); and for noncyclic operation for different types of plants. Table 4 shows the lower-bound costs for the different plant types.

Upper-bound costs were also used in this study. The raw

Type of Unit	Heat Input per Ramp (Millions Btu/MW)	NO_x per Ramp (lb/MW)	SO_2 per Ramp (lb/MW)
Coal	0.57	0.73	0.82
Gas CC	0.08	0.00	n/a
Gas CT	0.28	0.02	n/a
Gas steam	−0.09	0.05	n/a

TABLE 3

Ramping emissions per MW of capacity

Copyright 2017 Cengage Learning. All Rights Reserved. May not be copied, scanned, or duplicated, in whole or in part. Due to electronic rights, some third party content may be suppressed from the eBook and/or eChapter(s). Editorial review has deemed that any suppressed content does not materially affect the overall learning experience. Cengage Learning reserves the right to remove additional content at any time if subsequent rights restrictions require it.

	Small Subcritical Coal	Large Subcritical Coal	Super-Critical Coal	Gas, Combined Cycle	Gas, Large-Frame Combustion Turbine	Gas, Aero-derivative Combustion Turbine	Gas, Steam
Hot start (US$/MW)	94	59	54	35	32	19	36
Warm start (US$/MW)	157	65	64	55	126	24	58
Cold start (US$/MW)	147	105	104	79	103	32	75
Ramp (US$/MW)	3.34	2.45	1.96	0.64	1.59	0.63	1.92
Noncyclic operation (US$/MWh)	2.82	2.68	2.96	1.02	0.57	0.66	0.92

TABLE 4

Lower-bound median costs for cycling for various generation types

upper-bound data is confidential, however; only aggregated results can be presented here. All the cycling cost estimates used for this study are for typical units of various types; they are not unit-specific. The worst units for cycling are older base load power plants that should be retrofitted prior to significant cycling, using countermeasures such as procedure and chemistry changes and hardware retrofits. Without these measures, cycling could potentially lead to costly high-impact, low-probability events. Ongoing studies are examining the costs and benefits of retrofitting coal- and gas-fired power plants for increased flexibility.

Five Scenarios: Wind versus Solar

We used these new data sets in a commercial production simulation tool, PLEXOS, to model grid operations of the Western Interconnection on a 5-minute time step, because wind and solar output varies within the hour. We used the Western Electricity Coordinating Council (WECC) Transmission Expansion Policy Planning Committee (TEPPC) 2020 data set as a basis for our model, because it has been widely vetted among western U.S. utilities. A key change in assumptions was the natural gas price: the 2020 case average gas price was high, so we used the 2022 average gas price of US$4.60/million Btu.

We created five scenarios to examine increasing penetration levels of variable generation and also to compare wind with solar. Solar included rooftop photovoltaics (PV), utilityscale PV, and concentrating solar power (CSP) with six hours of

Copyright 2017 Cengage Learning. All Rights Reserved. May not be copied, scanned, or duplicated, in whole or in part. Due to electronic rights, some third party content may be suppressed from the eBook and/or eChapter(s). Editorial review has deemed that any suppressed content does not materially affect the overall learning experience. Cengage Learning reserves the right to remove additional content at any time if subsequent rights restrictions require it.

thermal storage. The scenarios were as follows:

- **No renewables:** 0 MW wind, 0 MW solar (0% wind, 0% solar)
- **TEPPC:** 27,900 MW wind; 7074 MW PV; 4352 MW CSP (9.4% wind, 3.6% solar)
- **High wind:** 63,840 MW wind; 20,064 MW PV; 6536 MW CSP (25% wind, 8% solar)
- **High mix:** 43,118 MW wind; 40,374 MW PV; 13,997 MW CSP (16.5% wind, 16.5% solar)
- **High solar:** 23,357 MW wind; 61,941 MW PV; 21,526 MW CSP (8% wind, 25% solar).

Penetration levels refer to energy, not capacity, and are penetration levels for the U.S. portion of the Western Interconnection only, because data for Canada and Mexico were lacking. The scenario without any renewables is an unrealistic one because existing wind and solar plants have been removed, but it was created to examine the impacts of all the wind and solar on the system.

Table 5 shows the penetration levels for each scenario. Wind and solar were nominally built to 33% energy penetration considering the historical weather patterns of 2004, 2005, and 2006. The analysis was for the load and weather pattern of 2006, which had a typical solar profile but better wind than the average of the years 2004–2006. After curtailment (curtailment includes CSP storage curtailment, some of which is built into the design of the generator), the 2006 penetration levels are 30–33% of U.S. load in the Western Interconnection and 24–26% of total load in the Western Interconnection. Because Canada and Mexico have relatively small connections with the United States in the Western Interconnection (compared with the total size of the U.S. portion), the impacts of renewables in the United States should be compared with the nominal 33% penetration numbers. Certain outputs, such as total change in emissions throughout the Western Interconnection, should be compared with the total Western Interconnection penetration levels (nominally 26%).

	2006 Penetration Level Across U.S. WECC After All Curtailment	2006 Penetration Level Across All WECC After All Curtailment
TEPPC	13.2	10.5
High wind	32.6	26.0
High mix	32.2	25.6
High solar	30.2	24.1

TABLE 5

Renewable energy penetration levels

To bring resources to load, we expanded the capabilities of existing transmission paths by iterating production cost runs until shadow prices across paths were within fixed, consistent cutoff values.

Simulating Western Grid Operations

We committed base load units one day ahead using synthesized day-ahead wind and solar forecasts. We

Copyright 2017 Cengage Learning. All Rights Reserved. May not be copied, scanned, or duplicated, in whole or in part. Due to electronic rights, some third party content may be suppressed from the eBook and/or eChapter(s). Editorial review has deemed that any suppressed content does not materially affect the overall learning experience. Cengage Learning reserves the right to remove additional content at any time if subsequent rights restrictions require it.

then committed gas units four hours ahead using synthesized four-hour-ahead wind and solar forecasts. Finally, we ran a 5-minute real-time dispatch.

Balancing the system can be more challenging with higher penetrations of variable generation. We therefore increased operating reserves to accommodate the wind and solar, as shown in Table 6. We used dynamic reserve requirements, and Table 6 shows the average level of operating reserves held throughout the year. We did not increase contingency reserves, which were held zonally, because neither wind nor solar plants were the single largest contingency. We adjusted other operating reserves, however, based on the wind and solar output during each hour of the year. Regulating reserves were held equivalent to 1% of load plus 90% of the 10-minutes wind and solar variability. The high wind and solar penetrations required up to 10% more regulating reserves than the scenario without any renewables. We also held a new reserve category—“flexibility reserves”—to account for the 60-minutes variability of wind and solar. These amounted to 1–3% of the installed capacity of the wind and solar generating facilities.

All of this work was overseen by a technical review committee consisting of about 50 utility staff members, researchers, and power plant experts. They met approximately every other month to review inputs, assumptions, methodologies, and results.

System Operation with High Penetrations of Wind and Solar

We analyzed the 5-minute operational simulations, with a focus on cycling impacts of the coal and gas units. All results reflect the specific characteristics of the generators and transmission of the Western Interconnection.

During the summer, load is high, and the impacts of variable generation on cycling are modest. In the spring and fall, however, load is low, and both wind and solar output are high, resulting in challenging operational conditions. This makes for a low net load: net load is the load minus the variable generation. Five-minute dispatch from the most challenging week of the year, as defined by the minimum net load condition,

Scenario	Contingency (MW)	Regulation (MW)	Flexibility (MW)
No renewables	3361	1120	0
TEPPC	3361	1158	1193
High wind	3361	1236	2599
High mix	3361	1211	2035
High solar	3361	1207	1545

TABLE 6

Contingency, regulating, and flexibility reserves

Copyright 2017 Cengage Learning. All Rights Reserved. May not be copied, scanned, or duplicated, in whole or in part. Due to electronic rights, some third party content may be suppressed from the eBook and/or eChapter(s). Editorial review has deemed that any suppressed content does not materially affect the overall learning experience. Cengage Learning reserves the right to remove additional content at any time if subsequent rights restrictions require it.

is shown in Figure 1. At low penetrations, as shown in Figure 1(a), there is little impact on the rest of the system except on the minimum net load day of March 29. For the high-wind scenario, shown in Figure 1(b), however, most of the gas CC generation has been displaced; there is curtailment on March 29; and coal generation declines markedly over the week. In the high-solar scenario, shown in Figure 1(c), the high midday

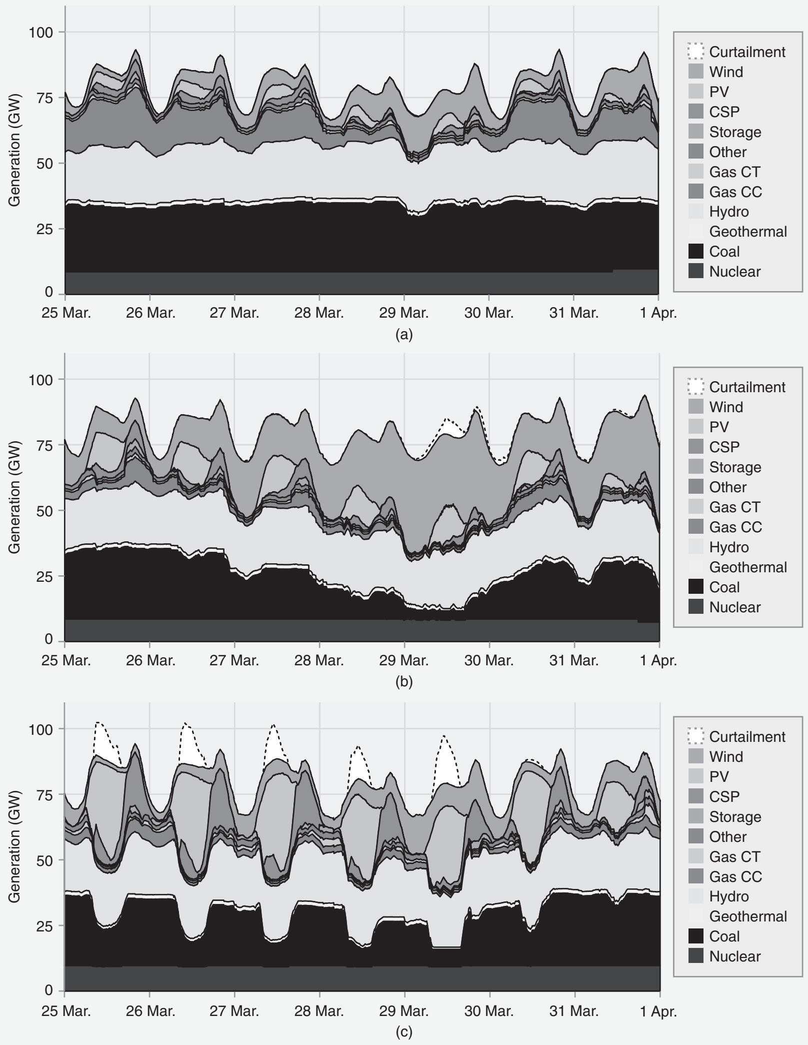

Figure 1 *Five-minute dispatch stacks for the (a) TEPPC, (b) high-wind, and (c) high-solar scenarios for a week in March. This week represented the most challenging week, as defined by the minimum net load condition.*

Copyright 2017 Cengage Learning. All Rights Reserved. May not be copied, scanned, or duplicated, in whole or in part. Due to electronic rights, some third party content may be suppressed from the eBook and/or eChapter(s). Editorial review has deemed that any suppressed content does not materially affect the overall learning experience. Cengage Learning reserves the right to remove additional content at any time if subsequent rights restrictions require it.

output leads to curtailment and the backing down of coal generation on a nearly daily basis in the middle of the day. Gas CT units turn on in the evening to help meet the evening load peak.

Despite these challenges, we find that the system can operate and balance load and generation. There were no regulating reserve violations and very few contingency reserve violations. Figure 2 shows that wind and solar mostly displace gas CC generation. Displacement of coal increased with increasing penetrations of wind because gas tends to be decommitted or backed down already at night, when there are high levels of wind. Curtailment of potential wind and solar generation on an annual basis was as much as 5% in the high-penetration scenarios. The high-mix scenario saw the least curtailment (1.6%).

The biggest impact from wind and solar on cycling of other generation is the increased ramping of the coal units, as shown in Figure 3(b). Starts for coal units, as shown in Figure 3(a), change little. Gas CCs start more with low wind and solar penetrations, but at high penetrations starts are similar to those in the scenario with no renewables. Gas CTs cycle more with high solar penetrations and less with high wind penetrations.

Figure 4 depicts coal starts and ramps for the challenging week in March. At low penetrations, there is little change in coal commitments, and the coal units are typically running at or near full output. In the high-penetration scenarios, coal capacity is shut down approximately each week, and the coal is ramped up and down each day, especially with high penetrations of solar.

Emissions Reductions Are Significant

We find that wind- and solar-induced cycling offsets a very small percentage of the wind- and solar-induced emissions reductions of CO_2, NO_x, and SO_2 across the Western Interconnection that are more than offset by the emissions reductions due

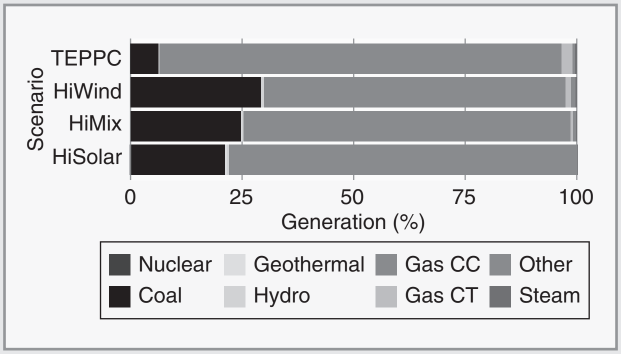

Figure 2 Generation displaced by wind and solar, as compared with the scenario without any renewables

Copyright 2017 Cengage Learning. All Rights Reserved. May not be copied, scanned, or duplicated, in whole or in part. Due to electronic rights, some third party content may be suppressed from the eBook and/or eChapter(s). Editorial review has deemed that any suppressed content does not materially affect the overall learning experience. Cengage Learning reserves the right to remove additional content at any time if subsequent rights restrictions require it.

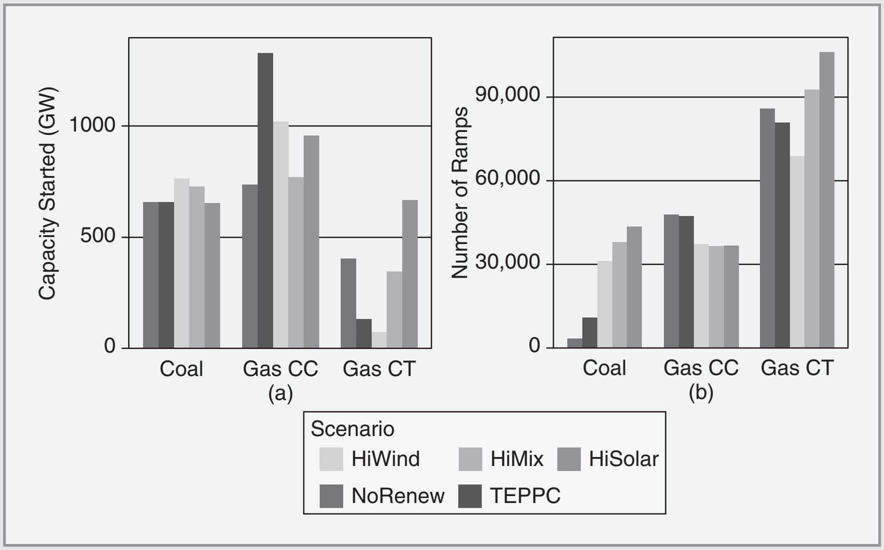

Figure 3 *(a) Capacity started and (b) total number of ramps for each plant type by scenario for one year*

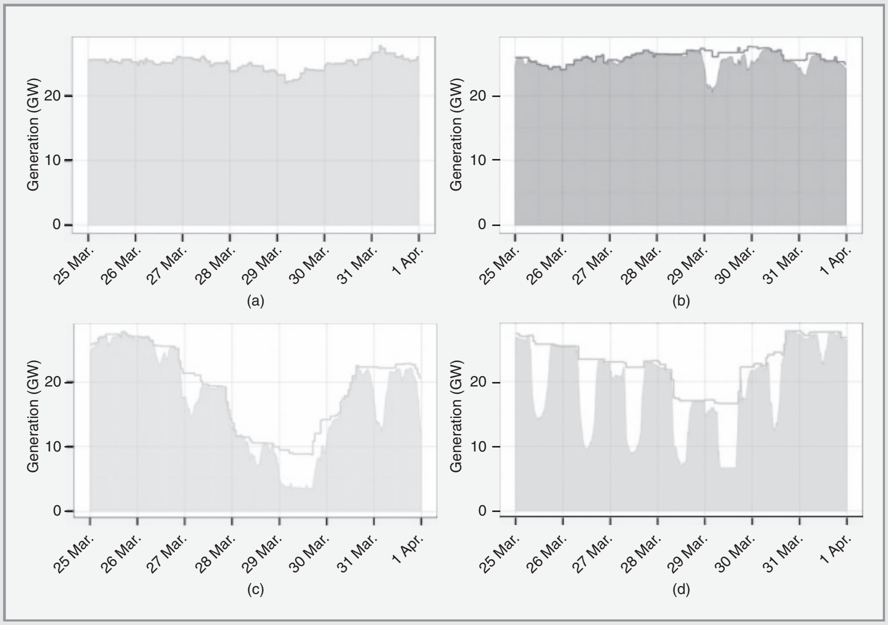

Figure 4 *Capacity committed (solid line) and dispatched (shaded area) for coal units during a sample week in March. The white area between the solid line and the shaded area illustrates how far the capacity is backed down (a) no renewables, (b) TEPPC, (c) high wind, and (d) high solar.*

Copyright 2017 Cengage Learning. All Rights Reserved. May not be copied, scanned, or duplicated, in whole or in part. Due to electronic rights, some third party content may be suppressed from the eBook and/or eChapter(s). Editorial review has deemed that any suppressed content does not materially affect the overall learning experience. Cengage Learning reserves the right to remove additional content at any time if subsequent rights restrictions require it.

to the displacement of fossil-fueled generation. Compared with the scenario without any renewables, the high-penetration scenarios (nominally 33% wind and solar in the U.S. portion of the Western Interconnection, resulting in 26% wind and solar across the interconnection) reduce CO_2 by 29–34%, NO_x by 16–22%, and SO_2 by 14–24%, including the cycling impacts. CO_2 emissions are reduced by a greater percentage than the wind and solar penetration level because wind and solar preferentially displace fossil-fueled generation, while typically the generation in the western United States is a combination of hydro, nuclear, fossil-fueled, and other renewable generation.

Figure 5(a) shows the total CO_2 emissions for each scenario. Ramping had no significant impact on CO_2 emissions, so those estimates are not shown. The start-up CO_2 emissions (shown by the thin, dark line at the top of each bar) were negligible in all cases. Figure 5(b) shows the CO_2 emissions saved by each MWh of wind/solar. Avoided CO_2—considering part-load, ramping, and start impacts—was 1100–1190 lb/MWh of wind and solar produced in the high-penetration scenarios (see Table 7). CO_2 emissions from starts were negligible here as well. We also calculated the part-load penalty— which was the incremental CO_2 emissions from part loading—as negligible. These values reflect aggregate emissions across the Western Interconnection; any specific plant might have lower or higher emissions than those shown here.

From the fossil-fueled plant perspective, average CO_2 emission rates of coal, CCs, and CTs change only slightly with wind and solar, as shown in Figure 6(a). Figure 6(b)

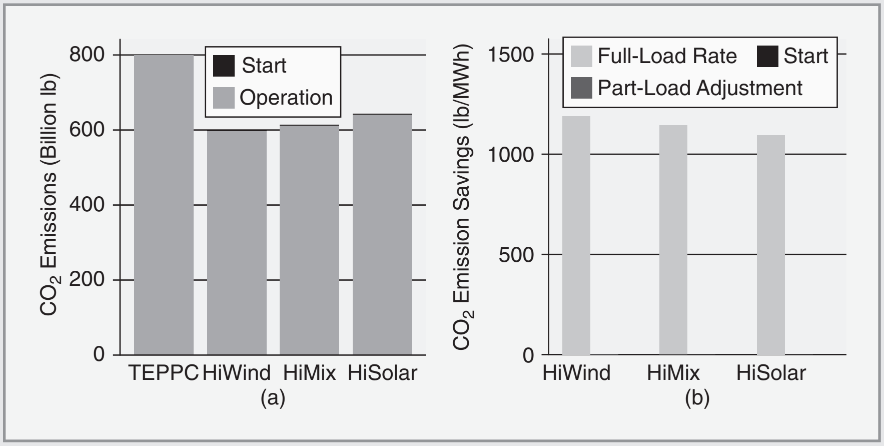

Figure 5 CO_2 emissions by scenario: (a) absolute CO_2 emissions for operation and starts and (b) CO_2 emissions reductions compared with the scenario without renewables, separated into the constant emissions rate assumption and adjustments for part load and starts. Ramping emissions are excluded because they have no significant impact on CO_2 emissions.

Copyright 2017 Cengage Learning. All Rights Reserved. May not be copied, scanned, or duplicated, in whole or in part. Due to electronic rights, some third party content may be suppressed from the eBook and/or eChapter(s). Editorial review has deemed that any suppressed content does not materially affect the overall learning experience. Cengage Learning reserves the right to remove additional content at any time if subsequent rights restrictions require it.

Scenario	Avoided CO_2 (lb/MWh)	Avoided NO_x (lb/MWh)	Avoided SO_2 (lb/MWh)
High wind	1190	0.92	0.56
High mix	1150	0.80	0.44
High solar	1100	0.72	0.35

TABLE 7

Emissions avoided per MWh of wind and solar, considering part-load, ramping, and start impacts. Part-load impacts were not included for SO_2 because of inadequate data

shows that adding wind and solar can positively or negatively affect emissions rates, depending on the plant type and scenario. For coal and CC units, wind and solar generally improves emissions rates by up to 1%. The largest negative impact of wind- and solar-induced cycling is found in the high-wind scenario and for the CT units, where the emissions rate increases by 2%. This is on average; individual units might be more or less affected.

Figure 7 shows the analysis for NO_x emissions. There was a negligible impact of starts on NO_x. Ramping

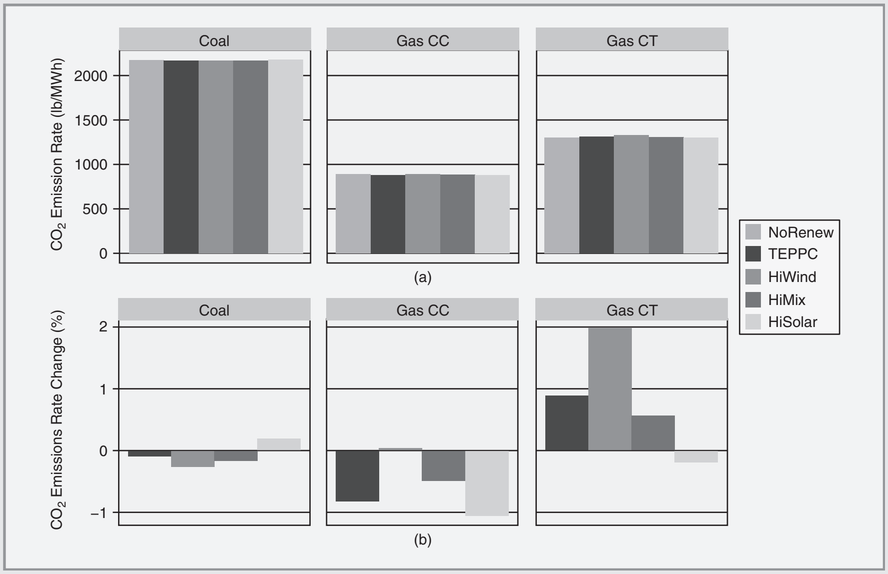

Figure 6 (a) Average CO_2 emission rates by plant type (defined as CO_2 emissions divided by MWh of coal, CC, or CT generation) for each scenario and (b) changes in emissions rates as compared with the scenario without renewables

Copyright 2017 Cengage Learning. All Rights Reserved. May not be copied, scanned, or duplicated, in whole or in part. Due to electronic rights, some third party content may be suppressed from the eBook and/or eChapter(s). Editorial review has deemed that any suppressed content does not materially affect the overall learning experience. Cengage Learning reserves the right to remove additional content at any time if subsequent rights restrictions require it.

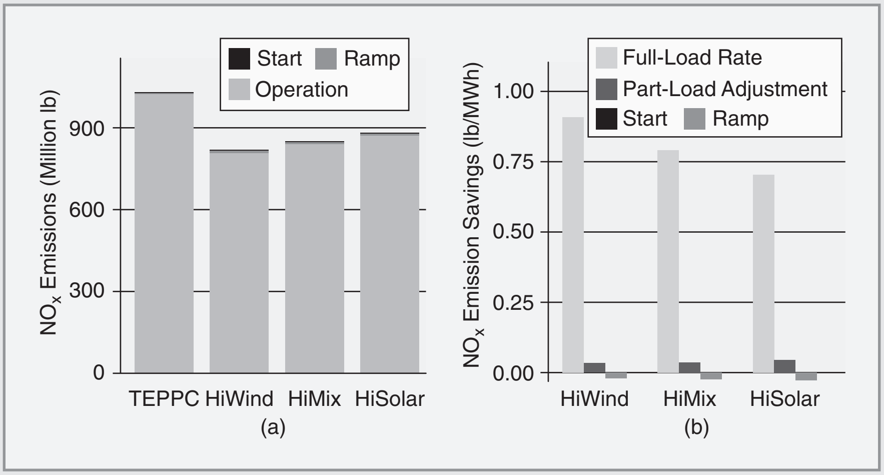

Figure 7 *NO_X emissions by scenario: (a) absolute NO_X emissions for operation, ramps, and starts, and (b) NO_X emissions reductions compared with the scenario without renewables, separated into the constant emissions rate assumption and adjustments for part-load, ramps, and start impacts*

reduced the avoided NO_x by 2–4%. This is shown in Figure 7(b) as a small negative contribution. Part-loading impacts, on the other hand, increased avoided NO_x by 4–6%. On average, coal units in the western United States emit less NO_x per MWh of generation at part load. The net impact of considering cycling improved avoided NO_x emissions from wind and solar by 1–2%.

Figure 8 shows the emissions analysis for SO_2. Because there were inadequate data to create SO_2 emission part-load curves, part-load impacts were not studied for SO_2. Ramping impacts on avoided SO_2 were modest for the high-penetration scenarios, reducing avoided SO_2 by 2–5%. Start-up emissions affected the avoided emissions rates by significantly less than 1%.

Wind- and Solar-Induced Cycling Operational Costs

The production simulation analysis undertaken in this study quantifies (1) the operational impacts of wind and solar displacing other generation and (2) the cycling costs induced by wind and solar. Operational costs (the industry term is production cost) include fuel, noncyclic VOM, and cycling costs. Cycling costs includes costs for starts, ramps and start-up fuel.

Under the scenarios studied, we find that the high wind and solar penetrations affect the grid by displacing US$7 billion/year in fuel costs and inducing an increase of US$35–157 million/year in cycling costs of fossil-fueled plants. The overall production cost for each scenario is shown in Figure 9, with the lower- and upper-bound uncertainty ranges shown.

Copyright 2017 Cengage Learning. All Rights Reserved. May not be copied, scanned, or duplicated, in whole or in part. Due to electronic rights, some third party content may be suppressed from the eBook and/or eChapter(s). Editorial review has deemed that any suppressed content does not materially affect the overall learning experience. Cengage Learning reserves the right to remove additional content at any time if subsequent rights restrictions require it.

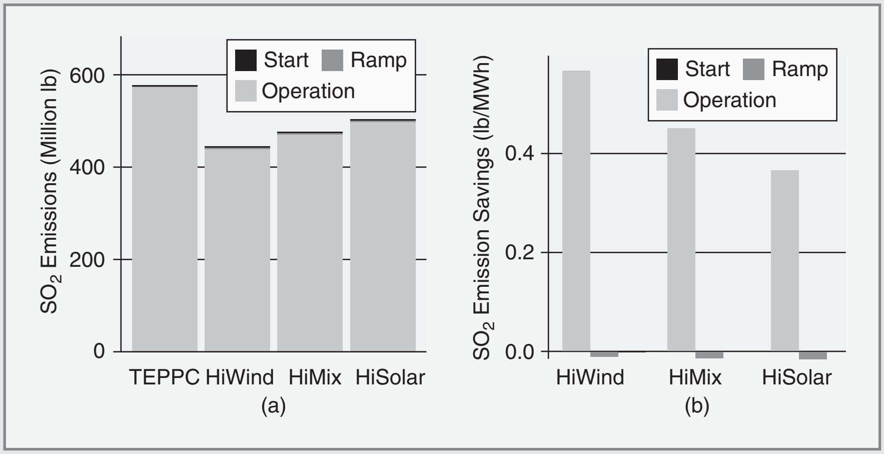

Figure 8 *SO$_2$ emissions by scenario: (a) absolute SO$_2$ emissions for operation, ramping, and starts and (b) SO$_2$ emission reductions compared with the scenario without renewables, separated into the constant emissions rate assumption and adjustments for ramps, and start impacts. Part-load impacts were not studied because of inadequate data.*

At an average gas price of US$4.60/million Btu, fuel dominates the production cost savings as wind and solar penetration increases. It is important to note that production cost does not include the capital costs of renewable or thermal generation or transmission.

Figure 10 details the cycling costs of each scenario. The cycling costs range from about US$270 million in the scenario without renewables, using lower-bound costs, to about US$800 million in the high-solar scenario, using upper-bound

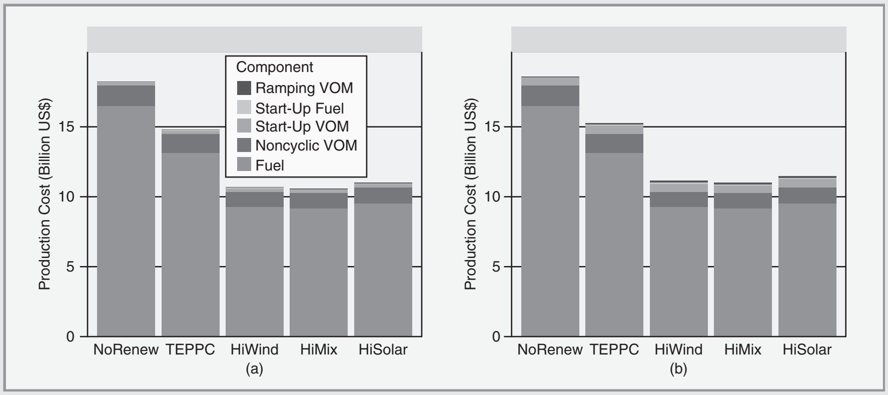

Figure 9 *Production cost for each scenario showing the (a) lower-bound and (b) upper-bound cycling costs. These costs do not include capital costs of renewable or thermal generation or transmission.*

Copyright 2017 Cengage Learning. All Rights Reserved. May not be copied, scanned, or duplicated, in whole or in part. Due to electronic rights, some third party content may be suppressed from the eBook and/or eChapter(s). Editorial review has deemed that any suppressed content does not materially affect the overall learning experience. Cengage Learning reserves the right to remove additional content at any time if subsequent rights restrictions require it.

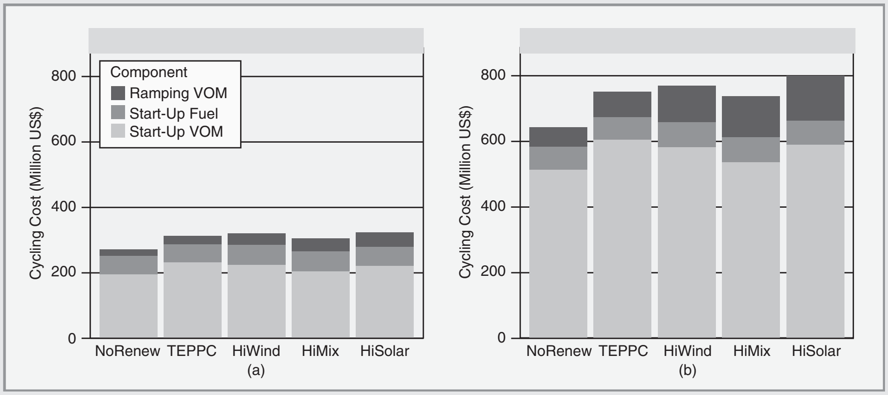

Figure 10 Production cost components resulting from cycling, showing the (a) lower-bound and (b) upper-bound wear-and-tear costs for each scenario. Cost components have been broken down into starts, start fuel, and ramping costs.

cycling costs. Interestingly, the high-mix scenario has a higher wind and solar penetration but lower cycling costs than the TEPPC scenario. In these scenarios, going from no wind and solar penetration to 13% nominal wind and solar penetration induces higher cycling costs than going from 13% to 33% penetration. On a per-MWh-of-fossil-fueled-generation basis, the increased cycling costs (compared with the scenario without any renewables) are US$0.18–0.44/MWh, US$0.52–1.24/MWh, US$0.47–1.14/MWh, and US$0.50–1.28/MWh for the TEPPC, high-wind, high-mix, and high-solar scenarios, respectively. The ranges represent the uncertainty range in the cycling cost inputs.

Figure 11 shows the lower-bound costs from the perspective of a coal, gas CC, or gas CT unit, in terms of cycling costs per MWh of that unit's generation. Must-run gas CT units were excluded from this plot, as they skew the results. Cycling costs for coal increase modestly with high penetrations of wind and solar. Cycling costs for gas CC units increase significantly with increased wind and solar penetration. But the largest cycling costs (per MWh) are borne by the gas CT units, which are operated as peakers and cycle the most. Interestingly, gas CT units see lower cycling costs in the TEPPC scenario than in the scenario without any renewables at all. And in the high-wind scenario, their cycling costs are similar to the scenario without renewables.

These cycling costs are comparable to the noncyclic VOM of approximately US$2/MWh. The impact of wind and solar on the economic viability of a fossil-fueled plant can be significant if that plant's energy production is displaced by wind and solar, its revenue is reduced, and it now bears an increased cycling cost. That fossil-fueled plant may still be needed to help balance the system or provide power on peak demand

Copyright 2017 Cengage Learning. All Rights Reserved. May not be copied, scanned, or duplicated, in whole or in part. Due to electronic rights, some third party content may be suppressed from the eBook and/or eChapter(s). Editorial review has deemed that any suppressed content does not materially affect the overall learning experience. Cengage Learning reserves the right to remove additional content at any time if subsequent rights restrictions require it.

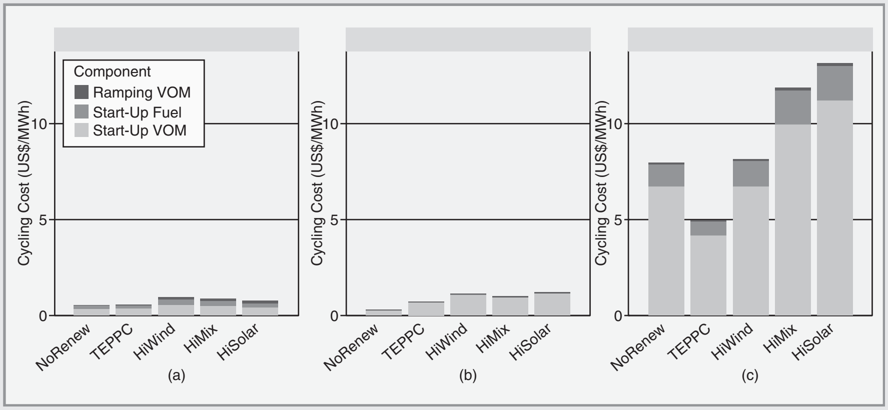

Figure 11 Lower-bound cycling cost for (a) coal, (b) gas CC units, and (c) gas CTs (excluding the must-run CTs). The total, system wide, lower-bound cycling costs were disaggregated by plant type and divided by MWh of generation for that plant type.

days. This raises a host of market and policy issues that require future analysis.

We performed a sensitivity analysis on the gas price to see if halving the price (to US$2.30/million Btu) or doubling it (to US$9.60/million Btu) significantly changed results. The US$9.60 gas price had little effect on operations. The US$2.30 gas price led to more gas usage and less coal usage, regardless of renewables on the system. The type of generation displaced by renewables was very similar for the three gas price estimates. Interestingly, the impact of wind and solar in the very low and very high gas price scenarios is to reduce overall cycling cost, because they displace starts for various unit types. The increase in cycling costs per MWh generated at fossil-fueled plants was similar in all the gas price scenarios. Units with increased cycling, however, will have a higher US$/MWh cost of generation and will probably see an increase in forced outage rates if adjustments to maintenance spending are not made.

An examination of the cycling impacts from a system perspective in Figure 12 shows the change in production cost (operational cost, not including capital or power purchase agreement costs) for each scenario as compared with the scenario without renewables. The primary operational impact of wind and solar is to displace a large amount of fuel cost (shown by the negative orange bars) and a small amount of noncyclic VOM (small negative blue bars). At this gas price (US$4.60/million Btu), the secondary impact of wind and solar is to incur the startup VOM, start-up fuel, and ramping VOM shown by the small positive bars. While it is important to remember that these operational costs do not include the capital costs of any generator or transmission, one can see

Copyright 2017 Cengage Learning. All Rights Reserved. May not be copied, scanned, or duplicated, in whole or in part. Due to electronic rights, some third party content may be suppressed from the eBook and/or eChapter(s). Editorial review has deemed that any suppressed content does not materially affect the overall learning experience. Cengage Learning reserves the right to remove additional content at any time if subsequent rights restrictions require it.

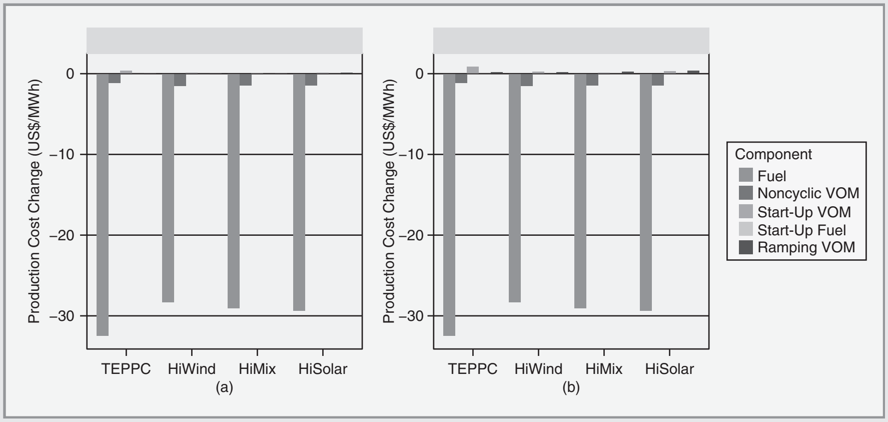

Figure 12 The change in production cost for each scenario relative to the scenario without renewables, per MWh of wind and solar generation, for the (a) lower-bound and (b) upper-bound wear-and-tear costs. Production costs do not include any fixed capital or power purchase agreement costs.

that the cycling costs are a small fraction of the costs of the fuel displaced. This cycling impact offsets the production cost reduction of wind and solar by US$0.14–0.67 per MWh of wind and solar generated. The net reduction in production cost compared with the scenario without renewables, including these cycling impacts, is approximately US$30 per MWh of wind and solar generated.

Wind Dominates Uncertainty, and Solar Dominates Variability

This study took advantage of recent advances in simulating large PV plants that allowed a comparison of the impacts of wind and solar on the grid. We conducted statistical analysis of variability and uncertainty (forecast error) to look at these impacts. We looked at extreme ramping events on an hourly and 5-minute basis and found that extreme ramping events were dominated by sunrise and sunset events. However, because we know when sunrise and sunset occur and, in fact, the path of the sun through the sky each day, we can plan for these events. When the solar diurnal variability is removed, PV variability due to weather is found to be similar to wind variability.

Statistical analysis of forecast errors showed that our day-ahead forecast errors were driven by wind uncertainty. Day-ahead solar forecasts were more accurate than day-ahead wind forecasts. Because forecast accuracy improves as one approaches the time in question, the four-hour-ahead forecasts were much more accurate, as shown in Figure 13. We used a four-hour-ahead unit commitment to commit gas units, similar to operations of the California Independent System Operator. This helped mitigate the uncertainty of the wind day-ahead forecasts.

Copyright 2017 Cengage Learning. All Rights Reserved. May not be copied, scanned, or duplicated, in whole or in part. Due to electronic rights, some third party content may be suppressed from the eBook and/or eChapter(s). Editorial review has deemed that any suppressed content does not materially affect the overall learning experience. Cengage Learning reserves the right to remove additional content at any time if subsequent rights restrictions require it.

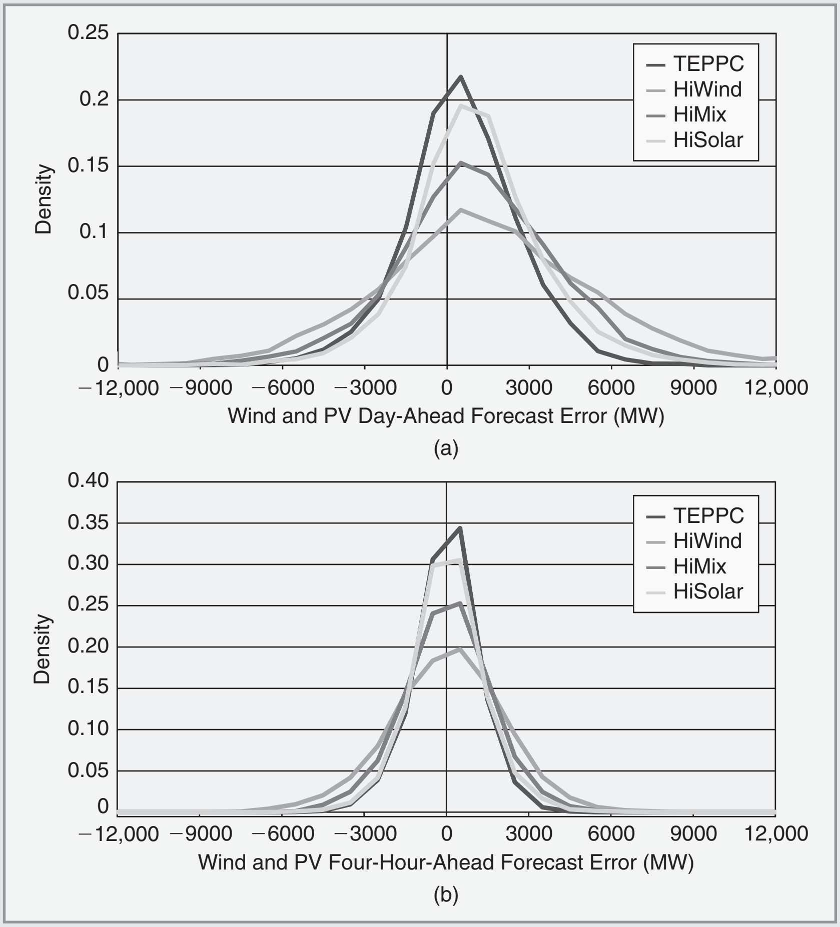

Figure 13 (a) Day-ahead and (b) four-hour-ahead wind and PV forecast errors for each scenario

Conclusions

For the first time, we have conducted an operational simulation of wind and solar impacts across the entire Western Interconnection using detailed data on cycling costs and cycling emissions. Our three high-penetration scenarios model a nominal 33% wind and solar penetration across the U.S. portion of the Western Interconnection, resulting in 26% nominal penetration across the entire Western Interconnection. We examine the primary operational impact of wind and solar in displacing fuel (and the costs and emissions associated with the fuel), along with the secondary impact of increased cycling (and the costs and emissions associated with cycling).

Copyright 2017 Cengage Learning. All Rights Reserved. May not be copied, scanned, or duplicated, in whole or in part. Due to electronic rights, some third party content may be suppressed from the eBook and/or eChapter(s). Editorial review has deemed that any suppressed content does not materially affect the overall learning experience. Cengage Learning reserves the right to remove additional content at any time if subsequent rights restrictions require it.

We found that wind- and solar-induced cycling has a small impact on avoided emissions of CO_2, NO_x, and SO_2. In our high-penetration scenarios, cycling reduces avoided CO_2 emissions by 0.2%, improves avoided NO_x by 1–2%, and lessens avoided SO_2 by up to 5%. The net result is that wind and solar in our high-penetration scenarios reduce CO_2 by 29–34%, NO_x by 16–22%, and SO_2 by 14–24%, inclusive of cycling impacts.

We also found that the secondary impact of increased cycling incurs costs that are a small fraction of the displaced fuel costs. In our high-penetration scenarios, wind and solar induce additional annual cycling costs of US$35–157 million. This same wind and solar also displaces about US$7 billion annually in fuel costs. In the high-penetration scenarios, the increase in cycling cost for the average fossil-fueled plant ranges from US$0.47–1.14 per MWh of fossil-fueled generation in the high-mix scenario to US$0.50–1.28 per MWh in the high-solar scenario. These additional costs, combined with reduced generation and revenue, beg the question of market and policy changes that may be required in a potential future with high levels of wind and solar energy.

For Further Reading

GE Energy. (2010). “Western wind and solar integration study.” NREL. Golden, CO. NREL/SR-550-47434 [Online]. Available: http://www.nrel.gov/docs/fy10osti/47434.pdf.

N. Kumar, P. Besuner, S. Lefton, D. Agan, and D. Hilleman. (2012). “Power plant cycling costs.” Intertek AIM. NREL. Sunnyvale, CA, Golden, CO. NREL/SR-5500-55433 [Online]. Available: http://www.nrel.gov/docs/fy12osti/55433.pdf.

D. Lew, G. Brinkman, E. Ibanez, A. Florita, M. Heaney, B.-M. Hodge, M. Hummon, G. Stark, J. King, S. Lefton, N. Kumar, D. Agan, G. Jordan, and S. Venkataraman. (2013). “The western wind and solar integration study phase 2.” NREL. Golden, CO. NREL/TP-5500-55588. [Online]. Available: http://www.nrel.gov/docs/fy13osti/55588.pdf.

M. Milligan, K. Clark, J. King, B. Kirby, T. Guo, and G. Liu. (2013). “Examination of potential benefits of an energy imbalance market in the western interconnection.” NREL. Golden, CO. NREL/TP-5500-57115. [Online]. Available: http://www.nrel.gov/docs/fy13osti/57115.pdf.

Biographies

Debra Lew is with the National Renewable Energy Laboratory, Golden, Colorado.

Greg Brinkman is with the National Renewable Energy Laboratory, Golden, Colorado.

Nikhil Kumar is with Intertek, Sunnyvale, California.

Steve Lefton is with Intertek and Global Utility Consultants LLC, Sunnyvale, California.

Gary Jordan is with GE Energy Consulting, Schenectady, New York.

Sundar Venkataraman is with GE Energy Consulting, Phoenix, Arizona. ■

Copyright 2017 Cengage Learning. All Rights Reserved. May not be copied, scanned, or duplicated, in whole or in part. Due to electronic rights, some third party content may be suppressed from the eBook and/or eChapter(s). Editorial review has deemed that any suppressed content does not materially affect the overall learning experience. Cengage Learning reserves the right to remove additional content at any time if subsequent rights restrictions require it.

6.1 DIRECT SOLUTIONS TO LINEAR ALGEBRAIC EQUATIONS: GAUSS ELIMINATION

Consider the following set of linear algebraic equations in matrix format:

$$\begin{bmatrix} A_{11} & A_{12} & \cdots & A_{1N} \\ A_{21} & A_{22} & \cdots & A_{2N} \\ \vdots & & \vdots & \\ A_{N1} & A_{N2} & \cdots & A_{NN} \end{bmatrix} \begin{bmatrix} x_1 \\ x_2 \\ \vdots \\ x_N \end{bmatrix} = \begin{bmatrix} y_1 \\ y_2 \\ \vdots \\ y_N \end{bmatrix} \tag{6.1.1}$$

or

$$\mathbf{Ax} = \mathbf{y} \tag{6.1.2}$$

where **x** and **y** are N vectors and **A** is an $N \times N$ square matrix. The components of **x**, **y**, and **A** may be real or complex. Given **A** and **y**, the objective is to solve for **x**. Assume the det(**A**) is nonzero, so a unique solution to (6.1.1) exists.

The solution **x** can be obtained easily when **A** is an upper triangular matrix with nonzero diagonal elements. Then (6.1.1) has the form

$$\begin{bmatrix} A_{11} & A_{12}\ldots & & A_{1N} \\ 0 & A_{22}\ldots & & A_{2N} \\ \vdots & & & \\ 0 & 0\ldots & A_{N-1,\,N-1} & A_{N-1,N} \\ 0 & 0\ldots 0 & & A_{NN} \end{bmatrix} \begin{bmatrix} x_1 \\ x_2 \\ \vdots \\ x_{N-1} \\ x_N \end{bmatrix} = \begin{bmatrix} y_1 \\ y_2 \\ \vdots \\ y_{N-1} \\ y_N \end{bmatrix} \tag{6.1.3}$$

Since the last equation in (6.1.3) involves only x_N,

$$x_N = \frac{y_N}{A_{NN}} \tag{6.1.4}$$

After x_N is computed, the next-to-last equation can be solved:

$$x_{N-1} = \frac{y_{N-1} - A_{N-1,\,N}x_N}{A_{N-1,\,N-1}} \tag{6.1.5}$$

In general, with $x_N, x_{N-1}, \ldots, x_{k+1}$ already computed, the kth equation can be solved as

$$x_k = \frac{y_k - \sum_{n=k+1}^{N} A_{kn}x_n}{A_{kk}} \qquad k = N, N-1, \ldots, 1 \tag{6.1.6}$$

This procedure for solving (6.1.3) is called *back substitution.*

If **A** is not an upper triangular, (6.1.1), it can be transformed to an equivalent equation with an upper triangular matrix. The transformation, called *Gauss*

Copyright 2017 Cengage Learning. All Rights Reserved. May not be copied, scanned, or duplicated, in whole or in part. Due to electronic rights, some third party content may be suppressed from the eBook and/or eChapter(s). Editorial review has deemed that any suppressed content does not materially affect the overall learning experience. Cengage Learning reserves the right to remove additional content at any time if subsequent rights restrictions require it.

elimination, is described by the following $(N - 1)$ steps. During Step 1, use the first equation in (6.1.1) to eliminate x_1 from the remaining equations. That is, Equation 1 is multiplied by A_{n1}/A_{11} and then subtracted from equation n, for $n = 2, 3, \ldots, N$. After completing Step 1, we have

$$\begin{bmatrix} A_{11} & A_{12} & \cdots & A_{1N} \\ 0 & \left(A_{22} - \dfrac{A_{21}}{A_{11}}A_{12}\right) & \cdots & \left(A_{2N} - \dfrac{A_{21}}{A_{11}}A_{1N}\right) \\ 0 & \left(A_{32} - \dfrac{A_{31}}{A_{11}}A_{12}\right) & \cdots & \left(A_{3N} - \dfrac{A_{31}}{A_{11}}A_{1N}\right) \\ \vdots & \vdots & & \vdots \\ 0 & \left(A_{N2} - \dfrac{A_{N1}}{A_{11}}A_{12}\right) & \cdots & \left(A_{NN} - \dfrac{A_{N1}}{A_{11}}A_{1N}\right) \end{bmatrix} \begin{bmatrix} x_1 \\ x_2 \\ x_3 \\ \vdots \\ x_N \end{bmatrix}$$

$$= \begin{bmatrix} y_1 \\ y_2 - \dfrac{A_{21}}{A_{11}}y_1 \\ y_3 - \dfrac{A_{31}}{A_{11}}y_1 \\ \vdots \\ y_N - \dfrac{A_{N1}}{A_{11}}y_1 \end{bmatrix} \tag{6.1.7}$$

Equation (6.1.7) has the following form:

$$\begin{bmatrix} A_{11}^{(1)} & A_{12}^{(1)} & \cdots & A_{1N}^{(1)} \\ 0 & A_{22}^{(1)} & \cdots & A_{2N}^{(1)} \\ 0 & A_{32}^{(1)} & \cdots & A_{3N}^{(1)} \\ \vdots & \vdots & & \vdots \\ 0 & A_{N2}^{(1)} & \cdots & A_{NN}^{(1)} \end{bmatrix} \begin{bmatrix} x_1 \\ x_2 \\ x_3 \\ \vdots \\ x_N \end{bmatrix} = \begin{bmatrix} y_1^{(1)} \\ y_2^{(1)} \\ y_3^{(1)} \\ \vdots \\ y_N^{(1)} \end{bmatrix} \tag{6.1.8}$$

where the superscript (1) denotes Step 1 of the Gauss elimination.

During Step 2, use the second equation in (6.1.8) to eliminate x_2 from the remaining (third, fourth, fifth, and so on) equations. That is, Equation 2 is multiplied by $A_{n2}^{(1)}/A_{22}^{(1)}$ and subtracted from equation n, for $n = 3, 4, \ldots, N$. After Step 2, there is

$$\begin{bmatrix} A_{11}^{(2)} & A_{12}^{(2)} & A_{13}^{(2)} & \cdots & A_{1N}^{(2)} \\ 0 & A_{22}^{(2)} & A_{23}^{(2)} & \cdots & A_{2N}^{(2)} \\ 0 & 0 & A_{33}^{(2)} & \cdots & A_{3N}^{(2)} \\ 0 & 0 & A_{43}^{(2)} & \cdots & A_{4N}^{(2)} \\ \vdots & \vdots & \vdots & & \vdots \\ 0 & 0 & A_{N3}^{(2)} & \cdots & A_{NN}^{(2)} \end{bmatrix} \begin{bmatrix} x_1 \\ x_2 \\ x_3 \\ x_4 \\ \vdots \\ x_N \end{bmatrix} = \begin{bmatrix} y_1^{(2)} \\ y_2^{(2)} \\ y_3^{(2)} \\ y_4^{(2)} \\ \vdots \\ y_N^{(2)} \end{bmatrix} \tag{6.1.9}$$

Copyright 2017 Cengage Learning. All Rights Reserved. May not be copied, scanned, or duplicated, in whole or in part. Due to electronic rights, some third party content may be suppressed from the eBook and/or eChapter(s). Editorial review has deemed that any suppressed content does not materially affect the overall learning experience. Cengage Learning reserves the right to remove additional content at any time if subsequent rights restrictions require it.

During step k, start with $\mathbf{A}^{(k-1)}\mathbf{x} = \mathbf{y}^{(k-1)}$. The first k of these equations, already triangularized, are left unchanged. Also, equation k is multiplied by $A_{nk}^{(k-1)}/A_{kk}^{(k-1)}$ and then subtracted from equation n, for $n = k+1, k+2, \ldots, N$.

After $(N-1)$ steps, the equivalent equation is $\mathbf{A}^{(N-1)}\mathbf{x} = \mathbf{y}^{(N-1)}$, where $\mathbf{A}^{(N-1)}$ is upper triangular.

EXAMPLE 6.1

Gauss elimination and back substitution: direct solution to linear algebraic equations

Solve

$$\left[\begin{array}{c|c} 10 & 5 \\ \hline 2 & 9 \end{array}\right]\begin{bmatrix} x_1 \\ x_2 \end{bmatrix} = \begin{bmatrix} 6 \\ 3 \end{bmatrix}$$

using Gauss elimination and back substitution.

SOLUTION

Since $N = 2$ for this example, there is $(N-1) = 1$ Gauss elimination step. Multiplying the first equation by $A_{21}/A_{11} = 2/10$ and then subtracting from the second,

$$\left[\begin{array}{c|c} 10 & 5 \\ \hline 0 & 9 - \frac{2}{10}(5) \end{array}\right]\begin{bmatrix} x_1 \\ x_2 \end{bmatrix} = \begin{bmatrix} 6 \\ 3 - \frac{2}{10}(6) \end{bmatrix}$$

or

$$\left[\begin{array}{c|c} 10 & 5 \\ \hline 0 & 8 \end{array}\right]\begin{bmatrix} x_1 \\ x_2 \end{bmatrix} = \begin{bmatrix} 6 \\ 1.8 \end{bmatrix}$$

which has the form $\mathbf{A}^{(1)}\mathbf{x} = \mathbf{y}^{(1)}$ where $\mathbf{A}^{(1)}$ is upper triangular. Now, using back substitution, (6.1.6) gives, for $k = 2$:

$$x_2 = \frac{y_2^{(1)}}{A_{22}^{(1)}} = \frac{1.8}{8} = 0.225$$

and, for $k = 1$,

$$x_1 = \frac{y_1^{(1)} - A_{12}^{(1)}x_2}{A_{11}^{(1)}} = \frac{6 - (5)(0.225)}{10} = 0.4875$$

Copyright 2017 Cengage Learning. All Rights Reserved. May not be copied, scanned, or duplicated, in whole or in part. Due to electronic rights, some third party content may be suppressed from the eBook and/or eChapter(s). Editorial review has deemed that any suppressed content does not materially affect the overall learning experience. Cengage Learning reserves the right to remove additional content at any time if subsequent rights restrictions require it.

EXAMPLE 6.2

Gauss elimination: triangularizing a matrix

Use Gauss elimination to triangularize

$$\begin{bmatrix} 2 & 3 & -1 \\ -4 & 6 & 8 \\ 10 & 12 & 14 \end{bmatrix} \begin{bmatrix} x_1 \\ x_2 \\ x_3 \end{bmatrix} = \begin{bmatrix} 5 \\ 7 \\ 9 \end{bmatrix}$$

SOLUTION

There are $(N-1) = 2$ Gauss elimination steps. During Step 1, subtract $A_{21}/A_{11} = -4/2 = -2$ times Equation 1 from Equation 2, and subtract $A_{31}/A_{11} = 10/2 = 5$ times Equation 1 from Equation 3, to give

$$\left[\begin{array}{c|c|c} 2 & 3 & -1 \\ \cline{1-3} 0 & 6-(-2)(3) & 8-(-2)(-1) \\ \cline{2-3} 0 & 12-(5)(3) & 14-(5)(-1) \end{array}\right] \begin{bmatrix} x_1 \\ x_2 \\ x_3 \end{bmatrix} = \begin{bmatrix} 5 \\ 7-(-2)(5) \\ 9-(5)(5) \end{bmatrix}$$

or

$$\begin{bmatrix} 2 & 3 & -1 \\ 0 & 12 & 6 \\ 0 & -3 & 19 \end{bmatrix} \begin{bmatrix} x_1 \\ x_2 \\ x_3 \end{bmatrix} = \begin{bmatrix} 5 \\ 17 \\ -16 \end{bmatrix}$$

which is $\mathbf{A}^{(1)}\mathbf{x} = \mathbf{y}^{(1)}$. During Step 2, subtract $A_{32}^{(1)}/A_{22}^{(1)} = -3/12 = -0.25$ times Equation 2 from Equation 3, to give

$$\left[\begin{array}{c|c|c} 2 & 3 & -1 \\ \cline{1-3} 0 & 12 & 6 \\ \cline{1-3} 0 & 0 & 19-(-.25)(6) \end{array}\right] \begin{bmatrix} x_1 \\ x_2 \\ x_3 \end{bmatrix} = \begin{bmatrix} 5 \\ 17 \\ -16-(-.25)(17) \end{bmatrix}$$

or

$$\begin{bmatrix} 2 & 3 & -1 \\ 0 & 12 & 6 \\ 0 & 0 & 20.5 \end{bmatrix} \begin{bmatrix} x_1 \\ x_2 \\ x_3 \end{bmatrix} = \begin{bmatrix} 5 \\ 17 \\ -11.75 \end{bmatrix}$$

which is triangularized. The solution $\mathbf{x}$ now can be easily obtained via back substitution.

Copyright 2017 Cengage Learning. All Rights Reserved. May not be copied, scanned, or duplicated, in whole or in part. Due to electronic rights, some third party content may be suppressed from the eBook and/or eChapter(s). Editorial review has deemed that any suppressed content does not materially affect the overall learning experience. Cengage Learning reserves the right to remove additional content at any time if subsequent rights restrictions require it.

Computer storage requirements for Gauss elimination and back substitution include N^2 memory locations for **A** and N locations for **y**. If there is no further need to retain **A** and **y**, then $A^{(k)}$ can be stored in the location of **A**, and $\mathbf{y}^{(k)}$, as well as the solution **x**, can be stored in the location of **y**. Additional memory is also required for iterative loops, arithmetic statements, and working space.

Computer time requirements can be evaluated by determining the number of arithmetic operations required for Gauss elimination and back substitution. One can show that Gauss elimination requires $(N^3 - N)/3$ multiplications, $(N)(N - 1)/2$ divisions, and $(N^3 - N)/3$ subtractions. Also, back substitution requires $(N)(N - 1)/2$ multiplications, N divisions, and $(N)(N - 1)/2$ subtractions. Therefore, for very large N, the approximate computer time for solving (6.1.1) by Gauss elimination and back substitution is the time required to perform $N^3/3$ multiplications and $N^3/3$ subtractions.

For example, consider a digital computer with a 2×10^{-9} s multiplication time and 1×10^{-9} s addition or subtraction time. Solving $N = 10{,}000$ equations would require

$$\frac{1}{3}N^3(2 \times 10^{-9}) + \frac{1}{3}N^3(1 \times 10^{-9}) = \frac{1}{3}(10{,}000)^3(3 \times 10^{-9}) = 1000 \quad \text{s}$$

approximately plus some additional bookkeeping time for indexing and managing loops.

Since the power flow problem often involves solving power systems with tens of thousands of equations, by itself Gauss elimination would not be a good solution. However, for matrixes that have relatively few nonzero elements, known as sparse matrices, special techniques can be employed to significantly reduce computer storage and time requirements. Since all large power systems can be modeled using sparse matrices, these techniques are briefly introduced in Section 6.8.

6.2 ITERATIVE SOLUTIONS TO LINEAR ALGEBRAIC EQUATIONS: JACOBI AND GAUSS-SEIDEL

A general iterative solution to (6.1.1) proceeds as follows. First select an initial guess $\mathbf{x}(0)$. Then use

$$\mathbf{x}(i+1) = \mathbf{g}[\mathbf{x}(i)] \qquad i = 0, 1, 2, \ldots \tag{6.2.1}$$

where $\mathbf{x}(i)$ is the ith guess and **g** is an N vector of functions that specify the iteration method. Continue this procedure until the following stopping condition is satisfied, as

$$\left| \frac{x_k(i+1) - x_k(i)}{x_k(i)} \right| < \varepsilon \qquad \text{for all } k = 1, 2, \ldots, N \tag{6.2.2}$$

where $x_k(i)$ is the kth component of $\mathbf{x}(i)$ and ε is a specified *tolerance level.*

Copyright 2017 Cengage Learning. All Rights Reserved. May not be copied, scanned, or duplicated, in whole or in part. Due to electronic rights, some third party content may be suppressed from the eBook and/or eChapter(s). Editorial review has deemed that any suppressed content does not materially affect the overall learning experience. Cengage Learning reserves the right to remove additional content at any time if subsequent rights restrictions require it.

The following questions are pertinent:

1. Will the iteration procedure converge to the unique solution?
2. What is the convergence rate (how many iterations are required)?
3. When using a digital computer, what are the computer storage and time requirements?

These questions are addressed for two specific iteration methods: *Jacobi* and *Gauss-Seidel.** The Jacobi method is obtained by considering the kth equation of (6.1.1), as follows:

$$y_k = A_{k1}x_1 + A_{k2}x_2 + \cdots + A_{kk}x_k + \cdots + A_{kN}x_N \tag{6.2.3}$$

Solving for x_k,

$$\begin{aligned} x_k &= \frac{1}{A_{kk}}[y_k - (A_{k1}x_1 + \cdots + A_{k,k-1}x_{k-1} + A_{k,k+1}x_{k+1} + \cdots + A_{kN}x_N)] \\ &= \frac{1}{A_{kk}}\left[y_k - \sum_{n=1}^{k-1} A_{kn}x_n - \sum_{n=k+1}^{N} A_{kn}x_n\right] \end{aligned} \tag{6.2.4}$$

The Jacobi method uses the "old" values of $\mathbf{x}(i)$ at iteration i on the right side of (6.2.4) to generate the "new" value $x_k(i+1)$ on the left side of (6.2.4). That is,

$$x_k(i+1) = \frac{1}{A_{kk}}\left[y_k - \sum_{n=1}^{k-1} A_{kn}x_n(i) - \sum_{n=k+1}^{N} A_{kn}x_n(i)\right] k = 1, 2, \ldots, N \tag{6.2.5}$$

The Jacobi method given by (6.2.5) also can be written in the following matrix format:

$$\mathbf{x}(i+1) = \mathbf{M}\mathbf{x}(i) + \mathbf{D}^{-1}\mathbf{y} \tag{6.2.6}$$

where

$$\mathbf{M} = \mathbf{D}^{-1}(\mathbf{D} - \mathbf{A}) \tag{6.2.7}$$

and

$$\mathbf{D} = \begin{bmatrix} A_{11} & 0 & 0 & \cdots & 0 \\ 0 & A_{22} & 0 & \cdots & 0 \\ 0 & \vdots & \vdots & & \vdots \\ \vdots & & & & 0 \\ 0 & 0 & 0 & \cdots & A_{NN} \end{bmatrix} \tag{6.2.8}$$

For Jacobi, **D** consists of the diagonal elements of the **A** matrix.

The Gauss-Seidel method is given by

$$x_k(i+1) = \frac{1}{A_{kk}}\left[y_k - \sum_{n=1}^{k-1} A_{kn}x_n(i+1) - \sum_{n=k+1}^{N} A_{kn}x_n(i)\right] \tag{6.2.9}$$

---

*The Jacobi method is also called the Gauss method.

Copyright 2017 Cengage Learning. All Rights Reserved. May not be copied, scanned, or duplicated, in whole or in part. Due to electronic rights, some third party content may be suppressed from the eBook and/or eChapter(s). Editorial review has deemed that any suppressed content does not materially affect the overall learning experience. Cengage Learning reserves the right to remove additional content at any time if subsequent rights restrictions require it.

EXAMPLE 6.3

Jacobi method: iterative solution to linear algebraic equations

Solve Example 6.1 using the Jacobi method. Start with $x_1(0) = x_2(0) = 0$ and continue until (6.2.2) is satisfied for $\varepsilon = 10^{-4}$.

SOLUTION

From (6.2.5) with $N = 2$,

$$k = 1 \qquad x_1(i+1) = \frac{1}{A_{11}}[y_1 - A_{12}x_2(i)] = \frac{1}{10}[6 - 5x_2(i)]$$

$$k = 2 \qquad x_2(i+1) = \frac{1}{A_{22}}[y_2 - A_{21}x_1(i)] = \frac{1}{9}[3 - 2x_1(i)]$$

Alternatively, in matrix format using (6.2.6) through (6.2.8),

$$\mathbf{D}^{-1} = \left[\begin{array}{c|c} 10 & 0 \\ \hline 0 & 9 \end{array}\right]^{-1} = \left[\begin{array}{c|c} \frac{1}{10} & 0 \\ \hline 0 & \frac{1}{9} \end{array}\right]$$

$$\mathbf{M} = \left[\begin{array}{c|c} \frac{1}{10} & 0 \\ \hline 0 & \frac{1}{9} \end{array}\right]\left[\begin{array}{c|c} 0 & -5 \\ \hline -2 & 0 \end{array}\right] = \left[\begin{array}{c|c} 0 & -\frac{5}{10} \\ \hline -\frac{2}{9} & 0 \end{array}\right]$$

$$\begin{bmatrix} x_1(i+1) \\ x_2(i+1) \end{bmatrix} = \left[\begin{array}{c|c} 0 & -\frac{5}{10} \\ \hline -\frac{2}{9} & 0 \end{array}\right]\begin{bmatrix} x_1(i) \\ x_2(i) \end{bmatrix} + \left[\begin{array}{c|c} \frac{1}{10} & 0 \\ \hline 0 & \frac{1}{9} \end{array}\right]\begin{bmatrix} 6 \\ 3 \end{bmatrix}$$

The above two formulations are identical. Starting with $x_1(0) = x_2(0) = 0$, the iterative solution is given in the following table:

Jacobi

i	0	1	2	3	4	5	6	7	8	9	10
$x_1(i)$	0	0.60000	0.43334	0.50000	0.48148	0.48889	0.48683	0.48766	0.48743	0.48752	0.48749
$x_2(i)$	0	0.33333	0.20000	0.23704	0.22222	0.22634	0.22469	0.22515	0.22496	0.22502	0.22500

As shown, the Jacobi method converges to the unique solution obtained in Example 6.1.

Copyright 2017 Cengage Learning. All Rights Reserved. May not be copied, scanned, or duplicated, in whole or in part. Due to electronic rights, some third party content may be suppressed from the eBook and/or eChapter(s). Editorial review has deemed that any suppressed content does not materially affect the overall learning experience. Cengage Learning reserves the right to remove additional content at any time if subsequent rights restrictions require it.

The convergence criterion is satisfied at the 10th iteration, since

$$\left|\frac{x_1(10) - x_1(9)}{x_1(9)}\right| = \left|\frac{0.48749 - 0.48752}{0.48749}\right| = 6.2 \times 10^{-5} < \varepsilon$$

and

$$\left|\frac{x_2(10) - x_2(9)}{x_2(9)}\right| = \left|\frac{0.22500 - 0.22502}{0.22502}\right| = 8.9 \times 10^{-5} < \varepsilon$$

Comparing (6.2.9) with (6.2.5), note that Gauss-Seidel is similar to Jacobi except that during each iteration, the "new" values, $x_n(i+1)$, for $n < k$ are used on the right side of (6.2.9) to generate the "new" value $x_k(i+1)$ on the left side.

The Gauss-Seidel method of (6.2.9) also can be written in the matrix format of (6.2.6) and (6.2.7), where

$$\mathbf{D} = \begin{bmatrix} A_{11} & 0 & 0 & \cdots & 0 \\ A_{21} & A_{22} & 0 & \cdots & 0 \\ \vdots & \vdots & & & \vdots \\ A_{N1} & A_{N2} & \cdots & & A_{NN} \end{bmatrix} \qquad (6.2.10)$$

For Gauss-Seidel, **D** in (6.2.10) is the lower triangular portion of **A**, whereas for Jacobi, **D** in (6.2.8) is the diagonal portion of **A**.

EXAMPLE 6.4

Gauss-Seidel method: iterative solution to linear algebraic equations

Rework Example 6.3 using the Gauss-Seidel method.

SOLUTION

From (6.2.9),

$$k = 1 \qquad x_1(i+1) = \frac{1}{A_{11}}[y_1 - A_{12}x_2(i)] = \frac{1}{10}[6 - 5x_2(i)]$$

$$k = 2 \qquad x_2(i+1) = \frac{1}{A_{22}}[y_2 - A_{21}x_1(i+1)] = \frac{1}{9}[3 - 2x_1(i+1)]$$

(Continued)

Copyright 2017 Cengage Learning. All Rights Reserved. May not be copied, scanned, or duplicated, in whole or in part. Due to electronic rights, some third party content may be suppressed from the eBook and/or eChapter(s). Editorial review has deemed that any suppressed content does not materially affect the overall learning experience. Cengage Learning reserves the right to remove additional content at any time if subsequent rights restrictions require it.

Using this equation for $x_1(i+1)$, $x_2(i+1)$ also can be written as

$$x_2(i+1) = \frac{1}{9}\left\{3 - \frac{2}{10}[6 - 5x_2(i)]\right\}$$

Alternatively, in matrix format, using (6.2.10), (6.2.6), and (6.2.7),

$$\mathbf{D}^{-1} = \left[\begin{array}{c|c} 10 & 0 \\ \hline 2 & 9 \end{array}\right]^{-1} = \left[\begin{array}{c|c} \frac{1}{10} & 0 \\ \hline -\frac{2}{90} & \frac{1}{9} \end{array}\right]$$

$$\mathbf{M} = \left[\begin{array}{c|c} \frac{1}{10} & 0 \\ \hline -\frac{2}{90} & \frac{1}{9} \end{array}\right] \left[\begin{array}{c|c} 0 & -5 \\ \hline 0 & 0 \end{array}\right] = \left[\begin{array}{c|c} 0 & -\frac{1}{2} \\ \hline 0 & \frac{1}{9} \end{array}\right]$$

$$\begin{bmatrix} x_1(i+1) \\ \\ x_2(i+1) \end{bmatrix} = \left[\begin{array}{c|c} 0 & -\frac{1}{2} \\ \hline 0 & \frac{1}{9} \end{array}\right] \begin{bmatrix} x_1(i) \\ \\ x_2(i) \end{bmatrix} + \left[\begin{array}{c|c} \frac{1}{10} & 0 \\ \hline -\frac{2}{90} & \frac{1}{9} \end{array}\right] \begin{bmatrix} 6 \\ \\ 3 \end{bmatrix}$$

These two formulations are identical. Starting with $x_1(0) = x_2(0) = 0$, the solution is given in the following table:

Gauss-Seidel

i	0	1	2	3	4	5	6
$x_1(i)$	0	0.60000	0.50000	0.48889	0.48765	0.48752	0.48750
$x_2(i)$	0	0.20000	0.22222	0.22469	0.22497	0.22500	0.22500

For this example, Gauss-Seidel converges in 6 iterations, compared to 10 iterations with Jacobi.

The convergence rate is faster with Gauss-Seidel for some **A** matrices, but faster with Jacobi for other **A** matrices. In some cases, one method diverges while the other converges. In other cases both methods diverge, as illustrated by the next example.

Copyright 2017 Cengage Learning. All Rights Reserved. May not be copied, scanned, or duplicated, in whole or in part. Due to electronic rights, some third party content may be suppressed from the eBook and/or eChapter(s). Editorial review has deemed that any suppressed content does not materially affect the overall learning experience. Cengage Learning reserves the right to remove additional content at any time if subsequent rights restrictions require it.

EXAMPLE 6.5

Divergence of Gauss-Seidel method

Using the Gauss-Seidel method with $x_1(0) = x_2(0) = 0$, solve

$$\left[\begin{array}{c|c} 5 & 10 \\ \hline 9 & 2 \end{array}\right]\begin{bmatrix} x_1 \\ x_2 \end{bmatrix} = \begin{bmatrix} 6 \\ 3 \end{bmatrix}$$

SOLUTION

Note that these equations are the same as those in Example 6.1, except that x_1 and x_2 are interchanged. Using (6.2.9),

$$k = 1 \qquad x_1(i+1) = \frac{1}{A_{11}}[y_1 - A_{12}x_2(i)] = \frac{1}{5}[6 - 10x_2(i)]$$

$$k = 2 \qquad x_2(i+1) = \frac{1}{A_{22}}[y_2 - A_{21}x_1(i+1)] = \frac{1}{2}[3 - 9x_1(i+1)]$$

Successive calculations of x_1 and x_2 are shown in the following table:

Gauss-Seidel

i	0	1	2	3	4	5
$x_1(i)$	0	1.2	9	79.2	711	6397
$x_2(i)$	0	−3.9	−39	−354.9	−3198	−28,786

The unique solution by matrix inversion is

$$\begin{bmatrix} x_1 \\ x_2 \end{bmatrix} = \left[\begin{array}{c|c} 5 & 10 \\ \hline 9 & 2 \end{array}\right]^{-1}\begin{bmatrix} 6 \\ 3 \end{bmatrix} = \frac{-1}{80}\left[\begin{array}{c|c} 2 & -10 \\ \hline -9 & 5 \end{array}\right]\begin{bmatrix} 6 \\ 3 \end{bmatrix} = \begin{bmatrix} 0.225 \\ 0.4875 \end{bmatrix}$$

As shown, Gauss-Seidel does not converge to the unique solution; instead it diverges. Jacobi also diverges for this example.

If any diagonal element A_{kk} equals zero, then Jacobi and Gauss-Seidel are undefined, because the right-hand sides of (6.2.5) and (6.2.9) are divided by A_{kk}. Also, if any one diagonal element has too small a magnitude, these methods will diverge. In Examples 6.3 and 6.4, Jacobi and Gauss-Seidel converge, since the diagonals (10 and 9) are both large; in Example 6.5, however, the diagonals (5 and 2) are small compared to the off-diagonals, and the methods diverge.

Copyright 2017 Cengage Learning. All Rights Reserved. May not be copied, scanned, or duplicated, in whole or in part. Due to electronic rights, some third party content may be suppressed from the eBook and/or eChapter(s). Editorial review has deemed that any suppressed content does not materially affect the overall learning experience. Cengage Learning reserves the right to remove additional content at any time if subsequent rights restrictions require it.

In general, convergence of Jacobi or Gauss-Seidel can be evaluated by recognizing that (6.2.6) represents a digital filter with input y and output $x(i)$. The z-transform of (6.2.6) may be employed to determine the filter transfer function and its poles. The output $x(i)$ converges if and only if all the filter poles have magnitudes less than 1 (see Problems 6.16 and 6.17).

Rate of convergence is also established by the filter poles. Fast convergence is obtained when the magnitudes of all the poles are small. In addition, experience with specific **A** matrices has shown that more iterations are required for Jacobi and Gauss-Seidel as the dimension N increases.

Computer storage requirements for Jacobi include N^2 memory locations for the **A** matrix and $3N$ locations for the vectors **y**, $\mathbf{x}(i)$, and $\mathbf{x}(i+1)$. Storage space is also required for loops, arithmetic statements, and working space to compute (6.2.5). Gauss-Seidel requires N fewer memory locations, since for (6.2.9) the new value $x_k(i+1)$ can be stored in the location of the old value $x_k(i)$.

Computer time per iteration is relatively small for Jacobi and Gauss-Seidel. Inspection of (6.2.5) or (6.2.9) shows that N^2 multiplications/divisions and $N(N-1)$ subtractions per iteration are required [one division, $(N-1)$ multiplications, and $(N-1)$ subtractions for each $k = 1, 2, \ldots, N$]. But as was the case with Gauss elimination, if the matrix is sparse (i.e., most of the elements are zero), special sparse matrix algorithms can be used to substantially decrease both the storage requirements and the computation time.

6.3 ITERATIVE SOLUTIONS TO NONLINEAR ALGEBRAIC EQUATIONS: NEWTON-RAPHSON

A set of nonlinear algebraic equations in matrix format is given by

$$\mathbf{f}(\mathbf{x}) = \begin{bmatrix} f_1(\mathbf{x}) \\ f_2(\mathbf{x}) \\ \vdots \\ f_N(\mathbf{x}) \end{bmatrix} = \mathbf{y} \tag{6.3.1}$$

where **y** and **x** are N vectors and $\mathbf{f}(\mathbf{x})$ is an N vector of functions. Given **y** and $\mathbf{f}(\mathbf{x})$, the objective is to solve for **x**. The iterative methods described in Section 6.2 can be extended to nonlinear equations as follows. Rewriting (6.3.1).

$$0 = \mathbf{y} - \mathbf{f}(\mathbf{x}) \tag{6.3.2}$$

Adding **Dx** to both sides of (6.3.2), where **D** is a square $N \times N$ invertible matrix.

$$\mathbf{Dx} = \mathbf{Dx} + \mathbf{y} - \mathbf{f}(\mathbf{x}) \tag{6.3.3}$$

Premultiplying by $\mathbf{D}^{-1}$.

$$\mathbf{x} = \mathbf{x} + \mathbf{D}^{-1}[\mathbf{y} - \mathbf{f}(\mathbf{x})] \tag{6.3.4}$$

The old values $\mathbf{x}(i)$ are used on the right side of (6.3.4) to generate the new values $\mathbf{x}(i+1)$ on the left side. That is,

Copyright 2017 Cengage Learning. All Rights Reserved. May not be copied, scanned, or duplicated, in whole or in part. Due to electronic rights, some third party content may be suppressed from the eBook and/or eChapter(s). Editorial review has deemed that any suppressed content does not materially affect the overall learning experience. Cengage Learning reserves the right to remove additional content at any time if subsequent rights restrictions require it.

$$\mathbf{x}(i+1) = \mathbf{x}(i) + \mathbf{D}^{-1}\{\mathbf{y} - \mathbf{f}[\mathbf{x}(i)]\} \tag{6.3.5}$$

For linear equations, $\mathbf{f}(\mathbf{x}) = \mathbf{A}\mathbf{x}$ and (6.3.5) reduces to

$$\mathbf{x}(i+1) = \mathbf{x}(i) + \mathbf{D}^{-1}[\mathbf{y} - \mathbf{A}\mathbf{x}(z)] = \mathbf{D}^{-1}(\mathbf{D} - \mathbf{A})\mathbf{x}(i) + \mathbf{D}^{-1}\mathbf{y} \tag{6.3.6}$$

which is identical to the Jacobi and Gauss-Seidel methods of (6.2.6). For nonlinear equations, the matrix **D** in (6.3.5) must be specified.

One method for specifying **D**, called *Newton-Raphson*, is based on the following Taylor series expansion of $\mathbf{f}(\mathbf{x})$ about an operating point $\mathbf{x}_0$.

$$\mathbf{y} = \mathbf{f}(\mathbf{x}_0) + \left.\frac{d\mathbf{f}}{d\mathbf{x}}\right|_{\mathbf{x}=\mathbf{x}_0}(\mathbf{x} - \mathbf{x}_0)\cdots \tag{6.3.7}$$

Neglecting the higher order terms in (6.3.7) and solving for **x**,

$$\mathbf{x} = \mathbf{x}_0 + \left[\left.\frac{d\mathbf{f}}{d\mathbf{x}}\right|_{\mathbf{x}=\mathbf{x}_0}\right]^{-1}[\mathbf{y} - \mathbf{f}(\mathbf{x}_0)] \tag{6.3.8}$$

The Newton-Raphson method replaces $\mathbf{x}_0$ by the old value $\mathbf{x}(i)$ and **x** by the new value $\mathbf{x}(i+1)$ in (6.3.8). Thus,

$$\mathbf{x}(i+1) = \mathbf{x}(i) + \mathbf{J}^{-1}(i)\{\mathbf{y} - \mathbf{f}[\mathbf{x}(i)]\} \tag{6.3.9}$$

where

$$\mathbf{J}(i) = \left.\frac{d\mathbf{f}}{d\mathbf{x}}\right|_{\mathbf{x}=\mathbf{x}(i)} = \begin{bmatrix} \frac{\partial f_1}{\partial x_1} & \frac{\partial f_1}{\partial x_2} & \cdots & \frac{\partial f_1}{\partial x_N} \\ \frac{\partial f_2}{\partial x_1} & \frac{\partial f_2}{\partial x_2} & \cdots & \frac{\partial f_2}{\partial x_N} \\ \vdots & \vdots & & \vdots \\ \frac{\partial f_N}{\partial x_1} & \frac{\partial f_N}{\partial x_2} & \cdots & \frac{\partial f_N}{\partial x_N} \end{bmatrix}_{\mathbf{x}=\mathbf{x}(i)} \tag{6.3.10}$$

The $N \times N$ matrix $\mathbf{J}(i)$, whose elements are the partial derivatives shown in (6.3.10), is called the Jacobian matrix. The Newton-Raphson method is similar to extended Gauss-Seidel, except that **D** in (6.3.5) is replaced by $\mathbf{J}(i)$ in (6.3.9).

EXAMPLE 6.6

Newton-Raphson method: solution to polynomial equations

Solve the scalar equation $f(x) = y$, where $y = 9$ and $f(x) = x^2$. Starting with $x(0) = 1$, use (a) Newton-Raphson and (b) extended Gauss-Seidel with $\mathbf{D} = 3$ until (6.2.2) is satisfied for $\varepsilon = 10^{-4}$. Compare the two methods.

(Continued)

Copyright 2017 Cengage Learning. All Rights Reserved. May not be copied, scanned, or duplicated, in whole or in part. Due to electronic rights, some third party content may be suppressed from the eBook and/or eChapter(s). Editorial review has deemed that any suppressed content does not materially affect the overall learning experience. Cengage Learning reserves the right to remove additional content at any time if subsequent rights restrictions require it.

SOLUTION

a. Using (6.3.10) with $f(x) = x^2$,

$$\mathbf{J}(i) = \frac{d}{dx}(x^2)\bigg|_{x=x(i)} = 2x\bigg|_{x=x(i)} = 2x(i)$$

Using $\mathbf{J}(i)$ in (6.3.9),

$$x(i+1) = x(i) + \frac{1}{2x(i)}[9 - x^2(i)]$$

Starting with $x(0) = 1$, successive calculations of the Newton-Raphson equation are shown in the following table.

Newton–Raphson

i	0	1	2	3	4	5
x(*i*)	1	5.00000	3.40000	3.02353	3.00009	3.00000

b. Using (6.3.5) with $\mathbf{D} = 3$, the Gauss-Seidel method is

$$x(i+1) = x(i) + \frac{1}{3}[9 - x^2(i)]$$

The corresponding Gauss-Seidel calculations are as follows:

Gauss-Seidel (D = 3)

i	0	1	2	3	4	5	6
x(*i*)	1	3.66667	2.18519	3.59351	2.28908	3.54245	2.35945

As shown, Gauss-Seidel oscillates about the solution, slowly converging, whereas Newton-Raphson converges in five iterations to the solution $x = 3$. Note that if $x(0)$ is negative, Newton-Raphson converges to the negative solution $x = -3$. Also, it is assumed that the matrix inverse $\mathbf{J}^{-1}$ exists. Thus, the initial value $x(0) = 0$ should be avoided for this example.

EXAMPLE 6.7

Newton-Raphson method: solution to nonlinear algebraic equations

Solve

$$\begin{bmatrix} x_1 + x_2 \\ x_1 x_2 \end{bmatrix} = \begin{bmatrix} 15 \\ 50 \end{bmatrix} \qquad \mathbf{x}(0) = \begin{bmatrix} 4 \\ 9 \end{bmatrix}$$

Copyright 2017 Cengage Learning. All Rights Reserved. May not be copied, scanned, or duplicated, in whole or in part. Due to electronic rights, some third party content may be suppressed from the eBook and/or eChapter(s). Editorial review has deemed that any suppressed content does not materially affect the overall learning experience. Cengage Learning reserves the right to remove additional content at any time if subsequent rights restrictions require it.

Use the Newton-Raphson method starting with the above **x**(0) and continue until (6.2.2) is satisfied with $\varepsilon = 10^{-4}$.

SOLUTION

Using (6.3.10) with $f_1 = (x_1 + x_2)$ and $f_2 = x_1 x_2$,

$$\mathbf{J}(i)^{-1} = \left[\begin{array}{c|c} \dfrac{\partial f_1}{\partial x_1} & \dfrac{\partial f_1}{\partial x_2} \\ \hline \dfrac{\partial f_2}{\partial x_1} & \dfrac{\partial f_2}{\partial x_2} \end{array}\right]^{-1}_{\mathbf{x}=\mathbf{x}(i)} = \left[\begin{array}{c|c} 1 & 1 \\ \hline x_2(i) & x_1(i) \end{array}\right]^{-1} = \frac{\left[\begin{array}{c|c} x_1(i) & -1 \\ \hline -x_2(i) & 1 \end{array}\right]}{x_1(i) - x_2(i)}$$

Using $\mathbf{J}(i)^{-1}$ in (6.3.9),

$$\begin{bmatrix} x_1(i+1) \\ x_2(i+1) \end{bmatrix} = \begin{bmatrix} x_1(i) \\ x_2(i) \end{bmatrix} + \frac{\left[\begin{array}{c|c} x_1(i) & -1 \\ \hline -x_2(i) & 1 \end{array}\right]}{x_1(i) - x_2(i)} \begin{bmatrix} 15 - x_1(i) - x_2(i) \\ 50 - x_1(i)x_2(i) \end{bmatrix}$$

Writing the preceding as two separate equations,

$$x_1(i+1) = x_1(i) + \frac{x_1(i)[15 - x_1(i) - x_2(i)] - [50 - x_1(i)x_2(i)]}{x_1(i) - x_2(i)}$$

$$x_2(i+1) = x_2(i) + \frac{-x_2(i)[15 - x_1(i) - x_2(i)] + [50 - x_1(i)x_2(i)]}{x_1(i) - x_2(i)}$$

Successive calculations of these equations are shown in the following table.

Newton-Raphson

i	0	1	2	3	4
$x_1(i)$	4	5.20000	4.99130	4.99998	5.00000
$x_2(i)$	9	9.80000	10.00870	10.00002	10.00000

Newton-Raphson converges in four iterations for this example.

Equation (6.3.9) contains the matrix inverse $\mathbf{J}^{-1}$. Instead of computing $\mathbf{J}^{-1}$, (6.3.9) can be rewritten as follows:

$$\mathbf{J}(i)\Delta\mathbf{x}(i) = \Delta\mathbf{y}(i) \tag{6.3.11}$$

where

$$\Delta\mathbf{x}(i) = \mathbf{x}(i+1) - \mathbf{x}(i) \tag{6.3.12}$$

and

$$\Delta\mathbf{y}(i) = \mathbf{y} - \mathbf{f}[\mathbf{x}(\mathrm{i})] \tag{6.3.13}$$

Copyright 2017 Cengage Learning. All Rights Reserved. May not be copied, scanned, or duplicated, in whole or in part. Due to electronic rights, some third party content may be suppressed from the eBook and/or eChapter(s). Editorial review has deemed that any suppressed content does not materially affect the overall learning experience. Cengage Learning reserves the right to remove additional content at any time if subsequent rights restrictions require it.

Then, during each iteration, the following four steps are completed:

STEP 1 Compute $\Delta\mathbf{y}(i)$ from (6.3.13).

STEP 2 Compute $\mathbf{J}(i)$ from (6.3.10).

STEP 3 Using Gauss elimination and back substitution, solve (6.3.11) for $\Delta\mathbf{x}(i)$.

STEP 4 Compute $\mathbf{x}(i+1)$ from (6.3.12).

Experience from power flow studies has shown that Newton-Raphson converges in many cases where Jacobi and Gauss-Seidel diverge. Furthermore, the number of iterations required for convergence is independent of the dimension

EXAMPLE 6.8

Newton-Raphson method in four steps

Complete the above four steps for the first iteration of Example 6.7.

SOLUTION

STEP 1 $\Delta\mathbf{y}(0) = \mathbf{y} - \mathbf{f}\,[\mathbf{x}(0)] = \begin{bmatrix} 15 \\ 20 \end{bmatrix} - \begin{bmatrix} 4+9 \\ (4)(9) \end{bmatrix} = \begin{bmatrix} 2 \\ 14 \end{bmatrix}$

STEP 2 $\mathbf{J}(0) = \left[\begin{array}{c|c} 1 & 1 \\ \hline x_2(0) & x_1(0) \end{array}\right] = \left[\begin{array}{c|c} 1 & 1 \\ \hline 9 & 4 \end{array}\right]$

STEP 3 Using $\Delta\mathbf{y}(0)$ and $\mathbf{J}(0)$, (6.3.11) becomes

$$\left[\begin{array}{c|c} 1 & 1 \\ \hline 9 & 4 \end{array}\right]\begin{bmatrix} \Delta x_1(0) \\ \Delta x_2(0) \end{bmatrix} = \begin{bmatrix} 2 \\ 14 \end{bmatrix}$$

Using Gauss elimination, subtract $J_{21}/J_{11} = 9/1 = 9$ times the first equation from the second equation, giving

$$\left[\begin{array}{c|c} 1 & 1 \\ \hline 0 & -5 \end{array}\right]\begin{bmatrix} \Delta x_1(0) \\ \Delta x_2(0) \end{bmatrix} = \begin{bmatrix} 2 \\ -4 \end{bmatrix}$$

Solving by back substitution,

$$\Delta x_2(0) = \frac{-4}{-5} = 0.8$$

$$\Delta x_1(0) = 2 - 0.8 = 1.2$$

STEP 4 $\mathbf{x}(1) = \mathbf{x}(0) + \Delta\mathbf{x}(0) = \begin{bmatrix} 4 \\ 9 \end{bmatrix} + \begin{bmatrix} 1.2 \\ 0.8 \end{bmatrix} = \begin{bmatrix} 5.2 \\ 9.8 \end{bmatrix}$

This is the same as computed in Example 6.7.

Copyright 2017 Cengage Learning. All Rights Reserved. May not be copied, scanned, or duplicated, in whole or in part. Due to electronic rights, some third party content may be suppressed from the eBook and/or eChapter(s). Editorial review has deemed that any suppressed content does not materially affect the overall learning experience. Cengage Learning reserves the right to remove additional content at any time if subsequent rights restrictions require it.

N for Newton-Raphson, but increases with N for Jacobi and Gauss-Seidel. Most Newton-Raphson power flow problems converge in fewer than 10 iterations [1].

6.4 THE POWER FLOW PROBLEM

The power flow problem is the computation of voltage magnitude and phase angle at each bus in a power system under balanced three-phase steady-state conditions. As a by-product of this calculation, real and reactive power flows in equipment such as transmission lines and transformers, as well as equipment losses, can be computed.

The starting point for a power flow problem is a single-line (oneline) diagram of the power system, from which the input data can be obtained. Input data consist of bus data, transmission line data, and transformer data.

As shown in Figure 6.1, the following four variables are associated with each bus k: voltage magnitude V_k, phase angle δ_k, net real power P_k, and reactive power Q_k supplied to the bus. At each bus, two of these variables are specified as input data, and the other two are unknowns to be computed by the power flow program. For convenience, the power delivered to bus k in Figure 6.1 is separated into generator and load terms. That is,

$$\begin{aligned} P_k &= P_{Gk} - P_{Lk} \\ Q_k &= Q_{Gk} - Q_{Lk} \end{aligned} \tag{6.4.1}$$

Each bus k is categorized into one of the following three bus types:

1. Swing bus (or slack bus)—There is only one swing bus, which for convenience is numbered bus 1 in this text. The swing bus is a reference bus for which $V_1\underline{/\delta_1}$, is input data with the angle typically zero degrees and the voltage magnitude close to 1.0 per unit. The power flow computes P_1 and Q_1.

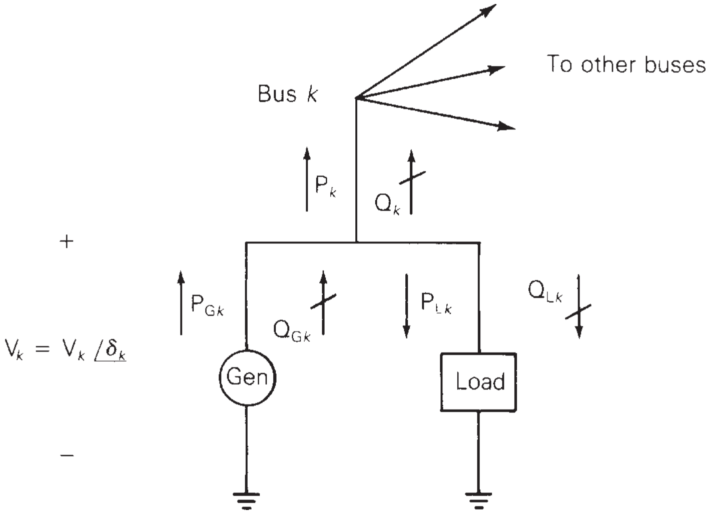

FIGURE 6.1 Bus variables V_k, δ_k, P_k, and Q_k

Copyright 2017 Cengage Learning. All Rights Reserved. May not be copied, scanned, or duplicated, in whole or in part. Due to electronic rights, some third party content may be suppressed from the eBook and/or eChapter(s). Editorial review has deemed that any suppressed content does not materially affect the overall learning experience. Cengage Learning reserves the right to remove additional content at any time if subsequent rights restrictions require it.

2. Load (PQ) bus—P_k and Q_k are input data. The power flow computes V_k and δ_k. Most buses in typical power flows are load buses.
3. Voltage controlled (PV) bus—P_k and V_k are input data. The power flow program computes Q_k and δ_k. Examples are buses to which generators, switched shunt capacitors, or static var systems are connected. Maximum and minimum reactive power (var) limits $Q_{Gk\max}$ and $Q_{Gk\min}$ that this equipment can supply are also input data. If an upper or lower reactive power limit is reached, then the reactive power output of the generator is held at the limit, and the bus is modeled as a PQ bus. Another example is a bus to which a tap-changing transformer is connected; the power flow then computes the tap setting.

Note that when bus k is a load bus with no generation, $P_k = -P_{Lk}$ is negative; that is, the real power supplied to bus k in Figure 6.1 is negative. If the load is inductive, $Q_k = -Q_{Lk}$ is negative.

Transmission lines are represented by the equivalent π circuit, shown in Figure 5.7. Transformers are also represented by equivalent circuits, as shown in Figure 3.9 for a two-winding transformer, Figure 3.20 for a three-winding transformer, or Figure 3.25 for a tap-changing transformer.

Input data for each transmission line include the per-unit equivalent π circuit series impedance Z' and shunt admittance Y', the two buses to which the line is connected, and maximum MVA rating. Similarly, input data for each transformer include per-unit winding impedances Z, the per-unit exciting branch admittance Y, the buses to which the windings are connected, and maximum MVA ratings. Input data for tap-changing transformers also include maximum tap settings.

The bus admittance matrix $\boldsymbol{Y}_{\text{bus}}$ can be constructed from the line and transformer input data. From (2.4.3) and (2.4.4), the elements of $\boldsymbol{Y}_{\text{bus}}$ are

$$\begin{aligned} &\text{Diagonal elements: } Y_{kk} = \text{sum of admittances connected to bus } k \\ &\text{Off-diagonal elements: } Y_{kn} = -(\text{sum of admittances connected} \\ &\qquad\qquad\qquad\text{between buses } k \text{ and } n)\ k \neq n \end{aligned} \tag{6.4.2}$$

EXAMPLE 6.9

Power flow input data and Y_{bus}

Figure 6.2 shows a single-line diagram of a five-bus power system. Input data are given in Tables 6.1, 6.2, and 6.3. As shown in Table 6.1, bus 1, to which a generator is connected, is the swing bus. Bus 3, to which a generator and a load are connected, is a voltage-controlled bus. Buses 2, 4, and 5 are load buses. Note that the loads at buses 2 and 3 are inductive since $Q_2 = -Q_{L2} = -2.8$ and $-Q_{L3} = -0.4$ are negative.

For each bus k, determine which of the variables V_k, δ_k, P_k, and Q_k are input data and which are unknowns. Also, compute the elements of the second row of $\boldsymbol{Y}_{\text{bus}}$.

Copyright 2017 Cengage Learning. All Rights Reserved. May not be copied, scanned, or duplicated, in whole or in part. Due to electronic rights, some third party content may be suppressed from the eBook and/or eChapter(s). Editorial review has deemed that any suppressed content does not materially affect the overall learning experience. Cengage Learning reserves the right to remove additional content at any time if subsequent rights restrictions require it.

FIGURE 6.2

Single-line diagram for Example 6.9

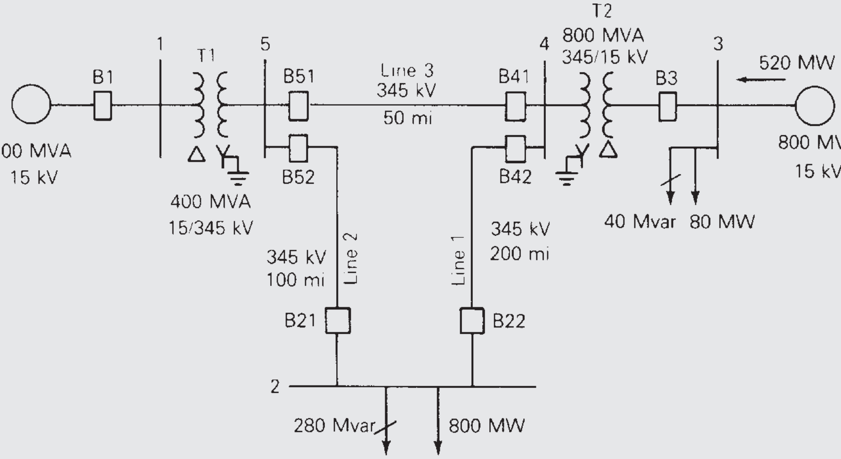
1
T1
5
B1
B51
Line 3
345 kV
50 mi
4
T2
800 MVA
345/15 kV
B41
3
B3
520 MW
400 MVA
15 kV
B52
400 MVA
15/345 kV
B42
40 Mvar
80 MW
800 MVA
15 kV
345 kV
200 mi
345 kV
100 mi
Line 2
Line 1
B21
B22
2
280 Mvar
800 MW

Bus	Type	V per unit	δ degrees	P_G per unit	Q_G per unit	P_L per unit	Q_L per unit	Q_{Gmax} per unit	Q_{Gmin} per unit
1	Swing	1.0	0	—	—	0	0	—	—
2	Load	—	—	0	0	8.0	2.8	—	—
3	Constant voltage	1.05	—	5.2	—	0.8	0.4	4.0	−2.8
4	Load	—	—	0	0	0	0	—	—
5	Load	—	—	0	0	0	0	—	—

TABLE 6.1

Bus input data for Example 6.9*

*S_{base} = 100 MVA, V_{base} = 15 kV at buses 1, 3, and 345 kV at buses 2, 4, 5

Bus-to-Bus	R′ per unit	X′ per unit	G′ per unit	B′ per unit	Maximum MVA per unit
2–4	0.0090	0.100	0	1.72	12.0
2–5	0.0045	0.050	0	0.88	12.0
4–5	0.00225	0.025	0	0.44	12.0

TABLE 6.2

Line input data for Example 6.9

(Continued)

Copyright 2017 Cengage Learning. All Rights Reserved. May not be copied, scanned, or duplicated, in whole or in part. Due to electronic rights, some third party content may be suppressed from the eBook and/or eChapter(s). Editorial review has deemed that any suppressed content does not materially affect the overall learning experience. Cengage Learning reserves the right to remove additional content at any time if subsequent rights restrictions require it.

Bus-to-Bus	R per unit	X per unit	G_c per unit	B_m per unit	Maximum MVA per unit	Maximum TAP Setting per unit
1–5	0.00150	0.02	0	0	6.0	—
3–4	0.00075	0.01	0	0	10.0	—

TABLE 6.3

Transformer input data for Example 6.9

Bus	Input Data	Unknowns
1	$V_1 = 1.0, \delta_1 = 0$	P_1, Q_1
2	$P_2 = P_{G2} - P_{L2} = -8$ $Q_2 = Q_{G2} - Q_{L2} = -2.8$	V_2, δ_2
3	$V_3 = 1.05$ $P_3 = P_{G3} - P_{L3} = 4.4$	Q_3, δ_4
4	$P_4 = 0, Q_4 = 0$	V_4, δ_4
5	$P_5 = 0, Q_5 = 0$	V_5, δ_5

TABLE 6.4

Input data and unknowns for Example 6.9

SOLUTION

The input data and unknowns are listed in Table 6.4. For bus 1, the swing bus, P_1 and Q_1 are unknowns. For bus 3, a voltage-controlled bus, Q_3 and δ_3 are unknowns. For buses 2, 4, and 5, load buses, V_2, V_4, V_5 and δ_2, δ_4, δ_5 are unknowns.

The elements of $\boldsymbol{Y}_{\text{bus}}$ are computed from (6.4.2). Since buses 1 and 3 are not directly connected to bus 2,

$$Y_{21} = Y_{23} = 0$$

Using (6.4.2),

$$Y_{24} = \frac{-1}{R'_{24} + jX'_{24}} = \frac{-1}{0.009 + j0.1} = -0.89276 + j9.91964 \quad \text{per unit}$$
$$= 9.95972\underline{/95.143^\circ} \quad \text{per unit}$$

$$Y_{25} = \frac{-1}{R'_{25} + jX'_{25}} = \frac{-1}{0.0045 + j0.05} = -1.78552 + j19.83932 \quad \text{per unit}$$
$$= 19.9195\underline{/95.143^\circ} \quad \text{per unit}$$

$$Y_{22} = \frac{1}{R'_{24} + jX'_{24}} + \frac{1}{R'_{25} + jX'_{25}} + j\frac{B'_{24}}{2} + j\frac{B'_{25}}{2}$$

Copyright 2017 Cengage Learning. All Rights Reserved. May not be copied, scanned, or duplicated, in whole or in part. Due to electronic rights, some third party content may be suppressed from the eBook and/or eChapter(s). Editorial review has deemed that any suppressed content does not materially affect the overall learning experience. Cengage Learning reserves the right to remove additional content at any time if subsequent rights restrictions require it.

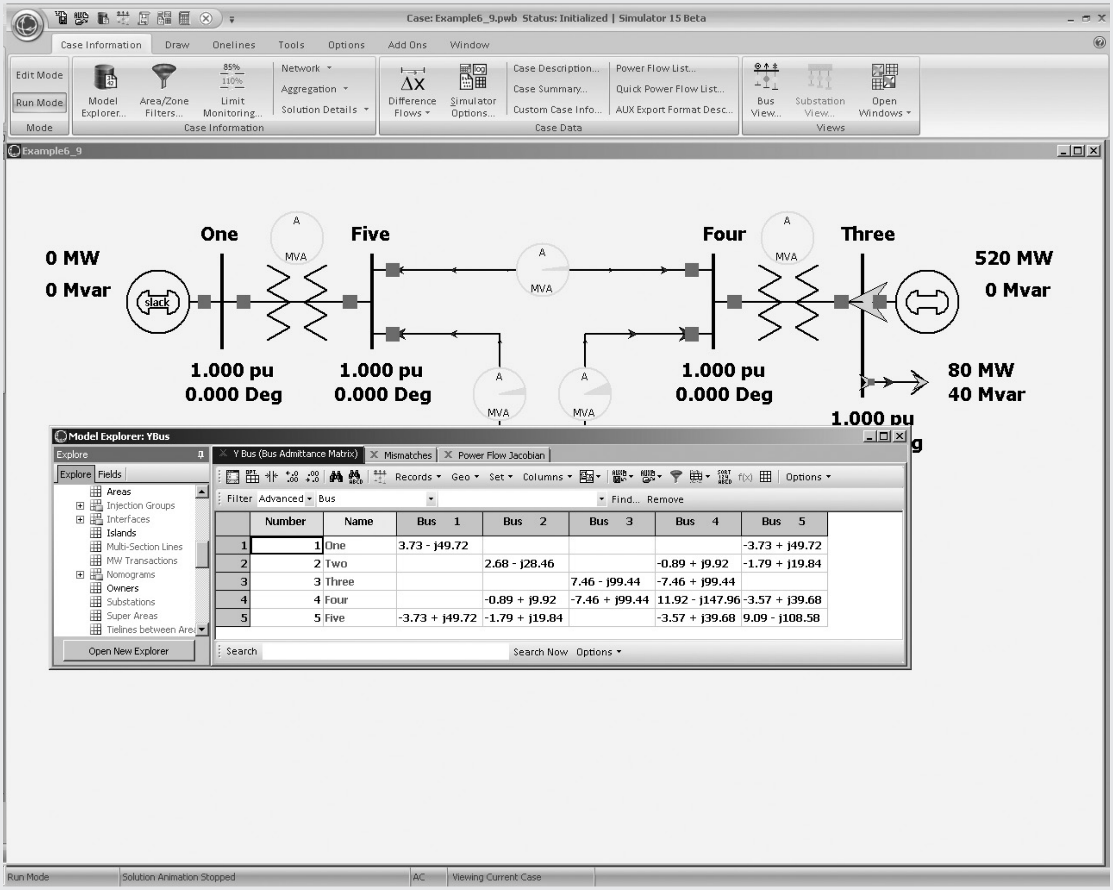
Case: Example6_9.pwb Status: Initialized | Simulator 15 Beta
Case Information
Draw
Onelines
Tools
Options
Add Ons
Window
Edit Mode
Run Mode
Mode
Model Explorer...
Area/Zone Filters...
Limit Monitoring...
Network
Aggregation
Solution Details
Case Information
Difference Flows
Simulator Options...
Case Description...
Case Summary...
Custom Case Info...
Power Flow List...
Quick Power Flow List...
AUX Export Format Desc...
Case Data
Bus View...
Substation View...
Open Windows
Views
Example6_9
One
Five
Four
Three
0 MW
0 Mvar
slack
520 MW
0 Mvar
1.000 pu
0.000 Deg
1.000 pu
0.000 Deg
1.000 pu
0.000 Deg
80 MW
40 Mvar
1.000 pu
A
MVA
Model Explorer: YBus
Explore
Fields
Areas
Injection Groups
Interfaces
Islands
Multi-Section Lines
MW Transactions
Nomograms
Owners
Substations
Super Areas
Tielines between Areas
Open New Explorer
Y Bus (Bus Admittance Matrix)
Mismatches
Power Flow Jacobian
Records
Geo
Set
Columns
Options
Filter Advanced
Bus
Find...
Remove
Search
Search Now
Options
Run Mode
Solution Animation Stopped
AC
Viewing Current Case

	Number	Name	Bus 1	Bus 2	Bus 3	Bus 4	Bus 5
1	1	One	3.73 - j49.72				-3.73 + j49.72
2	2	Two		2.68 - j28.46		-0.89 + j9.92	-1.79 + j19.84
3	3	Three			7.46 - j99.44	-7.46 + j99.44	
4	4	Four		-0.89 + j9.92	-7.46 + j99.44	11.92 - j147.96	-3.57 + j39.68
5	5	Five	-3.73 + j49.72	-1.79 + j19.84		-3.57 + j39.68	9.09 - j108.58

FIGURE 6.3

Screen for Example 6.9

$$= (0.89276 - j9.91964) + (1.78552 - j19.83932) + j\frac{1.72}{2} + j\frac{0.88}{2}$$

$$= 2.67828 - j28.4590 = 28.5847\underline{/-84.624^\circ} \quad \text{per unit}$$

where half of the shunt admittance of each line connected to bus 2 is included in Y_{22} (the other half is located at the other ends of these lines).

This five-bus power system is modeled in PowerWorld Simulator case Example 6_9 (see Figure 6.3). To view the input data, first click on the **Edit Mode** button (on the far left-hand side of the ribbon) to switch into the Edit mode (the Edit mode is used for modifying system parameters). Then by selecting the **Case Information** tab, you can view tabular displays showing the various parameters for

(Continued)

Copyright 2017 Cengage Learning. All Rights Reserved. May not be copied, scanned, or duplicated, in whole or in part. Due to electronic rights, some third party content may be suppressed from the eBook and/or eChapter(s). Editorial review has deemed that any suppressed content does not materially affect the overall learning experience. Cengage Learning reserves the right to remove additional content at any time if subsequent rights restrictions require it.

the system. For example, use **Network**, **Buses** to view the parameters for each bus, and **Network**, **Lines and Transformers** to view the parameters for the transmission lines and transformers. Fields shown in blue on the screen can be directly changed simply by typing over them, and those shown in green can be toggled by clicking on them. Note that the values shown on these displays match the per unit values from Tables 6.1 to 6.3, except the power values are shown in actual MW/Mvar units.

The elements of Y_{bus} also can be displayed by selecting **Solution Details**, Y_{bus}. Since the Y_{bus} entries are derived from other system parameters, they cannot be changed directly. Notice that several of the entries are blank, indicating that there is no transmission line or transformer directly connecting these two buses (a blank entry is equivalent to zero). For larger networks, most of the elements of the Y_{bus} are zero since any single bus usually only has a few incident lines (such sparse matrices are considered in Section 6.8). The elements of the Y_{bus} can be saved in a Matlab compatible format by first right-clicking within the Y_{bus} matrix to display the local menu, and then selecting **Save Y_{bus} in Matlab Format** from the local menu.

Finally, notice that no flows are shown on the oneline because the nonlinear power flow equations have not yet been solved, and the solution of these equations are covered next.

Using Y_{bus}, the nodal equations for a power system network are written as

$$\mathbf{I} = Y_{\text{bus}}\mathbf{V} \tag{6.4.3}$$

where **I** is the N vector of source currents injected into each bus and **V** is the N vector of bus voltages. For bus k, the kth equation in (6.4.3) is

$$I_k = \sum_{n=1}^{N} Y_{kn} V_n \tag{6.4.4}$$

The complex power delivered to bus k is

$$S_k = \mathrm{P}_k + j\mathrm{Q}_k = V_k I_k^* \tag{6.4.5}$$

Power flow solutions by Gauss-Seidel are based on nodal equations, (6.4.4), where each current source I_k is calculated from (6.4.5). Using (6.4.4) in (6.4.5),

$$\mathrm{P}_k + j\mathrm{Q}_k = V_k\left[\sum_{n=1}^{N} Y_{kn} V_n\right]^* \qquad k = 1, 2, \ldots, N \tag{6.4.6}$$

With the following notation,

$$V_n = \mathrm{V}_n e^{j\delta_n} \tag{6.4.7}$$

$$Y_{kn} = \mathrm{Y}_{kn} e^{j\theta_{kn}} = G_{kn} + jB_{kn} \qquad k,n = 1, 2, \ldots, N \tag{6.4.8}$$

(6.4.6) becomes

$$\mathrm{P}_k + j\mathrm{Q}_k = \mathrm{V}_k \sum_{n=1}^{N} \mathrm{Y}_{kn} \mathrm{V}_n e^{j(\delta_k - \delta_n - \theta_{kn})} \tag{6.4.9}$$

Copyright 2017 Cengage Learning. All Rights Reserved. May not be copied, scanned, or duplicated, in whole or in part. Due to electronic rights, some third party content may be suppressed from the eBook and/or eChapter(s). Editorial review has deemed that any suppressed content does not materially affect the overall learning experience. Cengage Learning reserves the right to remove additional content at any time if subsequent rights restrictions require it.

Taking the real and imaginary parts of (6.4.9), the power balance equations are written as either

$$\mathrm{P}_k = \mathrm{V}_k \sum_{n=1}^{N} \mathrm{Y}_{kn}\mathrm{V}_n \cos(\delta_k - \delta_n - \theta_{kn}) \tag{6.4.10}$$

$$\mathrm{Q}_k = \mathrm{V}_k \sum_{n=1}^{N} \mathrm{Y}_{kn}\mathrm{V}_n \sin(\delta_k - \delta_n - \theta_{kn}) \qquad k = 1, 2, \ldots, N \tag{6.4.11}$$

or when the Y_{kn} is expressed in rectangular coordinates as

$$\mathrm{P}_k = \mathrm{V}_k \sum_{n=1}^{N} V_n[G_{kn}\cos(\delta_k - \delta_n) + B_{kn}\sin(\delta_k - \delta_n)] \tag{6.4.12}$$

$$\mathrm{Q}_k = \mathrm{V}_k \sum_{n=1}^{N} V_n[G_{kn}\sin(\delta_k - \delta_n) - B_{kn}\cos(\delta_k - \delta_n)] \qquad k = 1, 2, \ldots, N \tag{6.4.13}$$

Power flow solutions by Newton-Raphson are based on the nonlinear power flow equations given by (6.4.10) and (6.4.11) [or alternatively by (6.4.12) and (6.4.13)].

6.5 POWER FLOW SOLUTION BY GAUSS-SEIDEL

Nodal equations $\mathbf{I} = \boldsymbol{Y}_{\text{bus}}\mathbf{V}$ are a set of linear equations analogous to $\mathbf{y} = \mathbf{Ax}$, solved in Section 6.2 using Gauss-Seidel. Since power flow bus data consists of P_k and Q_k for load buses or P_k and V_k for voltage-controlled buses, nodal equations do not directly fit the linear equation format; the current source vector $\mathbf{I}$ is unknown and the equations are actually nonlinear. For each load bus, I_k can be calculated from (6.4.5), giving

$$I_k = \frac{\mathrm{P}_k - j\mathrm{Q}_k}{V_k^*} \tag{6.5.1}$$

Applying the Gauss-Seidel method (6.2.9) to the nodal equations with I_k given above, obtain

$$V_k(i+1) = \frac{1}{Y_{kk}}\left[\frac{\mathrm{P}_k - j\mathrm{Q}_k}{V_k^*(i)} - \sum_{n=1}^{k-1} Y_{kn}V_n(i+1) - \sum_{n=k+1}^{N} Y_{kn}V_n(i)\right] \tag{6.5.2}$$

Equation (6.5.2) can be applied twice during each iteration for load buses, first using $V_k^*(i)$, then replacing $V_k^*(i)$, by $V_k^*(i+1)$ on the right side of (6.5.2).

For a voltage-controlled bus, Q_k is unknown but can be calculated from (6.4.11), giving

$$\mathrm{Q}_k = \mathrm{V}_k(i) \sum_{n=1}^{N} \mathrm{Y}_{kn}\mathrm{V}_n(i) \sin[\delta_k(i) - \delta_n(i) - \theta_{kn}] \tag{6.5.3}$$

Also,

$$\mathrm{Q}_{\mathrm{G}k} = \mathrm{Q}_k + \mathrm{Q}_{\mathrm{L}k}$$

Copyright 2017 Cengage Learning. All Rights Reserved. May not be copied, scanned, or duplicated, in whole or in part. Due to electronic rights, some third party content may be suppressed from the eBook and/or eChapter(s). Editorial review has deemed that any suppressed content does not materially affect the overall learning experience. Cengage Learning reserves the right to remove additional content at any time if subsequent rights restrictions require it.

If the calculated value of Q_{Gk} does not exceed its limits, then Q_k is used in (6.5.2) to calculate $V_k(i+1) = V_k(i+1)\angle\delta_k(i+1)$. Then the magnitude $V_k(i+1)$ is changed to V_k, which is input data for the voltage-controlled bus. Thus, use (6.5.2) to compute only the angle $\delta_k(i+1)$ for voltage-controlled buses.

If the calculated value exceeds its limit $Q_{Gk\max}$ or $Q_{Gk\min}$ during any iteration, then the bus type is changed from a voltage-controlled bus to a load bus, with Q_{Gk} set to its limit value. Under this condition, the voltage-controlling device (e.g., generator, capacitor bank, static var compensator) is not capable of maintaining V_k as specified by the input data. The power flow then calculates a new value of V_k.

For the swing bus, denoted bus 1, V_1 and δ_1 *are* input data. As such, no iterations are required for the swing bus. After the iteration process has converged, one pass through (6.4.10) and (6.4.11) can be made to compute P_1 and Q_1.

EXAMPLE 6.10

Power flow solution by Gauss-Seidel

For the power system of Example 6.9, use Gauss-Seidel to calculate $V_2(1)$, the phasor voltage at bus 2 after the first iteration. Use zero initial phase angles and 1.0 per-unit initial voltage magnitudes (except at bus 3, where $V_3 = 1.05$) to start the iteration procedure.

SOLUTION

Bus 2 is a load bus. Using the input data and bus admittance values from Example 6.9 in (6.5.2),

$$V_2(1) = \frac{1}{Y_{22}}\left\{\frac{P_2 - jQ_2}{V_2^*(0)} - [Y_{21}V_1(1) + Y_{23}V_3(0) + Y_{24}V_4(0) + Y_{25}V_5(0)]\right\}$$

$$= \frac{1}{28.5847\angle{-84.624°}}\left\{\frac{-8 - j(-2.8)}{1.0\angle 0°}\right.$$

$$\left. - [(-1.78552 + j19.83932)(1.0) + (-0.89276 + j9.91964)(1.0)]\right\}$$

$$= \frac{(-8 + j2.8) - (-2.67828 + j29.7589)}{28.5847\angle{-84.624°}}$$

$$= 0.96132\angle{-16.543°} \quad \text{per unit}$$

Next, the above value is used in (6.5.2) to recalculate $V_2(1)$;

$$V_2(1) = \frac{1}{28.5847\angle{-84.624°}}\left\{\frac{-8 + j2.8}{0.96132\angle 16.543°} - [-2.67828 + j29.75829]\right\}$$

Copyright 2017 Cengage Learning. All Rights Reserved. May not be copied, scanned, or duplicated, in whole or in part. Due to electronic rights, some third party content may be suppressed from the eBook and/or eChapter(s). Editorial review has deemed that any suppressed content does not materially affect the overall learning experience. Cengage Learning reserves the right to remove additional content at any time if subsequent rights restrictions require it.

$$= \frac{-4.4698 - j24.5973}{28.5847\underline{/-84.624^\circ}} = 0.87460\underline{/-15.675^\circ} \quad \text{per unit}$$

Computations are next performed at buses 3, 4, and 5 to complete the first Gauss-Seidel iteration.

To see the complete convergence of this case, open PowerWorld Simulator case Example 6_10. By default, PowerWorld Simulator uses the Newton-Raphson method described in the next section since Gauss-Seidel, while being a useful technique for introducing the power flow to students, is now seldom used commercially. However, the free educational version of PowerWorld still allows cases to be solved with the Gauss-Seidel approach by selecting **Tools, Solve, Gauss-Seidel Power Flow**. To avoid getting stuck in an infinite loop if a case does not converge, PowerWorld Simulator places a limit on the maximum number of iterations. Usually for a Gauss-Seidel procedure this number is rather high, perhaps equal to 100 iterations. However, in this example to demonstrate the convergence characteristics of the Gauss-Seidel method, it has been set to a single iteration, allowing the voltages to be viewed after each iteration. To step through the solution one iteration at a time, just repeatedly select **Tools, Solve, Gauss-Seidel Power Flow**.

A common stopping criterion for the Gauss-Seidel is to use the scaled differences in the voltages from one iteration to the next (6.2.2). When the voltage differences for each bus are below a specified convergence tolerance ε, the problem is considered solved. An alternative approach, implemented in PowerWorld Simulator, is to examine the real and reactive mismatch equations, defined as the difference between the right- and left-hand sides of (6.4.10) and (6.4.11). PowerWorld Simulator continues iterating until all the bus mismatches are below an MVA (or kVA) tolerance. When single-stepping through the solution, the bus mismatches can be viewed after each iteration on the **Case Information, Mismatches** display. The solution mismatch tolerance can be changed on the Power Flow Solution page of the PowerWorld Simulator Options dialog (select **Tools, Simulator Options**, then select the **Power Flow Solution** category to view this dialog); the maximum number of iterations can also be changed from this page. A typical convergence tolerance is about 0.1 MVA.

6.6 POWER FLOW SOLUTION BY NEWTON-RAPHSON

Equations (6.4.10) and (6.4.11) are analogous to the nonlinear equation $\mathbf{y} = \mathbf{f}(\mathbf{x})$, solved in Section 6.3 by Newton-Raphson. The $\mathbf{x}$, $\mathbf{y}$, and $\mathbf{f}$ vectors for the power flow problem are defined as

Copyright 2017 Cengage Learning. All Rights Reserved. May not be copied, scanned, or duplicated, in whole or in part. Due to electronic rights, some third party content may be suppressed from the eBook and/or eChapter(s). Editorial review has deemed that any suppressed content does not materially affect the overall learning experience. Cengage Learning reserves the right to remove additional content at any time if subsequent rights restrictions require it.

$$\mathbf{x} = \begin{bmatrix} \delta \\ \mathbf{V} \end{bmatrix} = \begin{bmatrix} \delta_2 \\ \vdots \\ \delta_N \\ \mathrm{V}_2 \\ \vdots \\ \mathrm{V}_N \end{bmatrix}; \quad \mathbf{y} = \begin{bmatrix} \mathbf{P} \\ \mathbf{Q} \end{bmatrix} = \begin{bmatrix} \mathrm{P}_2 \\ \vdots \\ \mathrm{P}_N \\ \mathrm{Q}_2 \\ \vdots \\ \mathrm{Q}_N \end{bmatrix}$$

$$\mathbf{f}(\mathbf{x}) = \begin{bmatrix} \mathbf{P}(\mathbf{x}) \\ \mathbf{Q}(\mathbf{x}) \end{bmatrix} = \begin{bmatrix} \mathrm{P}_2(\mathbf{x}) \\ \vdots \\ \mathrm{P}_N(\mathbf{x}) \\ \mathrm{Q}_2(\mathbf{x}) \\ \vdots \\ \mathrm{Q}_N(\mathbf{x}) \end{bmatrix} \tag{6.6.1}$$

where all V, P, and Q terms are in per-unit and δ terms are in radians. The swing bus variables δ_1 and V_1 are omitted from (6.6.1), since they are already known. Equations (6.4.10) and (6.4.11) then have the following form:

$$y_k = \mathrm{P}_k = \mathrm{P}_k(\mathrm{x}) = \mathrm{V}_k \sum_{n=1}^{N} \mathrm{Y}_{kn} \mathrm{V}_n \cos(\delta_k - \delta_n - \theta_{kn}) \tag{6.6.2}$$

$$\begin{gathered} y_{k+N} = \mathrm{Q}_k = \mathrm{Q}_k(\mathrm{x}) = \mathrm{V}_k \sum_{n=1}^{N} \mathrm{Y}_{kn} \mathrm{V}_n \sin(\delta_k - \delta_n - \theta_{kn}) \\ k = 2, 3, \ldots, N \end{gathered} \tag{6.6.3}$$

The Jacobian matrix of (6.3.10) has the form

$$\mathbf{J} = \begin{array}{c} \qquad\qquad \mathbf{J}1 \qquad\qquad\qquad\qquad\qquad \mathbf{J}2 \\ \left[\begin{array}{ccc|ccc} \dfrac{\partial \mathrm{P}_2}{\partial \delta_2} & \cdots & \dfrac{\partial \mathrm{P}_2}{\partial \delta_N} & \dfrac{\partial \mathrm{P}_2}{\partial \mathrm{V}_2} & \cdots & \dfrac{\partial \mathrm{P}_2}{\partial \mathrm{V}_N} \\ \vdots & & & \vdots & & \\ \dfrac{\partial \mathrm{P}_N}{\partial \delta_2} & \cdots & \dfrac{\partial \mathrm{P}_N}{\partial \delta_N} & \dfrac{\partial \mathrm{P}_N}{\partial \mathrm{V}_2} & \cdots & \dfrac{\partial \mathrm{P}_N}{\partial \mathrm{V}_N} \\ \hline \dfrac{\partial \mathrm{Q}_2}{\partial \delta_2} & \cdots & \dfrac{\partial \mathrm{Q}_2}{\partial \delta_N} & \dfrac{\partial \mathrm{Q}_2}{\partial \mathrm{V}_2} & \cdots & \dfrac{\partial \mathrm{Q}_2}{\partial \mathrm{V}_N} \\ \vdots & & & \vdots & & \\ \dfrac{\partial \mathrm{Q}_N}{\partial \delta_2} & \cdots & \dfrac{\partial \mathrm{Q}_N}{\partial \delta_N} & \dfrac{\partial \mathrm{Q}_N}{\partial \mathrm{V}_2} & \cdots & \dfrac{\partial \mathrm{Q}_N}{\partial \mathrm{V}_N} \end{array}\right] \\ \qquad\qquad \mathbf{J}3 \qquad\qquad\qquad\qquad\qquad \mathbf{J}4 \end{array} \tag{6.6.4}$$

Equation (6.6.4) is partitioned into four blocks. The partial derivatives in each block, derived from (6.6.2) and (6.6.3), are given in Table 6.5.

Copyright 2017 Cengage Learning. All Rights Reserved. May not be copied, scanned, or duplicated, in whole or in part. Due to electronic rights, some third party content may be suppressed from the eBook and/or eChapter(s). Editorial review has deemed that any suppressed content does not materially affect the overall learning experience. Cengage Learning reserves the right to remove additional content at any time if subsequent rights restrictions require it.

$n \neq k$

$$\mathrm{J1}_{kn} = \frac{\partial \mathrm{P}_k}{\partial \delta_n} = \mathrm{V}_k \mathrm{Y}_{\mathrm{kn}} \mathrm{V}_n \sin(\delta_k - \delta_n - \theta_{kn})$$

$$\mathrm{J2}_{kn} = \frac{\partial \mathrm{P}_k}{\partial \mathrm{V}_n} = \mathrm{V}_k \mathrm{Y}_{\mathrm{kn}} \cos(\delta_k - \delta_n - \theta_{kn})$$

$$\mathrm{J3}_{kn} = \frac{\partial \mathrm{Q}_k}{\partial \delta_n} = -\mathrm{V}_k \mathrm{Y}_{\mathrm{kn}} \mathrm{V}_n \cos(\delta_k - \delta_n - \theta_{kn})$$

$$\mathrm{J4}_{kn} = \frac{\partial \mathrm{Q}_k}{\partial \mathrm{V}_n} = \mathrm{V}_k \mathrm{Y}_{\mathrm{kn}} \sin(\delta_k - \delta_n - \theta_{kn})$$

$n = k$

$$\mathrm{J1}_{kk} = \frac{\partial \mathrm{P}_k}{\partial \delta_k} = -\mathrm{V}_k \sum_{\substack{n=1 \\ n \neq k}}^{N} \mathrm{Y}_{\mathrm{kn}} \mathrm{V}_n \sin(\delta_k - \delta_n - \theta_{kn})$$

$$\mathrm{J2}_{kk} = \frac{\partial \mathrm{P}_k}{\partial \mathrm{V}_k} = \mathrm{V}_k \mathrm{Y}_{\mathrm{kk}} \cos \theta_{kk} + \sum_{n=1}^{N} \mathrm{Y}_{\mathrm{kn}} \mathrm{V}_n \cos(\delta_k - \delta_n - \theta_{kn})$$

$$\mathrm{J3}_{kk} = \frac{\partial \mathrm{Q}_k}{\partial \delta_k} = \mathrm{V}_k \sum_{\substack{n=1 \\ n \neq k}}^{N} \mathrm{Y}_{\mathrm{kn}} \mathrm{V}_n \cos(\delta_k - \delta_n - \theta_{kn})$$

$$\mathrm{J4}_{kk} = \frac{\partial \mathrm{Q}_k}{\partial \mathrm{V}_k} = -\mathrm{V}_k \mathrm{Y}_{\mathrm{kk}} \sin \theta_{kk} + \sum_{n=1}^{N} \mathrm{Y}_{\mathrm{kn}} \mathrm{V}_n \sin(\delta_k - \delta_n - \theta_{kn})$$

$$k, n = 2, 3, \ldots, N$$

TABLE 6.5

Elements of the Jacobian matrix

Now apply to the power flow problem the four Newton-Raphson steps outlined in Section 6.3, starting with $\mathbf{x}(i) = \begin{bmatrix} \boldsymbol{\delta}(i) \\ \mathbf{V}(i) \end{bmatrix}$ at the ith iteration.

STEP 1 Use (6.6.2) and (6.6.3) to compute

$$\Delta \mathbf{y}(i) = \begin{bmatrix} \Delta \mathbf{P}(i) \\ \Delta \mathbf{Q}(i) \end{bmatrix} = \begin{bmatrix} \mathbf{P} - \mathbf{P}[\mathbf{x}(i)] \\ \mathbf{Q} - \mathbf{Q}[\mathbf{x}(i)] \end{bmatrix} \tag{6.6.5}$$

STEP 2 Use the equations in Table 6.5 to calculate the Jacobian matrix.

STEP 3 Use Gauss elimination and back substitution to solve

$$\left[\begin{array}{c|c} \mathbf{J1}(i) & \mathbf{J2}(i) \\ \hline \mathbf{J3}(i) & \mathbf{J4}(i) \end{array}\right] \begin{bmatrix} \Delta \boldsymbol{\delta}(i) \\ \Delta \mathbf{V}(i) \end{bmatrix} = \begin{bmatrix} \Delta \mathbf{P}(i) \\ \Delta \mathbf{Q}(i) \end{bmatrix} \tag{6.6.6}$$

Copyright 2017 Cengage Learning. All Rights Reserved. May not be copied, scanned, or duplicated, in whole or in part. Due to electronic rights, some third party content may be suppressed from the eBook and/or eChapter(s). Editorial review has deemed that any suppressed content does not materially affect the overall learning experience. Cengage Learning reserves the right to remove additional content at any time if subsequent rights restrictions require it.

STEP 4 Compute

$$\mathbf{x}(i+1) = \begin{bmatrix} \boldsymbol{\delta}(i+1) \\ \mathbf{V}(i+1) \end{bmatrix} = \begin{bmatrix} \boldsymbol{\delta}(i) \\ \mathbf{V}(i) \end{bmatrix} + \begin{bmatrix} \Delta\boldsymbol{\delta}(i) \\ \Delta\mathbf{V}(i) \end{bmatrix} \tag{6.6.7}$$

Starting with initial value $\mathbf{x}(0)$, the procedure continues until convergence is obtained or until the number of iterations exceeds a specified maximum. Convergence criteria are often based on $\Delta\mathbf{y}(i)$ (called *power mismatches*) rather than on $\Delta\mathbf{x}(i)$ (phase angle and voltage magnitude mismatches).

For each voltage-controlled bus, the magnitude V_k is already known, and the function $Q_k(\mathbf{x})$ is not needed. Therefore, V_k from the $\mathbf{x}$ vector can be omitted, as well as Q_k from the $\mathbf{y}$ vector. The column corresponding to partial derivatives with respect to V_k and the row corresponding to partial derivatives of $Q_k(\mathbf{x})$ can also be omitted from the Jacobian matrix. Alternatively, rows and corresponding columns for voltage-controlled buses can be retained in the Jacobian matrix. Then during each iteration, the voltage magnitude $V_k(i+1)$ of each voltage-controlled bus is reset to V_k which is input data for that bus.

At the end of each iteration, $Q_k(\mathbf{x})$ is computed using (6.6.3) and $Q_{Gk} = Q_k(\mathbf{x}) + Q_{Lk}$ for each voltage-controlled bus. If the computed value of Q_{Gk} exceeds its limits, then the bus type is changed to a load bus with Q_{Gk} set to its limit value. The power flow program also computes a new value for V_k.

EXAMPLE 6.11

Jacobian matrix and power flow solution by Newton-Raphson

Determine the dimension of the Jacobian matrix for the power system in Example 6.9. Also calculate $\Delta P_2(0)$ in Step 1 and $J1_{24}(0)$ in Step 2 of the first Newton-Raphson iteration. Assume zero initial phase angles and 1.0 per-unit initial voltage magnitudes (except $V_3 = 1.05$).

SOLUTION

Since there are $N = 5$ buses for Example 6.9, (6.6.2) and (6.6.3) constitute $2(N-1) = 8$ equations, for which $\mathbf{J}(i)$ has dimension 8×8. However, there is one voltage-controlled bus, bus 3. Therefore, V_3 and the equation for $Q_3(\mathbf{x})$ could be eliminated, with $\mathbf{J}(i)$ reduced to a 7×7 matrix.

From Step 1 and (6.6.2),

$$\begin{aligned} \Delta P_2(0) = P_2 - P_2(x) = P_2 - V_2(0)\{&Y_{21}V_1\cos[\delta_2(0) - \delta_1(0) - \theta_{21}] \\ &+ Y_{22}V_2\cos[-\theta_{22}] + Y_{23}V_3\cos[\delta_2(0) - \delta_3(0) - \theta_{23}] \\ &+ Y_{24}V_4\cos[\delta_2(0) - \delta_4(0) - \theta_{24}] \\ &+ Y_{25}V_5\cos[\delta_2(0) - \delta_5(0) - \theta_{25}]\} \end{aligned}$$

Copyright 2017 Cengage Learning. All Rights Reserved. May not be copied, scanned, or duplicated, in whole or in part. Due to electronic rights, some third party content may be suppressed from the eBook and/or eChapter(s). Editorial review has deemed that any suppressed content does not materially affect the overall learning experience. Cengage Learning reserves the right to remove additional content at any time if subsequent rights restrictions require it.

$$
\begin{aligned}
\Delta P_2(0) &= -8.0 - 1.0\{28.5847(1.0)\cos(84.624°) \\
&\quad + 9.95972(1.0)\cos(-95.143°) \\
&\quad + 19.9159(1.0)\cos(-95.143°)\} \\
&= -8.0 - (-2.89 \times 10^{-4}) = -7.99972 \text{ per unit}
\end{aligned}
$$

From Step 2 and J1 given in Table 6.5

$$
\begin{aligned}
J1_{24}(0) &= V_2(0)\,Y_{24}V_4(0)\sin[\delta_2(0) - \delta_4(0) - \theta_{24}] \\
&= (1.0)(9.95972)(1.0)\sin[-95.143°] \\
&= -9.91964 \text{ per unit}
\end{aligned}
$$

To see the complete convergence of this case, open PowerWorld Simulator case Example 6_11 (see Figure 6.4). Select **Case Information, Network, Mismatches** to see the initial mismatches, and **Case Information, Solution Details, Power Flow Jacobian** to view the initial Jacobian matrix. As is common in commercial power flows, PowerWorld Simulator actually includes rows in the Jacobian for voltage-controlled buses. When a generator is regulating its terminal voltage, this row corresponds to the equation setting the bus voltage magnitude equal to the generator voltage setpoint. However, if the generator hits a reactive power limit, the bus type is switched to a load bus.

To step through the Newton-Raphson solution, from the ribbon select **Solve, Single Solution–Full Newton**. Ordinarily this selection would perform a complete Newton-Raphson iteration, stopping only when all the mismatches are less than the desired tolerance. However, for this case, in order to allow you to see the solution process, the maximum number of iterations has been set to 1, allowing the voltages, mismatches and the Jacobian to be viewed after each iteration. To complete the solution, continue to select **Single Solution—Full Newton** until the solution convergence to the values shown in Tables 6.6, 6.7, and 6.8 (in about three iterations).

Bus #	Voltage Magnitude (per unit)	Phase Angle (degrees)	Generation PG (per unit)	Generation QG (per unit)	Load PL (per unit)	Load QL (per unit)
1	1.000	0.000	3.948	1.144	0.000	0.000
2	0.834	−22.407	0.000	0.000	8.000	2.800
3	1.050	−0.597	5.200	3.376	0.800	0.400
4	1.019	−2.834	0.000	0.000	0.000	0.000
5	0.974	−4.548	0.000	0.000	0.000	0.000
		TOTAL	9.148	4.516	8.800	3.200

TABLE 6.6

Bus output data for the power system given in Example 6.9

(Continued)

Copyright 2017 Cengage Learning. All Rights Reserved. May not be copied, scanned, or duplicated, in whole or in part. Due to electronic rights, some third party content may be suppressed from the eBook and/or eChapter(s). Editorial review has deemed that any suppressed content does not materially affect the overall learning experience. Cengage Learning reserves the right to remove additional content at any time if subsequent rights restrictions require it.

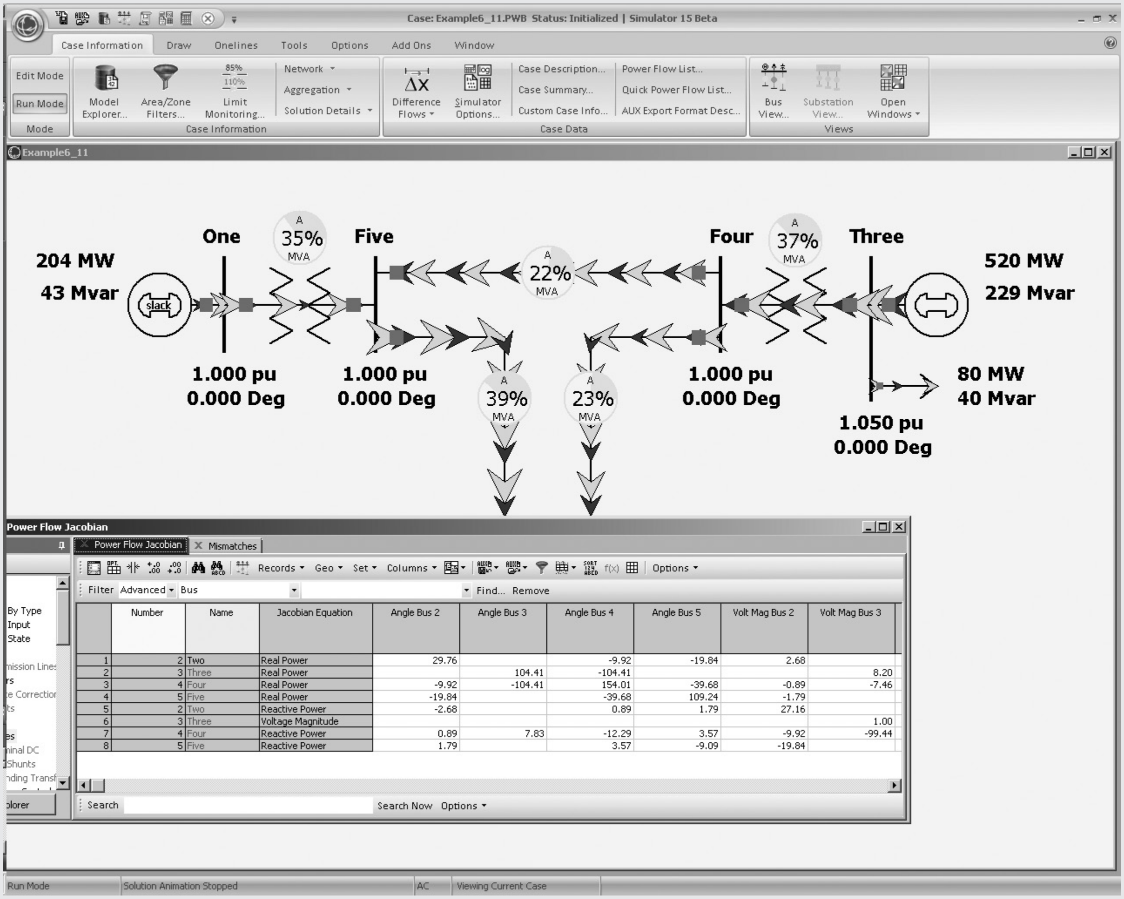
Case: Example6_11.PWB Status: Initialized | Simulator 15 Beta
Case Information
Draw
Onelines
Tools
Options
Add Ons
Window
Edit Mode
Run Mode
Mode
Model Explorer...
Area/Zone Filters...
Limit Monitoring...
Network
Aggregation
Solution Details
Case Information
Difference Flows
Simulator Options...
Case Description...
Case Summary...
Custom Case Info...
Power Flow List...
Quick Power Flow List...
AUX Export Format Desc...
Case Data
Bus View...
Substation View...
Open Windows
Views
Example6_11
One
Five
Four
Three
204 MW
43 Mvar
slack
35% MVA
22% MVA
37% MVA
520 MW
229 Mvar
1.000 pu
0.000 Deg
1.000 pu
0.000 Deg
39% MVA
23% MVA
1.000 pu
0.000 Deg
80 MW
40 Mvar
1.050 pu
0.000 Deg
Power Flow Jacobian
Power Flow Jacobian
Mismatches
Records
Geo
Set
Columns
Options
Filter Advanced
Bus
Find...
Remove
Search
Search Now
Options
Run Mode
Solution Animation Stopped
AC
Viewing Current Case

	Number	Name	Jacobian Equation	Angle Bus 2	Angle Bus 3	Angle Bus 4	Angle Bus 5	Volt Mag Bus 2	Volt Mag Bus 3
1	2	Two	Real Power	29.76		-9.92	-19.84	2.68	
2	3	Three	Real Power		104.41	-104.41			8.20
3	4	Four	Real Power	-9.92	-104.41	154.01	-39.68	-0.89	-7.46
4	5	Five	Real Power	-19.84		-39.68	109.24	-1.79	
5	2	Two	Reactive Power	-2.68		0.89	1.79	27.16	
6	3	Three	Voltage Magnitude						1.00
7	4	Four	Reactive Power	0.89	7.83	-12.29	3.57	-9.92	-99.44
8	5	Five	Reactive Power	1.79		3.57	-9.09	-19.84	

FIGURE 6.4

Screen for Example 6.11 showing Jacobian matrix at first iteration

Line #	Bus to Bus		P	Q	S
1	2	4	−2.920	−1.392	3.232
	4	2	3.036	1.216	3.272
2	2	5	−5.080	−1.408	5.272
	5	2	5.256	2.632	5.876
3	4	5	1.344	1.504	2.016
	5	4	−1.332	−1.824	2.260

TABLE 6.7

Line output data for the power system given in Example 6.9

Copyright 2017 Cengage Learning. All Rights Reserved. May not be copied, scanned, or duplicated, in whole or in part. Due to electronic rights, some third party content may be suppressed from the eBook and/or eChapter(s). Editorial review has deemed that any suppressed content does not materially affect the overall learning experience. Cengage Learning reserves the right to remove additional content at any time if subsequent rights restrictions require it.

Tran. #	Bus to Bus		P	Q	S
1	1	5	3.948	1.144	4.112
	5	1	−3.924	−0.804	4.004
2	3	4	4.400	2.976	5.312
	4	3	−4.380	−2.720	5.156

TABLE 6.8

Transformer output data for the power system given in Example 6.9

EXAMPLE 6.12

Power flow program: change in generation

Using the power-flow system given in Example 6.9, determine the acceptable generation range at bus 3, keeping each line and transformer loaded at or below 100% of its MVA limit.

SOLUTION

Load PowerWorld Simulator case Example 6_9. Select **Single Solution-Full Newton** to perform a single power flow solution using the Newton-Raphson approach. Then view the **Case Information** displays to verify that the PowerWorld Simulator solution matches the solution shown in Tables 6.6, 6.7, and 6.8. Additionally, the pie charts on the onelines show the percentage line and transformer loadings. Initially transformer Tl, between buses 1 and 5, is loaded at about 69% of its maximum MVA limit, while transformer T2, between buses 3 and 4, is loaded at about 53%.

Next, the bus 3 generation needs to be varied. This can be done a number of different ways in PowerWorld Simulator. The easiest (for this example) is to use the bus 3 generator MW oneline field to manually change the generation (see Figure 6.5). Right-click on the 520 MW field to the right of the bus 3 generator and select **Generator Field Information** dialog to view the **Generator Field Options** dialog. Set the Delta Per Mouse Click field to 10 and select OK. Small arrows are now visible next to this field on the oneline; clicking on the up arrow increases the generator's MW output by 10 MW, while clicking on the down arrow decreases the generation by 10 MW. Select **Tools, Play** to begin the simulation. Increase the generation until the pie chart for the transformer from bus 3 to 4 is loaded to 100%. This occurs at about 1000 MW. Notice that as the bus 3 generation is increased, the bus 1 slack generation decreases by a similar amount. Repeat the process, except now decreasing the generation. This unloads the transformer from bus 3 to 4, but increases the loading on the transformer from bus 1 to bus 5. The bus 1 to 5 transformer should reach 100% loading with the bus 3 generation equal to about 330 MW.

(Continued)

Copyright 2017 Cengage Learning. All Rights Reserved. May not be copied, scanned, or duplicated, in whole or in part. Due to electronic rights, some third party content may be suppressed from the eBook and/or eChapter(s). Editorial review has deemed that any suppressed content does not materially affect the overall learning experience. Cengage Learning reserves the right to remove additional content at any time if subsequent rights restrictions require it.

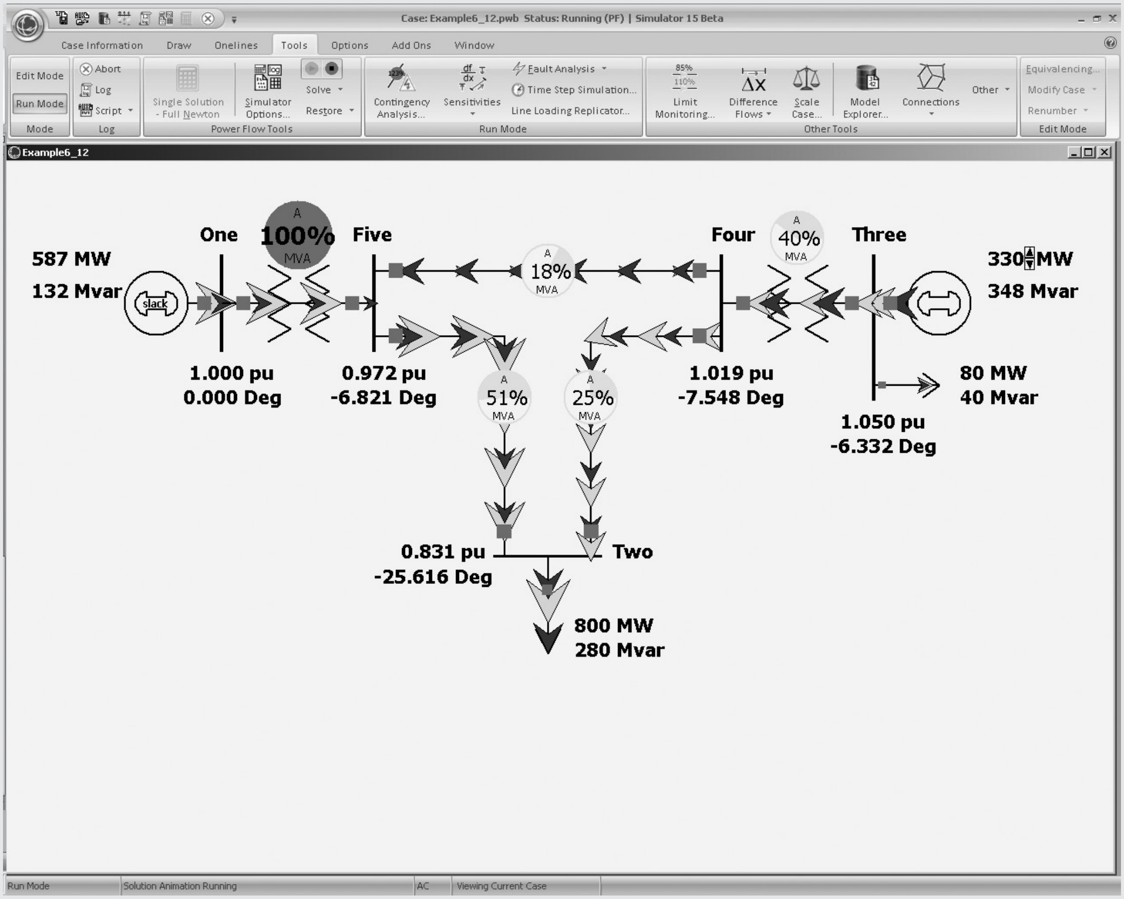
Case: Example6_12.pwb Status: Running (PF) | Simulator 15 Beta
Case Information
Draw
Onelines
Tools
Options
Add Ons
Window
Edit Mode
Run Mode
Mode
Abort
Log
Script
Log
Single Solution - Full Newton
Simulator Options...
Solve
Restore
Power Flow Tools
Contingency Analysis...
Sensitivities
Fault Analysis
Time Step Simulation...
Line Loading Replicator...
Run Mode
Limit Monitoring...
Difference Flows
Scale Case...
Model Explorer...
Connections
Other
Other Tools
Equivalencing...
Modify Case
Renumber
Edit Mode
Example6_12
One
Five
Four
Three
Two
587 MW
132 Mvar
slack
100%
MVA
18%
MVA
40%
MVA
51%
MVA
25%
MVA
330 MW
348 Mvar
1.000 pu
0.000 Deg
0.972 pu
-6.821 Deg
1.019 pu
-7.548 Deg
1.050 pu
-6.332 Deg
80 MW
40 Mvar
0.831 pu
-25.616 Deg
800 MW
280 Mvar
Run Mode
Solution Animation Running
AC
Viewing Current Case

FIGURE 6.5

Screen for Example 6.12, Minimum Bus 3 Generator Loading

Voltage-controlled buses to which tap-changing or voltage-regulating transformers are connected can be handled by various methods. One method is to treat each of these buses as a load bus. The equivalent π circuit parameters (Figure 3.25) are first calculated with tap setting $c = 1.0$ for starting. During each iteration, the computed bus voltage magnitude is compared with the desired value specified by the input data. If the computed voltage is low (or high), c is increased (or decreased) to its next setting, and the parameters of the equivalent π circuit as well as Y_{bus} are recalculated. The procedure continues until the computed bus voltage magnitude equals the desired value within a specified tolerance or until the high

Copyright 2017 Cengage Learning. All Rights Reserved. May not be copied, scanned, or duplicated, in whole or in part. Due to electronic rights, some third party content may be suppressed from the eBook and/or eChapter(s). Editorial review has deemed that any suppressed content does not materially affect the overall learning experience. Cengage Learning reserves the right to remove additional content at any time if subsequent rights restrictions require it.

or low tap-setting limit is reached. Phase-shifting transformers can be handled in a similar way by using a complex turns ratio $c = 1.0\underline{/\alpha}$ and by varying the phase-shift angle α.

A method with faster convergence makes c a variable and includes it in the $\mathbf{x}$ vector of (6.6.1). An equation is then derived to enter into the Jacobian matrix [4].

In comparing the Gauss-Seidel and Newton-Raphson algorithms, experience from power flow studies has shown that Newton-Raphson converges in many cases where Jacobi and Gauss-Seidel diverge. Furthermore, the number of iterations required for convergence is independent of the number of buses N for Newton-Raphson, but increases with N for Jacobi and Gauss-Seidel. The principal advantage of the Jacobi and Gauss-Seidel methods had been their more modest memory storage requirements and their lower computational requirements per iteration. However, with the vast increases in low-cost computer memory over the last several decades, coupled with the need to solve power flow problems with tens of thousands of buses, these advantages have been essentially eliminated. Therefore the Newton-Raphson, or one of the derivative methods discussed in Sections 6.9 and 6.10, are the preferred power flow solution approaches.

EXAMPLE 6.13

Power flow program: 37-bus system

To see a power flow example of a larger system, open PowerWorld Simulator case Example 6_13 (see Figure 6.6). This case models a 37-bus, 9-generator power system containing three different voltage levels (345 kV, 138 kV, and 69 kV) with 57 transmission lines or transformers. The oneline can be panned by pressing the arrow keys, and it can be zoomed by pressing the <ctrl> with the up arrow key to zoom in or with the down arrow key to zoom out. Use **Tools, Play** to animate the oneline and **Tools, Pause** to stop the animation.

Determine the lowest per-unit voltage and the maximum line/transformer loading both for the initial case and for the case with the line from bus OAK69 to WALNUT69 out of service.

SOLUTION

Use single solution to initially solve the power flow, and then **Case Information, Network, Buses…** to view a listing of all the buses in the case. To quickly determine the lowest per-unit voltage magnitude, left-click on the PU Volt column header to sort the column (clicking a second time reverses the sort). The lowest initial voltage magnitude is 0.990 at bus LOCUST69. Next, select **Case Information, Network, Lines and Transformers…** to view the Line and Transformer Records display. Left-click on % of Max Limit to sort the lines by percentage loading. Initially the highest percentage loading is 64.9% on the line between PEAR69 and PECAN69, circuit 1.

(*Continued*)

Copyright 2017 Cengage Learning. All Rights Reserved. May not be copied, scanned, or duplicated, in whole or in part. Due to electronic rights, some third party content may be suppressed from the eBook and/or eChapter(s). Editorial review has deemed that any suppressed content does not materially affect the overall learning experience. Cengage Learning reserves the right to remove additional content at any time if subsequent rights restrictions require it.

In the software, there are several ways to open the line between OAK69 and WALNUT69. One approach is to locate the line on the Line and Transformer Records display and then double-click on the Status field to change its value. An alternative approach is to find the line on the oneline (it is in the upper-lefthand portion) and then click on one of its circuit breakers. Once the line is removed, use single solution to resolve the power flow. The lowest per-unit voltage is now 0.911 at MAPLE69, and the highest percentage line loading is 135% on the line between PEACH69 to POPLAR69. Since there are now several bus and line violations, the power system is no longer at a reliable operating point. Control actions and/or design improvements are needed to correct these problems. The design projects at the end of the chapter discuss these options.

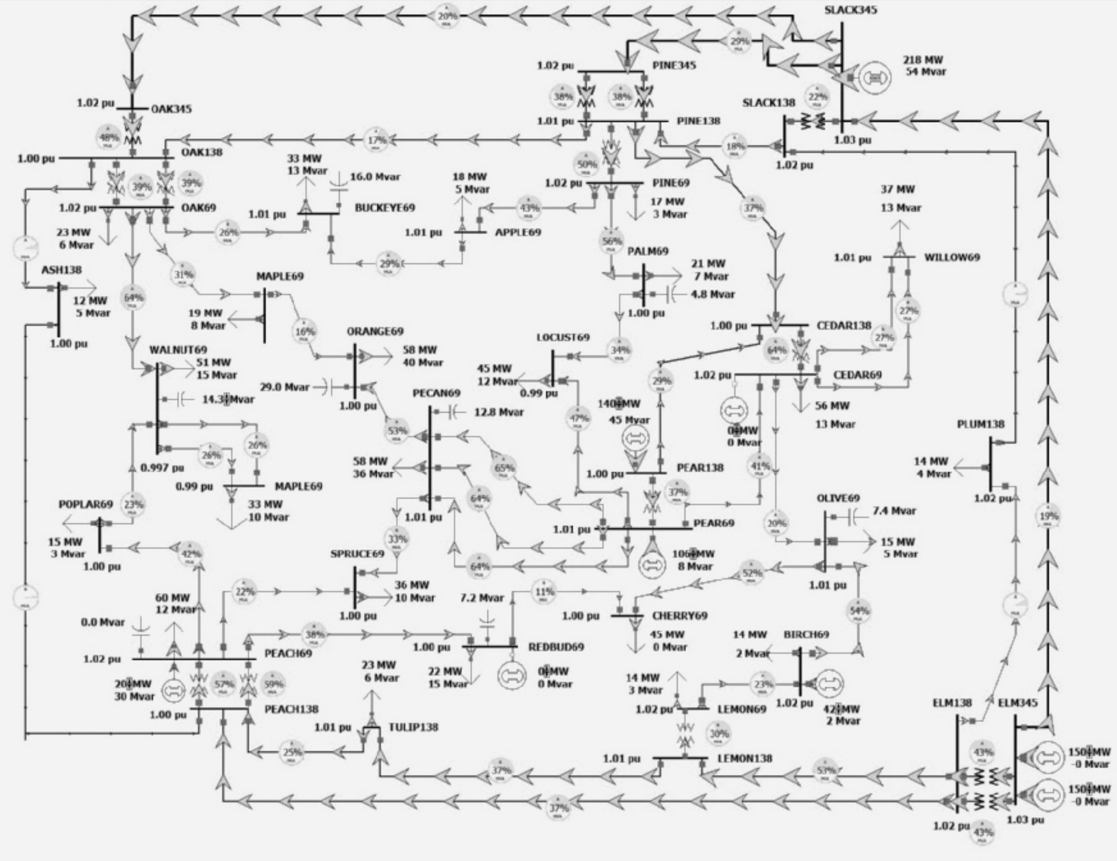
SLACK345
20%
29%
218 MW
54 Mvar
1.02 pu
PINE345
38%
38%
22%
SLACK138
1.01 pu
PINE138
1.03 pu
1.02 pu
OAK345
48%
17%
18%
1.02 pu
1.00 pu
OAK138
33 MW
13 Mvar
16.0 Mvar
50%
39%
39%
18 MW
5 Mvar
1.02 pu
PINE69
37 MW
13 Mvar
1.02 pu
OAK69
1.01 pu
BUCKEYE69
43%
17 MW
3 Mvar
37%
23 MW
6 Mvar
26%
1.01 pu
APPLE69
56%
PALM69
1.01 pu
WILLOW69
ASH138
31%
29%
21 MW
7 Mvar
MAPLE69
4.8 Mvar
12 MW
5 Mvar
64%
19 MW
8 Mvar
1.00 pu
27%
1.00 pu
16%
ORANGE69
1.00 pu
CEDAR138
LOCUST69
34%
27%
WALNUT69
58 MW
40 Mvar
64%
51 MW
15 Mvar
45 MW
12 Mvar
29%
1.02 pu
CEDAR69
29.0 Mvar
0.99 pu
14.3 Mvar
PECAN69
140 MW
56 MW
1.00 pu
12.8 Mvar
45 Mvar
13 Mvar
47%
0 MW
0 Mvar
PLUM138
53%
26%
26%
58 MW
36 Mvar
65%
41%
0.997 pu
1.00 pu
PEAR138
14 MW
4 Mvar
0.99 pu
MAPLE69
64%
37%
OLIVE69
1.02 pu
POPLAR69
23%
7.4 Mvar
33 MW
10 Mvar
1.01 pu
PEAR69
20%
19%
1.01 pu
15 MW
3 Mvar
33%
106 MW
15 MW
5 Mvar
42%
SPRUCE69
64%
8 Mvar
1.00 pu
52%
1.01 pu
36 MW
10 Mvar
60 MW
12 Mvar
22%
7.2 Mvar
11%
54%
1.00 pu
1.00 pu
CHERRY69
0.0 Mvar
38%
45 MW
0 Mvar
14 MW
2 Mvar
BIRCH69
1.02 pu
1.00 pu
PEACH69
REDBUD69
23 MW
6 Mvar
22 MW
15 Mvar
0 MW
0 Mvar
14 MW
3 Mvar
20 MW
30 Mvar
57%
59%
23%
PEACH138
1.02 pu
LEMON69
1.02 pu
42 MW
2 Mvar
ELM138
ELM345
1.00 pu
1.01 pu
TULIP138
30%
25%
43%
150 MW
-0 Mvar
1.01 pu
LEMON138
37%
53%
150 MW
-0 Mvar
37%
1.02 pu
43%
1.03 pu

FIGURE 6.6

Screen for Example 6.13 showing the initial flows

Copyright 2017 Cengage Learning. All Rights Reserved. May not be copied, scanned, or duplicated, in whole or in part. Due to electronic rights, some third party content may be suppressed from the eBook and/or eChapter(s). Editorial review has deemed that any suppressed content does not materially affect the overall learning experience. Cengage Learning reserves the right to remove additional content at any time if subsequent rights restrictions require it.

6.7 CONTROL OF POWER FLOW

The following means are used to control system power flows:

1. Prime mover and excitation control of generators
2. Switching of shunt capacitor banks, shunt reactors, and static var systems
3. Control of tap-changing and regulating transformers

A simple model of a generator operating under balanced steady-state conditions is the Thévenin equivalent shown in Figure 6.7. V_t is the generator terminal voltage, E_g is the excitation voltage, δ is the power angle, and X_g is the positive-sequence synchronous reactance. From the figure, the generator current is

$$I = \frac{E_g e^{j\delta} - V_t}{jX_g} \tag{6.7.1}$$

and the complex power delivered by the generator is

$$S = P + jQ = V_t I^* = V_t\left(\frac{E_g e^{-j\delta} - V_t}{-jX_g}\right)$$
$$= \frac{V_t E_g (j\cos\delta + \sin\delta) - jV_t^2}{X_g} \tag{6.7.2}$$

The real and reactive powers delivered are then

$$P = \text{Re}\, S = \frac{V_t E_g}{X_g}\sin\delta \tag{6.7.3}$$

$$Q = \text{Im}\, S = \frac{V_t}{X_g}(E_g\cos\delta - V_t) \tag{6.7.4}$$

Equation (6.7.3) shows that the real power P increases when the power angle δ increases. From an operational standpoint, when the prime mover increases the power input to the generator while the excitation voltage is held constant, the rotor speed increases. As the rotor speed increases, the power angle δ also increases, causing an increase in generator real power output P. There is also a decrease in reactive power output Q, given by (6.7.4). However, when δ is less than 15°, the increase in P is much larger than the decrease in Q. From the power flow standpoint, an increase in prime-move power corresponds to an increase in P at the constant-voltage bus to

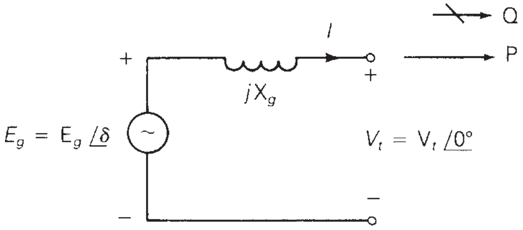

FIGURE 6.7 Generator Thévenin equivalent

Copyright 2017 Cengage Learning. All Rights Reserved. May not be copied, scanned, or duplicated, in whole or in part. Due to electronic rights, some third party content may be suppressed from the eBook and/or eChapter(s). Editorial review has deemed that any suppressed content does not materially affect the overall learning experience. Cengage Learning reserves the right to remove additional content at any time if subsequent rights restrictions require it.

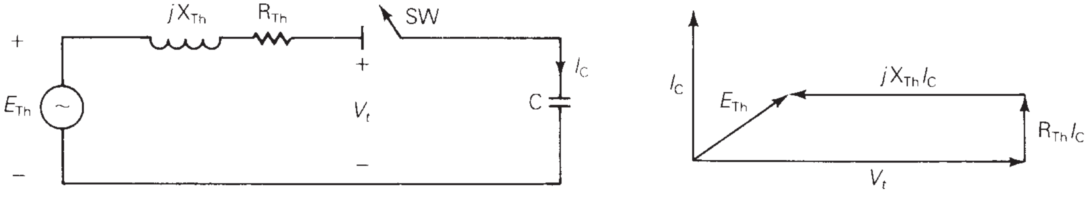

(a) Equivalent circuit (b) Phasor diagram with switch SW closed

FIGURE 6.8

Effect of adding a shunt capacitor bank to a power system bus

which the generator is connected. The power flow program computes the increase in δ along with the small change in Q.

Equation (6.7.4) shows that reactive power output Q increases when the excitation voltage E_g increases. From the operational standpoint, when the generator exciter output increases while holding the prime-mover power constant, the rotor current increases. As the rotor current increases, the excitation voltage E_g also increases, causing an increase in generator reactive power output Q. There is also a small decrease in δ required to hold P constant in (6.7.3). From the power flow standpoint, an increase in generator excitation corresponds to an increase in voltage magnitude at the constant-voltage bus to which the generator is connected. The power flow program computes the increase in reactive power Q supplied by the generator along with the small change in δ.

Figure 6.8 shows the effect of adding a shunt capacitor bank to a power system bus. The system is modeled by its Thévenin equivalent. Before the capacitor bank is connected, the switch SW is open and the bus voltage equals E_{Th}. After the bank is connected, SW is closed, and the capacitor current I_C leads the bus voltage V_t by 90°. The phasor diagram shows that V_t is larger than E_{Th} when SW is closed. From the power flow standpoint, the addition of a shunt capacitor bank to a load bus corresponds to the addition of a negative reactive load, since a capacitor absorbs negative reactive power. The power flow program computes the increase in bus voltage magnitude along with the small change in δ. Similarly, the addition of a shunt reactor corresponds to the addition of a positive reactive load, wherein the power flow program computes the decrease in voltage magnitude.

Tap-changing and voltage-magnitude-regulating transformers are used to control bus voltages as well as reactive power flows on lines to which they are connected. Similarly, phase-angle regulating transformers are used to control bus angles as well as real power flows on lines to which they are connected. Both tap-changing and regulating transformers are modeled by a transformer with an off-nominal turns ratio c (Figure 3.25). From the power flow standpoint, a change in tap setting or voltage regulation corresponds to a change in c. The power flow program computes the changes in $\boldsymbol{Y}_{bus}$, bus voltage magnitudes and angles, and branch flows.

Besides the above controls, the power flow program can be used to investigate the effect of switching in or out lines, transformers, loads, and generators. Proposed

Copyright 2017 Cengage Learning. All Rights Reserved. May not be copied, scanned, or duplicated, in whole or in part. Due to electronic rights, some third party content may be suppressed from the eBook and/or eChapter(s). Editorial review has deemed that any suppressed content does not materially affect the overall learning experience. Cengage Learning reserves the right to remove additional content at any time if subsequent rights restrictions require it.

system changes to meet future load growth, including new transmission, new transformers, and new generation can also be investigated. Power flow design studies are normally conducted by trial and error. Using engineering judgment, adjustments in generation levels and controls are made until the desired equipment loadings and voltage profile are obtained.

EXAMPLE 6.14

Power flow program: effect of shunt capacitor banks

Determine the effect of adding a 200-Mvar shunt capacitor bank at bus 2 on the power system in Example 6.9.

SOLUTION

Open PowerWorld Simulator case Example 6_14 (see Figure 6.9). This case is identical to Example 6.9 except that a 200-Mvar shunt capacitor bank has been added at bus 2. Initially this capacitor is open. Click on the capacitor's circuit to close the capacitor and then solve the case. The capacitor increases the bus 2 voltage from 0.834 per unit to a more acceptable 0.959 per unit. The insertion of the capacitor has also substantially decreased the losses, from 34.84 to 25.37 MW.

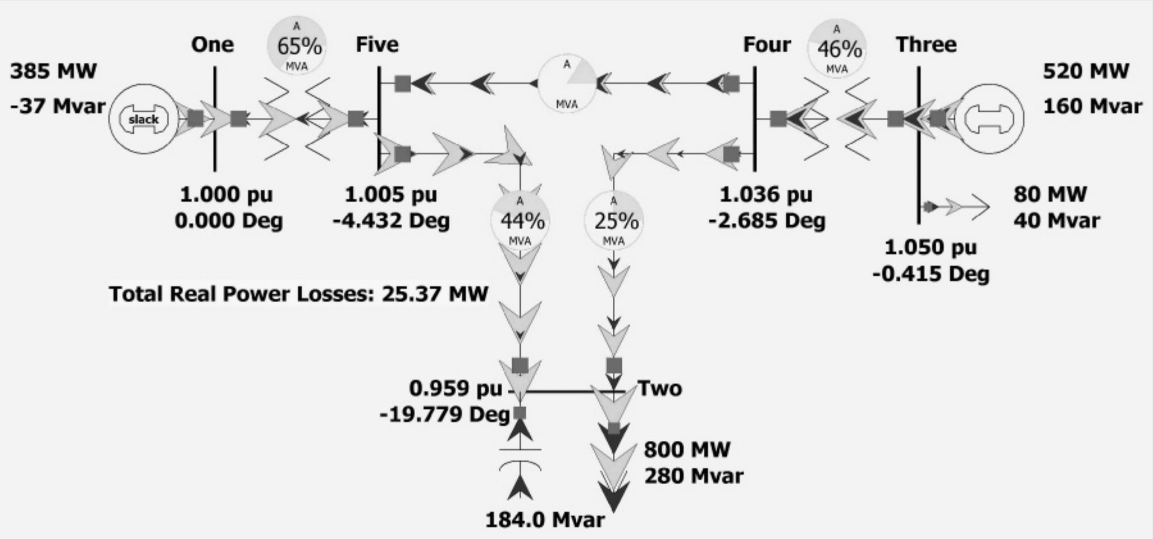
One
Five
Four
Three
385 MW
-37 Mvar
slack
65%
MVA
46%
MVA
MVA
520 MW
160 Mvar
1.000 pu
0.000 Deg
1.005 pu
-4.432 Deg
44%
MVA
25%
MVA
1.036 pu
-2.685 Deg
80 MW
40 Mvar
1.050 pu
-0.415 Deg
Total Real Power Losses: 25.37 MW
0.959 pu
-19.779 Deg
Two
800 MW
280 Mvar
184.0 Mvar

FIGURE 6.9

Screen for Example 6.14

(Continued)

Copyright 2017 Cengage Learning. All Rights Reserved. May not be copied, scanned, or duplicated, in whole or in part. Due to electronic rights, some third party content may be suppressed from the eBook and/or eChapter(s). Editorial review has deemed that any suppressed content does not materially affect the overall learning experience. Cengage Learning reserves the right to remove additional content at any time if subsequent rights restrictions require it.

Notice that the amount of reactive power actually supplied by the capacitor is only 184 Mvar. This discrepancy arises because a capacitor's reactive output varies with the square of the terminal voltage, $Q_{cap} = V_{cap}^2/X_c$ (see 2.3.5). A capacitor's Mvar rating is based on an assumed voltage of 1.0 per unit.

EXAMPLE 6.15

PowerWorld Simulator Case Example 6_15 (see Figure 6.10) modifies the Example 6.13 case by (1) opening one of the 138/69 kV transformers at the PEACH substation and (2) opening the 69-kV transmission line between CHERRY69 and OLIVE69. This causes a flow of 116 MVA on the remaining 138/69 kV

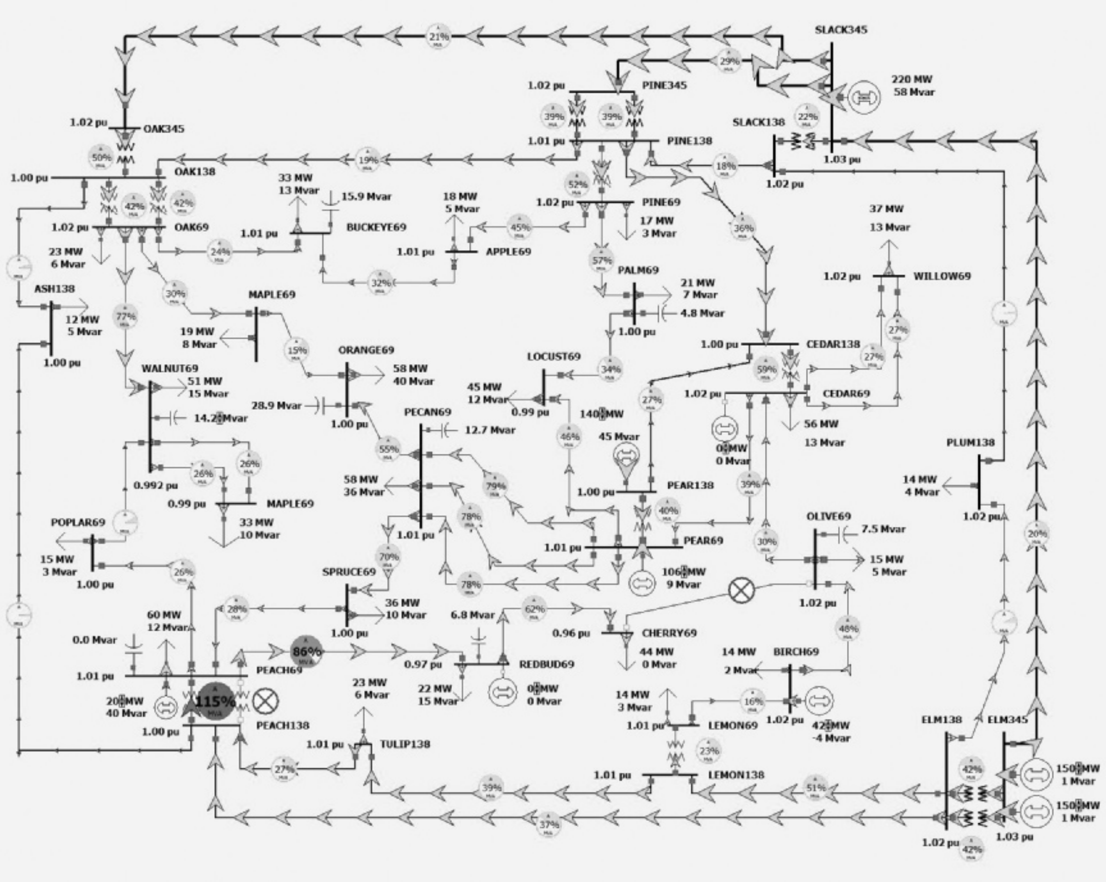
SLACK345
220 MW
58 Mvar
21%
29%
1.02 pu
PINE345
39%
39%
SLACK138
22%
1.01 pu
PINE138
1.03 pu
1.02 pu
OAK345
50%
19%
18%
1.00 pu
OAK138
1.02 pu
33 MW
13 Mvar
15.9 Mvar
18 MW
5 Mvar
52%
1.02 pu
PINE69
42%
42%
1.02 pu
OAK69
1.01 pu
BUCKEYE69
45%
17 MW
3 Mvar
36%
37 MW
13 Mvar
23 MW
6 Mvar
24%
1.01 pu
APPLE69
57%
PALM69
1.02 pu
WILLOW69
ASH138
32%
21 MW
7 Mvar
30%
MAPLE69
4.8 Mvar
12 MW
5 Mvar
77%
19 MW
8 Mvar
1.00 pu
1.00 pu
CEDAR138
27%
1.00 pu
15%
ORANGE69
LOCUST69
34%
27%
59%
WALNUT69
58 MW
40 Mvar
51 MW
15 Mvar
45 MW
12 Mvar
27%
1.02 pu
CEDAR69
28.9 Mvar
0.99 pu
14.2 Mvar
1.00 pu
PECAN69
140 MW
56 MW
12.7 Mvar
46%
45 Mvar
0 MW
0 Mvar
13 Mvar
PLUM138
55%
26%
26%
58 MW
36 Mvar
79%
1.00 pu
PEAR138
39%
14 MW
4 Mvar
0.992 pu
0.99 pu
MAPLE69
78%
40%
1.02 pu
POPLAR69
33 MW
10 Mvar
1.01 pu
OLIVE69
7.5 Mvar
1.01 pu
PEAR69
30%
20%
15 MW
3 Mvar
70%
15 MW
5 Mvar
1.00 pu
26%
SPRUCE69
106 MW
9 Mvar
78%
60 MW
12 Mvar
28%
36 MW
10 Mvar
6.8 Mvar
62%
1.02 pu
1.00 pu
0.96 pu
CHERRY69
48%
0.0 Mvar
86%
0.97 pu
44 MW
0 Mvar
14 MW
2 Mvar
BIRCH69
PEACH69
REDBUD69
1.01 pu
23 MW
6 Mvar
22 MW
15 Mvar
0 MW
0 Mvar
14 MW
3 Mvar
16%
20 MW
40 Mvar
115%
1.02 pu
42 MW
-4 Mvar
1.00 pu
PEACH138
1.01 pu
LEMON69
ELM138
ELM345
1.01 pu
TULIP138
23%
27%
1.01 pu
LEMON138
42%
150 MW
1 Mvar
39%
51%
150 MW
1 Mvar
37%
1.02 pu
42%
1.03 pu

FIGURE 6.10

Screen for Example 6.15

Copyright 2017 Cengage Learning. All Rights Reserved. May not be copied, scanned, or duplicated, in whole or in part. Due to electronic rights, some third party content may be suppressed from the eBook and/or eChapter(s). Editorial review has deemed that any suppressed content does not materially affect the overall learning experience. Cengage Learning reserves the right to remove additional content at any time if subsequent rights restrictions require it.

transformer at PEACH. Since this transformer has a limit of 101 MVA, it results in an overload at 115%. Redispatch the generators in order to remove this overload.

SOLUTION

There are a number of solutions to this problem and several solution techniques. One solution technique would be to use engineering intuition, along with a trial-and-error approach (see Figure 6.11). Since the overload is from the 138 kV level to the 69 kV level and there is a generator directly connected to at the PEACH 69 kV bus, it stands to reason that increasing this generation would decrease the overload. Using this approach, the overload is removed by increasing the PEACH generation until the transformer flow is reduced to 100%. This occurs when the generation is increased from 20 MW to 51 MW. Notice that as the generation is

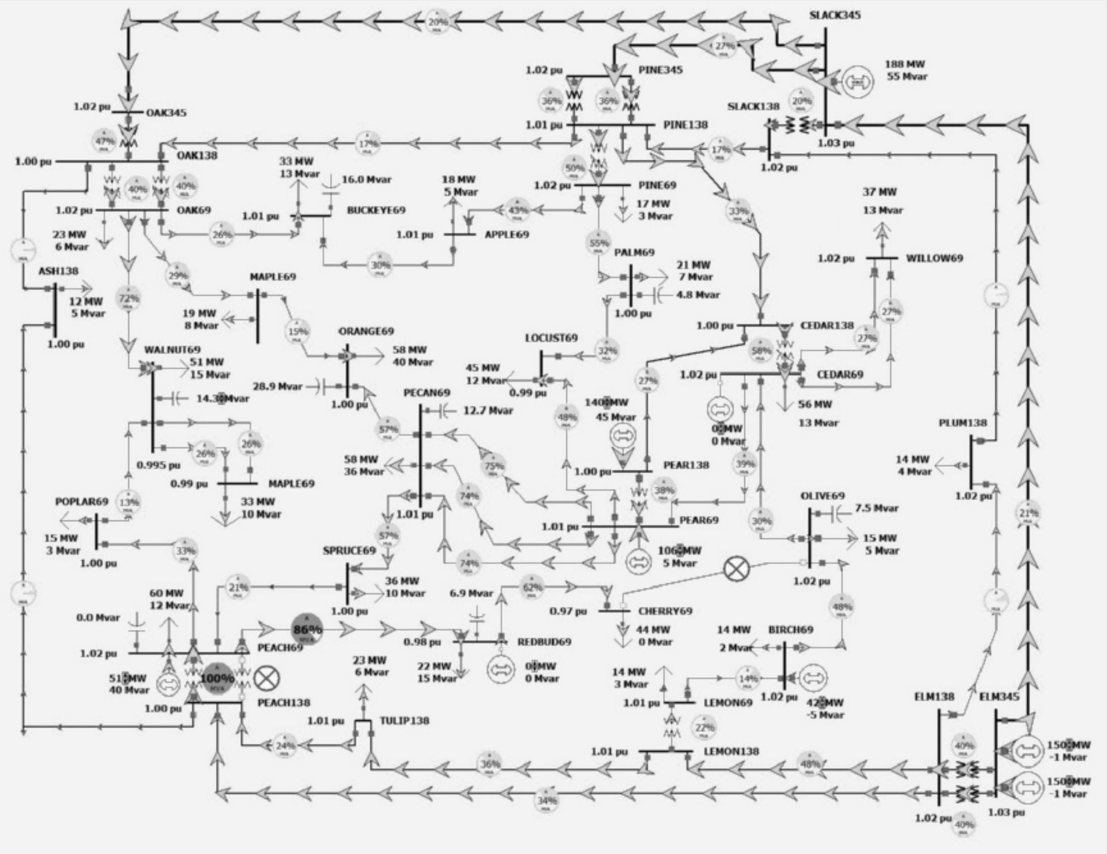

SLACK345
188 MW
55 Mvar
20%
27%
1.02 pu
PINE345
36%
36%
SLACK138
20%
1.01 pu
PINE138
1.03 pu
17%
1.02 pu
1.02 pu
OAK345
47%
17%
1.00 pu
OAK138
33 MW
13 Mvar
16.0 Mvar
18 MW
5 Mvar
50%
1.02 pu
PINE69
40%
40%
17 MW
3 Mvar
1.02 pu
OAK69
1.01 pu
BUCKEYE69
43%
33%
37 MW
13 Mvar
23 MW
6 Mvar
26%
1.01 pu
APPLE69
55%
PALM69
1.02 pu
WILLOW69
ASH138
29%
30%
21 MW
7 Mvar
MAPLE69
4.8 Mvar
12 MW
5 Mvar
72%
19 MW
8 Mvar
1.00 pu
27%
1.00 pu
15%
ORANGE69
1.00 pu
CEDAR138
27%
1.00 pu
LOCUST69
WALNUT69
58 MW
40 Mvar
32%
58%
51 MW
15 Mvar
45 MW
12 Mvar
27%
1.02 pu
CEDAR69
28.9 Mvar
0.99 pu
14.3 Mvar
1.00 pu
PECAN69
140 MW
45 Mvar
56 MW
13 Mvar
12.7 Mvar
48%
0 MW
0 Mvar
PLUM138
57%
26%
26%
58 MW
36 Mvar
75%
1.00 pu
PEAR138
39%
0.995 pu
14 MW
4 Mvar
0.99 pu
MAPLE69
38%
POPLAR69
13%
33 MW
10 Mvar
74%
OLIVE69
1.02 pu
1.01 pu
7.5 Mvar
PEAR69
21%
30%
1.01 pu
15 MW
3 Mvar
57%
15 MW
5 Mvar
1.00 pu
33%
SPRUCE69
74%
106 MW
5 Mvar
1.02 pu
60 MW
12 Mvar
21%
36 MW
10 Mvar
6.9 Mvar
62%
0.97 pu
CHERRY69
48%
0.0 Mvar
1.00 pu
86%
0.98 pu
REDBUD69
44 MW
0 Mvar
14 MW
BIRCH69
2 Mvar
1.02 pu
PEACH69
23 MW
6 Mvar
22 MW
15 Mvar
51 MW
40 Mvar
100%
0 MW
0 Mvar
14 MW
3 Mvar
14%
PEACH138
1.01 pu
LEMON69
1.02 pu
42 MW
-5 Mvar
ELM138
ELM345
1.00 pu
1.01 pu
TULIP138
22%
24%
1.01 pu
LEMON138
40%
150 MW
-1 Mvar
36%
48%
150 MW
-1 Mvar
34%
1.02 pu
40%
1.03 pu

FIGURE 6.11

A solution to Example 6.15

(Continued)

Copyright 2017 Cengage Learning. All Rights Reserved. May not be copied, scanned, or duplicated, in whole or in part. Due to electronic rights, some third party content may be suppressed from the eBook and/or eChapter(s). Editorial review has deemed that any suppressed content does not materially affect the overall learning experience. Cengage Learning reserves the right to remove additional content at any time if subsequent rights restrictions require it.

increased, the slack bus (SLACK345) generation automatically decreases in order to satisfy the requirement that total system load plus losses must be equal to total generation.

An alternative possible solution is seen by noting that, since the overload is caused by power flowing from the 138 kV bus, decreasing the generation at ELM345 might also decrease this flow. This is indeed the case, but now the trial-and-error approach requires a substantial amount of work and ultimately doesn't solve the problem. Even when the total ELM345 generation is decreased from 300 MW to 0 MW, the overload is still present, albeit with its percentage decreased to 105%.

Another solution approach would be to first determine the generators with the most sensitivity to this violation and then adjust these (see Figure 6.12). This

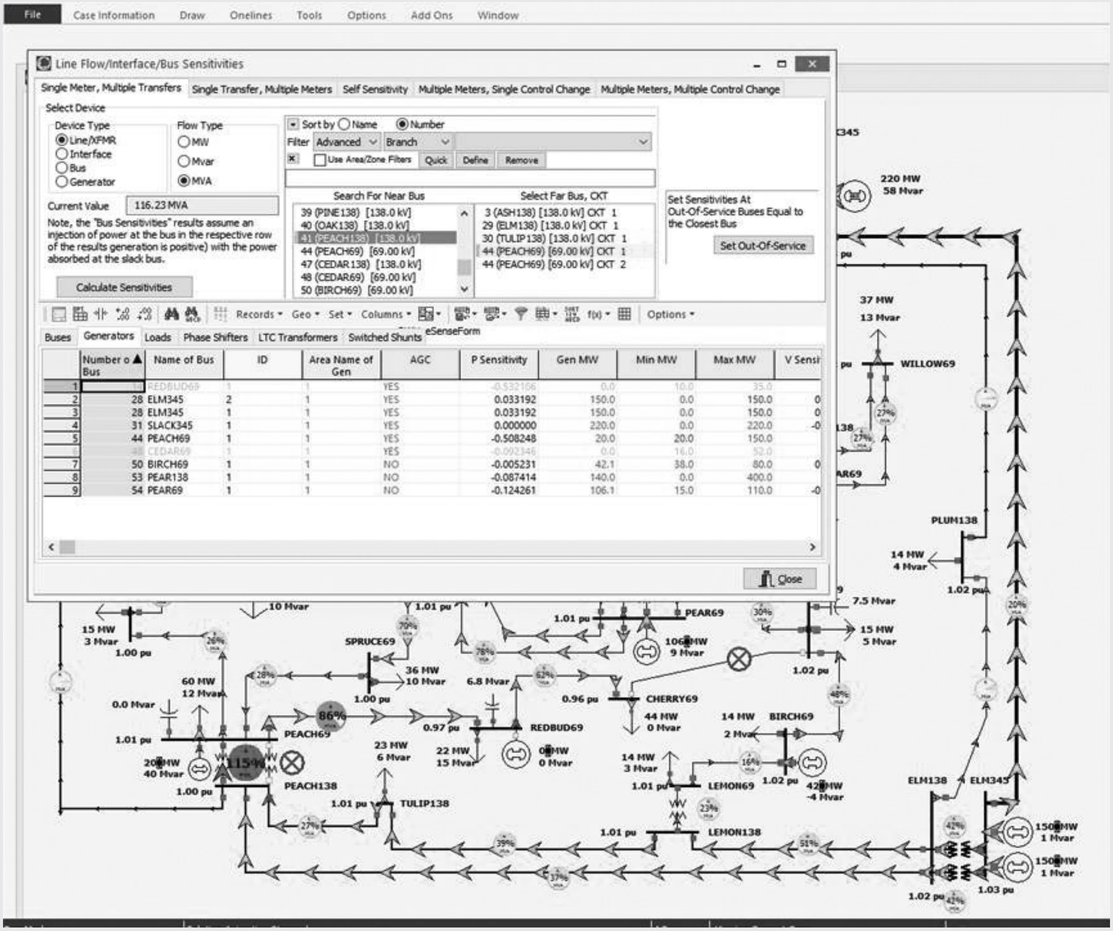
File
Case Information
Draw
Onelines
Tools
Options
Add Ons
Window
Line Flow/Interface/Bus Sensitivities
Single Meter, Multiple Transfers
Single Transfer, Multiple Meters
Self Sensitivity
Multiple Meters, Single Control Change
Multiple Meters, Multiple Control Change
Select Device
Device Type
Flow Type
Sort by
Filter
Quick
Define
Remove
Search For Near Bus
Select Far Bus, CKT
Calculate Sensitivities
Set Out-Of-Service
Records
Geo
Set
Columns
f(x)
Options
eSenseForm
Buses
Generators
Loads
Phase Shifters
LTC Transformers
Switched Shunts
Close
220 MW
58 Mvar
37 MW
13 Mvar
WILLOW69
PLUM138
14 MW
4 Mvar
1.02 pu
7.5 Mvar
15 MW
5 Mvar
1.02 pu
PEAR69
106 MW
9 Mvar
1.01 pu
15 MW
3 Mvar
1.00 pu
10 Mvar
1.01 pu
SPRUCE69
36 MW
10 Mvar
6.8 Mvar
60 MW
12 Mvar
0.0 Mvar
1.00 pu
0.96 pu
CHERRY69
44 MW
0 Mvar
14 MW
2 Mvar
BIRCH69
1.01 pu
PEACH69
0.97 pu
REDBUD69
20 MW
40 Mvar
23 MW
6 Mvar
22 MW
15 Mvar
0 MW
0 Mvar
14 MW
3 Mvar
1.00 pu
PEACH138
1.01 pu
LEMON69
1.02 pu
42 MW
-4 Mvar
ELM138
ELM345
1.01 pu
TULIP138
1.01 pu
LEMON138
150 MW
1 Mvar
150 MW
1 Mvar
1.02 pu
1.03 pu
86%
115%
70%
78%
62%
28%
26%
30%
27%
27%
16%
23%
39%
37%
51%
42%
42%
48%
20%

Device Type: ● Line/XFMR ○ Interface ○ Bus ○ Generator

Flow Type: ○ MW ○ Mvar ● MVA

Sort by ○ Name ● Number

Filter: Advanced | Branch

☐ Use Area/Zone Filters

Current Value: 116.23 MVA

Note, the "Bus Sensitivities" results assume an injection of power at the bus in the respective row of the results generation is positive) with the power absorbed at the slack bus.

Search For Near Bus:
39 (PINE138) [138.0 kV]
40 (OAK138) [138.0 kV]
41 (PEACH138) [138.0 kV]
44 (PEACH69) [69.00 kV]
47 (CEDAR138) [138.0 kV]
48 (CEDAR69) [69.00 kV]
50 (BIRCH69) [69.00 kV]

Select Far Bus, CKT:
3 (ASH138) [138.0 kV] CKT 1
29 (ELM138) [138.0 kV] CKT 1
30 (TULIP138) [138.0 kV] CKT 1
44 (PEACH69) [69.00 kV] CKT 1
44 (PEACH69) [69.00 kV] CKT 2

Set Sensitivities At Out-Of-Service Buses Equal to the Closest Bus

	Number of Bus	Name of Bus	ID	Area Name of Gen	AGC	P Sensitivity	Gen MW	Min MW	Max MW	V Sensi
1	14	REDBUD69	1	1	YES	-0.532106	0.0	10.0	35.0	
2	28	ELM345	2	1	YES	0.033192	150.0	0.0	150.0	0
3	28	ELM345	1	1	YES	0.033192	150.0	0.0	150.0	0
4	31	SLACK345	1	1	YES	0.000000	220.0	0.0	220.0	-0
5	44	PEACH69	1	1	YES	-0.508248	20.0	20.0	150.0	
6	48	CEDAR69	1	1	YES	-0.092346	0.0	16.0	52.0	
7	50	BIRCH69	1	1	NO	-0.005231	42.1	38.0	80.0	0
8	53	PEAR138	1	1	NO	-0.087414	140.0	0.0	400.0	
9	54	PEAR69	1	1	NO	-0.124261	106.1	15.0	110.0	-0

FIGURE 6.12

Example 6.15 Flow Sensitivities Dialog

Copyright 2017 Cengage Learning. All Rights Reserved. May not be copied, scanned, or duplicated, in whole or in part. Due to electronic rights, some third party content may be suppressed from the eBook and/or eChapter(s). Editorial review has deemed that any suppressed content does not materially affect the overall learning experience. Cengage Learning reserves the right to remove additional content at any time if subsequent rights restrictions require it.

can be done in PowerWorld Simulator by selecting **Tools, Sensitivities, Flows and Voltage Sensitivities** to calculate sensitivities. On the top of the page, select the PEACH138 to PEACH69 circuit 1 transformer; then click on the **Calculate Sensitivities** button, and select the Generator Sensitivities tab towards the bottom of the dialog. The "P Sensitivity" field tells how increasing the output of each generator by one MW would affect the MVA flow on this transformer. Note that the sensitivity for the PEACH69 generator is −0.508, indicating that if this generation is increased by 1 MW, the transformer MVA flow would decrease by 0.508 MVA. Hence, in order to decrease the flow by 15.2 MVA, increase the PEACH69 generator by 30 MW, which is exactly what was gotten by the trial-and-error approach. It is also clear that the ELM345 generators, with a sensitivity of just 0.033, would be relatively ineffective. In actual power system operation, these sensitivities, known as generator shift factors, are used extensively. These sensitivities are also used in the Optimal Power Flow (introduced in Section 6.13).

6.8 SPARSITY TECHNIQUES

A typical large power system has an average of fewer than three lines connected to each bus. As such, each row of Y_{bus} has an average of fewer than four nonzero elements: one off-diagonal for each line and the diagonal. Such a matrix, which has only a few nonzero elements, is said to be *sparse*.

Newton-Raphson power flow programs employ sparse matrix techniques to reduce computer storage and time requirements [2]. These techniques include compact storage of Y_{bus} and $\mathbf{J}(i)$ and reordering of buses to avoid fill-in of $\mathbf{J}(i)$ during Gauss elimination steps. Consider the following matrix:

$$\mathbf{S} = \begin{bmatrix} 1.0 & -1.1 & -2.1 & -3.1 \\ -4.1 & 2.0 & 0 & -5.1 \\ -6.1 & 0 & 3.0 & 0 \\ -7.1 & 0 & 0 & 4.0 \end{bmatrix} \tag{6.8.1}$$

One method for compact storage of S consists of the following four vectors:

$$\mathbf{DIAG} = [1.0\ 2.0\ 3.0\ 4.0] \tag{6.8.2}$$

$$\mathbf{OFFDIAG} = [1.1\ -2.1\ -3.1\ -4.1\ -5.1\ -6.1\ -7.1] \tag{6.8.3}$$

$$\mathbf{COL} = [2\ 3\ 4\ 1\ 4\ 1\ 1] \tag{6.8.4}$$

$$\mathbf{ROW} = [3\ 2\ 1\ 1] \tag{6.8.5}$$

Copyright 2017 Cengage Learning. All Rights Reserved. May not be copied, scanned, or duplicated, in whole or in part. Due to electronic rights, some third party content may be suppressed from the eBook and/or eChapter(s). Editorial review has deemed that any suppressed content does not materially affect the overall learning experience. Cengage Learning reserves the right to remove additional content at any time if subsequent rights restrictions require it.

DIAG contains the ordered diagonal elements and **OFFDIAG** contains the nonzero off-diagonal elements of **S**. **COL** contains the column number of each off-diagonal element. For example, the *fourth* element in **COL** is 1, indicating that the *fourth* element of **OFFDIAG**, −4.1, is located in column 1. **ROW** indicates the number of off-diagonal elements in each row of **S**. For example, the *first* element of **ROW** is 3, indicating the *first* three elements of **OFFDIAG**, −1.1, −2.1, and −3.1, are located in the *first* row. The *second* element of **ROW** is 2, indicating the next two elements of **OFFDIAG**, −4.1 and −5.1, are located in the *second* row. The **S** matrix can be completely reconstructed from these four vectors. Note that the dimension of **DIAG** and **ROW** equals the number of diagonal elements of **S**, whereas the dimension of **OFFDIAG** and **COL** equals the number of nonzero off-diagonals.

Now assume that computer storage requirements are 4 bytes to store each magnitude and 4 bytes to store each phase entry in Y_{bus} in an N-bus power system. Also assume Y_{bus} has an average of $3N$ nonzero off-diagonals (three lines per bus) along with its N diagonals. Using the preceding compact storage technique, $(4 + 4)3N = 24N$ bytes are required for **OFFDIAG** and $(4 + 4)N = 8N$ bytes for **DIAG**. Also, assuming 2 bytes to store each integer, $6N$ bytes are required for **COL** and $2N$ bytes for **ROW**. Total computer memory required is then $(24 + 8 + 6 + 2)N = 40N$ bytes with compact storage of Y_{bus}, compared to $8N^2$ bytes without compact storage. For a 1000-bus power system, this means 40 instead of 8000 kilobytes to store Y_{bus}.

The Jacobian matrix is also sparse. From Table 6.5, whenever $Y_{kn} = 0$, $\text{J1}_{kn} = \text{J2}_{kn} = \text{J3}_{kn} = \text{J4}_{kn} = 0$. Compact storage of **J** for a 30,000-bus power system requires less than 10 megabytes with the above assumptions.

The other sparsity technique is to reorder buses. Suppose Gauss elimination is used to triangularize **S** in (6.8.1). After one Gauss elimination step, as described in Section 6.1, the result is

$$\mathbf{S}^{(1)} = \begin{bmatrix} 1.0 & -1.1 & -2.1 & -3.1 \\ 0 & -2.51 & -8.61 & -7.61 \\ 0 & -6.71 & -9.81 & -18.91 \\ 0 & -7.81 & -14.91 & -18.01 \end{bmatrix} \tag{6.8.6}$$

Note that the zeros in columns 2, 3, and 4 of **S** are filled in with nonzero elements in $\mathbf{S}^{(1)}$. The original degree of sparsity is lost.

One simple reordering method is to start with those buses having the fewest connected branches and to end with those having the most connected branches. For example, **S** in (6.8.1) has three branches connected to bus 1 (three off-diagonals in row 1), two branches connected to bus 2, and one branch connected to buses 3 and 4. Reordering the buses 4, 3, 2, 1 instead of 1, 2, 3, 4 results in

$$\mathbf{S}_{\text{recordered}} = \begin{bmatrix} 4.0 & 0 & 0 & -7.1 \\ 0 & 3.0 & 0 & -6.1 \\ -5.1 & 0 & 2.0 & -4.1 \\ -3.1 & -2.1 & -1.1 & 1.0 \end{bmatrix} \tag{6.8.7}$$

Copyright 2017 Cengage Learning. All Rights Reserved. May not be copied, scanned, or duplicated, in whole or in part. Due to electronic rights, some third party content may be suppressed from the eBook and/or eChapter(s). Editorial review has deemed that any suppressed content does not materially affect the overall learning experience. Cengage Learning reserves the right to remove additional content at any time if subsequent rights restrictions require it.

Now, after one Gauss elimination step,

$$\mathbf{S}^{(1)}_{\text{recorderd}} = \begin{bmatrix} 4.0 & 0 & 0 & -7.1 \\ 0 & 3.0 & 0 & -6.1 \\ 0 & 0 & 2.0 & -13.15 \\ 0 & -2.1 & -1.1 & -4.5025 \end{bmatrix} \tag{6.8.8}$$

Note that the original degree of sparsity is not lost in (6.8.8).

Reordering buses according to the fewest connected branches can be performed once, before the Gauss elimination process begins. Alternatively, buses can be renumbered during each Gauss elimination step in order to account for changes during the elimination process.

Sparsity techniques similar to those described in this section are a standard feature of today's Newton-Raphson power flow programs. As a result of these techniques, typical 30,000-bus power flow solutions require less than 10 megabytes of storage, less than one second per iteration of computer time, and less than 10 iterations to converge.

EXAMPLE 6.16

Sparsity in a 37-bus system

To see a visualization of the sparsity of the power flow Y_{bus} and Jacobian matrices in a *37*-bus system, open PowerWorld Simulator case Example 6_13. Select **Case Information, Solution Details, Ybus** to view the bus admittance matrix. Then press <ctrl> Page Down to zoom the display out. Blank entries in the matrix correspond to zero entries. The 37 × 37 Y_{bus} has a total of 1369 entries, with only about 10% nonzero (see Figure 6.13). Select **Case Information, Solution Details, Power Flow Jacobian** to view the Jacobian matrix.

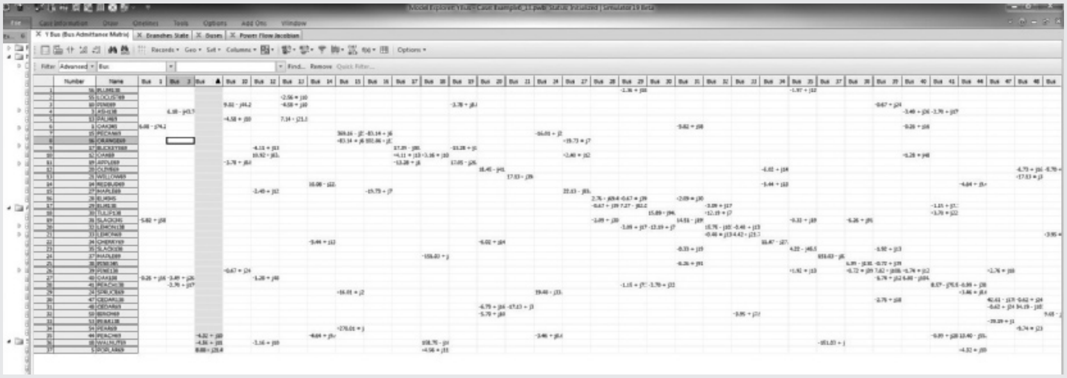

FIGURE 6.13

Screen for Example 6.16

Copyright 2017 Cengage Learning. All Rights Reserved. May not be copied, scanned, or duplicated, in whole or in part. Due to electronic rights, some third party content may be suppressed from the eBook and/or eChapter(s). Editorial review has deemed that any suppressed content does not materially affect the overall learning experience. Cengage Learning reserves the right to remove additional content at any time if subsequent rights restrictions require it.

6.9 FAST DECOUPLED POWER FLOW

Contingencies are a major concern in power system operations. For example, operating personnel need to know what power flow changes will occur due to a particular generator outage or transmission-line outage. Contingency information, when obtained in real time, can be used to anticipate problems caused by such outages and can be used to develop operating strategies to overcome the problems.

Fast power flow algorithms have been developed to give power flow solutions in seconds or less [8]. These algorithms are based on the following simplification of the Jacobian matrix. Neglecting $\mathbf{J}_2(i)$ and $\mathbf{J}_3(i)$, (6.6.6) reduces to two sets of decoupled equations:

$$\mathbf{J}_1(i)\,\boldsymbol{\Delta\delta}(i) = \Delta\mathrm{P}(i) \tag{6.9.1}$$

$$\mathbf{J}_4(i)\,\boldsymbol{\Delta}\mathbf{V}(0) = \Delta\mathbf{Q}(i) \tag{6.9.2}$$

The computer time required to solve (6.9.1) and (6.9.2) is significantly less than that required to solve (6.6.6). Further reduction in computer time can be obtained from additional simplification of the Jacobian matrix. For example, assume $\mathrm{V}_k \approx \mathrm{V}_n \approx 1.0$ per unit and that the angle differences are small so the sin terms can be ignored. Then $\mathbf{J}_1$ and $\mathbf{J}_4$ are constant matrices whose elements in Table 6.5 are the negative of the imaginary components of Y_{bus}. As such, $\mathbf{J}_1$ and $\mathbf{J}_4$ do not have to be recalculated during successive iterations.

The above simplifications can result in rapid power flow solutions for most systems. While the fast decoupled power flow usually takes more iterations to converge, it is usually significantly faster than the Newton-Raphson algorithm since the Jacobian does not need to be recomputed each iteration. And since the mismatch equations themselves have not been modified, the solution obtained by the fast decoupled algorithm is the same as that found with the Newton-Raphson algorithm. However, in some situations in which only an approximate power flow solution is needed, the fast decoupled approach can be used with a fixed number of iterations (typically one) to give an extremely fast, albeit approximate solution.

6.10 THE "DC" POWER FLOW

The power flow problem can be further simplified by extending the fast decoupled power flow to completely neglect the Q-V equations by assuming that the voltage magnitudes are constant at 1.0 per unit. With these simplifications, the power flow on the line from bus j to bus k with reactance X_{jk} becomes

Copyright 2017 Cengage Learning. All Rights Reserved. May not be copied, scanned, or duplicated, in whole or in part. Due to electronic rights, some third party content may be suppressed from the eBook and/or eChapter(s). Editorial review has deemed that any suppressed content does not materially affect the overall learning experience. Cengage Learning reserves the right to remove additional content at any time if subsequent rights restrictions require it.

$$P_{jk} = \frac{\delta_j - \delta_k}{X_{jk}} \tag{6.10.1}$$

and the real power balance equations reduce to a completely linear problem

$$-\mathbf{B}\boldsymbol{\delta} = \mathbf{P} \tag{6.10.2}$$

where **B** is the imaginary component of the of Y_{bus} calculated neglecting line resistance and excepting the slack bus row and column and **P** is the vector of real power injections (with generation assumed positive).

Because (6.10.2) is a linear equation with a form similar to that found in solving dc resistive circuits, this technique is referred to as the dc power flow. However, in contrast to the previous power flow algorithms, the dc power flow only gives an approximate solution with the degree of approximation system dependent. Nevertheless, with the advent of power system restructuring, the dc power flow has become a commonly used analysis technique.

EXAMPLE 6.17

Determine the dc power flow solution for the five bus system from Example 6.9.

SOLUTION

With bus 1 as the system slack, the **B** matrix and **P** vector for this system are

$$\mathbf{B} = \begin{bmatrix} -30 & 0 & 10 & 20 \\ 0 & -100 & 100 & 0 \\ 10 & 100 & -150 & 40 \\ 20 & 0 & 40 & -110 \end{bmatrix} \quad \mathbf{P} = \begin{bmatrix} -8.0 \\ 4.4 \\ 0 \\ 0 \end{bmatrix}$$

$$\boldsymbol{\delta} = -\mathbf{B}^{-1}\mathbf{P} = \begin{bmatrix} -0.3263 \\ 0.0091 \\ -0.0349 \\ -0.0720 \end{bmatrix} \text{radians} = \begin{bmatrix} -18.70 \\ 0.5214 \\ -2.000 \\ -4.125 \end{bmatrix} \text{degrees}$$

To view this example in PowerWorld Simulator, open case Example 6_17, which has this example solved using the dc power flow (see Figure 6.14). To view the dc power flow options, select **Options, Simulator Options** to show the PowerWorld Simulator Options dialog. Then select the Power Flow Solution category and the DC Options page.

(*Continued*)

Copyright 2017 Cengage Learning. All Rights Reserved. May not be copied, scanned, or duplicated, in whole or in part. Due to electronic rights, some third party content may be suppressed from the eBook and/or eChapter(s). Editorial review has deemed that any suppressed content does not materially affect the overall learning experience. Cengage Learning reserves the right to remove additional content at any time if subsequent rights restrictions require it.

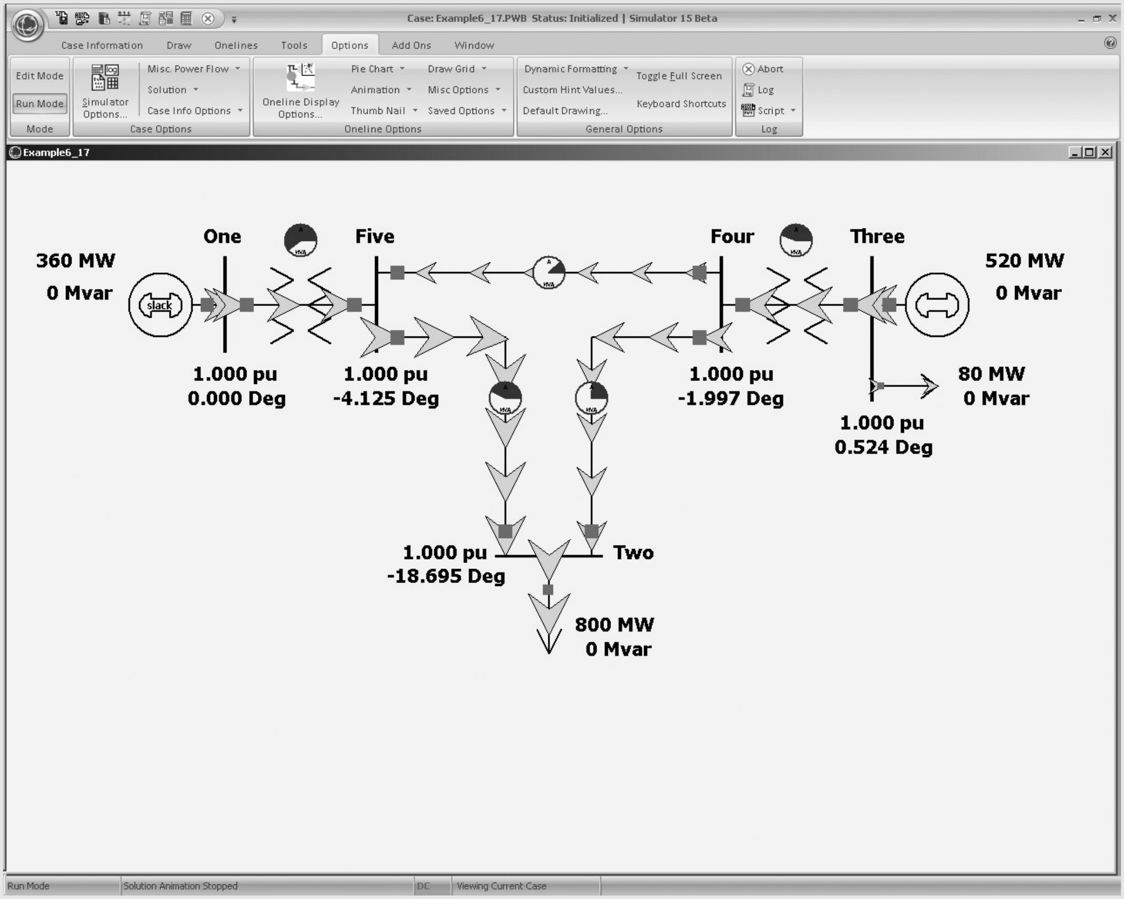
Case: Example6_17.PWB Status: Initialized | Simulator 15 Beta
Case Information
Draw
Onelines
Tools
Options
Add Ons
Window
Edit Mode
Run Mode
Mode
Simulator Options...
Misc. Power Flow
Solution
Case Info Options
Case Options
Oneline Display Options...
Pie Chart
Animation
Thumb Nail
Draw Grid
Misc Options
Saved Options
Oneline Options
Dynamic Formatting
Custom Hint Values...
Default Drawing...
Toggle Full Screen
Keyboard Shortcuts
General Options
Abort
Log
Script
Log
Example6_17
One
Five
Four
Three
Two
360 MW
0 Mvar
slack
1.000 pu
0.000 Deg
1.000 pu
-4.125 Deg
1.000 pu
-1.997 Deg
520 MW
0 Mvar
80 MW
0 Mvar
1.000 pu
0.524 Deg
1.000 pu
-18.695 Deg
800 MW
0 Mvar
MVA
Run Mode
Solution Animation Stopped
DC
Viewing Current Case

FIGURE 6.14

Screen for Example 6.17

6.11 POWER FLOW MODELING OF WIND GENERATION

As was mentioned in Chapter 1, the amount of renewable generation, particularly wind, being integrated into electric grids around the world is rapidly growing. For example, in 2013 Denmark obtained 33% of their total electric energy from wind while Spain got over 20%. In the United States the amount of wind capacity has been rapidly escalating from less than 2.5 GW in 2000 to more than 68 GW in 2015 (out of a total generation capacity of about 1065 GW), while worldwide, it was more than 360 GW in 2014.

Copyright 2017 Cengage Learning. All Rights Reserved. May not be copied, scanned, or duplicated, in whole or in part. Due to electronic rights, some third party content may be suppressed from the eBook and/or eChapter(s). Editorial review has deemed that any suppressed content does not materially affect the overall learning experience. Cengage Learning reserves the right to remove additional content at any time if subsequent rights restrictions require it.

Whereas most energy from traditional synchronous generators comes from large units with ratings of hundreds of MWs, comparatively speaking, individual wind turbine generator (WTG) power ratings are quite low, with common values for new land-based WTGs between one to three MWs, and offshore WTGs up to 6 MWs. This power is generated at low voltage (e.g., 600 V) and then usually stepped-up with a pad-mounted transformer at the base of the turbine to a distribution-level voltage (e.g., 34.5 kV). Usually dozens or even hundreds of individual WTGs are located in wind "farms" or "parks" that cover an area of many square miles, with most of the land still available for other uses such as farming. An underground and/or overhead collector system is used to transmit the power to a single interconnection point at which its voltage is stepped-up to a transmission level voltage (> 100 kV). The layout of such a system is shown in Figure 6.15.

From a power system analysis perspective for large-scale studies, the entire wind farm can usually be represented as a single equivalent generator that is either directly connected at the interconnection point transmission system bus or connected to this bus through an equivalent impedance that represents the impedance of the collector system and the step-up transformers. The parameters associated with the equivalent generator are usually just scaled values of the parameters for the individual WTGs.

There are four main types of WTGs [13,15] with more details on each type provided in Chapter 11. Here the focus is on their power flow characteristics. As is the case with traditional synchronous generators, the real power outputs for all the WTG types are considered to be a constant value in power flow studies. Of course how much real power a wind farm can actually produce at any moment depends upon the wind speed, with a typical wind speed versus power curve shown in Figure 6.16.

Type 1 WTGs are squirrel-cage induction machines. Since induction machines consume reactive power and their reactive power output cannot be independently

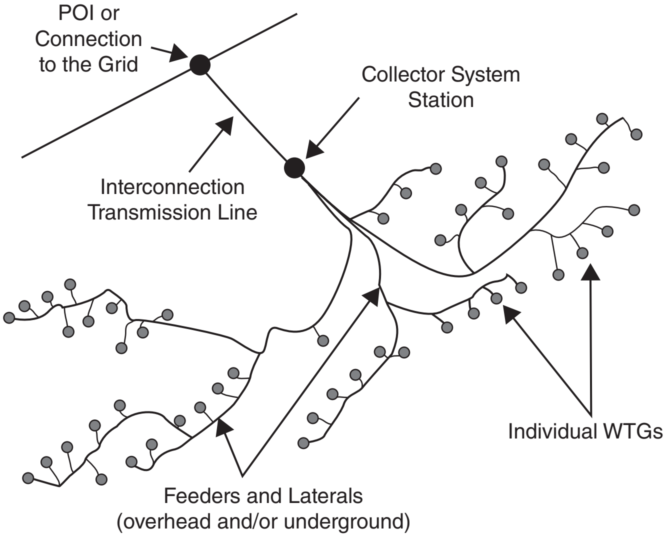

FIGURE 6.15

Wind power plant collector system topology [14] (Figure 1 from WECC Wind Generation Modeling Group, "WECC Wind Power Plant Power Flow Model Guide," WECC, May 2008, p. 2.)

Copyright 2017 Cengage Learning. All Rights Reserved. May not be copied, scanned, or duplicated, in whole or in part. Due to electronic rights, some third party content may be suppressed from the eBook and/or eChapter(s). Editorial review has deemed that any suppressed content does not materially affect the overall learning experience. Cengage Learning reserves the right to remove additional content at any time if subsequent rights restrictions require it.

FIGURE 6.16

Typical wind speed versus power curve

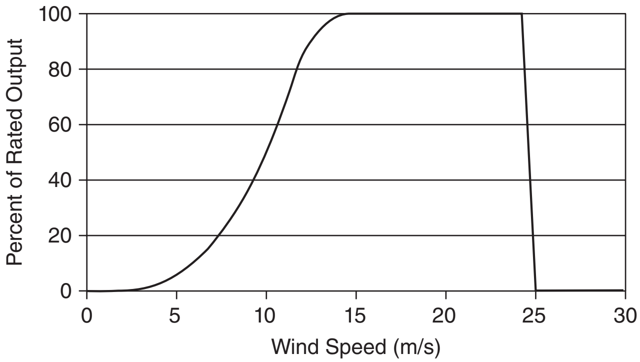

controlled, typically these machines are modeled as a constant power factor PQ bus. By themselves these machines have under-excited (consuming reactive power) power factors of between 0.85 and 0.9, but banks of switched capacitors are often used to correct the wind farm power factor. Type 2 WTGs are wound rotor induction machines in which the rotor resistance can be controlled. The advantages of this approach are discussed in Chapter 11; from a power flow perspective, they perform like Type 1 WTGs.

Most of the installed wind capacity and almost all new WTGs are either Type 3 or Type 4. Type 3 wind turbines are used to represent doubly-fed asynchronous generators (DFAGs), also sometimes referred to as doubly-fed induction generators (DFIGs). This type models induction machines in which the rotor circuit is also connected to the ac network through an ac-dc-ac converter, allowing for much greater control of the WTG. Type 4 wind turbines are fully asynchronous machines in which the full power output of the machine is coupled to the ac network through an ac-dc-ac converter. From a power flow perspective, both types are capable of full voltage control like a traditional bus generator with reactive power control between a power factor of up to ±0.9. However, like traditional synchronous generators, how their reactive power is actually controlled depends on commercial considerations, with many generator owners desiring to operate at unity power factor to maximize their real power outputs.

6.12 ECONOMIC DISPATCH

This section describes how the real power output of a controlled generating unit is selected to meet a given load and to minimize the total operating costs. This is the *economic dispatch* problem [16]. In interconnected power systems, economic dispatch is often solved for smaller portions of the system, known as *areas*, in which the total generation in each area is controlled to match the total area load; further details are provided in Chapter 12.

This section begins by considering only fossil-fuel generating units, with no constraints on maximum and minimum generator outputs, and with no transmission losses. The economic dispatch problem is first solved for this idealized case. Then it is

Copyright 2017 Cengage Learning. All Rights Reserved. May not be copied, scanned, or duplicated, in whole or in part. Due to electronic rights, some third party content may be suppressed from the eBook and/or eChapter(s). Editorial review has deemed that any suppressed content does not materially affect the overall learning experience. Cengage Learning reserves the right to remove additional content at any time if subsequent rights restrictions require it.

expanded to include inequality constraints on generator outputs and to consider the impact of transmission losses. Finally, the dispatch of other types of units including solar and wind, nuclear, pumped-storage hydro, and hydro units is briefly discussed.

FOSSIL-FUEL UNITS, NO INEQUALITY CONSTRAINTS, NO TRANSMISSION LOSSES

Figure 6.17 shows the operating cost C_i, of a fossil-fuel generating unit versus its real power output P_i. Fuel cost is the major portion of the variable cost of operation, although other variable costs, such as maintenance, could have been included in the figure. Fixed costs, such as the capital cost of installing the unit, are not included. Only those costs that are a function of unit power output—that is, those costs that can be controlled by operating strategy—enter into the economic dispatch formulation.

In practice, C_i is constructed of piecewise continuous functions valid for ranges of output P_i based on empirical data. The discontinuities in Figure 6.17 may be due to the firing of equipment such as additional boilers or condensers as power output is increased. It is often convenient to express C_i in terms of BTU/hr, which is relatively constant over the lifetime of the unit, rather than \$/hr, which can change monthly or daily. C_i can be converted to \$/hr by multiplying the fuel input in BTU/hr by the cost of fuel in \$/BTU.

Figure 6.18 shows the unit incremental operating cost dC_i/dP_i versus unit output P_i, which is the slope or derivative of the C_i versus P_i curve in Figure 6.17. When C_i consists of only fuel costs, dC_i/dP_i is the ratio of the incremental fuel energy input in BTU to incremental energy output in kWh, which is called the incremental *heat rate.* Note that the reciprocal of the heat rate, which is the ratio of output energy to input energy, gives a measure of fuel efficiency for the unit. For the unit shown in Figure 6.17, maximum efficiency occurs at $P_i = 600$ MW, where the heat rate is $C_i/P_i = 5.4 \times 10^9/600 \times 10^3 = 9000$ BTU/kWh. The efficiency at this output is

$$\text{percentage efficency} = \left(\frac{1}{9000}\,\frac{\text{kWh}}{\text{BTU}}\right)\left(3413\,\frac{\text{BTU}}{\text{kWh}}\right) \times 100 = 37.92\%$$

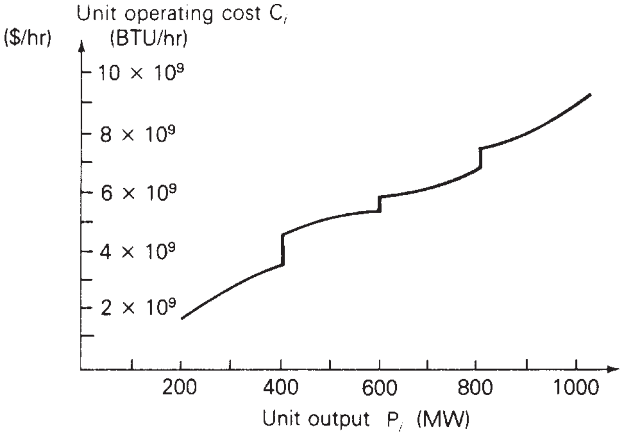

FIGURE 6.17

Unit operating cost versus real power output—fossil-fuel generating unit

Copyright 2017 Cengage Learning. All Rights Reserved. May not be copied, scanned, or duplicated, in whole or in part. Due to electronic rights, some third party content may be suppressed from the eBook and/or eChapter(s). Editorial review has deemed that any suppressed content does not materially affect the overall learning experience. Cengage Learning reserves the right to remove additional content at any time if subsequent rights restrictions require it.

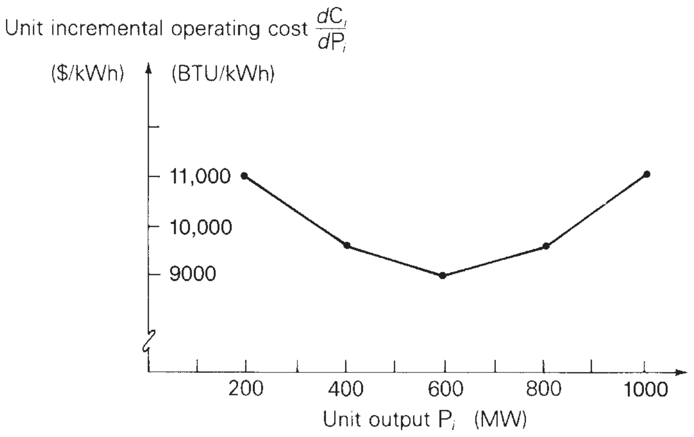

FIGURE 6.18 Unit incremental operating cost versus real power output—fossil-fuel generating unit

The dC_i/dP_i curve in Figure 6.18 is also represented by piecewise continuous functions valid for ranges of output P_i. For analytical work, the actual curves are often approximated by straight lines. The ratio dC_i/dP_i can also be converted to $/kWh by multiplying the incremental heat rate in BTU/kWh by the cost of fuel in $/BTU.

For the area of an interconnected power system consisting of N units operating on economic dispatch, the total variable cost C_T of operating these units is

$$C_T = \sum_{i=i}^{N} C_i$$

$$= C_1(P_1) + C_2(P_2) + \cdots + C_N(P_N) \quad \$/\text{hr} \tag{6.12.1}$$

where C_i, expressed in $/hr, includes fuel cost as well as any other variable costs of unit *i.* Let P_T equal the total load demand in the area. Neglecting transmission losses.

$$P_1 + P_2 + \cdots + P_N = P_T \tag{6.12.2}$$

Due to relatively slow changes in load demand, P_T may be considered constant for periods of 2 to 10 minutes. The economic dispatch problem can be stated as follows:

> Find the values of unit outputs $P_1, P_2, \ldots, P_N$ that minimize C_T given by (6.12.1), subject to the equality constraint given by (6.12.2).

A criterion for the solution to this problem is: All units on economic dispatch should operate at equal incremental operating cost. That is,

$$\frac{dC_1}{dP_1} = \frac{dC_2}{dP_2} = \cdots = \frac{dC_N}{dP_N} \tag{6.12.3}$$

An intuitive explanation of this criterion is the following. Suppose one unit is operating at a higher incremental operating cost than the other units. If the output power of that unit is reduced and transferred to units with lower incremental operating costs, then the total operating cost C_T decreases. That is, reducing the output of the unit with the *higher* incremental cost results in a *greater cost decrease* than the

Copyright 2017 Cengage Learning. All Rights Reserved. May not be copied, scanned, or duplicated, in whole or in part. Due to electronic rights, some third party content may be suppressed from the eBook and/or eChapter(s). Editorial review has deemed that any suppressed content does not materially affect the overall learning experience. Cengage Learning reserves the right to remove additional content at any time if subsequent rights restrictions require it.

cost increase of adding that same output reduction to units with lower incremental costs. Therefore, all units must operate at the same incremental operating cost (the economic dispatch criterion).

A mathematical solution to the economic dispatch problem also can be given. The minimum value of C_T occurs when the total differential dC_T is zero. That is,

$$dC_T = \frac{\partial C_T}{\partial P_1} dP_1 + \frac{\partial C_T}{\partial P_2} dP_2 + \cdots + \frac{\partial C_T}{\partial P_N} dP_N = 0 \tag{6.12.4}$$

Using (6.12.1), (6.12.4) becomes

$$dC_T = \frac{dC_1}{dP_1} dP_1 + \frac{dC_2}{dP_2} dP_2 + \cdots + \frac{dC_N}{dP_N} dP_N = 0 \tag{6.12.5}$$

Also, assuming P_T is constant, the differential of (6.12.2) is

$$dP_1 + dP_2 + \cdots + dP_N = 0 \tag{6.12.6}$$

Multiplying (6.12.6) by λ and subtracting the resulting equation from (6.12.5),

$$\left(\frac{dC_1}{dP_1} - \lambda\right) dP_1 + \left(\frac{dC_2}{dP_2} - \lambda\right) dP_2 + \cdots + \left(\frac{dC_N}{dP_N} - \lambda\right) dP_N = 0 \tag{6.12.7}$$

Equation (6.12.7) is satisfied when each term in parentheses equals zero. That is,

$$\frac{dC_1}{dP_1} = \frac{dC_2}{dP_2} = \cdots = \frac{dC_N}{dP_N} = \lambda \tag{6.12.8}$$

Therefore, all units have the same incremental operating cost, denoted here by λ, in order to minimize the total operating cost C_T.

EXAMPLE 6.18

Economic dispatch solution neglecting generator limits and line losses

An area of an interconnected power system has two fossil-fuel units operating on economic dispatch. The variable operating costs of these units are given by

$$C_1 = 10P_1 + 8 \times 10^{-3} P_1^2 \quad \$/\text{hr}$$

$$C_2 = 8P_2 + 9 \times 10^{-3} P_2^2 \quad \$/\text{hr}$$

where P_1 and P_2 are in megawatts. Determine the power output of each unit, the incremental operating cost, and the total operating cost C_T that minimizes C_T as the total load demand P_T varies from 500 to 1500 MW. Generating unit inequality constraints and transmission losses are neglected.

(Continued)

Copyright 2017 Cengage Learning. All Rights Reserved. May not be copied, scanned, or duplicated, in whole or in part. Due to electronic rights, some third party content may be suppressed from the eBook and/or eChapter(s). Editorial review has deemed that any suppressed content does not materially affect the overall learning experience. Cengage Learning reserves the right to remove additional content at any time if subsequent rights restrictions require it.

SOLUTION

The incremental operating costs of the units are

$$\frac{dC_1}{dP_1} = 10 + 16 \times 10^{-3}P_1 \quad \$/\text{MWh}$$

$$\frac{dC_2}{dP_2} = 8 + 18 \times 10^{-3}P_2 \quad \$/\text{MWh}$$

Using (6.12.8), the minimum total operating cost occurs when

$$\frac{dC_1}{dP_1} = 10 + 16 \times 10^{-3}P_1 = \frac{dC_2}{dP_2} = 8 + 18 \times 10^{-3}P_2$$

Using $P_2 = P_T - P_1$, the preceding equation becomes

$$10 + 16 \times 10^{-3}P_1 = 8 + 18 \times 10^{-3}(P_T - P_1)$$

Solving for P_1,

$$P_1 = \frac{18 \times 10^{-3}P_T - 2}{34 \times 10^{-3}} = 0.5294P_T - 58.82 \quad \text{MW}$$

Also, the incremental operating cost when C_T is minimized is

$$\frac{dC_2}{dP_2} = \frac{dC_1}{dP_1} = 10 + 16 \times 10^{-3}P_1 = 10 + 16 \times 10^{-3}(0.5294P_T - 58.82)$$

$$= 9.0589 + 8.4704 \times 10^{-3}P_T \quad \$/\text{MWh}$$

P_T MW	P_1 MW	P_2 MW	dC_i/dP_i \$/MWh	C_T \$/hr
500	206	294	13.29	5529
600	259	341	14.14	6901
700	312	388	14.99	8358
800	365	435	15.84	9899
900	418	482	16.68	11,525
1000	471	529	17.53	13,235
1100	524	576	18.38	15,030
1200	576	624	19.22	16,910
1300	629	671	20.07	18,875
1400	682	718	20.92	20,924
1500	735	765	21.76	23,058

TABLE 6.9

Economic dispatch solution for Example 6.18

Copyright 2017 Cengage Learning. All Rights Reserved. May not be copied, scanned, or duplicated, in whole or in part. Due to electronic rights, some third party content may be suppressed from the eBook and/or eChapter(s). Editorial review has deemed that any suppressed content does not materially affect the overall learning experience. Cengage Learning reserves the right to remove additional content at any time if subsequent rights restrictions require it.

and the minimum total operating cost is

$$C_T = C_1 + C_2 = (10P_1 + 8 \times 10^{-3}P_1^2) + (8P_2 + 9 \times 10^{-3}P_2^2) \quad \$/\text{hr}$$

The economic dispatch solution is shown in Table 6.9 for values of P_T from 500 to 1500 MW.

EFFECT OF INEQUALITY CONSTRAINTS

Each generating unit must not operate above its rating or below some minimum value. That is.

$$P_{i\min} < P_i < P_{i\max} \qquad i = 1, 2, \ldots, N \tag{6.12.9}$$

Other inequality constraints also may be included in the economic dispatch problem. For example, some unit outputs may be restricted so that certain transmission lines or other equipment are not overloaded. Also, under adverse weather conditions, generation at some units may be limited to reduce emissions.

When inequality constraints are included, modify the economic dispatch solution as follows. If one or more units reach their limit values, then these units are held at their limits, and the remaining units operate at equal incremental operating cost λ. The incremental operating cost of the area equals the common λ for the units that are not at their limits.

EXAMPLE 6.19

Economic dispatch solution including generator limits

Rework Example 6.18 if the units are subject to the following inequality constraints:

$$100 \leqq P_1 \leqq 600 \quad \text{MW}$$

$$400 \leqq P_2 \leqq 1000 \quad \text{MW}$$

SOLUTION

At light loads, unit 2 operates at its lower limit of 400 MW, where its incremental operating cost is $dC_2/dP_2 = 15.2$ \$/MWh. Additional load comes from unit 1 until $dC_1/dP_1 = 15.2$ \$/MWh, or

$$\frac{dC_1}{dP_1} = 10 + 16 \times 10^{-3}P_1 = 15.2$$

$$P_1 = 325 \quad \text{MW}$$

(*Continued*)

Copyright 2017 Cengage Learning. All Rights Reserved. May not be copied, scanned, or duplicated, in whole or in part. Due to electronic rights, some third party content may be suppressed from the eBook and/or eChapter(s). Editorial review has deemed that any suppressed content does not materially affect the overall learning experience. Cengage Learning reserves the right to remove additional content at any time if subsequent rights restrictions require it.

For P_T less than 725 MW, where P_1 is less than 325 MW, the incremental operating cost of the area is determined by unit 1 alone.

At heavy loads, unit 1 operates at its upper limit of 600 MW, where its incremental operating cost is $dC_1/dP_1 = 19.60$ \$/MWh. Additional load comes from unit 2 for all values of dC_2/dP_2 greater than 19.60 \$/MWh. At $dC_2/dP_2 =$ 19.60 \$/MWh,

$$\frac{dC_2}{dP_2} = 8 + 18 \times 10^{-3}P_2 = 19.60$$

$$P_2 = 644 \quad \text{MW}$$

For P_T greater than 1244 MW, where P_2 is greater than 644 MW, the incremental operating cost of the area is determined by unit 2 alone.

For $725 < P_T < 1244$ MW, neither unit has reached a limit value, and the economic dispatch solution is the same as that given in Table 6.9.

The solution to this example is summarized in Table 6.10 for values of P_T from 500 to 1500 MW.

P_T MW	P_1 MW	P_2 MW		dC/dP \$/MWh	C_T \$/hr
500	100	400	$\frac{dC_1}{dP_1}$	11.60	5720
600	200	400		13.20	6960
700	300	400		14.80	8360
725	325	400		15.20	8735
800	365	435		15.84	9899
900	418	482		16.68	11,525
1000	471	529		17.53	13,235
1100	524	576		18.38	15,030
1200	576	624		19.22	16,910
1244	600	644	$\frac{dC_2}{dP_2}$	19.60	17,765
1300	600	700		20.60	18,890
1400	600	800		22.40	21,040
1500	600	900		24.20	23,370

TABLE 6.10

Economic dispatch solution for Example 6.19

EXAMPLE 6.20

PowerWorld Simulator–economic dispatch, including generator limits

PowerWorld Simulator case Example 6_20 uses a five-bus, three-generator lossless case to show the interaction between economic dispatch and the transmission

Copyright 2017 Cengage Learning. All Rights Reserved. May not be copied, scanned, or duplicated, in whole or in part. Due to electronic rights, some third party content may be suppressed from the eBook and/or eChapter(s). Editorial review has deemed that any suppressed content does not materially affect the overall learning experience. Cengage Learning reserves the right to remove additional content at any time if subsequent rights restrictions require it.

system (see Figure 6.19). The variable operating costs for each of the units are given by

$$C_1 = 10P_1 + 0.016P_1^2 \quad \$/\text{hr}$$

$$C_2 = 8P_2 + 0.018P_2^2 \quad \$/\text{hr}$$

$$C_4 = 12P_4 + 0.018P_4^2 \quad \$/\text{hr}$$

where P_1, P_2, and P_4 are the generator outputs in megawatts. Each generator has minimum/maximum limits of

$$100 \le P_1 \le 400 \quad \text{MW}$$

$$150 \le P_2 \le 500 \quad \text{MW}$$

$$50 \le P_4 \le 300 \quad \text{MW}$$

In addition to solving the power flow equations, PowerWorld Simulator can simultaneously solve the economic dispatch problem to optimally allocate the generation in an area. To turn on this option, select **Case Information, Aggregation, Areas…** to view a list of each of the control areas in a case (just one in this example). Then toggle the AGC Status field to ED. Now anytime the power flow equations are solved, the generator outputs are also changed using the economic dispatch.

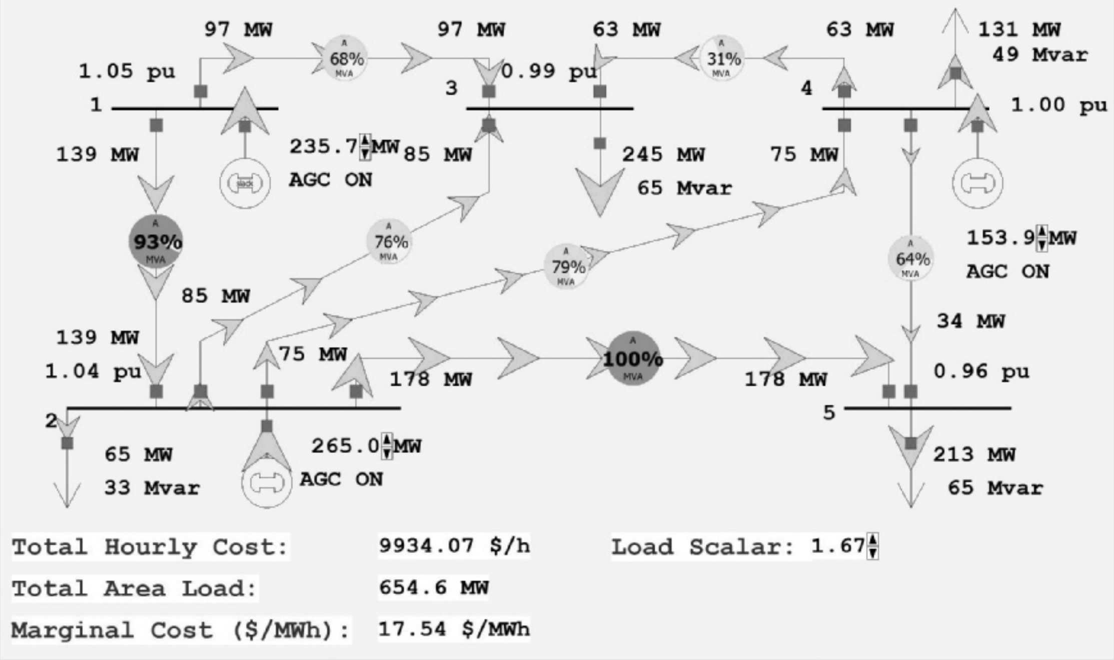
97 MW
97 MW
63 MW
63 MW
131 MW
49 Mvar
68% MVA
31% MVA
1.05 pu
1
0.99 pu
3
4
1.00 pu
139 MW
235.7 MW
AGC ON
85 MW
245 MW
65 Mvar
75 MW
93% MVA
76% MVA
79% MVA
64% MVA
153.9 MW
AGC ON
85 MW
34 MW
139 MW
1.04 pu
75 MW
178 MW
100% MVA
178 MW
0.96 pu
2
5
65 MW
33 Mvar
265.0 MW
AGC ON
213 MW
65 Mvar
Total Hourly Cost: 9934.07 $/h
Load Scalar: 1.67
Total Area Load: 654.6 MW
Marginal Cost ($/MWh): 17.54 $/MWh

FIGURE 6.19

Example 6.20 with maximum economic loading

(Continued)

Copyright 2017 Cengage Learning. All Rights Reserved. May not be copied, scanned, or duplicated, in whole or in part. Due to electronic rights, some third party content may be suppressed from the eBook and/or eChapter(s). Editorial review has deemed that any suppressed content does not materially affect the overall learning experience. Cengage Learning reserves the right to remove additional content at any time if subsequent rights restrictions require it.

Initially, the case has a total load of 392 MW with an economic dispatch of $P_1 = 141$ MW, $P_2 = 181$, and $P_4 = 70$, and an incremental operating cost, λ, of 14.52 \$/MWh. To view a graph showing the incremental cost curves for all of the area generators, right-click on any generator to display the generator's local menu, and then select All Area Gen IC Curves (right-click on the graph's axes to change their scaling).

To see how changing the load impacts the economic dispatch and power flow solutions, first select **Tools, Play** to begin the simulation. Then, on the oneline, click on the up/down arrows next to the Load Scalar field. This field is used to scale the load at each bus in the system. Notice that the change in the Total Hourly Cost field is well approximated by the change in the load multiplied by the incremental operating cost.

Determine the maximum amount of load this system can supply without overloading any transmission line with the generators dispatched using economic dispatch.

SOLUTION

The maximum system economic loading is determined numerically to be 655 MW (which occurs with a Load Scalar of 1.67) with the line from bus 2 to bus 5 being the critical element.

EFFECT OF TRANSMISSION LOSSES

Although one unit may be very efficient with a low incremental operating cost, it also may be located far from the load center. The transmission losses associated with this unit may be so high that the economic dispatch solution requires the unit to decrease its output, while other units with higher incremental operating costs but lower transmission losses increase their outputs.

When transmission losses are included in the economic dispatch problem, (6.12.2) becomes

$$P_1 + P_2 + \cdots + P_N - P_L = P_T \tag{6.12.10}$$

where P_T is the total load demand and P_L is the total transmission loss in the area. In general, P_L is not constant but depends on the unit outputs $P_1, P_2, \ldots, P_N$, The total differential of (6.12.10) is

$$(dP_1 + dP_2 + \cdots + dP_N) - \left(\frac{\partial P_L}{\partial P_1} dP_1 + \frac{\partial P_L}{\partial P_2} dP_2 + \cdots + \frac{\partial P_L}{\partial P_N} dP_N\right) = 0 \tag{6.12.11}$$

Multiplying (6.12.11) by λ and subtracting the resulting equation from (6.12.5),

$$\left(\frac{dC_1}{dP_1} + \lambda\frac{\partial P_L}{\partial P_1} - \lambda\right) dP_1 + \left(\frac{dC_2}{dP_2} + \lambda\frac{\partial P_L}{\partial P_2} - \lambda\right) dP_2$$

Copyright 2017 Cengage Learning. All Rights Reserved. May not be copied, scanned, or duplicated, in whole or in part. Due to electronic rights, some third party content may be suppressed from the eBook and/or eChapter(s). Editorial review has deemed that any suppressed content does not materially affect the overall learning experience. Cengage Learning reserves the right to remove additional content at any time if subsequent rights restrictions require it.

$$+ \cdots + \left(\frac{dC_N}{dP_N} + \lambda\frac{\partial P_L}{\partial P_N} - \lambda\right)dP_N = 0 \qquad (6.12.12)$$

Equation (6.12.12) is satisfied when each term in parentheses equals zero. That is.

$$\frac{dC_i}{dP_i} + \lambda\frac{\partial P_L}{\partial P_i} - \lambda = 0$$

or

$$\lambda = \frac{dC_i}{dP_i}(L_i) = \frac{dC_i}{dP_i}\left(\frac{1}{1 - \dfrac{\partial P_L}{\partial P_i}}\right) \qquad i = 1, 2, \ldots, N \qquad (6.12.13)$$

Equation (6.12.13) gives the economic dispatch criteria, including transmission losses. Each unit that is not at a limit value operates such that its incremental operating cost dC_i/dP_i multiplied by the *penalty factor* L_i is the same. Note that when transmission losses are negligible $\partial P_L/\partial P_i = 0$, $L_i = 1$, and (6.12.13) reduces to (6.12.8).

EXAMPLE 6.21

Economic dispatch solution including generator limits and line losses

Total transmission losses for the power system area given in Example 6.18 are given by

$$P_L = 1.5 \times 10^{-4}P_1^2 + 2 \times 10^{-5}P_1P_2 + 3 \times 10^{-5}P_2^2 \quad \text{MW}$$

where P_1 and P_2 are given in megawatts. Determine the output of each unit, total transmission losses, total load demand, and total operating cost C_T when the area $\lambda = 16.00$ \$/MWh.

SOLUTION

Using the incremental operating costs from Example 6.18 in (6.12.13),

$$\frac{dC_1}{dP_1}\left(\frac{1}{1 - \dfrac{\partial P_L}{\partial P_1}}\right) = \frac{10 + 16 \times 10^{-3}P_1}{1 - (3 \times 10^{-4}P_1 + 2 \times 10^{-5}P_2)} = 16.00$$

$$\frac{dC_2}{dP_2}\left(\frac{1}{1 - \dfrac{\partial P_L}{\partial P_2}}\right) = \frac{8 + 18 \times 10^{-3}P_2}{1 - (6 \times 10^{-5}P_2 + 2 \times 10^{-5}P_1)} = 16.00$$

(*Continued*)

Copyright 2017 Cengage Learning. All Rights Reserved. May not be copied, scanned, or duplicated, in whole or in part. Due to electronic rights, some third party content may be suppressed from the eBook and/or eChapter(s). Editorial review has deemed that any suppressed content does not materially affect the overall learning experience. Cengage Learning reserves the right to remove additional content at any time if subsequent rights restrictions require it.

Rearranging the two equations,

$$20.8 \times 10^{-3}P_1 + 32 \times 10^{-5}P_2 = 6.00$$
$$32 \times 10^{-5}P_1 + 18.96 \times 10^{-3}P_2 = 8.00$$

Solving,

$$P_1 = 282 \quad \text{MW} \qquad P_2 = 417 \quad \text{MW}$$

Using the equation for total transmission losses,

$$P_L = 1.5 \times 10^{-4}(282)^2 + 2 \times 10^{-5}(282)(417) + 3 \times 10^{-5}(417)^2$$
$$= 19.5 \quad \text{MW}$$

From (6.12.10), the total load demand is

$$P_T = P_1 + P_2\, P_L = 282 + 417 - 19.5 = 679.5 \quad \text{MW}$$

Also, using the cost formulas given in Example 6.18, the total operating cost is

$$C_T = C_1 + C_2 = 10(282) + 8 \times 10^{-3}(282)^2 + 8(417) + 9 \times 10^{-3}(417)^2$$
$$= 8357 \quad \$/\text{h}$$

Note that when transmission losses are included, λ given by (6.12.13) is no longer the incremental operating cost of the area. Instead, λ is the unit incremental operating cost dC_i/dP_i multiplied by the unit penalty factor L_i.

EXAMPLE 6.22

PowerWorld Simulator—economic dispatch, including generator limits and line losses

This example repeats the Example 6.19 power system, except that now losses are included with each transmission line modeled with an R/X ratio of 1/3 (see Figure 6.20). The current value of each generator's loss sensitivity, $\partial P_L/\partial P_i$, is shown immediately below the generator's MW output field. Calculate the penalty factors L_i, and verify that the economic dispatch shown in the figure is optimal. Assume a Load Scalar of 1.0.

SOLUTION

From (6.12.13), the condition for optimal dispatch is

$$\lambda = dC_i/dP_i(1/(1 - \partial P_L/\partial P_i) = dC_i/dP_i L_i \qquad i = 1, 2, \ldots, N$$

with

$$L_i = 1/(1 - \partial P_L/\partial P_i)$$

Therefore, $L_1 = 1.0$, $L_2 = 0.9733$, and $L_4 = 0.9238$.

$$\text{with } P_1 = 130.1 \text{ MW}, \quad dC_1/dP_1 * L_1 = (10 + 0.032 * 130.1) * 1.0$$
$$= 14.16 \quad \$/\text{MWh}$$

Copyright 2017 Cengage Learning. All Rights Reserved. May not be copied, scanned, or duplicated, in whole or in part. Due to electronic rights, some third party content may be suppressed from the eBook and/or eChapter(s). Editorial review has deemed that any suppressed content does not materially affect the overall learning experience. Cengage Learning reserves the right to remove additional content at any time if subsequent rights restrictions require it.

$$\text{With } P_2 = 181.8 \text{ MW}, \quad dC_2/dP_2 * L_2 = (8 + 0.036 * 181.8) * 0.9733$$
$$= 14.16 \quad \$/\text{MWh}$$
$$\text{With } P_4 = 92.4 \text{ MW}, \quad dC_4/dP_4 * L_4 = (12 + 0.036 * 92.4) * 0.9238$$
$$= 14.16 \quad \$/\text{MWh}$$

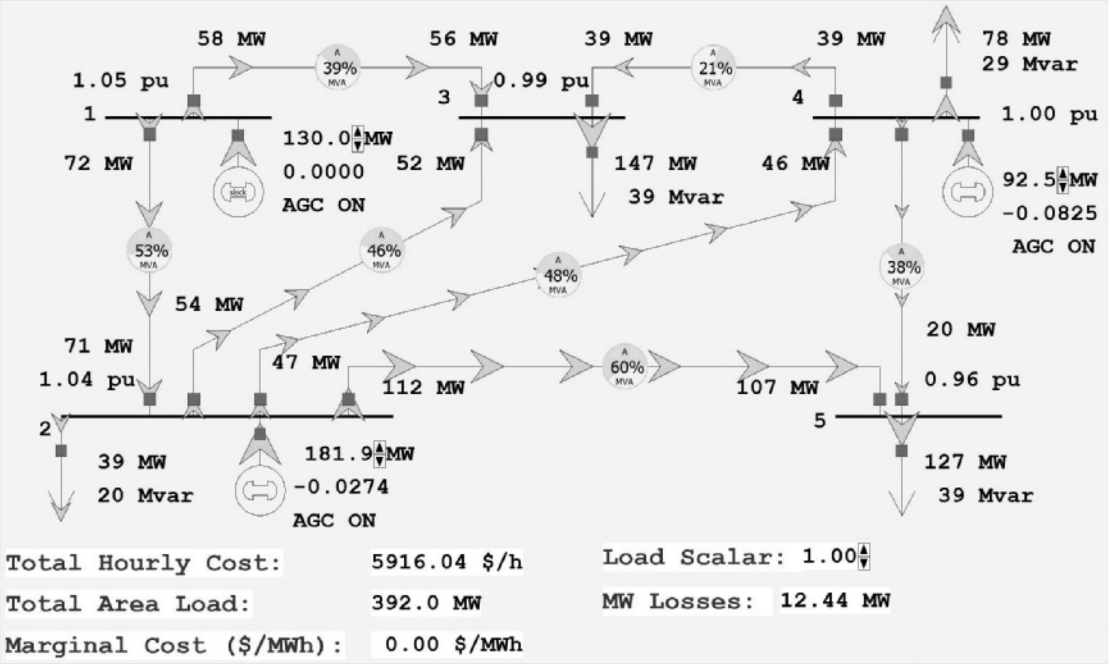
58 MW
56 MW
39 MW
39 MW
78 MW
29 Mvar
1.05 pu
1
39%
21%
3
0.99 pu
4
1.00 pu
130.0 MW
0.0000
AGC ON
72 MW
52 MW
147 MW
39 Mvar
46 MW
92.5 MW
-0.0825
AGC ON
53%
46%
48%
38%
54 MW
20 MW
71 MW
1.04 pu
47 MW
112 MW
60%
107 MW
0.96 pu
2
5
39 MW
20 Mvar
181.9 MW
-0.0274
AGC ON
127 MW
39 Mvar
Total Hourly Cost: 5916.04 $/h
Total Area Load: 392.0 MW
Marginal Cost ($/MWh): 0.00 $/MWh
Load Scalar: 1.00
MW Losses: 12.44 MW

FIGURE 6.20

Example 6.22 five-bus case with transmission line losses

In Example 6.21, total transmission losses are expressed as a quadratic function of unit output powers. For an area with N units, this formula generalizes to

$$P_L = \sum_{i=1}^{N} \sum_{j=1}^{N} P_i B_{ij} P_j \tag{6.12.14}$$

where the B_{ij} terms are called *loss coefficients* or B *coefficients.* The B coefficients are not truly constant but vary with unit loadings. However, the B coefficients are often assumed constant in practice since the calculation of $\partial P_L/\partial P_i$ is thereby simplified. Using (6.12.14),

$$\frac{\partial P_L}{\partial P_i} = 2\sum_{j=1}^{N} B_{ij} P_j \tag{6.12.15}$$

This equation can be used to compute the penalty factor L_i, in (6.12.13).

Copyright 2017 Cengage Learning. All Rights Reserved. May not be copied, scanned, or duplicated, in whole or in part. Due to electronic rights, some third party content may be suppressed from the eBook and/or eChapter(s). Editorial review has deemed that any suppressed content does not materially affect the overall learning experience. Cengage Learning reserves the right to remove additional content at any time if subsequent rights restrictions require it.

Various methods of evaluating B coefficients from power flow studies are available [17]. In practice, more than one set of B coefficients may be used during the daily load cycle.

When the unit incremental cost curves are linear, an analytic solution to the economic dispatch problem is possible, as illustrated by Examples 6.18 through 6.20. However, in practice, the incremental cost curves are nonlinear and contain discontinuities. In this case, an iterative solution can be obtained. Given the load demand P_T, the unit incremental cost curves, generator limits, and B coefficients, such an iterative solution can be obtained by the following nine steps. Assume that the incremental cost curves are stored in tabular form, such that a unique value of P_i can be read for each dC_i/dP_i.

STEP 1 Set iteration index $m = 1$.

STEP 2 Estimate mth value of λ.

STEP 3 Skip this step for all $m > 1$. Determine initial unit outputs P_i, ($i = 1, 2, \ldots, N$). Use $dC_i/dP_i = \lambda$ and read P_i from each incremental operating cost table. Transmission losses are neglected here.

STEP 4 Compute $\partial P_L/\partial P_i$ from (6.12.15) ($i = 1, 2, \ldots, N$).

STEP 5 Compute dC_i/dP_i from (6.12.13) ($i = 1, 2, \ldots, N$).

STEP 6 Determine updated values of unit output P_i ($i = 1, 2, \ldots, N$). Read P_i from each incremental operating cost table. If P_i exceeds a limit value, set P_i to the limit value.

STEP 7 Compare P_i determined in Step 6 with the previous value ($i = 1, 2, \ldots, N$). If the change in each unit output is less than a specified tolerance ε_1, go to Step 8. Otherwise, return to Step 4.

STEP 8 Compute P_L from (6.12.14).

STEP 9 If $\left|\left(\sum_{i=1}^{N} P_i\right) - P_L - P_T\right|$ is less than a specified tolerance ε_2, stop. Otherwise, set $m = m + 1$ and return to Step 2.

Instead of having their values stored in tabular form for this procedure, the incremental cost curves instead could be represented by nonlinear functions such as polynomials. Then, in Step 3 and Step 5, each unit output P_i would be computed from the nonlinear functions instead of being read from a table. Note that this procedure assumes that the total load demand P_T is constant. In practice, this economic dispatch program is executed every few minutes with updated values of P_T.

OTHER TYPES OF UNITS

The economic dispatch criterion has been derived for a power system area consisting of fossil-fuel generating units. In practice, however, an area has a mix of different types of units including fossil-fuel, nuclear, pumped-storage hydro, hydro, wind, and other types.

Wind and solar generation, which have no fuel costs, are represented with very low or negative cost. As such, they are preferred sources for economic dispatch and

Copyright 2017 Cengage Learning. All Rights Reserved. May not be copied, scanned, or duplicated, in whole or in part. Due to electronic rights, some third party content may be suppressed from the eBook and/or eChapter(s). Editorial review has deemed that any suppressed content does not materially affect the overall learning experience. Cengage Learning reserves the right to remove additional content at any time if subsequent rights restrictions require it.

are used by system operators whenever possible, unless there are generator operating limits or transmission constraints.

Although the fixed costs of a nuclear unit may be high, their operating costs are low due to inexpensive nuclear fuel. As such, nuclear units are normally base-loaded at their rated outputs. That is, the reference power settings of turbine-governors for nuclear units are held constant at rated output; therefore, these units do not participate in economic dispatch.

Pumped-storage hydro is a form of energy storage. During off-peak hours, these units are operated as synchronous motors to pump water to a higher elevation. Then during peak-load hours the water is released, and the units are operated as synchronous generators to supply power. As such, pumped-storage hydro units are used for light-load build-up and peak-load shaving. Economic operation of the area is improved by pumping during off-peak hours when the area λ is low, and by generating during peak-load hours when λ is high. Techniques are available for incorporating pumped-storage hydro units into economic dispatch of fossil-fuel units [18].

In an area consisting of hydro plants located along a river, the objective is to maximize the energy generated over the yearly water cycle rather than to minimize total operating costs. Reservoirs are used to store water during high-water or light-load periods, although some water may have to be released through spillways. Also, there are constraints on water levels due to river transportation, irrigation, or fishing requirements. Optimal strategies are available for coordinating outputs of plants along a river [19]. Economic dispatch strategies for mixed fossil-fuel/hydro systems are also available [20, 21, 22].

Techniques are also available for including reactive power flows in the economic dispatch formulation, whereby both active and reactive powers are selected to minimize total operating costs. In particular, reactive injections from generators, switched capacitor banks, and static var systems, along with transformer tap settings, can be selected to minimize transmission-line losses [22]. However, electric utility companies usually control reactive power locally. That is, the reactive power output of each generator is selected to control the generator terminal voltage, and the reactive power output of each capacitor bank or static var system located at a power system bus is selected to control the voltage magnitude at that bus. In this way, the reactive power flows on transmission lines are low, and the need for central dispatch of reactive power is eliminated.

6.13 OPTIMAL POWER FLOW

Economic dispatch has one significant shortcoming—it ignores the limits imposed by the devices in the transmission system. Each transmission line and transformer has a limit on the amount of power that can be transmitted through it, with the limits arising because of thermal, voltage, or stability considerations (Section 5.6). Traditionally, the transmission system was designed so that when the generation was dispatched economically there would be no limit violations. Hence, just solving economic dispatch was usually sufficient. However, with the worldwide trend toward deregulation of the electric utility industry, the transmission system is becoming

Copyright 2017 Cengage Learning. All Rights Reserved. May not be copied, scanned, or duplicated, in whole or in part. Due to electronic rights, some third party content may be suppressed from the eBook and/or eChapter(s). Editorial review has deemed that any suppressed content does not materially affect the overall learning experience. Cengage Learning reserves the right to remove additional content at any time if subsequent rights restrictions require it.

increasingly constrained (with these constraints sometimes called congestion). For example, in the PJM power market in the eastern United States, the costs associated with active transmission line and transformer limit violations (congestion) increased from \$65 million in 1999 to almost \$2.1 billion in 2005 and have averaged about \$1 billion per year from 2008 to 2013 [23].

The solution to the problem of optimizing the generation while enforcing the transmission lines is to combine economic dispatch with either the full ac power flow, or a dc power flow. The result is known as the optimal power flow (OPF). There are several methods for solving the OPF with [24] providing a nice summary. One common approach is sequential linear programming (LP); this is the technique used with the PowerWorld Simulator. The LP OPF solution algorithm iterates between solving the power flow to determine the flow of power in the system devices and solving an LP to economically dispatch the generation (and possibility other controls) subject to the transmission system limits. In the absence of system elements loaded to their limits, the OPF generation dispatch is identical to the economic dispatch solution, and the marginal cost of energy at each bus is identical to the system λ. However, when one or more elements are loaded to their limits, the economic dispatch becomes constrained, and the bus marginal energy prices are no longer identical. In some electricity markets, these marginal prices are known as the Locational Marginal Prices (LMPs) and are used to determine the wholesale price of electricity at various locations in the system. For example, the real-time LMPs for the Midcontinent ISO (MISO) are available online at www.misoenergy.org/MarketsOperations.

EXAMPLE 6.23

PowerWorld Simulator—optimal power flow

PowerWorld Simulator case Example 6_23 duplicates the five-bus case from Example 6.20, except that the case is solved using PowerWorld Simulator's LP OPF algorithm (see Figure 6.21). To turn on the OPF option, first select **Case Information, Aggregation, Areas…,** and toggle the AGC Status field to OPF. Then, rather than solving the case with the "Single Solution" button, select **Add-ons, Primal LP** to solve using the LP OPF. Initially the OPF solution matches the ED solution from Example 6.20 since there are no overloaded lines. The green-colored fields on the screen immediately to the right of the buses show the marginal cost of supplying electricity to each bus in the system (i.e., the bus LMPs). With the system initially unconstrained, the bus marginal prices are all identical at \$14.5/MWh, with a Load Scalar of 1.0.

Now increase the Load Scalar field from 1.00 to the maximum economic loading value, determined to be 1.67 in Example 6.20, and again select **Add-ons, Primal LP**. The bus marginal prices are still all identical, now at a value of \$17.5/MWh, and with the line from bus 2 to 5 just reaching its maximum value. For load scalar values above 1.67, the line from bus 2 to bus 5 becomes constrained, with a result that the bus marginal prices on the constrained side of the line become higher than those on the unconstrained side.

Copyright 2017 Cengage Learning. All Rights Reserved. May not be copied, scanned, or duplicated, in whole or in part. Due to electronic rights, some third party content may be suppressed from the eBook and/or eChapter(s). Editorial review has deemed that any suppressed content does not materially affect the overall learning experience. Cengage Learning reserves the right to remove additional content at any time if subsequent rights restrictions require it.

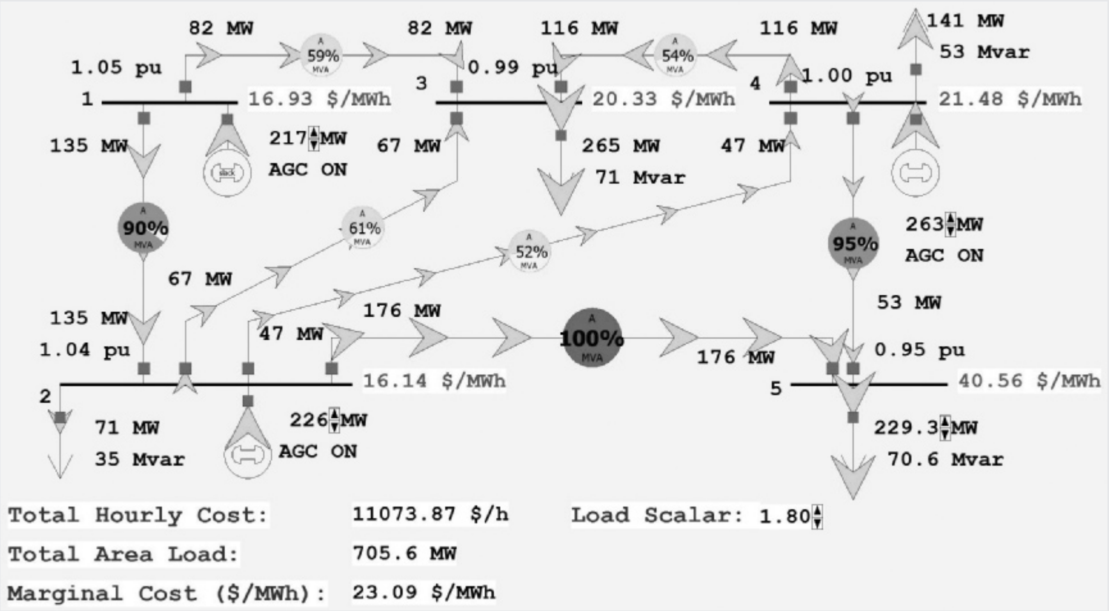
82 MW
82 MW
116 MW
116 MW
141 MW
53 Mvar
1.05 pu
59% MVA
0.99 pu
54% MVA
1.00 pu
1
16.93 $/MWh
3
20.33 $/MWh
4
21.48 $/MWh
135 MW
217 MW
AGC ON
67 MW
265 MW
71 Mvar
47 MW
90% MVA
61% MVA
52% MVA
95% MVA
263 MW
AGC ON
67 MW
53 MW
135 MW
1.04 pu
47 MW
176 MW
100% MVA
176 MW
0.95 pu
2
16.14 $/MWh
5
40.56 $/MWh
71 MW
35 Mvar
226 MW
AGC ON
229.3 MW
70.6 Mvar
Total Hourly Cost: 11073.87 $/h
Load Scalar: 1.80
Total Area Load: 705.6 MW
Marginal Cost ($/MWh): 23.09 $/MWh

FIGURE 6.21

Example 6.23 optimal power flow solution with load multiplier = 1.80

With the load scalar equal to 1.80, numerically verify that the price of power at bus 5 is approximately \$40.60/MWh.

SOLUTION

The easiest way to numerically verify the bus 5 price is to increase the load at bus 5 by a small amount and compare the change in total system operating cost. With a load scalar of 1.80, the bus 5 MW load is 229.3 MW with a case hourly cost of \$11,073.90. Increasing the bus 5 load by 0.9 MW and resolving the LP OPF gives a new cost of \$11,110.40, which is a change of about \$40.60/MWh (note that this increase in load also increases the bus 5 price to over \$41/MWh). Because of the constraint, the price of power at bus 5 is actually more than double the incremental cost of the most expensive generator!

MULTIPLE CHOICE QUESTIONS

SECTION 6.1

6.1 For a set of linear algebraic equations in matrix format, $\mathbf{Ax} - \mathbf{y}$, for a unique solution to exist, det(**A**) should be ________.

6.2 For an $N \times N$ square matrix **A**, in $(N - 1)$ steps, the technique of Gauss elimination can transform into an ________ matrix.

Copyright 2017 Cengage Learning. All Rights Reserved. May not be copied, scanned, or duplicated, in whole or in part. Due to electronic rights, some third party content may be suppressed from the eBook and/or eChapter(s). Editorial review has deemed that any suppressed content does not materially affect the overall learning experience. Cengage Learning reserves the right to remove additional content at any time if subsequent rights restrictions require it.

SECTION 6.2

6.3 For the iterative solution to linear algebraic equations $\mathbf{Ax} - \mathbf{y}$, the $\mathbf{D}$ matrix in the Jacobi method is the ________ portion of $\mathbf{A}$, whereas $\mathbf{D}$ for Gauss-Siedel is the ________ portion of $\mathbf{A}$.

6.4 Is convergence guaranteed always with Jacobi and Gauss-Siedel methods, as applied to iterative solutions of linear algebraic equations?
(a) Yes (b) No

SECTION 6.3

6.5 For the iterative solutions to nonlinear algebraic equations with the Newton-Raphson method, the Jacobian matrix $\mathbf{J}\,(i)$ consists of the partial derivatives. Write down the elements of first row of $\mathbf{J}\,(i)$.

6.6 For the Newton-Raphson method to work, one should make sure that $\mathbf{J}^{-1}$ exists.
(a) True (b) False

6.7 The Newton-Raphson method in four steps makes use of Gauss elimination and back substitution.
(a) True (b) False

6.8 The number of iterations required for convergence is dependent/independent of the dimension N for Newton-Raphson method. Choose one.

SECTION 6.4

6.9 The swing bus or slack bus is a reference bus for which $V_1\underline{/\delta_1}$, typically $1.0\underline{/0^\circ}$ per unit, is input data. The power flow program computes __________. Fill in the blank.

6.10 Most buses in a typical power flow program are load buses, for which P_k and Q_k are input data. The power flow program computes __________.

6.11 For a voltage-controlled bus k, __________ are input data, while the power flow program computes __________.

6.12 When the bus k is a load bus with no generation and inductive load, in terms of generation and load, $P_k =$ __________, and $Q_k =$ __________.

6.13 Starting from a single-line diagram of a power system, the input data for a power flow problem consists of __________, __________, and __________.

SECTION 6.5

6.14 Nodal equations $I = Y_{\text{bus}}\ V$ are a set of linear equations analogous to $y = Ax$.
(a) True (b) False

6.15 Because of the nature of the power flow bus data, nodal equations do not directly fit the linear-equation format, and power flow equations are

Copyright 2017 Cengage Learning. All Rights Reserved. May not be copied, scanned, or duplicated, in whole or in part. Due to electronic rights, some third party content may be suppressed from the eBook and/or eChapter(s). Editorial review has deemed that any suppressed content does not materially affect the overall learning experience. Cengage Learning reserves the right to remove additional content at any time if subsequent rights restrictions require it.

actually nonlinear. However, the Gauss-Siedel method can be used for the power flow solution.
(a) True (b) False

SECTION 6.6

6.16 The Newton-Raphson method is most well suited for solving the nonlinear power flow equations.
(a) True (b) False

6.17 By default, PowerWorld Simulator uses ___________ method for the power flow solution.

SECTION 6.7

6.18 Prime-mover control of a generator is responsible for a significant change in ___________, whereas excitation control significantly changes ___________.

6.19 From the power flow standpoint, the addition of a shunt-capacitor bank to a load bus corresponds to the addition of a positive/negative reactive load. Choose the right word.

6.20 Tap-changing and voltage-magnitude-regulating transformers are used to control bus voltages and reactive power flows on lines to which they are connected.
(a) True (b) False

SECTION 6.8

6.21 A matrix, which has only a few nonzero elements, is said to be ________.

6.22 Sparse-matrix techniques are used in Newton-Raphson power flow programs in order to reduce computer ___________ and ___________ requirements.

6.23 Reordering buses can be an effective sparsity technique in power flow solutions.
(a) True (b) False

SECTION 6.9

6.24 While the fast decoupled power flow usually takes more iterations to converge, it is usually significantly faster than the Newton-Raphson method.
(a) True (b) False

SECTION 6.10

6.25 The "dc" power flow solution, giving approximate answers, is based on completely neglecting the Q-V equation and solving the linear real-power balance equations.
(a) True (b) False

Copyright 2017 Cengage Learning. All Rights Reserved. May not be copied, scanned, or duplicated, in whole or in part. Due to electronic rights, some third party content may be suppressed from the eBook and/or eChapter(s). Editorial review has deemed that any suppressed content does not materially affect the overall learning experience. Cengage Learning reserves the right to remove additional content at any time if subsequent rights restrictions require it.

PROBLEMS

SECTION 6.1

6.1 Using Gauss elimination, solve the following linear algebraic equations:

$$\begin{aligned} -25x_1 + 10x_2 + 10x_3 + 10x_4 &= 0 \\ 5x_1 - 10x_2 + 10x_3 &= 2 \\ 10x_1 + 5x_2 - 10x_3 + 10x_4 &= 1 \\ 10x_1 - 20x_4 &= -2 \end{aligned}$$

6.2 Using Gauss elimination and back substitution, solve

$$\begin{bmatrix} 8 & 2 & 1 \\ 4 & 6 & 2 \\ 3 & 4 & 14 \end{bmatrix} \begin{bmatrix} x_1 \\ x_2 \\ x_3 \end{bmatrix} = \begin{bmatrix} 3 \\ 4 \\ 2 \end{bmatrix}$$

6.3 Rework Problem 6.2 with the value of 8 changed to 4.

6.4 What is the difficulty in applying Gauss elimination to the following linear algebraic equations?

$$\begin{aligned} -5x_1 + 5x_2 &= 5 \\ 10x_1 - 10x_2 &= -5 \end{aligned}$$

6.5 Show that, after triangularizing $\mathbf{Ax} = \mathbf{y}$, the back substitution method of solving $\mathbf{A}^{(N-1)}\mathbf{x} = \mathbf{y}^{(N-1)}$ requires N divisions, $N(N-1)/2$ multiplications, and $N(N-1)/2$ subtractions. Assume that all the elements of $\mathbf{A}^{(N-1)}$ and $\mathbf{y}^{(N-1)}$ are nonzero and real.

SECTION 6.2

6.6 Solve Problem 6.2 using the Jacobi iterative method. Start with $x_1(0) = x_2(0) = x_3(0) = 0$, and continue until (6.2.2) is satisfied with $\varepsilon = 0.01$.

6.7 Repeat Problem 6.6 using the Gauss-Seidel iterative method. Which method converges more rapidly?

6.8 Express the following set of equations in the form of (6.2.6), and then solve using the Jacobi iterative method with $\varepsilon = 0.05$ and with $x_1(0) = 1$, and $x_2(0) = 1$, $x_3(0) = 0$.

$$\begin{bmatrix} 10 & -2 & -4 \\ -2 & 6 & -2 \\ -4 & -2 & 10 \end{bmatrix} \begin{bmatrix} x_1 \\ x_2 \\ x_3 \end{bmatrix} = \begin{bmatrix} -2 \\ 3 \\ -1 \end{bmatrix}$$

Copyright 2017 Cengage Learning. All Rights Reserved. May not be copied, scanned, or duplicated, in whole or in part. Due to electronic rights, some third party content may be suppressed from the eBook and/or eChapter(s). Editorial review has deemed that any suppressed content does not materially affect the overall learning experience. Cengage Learning reserves the right to remove additional content at any time if subsequent rights restrictions require it.

6.9 Solve for x_1 and x_2 in the system of equations given by

$$x_2 - 3x_1 + 1.9 = 0$$
$$x_2 + x_1^2 - 3.0 = 0$$

using the Gauss method with an initial guess of $x_1 = 1$ and $x_2 = 1$.

6.10 Solve $x^2 - 4x + 1 = 0$ using the Jacobi iterative method with $x(0) = 1$. Continue until (6.2.2) is satisfied with $\varepsilon = 0.01$. Check using the quadratic formula.

6.11 Try to solve Problem 6.2 using the Jacobi and Gauss-Seidel iterative methods with the value of A_{33} changed from 14 to 0.14 and with $x_1(0) = x_2(0) = x_3(0) = 0$. Show that neither method converges to the unique solution.

6.12 Using the Jacobi method (also known as the Gauss method), solve for x_1 and x_2 in the following system of equations.

$$x_2 - 3x_1 + 1.9 = 0$$
$$x_2 + x_1^2 - 1.8 = 0$$

Use an initial guess of $x_1(0) = 1.0$ and $x_2 = (0) = 1.0$. Also, see what happens when you choose an uneducated initial guess of $x_1(0) = x_2(0) = 100$.

6.13 Use the Gauss-Seidel method to solve the following equations that contain terms that are often found in power flow equations.

$$x_1 = (1/(-20j)) * [(-1 + 0.5j)/(x_1)^* - (j10) * x_2 - (j10)]$$
$$x_2 = (1/(-20j)) * [(-3 + j)/(x_2)^* - (j10) * x_1 - (j10)]$$

Use an initial estimate of $x_1(0) = 1$ and $x_2(0) = 1$, and a stopping of $\varepsilon = 0.05$.

6.14 Find a root of the following equation by using the Gauss-Seidel method: (use an initial estimate of $x = 2$) $f(x) = x^3 - 6x^2 + 9x - 4 = 0$.

6.15 Use the Jacobi method to find a solution to $x^2 \cos x - x + 0.5 = 0$. Use $x(0) = 1$ and $\varepsilon = 0.01$. Experimentally determine the range of initial values that results in convergence.

6.16 Take the z-transform of (6.2.6) and show that $\mathbf{X}(z) = \mathbf{G}(z)\mathbf{Y}(z)$, where $\mathbf{G}(z) = (z\mathbf{U} - \mathbf{M})^{-1}\,\mathbf{D}^{-1}$ and $\mathbf{U}$ is the unit matrix.

Note: $\mathbf{G}(z)$ is the matrix transfer function of a digital filter that represents the Jacobi or Gauss-Seidel methods. The filter poles are obtained by solving $\det(z\mathbf{U} - \mathbf{M}) = 0$. The filter is stable if and only if all the poles have magnitudes less than 1.

6.17 Determine the poles of the Jacobi and Gauss-Seidel digital filters for the general two-dimensional problem ($N = 2$):

$$\left[\begin{array}{c|c} A_{11} & A_{12} \\ \hline A_{21} & A_{22} \end{array}\right]\begin{bmatrix} x_1 \\ x_2 \end{bmatrix} = \begin{bmatrix} y_1 \\ y_2 \end{bmatrix}$$

Then determine a necessary and sufficient condition for convergence of these filters when $N = 2$.

Copyright 2017 Cengage Learning. All Rights Reserved. May not be copied, scanned, or duplicated, in whole or in part. Due to electronic rights, some third party content may be suppressed from the eBook and/or eChapter(s). Editorial review has deemed that any suppressed content does not materially affect the overall learning experience. Cengage Learning reserves the right to remove additional content at any time if subsequent rights restrictions require it.

SECTION 6.3

6.18 Use Newton-Raphson to find a solution to the polynomial equation $f(x) = y$ where $y = 0$ and $f(x) = x^3 + 8x^2 + 2x - 40$. Start with $x(0) = 1$ and continue until (6.2.2) is satisfied with $\varepsilon = 0.001$.

6.19 Repeat 6.19 using $x(0) = -2$.

6.20 Use Newton-Raphson to find one solution to the polynomial equation $f(x) = y$, where $y = 7$ and $f(x) = x^4 + 3x^3 - 15x^2 - 19x + 30$. Start with $x(0) = 0$ and continue until (6.2.2) is satisfied with $\varepsilon = 0.001$.

6.21 Repeat Problem 6.20 with an initial guess of $x(0) = 4$.

6.22 For Problem 6.20, plot the function $f(x)$ between $x = 0$ and 4. Then provide a graphical interpretation why points close to $x = 2.2$ would be poorer initial guesses.

6.23 Use Newton-Raphson to find a solution to

$$\begin{bmatrix} e^{x_1 x_2} \\ \cos(x_1 + x_2) \end{bmatrix} = \begin{bmatrix} 1.2 \\ 0.5 \end{bmatrix}$$

where x_1 and x_2 are in radians. (a) Start with $x_1(0) = 1.0$ and $x_2(0) = 0.5$ and continue until (6.2.2) is satisfied with $\varepsilon = 0.005$. (b) Show that Newton-Raphson diverges for this example if $x_1(0) = 1.0$ and $x_2(0) = 2.0$.

6.24 Solve the following equations by the Newton-Raphson method:

$$2x_1 + x_2^2 - 8 = 0$$
$$x_1^2 - x_2^2 + x_1 x_2 - 3 = 0$$

Start with an initial guess of $x_1 = 1$ and $x_2 = 1$.

6.25 The following nonlinear equations contain terms that are often found in the power flow equations:

$$f_1(x) = 10x_1 \sin x_2 + 2 = 0$$
$$f_2(x) = 10\,(x_1)^2 - 10x_1 \cos x_2 + 1 = 0$$

Solve using the Newton-Raphson method starting with an initial guess of $x_1\,(0) = 1$ and $x_2(0) = 0$ radians and a stopping criteria of $\varepsilon = 10^{-4}$.

6.26 Repeat Problem 6.25 except using $x_1(0) = 0.25$ and $x_2(0) = 0$ radians as an initial guess.

6.27 For the Newton-Raphson method, the *region of attraction* (or *basin of attraction)* for a particular solution is the set of all initial guesses that converge to that solution. Usually initial guesses close to a particular solution will converge to that solution. However, for all but the simplest of multi-dimensional, nonlinear problems, the region of attraction boundary is often fractal. This makes it impossible to quantify the region of attraction and hence to guarantee convergence. Problem 6.25 has two

Copyright 2017 Cengage Learning. All Rights Reserved. May not be copied, scanned, or duplicated, in whole or in part. Due to electronic rights, some third party content may be suppressed from the eBook and/or eChapter(s). Editorial review has deemed that any suppressed content does not materially affect the overall learning experience. Cengage Learning reserves the right to remove additional content at any time if subsequent rights restrictions require it.

solutions when x_2 is restricted to being between $-\pi$ and π. With the x_2 initial guess fixed at 0 radians, numerically determine the values of the x_1 initial guesses that converge to the Problem 6.25 solution. Restrict your search to values of x_1 between 0 and 1.

SECTION 6.4

6.28 Consider the simplified electric power system shown in Figure 6.22 for which the power flow solution can be obtained without resorting to iterative techniques. (a) Compute the elements of the bus admittance matrix $\boldsymbol{Y}_{\text{bus}}$. (b) Calculate the phase angle δ_2 by using the real power equation at bus 2 (voltage-controlled bus). (c) Determine $|V_3|$ and δ_3 by using both the real and reactive power equations at bus 3 (load bus). (d) Find the real power generated at bus 1 (swing bus). (e) Evaluate the total real power losses in the system.

6.29 In Example 6.9, double the impedance on the line from bus 2 to bus 5. Determine the new values for the second row of $\boldsymbol{Y}_{\text{bus}}$. Verify your result using PowerWorld Simulator case Example 6_9.

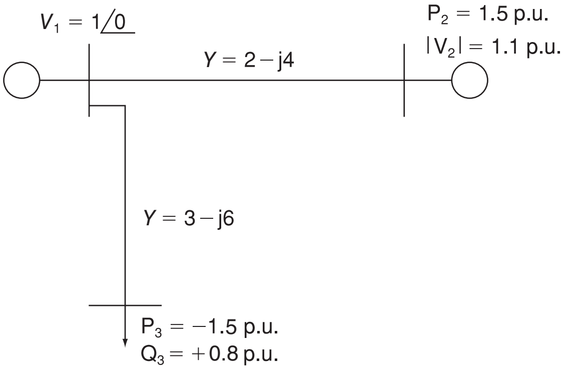

FIGURE 6.22

Problem 6.28

6.30 Determine the bus admittance matrix ($\boldsymbol{Y}_{\text{bus}}$) for the three-phase power system shown in Figure 6.23 with input data given in Table 6.11 and partial results in Table 6.12. Assume a three-phase 100 MVA per unit base.

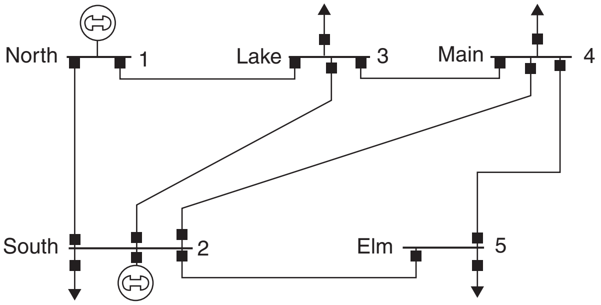

FIGURE 6.23

Sample System Diagram for Problem 6.30

Copyright 2017 Cengage Learning. All Rights Reserved. May not be copied, scanned, or duplicated, in whole or in part. Due to electronic rights, some third party content may be suppressed from the eBook and/or eChapter(s). Editorial review has deemed that any suppressed content does not materially affect the overall learning experience. Cengage Learning reserves the right to remove additional content at any time if subsequent rights restrictions require it.

Bus-to-Bus	R per unit	X per unit	B per unit
1-2	0.02	0.06	0.06
1-3	0.08	0.24	0.05
2-3	0.06	0.18	0.04
2-4	0.08	0.24	0.05
2-5	0.02	0.06	0.02
3-4	0.01	0.04	0.01
4-5	0.03	0.10	0.04

TABLE 6.11

Bus input data for Problem 6.30

$6.25 - j18.695$	$-5.00 + j15.00$	$-1.25 + j3.75$	0	0
$-5.00 + j15.00$				

TABLE 6.12

Partially Completed Bus Admittance Matrix ($\boldsymbol{Y}_{\text{bus}}$) for Problem 6.30

6.31 For the system from Problem 6.30, assume that a 75-Mvar shunt capacitance (three phase assuming one per unit bus voltage) is added at bus 4. Calculate the new value of Y_{44}.

SECTION 6.5

6.32 For a two-bus power system, a $0.7 + j0.4$ per unit load at bus 2 is supplied by a generator at bus 1 through a transmission line with series impedance of $0.05 + j0.1$ per unit. With bus 1 as the slack bus with a fixed per-unit voltage of $1.0\angle 0$, use the Gauss-Seidel method to calculate the voltage at bus 2 after three iterations.

6.33 Repeat Problem 6.32 with the slack bus voltage changed to $1.0\angle 30°$ per unit.

6.34 For the three-bus system whose $\boldsymbol{Y}_{\text{bus}}$ is given, calculate the second iteration value of V_3 using the Gauss-Seidel method. Assume bus 1 as the slack (with $V_1 = 1.0\angle 0°$), and buses 2 and 3 are load buses with a per-unit load of $S_2 = 1 + j0.5$ and $S_3 = 1.5 + j0.75$. Use voltage guesses of $1.0\angle 0°$ at both buses 2 and 3. The bus admittance matrix for a three-bus system is

$$\boldsymbol{Y}_{\text{bus}} = \begin{bmatrix} -j10 & j5 & j5 \\ j5 & -j10 & j5 \\ j5 & j5 & -j10 \end{bmatrix}$$

Copyright 2017 Cengage Learning. All Rights Reserved. May not be copied, scanned, or duplicated, in whole or in part. Due to electronic rights, some third party content may be suppressed from the eBook and/or eChapter(s). Editorial review has deemed that any suppressed content does not materially affect the overall learning experience. Cengage Learning reserves the right to remove additional content at any time if subsequent rights restrictions require it.

6.35 Repeat Problem 6.34 except assume the bus 1 (slack bus) voltage of $V_1 = 1.05\underline{/0°}$.

6.36 The bus admittance matrix for the power system shown in Figure 6.24 is given by

$$\boldsymbol{Y}_{\text{bus}} = \begin{bmatrix} 3 - j9 & -2 + j6 & -1 + j3 & 0 \\ -2 + j6 & 3.666 - j11 & -0.666 + j2 & -1 + j3 \\ -1 + j3 & -0.666 + j2 & 3.666 - j11 & -2 + j6 \\ 0 & -1 + j3 & -2 + j6 & 3 - j9 \end{bmatrix} \text{ per unit}$$

With the complex powers on load buses 2, 3, and 4 as shown in Figure 6.24, determine the value for V_2 that is produced by the first and second iterations of the Gauss-Seidel procedure. Choose the initial guess $V_2(0) = V_3(0) = V_4(0) = 1.0\underline{/0°}$ per unit.

FIGURE 6.24

Problem 6.36

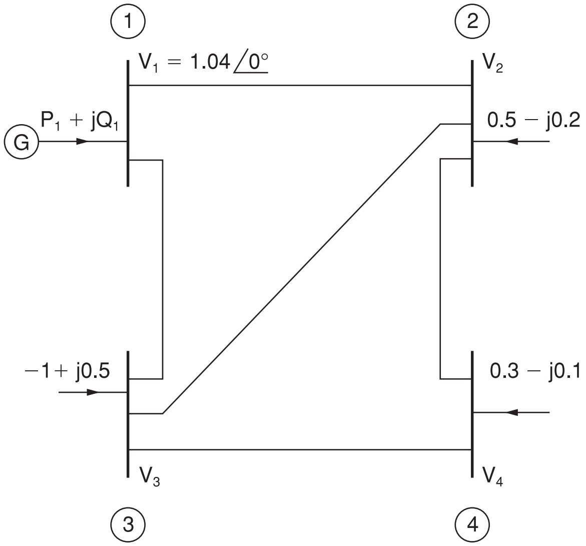

6.37 The bus admittance matrix of a three-bus power system is given by

$$\boldsymbol{Y}_{\text{bus}} = -j\begin{bmatrix} 7 & -2 & -5 \\ -2 & 6 & -4 \\ -5 & -4 & 9 \end{bmatrix} \text{ per unit}$$

with $V_1 = 1.0\underline{/0°}$ per unit; $V_2 = 1.0$ per unit; $P_2 = 60$ MW; $P_3 = -80$ MW; $Q_3 = -60$ Mvar (lagging) as a part of the power flow solution of the system. Find V_2 and V_3 within a tolerance of 0.01 per unit by using the Gauss-Seidel iteration method. Start with $\delta_2 = 0$, $V_3 = 1.0$ per unit, and $\delta_3 = 0$.

Copyright 2017 Cengage Learning. All Rights Reserved. May not be copied, scanned, or duplicated, in whole or in part. Due to electronic rights, some third party content may be suppressed from the eBook and/or eChapter(s). Editorial review has deemed that any suppressed content does not materially affect the overall learning experience. Cengage Learning reserves the right to remove additional content at any time if subsequent rights restrictions require it.

SECTION 6.6

6.38 A generator bus (with a 1.0 per unit voltage) supplies a 180 MW, 60 Mvar load through a lossless transmission line with per unit (100 MVA base) impedance of $j0.1$ and no line charging. Starting with an initial voltage guess of $1.0\angle 0°$, iterate until converged using the Newton-Raphson power flow method. For convergence criteria, use a maximum power flow mismatch of 0.1 MVA.

6.39 Repeat Problem 6.38 except use an initial voltage guess of $1.0\angle 30°$.

6.40 Repeat Problem 6.38 except use an initial voltage guess of $0.25\angle 0°$.

6.41 Determine the initial Jacobian matrix for the power system described in Problem 6.34.

6.42 Use the Newton-Raphson power flow to solve the power system described in Problem 6.34. For convergence criteria, use a maximum power flow mismatch of 0.1 MVA.

6.43 For a three-bus power system, assume bus 1 is the slack with a per unit voltage of $1.0\angle 0°$, bus 2 is a PQ bus with a per unit load of $2.0 + j0.5$, and bus 3 is a PV bus with 1.0 per unit generation and a 1.0 voltage setpoint. The per unit line impedances are $j0.1$ between buses 1 and 2, $j0.4$ between buses 1 and 3, and $j0.2$ between buses 2 and 3. Using a flat start, use the Newton-Raphson approach to determine the first iteration phasor voltages at buses 2 and 3.

6.44 Repeat Problem 6.43 except with the bus 2 real power load changed to 1.0 per unit.

PW **6.45** Load PowerWorld Simulator case Example 6_11; this case is set to perform a single iteration of the Newton-Raphson power flow each time **Single Solution** is selected. Verify that initially the Jacobian element J_{33} is 104.41. Then, give and verify the value of this element after each of the next three iterations (until the case converges).

PW **6.46** Load PowerWorld Simulator case Problem 6_46. Using a 100 MVA base, each of the three transmission lines have an impedance of $0.05 + j0.1$ p.u. There is a single 180 MW load at bus 3, while bus 2 is a PV bus with generation of 80 MW and a voltage setpoint of 1.0 p.u. Bus 1 is the system slack with a voltage setpoint of 1.0 p.u. Manually solve this case using the Newton-Raphson approach with a convergence criteria of 0.1 MVA. Show all your work. Then verify your solution by solving the case with PowerWorld Simulator.

PW **6.47** As was mentioned in Section 6.4, if a generator's reactive power output reaches its limit, then it is modeled as though it were a PQ bus. Repeat Problem 6.46, except assume the generator at bus 2 is operating with its reactive power limited to a maximum of 50 Mvar. Then verify your solution by solving the case with PowerWorld Simulator. To increase the reactive power output of the bus 2 generator, select **Tools, Play** to

Copyright 2017 Cengage Learning. All Rights Reserved. May not be copied, scanned, or duplicated, in whole or in part. Due to electronic rights, some third party content may be suppressed from the eBook and/or eChapter(s). Editorial review has deemed that any suppressed content does not materially affect the overall learning experience. Cengage Learning reserves the right to remove additional content at any time if subsequent rights restrictions require it.

begin the power flow simulation, then click on the up arrow on the bus 2 magenta voltage setpoint field until the reactive power output reaches its maximum.

PW **6.48** Load PowerWorld Simulator case Problem 6_46. Plot the reactive power output of the generator at bus 2 as a function of its voltage setpoint value in 0.005 p.u. voltage steps over the range between its lower limit of −50 Mvar and its upper limit of 50 Mvar. To change the generator 2 voltage set point first select **Tools, Play** to begin the power flow simulation, and then click on the up/down arrows on the bus 2 magenta voltage setpoint field.

SECTION 6.7

PW **6.49** Open PowerWorld Simulator case Problem 6_49. This case is identical to Example 6.9, except that the transformer between buses 1 and 5 is now a tap-changing transformer with a tap range between 0.9 and 1.1 and a tap step size of 0.00625. The tap is on the high side of the transformer. As the tap is varied between 0.975 and 1.1, show the variation in the reactive power output of generator 1, V_5, V_2, and the total real power losses.

PW **6.50** Use PowerWorld Simulator to determine the Mvar rating of the shunt capacitor bank in the Example 6_14 case that increases V_2 to 1.0 per unit. Also determine the effect of this capacitor bank on line loadings and the total real power losses (shown immediately below bus 2 on the oneline). To vary the capacitor's nominal Mvar rating, right-click on the capacitor symbol to view the Switched Shunt Dialog, and then change Nominal Mvar field.

PW **6.51** Use PowerWorld Simulator to modify the Example 6_9 case by inserting a second line between bus 2 and bus 5. Give the new line a circuit identifier of "2" to distinguish it from the existing line. The line parameters of the added line should be identical to those of the existing lines 2 to 5. Determine the new line's effect on V_2, the line loadings, and on the total real power losses.

PW **6.52** Open PowerWorld Simulator case Problem 6_52. Open the 69 kV line between buses REDBUD69 and PEACH69 (shown towards the bottom of the oneline). With the line open, determine the amount of Mvar (to the nearest 1 Mvar) needed from the REDBUD69 capacitor bank to correct the REDBUD69 voltage to at least 1.0 p.u.

PW **6.53** Open PowerWorld Simulator case Problem 6_53. Plot the variation in the total system real power losses as the generation at bus PEAR138 is varied in 20 MW blocks between 0 MW and 400 MW. What value of PEAR138 generation minimizes the total system losses?

PW **6.54** Repeat Problem 6.53, except first remove the 69 kV line between LOCUST69 and PEAR69.

Copyright 2017 Cengage Learning. All Rights Reserved. May not be copied, scanned, or duplicated, in whole or in part. Due to electronic rights, some third party content may be suppressed from the eBook and/or eChapter(s). Editorial review has deemed that any suppressed content does not materially affect the overall learning experience. Cengage Learning reserves the right to remove additional content at any time if subsequent rights restrictions require it.

SECTION 6.8

6.55 Using the compact storage technique described in Section 6.8, determine the vectors **DIAG**, **OFFDIAG**, **COL**, and **ROW** for the following matrix:

$$\mathrm{S}=\begin{bmatrix} 17 & -9.1 & 0 & 0 & -2.1 & -7.1 \\ -9.1 & 25 & -8.1 & -1.1 & -6.1 & 0 \\ 0 & -8.1 & 9 & 0 & 0 & 0 \\ 0 & -1.1 & 0 & 2 & 0 & 0 \\ -2.1 & -6.1 & 0 & 0 & 14 & -5.1 \\ -7.1 & 0 & 0 & 0 & -5.1 & 15 \end{bmatrix}$$

6.56 For the triangular factorization of the corresponding Y_{bus}, number the nodes of the graph shown in Figure 6.9 in an optimal order.

SECTION 6.10

6.57 Compare the angles and line flows between the Example 6_17 case and results shown in Tables 6.6, 6.7, and 6.8.

6.58 Redo Example 6.17 with the assumption that the per-unit reactance on the line between buses 2 and 5 is changed from 0.05 to 0.03.

PW **6.59** Open PowerWorld Simulator case Problem 6_59, which models a seven-bus system using the dc power flow approximation. Bus 7 is the system slack. The real power generation/load at each bus is as shown, while the per-unit reactance of each of the lines (on a 100 MVA base) is as shown in yellow on the oneline. (a) Determine the six-by-six **B** matrix for this system and the **P** vector. (b) Use a matrix package such as Matlab to verify the angles as shown on the oneline.

PW **6.60** Using the PowerWorld Simulator case from Problem 6.59, if the rating on the line between buses 1 and 2 is 150 MW, the current flow is 101 MW (from bus 1 to bus 3), and the bus 1 generation is 160 MW, analytically determine the amount this generation can increase until this line reaches 100% flow. Assume any change in the bus 1 generation is absorbed at the system slack.

SECTION 6.11

PW **6.61** PowerWorld Simulator cases Problem 6_61_PQ and 6_61_PV model a seven-bus power system in which the generation at bus 4 is modeled as a Type 1 or 2 wind turbine in the first case and as a Type 3 or 4 wind turbine in the second. A shunt capacitor is used to make the net reactive power injection at the bus the same in both cases. Compare the bus 4 voltage between the two cases for a contingency in which the line between buses 2 and 4 is opened. What is an advantage of a Type 3 or 4 wind turbine with respect to voltage regulation following a contingency? What is the variation in the Mvar output of a shunt capacitor with respect to bus voltage magnitude?

Copyright 2017 Cengage Learning. All Rights Reserved. May not be copied, scanned, or duplicated, in whole or in part. Due to electronic rights, some third party content may be suppressed from the eBook and/or eChapter(s). Editorial review has deemed that any suppressed content does not materially affect the overall learning experience. Cengage Learning reserves the right to remove additional content at any time if subsequent rights restrictions require it.

SECTION 6.12

6.62 The fuel-cost curves for two generators are given as follows:

$$C_1(P_1) = 600 + 18 \cdot P_1 + 0.04 \cdot (P_1)^2$$

$$C_2(P_2) = 700 + 20 \cdot P_2 + 0.03 \cdot (P_2)^2$$

Assuming the system is lossless, calculate the optimal dispatch values of P_1 and P_2 for a total load of 1000 MW, the incremental operating cost, and the total operating cost.

6.63 Rework Problem 6.62, except assume that the limit outputs are subject to the following inequality constraints:

$$200 \le P_1 \le 800 \text{ MW}$$

$$100 \le P_2 \le 400 \text{ MW}$$

6.64 Rework Problem 6.62, except assume the 1000 MW value also includes losses, and the penalty factor for the first unit is 1.0 and for the second unit 0.95.

6.65 The fuel-cost curves for a two-generator power system are given as follows:

$$C_1(P_1) = 600 + 15 \cdot P_1 + 0.05 \cdot (P_1)^2$$

$$C_2(P_2) = 700 + 20 \cdot P_2 + 0.04 \cdot (P_2)^2$$

while the system losses can be approximated as

$$P_L = 2 \times 10^{-4}(P_1)^2 + 3 \times 10^{-4}(P_2)^2 - 4 \times 10^{-4} P_1 P_2 \quad \text{MW}$$

If the system is operating with a marginal cost (λ) of \$60/hr, determine the output of each unit, the total transmission losses, the total load demand, and the total operating cost.

6.66 Expand the summations in (6.12.14) for $N = 2$, and verify the formula for $\partial P_L/\partial P_i$ given by (6.12.15). Assume $B_{ij} = B_{ji}$.

6.67 Given two generating units with their respective variable operating costs as

$$C_1 = 0.01P_{G1}^2 + 2P_{G1} + 100 \quad \$/\text{hr} \qquad \text{for } 25 \le P_{G1} \le 150 \quad \text{MW}$$
$$C_2 = 0.004P_{G2}^2 + 2.6P_{G2} + 80 \quad \$/\text{hr} \qquad \text{for } 30 \le P_{G2} \le 200 \quad \text{MW}$$

determine the economically optimum division of generation for $55 \le P_L \le 350$ MW. In particular, for $P_L = 282$ MW, compute P_{G1} and P_{G2}. Neglect transmission losses.

PW **6.68** Resolve Example 6.20, except with the generation at bus 2 set to a fixed value (i.e., modeled as off of Automatic Generation Control). Plot the variation in the total hourly cost as the generation at bus 2 is varied between 1000 and 200 MW in 5 MW steps, resolving the economic dispatch at each step. What is the relationship between bus 2 generation at the minimum point on this plot and the value from economic dispatch in Example 6.20? Assume a Load Scalar of 1.0.

Copyright 2017 Cengage Learning. All Rights Reserved. May not be copied, scanned, or duplicated, in whole or in part. Due to electronic rights, some third party content may be suppressed from the eBook and/or eChapter(s). Editorial review has deemed that any suppressed content does not materially affect the overall learning experience. Cengage Learning reserves the right to remove additional content at any time if subsequent rights restrictions require it.

PW **6.69** Using PowerWorld case Example 6_22 with the Load Scalar equal to 1.0, determine the generation dispatch that minimizes system losses *(Hint:* Manually vary the generation at buses 2 and 4 until their loss sensitivity values are zero). Compare the operating cost between this solution and the Example 6_22 economic dispatch result. Which is better?

PW **6.70** Repeat Problem 6.69, except with the Load Scalar equal to 1.4.

SECTION 6.13

PW **6.71** Using LP OPF with PowerWorld Simulator case Example 6_23, plot the variation in the bus 5 marginal price as the Load Scalar is increased from 1.0 in steps of 0.02. What is the maximum possible load scalar without overloading any transmission line? Why is it impossible to operate without violations above this value?

PW **6.72** Load PowerWorld Simulator case Problem 6_72. This case models a slightly modified, lossless version of the 37-bus case from Example 6.13 with generator cost information, but also with the transformer between buses PEAR138 and PEAR69 open. When the case is loaded, the "Total Cost" field shows the economic dispatch solution, which results in an overload on several lines. Before solving the case, select **Add-Ons, OPF Case Info, OPF Buses** to view the bus LMPs, noting that they are all identical. Then Select **Add-Ons, Primal LP** to solve the case using the OPF, and again view the bus LMPs. Verify the LMP at the PECAN69 bus by manually changing the load at the bus by one MW, and then noting the change in the Total Cost field. Repeat for the LOCUST69 bus. *Note*: Because of solution convergence tolerances, the manually calculated results may not exactly match the OFP calculated bus LMPs.

CASE STUDY QUESTIONS

a. What are the operational impacts on fossil-fueled power plants due to high penetrations of wind and solar generation into a power grid?

b. Do high penetrations of wind and solar generation increase the wear and tear costs of fossil-fueled generation? Why?

c. Which has more forecast uncertainty, wind generation or solar generation? Why?

DESIGN PROJECT I: NEW LOAD

As a result of the low electric rates from the local utility, Metropolis Light and Power (MLP), several large server farms and a new factory are going to be built in the eastern portion of the MLP service territory (see Figure 6.25). With an anticipated peak load of about 75 MW and 20 Mvar, this new load also brings additional revenue to MLP. However, in order to supply this additional load, the new TULIP substation will need to be constructed. While they would like to receive electricity at the

Copyright 2017 Cengage Learning. All Rights Reserved. May not be copied, scanned, or duplicated, in whole or in part. Due to electronic rights, some third party content may be suppressed from the eBook and/or eChapter(s). Editorial review has deemed that any suppressed content does not materially affect the overall learning experience. Cengage Learning reserves the right to remove additional content at any time if subsequent rights restrictions require it.

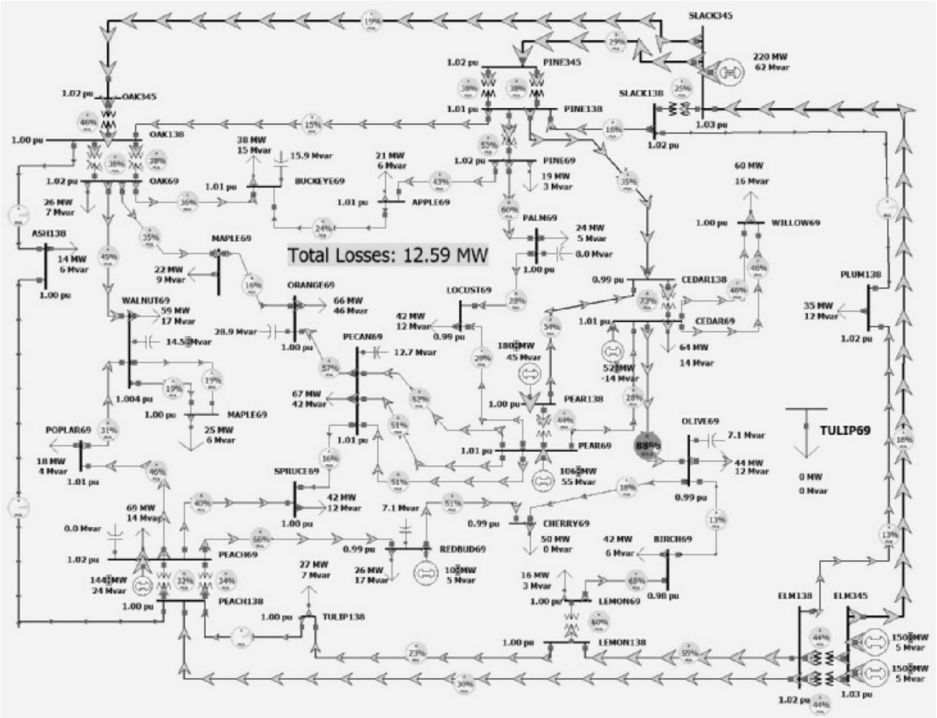
SLACK345
220 MW
62 Mvar
1.02 pu
PINE345
1.02 pu
OAK345
SLACK138
1.01 pu
PINE138
1.03 pu
1.00 pu
OAK138
38 MW
15 Mvar
15.9 Mvar
21 MW
6 Mvar
1.02 pu
PINE69
1.02 pu
1.02 pu
OAK69
1.01 pu
BUCKEYE69
19 MW
3 Mvar
60 MW
16 Mvar
26 MW
7 Mvar
1.01 pu
APPLE69
PALM69
1.00 pu
WILLOW69
ASH138
24 MW
5 Mvar
8.0 Mvar
MAPLE69
14 MW
6 Mvar
Total Losses: 12.59 MW
1.00 pu
22 MW
9 Mvar
0.99 pu
CEDAR138
PLUM138
1.00 pu
ORANGE69
LOCUST69
WALNUT69
59 MW
17 Mvar
66 MW
46 Mvar
42 MW
12 Mvar
1.01 pu
CEDAR69
35 MW
12 Mvar
28.9 Mvar
0.99 pu
14.5 Mvar
1.00 pu
PECAN69
12.7 Mvar
180 MW
45 Mvar
64 MW
14 Mvar
1.02 pu
52 MW
-14 Mvar
1.004 pu
67 MW
42 Mvar
1.00 pu
PEAR138
1.00 pu
MAPLE69
OLIVE69
POPLAR69
25 MW
6 Mvar
7.1 Mvar
TULIP69
1.01 pu
1.01 pu
PEAR69
18 MW
4 Mvar
44 MW
12 Mvar
SPRUCE69
106 MW
55 Mvar
1.01 pu
0 MW
0 Mvar
42 MW
12 Mvar
0.99 pu
69 MW
14 Mvar
7.1 Mvar
1.00 pu
0.99 pu
CHERRY69
0.0 Mvar
50 MW
0 Mvar
42 MW
6 Mvar
BIRCH69
PEACH69
0.99 pu
REDBUD69
1.02 pu
27 MW
7 Mvar
26 MW
17 Mvar
10 MW
5 Mvar
16 MW
3 Mvar
144 MW
24 Mvar
0.98 pu
1.00 pu
PEACH138
1.00 pu
LEMON69
ELM138
ELM345
1.00 pu
TULIP138
1.00 pu
LEMON138
150 MW
5 Mvar
150 MW
5 Mvar
1.02 pu
1.03 pu
19%
29%
38%
38%
25%
46%
15%
16%
53%
38%
38%
43%
36%
35%
24%
60%
35%
45%
16%
46%
73%
46%
28%
34%
20%
57%
19%
19%
52%
28%
44%
31%
51%
88%
16%
46%
51%
18%
40%
51%
13%
66%
13%
32%
34%
65%
60%
23%
55%
44%
30%
44%
16%

FIGURE 6.25

Design Case 1 System Oneline Diagram

69 kV level, the new substation location is large enough to accommodate a 138/69 kV transformer if needed. Additionally, for reliability purposes, the TULIP substation needs to have at least two separate lines into their substation.

As a planning engineer for MLP, your job is to make recommendations to ensure that, with new TULIP loads under peak loading conditions, the transmission system in the eastern region is adequate for any base case or first contingency loading situation. This is also a good opportunity not only to meet the new load, but also to fix some existing first contingency violations in the eastern portion of the MLP service territory. Table 6.13 shows the available right-of-way distances that

Right-of-Way/Substation	Right-of-Way Distance (km)
TULIP to ELM	15
TULIP to PLUM	12
TULIP to OLIVE	8
TULIP to CEDAR	10
TULIP to BIRCH	14
CEDAR to PLUM	13
WILLOW to PLUM	8
OLIVE TO CEDAR	10

TABLE 6.13

Available New Rights-of-Way

Copyright 2017 Cengage Learning. All Rights Reserved. May not be copied, scanned, or duplicated, in whole or in part. Due to electronic rights, some third party content may be suppressed from the eBook and/or eChapter(s). Editorial review has deemed that any suppressed content does not materially affect the overall learning experience. Cengage Learning reserves the right to remove additional content at any time if subsequent rights restrictions require it.

can be used for the construction of new 69 kV and/or new 138 kV lines. All existing 69 kV-only substations are large enough to accommodate 138 kV as well. The DesignCase1_2015 provides a power flow model of the initial conditions.

Design Procedure

1. Load DesignCase1_2015 into PowerWorld Simulator. Perform an initial power-flow solution to verify the base case system operation without the TULIP load. Note that the entire line flows and bus voltage magnitudes are within their limits. Assume all line MVA flows must be at or below 100% of the limit A values, and all voltages must be between 0.95 and 1.10 per unit.
2. Repeat the above analysis considering the impact of any single transmission line or transformer outage. This is known as contingency analysis. To simplify this analysis, PowerWorld Simulator has the ability to automatically perform a contingency analysis study. Select **Tools, Contingency Analysis** to show the Contingency Analysis display. Note that the 57 single line/transformer contingencies are already defined. Select **Start Run** to automatically see the impact of removing any single element. This system has line violations for several different contingencies.
3. Using the rights-of-way and the transmission line parameters/costs given in the cost section (see page 409), iteratively determine the least expensive system additions so that the base case and all the contingences result in reliable operation points (i.e., one with no violations) with the new TULIP load. The parameters of the new transmission lines(s) need to be derived using the tower configurations and conductor types. Tower configurations are provided by the instructor with default values given with the cost data. Several different conductor types are available in the cost section. The total cost of an addition is defined as the construction costs minus the savings associated with any decrease in system losses over the next 5 years.
4. Write a detailed report discussing the initial system problems, your approach to optimally solving the system problems, and the justification for your final recommendation.

Simplifying Assumptions

To simplify the analysis, several assumptions are made:

1. You need only consider the base case loading level given in DesignCase1_2015. In a real design, typically a number of different operating points/loading levels must be considered.
2. You should consider the generator outputs as fixed values; any changes in the losses and the new TULIP load are always picked up by the system slack generator.
3. You should not modify the status of the capacitors or the transformer taps.
4. You should assume that the system losses remain constant over the 5-year period and need only consider the impact the new design has on the base case losses. Electricity is priced at \$60/MWh.

Copyright 2017 Cengage Learning. All Rights Reserved. May not be copied, scanned, or duplicated, in whole or in part. Due to electronic rights, some third party content may be suppressed from the eBook and/or eChapter(s). Editorial review has deemed that any suppressed content does not materially affect the overall learning experience. Cengage Learning reserves the right to remove additional content at any time if subsequent rights restrictions require it.

DESIGN PROJECT 2: NEW WIND GENERATION AND GENERATION RETIREMENT

As a planning engineer for Island Electric Company (IEC), you have been tasked with determining the transmission system changes required to locate a new 600 MW wind farm in the western portion of your service territory (see Figure 6.26). IEC uses 345 and 161 kV transmission grids, so your changes are restricted to these existing voltages. The wind farm would like to connect at the 161 kV level and requires at least two transmission lines into the NewWind substation (which can be at either 161 and/or 345 kV). Since the location is usually quite windy, it is expected to have a capacity factor of at least 40%. However, the wind also can be quite variable, including during times of maximum system loading, so this generation cannot be counted on for firm capacity. Simultaneous with the addition of the new wind farm, IEC would like to retire the existing 300 MW generator at the Pheasant substation.

Hence, your job is to make recommendations on the least-cost design for the construction of new lines and transformers to ensure that the transmission system in the IEC system is adequate for any base case or first-contingency loading situation when then wind farm is installed and operating at either its maximum output of 600 or 0 MW and with the Pheasant generator removed from service. Note, this will also involve fixing some existing first-contingency violations. Since the wind farm will be built with Type 3 DFAG wind turbines, you can model the wind farm in the power flow as a single equivalent, traditional PV bus generator with a fixed output of either 0 or 600 MW, a voltage setpoint of 1.03 per unit, and with reactive power limits of ±250 Mvar.

Table 6.14 shows the right-of-way distances that are available for the construction of new 161 kV and/or new 345 kV lines. All existing 161-kV only substations are large enough to accommodate 345 kV as well, as is the NewWind substation.

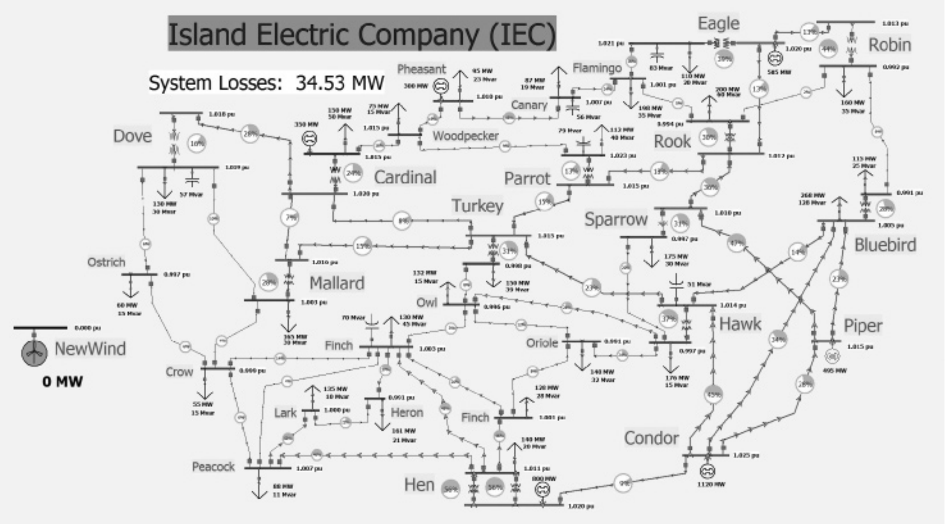

FIGURE 6.26 Design Case 2 System Oneline Diagram

Copyright 2017 Cengage Learning. All Rights Reserved. May not be copied, scanned, or duplicated, in whole or in part. Due to electronic rights, some third party content may be suppressed from the eBook and/or eChapter(s). Editorial review has deemed that any suppressed content does not materially affect the overall learning experience. Cengage Learning reserves the right to remove additional content at any time if subsequent rights restrictions require it.

Right-of-Way/Substation	Right-of-Way Distance (km)
NewWind to Ostrich	15
NewWind to Dove	55
NewWind to Crow	30
NewWind to Peacock	53
NewWind to Hen	70
Ostrich to Mallard	45
Peakcock to Hen	20
Dove to Cardinal	40

TABLE 6.14

Available New Rights-of-Way

Design Procedure

1. Load DesignCase2_2015 into PowerWorld Simulator, which contains the system power flow case and the disconnected NewWind generator and bus. Perform an initial power flow solution to verify the base case system operation. Note that all of the line flows and bus voltage magnitudes are within their limits. Assume all line MVA flows must be at or below 100% of their limit values, and all voltages must be between 0.92 and 1.10 per unit.
2. Repeat the above analysis, considering the impact of any single transmission line or transformer outage. This is known as contingency analysis. To simplify this analysis, PowerWorld Simulator has the ability to automatically perform a contingency analysis study. Select **Tools, Contingency Analysis** to show the Contingency Analysis display. Note that the 60 single line/transformer contingencies are already defined. Select **Start Run** (towards the bottom right corner of the display) to automatically see the impact of removing any single element. Note that there are several existing violations.
3. Open the existing 300 MW generator at the Pheasant substation, and repeat parts 1 and 2.
4. Using the rights-of-way given in Table 6.14 and the transmission line parameters/costs, iteratively determine the least-expensive system additions so that the base case and all the contingences result in reliable operation points with the NewWind generation connected with an output of either 0 or 600 MW. When the output is at 0 MW, the wind farm is still considered on-line and hence should be modeled as a PV bus regulating its voltage to 1.03 p.u. The parameters of the new transmission lines(s) need to be derived using the tower configurations and conductor types provided by the instructor. In addition, the transmission changes you propose will modify the total system losses, indicated by the large field

Copyright 2017 Cengage Learning. All Rights Reserved. May not be copied, scanned, or duplicated, in whole or in part. Due to electronic rights, some third party content may be suppressed from the eBook and/or eChapter(s). Editorial review has deemed that any suppressed content does not materially affect the overall learning experience. Cengage Learning reserves the right to remove additional content at any time if subsequent rights restrictions require it.

on the oneline diagram. In your design, you should consider the impact on total system losses in the studied condition for the next 5 years. Hence, you should minimize the total construction costs minus the savings associated with any decrease in system losses over the next 5 years.

5. Write a detailed report discussing the initial system problems, your approach to optimally solving the system problems, and the justification for your final recommendation.

Simplifying Assumptions

To simplify the analysis, several assumptions are made:

1. You need only consider the base case loading level given with the modification of opening the Pheasant generation. In a real design, typically a number of different operating points/loading levels must be considered.
2. You should consider all the generator real power outputs as fixed values with the exception that the NewWind generator should be studied at both 0 and 600 MW. The change in the total system generation and any changes in the system losses are always picked up by the system slack.
3. You should not modify the status of the capacitors or the transformer taps.
4. You should assume that the system losses remain constant over the 5-year period and need only consider the impact the new design has on the base case losses, assuming the NewWind generation is at 600 MW. The price for losses can be assumed to be \$50/MWh.
5. You do not need to consider contingencies involving the new transmission lines and possibly any transformers you may be adding.
6. While an appropriate control response to a contingency might be to decrease the wind farm output (by changing the pitch on the wind turbine blades), your supervisor has specifically asked you not to consider this possibility. Therefore the NewWind generator should always have either a 0 or 600 MW output.

DESIGN PROJECTS 1 AND 2: SAMPLE TRANSMISSION SYSTEM DESIGN COSTS

Transmission Lines (69 kV, 138 kV, 161 kV, 345 kV)

New transmission lines include a fixed cost and a variable cost. The fixed cost is for the design work, the purchase/installation of the three-phase circuit breakers, associated relays, and changes to the substation bus structure. The fixed costs are \$2,400,000 for a 345 kV line, \$1,100,000 for at 161 kV line, \$850,000 for a 138 kV line, and \$500,000 for a 69 kV line. The variable costs depend on the type of conductor and the length of the line. The assumed cost in \$/km are given in Table 6.15.

Copyright 2017 Cengage Learning. All Rights Reserved. May not be copied, scanned, or duplicated, in whole or in part. Due to electronic rights, some third party content may be suppressed from the eBook and/or eChapter(s). Editorial review has deemed that any suppressed content does not materially affect the overall learning experience. Cengage Learning reserves the right to remove additional content at any time if subsequent rights restrictions require it.

Conductor Type	Current Rating (Amps)	345-kV Lines	161-kV Lines	138-kV Lines	69-kV Lines
Rook	770				\$200,000/km
Crow	830		\$390,000/km	\$330,000/km	\$220,000/km
Condor	900		\$410,000/km	\$350,000/km	\$240,000/km
Cardinal	1110	\$600,000/km	\$430,000/km	\$370,000/km	
Pheasant	1200	\$650,000/km	\$450,000/km		
Falcon	1380	\$700,000/km			

TABLE 6.15

Assumed costs

Lined impedance data and MVA ratings are determined based on the conductor type and tower configuration. The conductor characteristics are given in Table A.4 of the book. For these design problems, assume a symmetric tower configurations. Often the spacings between conductors are provided by the instructor and may be student specific. If no values are given, assume a GMD of 2 m for 69 kV, 4 m for 138 kV, 5 m for 161 kV, and 8 m for 345 kV.

Transformers

Transformer costs include associated circuit breakers, relaying, and installation.

138/69 kV, 101 MVA	\$1,500,000
138/69 kV, 168 MVA	\$1,800,000
345/161 kV, 560 MVA	\$7,500,000

Assume any new 138/69 kV transformer has 0.0025 per unit resistance and 0.07 per unit reactance, and any new 345/161 kV transformer has 0.0004 per unit resistance and 0.025 per unit reactance (all on a 100 MVA base).

Bus Work

Upgrade 69-kV substation to also include 138 kV	\$900,000
Upgrade 161-kV substation to also include 345 kV	\$3,500,000

DESIGN PROJECT 3: POWER FLOW/SHORT CIRCUITS

Time given: 3 weeks
Approximate time required: 15 hours
Each student is assigned one of the single-line diagrams shown in Figures 6.27 and 6.28. Also, the length of line 2 in these figures is varied for each student.

Assignment I: Power Flow Preparation

For the single-line diagram that you have been assigned (Figure 6.27 or 6.28), convert all positive-sequence impedance, load, and voltage data to per unit using the given

Copyright 2017 Cengage Learning. All Rights Reserved. May not be copied, scanned, or duplicated, in whole or in part. Due to electronic rights, some third party content may be suppressed from the eBook and/or eChapter(s). Editorial review has deemed that any suppressed content does not materially affect the overall learning experience. Cengage Learning reserves the right to remove additional content at any time if subsequent rights restrictions require it.

system base quantities. Then using the PowerWorld Simulator, create three input data files: bus input data, line input data, and transformer input data. Note that bus 1 is the swing bus. Your output for this assignment consists of three power-flow input data files.

The purpose of this assignment is to get started and to correct errors before going to the next assignment. It requires a knowledge of the per-unit system, which was covered in Chapter 3, but may need review.

Assignment 2: Power Flow

Case 1. Run the power flow program and obtain the bus, line, and transformer input/output data files that you prepared in Assignment 1.

Case 2. Suggest one method of increasing the voltage magnitude at bus 4 by 5%. Demonstrate the effectiveness of your method by making appropriate changes to the input data of case 1 and by running the power flow program.

Your output for this assignment consists of 12 data files, 3 input, and 3 output data files for each case, along with a one-paragraph explanation of your method for increasing the voltage at bus 4 by 5%.

During this assignment, course material contains voltage control methods, including use of generator excitation control, tap changing and regulating transformers, static capacitors, static var systems, and parallel transmission lines.

This project continues in Chapters 7 and 9.

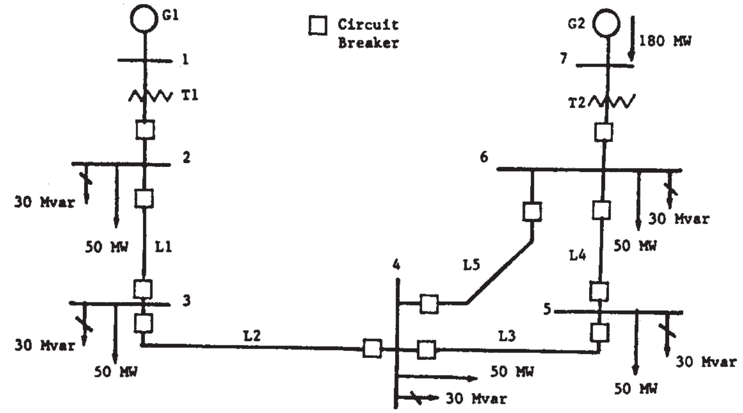

FIGURE 6.27 Single-line diagram for Design Project 3—transmission loop

Generator Ratings

G1: 100 MVA, 13.8 kV, $x'' = 0.12, x_2 = 0.14, x_0 = 0.05$ per unit

G2: 200 MVA, 15.0 kV, $x'' = 0.12, x_2 = 0.14, x_0 = 0.05$ per unit

The generator neutrals are solidly grounded

Transformer Ratings

T1: 100 MVA, 13.8 kVΔ/230 kVY, $x = 0.1$ per unit

T2: 200 MVA, 15 kVΔ/230 kVY, $x = 0.1$ per unit

The transformer neutrals are solidly grounded

Transmission Line Ratings

All Lines: 230 kV, $z_1 = 0.08 + j0.5$ Ω/km,

$z_0 = 0.2 + j1.5$ Ω/km, $y_1 = j3.3$ E-6 S/km,

Maximum MVA = 400

Line Lengths: $L_1 = 15$ km, L_2 assigned by the instructor (20 to 50 km), $L_3 = 40$ km, $L_4 = 15$ km, $L_5 = 50$ km.

Power Flow Data

Bus 1 : Swing bus, $V_1 = 13.8$ kV, $\partial_1 = 0°$

Bus 2,3,4,5,6 : Load buses

Bus 7 : Constant voltage magnitude bus, $V_7 = 15$ kV,

$P_{G7} = 180$ MW, $-87 \text{ Mvar} < Q_{G7} < +87 \text{ Mvar}$

System Base Quantities

$S_{base} = 100$ MVA (three-phase)

$V_{base} = 13.8$ kV (line-to-line) in the zone of G1

Copyright 2017 Cengage Learning. All Rights Reserved. May not be copied, scanned, or duplicated, in whole or in part. Due to electronic rights, some third party content may be suppressed from the eBook and/or eChapter(s). Editorial review has deemed that any suppressed content does not materially affect the overall learning experience. Cengage Learning reserves the right to remove additional content at any time if subsequent rights restrictions require it.

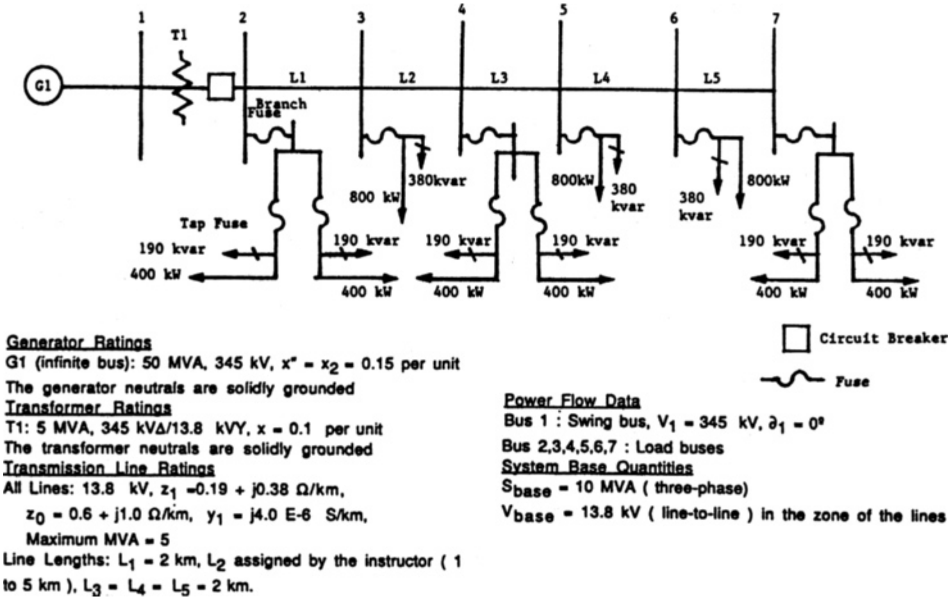

Generator Ratings
G1 (infinite bus): 50 MVA, 345 kV, $x'' = x_2 = 0.15$ per unit
The generator neutrals are solidly grounded
Transformer Ratings
T1: 5 MVA, 345 kVΔ/13.8 kVY, x = 0.1 per unit
The transformer neutrals are solidly grounded
Transmission Line Ratings
All Lines: 13.8 kV, $z_1 = 0.19 + j0.38$ Ω/km,
$z_0 = 0.6 + j1.0$ Ω/km, $y_1 = j4.0$ E-6 S/km,
Maximum MVA = 5
Line Lengths: $L_1 = 2$ km, L_2 assigned by the instructor (1 to 5 km), $L_3 = L_4 = L_5 = 2$ km.

Power Flow Data
Bus 1 : Swing bus, $V_1 = 345$ kV, $\delta_1 = 0°$
Bus 2,3,4,5,6,7 : Load buses
System Base Quantities
$S_{base} = 10$ MVA (three-phase)
$V_{base} = 13.8$ kV (line-to-line) in the zone of the lines

FIGURE 6.28 Single-line diagram for Design Project 3—radial distribution feeder

REFERENCES

1. W. F. Tinney and C. E. Hart, "Power Flow Solutions by Newton's Method," *IEEE Trans. PAS*, *86* (November 1967), p. 1449.
2. W. F. Tinney and J. W. Walker, "Direct Solution of Sparse Network Equations by Optimally Ordered Triangular Factorization," *Proc. IEEE*, *55* (November 1967), pp. 1801–1809.
3. Glenn W. Stagg and Ahmed H. El-Abiad, *Computer Methods in Power System Analysis* (New York: McGraw-Hill, 1968).
4. N. M. Peterson and W. S. Meyer, "Automatic Adjustment of Transformer and Phase Shifter Taps in Newton Power Flow," *IEEE Trans. PAS*, *90* (January-February 1971), pp. 103–108.
5. W. D. Stevenson, Jr., *Elements of Power Systems Analysis*, 4th ed. (New York: McGraw-Hill, 1982).
6. A. Bramellar and R. N. Allan, *Sparsity* (London: Pitman, 1976).
7. C. A. Gross, *Power Systems Analysis* (New York: Wiley, 1979).
8. B. Stott, "Fast Decoupled Load Flow," *IEEE Trans. PAS*, Vol. PAS 91 (September–October 1972), pp. 1955–1959.
9. T. Overbye and J. Weber, "Visualizing the Electric Grid," *IEEE Spectrum*, 38, 2 (February 2001), pp. 52–58.
10. Westinghouse Electric Corporation, *Transmission and Distribution Reference Book*, 4th ed. (Pittsburgh: Westinghouse, 1964).

Copyright 2017 Cengage Learning. All Rights Reserved. May not be copied, scanned, or duplicated, in whole or in part. Due to electronic rights, some third party content may be suppressed from the eBook and/or eChapter(s). Editorial review has deemed that any suppressed content does not materially affect the overall learning experience. Cengage Learning reserves the right to remove additional content at any time if subsequent rights restrictions require it.

11. Aluminum Association, *The Aluminum Electrical Conductor Handbook* (Washington, D.C.: Aluminum Association).

12. A. J. Wood and B. F. Wollenberg, *Power Generation*, *Operation and Control*, 2nd ed. (New York: John Wiley & Sons, 1996).

13. A. Ellis, "Wind Power Plant Models for System Studies," Tutorial on Fundamentals of Wind Energy, Section V, *IEEE PES GM* (Calgary, AB: July 2009).

14. WECC Wind Generator Modeling Group, "WECC Wind Power Plant Power Flow Modeling Guide," *WECC*, May 2008.

15. E.H. Camm et al., "Characteristics of Wind Turbine Generators for Wind Power Plants," *Proc. IEEE* 2009 General Meeting (Calgary, AB: July 2009).

16. L. K. Kirchmayer, *Economic Operation of Power Systems* (New York: Wiley, 1958).

17. L. K. Kirchmayer and G. W. Stagg, "Evaluation of Methods of Coordinating Incremental Fuel Costs and Incremental Transmission Losses," *Transactions AIEE*, vol. 71, part III (1952), pp. 513–520.

18. G. H. McDaniel and A. F. Gabrielle, "Dispatching Pumped Storage Hydro," *IEEE Transmission PAS*, vol. PAS-85 (May 1966), pp. 465–471.

19. E. B. Dahlin and E. Kindingstad, "Adaptive Digital River Flow Predictor for Power Dispatch," *IEEE Transactions PAS*, vol. PAS-83 (April 1964), pp. 320–327.

20. L. K. Kirchmayer, *Economic Control of Interconnected Systems* (New York: Wiley, 1959).

21. J. H. Drake et al., "Optimum Operation of a Hydrothermal System," *Transactions AIEE* (*Power Apparatus and Systems*), vol. 62 (August 1962), pp. 242–250.

22. A. J. Wood and B. F. Wollenberg, *Power Generation*, *Operation*, *and Control* (New York: Wiley, 1989).

23. 2005 and 2014 PJM State of the Market Report, available online at http://www.monitoringanalytics.com/reports/PJM_State_of_the_Market/2014.shtml.

24. A. Castillo and R. P. O'Neill, "Survey of Approaches to Solving the ACOPF," *U.S. FERC* (March 2013).

Copyright 2017 Cengage Learning. All Rights Reserved. May not be copied, scanned, or duplicated, in whole or in part. Due to electronic rights, some third party content may be suppressed from the eBook and/or eChapter(s). Editorial review has deemed that any suppressed content does not materially affect the overall learning experience. Cengage Learning reserves the right to remove additional content at any time if subsequent rights restrictions require it.

Copyright 2017 Cengage Learning. All Rights Reserved. May not be copied, scanned, or duplicated, in whole or in part. Due to electronic rights, some third party content may be suppressed from the eBook and/or eChapter(s). Editorial review has deemed that any suppressed content does not materially affect the overall learning experience. Cengage Learning reserves the right to remove additional content at any time if subsequent rights restrictions require it.

7 Symmetrical Faults

345-kV SF6 circuit breaker installation at Goshen Substation, Idaho Falls, Idaho, USA. This circuit breaker has a continuous current rating of 2000A and an interrupting current rating of 40 kA (Courtesy of PacifiCorp.)

Short circuits occur in power systems when equipment insulation fails due to system overvoltages caused by lightning or switching surges, to insulation contamination (salt spray or pollution), or to other mechanical causes. The resulting short circuit or "fault" current is determined by the internal voltages of the synchronous machines and by the system impedances between the machine voltages and the fault. Short-circuit currents may be several orders of magnitude larger than normal operating currents and, if allowed to persist, may cause thermal damage to equipment. Windings and busbars may also suffer mechanical damage due to high

Copyright 2017 Cengage Learning. All Rights Reserved. May not be copied, scanned, or duplicated, in whole or in part. Due to electronic rights, some third party content may be suppressed from the eBook and/or eChapter(s). Editorial review has deemed that any suppressed content does not materially affect the overall learning experience. Cengage Learning reserves the right to remove additional content at any time if subsequent rights restrictions require it.

magnetic forces during faults. It is therefore necessary to remove faulted sections of a power system from service as soon as possible. Standard EHV protective equipment is designed to clear faults within 3 cycles (50 ms at 60 Hz). Lower voltage protective equipment operates more slowly (for example, 5 to 20 cycles).

Section 7.1 begins by reviewing series R–L circuit transients followed in Section 7.2 by a description of three-phase short-circuit currents at unloaded synchronous machines, analyzing both the ac component, including subtransient, transient, and steady-state currents, and the dc component of fault current. These results are extended in Sections 7.3 and 7.4 to power system three-phase short circuits by means of the superposition principle. We observe that the bus impedance matrix is the key to calculating fault currents. Section 7.5 discusses circuit breaker and fuse selection.

Balanced three-phase power systems are assumed throughout this chapter, working in per unit.

CASE STUDY

The following case study investigates the short-circuit behavior of wind power plants (WPPs) [11]. Conventional power plants including fossil-fueled, nuclear, and hydro plants consist of single or several synchronous generating units, wherein for each unit the rotational speed is fixed and the magnetic flux is controlled via exciter windings; the magnetic flux and the rotor rotate synchronously. A WPP consists of several wind turbine generators (WTGs), presently available in sizes between 1 and 5 MW, which are dispersed over a wide geographical area. There are four main types of WTGs: Type 1—fixed-speed turbine with a squirrel-cage induction generator; Type 2—variable-speed turbine with a wound-rotor induction generator that has a variable resistor in series with the rotor winding; Type 3—variable-speed turbine with a doubly fed induction generator; and Type 4—variable-speed turbine with a permanent-magnet synchronous generator and ac-dc-ac power-electronic converter. The short-circuit current characteristics for both symmetrical and unsymmetrical faults are examined for each of the four types of WTGs.

Short-Circuit Modeling of a Wind Power Plant

E. Muljadi V. Gevorgian
Fellow, IEEE Member, IEEE
National Renewable Energy Laboratory

Copyright 2017 Cengage Learning. All Rights Reserved. May not be copied, scanned, or duplicated, in whole or in part. Due to electronic rights, some third party content may be suppressed from the eBook and/or eChapter(s). Editorial review has deemed that any suppressed content does not materially affect the overall learning experience. Cengage Learning reserves the right to remove additional content at any time if subsequent rights restrictions require it.

Introduction

Energy and environmental issues have become one of the biggest challenges facing the world. In response to energy needs and environmental concerns, renewable energy technologies are considered the future technologies of choice [1, 2]. Renewable energy is harvested from nature, and it is clean and free. However, it is widely accepted that renewable energy is not a panacea that comes without challenges. With the federal government's aggressive goal of achieving 20% wind energy penetration by 2030, it is necessary to understand the challenges that must be overcome when using renewable energy.

In the years to come, there will be more and more wind power plants (WPPs) connected to the grid. With the goal of 20% wind penetration by 2030, the WPP's operation should be well planned. The power system switchgear and power system protection for WPPs should be carefully designed to be compatible with the operation of conventional synchronous generators connected to the same grid. This paper attempts to illustrate the behavior of short-circuit current (SCC) contributions for different types of WTGs.

Conventional Power Plants versus Wind Power Plants

A conventional power plant consists of a single or several large (e.g., 100 MW) generators. The prime mover of the generator can be steam, gas, or a combustion engine. The generator is controllable and is adjustable up to a maximum limit and down to minimum limit. The power output is dispatched according to the load forecast, influenced by human operation, and is based on optimum operation (i.e., scheduled operation). The power plant is usually located relatively close to the load center.

The typical conventional generator used is a synchronous generator. The rotational speed is fixed—no slip; and the flux is controlled via exciter windings. The magnetic flux and the rotor rotate synchronously.

A WPP consists of many (hundreds) of wind turbine generators (WTGs). Currently, available WTG sizes are between 1 MW and 5 MW. The prime mover of the WTG is wind, and it is free, natural, and pollution-free. The controllability of the WPP is typically curtailment (spilling the wind). The energy production of a WPP depends on the wind variability, and its dispatch capability is based on wind forecasting. It is influenced more by nature (wind) than human factors, with the goal set on maximizing energy production from renewable resources (i.e., unscheduled operation). Large-scale WPPs are located in high-wind resource regions, and these may be far from the load center.

Because a WPP covers a very large area, there are power output diversities found in a typical WPP. Each WTG in a WPP will be located at different electrical distances from the substation (diversity in line impedance). Each turbine may be driven by different instantaneous wind speeds.

Short-Circuit Modeling of a Wind Power Plant by E. Muljadi and V. Gevorgian, Conference Paper NREL/CP-5500-50632, *Power & Energy Society General Meeting*, July 24–29, 2011, Detroit MI, p i–ii, 1–10.

Copyright 2017 Cengage Learning. All Rights Reserved. May not be copied, scanned, or duplicated, in whole or in part. Due to electronic rights, some third party content may be suppressed from the eBook and/or eChapter(s). Editorial review has deemed that any suppressed content does not materially affect the overall learning experience. Cengage Learning reserves the right to remove additional content at any time if subsequent rights restrictions require it.

Thus, the operating condition of each turbine may be slightly different from others within the WPP.

Operation of Wind Turbine Generators

The generator at each turbine should be protected individually and independently because of the electrical diversity of the WPP. In practice, this is an advantage of a WPP compared to a conventional power plant. During a disturbance, the electrical characteristics at each terminal of the turbine is different from the other turbines, and only the most affected WTGs will be disconnected from the grid. For general faults (distance faults at the transmission point), only 5%–15% of the turbines are disconnected from the grid [3]. This is partially because WPPs are required to have zero voltage ride-through capability. Thus, the loss of generation is not as severe as in a power plant with large generators.

At the turbine level, the WTG generates at low voltage levels (480 V to 690 V). For the Type 1 and Type 2 WTGs, it is typically compensated by switched capacitor banks to generate at a unity power factor. Type 3 and Type 4 generators are operated to generate a constant voltage at a designated bus, or may be operated at constant power factor or constant reactive power. The generator is connected to a pad-mounted transformer to step up the voltage to 34.5 kV.

Collector System

The collector system consists of miles of line feeders connecting the high side of the pad-mounted transformer to the substation. Usually, wind turbines are divided into groups of turbines connected in a daisy-chain fashion using underground cables. These groupings are then connected to the substation by either underground cables or overhead lines at 34.5 kV. Since it is not practical to model hundreds of tur bines in a power flow calculation or in a dynamic simulation, it is common to find the equivalent of the turbines as either a single equivalent turbine representation or multiple turbine representation [4, 5].

Short Circuit Behavior under Symmetrical Faults

A utility-sized wind turbine is larger than non-grid wind turbine applications. In the early days, the turbines were sized from 10 kW to 100 kW. Nowadays, wind turbines are sized above 1000 kW (1 MW).

R–L Circuits

Short-circuit faults can occur in various locations of the power system in a number of different ways including line-to-ground and line-to-line faults. For simplicity purposes, we'll consider a symmetrical three-phase fault since it is the easiest to analyze. A simple equivalent diagram of a power system under such fault conditions is shown in Figure 1(a).

The fault in Figure 1(a) is represented by a shorting switch. Immediately after the fault, the SCC contribution from the generator can be found using the following equation:

$$u_g = L\frac{di}{dt} + iR \tag{1}$$

Where u_g is the instantaneous voltage on the generator terminals, and

Copyright 2017 Cengage Learning. All Rights Reserved. May not be copied, scanned, or duplicated, in whole or in part. Due to electronic rights, some third party content may be suppressed from the eBook and/or eChapter(s). Editorial review has deemed that any suppressed content does not materially affect the overall learning experience. Cengage Learning reserves the right to remove additional content at any time if subsequent rights restrictions require it.

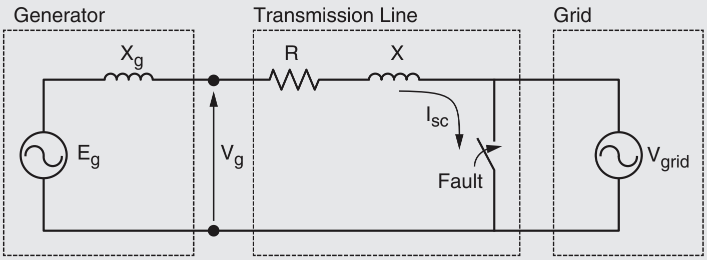

(a) Equivalent diagram of symmetrical fault

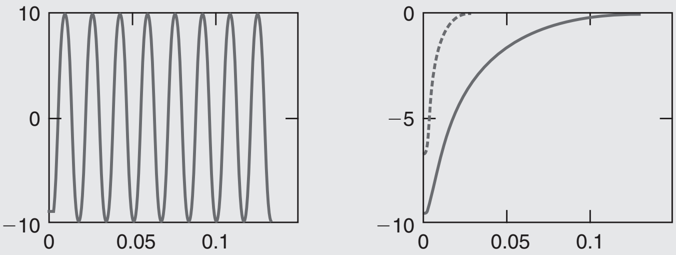

(b) ac component

(c) dc component

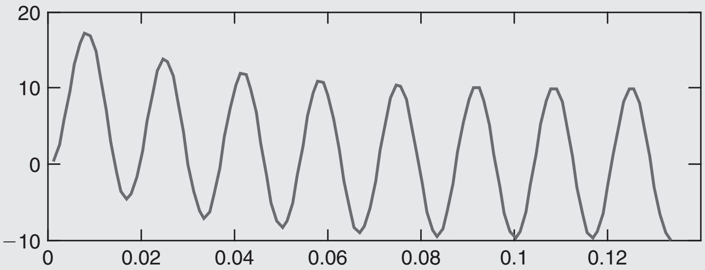

(d) Fault current

Figure 1 Symmetrical Three-Phase Fault

R and L are line resistance and inductance. Solving equation (1) for current

$$i = \frac{V_g}{Z}\sin\left(\omega t + \alpha - \operatorname{atan}\left(\frac{X}{R}\right)\right) - e^{-\frac{R}{L}t}\left[\frac{V_g}{Z}\sin\left(\alpha - \operatorname{atan}\left(\frac{X}{R}\right)\right)\right] \quad (2)$$

Where V_g is peak generator voltage, $Z = \sqrt{R^2 + X^2}$ is line impedance, and α is the voltage phase. The solution (2) has two components; the first component is stationary and varies sinusoidally with time as shown in Figure 1(b). It represents the steady SCC driven by the voltage source E_g.

Copyright 2017 Cengage Learning. All Rights Reserved. May not be copied, scanned, or duplicated, in whole or in part. Due to electronic rights, some third party content may be suppressed from the eBook and/or eChapter(s). Editorial review has deemed that any suppressed content does not materially affect the overall learning experience. Cengage Learning reserves the right to remove additional content at any time if subsequent rights restrictions require it.

The second component decays exponentially [as shown in Figure 1(c)] with a time constant equal to $\frac{R}{L}$. It represents the dc component of the current and the natural response of the circuit without the excitation provided by E_g.

The steady-state symmetrical fault rms value of the SCC I_{sc} from the generator can be calculated from the first component of equation (2) and is shown in

$$I_{sc} = \frac{V_g/\sqrt{2}}{\sqrt{R^2 + X^2}} \qquad (3)$$

Obviously, the steady-state fault current depends on the impedance of the line. The closer the fault occurrence location to generator terminals, the larger the SCC contributed to the fault.

The peak magnitude of the transient component in equation (2) depends on line impedance as well, but it also depends on impedance angle $\varphi = \text{atan}\left(\frac{X}{R}\right)$ at the point of the fault. The dc term does not exist if $\phi = 0$, and will have its maximum initial value of $\frac{V_g}{Z}$, where $\alpha - \varphi = \pm\frac{\pi}{2}$.

The worst case scenario for the SCC peak value (including the dc component) for the circuit presented in Figure 1(a) is shown in equation (3).

So, depending on the time when the fault occurs, the circuit characteristics and the transient current waveform will be different. This means that in three-phase systems, the phase transient currents will have different peaks due to a 120° shift in voltages.

In large power systems with many generators and transmission lines, the actual fault current at any location in the grid will be the sum of collective contributions from all generators, making the above described analysis extremely complicated. So, some sort of simplification is needed for the fault current calculation in such a case.

SCC from a Type 1 WTG

The first generation of utility-sized WTGs is a fixed-speed turbine with a squirrel-cage induction generator (SCIG) and is called a Type 1 generator in wind-related applications. The SCIG generates electricity when it is driven above synchronous speed. The difference between the synchronous speed and the operating speed of the induction generator is measured by its slip (in per unit or in percent). A negative slip indicates that the wind turbine operates in generating mode. Normal operating slips for an induction generator are between 0% and −1%. The simplified single-phase equivalent circuit of a squirrel-cage induction machine is shown in Figure 2 [6].

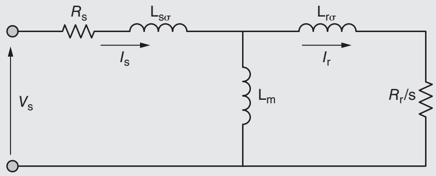

Figure 2 Equivalent circuit of a Type 1 generator

The circuit in Figure 2 is referred to the stator where R_S and R_r are stator and rotor resistances, $L_{s\sigma}$ and $L_{r\sigma}$ are stator and rotor leakage inductances, L_m is magnetizing reactance, and s is rotor slip. The example single-line connection diagram of a Type 1 generator is shown in Figure 3. In the case of a voltage fault, the inertia of the wind rotor drives the generator after the voltage drops at the generator

Copyright 2017 Cengage Learning. All Rights Reserved. May not be copied, scanned, or duplicated, in whole or in part. Due to electronic rights, some third party content may be suppressed from the eBook and/or eChapter(s). Editorial review has deemed that any suppressed content does not materially affect the overall learning experience. Cengage Learning reserves the right to remove additional content at any time if subsequent rights restrictions require it.

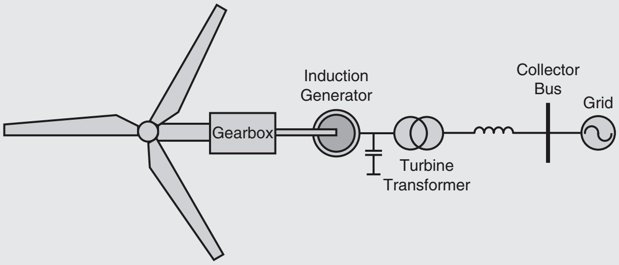

Figure 3 Type 1 WTG

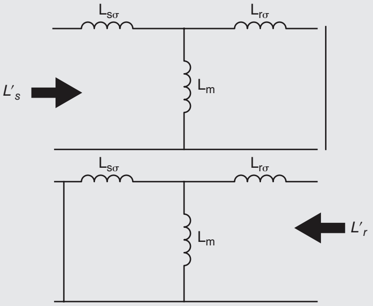

Figure 4 Stator and rotor transient inductances

terminals. The rotor flux may not change instantaneously right after the voltage drop due to a fault. Therefore, voltage is produced at the generator terminals causing fault current flow into the fault until the rotor flux decays to zero. This process takes a few electrical cycles. The fault current produced by an induction generator must be considered when selecting the rating for circuit breakers and fuses. The fault current is limited by generator impedance (and can be calculated from parameters in Figure 2) and impedance of the system from the short circuit to the generator terminals.

The initial value of fault current fed in by the induction generator is close to the locked rotor-inrush current. Assuming a three-phase symmetrical fault, an analytical solution can be found to estimate the current contribution of the generator. The SCC of an induction generator can be calculated as [7]:

$$i(t) = \frac{\sqrt{2}V_S}{Z'_S}\left[e^{-\frac{t}{T'_S}}\sin(\alpha) - (1-\sigma)e^{-\frac{t}{T'_r}}\sin(\omega t + \alpha)\right] \quad (4)$$

where α is the voltage phase angle for a given phase, σ is the leakage factor, $Z'_S = X'_S = \omega L'_S$ is stator transient reactance, and T'_S and T'_r are stator and rotor time constants representing the damping of the dc component in stator and rotor windings. The transient stator and rotor inductances L'_S and L'_r can be determined from the circuits shown in Figure 4.

$$L'_S = L_{S\sigma} + \frac{L_{r\sigma}L_m}{L_{r\sigma} + L_m}$$
$$L'_r = L_{r\sigma} + \frac{L_{S\sigma}L_m}{L_{S\sigma} + L_m} \quad (5)$$

$$T'_S = \frac{L'_S}{R_S} \qquad T'_r = \frac{L'_r}{R_r} \quad (6)$$

$$\sigma = 1 - \frac{L_m^2}{L_S L_r} \quad (7)$$

$$L_S = L_{S\sigma} + L_m$$
$$L_r = L_{r\sigma} + L_m \quad (8)$$

Copyright 2017 Cengage Learning. All Rights Reserved. May not be copied, scanned, or duplicated, in whole or in part. Due to electronic rights, some third party content may be suppressed from the eBook and/or eChapter(s). Editorial review has deemed that any suppressed content does not materially affect the overall learning experience. Cengage Learning reserves the right to remove additional content at any time if subsequent rights restrictions require it.

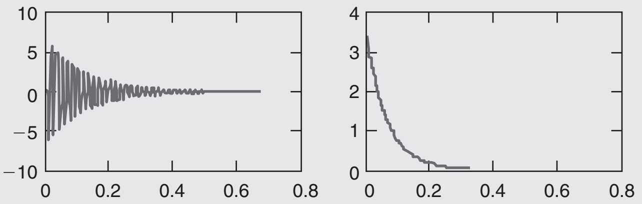

(a) ac component (b) dc component

Figure 5 The two components of the SCC for a Type 1 WTG

Equation (4) is different from equation (2). The first distinction is that there is no voltage source driving the fault current as in equation (2). The fault current is driven by the decaying flux trapped in the rotor winding as represented by the right portion of the equation (4). The second distinction is the rotor time constant T'_r governs the dynamic of the decaying rotor flux [ac component of the SCC as shown in Figure 5(a)] and the decaying dc component of the fault current [refer to Figure 5(b)] is governed by the stator time constant T'_S. The larger the leakage inductances (σ), the smaller is the fault current amplitude. The third distinction is that the fault current dies out after the flux driving the fault current depleted to zero. Note, the dc and ac transient components of the SCC flowing out of the stator windings induce fault currents in the rotor winding and vice versa until the magnetic flux is depleted.

The current calculated from equation (4) is shown in Figure 6 using parameters for a typical 2-MW induction generator when the prefault voltage is 0.7 p.u. As can be seen from Figure 6, the current reaches the maximum value at π (first half a period). Therefore, it may be a good approximation to calculate the maximum (peak) current by substituting $t = \mathrm{T}/2$ into equation (4). The resulting equation for peak current will be

$$i_{\max} = \frac{\sqrt{2}V_S}{Z'_S}\left[e^{-\frac{\mathrm{T}}{2\mathrm{T}'_S}} + (1-\sigma)e^{-\frac{\mathrm{T}}{2\mathrm{T}'_r}}\right] \quad (9)$$

It was demonstrated experimentally in [8] that equation (9) gives satisfactory accuracy for peak current assessment. The resulting current is shown in Figure 7. A detailed dynamic model of a Type 1 WTG is simulated in PSCAD™. A symmetrical three-phase fault is simulated and the resulting SCC is compared to the simulation result of the simplified representation as described in equation (4). It is shown in Figure 7 that the two traces are very closely matched.

From equation (4), it is shown that the operating slip does not influence the short-circuit transient behavior. To check the influence of the slip, we performed symmetrical three-phase faults on a Type 1 WTG for two different slips using the detailed model. As shown in Figure 8, the prefault current and the postfault current for the two different operating slips are very distinct. Similarly, the frequencies of the

Copyright 2017 Cengage Learning. All Rights Reserved. May not be copied, scanned, or duplicated, in whole or in part. Due to electronic rights, some third party content may be suppressed from the eBook and/or eChapter(s). Editorial review has deemed that any suppressed content does not materially affect the overall learning experience. Cengage Learning reserves the right to remove additional content at any time if subsequent rights restrictions require it.

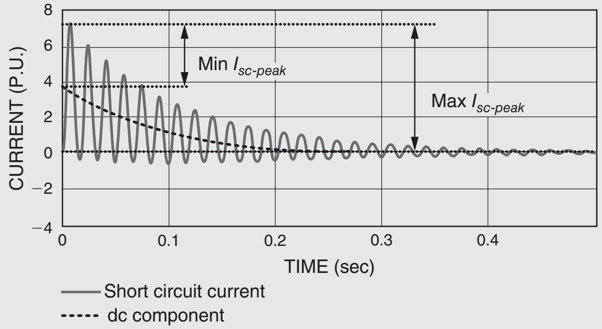

Figure 6 SCC from a Type 1 WTG

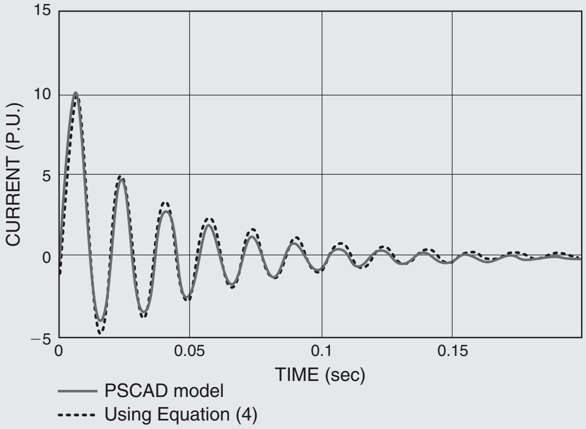

Figure 7 SCC comparison between the output of the detailed model and the output of the simplified model simulated for a Type 1 WTG

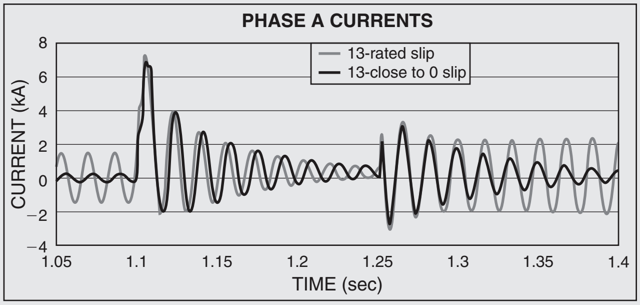

Figure 8 SCC comparison for two different slips

Copyright 2017 Cengage Learning. All Rights Reserved. May not be copied, scanned, or duplicated, in whole or in part. Due to electronic rights, some third party content may be suppressed from the eBook and/or eChapter(s). Editorial review has deemed that any suppressed content does not materially affect the overall learning experience. Cengage Learning reserves the right to remove additional content at any time if subsequent rights restrictions require it.

SCC during the fault are not the same for two different operating slips. However, the peak values of the SCC of the induction generator operating at two different slips are very closely matched.

SCC from a Type 2 WTG

The variable slip generator is essentially a wound-rotor induction generator with a variable resistor connected in series to the rotor winding (Type 2 generator). This external resistor is controlled by a high-frequency switch. Below rated power, the resistor control is inactive, so the system operates as a conventional induction generator. Above rated power, the resistor control allows the slip to vary, so variable speed operation is possible for a speed range of about 10% [9]. If the blade pitch angle is kept constant at zero degrees, the rotor speed, and thus the slip, will vary with wind speed. However, operation at higher slips generate a lot of loss because of the rotor resistance. Thus, the heat loss can be excessive. On the other hand, if the blade pitch angle is controlled to keep the rotor speeds within a small deviation from the rated slip, the losses in rotor resistance can be minimized. An equivalent electrical diagram of a variable-slip induction generator is shown in Figure 9, with a variable external resistor R_{ext}.

The connection diagram example for this type of generator is shown in Figure 10. In case of three-phase symmetrical fault, the same equations as for a Type 1 generator are applied. The only difference is for rotor time constant that needs to account for additional external resistance.

The modified rotor time constant can be calculated by adding the effect of the external resistor R_{ext} (refer to Table 2, p. 429), where R_{ext} is the value of external resistance that happens to be in the circuit at the time of the fault. The effect of such additional resistance on SCC is shown in Figure 11. So, adding the external resistors doubles the overall rotor resistance. The modified equation for SCC, maximum current, and the rotor transient time constant can then be derived using the values shown in Table 1 (see p. 428).

The maximum current occurs at ΔT, the time after a fault when current reaches its first peak. In this case, this additional resistance decreases the overall ac component in current, but does not much affect the first peak value of the current since the increase in resistance is relatively small. The same conclusion can be made by analyzing equations (4) and (9), where the additional external resistance has an effect on a second term that represents

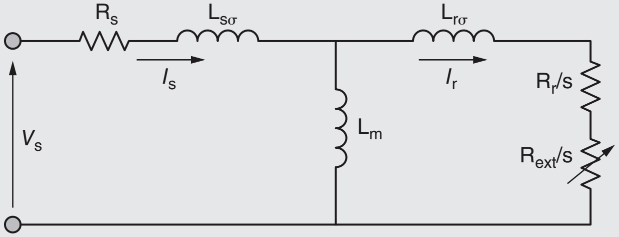

Figure 9 Equivalent circuit for a Type 2 generator

Copyright 2017 Cengage Learning. All Rights Reserved. May not be copied, scanned, or duplicated, in whole or in part. Due to electronic rights, some third party content may be suppressed from the eBook and/or eChapter(s). Editorial review has deemed that any suppressed content does not materially affect the overall learning experience. Cengage Learning reserves the right to remove additional content at any time if subsequent rights restrictions require it.

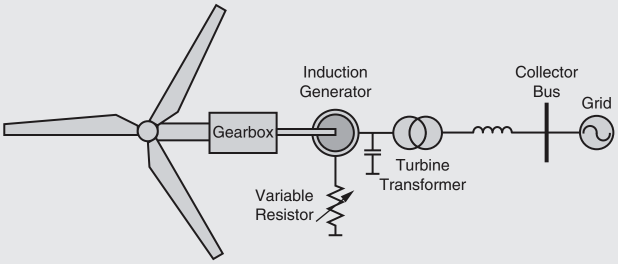

Figure 10 Connection diagram for a Type 2 WTG

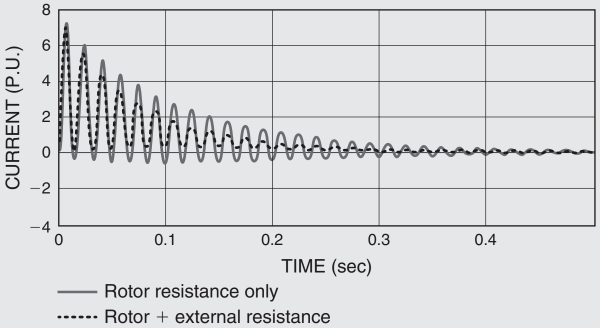

Figure 11 Effect of external resistance for a Type 2 WTG

the ac component of the current. As shown in Tables 1 and 2, the impact of the external rotor resistance on the SCC is two-fold: it reduces the SCC magnitude, and it shortens the rotor time constant (decay time of the SCC).

SCC from a Type 3 WTG

A Type 3 WTG is implemented by a doubly fed induction generator (DFIG). It is a variable-speed WTG where the rotor speed is allowed to vary within a slip range of ±30%. Thus, the power converter can be sized to about 30% of rated power. The equivalent electrical diagram of a DFIG is shown in Figure 12.

It is similar to one for a regular induction generator except for additional rotor voltage, representing voltage produced by a power converter. Under normal operation, this voltage is actually from a current-controlled power converter with the ability to control the real and reactive power output instantaneously and independently. The capability to control flux (flux-oriented controller—FOC) in induction machines has been used in the motor drive industry since the seventies.

The typical connection diagram for a DFIG (Type 3) WTG is shown in Figure 12. In an ideal situation, the power converter connected to the rotor winding should be able to withstand the currents induced by the dc and ac components flowing in the stator winding. However, the components of the power converter (IGBT, diode, capacitor, etc.) are designed to handle only normal currents and normal dc bus voltage. A crowbar system is

Copyright 2017 Cengage Learning. All Rights Reserved. May not be copied, scanned, or duplicated, in whole or in part. Due to electronic rights, some third party content may be suppressed from the eBook and/or eChapter(s). Editorial review has deemed that any suppressed content does not materially affect the overall learning experience. Cengage Learning reserves the right to remove additional content at any time if subsequent rights restrictions require it.

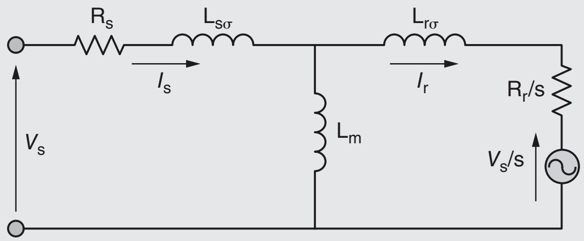
R_s
$L_{s\sigma}$
$L_{r\sigma}$
I_s
I_r
R_r/s
V_s
L_m
V_s/s

Figure 12 Simplified equivalent circuit of a DFIG

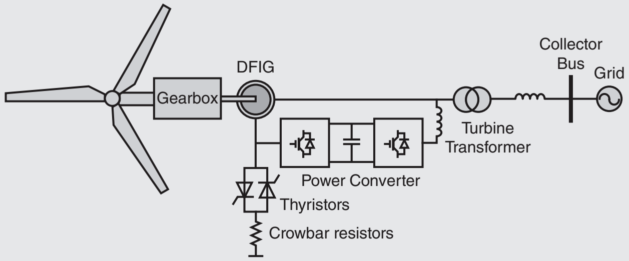
Gearbox
DFIG
Collector Bus
Grid
Turbine Transformer
Power Converter
Thyristors
Crowbar resistors

Figure 13 Connection diagram for a Type 3 WTG

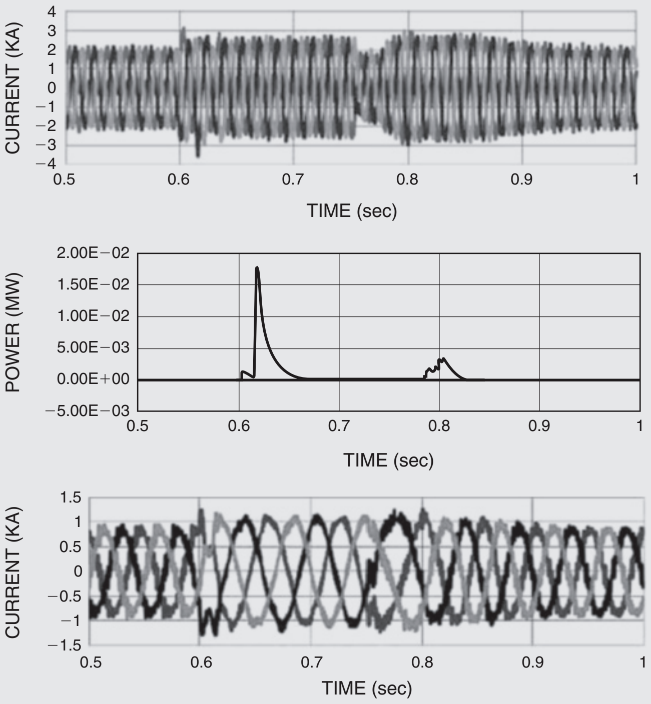

Figure 14 The fault currents, the rotor currents, and the power consumed by the crowbar circuits in a Type 3 WTG

Copyright 2017 Cengage Learning. All Rights Reserved. May not be copied, scanned, or duplicated, in whole or in part. Due to electronic rights, some third party content may be suppressed from the eBook and/or eChapter(s). Editorial review has deemed that any suppressed content does not materially affect the overall learning experience. Cengage Learning reserves the right to remove additional content at any time if subsequent rights restrictions require it.

usually used for protecting the power electronics converter from overvoltage and thermal breakdown during short-circuit faults. A crowbar is usually implemented to allow the insertion of additional resistance into the rotor winding to divert the SCC in the rotor winding from damaging the power converter. Additional dynamic braking on the dc bus is also used to limit the dc bus voltage.

During faults, the rotor windings are essentially short circuited by an equivalent adjustable crowbar resistance R_{CB}. The modified equation for SCC, maximum current, and the rotor transient time constant can then be derived using the values shown in Table 1 [7]. In a Type 3 WTG, however, the size of the crowbar is usually controlled, such that the actual fault current is more controllable than the simplified assumption. In Figure 14, three-phase fault currents are shown to be well regulated by proper control of the crowbar resistance. In this case, the crowbar circuit installed on the rotor winding is controlled to maintain the dc bus voltage constant.

A dynamic braking resistor is also installed on the dc bus to help regulate the dc bus. Figure 14 shows the size of the real power modulated in the crowbar during the faults. There are also dynamic braking resistors and a dc chopper installed on the dc bus to help regulate the dc bus voltage during transients. The corresponding rotor currents are also shown in Figure 14. Because of differences in crowbar implementation from one turbine manufacturer to the other, a protection engineer should evaluate the recommended value provided by the manufacturers. However, if none is available, the values of minimum and maximum SCCs presented in Table 1 can be used.

Type 4 WTGs

An example of a Type 4 direct-drive WTG with permanent-magnet synchronous generator (PMSG) is shown in Figure 15. This is a variable-speed WTG implemented with full power conversion. Recent advances and lower cost of power electronics make it feasible to build variable-speed wind turbines with power converters with the same rating as the turbines. The full power conversion allows separation between the WTG and the grid, thus, the mechanical dynamic can be buffered from entering the grid and the transient dynamic on the grid can be buffered from entering the wind turbine dynamic. Thus, while the grid is at 60 Hz, the stator winding of the generator may operate at variable frequencies. The temporary imbalance between aerodynamic power and generated power during a transient is handled by the pitch control, dynamic brake, and power converter control.

The SCC contribution for a three-phase fault is limited to its rated current or a little above its rated current. It is common to design a power converter for a Type 4 wind turbine with an overload capability of 10% above rated. Note that in any fault condition, the generator stays connected to the power converter and is buffered from the faulted lines on the grid. Thus, although there is a fault on the grid, the generator output current is controlled to stay within the current limit (e.g., 1.1 p.u.). However, keep in mind that with a fault on the grid, the

Copyright 2017 Cengage Learning. All Rights Reserved. May not be copied, scanned, or duplicated, in whole or in part. Due to electronic rights, some third party content may be suppressed from the eBook and/or eChapter(s). Editorial review has deemed that any suppressed content does not materially affect the overall learning experience. Cengage Learning reserves the right to remove additional content at any time if subsequent rights restrictions require it.

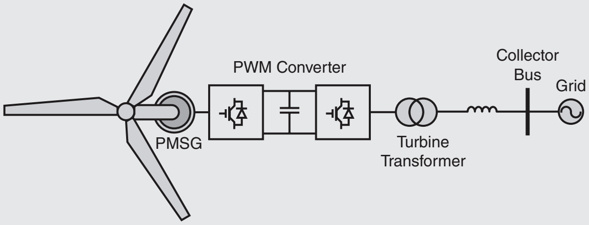

Figure 15 PMSG direct-drive WTG diagram

output power delivered to the grid is less than rated power. Although the currents can be made to balance, due to reduced voltage and/or unbalanced voltage, only a reduced output power can be delivered. In Type 4 WTGs, the SCC is a controlled parameter. So, such WTGs can be represented as a constant three-phase balanced current source in a short-circuit models. The priority of the real power versus reactive power during the fault depends on the prior setting of the controller. However, the current limit of the power converter must be followed to protect the power switches.

SCC Comparison for Symmetrical Faults

The SCCs for different types of wind turbines are not the same. For each turbine type, the peak value of the magnitude of the SCC is affected by the transient reactance, the prefault voltage, the effective rotor resistances, and the instant the fault occurs.

For turbine Types 1 through 3, the SCC declines as the fault progresses and eventually ceases as the rotor flux is depleted. For Type 4 WTGs, the SCC can be maintained constant.

The SCC transient behavior is affected by the stator time constant and the rotor time constant for Type 1 through Type 3 WTGs. The Type 4 generators can generate constant current during the fault.

In Table 1, the list parameters are shown. These parameters can be used to substitute the parameters from equation (4) and equation (6) for different types of WTGs. Table 2 lists the maximum and minimum possible values of the peak of SCC. It is shown that the Type 1 WTG can produce the largest SCC. The instant of the fault has affects on the magnitude of the SCC. The maximum value is based on the peak of the ac component and the highest value of the dc component, and the minimum value is based on the peak value of the ac component only.

For a Type 2 WTG, the maximum value is computed when $R_{\text{ext}} = 0\ \Omega$.

WTG	Type 1	Type 2	Type 3
$\mathbf{Z}'_S$	$X'_S = \omega L'_S$	$\sqrt{X'^2_S + R^2_{\text{ext}}}$	$\sqrt{X'^2_S + R^2_{CB}}$
$\mathbf{T}'_r$	$\dfrac{L'_r}{R_r}$	$\dfrac{L'_r}{R_r + R_{\text{ext}}}$	$\dfrac{L'_r}{R_r + R_{CB}}$

TABLE 1

Modified Values for SCC Calculation for Different Types of WTGs

Copyright 2017 Cengage Learning. All Rights Reserved. May not be copied, scanned, or duplicated, in whole or in part. Due to electronic rights, some third party content may be suppressed from the eBook and/or eChapter(s). Editorial review has deemed that any suppressed content does not materially affect the overall learning experience. Cengage Learning reserves the right to remove additional content at any time if subsequent rights restrictions require it.

WTG	Type 1	Type 2	Type 3	Type 4
Max I_{SC_PEAK}	$2\frac{\sqrt{2}V_s}{X'_S}$	$2\frac{\sqrt{2}V_s}{X'_S}$	$2\frac{\sqrt{2}V_s}{X'_S}$	1.1 I_{RATED}
Min I_{SC_PEAK}	$\frac{\sqrt{2}V_s}{X'_S}$	$\frac{\sqrt{2}V_s}{\sqrt{X'^2_S + (9R'_r)^2}}$	1.1 I_{RATED}	0

TABLE 2

Maximum and Minimum Possible Value of the SCC

The minimum value is computed when the slip reaches 10% above synchronous speed. And for a Type 3 WTG, the maximum value is computed when the crowbar shorts the rotor winding and the minimum value is computed when the power converter can follow the commanded current (i.e., in case the fault occurs far away from the point of interconnection, the remaining terminal voltage is relatively high enough to let the power converter operate normally and supply the commanded currents). Note, that for a symmetrical fault, the actual fault current for each phase is different from the other phases due to the fact that the time of the fault occurs at a different phase angle for different phases, thus affecting the dc offset. For a Type 4 WTG, the stator current can always be controlled because of the nature of power converter which is based on current controlled voltage source converter.

An example of SCC for Type 4 WTGs is given in the next section. In this section, the SCC is analyzed at the terminals of the generator. In an actual WPP, the faults will likely occur at the transmission side. Thus, the impact of the cable capacitance, plant level reactive compensation, and wind plant transformer connections are not included. References [10–14] provide good sources of information for the WPP environment.

Unsymmetrical Faults

The nature of the fault produces a different response for different wind turbine types. In this section, the observation of the short-circuit behavior for unsymmetrical faults on different types of WTGs is presented. Note that operating an induction generator under an unbalanced condition creates torque pulsation and unbalanced currents. If this condition persists for a long period of time, it may excite other parts of the wind turbine, and the unbalanced currents may create unequal heating in the three-phase windings and, thus, shorten the life of the winding insulation.

Unlike in a symmetrical three-phase fault, the positive-sequence voltage source continues to drive the fault current until the fault or the generator is removed from the circuit. The remaining un-faulted (normal) phases continue to maintain the air gap flux. The initial conditions of the fault currents are different for each phase. The three line currents usually

Copyright 2017 Cengage Learning. All Rights Reserved. May not be copied, scanned, or duplicated, in whole or in part. Due to electronic rights, some third party content may be suppressed from the eBook and/or eChapter(s). Editorial review has deemed that any suppressed content does not materially affect the overall learning experience. Cengage Learning reserves the right to remove additional content at any time if subsequent rights restrictions require it.

show a different dc offset, which eventually settles out over time.

To explore the short-circuit behavior of unsymmetrical faults presented in this section, a detailed model of the system is developed in PSCAD™.

Single Line-to-Ground (SLG) Faults

The single line-to-ground fault is the most likely to occur in the power system. The magnetic flux in the air gap, although smaller than normal and unbalanced, is maintained by the remaining un-faulted lines. Thus, the short circuit in SLG faults will continue to flow until the circuit breaker removes the fault from the circuit.

Figure 16 shows the SCC of a Type 1 WTG for three lines-to-ground (3LG) and an SLG fault. In the symmetrical fault, the SCC dies out rather quickly, while in a SLG fault, the SCC is driven by the remaining two phases and it continues to flow until the short circuit is removed from the circuit. The peak current during a SLG fault is typically higher than for a 3LG fault (there is a quicker decay of current during symmetrical a 3LG fault due to magnetic field collapse). The difference in peak currents for both 3LG and SLG faults depends on generator parameters, fault location, etc. Note also that the presence of the positive sequence, the negative sequence, and zero sequence currents in the unsymmetrical faults influence the size of the SCC. No comparison has been made between dynamic simulation results and results obtained via symmetrical component calculations (this is planned for future work).

In Figure 17, the SCC for a Type 3 WTG is shown both for the three-phase currents and the corresponding sequence components. The changes in positive sequence and the sudden appearance of the negative sequence are also shown. The absence of the zero sequence current is a consequence of transformer winding connections.

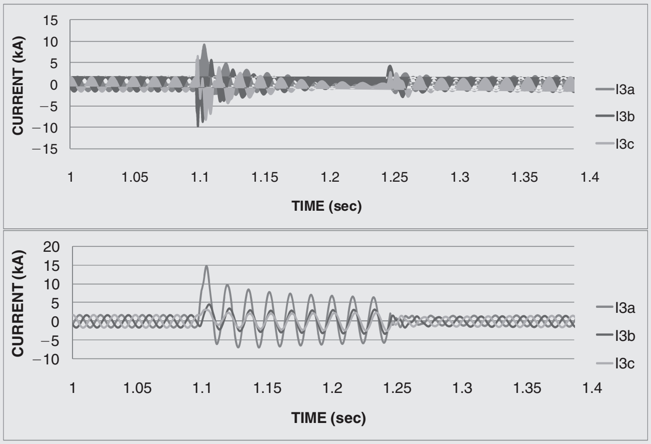

Figure 16 Voltage and SCC for 3LG and SLG for a Type 1 WTG

Copyright 2017 Cengage Learning. All Rights Reserved. May not be copied, scanned, or duplicated, in whole or in part. Due to electronic rights, some third party content may be suppressed from the eBook and/or eChapter(s). Editorial review has deemed that any suppressed content does not materially affect the overall learning experience. Cengage Learning reserves the right to remove additional content at any time if subsequent rights restrictions require it.

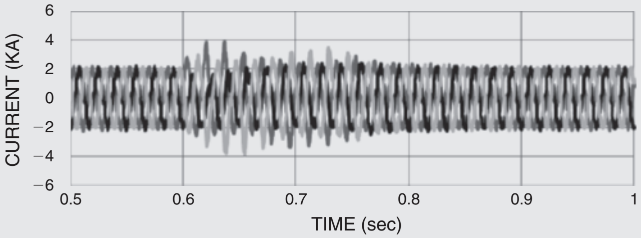

(a) Three phase currents

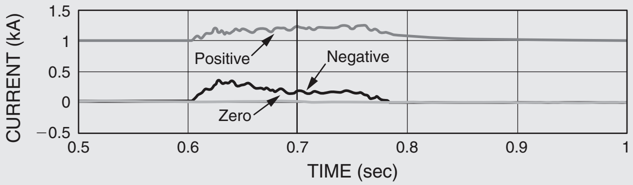

(b) Positive, negative and zero sequence currents

Figure 17 SCC for SLG for a Type 3 WTG

Line-to-Line (LL) and Line-to-Line-to-Ground (LLG) Faults

The line-to-line fault and the line-to-line-to-ground fault also maintain the air-gap flux during the fault. Output power of the generator will be limited and pulsating due to an unbalanced condition. The SCC will continue to flow until the circuit breaker removes the fault from the circuit.

As shown on Figures 18 and 19, the type of fault affects the existence of the zero sequence component in the SCC of the WPP. Thus, the line currents in the three phases are distributed differently based on its positive sequence, negative sequence, and the zero sequence magnitudes and phase angles.

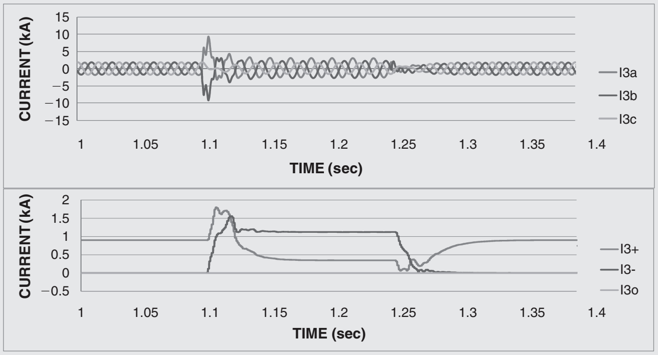

Figure 18 The SCC for a LL fault of a Type 2 WTG

Copyright 2017 Cengage Learning. All Rights Reserved. May not be copied, scanned, or duplicated, in whole or in part. Due to electronic rights, some third party content may be suppressed from the eBook and/or eChapter(s). Editorial review has deemed that any suppressed content does not materially affect the overall learning experience. Cengage Learning reserves the right to remove additional content at any time if subsequent rights restrictions require it.

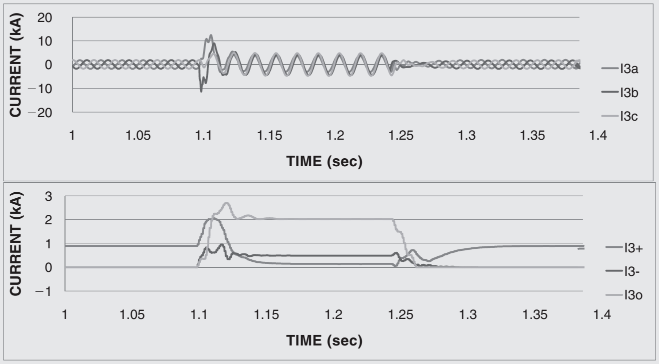

Figure 19 The SCC for LLG fault of a Type 2 WTG

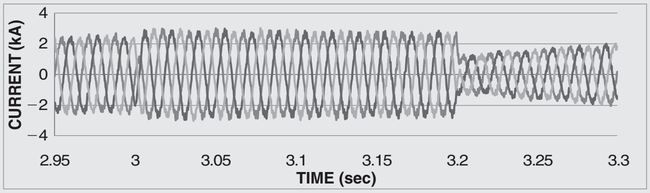

(a) 3 LG

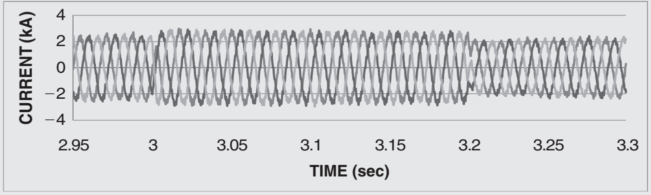

(b) SLG

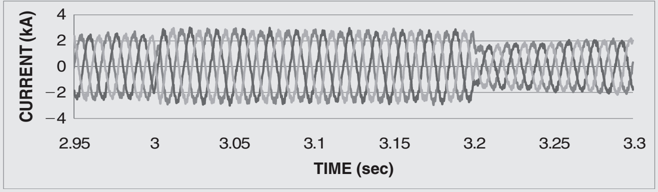

(c) LLG

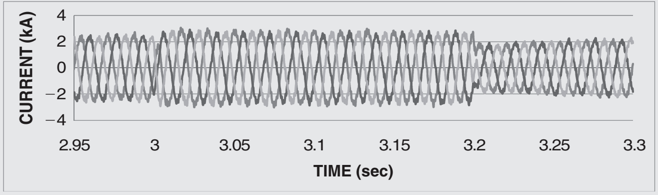

(d) LL

Figure 20 SCC for Type 4 WTG for different types of faults

Copyright 2017 Cengage Learning. All Rights Reserved. May not be copied, scanned, or duplicated, in whole or in part. Due to electronic rights, some third party content may be suppressed from the eBook and/or eChapter(s). Editorial review has deemed that any suppressed content does not materially affect the overall learning experience. Cengage Learning reserves the right to remove additional content at any time if subsequent rights restrictions require it.

SCC for the Type 4 WTG under Different Faults

In Figure 20, the fault currents for a Type 4 WTG are shown. Note, that the power converter buffers the generator from the grid. The SCC is basically controlled by the power converter. Hence, the line currents are symmetrical currents at different types of unsymmetrical faults. The postfault recovery may slightly differ for different faults.

Conclusions

In this case study, the SCC contributions of different WTGs for faults at the terminal of the generator were simulated using simplified model to determine SCC characteristics for symmetrical faults. The simplified model represents the size and the time constants governing the SCC behavior. A table summarizing different fault impedance and transient rotor time constants is provided. Another table summarizing the range of SCCs for different types of WTGs is presented in Table 2. For Type 1 and Type 2 WTGs, the maximum and the minimum values depend on timing of the fault and the parameters and the operating condition of the induction generator. For Type 3 WTGs, the control and the operation of the crowbar and dynamic braking affects the characteristics of the SCC. For Type 4 WTGs, the SCC is controllable by the power converter.

To compute unsymmetrical faults, detailed models were used to demonstrate the behavior of SCCs of different WTGs. As expected, the SCC continues to flow until the fault is cleared from the circuit or the generator is disconnected from the grid. The terminal voltage and currents are sustained longer because the line voltages, except from the faulted phase, are able to sustain air gap flux. The nature of SCC is not only affected by the type of WTG, but also by the nature of the faults, the winding connections of the generator, and the transformers between the fault and the generator. Auxiliary components (reactive compensations), cable length and capacitance, and the diversity of the WPP contribute to the size and nature of the SCC, one way or another.

Each WPP is unique. Therefore, recommended practice from local reliability organizations, the manufacturers, transmission planners, wind plant developers, and the local utilities should be followed very closely.

Acknowledgment

This work is supported by the U.S. Department of Energy and California Energy Commission.

References

1. U.S. Department of Energy—Energy Efficiency and Renewable Energy, “20% Wind Energy by 2030—Increasing Wind Energy’s Contribution to U.S. Electricity Supply,” May, 2008.
2. J. Charles Smith, Michael R. Milligan, Edgar A. DeMeo, and Brian Parsons, “Utility wind Integration and operating impact state of the art,” *IEEE Trans. Power Systems,* vol. 22, pp. 900–908, Aug. 2007.

Copyright 2017 Cengage Learning. All Rights Reserved. May not be copied, scanned, or duplicated, in whole or in part. Due to electronic rights, some third party content may be suppressed from the eBook and/or eChapter(s). Editorial review has deemed that any suppressed content does not materially affect the overall learning experience. Cengage Learning reserves the right to remove additional content at any time if subsequent rights restrictions require it.

3. E. Muljadi, Z. Mills, A. Ellis, and R. Foster, “Fault Analysis at a Wind Power Plant for a One Year of Observation,” presented at the *IEEE Power Engineering Society, General Meeting*, Pittsburgh, PA, July 20–24, 2008.

4. E. Muljadi, S. Pasupulati, A. Ellis, and D. Kosterev, “Method of Equivalencing for a Large Wind Power Plant with Multiple Turbine Representation,” presented at the *IEEE Power Engineering Society, General Meeting*, Pittsburgh, PA, July 20–24, 2008.

5. E. Muljadi, C. P. Butterfield, A. Ellis, J. Mechenbier, J. Hochheimer, R. Young, N. Miller, R. Delmerico, R. Zavadil, and J. C. Smith, “Equivalencing the collector system of a large wind power plant,” in *Proc. 2006 IEEE Power Engineering Society General Meeting.* June 18–22, 2006.

6. Nader Samaan, Robert Zavadil, J. Charles Smith, and Jose Conto, “Modeling of Wind Power Plants for Short Circuit Analysis in the Transmission Network,” in *Proc. of IEEE/PES Transmission and Distribution Conference*, Chicago, USA, April 2008.

7. J. Moren, and S.W.H. de Haan, “Short-Circuit Current of Wind Turbines with Doubly Fed Induction Generator,” *IEEE Transactions on Energy Conversion*, Vol. 22, No. 1, March 2007.

8. Sulawa, Zabara, et al. “Short circuit current of induction generators.” *IEEE ISCAS 2007 proceedings*.

9. O. Anaya-Lara, N. Jenkins, et al. *Wind energy generation: modeling and control*. Wiley. ISBN 9780470714331.

10. IEEE PES Wind Plant Collector System Design Working Group,“Wind Power Plant Substation and Collector System Redundancy, Reliability and Economics,” *Proceedings of the 2009 IEEE Power and Energy* Society General Meeting.

11. IEEE PES Wind Plant Collector System Design Working Group, “Power Transformer Application for Wind Plant Substation,” *Proceedings of the 2009 IEEE Power and Energy Society General Meeting*.

12. IEEE PES Wind Plant Collector System Design Working Group, “Wind Power Plant Grounding, Overvoltage Protection, and Insulation Coordination,” *Proceedings of the 2009 IEEE Power and Energy Society General Meeting*.

13. WECC Modeling and Validation Work Group, “WECC Wind Power Plant Power Flow Modeling Guide Prepared.” May 2008.

14. “Short-circuit currents in three-phase a.c. systems–Part 0: Calculation of currents,” *IEC Standard* 60909-0, July 2001.

Copyright 2017 Cengage Learning. All Rights Reserved. May not be copied, scanned, or duplicated, in whole or in part. Due to electronic rights, some third party content may be suppressed from the eBook and/or eChapter(s). Editorial review has deemed that any suppressed content does not materially affect the overall learning experience. Cengage Learning reserves the right to remove additional content at any time if subsequent rights restrictions require it.

Biographies

Eduard Muljadi (M'82-SM'94-F'10) received his PhD (in Electrical Engineering) from the University of Wisconsin, Madison. From 1988 to 1992, he taught at California State University, Fresno, California. In June 1992, he joined the National Renewable Energy Laboratory in Golden, Colorado. His current research interests are in the fields of electric machines, power electronics, and power systems in general with emphasis on renewable energy applications. He is a member of Eta Kappa Nu, Sigma Xi, and a Fellow of the IEEE. He is involved in the activities of the IEEE Industry Application Society (IAS), Power Electronics Society, and Power and Energy Society (PES).

He is currently a member of various committees of the IAS, and a member of the Working Group on Renewable Technologies and Dynamic Performance Wind Generation Task Force of the PES. He holds two patents in power conversion for renewable energy.

Vahan Gevorgian (M'97) graduated from the Yerevan Polytechnic Institute (Armenia) in 1986. During his studies, he concentrated on electrical machines. His thesis research dealt with doubly fed induction generators for stand-alone power systems. He obtained his PhD degree in electrical engineering from the State Engineering University of Armenia in 1993. His dissertation was devoted to a modeling of electrical transients in large wind turbine generators.

Dr. Gevorgian is currently working at the National Wind Technology Center (NWTC) of National Renewable Energy Laboratory (NREL) in Golden, Colorado, USA, as a research engineer. His current interests include modeling and testing of various applications of small wind turbine based power systems. ■

7.1 SERIES R–L CIRCUIT TRANSIENTS

Consider the series R–L circuit shown in Figure 7.1. The closing of switch SW at $t = 0$ represents to a first approximation a three-phase short circuit at the terminals of an unloaded synchronous machine. For simplicity, assume zero fault impedance; that is, the short circuit is a solid or "bolted" fault. The current is assumed to be zero before SW closes, and the source angle α determines the source voltage at $t = 0$. Writing a KVL equation for the circuit,

$$\frac{\mathrm{L}di(t)}{dt} + \mathrm{R}i(t) = \sqrt{2}V \sin(\omega t + \alpha) \quad t \geq 0 \tag{7.1.1}$$

Copyright 2017 Cengage Learning. All Rights Reserved. May not be copied, scanned, or duplicated, in whole or in part. Due to electronic rights, some third party content may be suppressed from the eBook and/or eChapter(s). Editorial review has deemed that any suppressed content does not materially affect the overall learning experience. Cengage Learning reserves the right to remove additional content at any time if subsequent rights restrictions require it.

FIGURE 7.1

Current in a series R–L circuit with ac voltage source

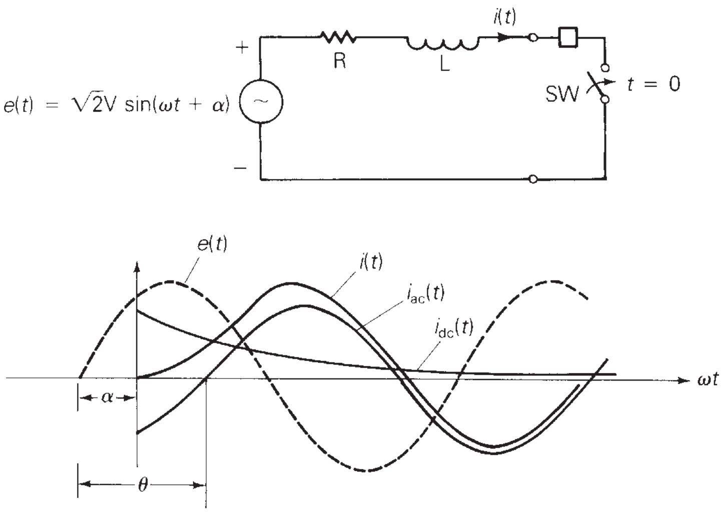

The solution to (7.1.1) is

$$i(t) = i_{ac}(t) + i_{dc}(t)$$

$$= \frac{\sqrt{2}V}{Z}\left[\sin(\omega t + \alpha - \theta) - \sin(\alpha - \theta)e^{-t/T}\right] \quad \text{A} \tag{7.1.2}$$

where

$$i_{ac}(t) = \frac{\sqrt{2}V}{Z}\sin(\omega t + \alpha - \theta) \quad \text{A} \tag{7.1.3}$$

$$i_{dc}(t) = -\frac{\sqrt{2}V}{Z}\sin(\alpha - \theta)e^{-t/T} \quad \text{A} \tag{7.1.4}$$

$$Z = \sqrt{R^2 + (\omega L)^2} = \sqrt{R^2 + X^2} \quad \Omega \tag{7.1.5}$$

$$\theta = \tan^{-1}\frac{\omega L}{R} = \tan^{-1}\frac{X}{R} \tag{7.1.6}$$

$$T = \frac{L}{R} = \frac{X}{\omega R} = \frac{X}{2\pi f R} \quad \text{s} \tag{7.1.7}$$

The total fault current in (7.1.2), called the *asymmetrical fault current*, is plotted in Figure 7.1 along with its two components. The ac fault current (also called *symmetrical* or *steady-state fault current*), given by (7.1.3), is a sinusoid. The *dc offset current*, given by (7.1.4), decays exponentially with time constant T = L/R.

The rms ac fault current is $I_{ac} = V/Z$. The magnitude of the dc offset, which depends on α, varies from 0 when $\alpha = \theta$ to $\sqrt{2}I_{ac}$ when $\alpha = (\theta \pm \pi/2)$. Note that a short circuit may occur at any instant during a cycle of the ac source; that is, α can

Copyright 2017 Cengage Learning. All Rights Reserved. May not be copied, scanned, or duplicated, in whole or in part. Due to electronic rights, some third party content may be suppressed from the eBook and/or eChapter(s). Editorial review has deemed that any suppressed content does not materially affect the overall learning experience. Cengage Learning reserves the right to remove additional content at any time if subsequent rights restrictions require it.

have any value. To find the largest fault current, choose $\alpha = (\theta - \pi/2)$. Then (7.1.2) becomes

$$i(t) = \sqrt{2}\mathrm{I}_{\mathrm{ac}}[\sin(\omega t - \pi/2) + e^{-t/\mathrm{T}}] \quad \mathrm{A} \tag{7.1.8}$$

where

$$\mathrm{I}_{\mathrm{ac}} = \frac{\mathrm{V}}{\mathrm{Z}} \quad \mathrm{A} \tag{7.1.9}$$

The rms value of $i(t)$ is of interest. Since $i(t)$ in (7.1.8) is not strictly periodic, its rms value is not strictly defined. However, to calculate the rms asymmetrical fault current with maximum dc offset, treat the exponential term as a constant, stretching the rms concept as follows:

$$\begin{aligned}\mathrm{I}_{\mathrm{rms}}(t) &= \sqrt{[\mathrm{I}_{\mathrm{ac}}]^2 + [\mathrm{I}_{\mathrm{dc}}(t)]^2}\\ &= \sqrt{[\mathrm{I}_{\mathrm{ac}}]^2 + [\sqrt{2}\mathrm{I}_{\mathrm{ac}}e^{-t/\mathrm{T}}]^2}\\ &= \mathrm{I}_{\mathrm{ac}}\sqrt{1 + 2e^{-2t/\mathrm{T}}} \quad \mathrm{A}\end{aligned} \tag{7.1.10}$$

It is convenient to use $\mathrm{T} = \mathrm{X}/(2\pi f\,\mathrm{R})$ and $t = \tau/f$, where τ is time in cycles, and write (7.1.10) as

$$\mathrm{I}_{\mathrm{rms}}(\tau) = \mathrm{K}(\tau)\mathrm{I}_{\mathrm{ac}} \quad \mathrm{A} \tag{7.1.11}$$

where

$$\mathrm{K}(\tau) = \sqrt{1 + 2e^{-4\pi\tau/(\mathrm{X}/\mathrm{R})}} \quad \text{per unit} \tag{7.1.12}$$

From (7.1.11) and (7.1.12), the rms asymmetrical fault current equals the rms ac fault current times an "asymmetry factor," $\mathrm{K}(\tau)$. $\mathrm{I}_{\mathrm{rms}}(\tau)$ decreases from $\sqrt{3}\mathrm{I}_{\mathrm{ac}}$ when $\tau = 0$ to I_{ac} when τ is large. Also, higher X to R ratios (X/R) give higher values of $\mathrm{I}_{\mathrm{rms}}(\tau)$. The above series R–L short-circuit currents are summarized in Table 7.1.

Component	Instantaneous Current (A)	rms Current (A)
Symmetrical (ac)	$i_{\mathrm{ac}}(t) = \frac{\sqrt{2}\mathrm{V}}{\mathrm{Z}}\sin(\omega t + \alpha - \theta)$	$\mathrm{I}_{\mathrm{ac}} = \frac{\mathrm{V}}{\mathrm{Z}}$
dc offset	$i_{\mathrm{dc}}(t) = \frac{-\sqrt{2}\mathrm{V}}{\mathrm{Z}}\sin(\alpha - \theta)e^{-t/\mathrm{T}}$	
Asymmetrical (total)	$i(t) = i_{\mathrm{ac}}(t) + i_{\mathrm{dc}}(t)$	$\mathrm{I}_{\mathrm{rms}}(t) = \sqrt{\mathrm{I}_{\mathrm{ac}}^2 + i_{\mathrm{dc}}(t)^2}$ with maximum dc offset: $\mathrm{I}_{\mathrm{rms}}(\tau) = \mathrm{K}(\tau)\mathrm{I}_{\mathrm{ac}}$

TABLE 7.1

Short-circuit current—series R–L circuit*

*See Figure 7.1 and (7.1.l) through (7.1.12).

Copyright 2017 Cengage Learning. All Rights Reserved. May not be copied, scanned, or duplicated, in whole or in part. Due to electronic rights, some third party content may be suppressed from the eBook and/or eChapter(s). Editorial review has deemed that any suppressed content does not materially affect the overall learning experience. Cengage Learning reserves the right to remove additional content at any time if subsequent rights restrictions require it.

EXAMPLE 7.1

Fault currents: R–L circuit with ac source

A bolted short circuit occurs in the series R–L circuit of Figure 7.1 with $V = 20$ kV, $X = 8\ \Omega$, $R = 0.8\ \Omega$, and with maximum dc offset. The circuit breaker opens 3 cycles after fault inception. Determine (a) the rms ac fault current, (b) the rms "momentary" current at $\tau = 0.5$ cycle, which passes through the breaker before it opens, and (c) the rms asymmetrical fault current that the breaker interrupts.

SOLUTION

a. From (7.1.9),

$$I_{ac} = \frac{20 \times 10^3}{\sqrt{(8)^2 + (0.8)^2}} = \frac{20 \times 10^3}{8.040} = 2.488 \quad \text{kA}$$

b. From (7.1.11) and (7.1.12) with $(X/R) = 8/(0.8) = 10$ and $\tau = 0.5$ cycle,

$$K(0.5\ \text{cycle}) = \sqrt{1 + 2e^{-4\pi(0.5)/10}} = 1.438$$

$$I_{\text{momentary}} = K(0.5\ \text{cycle})I_{ac} = (1.438)(2.488) = 3.576 \quad \text{kA}$$

c. From (7.1.11) and (7.1.12) with $(X/R) = 10$ and $\tau = 3$ cycles,

$$K(3\ \text{cycles}) = \sqrt{1 + 2e^{-4\pi(3)/10}} = 1.023$$

$$I_{\text{rms}}(3\ \text{cycles}) = (1.023)(2.488) = 2.544 \quad \text{kA}$$

7.2 THREE-PHASE SHORT CIRCUIT—UNLOADED SYNCHRONOUS MACHINE

One way to investigate a three-phase short circuit at the terminals of a synchronous machine is to perform a test on an actual machine. Figure 7.2 shows an oscillogram of the ac fault current in one phase of an unloaded synchronous machine during such a test. The dc offset has been removed from the oscillogram. As shown, the amplitude of the sinusoidal waveform decreases from a high initial value to a lower steady-state value.

A physical explanation for this phenomenon is that the magnetic flux caused by the short-circuit armature currents (or by the resultant armature MMF) is initially forced to flow through high-reluctance paths that do not link the field winding or damper circuits of the machine. This is a result of the theorem of constant flux linkages that states that the flux linking a closed winding cannot change instantaneously. The armature inductance, which is inversely proportional to reluctance, is therefore

Copyright 2017 Cengage Learning. All Rights Reserved. May not be copied, scanned, or duplicated, in whole or in part. Due to electronic rights, some third party content may be suppressed from the eBook and/or eChapter(s). Editorial review has deemed that any suppressed content does not materially affect the overall learning experience. Cengage Learning reserves the right to remove additional content at any time if subsequent rights restrictions require it.

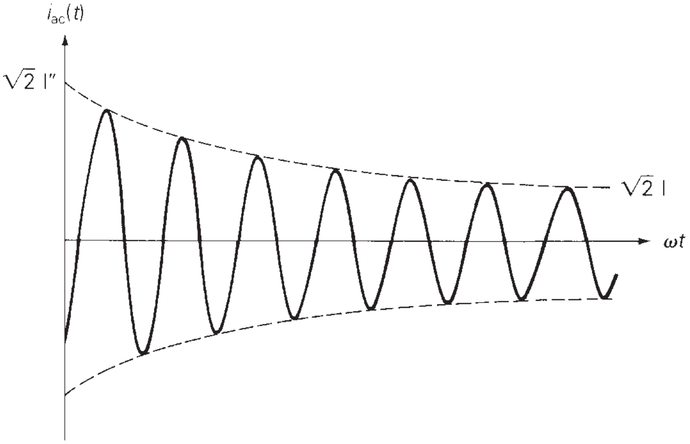

FIGURE 7.2

The ac fault current in one phase of an unloaded synchronous machine during a three-phase short circuit (the dc offset current is removed)

initially low. As the flux then moves toward the lower reluctance paths, the armature inductance increases.

The ac fault current in a synchronous machine can be modeled by the series R–L circuit of Figure 7.1 if a time-varying inductance $L(t)$ or reactance $X(t) = \omega L(t)$ is employed. In standard machine theory texts [3, 4], the following reactances are defined:

X''_d = direct axis subtransient reactance
X'_d = direct axis transient reactance
X_d = direct axis synchronous reactance

where $X''_d < X'_d < X_d$. The subscript d refers to the direct axis. There are similar quadrature axis reactances X''_q, X'_q, and X_q [3, 4]. However, if the armature resistance is small, the quadrature axis reactances do not significantly affect the short-circuit current. Using the above direct axis reactances, the instantaneous ac fault current can be written as

$$i_{ac}(t) = \sqrt{2}E_g\left[\left(\frac{1}{X''_d} - \frac{1}{X'_d}\right)e^{-t/T''_d} + \left(\frac{1}{X'_d} - \frac{1}{X_d}\right)e^{-t/T'_d} + \frac{1}{X_d}\right]\sin\left(\omega t + \alpha - \frac{\pi}{2}\right) \tag{7.2.1}$$

where E_g is the rms line-to-neutral prefault terminal voltage of the unloaded synchronous machine. Armature resistance is neglected in (7.2.1). Note that at $t = 0$, when the fault occurs, the rms value of $i_{ac}(t)$ in (7.2.1) is

$$I_{ac}(0) = \frac{E_g}{X''_d} = I'' \tag{7.2.2}$$

which is called the rms *subtransient fault current*, I''. The duration of I'' is determined by the time constant T''_d, called the *direct axis short-circuit sub-transient time constant*.

Copyright 2017 Cengage Learning. All Rights Reserved. May not be copied, scanned, or duplicated, in whole or in part. Due to electronic rights, some third party content may be suppressed from the eBook and/or eChapter(s). Editorial review has deemed that any suppressed content does not materially affect the overall learning experience. Cengage Learning reserves the right to remove additional content at any time if subsequent rights restrictions require it.

At a later time, when t is large compared to T''_d but small compared to the *direct axis short-circuit transient time constant* T'_d, the first exponential term in (7.2.1) has decayed almost to zero, but the second exponential has not decayed significantly. The rms ac fault current then equals the rms *transient fault current*, given by

$$I' = \frac{E_g}{X'_d} \tag{7.2.3}$$

When t is much larger than T'_d, the rms ac fault current approaches its steady-state value, given by

$$I_{ac}(\infty) = \frac{E_g}{X_d} = I \tag{7.2.4}$$

Since the three-phase no-load voltages are displaced 120° from each other, the three-phase ac fault currents are also displaced 120° from each other. In addition to the ac fault current, each phase has a different dc offset. The maximum dc offset in any one phase, which occurs when $\alpha = 0$ in (7.2.1), is

$$i_{\text{dcmax}}(t) = \frac{\sqrt{2}E_g}{X''_d} e^{-t/T_A} = \sqrt{2}I'' e^{-t/T_A} \tag{7.2.5}$$

where T_A is called the *armature time constant*. Note that the magnitude of the maximum dc offset depends only on the rms subtransient fault current I''. The above synchronous machine short-circuit currents are summarized in Table 7.2.

Component	Instantaneous Current (A)	rms Current (A)
Symmetrical (ac)	(7.2.1)	$I_{ac}(t) = E_g\left[\left(\frac{1}{X''_d} - \frac{1}{X'_d}\right)e^{-t/T''_d} + \left(\frac{1}{X'_d} - \frac{1}{X_d}\right)e^{-t/T'_d} + \frac{1}{X_d}\right]$
Subtransient		$I'' = E_g/X''_d$
Transient		$I' = E_g/X'_d$
Steady-state		$I = E_g/X_d$
Maximum dc offset	$i_{dc}(t) = \sqrt{2}I''e^{-t/T_A}$	
Asymmetrical (total)	$i(t) = i_{ac}(t) + i_{dc}(t)$	$I_{rms}(t) = \sqrt{I_{ac}(t)^2 + i_{dc}(t)^2}$ with maximum dc offset: $I_{rms}(t) = \sqrt{I_{ac}(t)^2 + [\sqrt{2}I''e^{-t/T_A}]^2}$

TABLE 7.2

Short-circuit current—unloaded synchronous machine*

*See Figure 7.2 and (7.2.1) through (7.2.5).

Copyright 2017 Cengage Learning. All Rights Reserved. May not be copied, scanned, or duplicated, in whole or in part. Due to electronic rights, some third party content may be suppressed from the eBook and/or eChapter(s). Editorial review has deemed that any suppressed content does not materially affect the overall learning experience. Cengage Learning reserves the right to remove additional content at any time if subsequent rights restrictions require it.

Machine reactances X''_d, X'_d, and X_d as well as time constants T''_d, T'_d, and T_A are usually provided by synchronous machine manufacturers. They also can be obtained from a three-phase short-circuit test by analyzing an oscillogram such as that in Figure 7.2 [2]. Typical values of synchronous machine reactances and time constants are given in Appendix Table A.1.

EXAMPLE 7.2

Three-phase short-circuit currents, unloaded synchronous generator

A 500-MVA, 20-kV, 60-Hz synchronous generator with reactances $X''_d = 0.15$, $X'_d = 0.24$, and $X_d = 1.1$ per unit and time constants $T''_d = 0.035$, $T'_d = 2.0$, $T_A = 0.20$ s is connected to a circuit breaker. The generator is operating at 5% above rated voltage and at no-load when a bolted three-phase short circuit occurs on the load side of the breaker. The breaker interrupts the fault three cycles after fault inception. Determine (a) the subtransient fault current in per-unit and kA rms; (b) maximum dc offset as a function of time; and (c) rms asymmetrical fault current, which the breaker interrupts, assuming maximum dc offset.

SOLUTION

a. The no-load voltage before the fault occurs is $E_g = 1.05$ per unit. From (7.2.2), the subtransient fault current that occurs in each of the three phases is

$$I'' = \frac{1.05}{0.15} = 7.0 \quad \text{per unit}$$

The generator base current is

$$I_{\text{base}} = \frac{S_{\text{rated}}}{\sqrt{3}V_{\text{rated}}} = \frac{500}{(\sqrt{3})(20)} = 14.43 \quad \text{kA}$$

The rms subtransient fault current in kA is the per-unit value multiplied by the base current:

$$I'' = (7.0)(14.43) = 101.0 \quad \text{kA}$$

b. From (7.2.5), the maximum dc offset that may occur in any one phase is

$$i_{\text{dcmax}}(t) = \sqrt{2}(101.0)e^{-t/0.20} = 142.9e^{-t/0.20} \quad \text{kA}$$

(Continued)

Copyright 2017 Cengage Learning. All Rights Reserved. May not be copied, scanned, or duplicated, in whole or in part. Due to electronic rights, some third party content may be suppressed from the eBook and/or eChapter(s). Editorial review has deemed that any suppressed content does not materially affect the overall learning experience. Cengage Learning reserves the right to remove additional content at any time if subsequent rights restrictions require it.

c. From (7.2.1), the rms ac fault current at $t = 3$ cycles $= 0.05$ s is

$$\begin{aligned} I_{ac}(0.05\text{ s}) &= 1.05\left[\left(\frac{1}{0.15} - \frac{1}{0.24}\right)e^{-0.05/0.035}\right. \\ &\qquad \left. + \left(\frac{1}{0.24} - \frac{1}{1.1}\right)e^{-0.05/2.0} + \frac{1}{1.1}\right] \\ &= 4.920 \quad \text{per unit} \\ &= (4.920)(14.43) = 71.01 \quad \text{kA} \end{aligned}$$

Modifying (7.1.10) to account for the time-varying symmetrical component of fault current,

$$\begin{aligned} I_{rms}(0.05) &= \sqrt{[I_{ac}(0.05)]^2 + [\sqrt{2}I''e^{-t/T_a}]^2} \\ &= I_{ac}(0.05)\sqrt{1 + 2\left[\frac{I''}{I_{ac}(0.05)}\right]^2 e^{-2t/T_a}} \\ &= (71.01)\sqrt{1 + 2\left[\frac{101}{71.01}\right]^2 e^{-2(0.05)/0.20}} \\ &= (71.01)(1.8585) \\ &= 132 \quad \text{kA} \end{aligned}$$

7.3 POWER SYSTEM THREE-PHASE SHORT CIRCUITS

In order to calculate the subtransient fault current for a three-phase short circuit in a power system, make the following assumptions:

1. Transformers are represented by their leakage reactances. Winding resistances, shunt admittances, and Δ–Y phase shifts are neglected.
2. Transmission lines are represented by their equivalent series reactances. Neglect series resistances and shunt admittances.
3. Synchronous machines are represented by constant-voltage sources behind subtransient reactances. Neglect armature resistance, saliency, and saturation.
4. Neglect all nonrotating impedance loads.
5. Especially for small motors rated less than 50 hp, either neglect induction motors or represent them in the same manner as synchronous machines.

These assumptions are made for simplicity in this text, and in practice they should not be made for all cases. For example, in distribution systems, resistances of primary and secondary distribution lines may in some cases significantly reduce fault current magnitudes.

Figure 7.3 shows a single-line diagram consisting of a synchronous generator feeding a synchronous motor through two transformers and a transmission line.

Copyright 2017 Cengage Learning. All Rights Reserved. May not be copied, scanned, or duplicated, in whole or in part. Due to electronic rights, some third party content may be suppressed from the eBook and/or eChapter(s). Editorial review has deemed that any suppressed content does not materially affect the overall learning experience. Cengage Learning reserves the right to remove additional content at any time if subsequent rights restrictions require it.

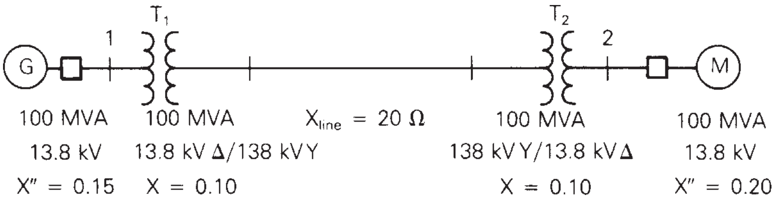
T$_1$
T$_2$
1
2
G
M
100 MVA
13.8 kV
X″ = 0.15
100 MVA
13.8 kV Δ/138 kV Y
X = 0.10
X$_{\text{line}}$ = 20 Ω
100 MVA
138 kV Y/13.8 kV Δ
X = 0.10
100 MVA
13.8 kV
X″ = 0.20

FIGURE 7.3 Single-line diagram of a synchronous generator feeding a synchronous motor

Consider a three-phase short circuit at bus 1. The positive-sequence equivalent circuit is shown in Figure 7.4(a), where the voltages E_g'' and E_m'' are the prefault internal voltages behind the subtransient reactances of the machines, and the closing of switch SW represents the fault. For purposes of calculating the subtransient fault current, E_g'' and E_m'' are assumed to be constant-voltage sources.

In Figure 7.4(b) the fault is represented by two opposing voltage sources with equal phasor values V_F. Using superposition, the fault current then can be calculated from the two circuits shown in Figure 7.4(c). However, if V_F equals the prefault

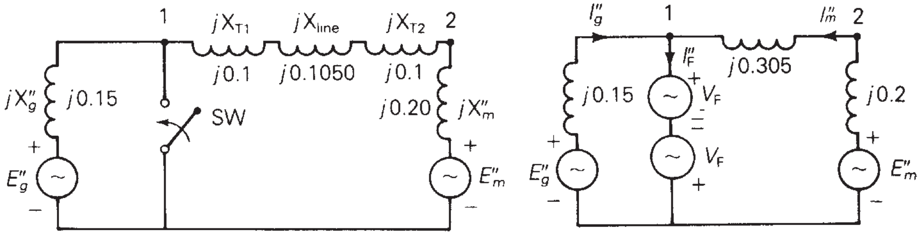
1
jX$_{T1}$
jX$_{\text{line}}$
jX$_{T2}$
2
j0.1
j0.1050
j0.1
jX″$_g$
j0.15
SW
j0.20
jX″$_m$
E″$_g$
E″$_m$
+
−
I″$_g$
1
I″$_m$
2
I″$_F$
j0.305
j0.15
V$_F$
j0.2
V$_F$
E″$_g$
E″$_m$

(a) Three-phase short circuit

(b) Short circuit represented by two opposing voltage sources

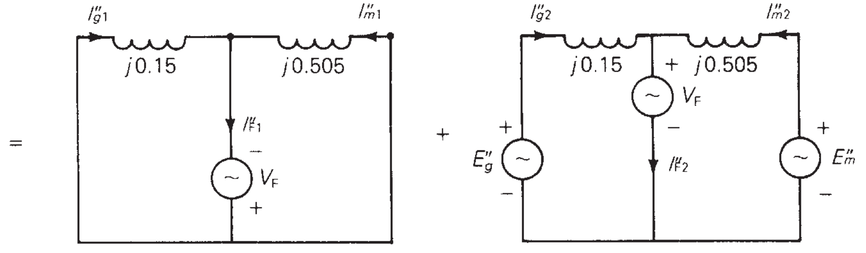
=
I″$_{g1}$
I″$_{m1}$
j0.15
j0.505
I″$_{F1}$
V$_F$
+
I″$_{g2}$
I″$_{m2}$
j0.15
j0.505
V$_F$
E″$_g$
I″$_{F2}$
E″$_m$

(c) Application of superposition

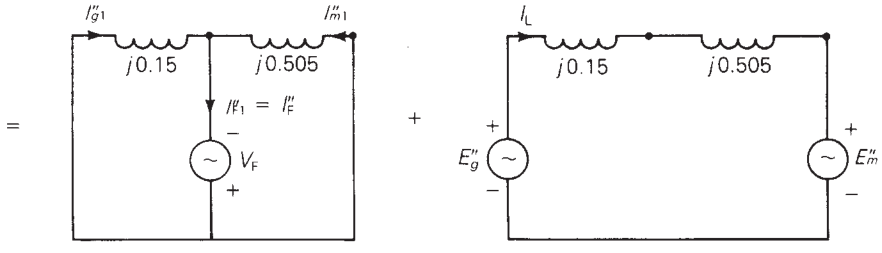
=
I″$_{g1}$
I″$_{m1}$
j0.15
j0.505
I″$_{F1}$ = I″$_F$
V$_F$
+
I$_L$
j0.15
j0.505
E″$_g$
E″$_m$

(d) V_F set equal to prefault voltage at fault

FIGURE 7.4 Application of superposition to a power system three-phase short circuit

Copyright 2017 Cengage Learning. All Rights Reserved. May not be copied, scanned, or duplicated, in whole or in part. Due to electronic rights, some third party content may be suppressed from the eBook and/or eChapter(s). Editorial review has deemed that any suppressed content does not materially affect the overall learning experience. Cengage Learning reserves the right to remove additional content at any time if subsequent rights restrictions require it.

voltage at the fault, then the second circuit in Figure 7.4(c) represents the system before the fault occurs. As such, $I''_{F2} = 0$ and V_F, which has no effect, can be removed from the second circuit, as shown in Figure 7.4(d). The subtransient fault current is then determined from the first circuit in Figure 7.4(d), $I''_F = I''_{F1}$. The contribution to the fault from the generator is $I''_g = I''_{g1} + I''_{g2} = I''_{g1} + I_L$, where I_L is the prefault generator current. Similarly, $I''_m = I''_{m1} - I_L$.

EXAMPLE 7.3

Three-phase short-circuit currents, power system

The synchronous generator in Figure 7.3 is operating at rated MVA, 0.95 p.f. lagging and at 5% above rated voltage when a bolted three-phase short circuit occurs at bus 1. Calculate the per-unit values of (a) subtransient fault current; (b) subtransient generator and motor currents neglecting prefault current; and (c) subtransient generator and motor currents including prefault current.

SOLUTION

a. Using a 100-MVA base, the base impedance in the zone of the transmission line is

$$Z_{\text{base, line}} = \frac{(138)^2}{100} = 190.44 \quad \Omega$$

and

$$X_{\text{line}} = \frac{20}{190.44} = 0.1050 \quad \text{per unit}$$

Figure 7.4 shows the per-unit reactances. From the first circuit in Figure 7.4(d), the Thévenin impedance as viewed from the fault is

$$Z_{Th} = jX_{Th} = j\frac{(0.15)(0.505)}{(0.15 + 0.505)} = j0.11565 \quad \text{per unit}$$

and the prefault voltage at the generator terminals is

$$V_F = 1.05\underline{/0^\circ} \quad \text{per unit}$$

The subtransient fault current is then

$$I''_F = \frac{V_F}{Z_{Th}} = \frac{1.05\underline{/0^\circ}}{j0.11565} = -j9.079 \quad \text{per unit}$$

b. Using current division in the first circuit of Figure 7.4(d),

$$I''_{g1} = \left(\frac{0.505}{0.505 + 0.15}\right) I''_F = (0.7710)(-j9.079) = -j7.000 \quad \text{per unit}$$

Copyright 2017 Cengage Learning. All Rights Reserved. May not be copied, scanned, or duplicated, in whole or in part. Due to electronic rights, some third party content may be suppressed from the eBook and/or eChapter(s). Editorial review has deemed that any suppressed content does not materially affect the overall learning experience. Cengage Learning reserves the right to remove additional content at any time if subsequent rights restrictions require it.

$$I''_{m1} = \left(\frac{0.15}{0.505 + 0.15}\right) I''_F = (0.2290)(-j9.079) = -j2.079 \quad \text{per unit}$$

c. The generator base current is

$$\text{I}_{\text{base,gen}} = \frac{100}{(\sqrt{3})(13.8)} = 4.1837 \quad \text{kA}$$

and the prefault generator current is

$$\begin{aligned} I_L &= \frac{100}{(\sqrt{3})(1.05 \times 13.8)} \underline{/-\cos^{-1} 0.95} = 3.9845 \underline{/-18.19^\circ} \quad \text{kA} \\ &= \frac{3.9845\underline{/-18.19^\circ}}{4.1837} = 0.9524\underline{/-18.19^\circ} \\ &= 0.9048 - j0.2974 \quad \text{per unit} \end{aligned}$$

The subtransient generator and motor currents, including prefault current, are then

$$\begin{aligned} I''_g = I''_{g1} + I_L &= -j7.000 + 0.9048 - j0.2974 \\ &= 0.9048 - j7.297 = 7.353\underline{/-82.9^\circ} \quad \text{per unit} \\ I''_m = I''_{m1} - I_L &= -j2.079 - 0.9048 + j0.2974 \\ &= -0.9048 - j1.782 = 1.999\underline{/243.1^\circ} \quad \text{per unit} \end{aligned}$$

An alternate method of solving Example 7.3 is to first calculate the internal voltages E''_g and E''_m using the prefault load current I_L. Then, instead of using superposition, the fault currents can be resolved directly from the circuit in Figure 7.4(a) (see Problem 7.11). However, in a system with many synchronous machines, the superposition method has the advantage that all machine voltage sources are shorted, and the prefault voltage is the only source required to calculate the fault current. Also, when calculating the contributions to fault current from each branch, prefault currents are usually small, and hence can be neglected. Otherwise, prefault load currents could be obtained from a power-flow program.

7.4 BUS IMPEDANCE MATRIX

Now to extend the results of the previous section to calculate subtransient fault currents for three-phase faults in an N-bus power system, the system is modeled by its positive-sequence network, where lines and transformers are represented by series reactances and synchronous machines are represented by constant-voltage sources behind subtransient reactances. As before, all resistances, shunt admittances, and nonrotating impedance loads, and also for simplicity prefault load currents, are neglected.

Consider a three-phase short circuit at any bus n. To analyze two separate circuits, use the superposition method described in Section 7.3. [For example, see Figure 7.4(d).]

Copyright 2017 Cengage Learning. All Rights Reserved. May not be copied, scanned, or duplicated, in whole or in part. Due to electronic rights, some third party content may be suppressed from the eBook and/or eChapter(s). Editorial review has deemed that any suppressed content does not materially affect the overall learning experience. Cengage Learning reserves the right to remove additional content at any time if subsequent rights restrictions require it.

In the first circuit, all machine-voltage sources are short-circuited, and the only source is due to the prefault voltage at the fault. Writing nodal equations for the first circuit,

$$\boldsymbol{Y}_{\text{bus}}\boldsymbol{E}^{(1)} = \boldsymbol{I}^{(1)} \tag{7.4.1}$$

where $\boldsymbol{Y}_{\text{bus}}$ is the positive-sequence bus admittance matrix, $\boldsymbol{E}^{(1)}$ is the vector of bus voltages, and $\boldsymbol{I}^{(1)}$ is the vector of current sources. The superscript (1) denotes the first circuit. Solving (7.4.1),

$$\boldsymbol{Z}_{\text{bus}}\boldsymbol{I}^{(1)} = \boldsymbol{E}^{(1)} \tag{7.4.2}$$

where

$$\boldsymbol{Z}_{\text{bus}} = \boldsymbol{Y}_{\text{bus}}^{-1} \tag{7.4.3}$$

$\boldsymbol{Z}_{\text{bus}}$, the inverse of $\boldsymbol{Y}_{\text{bus}}$, is called the positive-sequence *bus impedance matrix*. Both $\boldsymbol{Z}_{\text{bus}}$ and $\boldsymbol{Y}_{\text{bus}}$ are symmetric matrices.

Since the first circuit contains only one source, located at faulted bus n, the current source vector contains only one nonzero component, $I_n^{(1)} = -I''_{\text{F}n}$. Also, the voltage at faulted bus n in the first circuit is $E_n^{(1)} = -V_{\text{F}}$. Rewriting (7.4.2),

$$\begin{bmatrix} Z_{11} & Z_{12} & \cdots & Z_{1n} & \cdots & Z_{1N} \\ Z_{21} & Z_{22} & \cdots & Z_{2n} & \cdots & Z_{2N} \\ \vdots & & & & & \\ Z_{n1} & Z_{n2} & \cdots & Z_{nn} & \cdots & Z_{nN} \\ \vdots & & & & & \\ Z_{N1} & Z_{N2} & \cdots & Z_{Nn} & \cdots & Z_{NN} \end{bmatrix} \begin{bmatrix} 0 \\ 0 \\ \vdots \\ -I''_{\text{F}n} \\ \vdots \\ 0 \end{bmatrix} = \begin{bmatrix} E_1^{(1)} \\ E_2^{(1)} \\ \vdots \\ -V_{\text{F}} \\ \vdots \\ E_N^{(1)} \end{bmatrix} \tag{7.4.4}$$

The minus sign associated with the current source in (7.4.4) indicates that the current injected into bus n is the negative of I''_{Fn}, since I''_{Fn} flows away from bus n to the neutral. From (7.4.4), the subtransient fault current is

$$I''_{\text{F}n} = \frac{V_{\text{F}}}{Z_{nn}} \tag{7.4.5}$$

Also from (7.4.4) and (7.4.5), the voltage at any bus k in the first circuit is

$$E_k^{(1)} = Z_{kn}(-I''_{\text{F}n}) = \frac{-Z_{kn}}{Z_{nn}}V_{\text{F}} \tag{7.4.6}$$

The second circuit represents the prefault conditions. Neglecting prefault load current, all voltages throughout the second circuit are equal to the prefault voltage; that is, $E_k^{(2)} = V_{\text{F}}$ for each bus k. Applying superposition,

$$\begin{aligned} E_k &= E_k^{(1)} + E_k^{(2)} = \frac{-Z_{kn}}{Z_{nn}}V_{\text{F}} + V_{\text{F}} \\ &= \left(1 - \frac{Z_{kn}}{Z_{nn}}\right)V_{\text{F}} \qquad k = 1, 2, \ldots, N \end{aligned} \tag{7.4.7}$$

Copyright 2017 Cengage Learning. All Rights Reserved. May not be copied, scanned, or duplicated, in whole or in part. Due to electronic rights, some third party content may be suppressed from the eBook and/or eChapter(s). Editorial review has deemed that any suppressed content does not materially affect the overall learning experience. Cengage Learning reserves the right to remove additional content at any time if subsequent rights restrictions require it.

EXAMPLE 7.4

Using Z_{bus} to compute three-phase short-circuit currents in a power system

The faults at bus 1 and 2 in Figure 7.3 are of interest. The prefault voltage is 1.05 per unit, and prefault load current is neglected. (a) Determine the 2 × 2 positive-sequence bus impedance matrix. (b) For a bolted three-phase short circuit at bus 1, use $\boldsymbol{Z}_{\text{bus}}$ to calculate the subtransient fault current and the contribution to the fault current from the transmission line. (c) Repeat part (b) for a bolted three-phase short circuit at bus 2.

SOLUTION

a. The circuit of Figure 7.4(a) is redrawn in Figure 7.5 showing per-unit admittance rather than per-unit impedance values. Neglecting prefault load current, $E''_g = E''_m = V_F = 1.05\underline{/0^\circ}$ per unit. From Figure 7.5, the positive-sequence bus admittance matrix is

$$\boldsymbol{Y}_{\text{bus}} = -j\begin{bmatrix} 9.9454 & -3.2787 \\ -3.2787 & 8.2787 \end{bmatrix} \quad \text{per unit}$$

Inverting $\boldsymbol{Y}_{\text{bus}}$,

$$\boldsymbol{Z}_{\text{bus}} = \boldsymbol{Y}_{\text{bus}}^{-1} = +j\begin{bmatrix} 0.11565 & 0.04580 \\ 0.04580 & 0.13893 \end{bmatrix} \quad \text{per unit}$$

b. Using (7.4.5), the subtransient fault current at bus 1 is

$$I''_{F1} = \frac{V_F}{Z_{11}} = \frac{1.05\underline{/0^\circ}}{j0.11565} = -j9.079 \quad \text{per unit}$$

which agrees with the result in Example 7.3, part (a). The voltages at buses 1 and 2 during the fault are, from (7.4.7),

FIGURE 7.5

Circuit of Figure 7.4(a) showing per-unit admittance values

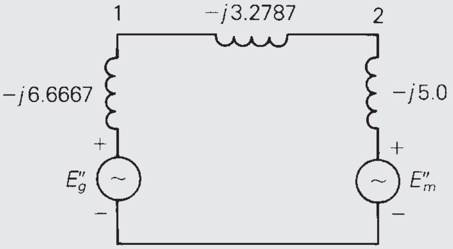

(*Continued*)

Copyright 2017 Cengage Learning. All Rights Reserved. May not be copied, scanned, or duplicated, in whole or in part. Due to electronic rights, some third party content may be suppressed from the eBook and/or eChapter(s). Editorial review has deemed that any suppressed content does not materially affect the overall learning experience. Cengage Learning reserves the right to remove additional content at any time if subsequent rights restrictions require it.

$$E_1 = \left(1 - \frac{Z_{11}}{Z_{11}}\right)V_F = 0$$

$$E_2 = \left(1 - \frac{Z_{21}}{Z_{11}}\right)V_F = \left(1 - \frac{j0.04580}{j0.11565}\right)1.05\underline{/0°} = 0.6342\underline{/0°}$$

The current to the fault from the transmission line is obtained from the voltage drop from bus 2 to 1 divided by the impedance of the line and transformers T_1 and T_2:

$$I_{21} = \frac{E_2 - E_1}{j(X_{\text{line}} + X_{T1} + X_{T2})} = \frac{0.6342 - 0}{j0.3050} = -j2.079 \quad \text{per unit}$$

which agrees with the motor current calculated in Example 7.3, part (b), where prefault load current is neglected.

c. Using (7.4.5), the subtransient fault current at bus 2 is

$$I''_{F2} = \frac{V_F}{Z_{22}} = \frac{1.05\underline{/0°}}{j0.13893} = -j7.558 \quad \text{per unit}$$

and from (7.4.7),

$$E_1 = \left(1 - \frac{Z_{12}}{Z_{22}}\right)V_F = \left(1 - \frac{j0.04580}{j0.13893}\right)1.05\underline{/0°} = 0.7039\underline{/0°}$$

$$E_2 = \left(1 - \frac{Z_{22}}{Z_{22}}\right)V_F = 0$$

The current to the fault from the transmission line is

$$I_{12} = \frac{E_1 - E_2}{j(X_{\text{line}} + X_{T1} + X_{T2})} = \frac{0.7039 - 0}{j0.3050} = -j2.308 \quad \text{per unit}$$

Figure 7.6 shows a bus impedance equivalent circuit that illustrates the short-circuit currents in an N-bus system. This circuit is given the name *rake equivalent* in Neuenswander [5] due to its shape, which is similar to a garden rake.

The diagonal elements Z_{11}, Z_{22}, …, Z_{NN} of the bus impedance matrix, which are the *self-impedances*, are shown in Figure 7.6. The off-diagonal elements, or the *mutual impedances*, are indicated by the brackets in the figure.

Neglecting prefault load currents, the internal voltage sources of all synchronous machines are equal both in magnitude and phase. As such, they can be connected, as shown in Figure 7.7, and replaced by one equivalent source V_F from neutral bus 0 to a references bus, denoted r. This equivalent source is also shown in the rake equivalent of Figure 7.6.

Copyright 2017 Cengage Learning. All Rights Reserved. May not be copied, scanned, or duplicated, in whole or in part. Due to electronic rights, some third party content may be suppressed from the eBook and/or eChapter(s). Editorial review has deemed that any suppressed content does not materially affect the overall learning experience. Cengage Learning reserves the right to remove additional content at any time if subsequent rights restrictions require it.

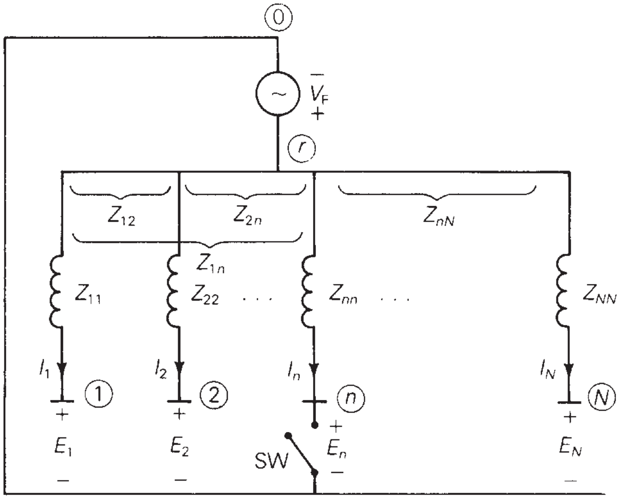

FIGURE 7.6

Bus impedance equivalent circuit (*rake equivalent*)

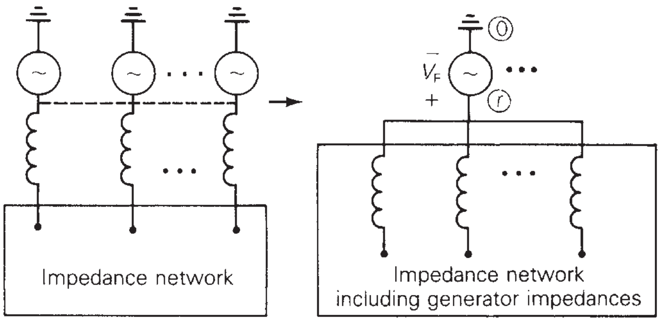

FIGURE 7.7

Parallel connection of unloaded synchronous machine internal-voltage sources

Using Z_{bus}, the fault currents in Figure 7.6 are given by

$$\begin{bmatrix} Z_{11} & Z_{12} & \cdots & Z_{1n} & \cdots & Z_{1N} \\ Z_{21} & Z_{22} & \cdots & Z_{2n} & \cdots & Z_{2N} \\ \vdots & & & & & \\ Z_{n1} & Z_{n2} & \cdots & Z_{nn} & \cdots & Z_{nN} \\ \vdots & & & & & \\ Z_{N1} & Z_{N2} & \cdots & Z_{Nn} & \cdots & Z_{NN} \end{bmatrix} \begin{bmatrix} I_1 \\ I_2 \\ \vdots \\ I_n \\ \vdots \\ I_N \end{bmatrix} = \begin{bmatrix} V_F - E_1 \\ V_F - E_2 \\ \vdots \\ V_F - E_n \\ \vdots \\ V_F - E_N \end{bmatrix} \tag{7.4.8}$$

where I_1, I_2, … are the branch currents and ($V_F - E_1$), ($V_F - E_2$), … are the voltages across the branches.

If switch SW in Figure 7.6 is open, all currents are zero and the voltage at each bus with respect to the neutral equals V_F. This corresponds to prefault conditions, neglecting prefault load currents. If switch SW is closed, corresponding to a short circuit at bus n, $E_n = 0$ and all currents except I_n remain zero. The fault current is

Copyright 2017 Cengage Learning. All Rights Reserved. May not be copied, scanned, or duplicated, in whole or in part. Due to electronic rights, some third party content may be suppressed from the eBook and/or eChapter(s). Editorial review has deemed that any suppressed content does not materially affect the overall learning experience. Cengage Learning reserves the right to remove additional content at any time if subsequent rights restrictions require it.

$I''_{Fn} = I_n = V_F/Z_{nn}$, which agrees with (7.4.5). This fault current also induces a voltage drop $Z_{kn}I_n = (Z_{kn}/Z_{nn})V_F$ across each branch k. The voltage at bus k with respect to the neutral then equals V_F minus this voltage drop, which agrees with (7.4.7).

As shown by Figure 7.6 as well as (7.4.5), subtransient fault currents throughout an N-bus system can be determined from the bus impedance matrix and the prefault voltage. $\boldsymbol{Z}_{bus}$ can be computed by first constructing $\boldsymbol{Y}_{bus}$, via nodal equations, and then inverting $\boldsymbol{Y}_{bus}$. Once $\boldsymbol{Z}_{bus}$ has been obtained, these fault currents are easily computed.

EXAMPLE 7.5

PowerWorld Simulator case Example 7_5 models the 5-bus power system whose oneline diagram is shown in Figure 6.2. Machine, line, and transformer data are given in Tables 7.3, 7.4, and 7.5. This system is initially unloaded. Prefault voltages at all the buses are 1.05 per unit. Use PowerWorld Simulator to determine the fault current for three-phase faults at each of the buses.

Bus	Machine Subtransient Reactance—X''_d
1	0.045
3	0.0225

TABLE 7.3

Synchronous machine data for the SYMMETRICAL SHORT CIRCUITS program*

$*S_{base} = 100\text{MVA}$
$V_{base} = 15$ kV at buses 1, 3
$= 345$ kV at buses 2, 4, 5

Bus-to-Bus	Equivalent Positive-Sequence Series Reactance (per unit)
2–4	0.1
2–5	0.05
4–5	0.025

TABLE 7.4

Line data for the SYMMETRICAL SHORT CIRCUITS program

Bus-to-Bus	Leakage Reactance—X (per unit)
1–5	0.02
3–4	0.01

TABLE 7.5

Transformer data for the SYMMETRICAL SHORT CIRCUITS program

Copyright 2017 Cengage Learning. All Rights Reserved. May not be copied, scanned, or duplicated, in whole or in part. Due to electronic rights, some third party content may be suppressed from the eBook and/or eChapter(s). Editorial review has deemed that any suppressed content does not materially affect the overall learning experience. Cengage Learning reserves the right to remove additional content at any time if subsequent rights restrictions require it.

SOLUTION

To fault a bus from the oneline, first right-click on the bus symbol to display the local menu, and then select **Fault** to display the Fault Analysis dialog (see Figure 7.8). In the list on the left side of the dialog, set the **Fault Definitions** to Single Fault; the Faulted Bus should be automatically selected to the selected bus location. Verify that the Fault Location field is Bus Fault and the Fault Type is 3-Phase Balanced (unbalanced faults are covered in Chapter 9). Then select **Calculate**, located in the upper left portion of the dialog, to determine the fault currents and voltages. The results are shown in the tables at the bottom of the dialog. Additionally, the fault currents can be shown on the oneline by selecting **Options** in the left list, and changing the Oneline Display Field value. Since with a three-phase fault the system remains balanced, the magnitudes of the a phase, b phase, and c phase values are identical. The 5 × 5 $\boldsymbol{Z}_{\text{bus}}$ matrix for this system is shown in Table 7.6, and the fault currents and bus voltages for faults at each of the buses are given in Table 7.7. Note that these fault currents are subtransient fault currents, since the machine reactance input data consist of direct axis subtransient reactances.

$$
j\begin{bmatrix}
0.0279725 & 0.0177025 & 0.0085125 & 0.0122975 & 0.020405 \\
0.0177025 & 0.0569525 & 0.0136475 & 0.019715 & 0.02557 \\
0.0085125 & 0.0136475 & 0.0182425 & 0.016353 & 0.012298 \\
0.0122975 & 0.019715 & 0.016353 & 0.0236 & 0.017763 \\
0.020405 & 0.02557 & 0.012298 & 0.017763 & 0.029475
\end{bmatrix}
$$

TABLE 7.6

Z_{bus} for Example 7.5

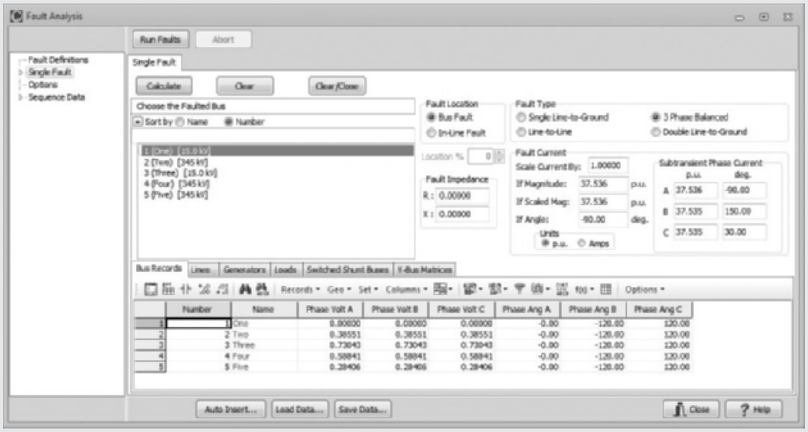

Choose the Faulted Bus

Sort by ○ Name ● Number

1 (One) [15.0 kV]
2 (Two) [345 kV]
3 (Three) [15.0 kV]
4 (Four) [345 kV]
5 (Five) [345 kV]

Fault Location: ● Bus Fault ○ In-Line Fault

Location %: 0

Fault Impedance
R: 0.00000
X: 0.00000

Fault Type: ○ Single Line-to-Ground ○ Line-to-Line ● 3 Phase Balanced ○ Double Line-to-Ground

Fault Current
Scale Current By: 1.00000
If Magnitude: 37.536 p.u.
If Scaled Mag: 37.536 p.u.
If Angle: -90.00 deg.
Units: ● p.u. ○ Amps

Subtransient Phase Current

	p.u.	deg.
A	37.536	-90.00
B	37.535	150.00
C	37.535	30.00

	Number	Name	Phase Volt A	Phase Volt B	Phase Volt C	Phase Ang A	Phase Ang B	Phase Ang C
1	1	One	0.00000	0.00000	0.00000	-0.00	-120.00	120.00
2	2	Two	0.38551	0.38551	0.38551	-0.00	-120.00	120.00
3	3	Three	0.73043	0.73043	0.73043	-0.00	-120.00	120.00
4	4	Four	0.58841	0.58841	0.58841	-0.00	-120.00	120.00
5	5	Five	0.28406	0.28406	0.28406	-0.00	-120.00	120.00

FIGURE 7.8

Fault Analysis Dialog for Example 7.5—fault at bus 1

(*Continued*)

Copyright 2017 Cengage Learning. All Rights Reserved. May not be copied, scanned, or duplicated, in whole or in part. Due to electronic rights, some third party content may be suppressed from the eBook and/or eChapter(s). Editorial review has deemed that any suppressed content does not materially affect the overall learning experience. Cengage Learning reserves the right to remove additional content at any time if subsequent rights restrictions require it.

		Contributions to Fault Current		
Fault Bus	Fault Current (per unit)	Gen Line or TRSF	Bus-to-Bus	Current (per unit)
1	37.536			
		G 1	GRND–1	23.332
		T 1	5–1	14.204
2	18.436			
		L 1	4–2	6.864
		L 2	5–2	11.572
3	57.556			
		G 2	GRND-3	46.668
		T 2	4–3	10.888
4	44.456			
		L 1	2–4	1.736
		L 3	5–4	10.412
		T 2	3–4	32.308
5	35.624			
		L 2	2–5	2.78
		L 3	4–5	16.688
		T 1	1–5	16.152

$V_F = 1.05$	Per-Unit Bus Voltage Magnitudes during the Fault				
Fault Bus	Bus 1	Bus 2	Bus 3	Bus 4	Bus 5
1	0.0000	0.7236	0.5600	0.5033	0.3231
2	0.3855	0.0000	0.2644	0.1736	0.1391
3	0.7304	0.7984	0.0000	0.3231	0.6119
4	0.5884	0.6865	0.1089	0.0000	0.4172
5	0.2840	0.5786	0.3422	0.2603	0.0000

TABLE 7.7

Fault currents and bus voltages for Example 7.5

Copyright 2017 Cengage Learning. All Rights Reserved. May not be copied, scanned, or duplicated, in whole or in part. Due to electronic rights, some third party content may be suppressed from the eBook and/or eChapter(s). Editorial review has deemed that any suppressed content does not materially affect the overall learning experience. Cengage Learning reserves the right to remove additional content at any time if subsequent rights restrictions require it.

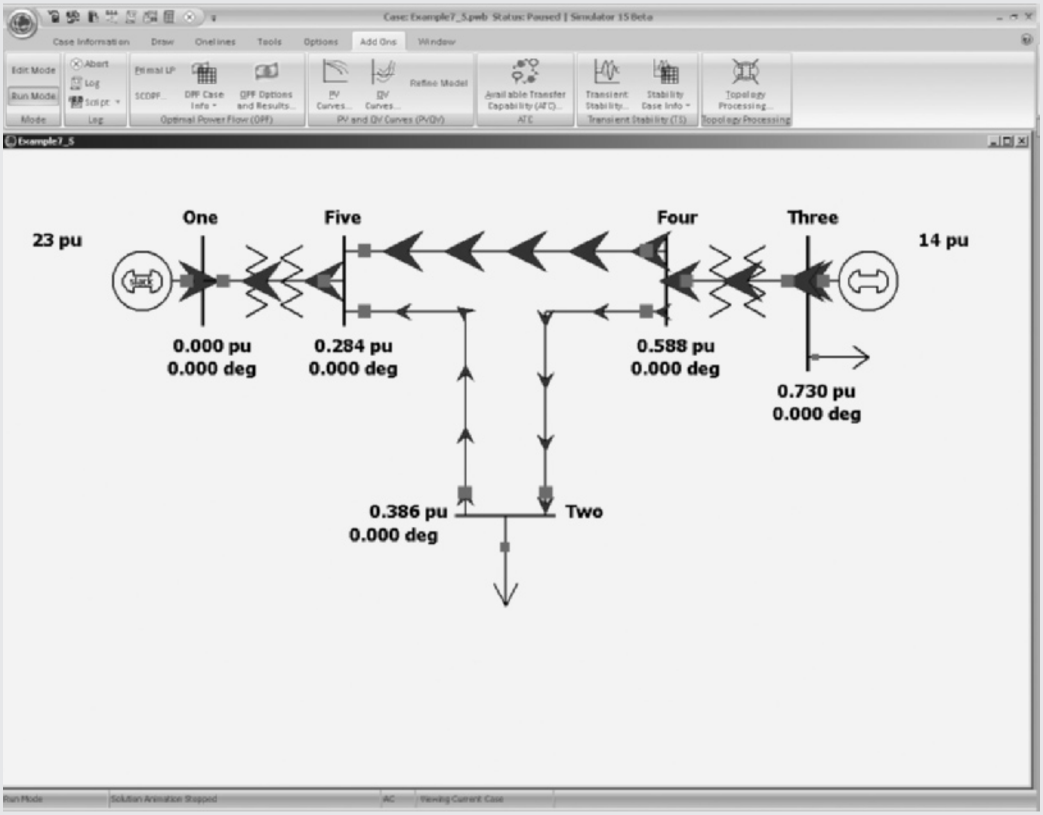
Case: Example7_5.pwb Status: Paused | Simulator 15 Beta
Example7_5
23 pu
One
Five
Four
Three
14 pu
0.000 pu
0.000 deg
0.284 pu
0.000 deg
0.588 pu
0.000 deg
0.730 pu
0.000 deg
0.386 pu
0.000 deg
Two

FIGURE 7.9

Screen for Example 7.5—fault at bus 1

EXAMPLE 7.6

Redo Example 7.5 with an additional line installed between buses 2 and 4. This line, whose reactance is 0.075 per unit, is not mutually coupled to any other line.

SOLUTION

The modified system is contained in PowerWorld Simulator case Example 7_6. The Z_{bus} along with the fault currents and bus voltages are shown in Tables 7.8 and 7.9. Notice the fault currents have increased, particularly at bus 2, since with the new line the total impedance between the faulted bus and the generators has decreased.

(Continued)

Copyright 2017 Cengage Learning. All Rights Reserved. May not be copied, scanned, or duplicated, in whole or in part. Due to electronic rights, some third party content may be suppressed from the eBook and/or eChapter(s). Editorial review has deemed that any suppressed content does not materially affect the overall learning experience. Cengage Learning reserves the right to remove additional content at any time if subsequent rights restrictions require it.

$$j\begin{bmatrix} 0.027723 & 0.01597 & 0.00864 & 0.01248 & 0.02004 \\ 0.01597 & 0.04501 & 0.01452 & 0.02097 & 0.02307 \\ 0.00864 & 0.01452 & 0.01818 & 0.01626 & 0.01248 \\ 0.01248 & 0.02097 & 0.01626 & 0.02349 & 0.01803 \\ 0.02004 & 0.02307 & 0.01248 & 0.01803 & 0.02895 \end{bmatrix}$$

TABLE 7.8

Z_{bus} for Example 7.6

		Contributions to Fault Current		
Fault Bus	Fault Current (per unit)	Gen Line or TRSF	Bus-to-Bus	Current (per unit)
1	37.872			
		G 1	GRND–1	23.332
		T 1	5–1	14.544
2	23.328			
		L 1	4–2	5.608
		L 2	5–2	10.24
		L 4	4–2	7.48
3	57.756			
		G 2	GRND–3	46.668
		T 2	4–3	11.088
4	44.704			
		L 1	2–4	1.128
		L 3	5–4	9.768
		L 4	2–4	1.504
		T 2	3–4	32.308
5	36.268			
		L 2	2–5	4.268
		L 3	4–5	15.848
		T 1	1–5	16.152

$V_F = 1.05$	Per-Unit Bus Voltage Magnitudes during the Fault				
Fault Bus	Bus 1	Bus 2	Bus 3	Bus 4	Bus 5
1	0.0000	0.6775	0.5510	0.4921	0.3231
2	0.4451	0.0000	0.2117	0.1127	0.2133
3	0.7228	0.7114	0.0000	0.3231	0.5974
4	0.5773	0.5609	0.1109	0.0000	0.3962
5	0.2909	0.5119	0.3293	0.2442	0.0000

TABLE 7.9

Fault currents and bus voltages for Example 7.6

Copyright 2017 Cengage Learning. All Rights Reserved. May not be copied, scanned, or duplicated, in whole or in part. Due to electronic rights, some third party content may be suppressed from the eBook and/or eChapter(s). Editorial review has deemed that any suppressed content does not materially affect the overall learning experience. Cengage Learning reserves the right to remove additional content at any time if subsequent rights restrictions require it.

7.5 CIRCUIT BREAKER AND FUSE SELECTION

A SHORT CIRCUITS computer program may be utilized in power system design to select, set, and coordinate protective equipment such as circuit breakers, fuses, relays, and instrument transformers. In this section, basic principles of circuit breaker and fuse selection are discussed.

AC CIRCUIT BREAKERS

A *circuit breaker* is a mechanical switch capable of interrupting fault currents and of reclosing. When circuit-breaker contacts separate while carrying current, an arc forms. The breaker is designed to extinguish the arc by elongating and cooling it. The fact that ac arc current naturally passes through zero twice during its 60 Hz cycle aids the arc extinction process.

Circuit breakers are classified as *power* circuit breakers when they are intended for service in ac circuits above 1500 V and as *low-voltage* circuit breakers in ac circuits up to 1500 V. There are different types of circuit breakers depending on the medium—air, oil, SF_6 gas, or vacuum—in which the arc is elongated. Also, the arc can be elongated either by a magnetic force or by a blast of air.

Some circuit breakers are equipped with a high-speed automatic reclosing capability. Since most faults are temporary and self-clearing, reclosing is based on the idea that, if a circuit is deenergized for a short time, it is likely that whatever caused the fault has disintegrated and the ionized arc in the fault has dissipated.

When reclosing breakers are employed in EHV systems, standard practice is to reclose only once, approximately 15 to 50 cycles (depending on operating voltage) after the breaker interrupts the fault. If the fault persists and the EHV breaker recloses into it, the breaker reinterrupts the fault current and then “locks out,” requiring operator resetting. Multiple-shot reclosing in EHV systems is not standard practice because transient stability (Chapter 11) may be compromised. However, for distribution systems (2.4 to 46 kV) where customer outages are of concern, standard reclosers are equipped for two or more reclosures.

For low-voltage applications, molded case circuit breakers with dual trip capability are available. There is a magnetic instantaneous trip for large fault currents above a specified threshold and a thermal trip with time delay for smaller fault currents.

Modern circuit-breaker standards are based on symmetrical interrupting current (Table 7.10). It is usually necessary to calculate only symmetrical fault current at a system location, and then select a breaker with a symmetrical interrupting capability equal to or above the calculated current. The breaker has the additional capability to interrupt the asymmetrical (or total) fault current if the dc offset is not too large.

Recall from Section 7.1 that the maximum asymmetry factor $K(\tau = 0)$ is $\sqrt{3}$, which occurs at fault inception ($\tau = 0$). After fault inception, the dc fault current decays exponentially with time constant $T = (L/R) = (X/\omega R)$, and the asymmetry factor decreases. Power circuit breakers with a 2-cycle rated interruption time are designed for an asymmetrical interrupting capability up to 1.4 times their symmetrical interrupting capability, whereas slower circuit breakers have a lower asymmetrical interrupting capability.

Copyright 2017 Cengage Learning. All Rights Reserved. May not be copied, scanned, or duplicated, in whole or in part. Due to electronic rights, some third party content may be suppressed from the eBook and/or eChapter(s). Editorial review has deemed that any suppressed content does not materially affect the overall learning experience. Cengage Learning reserves the right to remove additional content at any time if subsequent rights restrictions require it.

		Rated Values					
				Insulation Level		Current	
Identification		Voltage		Rated Withstand Test Voltage		Rated Continuous	Rated Short-Circuit
Nominal Voltage Class (kV, rms)	Nominal 3-Phase MVA Class	Rated Max Voltage (kV, rms)	Rated Voltage Range Factor (*K*)	Low Frequency (kV, rms)	Impulse (kV, Crest)	Current at 60 Hz (Amperes, rms)	Current at Rated Max kV (kA, rms)
Col 1	Col 2	Col 3	Col 4	Col 5	Col 6	Col 7	Col 8
14.4	250	15.5	2.67			600	8.9
14.4	500	15.5	1.29			1200	18
23	500	25.8	2.15			1200	11
34.5	1500	38	1.65			1200	22
46	1500	48.3	1.21			1200	17
69	2500	72.5	1.21			1200	19
115		121	1.0			1200	20
115		121	1.0			1600	40
115		121	1.0			2000	40
115		121	1.0			2000	63
115		121	1.0			3000	40
115		121	1.0			3000	63
138		145	1.0			1200	20
138	Not	145	1.0			1600	40
138		145	1.0			2000	40
138		145	1.0			2000	63
138		145	1.0			2000	80
138	Applicable	145	1.0			3000	40
138		145	1.0			3000	63
138		145	1.0			3000	80
161		169	1.0			1200	16
161		169	1.0			1600	31.5
161		169	1.0			2000	40
161		169	1.0			2000	50
230		242	1.0			1600	31.5
230		242	1.0			2000	31.5
230		242	1.0			3000	31.5
230		242	1.0			2000	40
230		242	1.0			3000	40
230		242	1.0			3000	63
345		362	1.0			2000	40
345		362	1.0			3000	40
500		550	1.0			2000	40
500		550	1.0			3000	40
700		765	1.0			2000	40
700		765	1.0			3000	40

TABLE 7.10

Preferred ratings for outdoor circuit breakers (symmetrical current basis of rating) [10]
Source: ANSI C 37.010-1999 (R 2005) Application Guide for AC High-Voltage Circuit Breakers Rated on a Symmetrical Current Basis. Reprinted with permission from IEEE. Copyright IEEE 1972. All rights reserved.

Copyright 2017 Cengage Learning. All Rights Reserved. May not be copied, scanned, or duplicated, in whole or in part. Due to electronic rights, some third party content may be suppressed from the eBook and/or eChapter(s). Editorial review has deemed that any suppressed content does not materially affect the overall learning experience. Cengage Learning reserves the right to remove additional content at any time if subsequent rights restrictions require it.

Rated Values		Related Required Capabilities			
			Current Values		
			Max Symmetrical Interrupting Capability	3-Second Short-Time Current Carrying Capability	Closing and Latching Capability 1.6K Times Rated Short-Circuit Current
			K Times Rated Short-Circuit Current		
Rated Interrupting Time (Cycles)	Rated Permissible Tripping Delay (Seconds)	Rated Max Voltage Divided by K (kV, rms)	(kA, rms)	(kA, rms)	(kA, rms)
Col 9	Col 10	Col 11	Col 12	Col 13	Col 14
5	2	5.8	24	24	38
5	2	12	23	23	37
5	2	12	24	24	38
5	2	23	36	36	58
5	2	40	21	21	33
5	2	60	23	23	37
3	1	121	20	20	32
3	1	121	40	40	64
3	1	121	40	40	64
3	1	121	63	63	101
3	1	121	40	40	64
3	1	121	63	63	101
3	1	145	20	20	32
3	1	145	40	40	64
3	1	145	40	40	64
3	1	145	63	63	101
3	1	145	80	80	128
3	1	145	40	40	64
3	1	145	63	63	101
3	1	145	80	80	128
3	1	169	16	16	26
3	1	169	31.5	31.5	50
3	1	169	40	40	64
3	1	169	50	50	80
3	1	242	31.5	31.5	50
3	1	242	31.5	31.5	50
3	1	242	31.5	31.5	50
3	1	242	40	40	64
3	1	242	40	40	64
3	1	242	63	63	101
3	1	362	40	40	64
3	1	362	40	40	64
2	1	550	40	40	64
2	1	550	40	40	64
2	1	765	40	40	64
2	1	765	40	40	64

Copyright 2017 Cengage Learning. All Rights Reserved. May not be copied, scanned, or duplicated, in whole or in part. Due to electronic rights, some third party content may be suppressed from the eBook and/or eChapter(s). Editorial review has deemed that any suppressed content does not materially affect the overall learning experience. Cengage Learning reserves the right to remove additional content at any time if subsequent rights restrictions require it.

A simplified method for breaker selection is called the "E/X simplified method" [1, 7]. The maximum symmetrical short-circuit current at the system location in question is calculated from the prefault voltage and system reactance characteristics using computer programs. Resistances, shunt admittances, nonrotating impedance loads, and prefault load currents are neglected. Then, if the X/R ratio at the system location is less than 15, a breaker with a symmetrical interrupting capability equal to or above the calculated current at the given operating voltage is satisfactory. However, if X/R is greater than 15, the dc offset may not have decayed to a sufficiently low value. In this case, a method for correcting the calculated fault current to account for dc and ac time constants as well as breaker speed can be used [10]. If X/R is unknown, the calculated fault current should not be greater than 80% of the breaker interrupting capability.

When selecting circuit breakers for generators, two cycle breakers are employed in practice, and the subtransient fault current is calculated; therefore subtransient machine reactances X_d'' are used in fault calculations. For synchronous motors, subtransient reactances X_d'' or transient reactances X_d' are used, depending on breaker speed. Also, induction motors can momentarily contribute to fault current. Large induction motors are usually modeled as sources in series with X_d'' or X_d', depending on breaker speed. Smaller induction motors (below 50 hp) are often neglected entirely.

Table 7.10 shows a schedule of preferred ratings for outdoor power circuit breakers. Some of the more important ratings shown are described next.

Voltage ratings

Rated maximum voltage: Designates the maximum rms line-to-line operating voltage. The breaker should be used in systems with an operating voltage less than or equal to this rating.

Rated low frequency withstand voltage: The maximum 60-Hz rms line-to-line voltage that the circuit breaker can withstand without insulation damage.

Rated impulse withstand voltage: The maximum crest voltage of a voltage pulse with standard rise and delay times that the breaker insulation can withstand.

Rated voltage range factor K: The range of voltage for which the symmetrical interrupting capability times the operating voltage is constant.

Current ratings

Rated continuous current: The maximum 60-Hz rms current that the breaker can carry continuously while it is in the closed position without overheating.

Rated short-circuit current: The maximum rms symmetrical current that the breaker can safely interrupt at rated maximum voltage.

Rated momentary current: The maximum rms asymmetrical current that the breaker can withstand while in the closed position without damage. Rated momentary current for standard breakers is 1.6 times the symmetrical interrupting capability.

Rated interrupting time: The time in cycles on a 60-Hz basis from the instant the trip coil is energized to the instant the fault current is cleared.

Rated interrupting MVA: For a three-phase circuit breaker, this is $\sqrt{3}$ times the rated maximum voltage in kV times the rated short-circuit current in

Copyright 2017 Cengage Learning. All Rights Reserved. May not be copied, scanned, or duplicated, in whole or in part. Due to electronic rights, some third party content may be suppressed from the eBook and/or eChapter(s). Editorial review has deemed that any suppressed content does not materially affect the overall learning experience. Cengage Learning reserves the right to remove additional content at any time if subsequent rights restrictions require it.

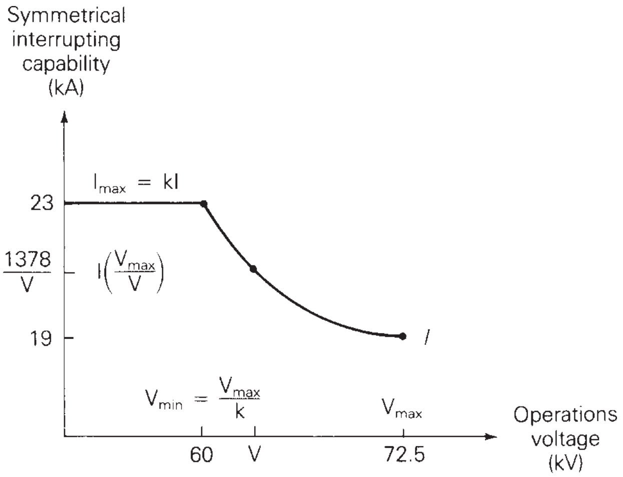

FIGURE 7.10

Symmetrical interrupting capability of a 69-kV class breaker

kA. It is more common to work with current and voltage ratings than with MVA rating.

As an example, the symmetrical interrupting capability of the 69-kV class breaker listed in Table 7.10 is plotted versus operating voltage in Figure 7.10. As shown, the symmetrical interrupting capability increases from its rated short-circuit current $I = 19$ kA at rated maximum voltage $V_{max} = 72.5$ kV up to $I_{max} = KI = (1.21)(19) = 23$ kA at an operating voltage $V_{max} = V_{max}/K = 72.5/1.21 = 60$ kV. At operating voltages V between V_{min} and V_{max}, the symmetrical interrupting capability is $I \times V_{max}/V = 1378/V$ kA. At operating voltages below V_{min}, the symmetrical interrupting capability remains at $I_{max} = 23$ kA.

Breakers of the 115 kV class and higher have a voltage range factor $K = 1.0$; that is, their symmetrical interrupting current capability remains constant.

EXAMPLE 7.7

Circuit breaker selection

The calculated symmetrical fault current is 17 kA at a three-phase bus where the operating voltage is 64 kV. The X/R ratio at the bus is unknown. Select a circuit breaker from Table 7.10 for this bus.

SOLUTION

The 69-kV-class breaker has a symmetrical interrupting capability $I(V_{max}/V) = 19(72.5/64) = 21.5$ kA at the operating voltage $V = 64$ kV. The calculated symmetrical fault current, 17 kA, is less than 80% of this capability (less than $0.80 \times 21.5 = 17.2$ kA), which is a requirement when X/R is unknown. Therefore, select the 69-kV-class breaker from Table 7.10.

Copyright 2017 Cengage Learning. All Rights Reserved. May not be copied, scanned, or duplicated, in whole or in part. Due to electronic rights, some third party content may be suppressed from the eBook and/or eChapter(s). Editorial review has deemed that any suppressed content does not materially affect the overall learning experience. Cengage Learning reserves the right to remove additional content at any time if subsequent rights restrictions require it.

FUSES

Figure 7.11(a) shows a cutaway view of a fuse, which is one of the simplest overcurrent devices. The fuse consists of a metal "fusible" link or links encapsulated in a tube, packed in filler material, and connected to contact terminals. Silver is a typical link metal, and sand is a typical filler material.

During normal operation, when the fuse is operating below its continuous current rating, the electrical resistance of the link is so low that it simply acts as a conductor. If an overload current from one to about six times its continuous current rating occurs and persists for more than a short interval of time, the temperature of the link eventually reaches a level that causes a restricted segment of the link to melt. As shown in Figure 7.11(b), a gap is then formed and an electric arc is established. As the arc causes the link metal to burn back, the gap width increases. The resistance of the arc eventually reaches such a high level that the arc cannot be sustained and it is extinguished, as in Figure 7.11(c). The current flow within the fuse is then completely cut off.

FIGURE 7.11

Typical fuse

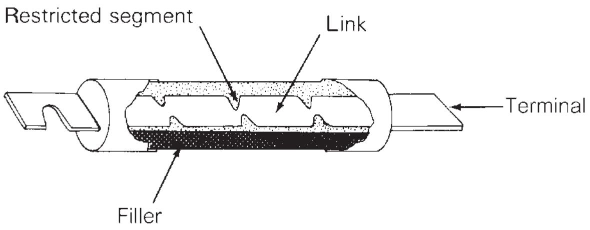

(a) Cutaway view

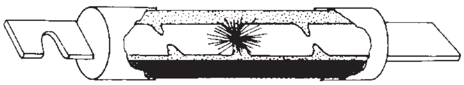

(b) The link melts and an arc is established under sustained overload current

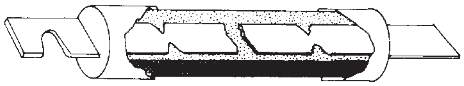

(c) The "open" link after clearing the overload current

Copyright 2017 Cengage Learning. All Rights Reserved. May not be copied, scanned, or duplicated, in whole or in part. Due to electronic rights, some third party content may be suppressed from the eBook and/or eChapter(s). Editorial review has deemed that any suppressed content does not materially affect the overall learning experience. Cengage Learning reserves the right to remove additional content at any time if subsequent rights restrictions require it.

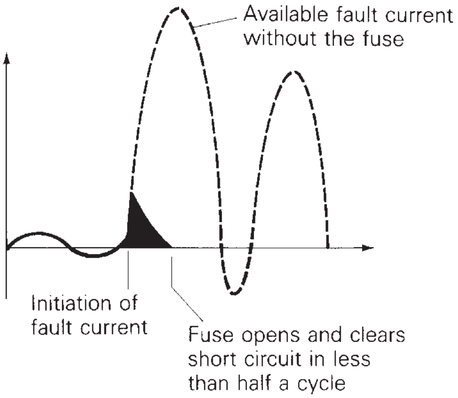
Available fault current without the fuse
Initiation of fault current
Fuse opens and clears short circuit in less than half a cycle

FIGURE 7.12 Operation of a current-limiting fuse

If the fuse is subjected to fault currents higher than about six times its continuous current rating, several restricted segments melt simultaneously, resulting in rapid arc suppression and fault clearing. Arc suppression is accelerated by the filler material in the fuse.

Many modern fuses are current limiting. As shown in Figure 7.12, a current-limiting fuse has such a high speed of response that it cuts off a high fault current in less than a half cycle—before it can build up to its full peak value. By limiting fault currents, these fuses permit the use of motors, transformers, conductors, and bus structures that could not otherwise withstand the destructive forces of high fault currents.

Fuse specification is normally based on the following four factors.

1. *Voltage rating*. This rms voltage determines the ability of a fuse to suppress the internal arc that occurs after the fuse link melts. A blown fuse should be able to withstand its voltage rating. Most low-voltage fuses have 250 or 600 V ratings. Ratings of medium-voltage fuses range from 2.4 to 34.5 kV.
2. *Continuous current rating*. The fuse should carry this rms current indefinitely, without melting and clearing.
3. *Interrupting current rating*. This is the largest rms asymmetrical current that the fuse can safely interrupt. Most modern, low-voltage current-limiting fuses have a 200-kA interrupting rating. Standard interrupting ratings for medium-voltage current-limiting fuses include 65, 80, and 100 kA.
4. *Time response*. The melting and clearing time of a fuse depends on the magnitude of the overcurrent or fault current and is usually specified by a "time-current" curve. Figure 7.13 shows the time-current curve of a 15.5-kV, 100-A (continuous) current-limiting fuse. As shown, the fuse link melts within 2 s and clears within 5 s for a 500-A current. For a 5 kA current, the fuse link melts in less than 0.01 s and clears within 0.015 s.

Copyright 2017 Cengage Learning. All Rights Reserved. May not be copied, scanned, or duplicated, in whole or in part. Due to electronic rights, some third party content may be suppressed from the eBook and/or eChapter(s). Editorial review has deemed that any suppressed content does not materially affect the overall learning experience. Cengage Learning reserves the right to remove additional content at any time if subsequent rights restrictions require it.

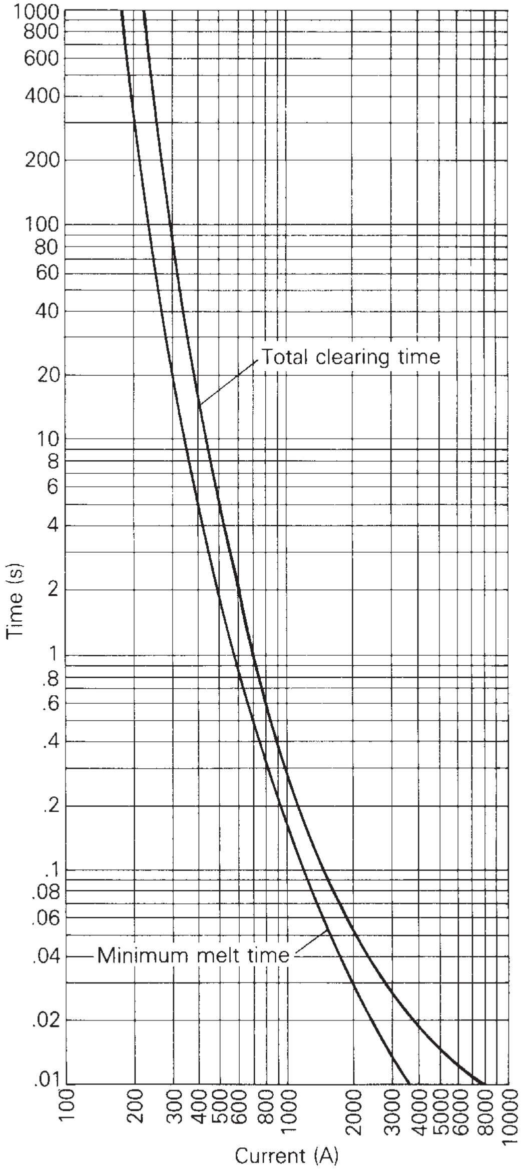

FIGURE 7.13

Time-current curves for a 15.5-kV, 100-A current-limiting fuse

It is usually a simple matter to coordinate fuses in a power circuit such that only the fuse closest to the fault opens the circuit. In a radial circuit, fuses with larger continuous-current ratings are located closer to the source, such that the fuse closest to the fault clears before other, upstream fuses melt.

Fuses are inexpensive, fast operating, easily coordinated, and reliable, and they do not require protective relays or instrument transformers. Their chief disadvantage is that the fuse or the fuse link must be manually replaced after it melts. They are basically one-shot devices that are, for example, incapable of high-speed reclosing.

Copyright 2017 Cengage Learning. All Rights Reserved. May not be copied, scanned, or duplicated, in whole or in part. Due to electronic rights, some third party content may be suppressed from the eBook and/or eChapter(s). Editorial review has deemed that any suppressed content does not materially affect the overall learning experience. Cengage Learning reserves the right to remove additional content at any time if subsequent rights restrictions require it.

MULTIPLE CHOICE QUESTIONS

SECTION 7.1

7.1 The asymmetrical short-circuit current in series R–L circuit for a simulated solid or "bolted fault" can be considered as a combination of symmetrical (ac) component that is a _____, and dc-offset current that decays _____ and depends on _____.

7.2 Even though the fault current is not symmetrical and not strictly periodic, the rms asymmetrical fault current is computed as the rms ac fault current times an "asymmetry factor," which is a function of _____.

SECTION 7.2

7.3 The amplitude of the sinusoidal symmetrical ac component of the three-phase short-circuit current of an unloaded synchronous machine decreases from a high initial value to a lower steady-state value, going through the stages of _____ and _____ periods.

7.4 The duration of subtransient fault current is dictated by _____ time constant and that of transient fault current is dictated by _____ time constant.

7.5 The reactance that plays a role under steady-state operation of a synchronous machine is called _____.

7.6 The dc-offset component of the three-phase short-circuit current of an unloaded synchronous machine is different in the three phases and its exponential decay is dictated by _____.

SECTION 7.3

7.7 Generally, in power-system short-circuit studies, for calculating subtransient fault currents, transformers are represented by their _____, transmission lines by their equivalent _____, and synchronous machines by _____ behind their subtransient reactances.

7.8 In power-system fault studies, all nonrotating impedance loads are usually neglected.

(a) True (b) False

7.9 Can superposition be applied in power-system short-circuit studies for calculating fault currents?

(a) Yes (b) No

7.10 Before proceeding with per-unit fault current calculations, based on the single-line diagram of the power system, a positive-sequence equivalent circuit is set up on a chosen base system.

(a) True (b) False

Copyright 2017 Cengage Learning. All Rights Reserved. May not be copied, scanned, or duplicated, in whole or in part. Due to electronic rights, some third party content may be suppressed from the eBook and/or eChapter(s). Editorial review has deemed that any suppressed content does not materially affect the overall learning experience. Cengage Learning reserves the right to remove additional content at any time if subsequent rights restrictions require it.

SECTION 7.4

7.11 The inverse of the bus-admittance matrix is called a _____ matrix.

7.12 For a power system, modeled by its positive-sequence network, both bus-admittance matrix and bus-impedance matrix are symmetric.
(a) True (b) False

7.13 The bus-impedance equivalent circuit can be represented in the form of a "rake" with the diagonal elements, which are _____, and the non-diagonal (off-diagonal) elements, which are _____.

SECTION 7.5

7.14 A circuit breaker is designed to extinguish the arc by _____.

7.15 Power-circuit breakers are intended for service in the ac circuit above _____ V.

7.16 In circuit breakers, besides air or vacuum, what gaseous medium, in which the arc is elongated, is used?

7.17 Oil can be used as a medium to extinguish the arc in circuit breakers.
(a) True (b) False

7.18 Besides a blast of air/gas, the arc in a circuit breaker can be elongated by _____.

7.19 For distribution systems, standard reclosers are equipped for two or more reclosures, whereas multiple-shot reclosing in EHV systems is not a standard practice.
(a) True (b) False

7.20 Breakers of the 115 kV class and higher have a voltage range factor K = _____, such that their symmetrical interrupting current capability remains constant.

7.21 A typical fusible link metal in fuses is _____, and a typical filler material is _____.

7.22 The melting and clearing time of a current-limiting fuse is usually specified by a _____ curve.

PROBLEMS

SECTION 7.1

7.1 In the circuit of Figure 7.1, $V = 277$ volts, $L = 2$ mH, $R = 0.4\ \Omega$, and $\omega = 2\pi 60$ rad/s. Determine (a) the rms symmetrical fault current; (b) the rms asymmetrical fault current at the instant the switch closes, assuming maximum dc offset; (c) the rms asymmetrical fault current five cycles after the switch closes, assuming maximum dc offset; and (d) the dc offset

Copyright 2017 Cengage Learning. All Rights Reserved. May not be copied, scanned, or duplicated, in whole or in part. Due to electronic rights, some third party content may be suppressed from the eBook and/or eChapter(s). Editorial review has deemed that any suppressed content does not materially affect the overall learning experience. Cengage Learning reserves the right to remove additional content at any time if subsequent rights restrictions require it.

as a function of time if the switch closes when the instantaneous source voltage is 300 volts.

7.2 Repeat Example 7.1 with V = 4 kV, X = 2 Ω, and R = 1 Ω

7.3 In the circuit of Figure 7.1, let R = 0.125 Ω., L = 10 mH, and the source voltage is $e(t) = 151\sin(377t + \alpha)$ V. Determine the current response after closing the switch for the following cases: (a) no dc offset or (b) maximum dc offset. Sketch the current waveform up to t = 0.10 s corresponding to parts (a) and (b).

7.4 Consider the expression for $i(t)$ given by

$$i(t) = \sqrt{2}I_{\text{rms}}[\sin(\omega t - \theta_z) + \sin\theta_z . e^{-(\omega R/X)t}]$$

where $\theta_z = \tan^{-1}(\omega L/R)$.

(a) For (X/R) equal to zero and infinity, plot $i(t)$ as a function of (ωt).

(b) Comment on the dc offset of the fault current waveforms.

(c) Find the asymmetrical current factor and the time of peak, t_p, in milliseconds, for (X/R) ratios of zero and infinity.

7.5 If the source impedance at a 13.2-kV distribution substation bus is (0.5 + j1.5) Ω per phase, compute the rms and maximum peak instantaneous value of the fault current for a balanced three-phase fault. For the system (X/R) ratio of 3.0, the asymmetrical factor is 1.9495 and the time of peak is 7.1 ms (see Problem 7.4). Comment on the withstanding peak current capability to which all substation electrical equipment need to be designed.

SECTION 7.2

7.6 A 1000-MVA, 20-kV, 60-Hz, three-phase generator is connected through a 1000-MVA, 20-kV, Δ/345-kV, Y transformer to a 345-kV circuit breaker and a 345-kV transmission line. The generator reactances are $X_d'' = 0.17$, $X_d' = 0.30$, and $X_d = 1.5$ per unit, and its time constants are $T_d'' = 0.05$, $T_d' = 1.0$, and $T_A = 0.10$ s. The transformer series reactance is 0.10 per unit; transformer losses and exciting current are neglected. A three-phase short-circuit occurs on the line side of the circuit breaker when the generator is operated at rated terminal voltage and at no-load. The breaker interrupts the fault three cycles after fault inception. Determine (a) the subtransient current through the breaker in per-unit and in kA rms and (b) the rms asymmetrical fault current the breaker interrupts, assuming maximum dc offset. Neglect the effect of the transformer on the time constants.

7.7 For Problem 7.6, determine (a) the instantaneous symmetrical fault current in kA in phase *a* of the generator as a function of time, assuming maximum dc offset occurs in this generator phase, and (b) the maximum dc offset current in kA as a function of time that can occur in any one generator phase.

Copyright 2017 Cengage Learning. All Rights Reserved. May not be copied, scanned, or duplicated, in whole or in part. Due to electronic rights, some third party content may be suppressed from the eBook and/or eChapter(s). Editorial review has deemed that any suppressed content does not materially affect the overall learning experience. Cengage Learning reserves the right to remove additional content at any time if subsequent rights restrictions require it.

7.8 A 300-MVA, 13.8-kV, three-phase, 60-Hz, Y-connected synchronous generator is adjusted to produce rated voltage on open circuit. A balanced three-phase fault is applied to the terminals at t = 0. After analyzing the raw data, the symmetrical transient current is obtained as

$$i_{ac}(t) = 10^4(1 + e^{-t/\tau_1} + 6e^{-t/\tau_2}) \quad A$$

where $\tau_1 = 200$ ms and $\tau_2 = 15$ ms. (a) Sketch $i_{ac}(t)$ as a function of time for $0 \leq t \leq 500$ ms. (b) Determine X_d'' and X_d in per unit based on the machine ratings.

7.9 Two identical synchronous machines, each rated 60 MVA and 15 kV with a subtransient reactance of 0.1 p.u., are connected through a line of reactance 0.1 p.u. on the base of the machine rating. One machine is acting as a synchronous generator, while the other is working as a motor drawing 40 MW at 0.8 p.f. leading with a terminal voltage of 14.5 kV, when a symmetrical three-phase fault occurs at the motor terminals. Determine the subtransient currents in the generator, the motor, and the fault by using the internal voltages of the machines. Choose a base of 60 MVA and 15 kV in the generator circuit.

SECTION 7.3

7.10 Recalculate the subtransient current through the breaker in Problem 7.6 if the generator is initially delivering rated MVA at 0.80 p.f. lagging and at rated terminal voltage.

7.11 Solve Example 7.3 parts (a) and (c) without using the superposition principle. First calculate the internal machine voltages E_g'' and E_m'' using the prefault load current. Then determine the subtransient fault, generator, and motor currents directly from Figure 7.4(a). Compare your answers with those of Example 7.3.

7.12 Equipment ratings for the four-bus power system shown in Figure 7.14 are as follows:

Generator Gl:	500 MVA, 13.8 kV, $X'' = 0.20$ per unit
Generator G2:	750 MVA, 18 kV, $X'' = 0.18$ per unit
Generator G3:	1000 MVA, 20 kV, $X'' = 0.17$ per unit
Transformer Tl:	500 MVA, 13.8 Δ/500 Y kV, $X = 0.12$ per unit
Transformer T2:	750 MVA, 18 Δ/500 Y kV, $X = 0.10$ per unit
Transformer T3:	1000 MVA, 20 Δ/500 Y kV, $X = 0.10$ per unit
Each 500 kV line:	$X_1 = 50\ \Omega$.

A three-phase short circuit occurs at bus 1, where the prefault voltage is 525 kV. Prefault load current is neglected. Draw the positive-sequence reactance diagram in per unit on a 1000-MVA, 20-kV base in the zone of generator G3. Determine (a) the Thévenin reactance in per unit at the fault, (b) the subtransient fault current in per unit and in kA rms, and (c) contributions to the fault current from generator Gl and from line 1–2.

Copyright 2017 Cengage Learning. All Rights Reserved. May not be copied, scanned, or duplicated, in whole or in part. Due to electronic rights, some third party content may be suppressed from the eBook and/or eChapter(s). Editorial review has deemed that any suppressed content does not materially affect the overall learning experience. Cengage Learning reserves the right to remove additional content at any time if subsequent rights restrictions require it.

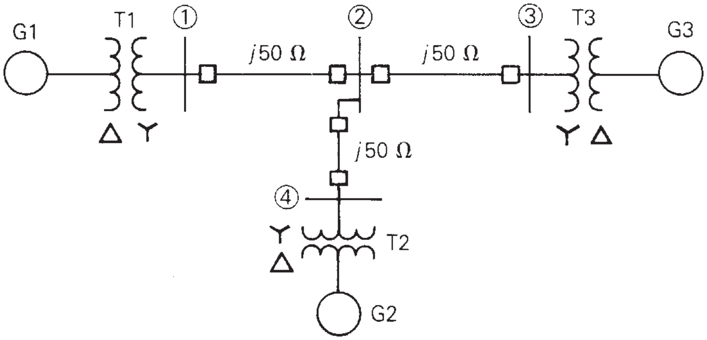

FIGURE 7.14

Problems 7.12, 7.13, 7.19, 7.24, 7.25, and 7.26

7.13 For the power system given in Problem 7.12, a three-phase short circuit occurs at bus 2, where the prefault voltage is 525 kV. Prefault load current is neglected. Determine the (a) Thévenin equivalent at the fault, (b) subtransient fault current in per unit and in kA rms, and (c) contributions to the fault from lines 1–2, 2–3, and 2–4.

7.14 Equipment ratings for the five-bus power system shown in Figure 7.15 are as follows:

Generator Gl: 50 MVA, 12 kV, $X'' = 0.2$ per unit
Generator G2: 100 MVA, 15 kV, $X'' = 0.2$ per unit
Transformer Tl: 50 MVA, 10 kV Y/138 kV Y, $X = 0.10$ per unit
Transformer T2: 100 MVA, 15 kV Δ/138 kV Y, $X = 0.10$ per unit
Each 138-kV line: $X_1 = 40\ \Omega$.

A three-phase short circuit occurs at bus 5, where the prefault voltage is 15 kV. Prefault load current is neglected. (a) Draw the positive-sequence reactance diagram in per unit on a 100-MVA, 15-kV base in the zone of generator G2. Determine (b) the Thévenin equivalent at the fault, (c) the subtransient fault current in per unit and in kA rms, and (d) contributions to the fault from generator G2 and from transformer T2.

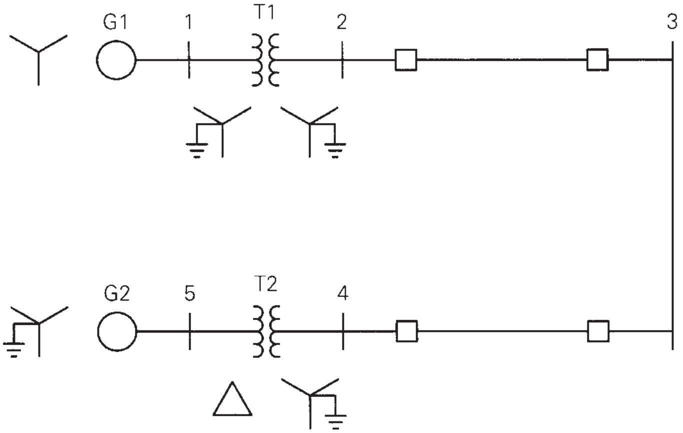

FIGURE 7.15

Problems 7.14, 7.15, 7.20

Copyright 2017 Cengage Learning. All Rights Reserved. May not be copied, scanned, or duplicated, in whole or in part. Due to electronic rights, some third party content may be suppressed from the eBook and/or eChapter(s). Editorial review has deemed that any suppressed content does not materially affect the overall learning experience. Cengage Learning reserves the right to remove additional content at any time if subsequent rights restrictions require it.

7.15 For the power system given in Problem 7.14, a three-phase short circuit occurs at bus 4, where the prefault voltage is 138 kV. Prefault load current is neglected. Determine (a) the Thévenin equivalent at the fault, (b) the subtransient fault current in per unit and in kA rms, and (c) contributions to the fault from transformer T2 and from line 3–4.

7.16 In the system shown in Figure 7.16, a three-phase short circuit occurs at point F. Assume that prefault currents are zero and that the generators are operating at rated voltage. Determine the fault current.

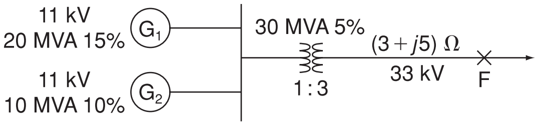

FIGURE 7.16

Problem 7.16

7.17 A three-phase short circuit occurs at the generator bus (bus 1) for the system shown in Figure 7.17. Neglecting prefault currents and assuming that the generator is operating at its rated voltage, determine the subtransient fault current using superposition.

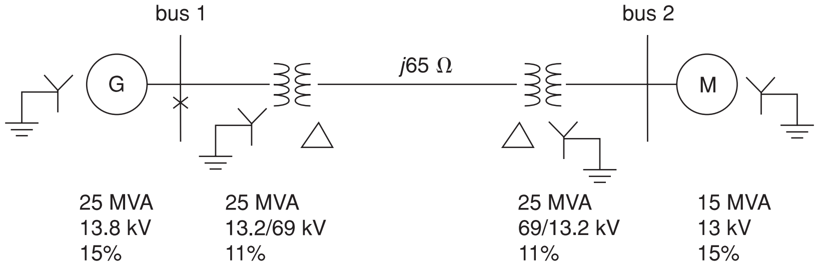

FIGURE 7.17

Problem 7.17

SECTION 7.4

7.18 (a) The bus impedance matrix for a three-bus power system is

$$\boldsymbol{Z}_{\text{bus}} = j\begin{bmatrix} 0.12 & 0.08 & 0.04 \\ 0.08 & 0.12 & 0.06 \\ 0.04 & 0.06 & 0.08 \end{bmatrix} \quad \text{per unit}$$

where subtransient reactances were used to compute $\boldsymbol{Z}_{\text{bus}}$. Prefault voltage is 1.0 per unit and prefault current is neglected. (a) Draw the bus impedance matrix equivalent circuit (rake equivalent). Identify the per-unit self- and mutual impedances as well as the prefault voltage in the circuit. (b) A three-phase short circuit occurs at bus 2. Determine the subtransient fault current and the voltages at buses 1, 2, and 3 during the fault.

Copyright 2017 Cengage Learning. All Rights Reserved. May not be copied, scanned, or duplicated, in whole or in part. Due to electronic rights, some third party content may be suppressed from the eBook and/or eChapter(s). Editorial review has deemed that any suppressed content does not materially affect the overall learning experience. Cengage Learning reserves the right to remove additional content at any time if subsequent rights restrictions require it.

(c) Repeat for the case of

$$\boldsymbol{Z}_{\text{bus}} = j\begin{bmatrix} 0.4 & 0.1 & 0.3 \\ 0.1 & 0.8 & 0.5 \\ 0.3 & 0.5 & 1.2 \end{bmatrix} \text{ per unit}$$

7.19 Determine $\boldsymbol{Y}_{\text{bus}}$ in per unit for the circuit in Problem 7.12. Then invert $\boldsymbol{Y}_{\text{bus}}$ to obtain $\boldsymbol{Z}_{\text{bus}}$.

7.20 Determine $\boldsymbol{Y}_{\text{bus}}$ in per unit for the circuit in Problem 7.14. Then invert $\boldsymbol{Y}_{\text{bus}}$ to obtain $\boldsymbol{Z}_{\text{bus}}$.

7.21 Figure 7.18 shows a system reactance diagram. (a) Draw the admittance diagram for the system by using source transformations. (b) Find the bus admittance matrix $\boldsymbol{Y}_{\text{bus}}$. (c) Find the bus impedance $\boldsymbol{Z}_{\text{bus}}$ matrix by inverting $\boldsymbol{Y}_{\text{bus}}$.

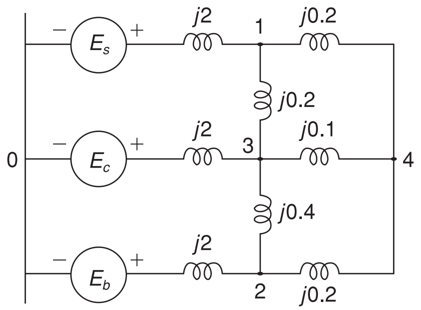

FIGURE 7.18

Problem 7.21

7.22 For the network shown in Figure 7.19, impedances labeled 1 through 6 are in per unit. (a) Determine $\boldsymbol{Y}_{\text{bus}}$, preserving all buses. (b) Using MATLAB or a similar computer program, invert $\boldsymbol{Y}_{\text{bus}}$ to obtain $\boldsymbol{Z}_{\text{bus}}$.

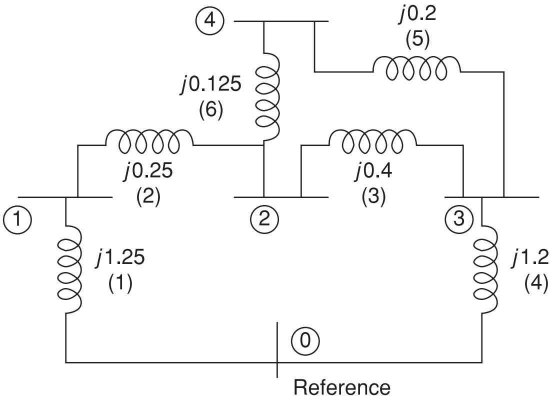

FIGURE 7.19

Problem 7.22

Copyright 2017 Cengage Learning. All Rights Reserved. May not be copied, scanned, or duplicated, in whole or in part. Due to electronic rights, some third party content may be suppressed from the eBook and/or eChapter(s). Editorial review has deemed that any suppressed content does not materially affect the overall learning experience. Cengage Learning reserves the right to remove additional content at any time if subsequent rights restrictions require it.

7.23 A single-line diagram of a four-bus system is shown in Figure 7.20, for which $\boldsymbol{Z}_{\text{bus}}$ is given below:

$$\boldsymbol{Z}_{\text{bus}} = j\begin{bmatrix} 0.25 & 0.2 & 0.16 & 0.14 \\ 0.2 & 0.23 & 0.15 & 0.151 \\ 0.16 & 0.15 & 0.196 & 0.1 \\ 0.14 & 0.151 & 0.1 & 0.195 \end{bmatrix} \text{ per unit}$$

Let a three-phase fault occur at bus 2 of the network.

(a) Calculate the initial symmetrical rms current in the fault.

(b) Determine the voltages during the fault at buses 1, 3, and 4.

(c) Compute the fault currents contributed to bus 2 by the adjacent unfaulted buses 1, 3, and 4.

(d) Find the current flow in the line from bus 3 to bus 1. Assume the prefault voltage V_f at bus 2 to be $1\underline{/0^\circ}$ p.u., and neglect all prefault currents.

FIGURE 7.20

Single-line diagram for Problem 7.23

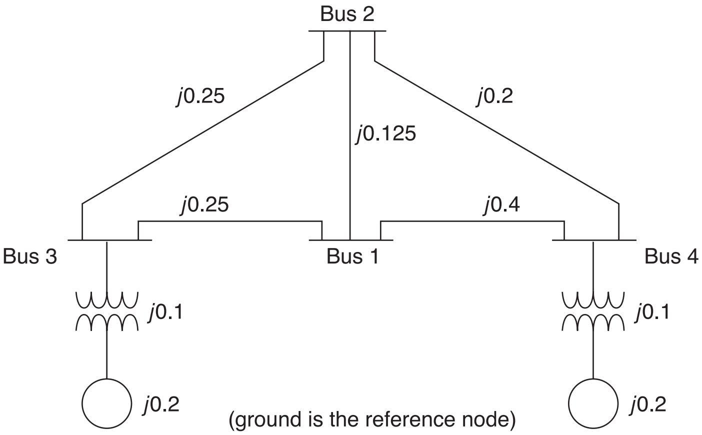

PW **7.24** PowerWorld Simulator case Problem 7_24 models the system shown in Figure 7.14 with all data on a 1000 MVA base. Using PowerWorld Simulator, determine the current supplied by each generator and the per-unit bus voltage magnitudes at each bus for a fault at bus 3.

PW **7.25** Repeat Problem 7.24, except place the fault at bus 4.

PW **7.26** Repeat Problem 7.24, except place the fault midway between buses 2 and 3. Determining the values for line faults requires that the line be split with a fictitious bus added at the point of the fault. The original line's impedance is then allocated to the two new lines based on the fault location, which is 50% each for this problem. Fault calculations are then the same as for a bus fault. This is done automatically in PowerWorld Simulator by first right-clicking on a line, and then selecting Fault. The Fault dialog appears as before, except now the fault type is changed to In-Line Fault.

Copyright 2017 Cengage Learning. All Rights Reserved. May not be copied, scanned, or duplicated, in whole or in part. Due to electronic rights, some third party content may be suppressed from the eBook and/or eChapter(s). Editorial review has deemed that any suppressed content does not materially affect the overall learning experience. Cengage Learning reserves the right to remove additional content at any time if subsequent rights restrictions require it.

Set the location percentage field to 50% to model a fault midway between buses 2 and 4.

PW **7.27** One technique for limiting fault current is to place reactance in series with the generators. Such reactance can be modeled in PowerWorld Simulator by increasing the value of the generator's positive sequence internal impedance. For the Problem 7.24 case, how much per-unit reactance must be added to G2 to limit its maximum fault current to 2.5 per unit for all three-phase bus faults? Where is the location of the most severe bus fault?

PW **7.28** Using PowerWorld Simulator case Example 6_13, determine the per-unit current and actual current in amps supplied by each of the generators for a fault at the POPLAR69 bus. During the fault, what percentage of the system buses have voltage magnitudes below 0.75 per unit?

PW **7.29** Repeat Problem 7.28, except place the fault at the REDBUD69 bus.

PW **7.30** Using PowerWorld Simulator case Example 7_5, open the line connecting buses 4 and 5. Then, determine the per unit current supplied by the generator at bus 3 due a fault at bus 2.

SECTION 7.5

7.31 A three-phase circuit breaker has a 15.5-kV rated maximum voltage, 9.0-kA rated short-circuit current, and a 2.50-rated voltage range factor. (a) Determine the symmetrical interrupting capability at 10-kV and 5-kV operating voltages. (b) Can this breaker be safely installed at a three-phase bus where the symmetrical fault current is 10 kA, the operating voltage is 13.8 kV, and the (X/R) ratio is 12?

7.32 A 345-kV, three-phase transmission line has a 2.2-kA continuous current rating and a 2.5-kA maximum short-time overload rating with a 356-kV maximum operating voltage. The maximum symmetrical fault current on the line is 30 kA. Select a circuit breaker for this line from Table 7.10.

7.33 A 69-kV circuit breaker has a voltage range factor K = 1.25, a continuous current rating of 1200 A, and a rated short-circuit current of 19,000 A at the maximum rated voltage of 72.5 kV. Determine the maximum symmetrical interrupting capability of the breaker. Also, explain its significance at lower operating voltages.

7.34 As shown in Figure 7.21, a 25-MVA, 13.8-kV, 60-Hz, synchronous generator with $X_d'' = 0.15$ per unit is connected through a transformer to a bus that supplies four identical motors. The rating of the three-phase transformer is 25 MVA and 13.8/6.9 kV with a leakage reactance of 0.1 per unit. Each motor has a subtransient reactance $X_d'' = 0.2$ per unit on a base of 5 MVA and 6.9 kV. A three-phase fault occurs at point P, when the bus voltage at the motors is 6.9 kV. Determine (a) the subtransient fault current, (b) the subtransient current through breaker A, and (c) the symmetrical short-circuit interrupting current (as defined for circuit breaker applications) in the fault and in breaker A.

Copyright 2017 Cengage Learning. All Rights Reserved. May not be copied, scanned, or duplicated, in whole or in part. Due to electronic rights, some third party content may be suppressed from the eBook and/or eChapter(s). Editorial review has deemed that any suppressed content does not materially affect the overall learning experience. Cengage Learning reserves the right to remove additional content at any time if subsequent rights restrictions require it.

FIGURE 7.21

Problem 7.34

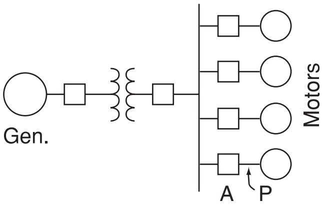

CASE STUDIES QUESTIONS

a. What are the four main types of wind-turbine generators (WTG)? How do WTGs differ from conventional generators?

b. Which type of WTG can produce the largest three-phase short-circuit current?

c. For which type of WTG can the short-circuit current be controlled? Why?

DESIGN PROJECT 3 (*CONTINUED*): POWER FLOW/ SHORT CIRCUITS

Additional time given: 3 weeks

Additional time required: 10 hours

This is a continuation of Design Project 3. Assignments 1 and 2 are given in Chapter 6.

Assignment 3: Symmetrical Short Circuits

For the single-line diagram that you have been assigned (Figure 6.13 or 6.14), convert the positive-sequence reactance data to per unit using the given base quantities. For synchronous machines, use subtransient reactance. Then using PowerWorld Simulator, create the machine, transmission line, and transformer input data files. Next, run the program to compute subtransient fault currents for a bolted three-phase-to-ground fault at bus 1, then at bus 2, then at bus 3, and so on. Also compute bus voltages during the faults and the positive-sequence bus impedance matrix. Assume 1.0 per-unit prefault voltage. Neglect prefault load currents and all losses.

Your output for this assignment consists of three input data files and three output data (fault currents, bus voltages, and the bus impedance matrix) files.

This project continues in Chapter 9.

Copyright 2017 Cengage Learning. All Rights Reserved. May not be copied, scanned, or duplicated, in whole or in part. Due to electronic rights, some third party content may be suppressed from the eBook and/or eChapter(s). Editorial review has deemed that any suppressed content does not materially affect the overall learning experience. Cengage Learning reserves the right to remove additional content at any time if subsequent rights restrictions require it.

REFERENCES

1. Westinghouse Electric Corporation, *Electrical Transmission and Distribution Reference Book*, 4th ed. (East Pittsburgh, PA: 1964).
2. E. W. Kimbark, *Power System Stability*, *Synchronous Machines*, vol. 3 (New York: Wiley, 1956).
3. A. E. Fitzgerald, C. Kingsley, and S. Umans, *Electric Machinery*, 5th ed. (New York: McGraw-Hill, 1990).
4. M. S. Sarma, *Electric Machines,* 2nd ed. (Boston: PWS Publishing, 1994).
5. J. R. Neuenswander, *Modern Power Systems* (New York: Intext Educational Publishers, 1971).
6. H. E. Brown, *Solution of Large Networks by Matrix Methods* (New York: Wiley, 1975).
7. G. N. Lester, "High Voltage Circuit Breaker Standards in the USA—Past, Present and Future," *IEEE Transactions PAS*, vol. PAS-93 (1974): pp. 590–600.
8. W. D. Stevenson, Jr., *Elements of Power System Analysis*, 4th ed. (New York: McGraw-Hill, 1982).
9. C. A. Gross, *Power System Analysis* (New York: Wiley, 1979).
10. *Application Guide for AC High-Voltage Circuit Breakers Rated on a Symmetrical Current Basis*, ANSI C 37.010 (New York: American National Standards Institute, 1999/R2005).
11. E. Muljadi and V. Grevorgian, "Short-Circuit Modeling of a Wind Power Plant," Conference Paper NREL/CP-5500-50632, *Power & Energy Society General Meeting*, July 24–29, 2011.

Copyright 2017 Cengage Learning. All Rights Reserved. May not be copied, scanned, or duplicated, in whole or in part. Due to electronic rights, some third party content may be suppressed from the eBook and/or eChapter(s). Editorial review has deemed that any suppressed content does not materially affect the overall learning experience. Cengage Learning reserves the right to remove additional content at any time if subsequent rights restrictions require it.

Copyright 2017 Cengage Learning. All Rights Reserved. May not be copied, scanned, or duplicated, in whole or in part. Due to electronic rights, some third party content may be suppressed from the eBook and/or eChapter(s). Editorial review has deemed that any suppressed content does not materially affect the overall learning experience. Cengage Learning reserves the right to remove additional content at any time if subsequent rights restrictions require it.